TECHNISCHE UNIVERSITÄT WIEN

DISSERTATION

Second-order in time numerical integration of the Landau–Lifshitz–Gilbert equation

ausgeführt zum Zwecke der Erlangung des akademischen Grades eines Doktors der technischen Wissenschaften unter der Leitung von

Univ.Prof. Dipl.Math. Dr.techn. Dirk Praetorius
E101 – Institut für Analysis und Scientific Computing, TU Wien

eingereicht an der Technischen Universität Wien
Fakultät für Mathematik und Geoinformation

von

Dipl.-Ing. Bernhard Erwin Stiftner, BSc.
Matrikelnummer: 0727954
Praterstraße 8/14
A-1020 Wien

Diese Dissertation haben begutachtet:

1. **Prof. Dr. Johannes Kraus**
Mathematische Fakultät, Universität Duisburg-Essen
2. **Univ.Prof. Dipl.Math. Dr.techn. Dirk Praetorius**
Institut für Analysis und Scientific Computing, Technische Universität Wien
3. **Prof. Dr. Andreas Prohl**
Mathematisches Institut, Universität Tübingen

Wien, am 15. Juni 2018

Für meine Eltern.

Kurzfassung

Die Landau–Lifshitz–Gilbert Gleichung (LLG) ist das fundamentale mathematische Modell für Verständnis und Simulation zeitabhängiger mikromagnetischer Phänomene. Schwierigkeiten bei der Entwicklung effizienter numerischer Verfahren sind die Nichtlinearität der Gleichung, eine nicht-konvexe Nebenbedingung, und die Nicht-Eindeutigkeit von Lösungen. Mit dem (zweite Ordnung) Tangent-Plane-Verfahren aus [Alouges et al. (Numer. Math., 128, 2014)] und dem Midpoint-Verfahren aus [Bartels und Prohl (SIAM J. Numer. Anal., 44, 2006)] verfügen wir über zwei Algorithmen mit (formal) zweiter Konvergenzordnung in der Zeit. Beide Algorithmen basieren auf der Finite-Elemente-Methode und konvergieren unbedingt.

Die spezielle Struktur beider Algorithmen legt bei Erweiterungen die aufwändige implizite Behandlung von etwaigen Termen niedriger Ordnung und von gekoppelten Gleichungen, wie etwa Streufeld-Berechnungen oder die Kopplung von LLG mit der Maxwell-Gleichung, nahe. Um dieses Problem zu umgehen, bedienen wir uns eines implizit-expliziten Adams–Bashforth-artigen Ansatzes, mit dem wir die Terme niedriger Ordnung explizit behandeln. Bei Kopplungen von LLG mit anderen Gleichungen entkoppeln wir die näherungsweise Berechnung der Magnetisierung (als Lösung von LLG) und der Lösung der gekoppelten Gleichung (z.B. elektrisches und magnetisches Feld bei der Kopplung von LLG mit der Maxwell-Gleichung). Die so erhaltenen Algorithmen sind (formal) zweiter Konvergenzordnung in der Zeit. Für die Kopplung mit der Eddy-Current-Gleichung erhalten wir so ein entkoppeltes Tangent-Plane-Verfahren mit Konvergenz zweiter Ordnung in der Zeit. Für die Kopplung mit der Spin-Diffusion-Gleichung erhalten wir so ein entkoppeltes Midpoint-Verfahren mit Konvergenz zweiter Ordnung in der Zeit. Darüber hinaus organisieren wir die Annahmen beider Verfahren in einem einheitlichen Rahmen, der insbesondere physikalisch relevante nicht-lineare dissipative Effekte abdeckt. Wir erweitern die vorhandene numerische Analysis und beweisen die unbedingte Konvergenz all unserer erweiterten Algorithmen. Zusätzlich behandeln wir Lösungsstrategien für die entsprechenden Variationsformulierungen. Schließlich führen wir mit unseren erweiterten Algorithmen numerische Experimente durch. Diese Experimente bestätigen die Konvergenz zweiter Ordnung in der Zeit, den reduzierten Aufwand und die Anwendbarkeit auf physikalisch relevante Beispiele.

Abstract

In computational micromagnetism, the Landau–Lifshitz–Gilbert equation (LLG) is the fundamental mathematical model for the understanding and simulation of time-dependent micromagnetic phenomena. The non-linear nature of the equation, a non-convex side constraint, and the non-uniqueness of solutions aggravate the development of efficient numerical algorithms. The (second-order) tangent plane scheme from [Alouges et al. (Numer. Math., 128, 2014)] and the midpoint scheme from [Bartels and Prohl (SIAM J. Numer. Anal., 44, 2006)] provide us with two finite-element-based algorithms, which are both (formally) second-order in time and unconditionally convergent.

The particular structure of both algorithms suggests the numerically expensive implicit treatment of possible lower-order terms and of coupled systems like, e.g., the computation of the stray field or, more generally, the coupling of LLG with the full Maxwell system. To avoid this and to conserve the second-order in time convergence, we employ an implicit-explicit second-order in time Adams–Bashforth-type approach, where we treat the lower-order terms explicitly in time. For couplings with other equations, this decouples the approximate computation of the magnetization (i.e., the solution of LLG), and of the coupled equation (e.g., electrical and magnetic field of the coupling of LLG with the full Maxwell system). The resulting algorithms are (formally) second-order in time. For the coupling with eddy currents, this yields a decoupled second-order in time tangent plane scheme. For the coupling with the spin diffusion equation, this yields a decoupled second-order in time midpoint scheme. Moreover, we provide certain assumptions in a unified framework, which covers, in particular, physically relevant non-linear dissipative effects. We extend the existing convergence analysis and prove unconditional convergence of our extended algorithms. Moreover, we discuss the efficient solution of the corresponding (linear and non-linear) variational problems. Numerical experiments with our extensions confirm the preservation of the second-order in time convergence, reduced computational costs, and the applicability to physically relevant examples of our algorithms.

Danksagung

Mein besonderer Dank gilt meinem PhD-Supervisor Prof. Dirk Praetorius für die Vergabe und das Heranführen an dieses schöne und gleichzeitig herausfordernde Thema. Ohne ihn hätte ich nicht mal gewusst, dass sich Mathematiker mit Mikromagnetismus befassen. Noch wichtiger war aber seine ausgezeichnete Betreuung, sein ganzer Zuspruch, als es nicht so lief, und das tolle Arbeitsklima, das ich in den letzten drei Jahren sehr genossen habe.

Ich danke besonders Prof. Andreas Prohl (Universität Tübingen) und Prof. Johannes Kraus (Universität Duisburg Essen) für das Lesen und Begutachten dieser Arbeit.

Weiters danke ich Prof. Markus Melenk (TU Wien). Durch die ausgezeichnete Betreuung meiner Diplomarbeit hat er wesentlich dazu beigetragen, dass ich mich dazu entschieden habe, ein Doktorat 'dranzuhängen'.

Besonders wichtig war in den letzten drei Jahren das freundschaftliche Umfeld in der (erweiterten) Arbeitsgruppe. Mein Dank gilt Gregor Gantner, Stefan Schimanko, Michael Innerberger, Giovanni Di Fratta, Markus Faustmann, Maximilian Bernkopf, Thomas Führer und Michael Feischl. Besonders hervorheben möchte ich meine Mikromagnetismus- und Bürokollegen Michele Ruggeri und Carl-Martin Pfeiler. Michele Ruggeri danke ich besonders dafür, dass er mir speziell am Anfang meines Doktorats mit Rat und Tat zur Seite gestanden ist. Seine Vorlesung zu Mikromagnetismus hat mir den Einstieg wesentlich erleichtert. Carl-Martin Pfeiler danke ich besonders dafür, dass er im Wesentlichen den `Python`-basierten Teil unseres Mikromagnetismus-Code geschrieben hat. Ein Teil der numerischen Experimente dieser Arbeit wurden mit diesem Code gerechnet. Weiters gilt mein besonderer Dank Alexander Haberl und Alexander Rieder für die Hilfe bei Fragen zu `BEM++`. Alexander Rieder danke ich auch dafür, dass er sein Software-Tool `NGBEM` für die Kopplung von `NGS/Py` und `BEM++` zur Verfügung gestellt hat. Darüber hinaus ist er mir ein treuer Freund seit Beginn meiner Studienzeit und hat geholfen, Teile dieser Arbeit korrekturzulesen. Schließlich danke ich unserer Sekretärin Frau Schweigler, ohne deren Hilfe ich wohl an einigen Hürden in der Verwaltung verzweifelt wäre.

Im Umfeld des Instituts danke ich Prof. Joachim Schöberl und seiner gesamten Arbeitsgruppe für die Unterstützung bei Fragen zur Implementierung mit `NGS/Py`. Besonders hervorheben möchte ich hierbei Christoph Wintersteiger, Philip Lederer und Matthias Hochsteger für die unkomplizierte Beantwortung der einen oder anderen (naiven) Frage.

Außerhalb der TU Wien danke ich allen Pubquiz-Leuten (wechselnde Besetzungen) und allen Fladerei-Leuten für etliche lustige Abende. Mein besonderer Dank gilt Florian Fuchs für seine Freundschaft seit bald 20 Jahren und weil er den Mut hat, mit mir im Anschluss an mein Doktorat auf Weltreise zu gehen.

Weiters danke ich dem gesamten Walder-Clan und allen Stiftners für den familiären Rückhalt in den letzten Jahren.

Am meisten danke ich meinen Eltern Monika Stiftner-Walder und Erwin Stiftner für ihre bedingungslose Unterstützung und Motivation, seit ich denken kann. Ihre Unverwüstlichkeit war mir oft Inspiration in den letzten Jahren. Diese Arbeit widme ich ihnen.

Diese Arbeit wurde dankenswerterweise vom Wiener Wissenschaftsfonds (WWTF) durch das Projekt *Thermally controlled magnetization dynamics* (Grant: MA14-44) unterstützt.

Eidesstattliche Erklärung

Ich erkläre an Eides statt, dass ich die vorliegende Dissertation selbstständig und ohne fremde Hilfe verfasst, andere als die angegebenen Quellen und Hilfsmittel nicht benutzt bzw. die wörtlich oder sinngemäß entnommenen Stellen als solche kenntlich gemacht habe.

Wien, am 15. Juni 2018

Bernhard Erwin Stiftner

Contents

1. Introduction

1.1. Motivation

In computational micromagnetics, the Landau–Lifshitz–Gilbert equation (LLG) [Gil55, LL08] is a widely accepted model for the simulation of magnetization dynamics; see Figure 1.1. In particular, LLG is applied for the modelling and simulation of the writing process on a hard disk drive (HDD). Hard disk drives store information coded in the average magnetization of a tiny compartment of a ferromagnetic material. In the writing process, a recording head generates a magnetic field and the resulting magnetization dynamics reverse the magnetization. For details, we refer to, e.g., [HS98, Chapter 6.4] and the references therein.

1.2. Mathematical model

On a mathematical level, magnetization dynamics (e.g., the HDD writing process) are modelled in the evolution of the magnetization $\boldsymbol{m}$ on a bounded and polyhedral Lipschitz domain $\omega \subset \mathbb{R}^3$. In the following, we provide a basic configuration and discuss certain aspects of the model; cf., e.g., [HS98, BMS09].

For low temperatures, the modulus of $\boldsymbol{m}$ can be assumed to be material dependent and constant. Without loss of generality, we restrict ourselves to the case $|\boldsymbol{m}| = 1$, i.e., we seek

$$\boldsymbol{m}(t) : \omega \to \mathbb{S}^2 := \{\boldsymbol{x} \in \mathbb{R}^3 : |\boldsymbol{x}| = 1\}, \tag{1.1}$$

where $\boldsymbol{m}$ is a solution of the Landau–Lifshitz–Gilbert equation [Gil55, LL08] (LLG). Given a final time $T > 0$, LLG reads

$$\begin{aligned} \partial_t \boldsymbol{m} &= -\boldsymbol{m} \times (\boldsymbol{h}_{\text{eff}}(\boldsymbol{m}) + \boldsymbol{\Pi}(\boldsymbol{m})) + \alpha \boldsymbol{m} \times \partial_t \boldsymbol{m} && \text{in} \quad (0,T) \times \omega, && (1.2a)\\ \partial_{\boldsymbol{n}} \boldsymbol{m} &= \boldsymbol{0} && \text{on} \quad (0,T) \times \partial\omega, && (1.2b)\\ \boldsymbol{m}(0) &= \boldsymbol{m}^0 \quad \text{with} \quad |\boldsymbol{m}^0| = 1 && \text{on} \quad \omega. && (1.2c) \end{aligned}$$

LLG describes the magnetization $\boldsymbol{m}$ under the influence of the so-called effective field $\boldsymbol{h}_{\text{eff}}(\boldsymbol{m}) : \omega \to \mathbb{R}^3$, which reads

$$\boldsymbol{h}_{\text{eff}}(\boldsymbol{m}) \,=\, C_{\mathbf{ex}}\, \Delta \boldsymbol{m} \,+\, \boldsymbol{\pi}(\boldsymbol{m}) \,+\, \boldsymbol{f}. \tag{1.3}$$

Here, $C_{\mathbf{ex}} \Delta \boldsymbol{m}$ is the so-called exchange field with the exchange constant $C_{\mathbf{ex}} > 0$, which models the tendency of the magnetization $\boldsymbol{m}$ to locally align itself into the same direction. In $\boldsymbol{\pi}(\boldsymbol{m}) : \omega \to \mathbb{R}^3$, we collect $\boldsymbol{m}$-dependent lower-order terms such as anisotropy or stray field. We refer to Section 2.2 for a precise definition. Finally, $\boldsymbol{f} : \omega \to \mathbb{R}^3$ models an applied

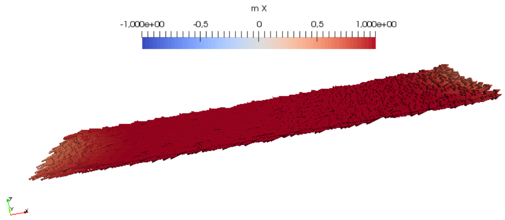

(a) $t = 0$ns

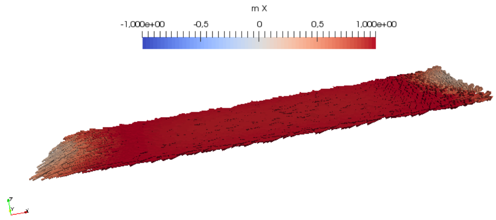

(b) $t = 0.05$ns

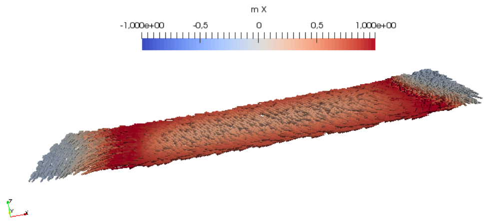

(c) $t = 0.1$ns

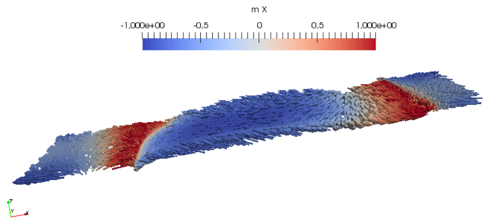

(d) $t = 0.15$ns

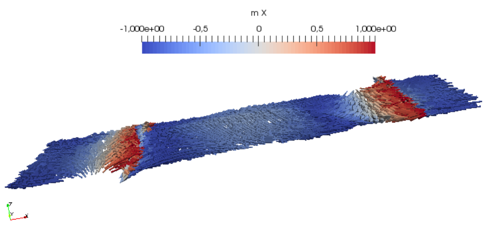

(e) $t = 0.2$ns

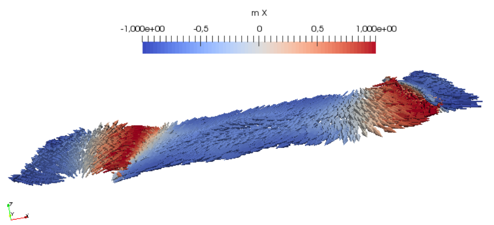

(f) $t = 0.3$ns

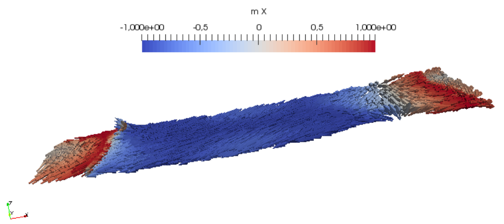

(g) $t = 0.4$ns

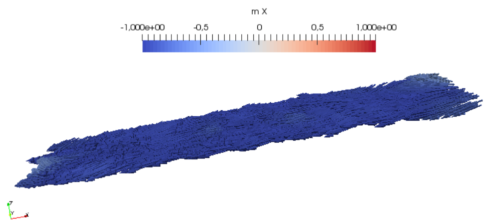

(h) $t = 1$ns

Figure 1.1.: Experiment of Chapter 1: Snapshots of the switching of a magnetization on a thin film of permalloy. The simulation follows the setting of the μ-MAG standard problem #4 [mum] (second configuration). The simulation was performed with a `C++`-based extension of `NGS/Py` [ngs], which was mainly developed by the author. The visualization was done with `ParaView` [AGL05].

magnetic field (e.g., the field generated by a recording head). Associated with the effective field $\boldsymbol{h}_{\mathrm{eff}}(\boldsymbol{m})$, the energy functional of LLG (1.2) is defined as

$$\mathcal{E}_{\mathrm{LLG}}(\boldsymbol{m}) := \frac{C_{\mathbf{ex}}}{2} \int_\omega |\nabla \boldsymbol{m}|^2 \,\mathrm{d}\boldsymbol{x} - \frac{1}{2} \int_\omega \boldsymbol{\pi}(\boldsymbol{m}) \cdot \boldsymbol{m} \,\mathrm{d}\boldsymbol{x} - \int_\omega \boldsymbol{f} \cdot \boldsymbol{m} \,\mathrm{d}\boldsymbol{x} \,. \tag{1.4}$$

Indeed, there holds the formal relation

$$\boldsymbol{h}_{\mathrm{eff}}(\boldsymbol{m}) = -\frac{\delta \mathcal{E}_{\mathrm{LLG}}(\boldsymbol{m})}{\delta \boldsymbol{m}},$$

i.e., $\boldsymbol{h}_{\mathrm{eff}}(\boldsymbol{m})$ is the negative variational derivative of the ferromagnetic bulk energy. Over time, the magnetization $\boldsymbol{m}$ tends to attain a state of minimum energy, where the so-called Gilbert damping constant $0 < \alpha \leq 1$ governs how fast this energy minimum is reached. The larger α, the faster the magnetization $\boldsymbol{m}$ reaches an eventual equilibrium.

Moreover, $\boldsymbol{\Pi}(\boldsymbol{m}) : \omega \to \mathbb{R}^3$ collects lower-order terms, which model external effects, such as the Slonczewski field [Ber96, Slo96] and the Zhang–Li field [ZL04, TNMS05]. Such effects are usually referred to as dissipative effects, and, in contrast to $\boldsymbol{\pi}(\boldsymbol{m})$, do not contribute to the energy functional (1.4). We refer to Section 2.2 for a precise definition.

Finally, let $\boldsymbol{m}$ be a solution of (1.2). Formally testing (1.2a) with $\boldsymbol{m}$, we infer that

$$\frac{\mathrm{d}}{\mathrm{d}t} |\boldsymbol{m}|^2 = \partial_t \boldsymbol{m} \cdot \boldsymbol{m} \stackrel{(1.2a)}{=} 0.$$

If the initial condition $\boldsymbol{m}^0$ satisfies $|\boldsymbol{m}^0| = 1$ on ω, it thus follows that $|\boldsymbol{m}| = 1$ in the space-time cylinder. Hence, regardless of the precise definition of $\boldsymbol{h}_{\mathrm{eff}}(\boldsymbol{m})$ and $\boldsymbol{\Pi}(\boldsymbol{m})$, any solution $\boldsymbol{m}$ of LLG (1.2) satisfies the constraint (1.1).

1.2.1. Couplings with other equations

More advanced mathematical models in computational micromagnetism take into account the effects which stem from a bounded and polyhedral Lipschitz domain $\Omega \subset \mathbb{R}^3$ with $\omega \subsetneqq \Omega$, i.e., from outside of ω. Naturally, this leads to the coupling of LLG with another PDE which is defined on Ω. In this work, we consider the coupling with the eddy current equation (ELLG) (see, e.g., [LT13, LPPT15]) as well as the coupling with the spin diffusion equation (SDLLG) [GW07]; see Chapter 2 for details.

1.3. State of the art

As far as the analysis of LLG is concerned, the notion of a weak solution of LLG goes back to [Vis85, AS92]. Weak solutions of LLG exist globally in time but are in general not unique [AS92]. However, [CF01] proves that strong solutions exist locally in time up to some (possibly very small) time $T > 0$. Moreover, the work [DS14] proves a weak-strong uniqueness principle of LLG in the sense that, if $\boldsymbol{m}_1$ is a smooth solution of LLG on $[0, T]$ and $\boldsymbol{m}_2$ is a weak solution on $[0, T]$, then $\boldsymbol{m}_1 = \boldsymbol{m}_2$ on $[0, T]$.

For couplings with other equations, the notion of weak solutions extends that from [AS92]: We refer to [LT13] for the coupling of LLG with the eddy current equation, to [CF98] for the coupling with the full Maxwell system (MLLG), and to [GW07] for the coupling with the spin diffusion equation (SDLLG). In all the latter references, existence of weak solutions to the corresponding coupled LLG systems is proved. Moreover, the weak-strong uniqueness principle for LLG applies also to MLLG [DS14].

The numerical integration of LLG and its coupled systems has received much attention in the recent years. For an introduction, we refer to, e.g., the monographs [Pro01, BBNP14] or the review articles [KP06, GW07, Cim08] and the references therein. This work is concerned with advances and extension of the following two numerical schemes, which are both based on the finite element method (FEM).

- **The tangent plane scheme (TPS):** The tangent plane scheme in its present form goes back to the work [Alo08]. It is based on an equivalent reformulation of LLG and requires only the solution of one linear FEM system per time-step; see Section 1.3.1 below for details.
- **The midpoint scheme (MPS):** The midpoint scheme was first analyzed in the work [BP06]. It is based on the implicit midpoint rule for time-integration and FEM in space; see Section 1.3.2 below for details.

As far as convergence is concerned, the tangent plane scheme as well as the midpoint scheme, and the corresponding extensions usually yield only formal convergence rates; see, e.g., [BP06, Alo08, BBP08, LT13, AKST14]. This is due to the fact that the convergence proofs in these works employ an energy argument for the existence of solutions of parabolic problems; see, e.g., [Eva10]. Usually, one only has convergence of a subsequence of the algorithm's output and ideally requires no CFL-type coupling of the time-step size $k > 0$ and the mesh-size $h > 0$. In this virtue, we make the following standard convention.

Convention 1.3.1 (Unconditional convergence)**.** *We say that a time-marching algorithm is unconditionally convergent, if a subsequence of the (postprocessed) output converges towards a weak solution of LLG (or a coupled LLG system) and if this requires no coupling of the time-step size $k > 0$ and the mesh-size $h > 0$.*

Finally, note that there exists a variety of micromagnetic software. We mention the popular `OOMMF`-package [DP99], which employs a finite difference method. Moreover, the `Python`-based software tool `magnum.fe` [AEB$^+$13] contributes to the well-known open source `FEniCS`-project. Besides, we refer to the μ-MAG homepage [mum] of the National Institute of Science and Technology (NIST) for benchmark problems, solution reports, and links to more micromagnetic software.

1.3.1. The tangent plane scheme (TPS)

The so-called tangent plane scheme (TPS) is a popular approach for the numerical integration of LLG. The fully explicit prototype of the first-order tangent plane scheme was first formulated and analyzed in [AJ06] with a refined analysis in [BKP08]. In [Alo08], an additional implicit stabilization term was introduced.

The tangent plane scheme relies on the equivalent reformulation of LLG (1.2a)

$$\alpha\,\partial_t \boldsymbol{m} + \boldsymbol{m} \times \partial_t \boldsymbol{m} = \big[\,\boldsymbol{h}_{\mathrm{eff}}(\boldsymbol{m}) + \boldsymbol{\Pi}(\boldsymbol{m})\,\big] - \big(\boldsymbol{h}_{\mathrm{eff}}(\boldsymbol{m}) \cdot \boldsymbol{m}\big)\boldsymbol{m} - \big(\boldsymbol{\Pi}(\boldsymbol{m}) \cdot \boldsymbol{m}\big)\boldsymbol{m}. \qquad (1.5)$$

It employs uniform time-stepping with time-step size $k > 0$ for time discretization and standard lowest-order Courant finite elements in $3D$ for space discretization. At time t_i and for given $\boldsymbol{m}_h^i \approx \boldsymbol{m}(t_i)$, one solves *one* linear system for $\boldsymbol{v}_h^i \approx \boldsymbol{v}(t_i) := \partial_t \boldsymbol{m}(t_i)$ in an $\boldsymbol{m}_h^i$-dependent subspace, which mimics $\boldsymbol{v} \cdot \boldsymbol{m} = 0$ nodewise. Then, $\boldsymbol{m}_h^{i+1} \approx \boldsymbol{m}(t_i + k)$ is the nodewise normalization of $\boldsymbol{m}_h^i + k\boldsymbol{v}_h^i$.

For the first-order tangent plane scheme, [Alo08] proves unconditional convergence in the sense of Convention 1.3.1. Starting from the basic configuration $\boldsymbol{h}_{\text{eff}}(\boldsymbol{m}) = \Delta \boldsymbol{m}$ and $\boldsymbol{\Pi}(\boldsymbol{m}) = \boldsymbol{0}$, the scheme as well as the convergence results of [Alo08] were extended to lower-order contributions [AKT12, Gol12, Pag13, BSF$^+$14], the couplings with the eddy current equation [LPPT15, LT13, Pag13], the coupling with the full Maxwell system [Pag13, BPP15], the coupling with the spin diffusion equation [AHP$^+$14, ARB$^+$15, Rug16], and the coupling with magnetostriction [Pag13, BPPR14]. Even stochastic effects were considered in [GLT16] and [AdBH14], where the latter work considers only a semi-discretization in time. Finally, [AHP$^+$14, Rug16] show that the normalization of the update in the computation of $\boldsymbol{m}_h^{i+1} \approx \boldsymbol{m}(t_i + k)$ can be omitted.

All the latter algorithms are formally first-order in time. Moreover, in the recent work [FT17], the authors derive a-priori estimates for the tangent plane scheme without normalization for LLG and ELLG, provided that the solution is smooth enough.

For (almost) second-order convergence in time, [AKST14] introduces a variant of the tangent plane scheme for plain LLG, which relies on a smarter choice of the unknown $\boldsymbol{v}$, but still requires only the solution of *one* adapted linear system per time-step. The resulting integrator (TPS2) is formally and experimentally of (almost) second-order in time in the sense that for the time-step size $k > 0$, one expects a consistency error of the size $\mathcal{O}(k^{2-\varepsilon})$ for all $\varepsilon > 0$. Moreover, [AKST14] proves unconditional convergence in the sense of Convention 1.3.1. However, the scheme treats the lower-order terms implicitly in time, and, for example, for non-local stray field computations one either has to solve a linear system with a fully populated system matrix or to employ a fixed-point iteration. Both approaches complicate the computations and increase the computational costs.

1.3.2. The midpoint scheme (MPS)

The so-called midpoint scheme is another popular approach for the numerical integration of LLG. It was first analyzed in [BP06] with $\boldsymbol{h}_{\text{eff}}(\boldsymbol{m}) := \Delta \boldsymbol{m}$ and $\boldsymbol{\Pi}(\boldsymbol{m}) = \boldsymbol{0}$.

The basic idea is summarized as follows: Let $k > 0$ be the uniform time-step size. At time t_i and for given $\boldsymbol{m}^i \approx \boldsymbol{m}(t_i)$, the standard semi-discrete midpoint rule in time employed to LLG (1.2a) solves for $\boldsymbol{m}^{i+1} \approx \boldsymbol{m}(t_i + k)$ the *non-linear* system

$$\mathrm{d}_t \boldsymbol{m}^{i+1} = -\boldsymbol{m}^{i+1/2} \times \Delta \boldsymbol{m}^{i+1/2} + \alpha\, \boldsymbol{m}^{i+1/2} \times \mathrm{d}_t \boldsymbol{m}^{i+1}, \tag{1.6}$$

where $\boldsymbol{m}^{i+1/2} := (\boldsymbol{m}^{i+1} + \boldsymbol{m}^i)/2$ and $\mathrm{d}_t \boldsymbol{m}^{i+1} := (\boldsymbol{m}^{i+1} - \boldsymbol{m}^i)/k$. Then, [BP06] additionally employs lowest-order Courant finite elements in $3D$ for space discretization and solves (1.6) on a discrete variational level.

The resulting integrator is unconditionally convergent in the sense of Convention 1.3.1 [BP06]. Moreover, [Cim09] and [BP07, BP08] transfer the midpoint scheme and the convergence result of [BP06] to the formally equivalent Landau–Lifshitz form of LLG and the related (p-)harmonic heat flow, respectively. The midpoint scheme and the convergence results of [BP06] were extended to applications in thermally assisted recording [BPS09, BPS12], where the modulus constraint $|\boldsymbol{m}| = 1$ from (1.1) is relaxed, and to stochastic effects [BBP13, BBNP14]. Moreover, [BBP08] considers the coupling of LLG with the full Maxwell system. There, the computation of the approximations to the magnetization $\boldsymbol{m}$ and the magnetic and electric field requires the solution of a fully-coupled non-linear system.

To solve the non-linear system, the only rigorous method is a fixed-point iteration; see, e.g., [BP06, BBP08, BPS09]. However, for the convergence of the fixed-point iteration, we require the CFL-type condition $k = \mathbf{o}(h^2)$. Naturally, this iteration is stopped when a given tolerance is reached. The resulting inexact midpoint scheme still conserves the modulus constraint (1.1) nodewise [Bar06]. Moreover, [Bar06] extends the convergence result of [BP06] in the sense that it takes into account the inexact solution of the non-linear system by the fixed-point iteration.

Formally and experimentally, the midpoint scheme is second-order in time, but, to our knowledge, the thorough a priori analysis is still open. However, in contrast to the tangent plane scheme from the latter section, the midpoint scheme conserves the (discrete) energy and the nodal modulus and requires no nodewise normalization.

1.4. Outline & Contributions

In this section, we give a short overview on the structure and contributions of this work. To this end, we start with the following crucial convention.

Convention 1.4.1 (IMEX). *We say that a time-marching scheme is implicit-explicit (IMEX), if it treats only the higher-order terms implicitly, while the lower-order terms are integrated explicitly in time.*

We will encounter the latter term at several places in this work. In particular, it is relevant the following two general concepts of this work.

- **Second-order in time IMEX integration:** For analytical reasons as well as for numerical stability, both, the (almost) second-order tangent plane scheme as well as the midpoint scheme require an implicit-in-time treatment of higher-order terms. In their basic forms from [BP06, AKST14], both algorithms suggest the numerically expensive implicit treatment of the lower-order terms $\boldsymbol{\pi}$ and $\boldsymbol{\Pi}$. As an improvement, we employ an explicit second-order in time Adams–Bashforth-type approach to the lower-order terms $\boldsymbol{\pi}$ and $\boldsymbol{\Pi}$. As a result, we obtain IMEX algorithms in the sense of Convention 1.4.1, which preserve the formal convergence order, but significantly reduce the computational costs.

- **Decoupled second-order time-stepping:** We extend the second-order in time IMEX integration to coupled LLG system (e.g., the coupling with eddy currents). The benefit is that (from the second time-step on) we decouple the time-stepping of LLG and the coupled equation. As before, this reduces the computational effort of the integrator, but preserves the formal convergence order.

Throughout this work, we keep assumptions (e.g., to $\boldsymbol{\pi}$) general. However, we note that our exemplary contributions to $\boldsymbol{\pi}$ (e.g., the stray field), $\boldsymbol{\Pi}$, as well as the corresponding approximations, (mostly) fall into our setting and refer to Appendix A for the verifications. Besides, the assumptions of this work are organized as follows.

- **Abstract assumption framework:** We label general assumptions to the lower-order terms and to the discretization with **(L $\cdot$)** and **(D $\cdot$)**, respectively. As an example, **(L2)** supposes the boundedness of the operator $\boldsymbol{\pi}(\cdot)$. Moreover, we label specific assumptions to the (almost) second-order tangent plane scheme and the extension to the coupled ELLG system with **(T $\cdot$)** and **(E $\cdot$)**, respectively. Similarly, we label the specific assumptions to the midpoint scheme and the extension to the coupled SDLLG system with **(M $\cdot$)** and **(S $\cdot$)**, respectively.

Chapter 2 and Chapter 3 collect the preliminaries of this work. In these chapters, we unify and extend the analytical and numerical framework of the own works [DPP$^+$17, PRS18].

- **Chapter 2 (Analytical framework):** We collect basic notations, function spaces, assumptions, the coupling of LLG with the eddy current equation (ELLG), and the spin diffusion equation (SDLLG). Moreover, we introduce the notion of weak solutions of LLG, the coupled ELLG system, and the coupled SDLLG system.

- **Chapter 3 (Discretization):** We introduce meshes, FEM spaces, and fix the time- and space discretization. Moreover, we introduce the discretization of the LLG data and make all assumptions which are not associated with the specific algorithms in this work. Specific assumptions for the tangent plane scheme or midpoint scheme and couplings are made in the corresponding chapters.

In Chapter 4–7, we present, elaborate, and extend findings from the own works [DPP$^+$17, PRS18], which we supplement with findings from our work [KPP$^+$18]. In particular, this involves the following contributions:

- **Chapter 4 (IMEX TPS2):** Based on [DPP$^+$17], we extend the (almost) second-order tangent plane scheme from [AKST14] and additionally cover non-constant external fields and dissipative effects, i.e., $\partial_t \boldsymbol{f} \neq \boldsymbol{0}$ and $\boldsymbol{\Pi} \neq \boldsymbol{0}$. To reduce the computational costs, we introduce a second-order in time IMEX approach. We prove unconditional convergence in the sense of Convention 1.3.1 of our extended algorithm. Based on [DPP$^+$17, KPP$^+$18], we also discuss strategies for the non-trivial solution of the underlying discrete variational problem of the method.

- **Chapter 5 (Decoupled TPS2 for ELLG):** We extend the findings of the latter section to the coupled ELLG system. Based on [DPP$^+$17], we formulate an (almost) second-order in time tangent plane scheme. In particular, this involves a decoupled second-order time-stepping. The benefit is that we only have to sequentially solve only two linear systems per time-step, which reduces the computational costs. Then, we prove unconditional convergence in the sense of Convention 1.3.1 of our extended algorithm.

- **Chapter 6 (IMEX MPS):** Based on [PRS18], we formulate an extension of the midpoint scheme of [BP06], which additionally takes into account the lower-order terms $\boldsymbol{\pi}$, $\boldsymbol{f}$, and, $\boldsymbol{\Pi}$. In particular, this involves a second-order in time IMEX approach, which conserves the second-order in time convergence of the overall scheme. As a benefit, this approach saves us the time-consuming (approximate) evaluation of $\boldsymbol{\pi}$ and $\boldsymbol{\Pi}$ at each iteration of the fixed-point iteration for the solution of the non-linear system. Instead, we only require *one* (approximate) evaluation of $\boldsymbol{\pi}$ and $\boldsymbol{\Pi}$ per time-step. Then, we prove unconditional convergence in the sense of Convention 1.3.1 of our extended algorithm as well as convergence of the algorithm resulting from the inexact solution of the non-linear system by the fixed-point iteration. Finally, extending [PRS18], we present a strategy to compute the fixed-point iterates on a linear algebra level, and prove a refined uniqueness result of the discrete solutions of the non-linear problem.

- **Chapter 7 (Decoupled MPS for SDLLG):** Based on new ideas, we extend the findings of the latter section to the coupled SDLLG system, i.e., we formulate and analyze a corresponding midpoint scheme. This chapter and the results therein are the natural counterpart of Chapter 5 for the tangent plane scheme, i.e., we employ a decoupled second-order time-stepping, and prove unconditional convergence in the sense of Convention 1.3.1 of our extended algorithm.

Moreover, we underpin the theoretical findings (e.g., formal convergence rates) and the practical applicability of our extensions from Chapter 4–6 with numerical experiments, which are based on the following implementations.

- **Implementation:** We employ a `C++`-based and a `Python`-based extension of the FEM software package `NGS/Py` [ngs]. The `C++`-based extension was mostly developed by the author in the time of his Phd thesis. The `Python`-based extension was mostly developed by *Carl-Martin Pfeiler*[1] in the course of his co-supervised master thesis. These implementations will also be part of the joint work [EHM⁺18] with *Lukas Exl*[2], *Carl-Martin Pfeiler*[1], *Norbert Mauser*[2], *Dirk Praetorius*[1], *Michele Ruggeri*[2], and *Joachim Schöberl*[1]. For both, the `C++`-extension and the `Python`-extension, we require couplings with the `BEM` software `BEM++` [ŚBA⁺15]. To this end, we employ the software tool `NGBem` [Rie], which was developed by *Alexander Rieder*[1].

Finally, we point out that the present work stands in line with the PhD-theses [Gol12, Pag13, Rug16], the master thesis [Kem14], and the co-supervised master thesis [Pfe17] on computational micromagnetism, which were all written in the work-group and which laid the foundations to this work.

[1] TU Wien
[2] Universität Wien

2. The analytical framework

The goal of this chapter is to unify, elaborate, and extend the analytical framework of the LLG model and the coupled LLG systems from our works [DPP⁺17, PRS18]. It covers:

- **General framework:** We collect general notations, definitions, spaces, and results. In particular, we introduce (time-dependent) L^p- and Sobolev spaces in Section 2.1.
- **Precise LLG:** We state the LLG model with all necessary general assumptions. In particular, we introduce the $\boldsymbol{m}$-dependent lower-order contributions $\boldsymbol{\pi}(\boldsymbol{m})$ and $\boldsymbol{\Pi}(\boldsymbol{m})$ as general operators. Moreover, we introduce the notion of a weak solution of LLG; see Section 2.2.
- **Coupled systems:** We extend the model by coupling LLG with eddy currents (ELLG) and spin diffusion (SDLLG) and introduce the corresponding notions of weak solutions; see Section 2.2.1 for ELLG and Section 2.2.2 for SDLLG.

Meshes and approximation spaces do not belong here. They are introduced in Chapter 3.

2.1. General notations, definitions, spaces, and results

We recall the following standard notations:

- $\boldsymbol{A \lesssim B}$: For $A, B \in \mathbb{R}$, we write $A \lesssim B$, if there exists a generic constant $C > 0$ (which is clear from the context), such that $A \leq CB$[1].
- $\boldsymbol{A \gtrsim B}$**:** For $A, B \in \mathbb{R}$, we write $A \gtrsim B$, if $B \lesssim A$[1].
- $\boldsymbol{A \simeq B}$**:** For $A, B \in \mathbb{R}$, we write $A \simeq B$ if $A \lesssim B$ and $B \lesssim A$[1].
- `Matlab` **notation:** Let $d \in \mathbb{N}$ and $\mathbf{b}_1, \dots, \mathbf{b}_m \in \mathbb{R}^d$. We write $[\mathbf{b}_1, \dots, \mathbf{b}_m] \in \mathbb{R}^{d\times m}$ for the matrix, whose ℓ-th column is $\mathbf{b}_\ell$ for all $\ell \in \{1, \dots, m\}$.
- $\mathbf{a} \times \mathbf{B}$**:** Given $\mathbf{a} \in \mathbb{R}^3$ and $\mathbf{B} := [\mathbf{b}_1, \mathbf{b}_2, \mathbf{b}_3]$ with $\mathbf{b}_1, \mathbf{b}_2, \mathbf{b}_3 \in \mathbb{R}^3$, we write

$$\mathbf{a} \times \mathbf{B} := \Big[\mathbf{a} \times \mathbf{b}_1 \, , \, \mathbf{a} \times \mathbf{b}_2 \, , \, \mathbf{a} \times \mathbf{b}_3\Big] \in \mathbb{R}^{3\times 3}.$$

- **Dual spaces:** Let B be a Banach space with the corresponding norm $\|\cdot\|_B$. By B', we denote the space of linear and continuous functionals on B. With the norm

$$\|f\|_{B'} := \sup_{B \ni x \neq \mathbf{0}} \frac{|f(x)|}{\|x\|_B},$$

[1] In particular, this notation implies that the constant $C > 0$ depends on the data of the model but not on discretization parameters such as time-step size $k > 0$ or mesh-size $h > 0$

B' is a Banach space. Moreover, we adopt the standard duality pairing with

$$\langle f, x\rangle_{B'\times B} := f(x) \quad \text{for all } f \in B' \quad \text{and for all } x \in B.$$

- **Polynomials:** For a domain $D \subset \mathbb{R}^d$, where $d \geq 1$, we write $\mathcal{P}^k(D)$ for the polynomials of degree at most $k \in \mathbb{N}_0$ on D.
- **Space-time domain:** Given $d \in \mathbb{N}$, a domain $D \subset \mathbb{R}^d$, and $T > 0$, we write $D_T := (0,T) \times D$.
- **Zero extension/Restriction:** Given two domains $D \subsetneq D' \subset \mathbb{R}^d$, where $d \geq 1$, we interpret functions on D as functions on D' with zero-extension, and functions on D' as functions on D via restriction.

Finally, we recall the following standard concepts of convergence on a Banach space B; cf, e.g., [Yos95, Chapter 5]:

- **Weak convergence:** Let $(x_\ell)_{\ell\in\mathbb{N}} \subset B$ and $x \in B$. We say that $(x_\ell)_{\ell\in\mathbb{N}}$ converges weakly in B to x as $\ell \to \infty$, if

  $$f(x_\ell) \to f(x) \quad \text{as } \ell \to \infty \quad \text{for all } f \in B'.$$

  Then, we write $x_\ell \rightharpoonup x$ as $\ell \to \infty$ in B.
- **Weak* convergence:** Let $(f_\ell)_{\ell\in\mathbb{N}} \subset B'$ and $f \in B'$. We say that $(f_\ell)_{\ell\in\mathbb{N}}$ is weak* convergent in B' towards f as $\ell \to \infty$, if

  $$f_\ell(x) \to f(x) \quad \text{as } \ell \to \infty \quad \text{for all } x \in B.$$

  Then, we write $f_\ell \overset{*}{\rightharpoonup} f$ as $\ell \to \infty$ in B.

2.1.1. L^p- and Sobolev spaces

In this section, we collect definitions, notations, and results for the well-known L^p- and Sobolev spaces; see, e.g., [AF03, Eva10, Maz11]. Throughout this section, let $d \in \mathbb{N}$ and let $D \subset \mathbb{R}^d$ be a domain.

- **L^p-spaces:** For $p \in [1,\infty]$ we denote the space of p-integrable functions on D with $L^p(D)$, and recall that for $\varphi \in L^p(D)$ the corresponding norm reads

$$\|\varphi\|_{L^p(D)} := \begin{cases} \big(\int_D |\varphi|^p \,\mathrm{d}x\big)^{1/p} & \text{for } p \in [1,\infty), \\ \operatorname{ess\,sup}_D |\varphi| & \text{for } p = \infty. \end{cases}$$

It is well-known that $L^p(D)$ is a Banach space, separable for $1 \leq p < \infty$, reflexive for $1 < p < \infty$, and a Hilbert space for $p = 2$, where we denote the generic scalar product with

$$\langle \varphi, \psi\rangle_{L^2(D)} := \int_D \varphi\,\psi \,\mathrm{d}x \quad \text{for all } \varphi, \psi \in L^2(D).$$

For details on L^p-spaces, we refer to, e.g., [AF03, Section 2]. Moreover, there holds the following well-known interpolation estimate.

Proposition 2.1.1 (Interpolation estimate, [AF03, Theorem 2.11])**.** *Let $D \subset \mathbb{R}^d$ be a domain. Let $1 \le p < q < r \le \infty$ and $\Theta \in (0,1)$ such that*

$$\frac{1}{q} = \frac{\Theta}{p} + \frac{1-\Theta}{r}.$$

Let $\varphi \in L^p(D) \cap L^r(D)$. Then, $\varphi \in L^q(D)$ and it holds that

$$\|\varphi\|_{L^q(D)}^2 \;\le\; \|\varphi\|_{L^p(D)}^{\Theta}\, \|\varphi\|_{L^r(D)}^{1-\Theta}. \qquad \square$$

- **Sobolev spaces:** Let $\boldsymbol{\alpha} := (\boldsymbol{\alpha}_1, \dots, \boldsymbol{\alpha}_d) \in (\mathbb{N}_0)^d$ be a given multi-index and $|\boldsymbol{\alpha}| := \sum_{m=1}^d |\boldsymbol{\alpha}_m|$. For $\varphi \in C^\infty(D)$, we denote the derivative of order $\boldsymbol{\alpha}$ by

$$D^{\boldsymbol{\alpha}}\varphi := \partial \boldsymbol{x}_1^{\boldsymbol{\alpha}_1} \cdots \partial \boldsymbol{x}_d^{\boldsymbol{\alpha}_d}\, \phi \in C^\infty(D) \quad \text{with } D^{\boldsymbol{\alpha}}\varphi = \varphi \text{ for } |\boldsymbol{\alpha}| = 0.$$

The standard generalization to weak derivatives in the distributional sense allows to define $D^{\boldsymbol{\alpha}}\phi$ even if ϕ is not differentiable; see, e.g., [AF03, Section 1]. For $p \in [1,\infty]$ and $k \in \mathbb{N}_0$, this leads us to the Sobolev spaces

$$W^{k,p}(D) := \{\varphi \in L^p(D) : D^{\boldsymbol{\alpha}}\varphi \in L^p(D) \text{ for all } \boldsymbol{\alpha} \in (\mathbb{N}_0)^d \text{ with } |\boldsymbol{\alpha}| \le k\},$$

and we interpret $W^{0,p} = L^p(D)$. For $\varphi \in W^{k,p}(D)$, we denote the corresponding norm by

$$\|\varphi\|_{W^{k,p}(D)} := \begin{cases} \Big(\sum_{|\boldsymbol{\alpha}| \le k} \|D^{\boldsymbol{\alpha}}\varphi\|_{L^p(D)}^p \Big)^{1/p} & \text{for } p \in [1,\infty), \\ \max_{|\boldsymbol{\alpha}| \le k} \|D^{\boldsymbol{\alpha}}\varphi\|_{L^\infty(D)} & \text{for } p = \infty. \end{cases}$$

It is well-known that $W^{k,p}(D)$ is Banach space, separable for $1 \le p < \infty$, and reflexive for $1 < p < \infty$. For $p = 2$, we use the standard notation $H^k(D) := W^{k,2}(D)$ and note that $H^k(D)$ is a separable Hilbert space. Then, we denote the generic scalar product by

$$\langle \varphi, \psi \rangle_{H^k(D)} := \sum_{|\boldsymbol{\alpha}| \le k} \int_D D^{\boldsymbol{\alpha}}\varphi\, D^{\boldsymbol{\alpha}}\psi \,\mathrm{d}x \quad \text{for all } \varphi, \psi \in H^k(D),$$

and write $\|\cdot\|_{H^k(D)}$ for the corresponding norm. For details on Sobolev spaces, we refer to, e.g., [AF03, Section 3] and [Eva10, Section 5]. Moreover, there hold the following well-known embedding theorems.

Theorem 2.1.2 (Rellich–Kondrachov theorem, [AF03, Theorem 6.3(i)])**.** *Let $d \in \mathbb{N}$ and let $D \subset \mathbb{R}^d$ be a bounded Lipschitz domain. Then, the embedding from $H^1(D)$ into $L^2(D)$ is compact. In particular, for any sequence $(\varphi_n)_{n\in\mathbb{N}} \subset H^1(D)$ and $\varphi \in H^1(D)$, we get that*

$$\varphi_n \rightharpoonup \varphi \quad \text{in } H^1(D) \text{ as } n \to \infty \quad \Rightarrow \quad \varphi_n \to \varphi \quad \text{in } L^2(D) \text{ as } n \to \infty. \qquad \square$$

Theorem 2.1.3 (Sobolev embedding, [AF03, Theorem 4.12, Case C])**.** *Let $D \subset \mathbb{R}^3$ be a bounded Lipschitz domain. Then, for $2 \le p \le 6$, the embedding from $H^1(D)$ in $L^p(D)$ is continuous.* $\square$

Finally, we define for $\varphi \in W^{k,p}(D)$ the semi-norm

$$|\varphi|_{W^{k,p}(D)} := \begin{cases} \Big(\sum_{|\boldsymbol{\alpha}| = k} \|D^{\boldsymbol{\alpha}}\varphi\|_{L^p(D)}^p \Big)^{1/p} & \text{for } p \in [1,\infty), \\ \max_{|\boldsymbol{\alpha}| = k} \|D^{\boldsymbol{\alpha}}\varphi\|_{L^\infty(D)} & \text{for } p = \infty. \end{cases}$$

2.1.2. Vector-valued spaces

In this section, we collect standard notations and definitions for vector-valued spaces. Given a space B, we use bold letter for the corresponding vector-valued version, i.e., we write

$$\boldsymbol{B} := (B)^3.$$

For given a domain $D \in \mathbb{R}^d$ with $d \in \mathbb{N}$, we write, for example

$$\boldsymbol{C}^\infty(D) := \big(\, C^\infty(D)\,\big)^3, \quad \boldsymbol{C}(D) := \big(\, C(D)\,\big)^3,$$
$$\boldsymbol{C}^\infty(\overline{D}) := \big(\, C^\infty(\overline{D})\,\big)^3, \quad \boldsymbol{C}(\overline{D}) := \big(\, C(\overline{D})\,\big)^3.$$

In particular, this extends the notations for L^p-spaces and Sobolev spaces from Section 2.1.1 to product spaces in three dimensions for vector-valued functions. For $p \in [1,\infty]$ and $k \in \mathbb{N}_0$, we write

$$\boldsymbol{L}^p(D) := (L^p(D))^3, \quad \boldsymbol{W}^{k,p}(D) := (W^{k,p}(D))^3, \quad \text{and} \quad \boldsymbol{H}^k(D) := (H^k(D))^3.$$

With $\boldsymbol{\varphi} \in \boldsymbol{L}^p(D)$, the corresponding norm on the product space $\boldsymbol{L}^p(D)$ reads

$$\|\boldsymbol{\varphi}\|_{\boldsymbol{L}^p(D)} := \begin{cases} \big(\int_D |\boldsymbol{\varphi}|^p \,\mathrm{d}x\,\big)^{1/p} & \text{for } p \in [1,\infty), \\ \operatorname{ess\,sup}_D |\boldsymbol{\varphi}| & \text{for } p = \infty. \end{cases}$$

For $p = 2$, we use the standard scalar product for product spaces and write

$$\langle \boldsymbol{\varphi}, \boldsymbol{\psi} \rangle_{\boldsymbol{L}^2(D)} := \sum_{\ell=1}^{3} \int_D \boldsymbol{\varphi}_\ell \cdot \boldsymbol{\psi}_\ell \,\mathrm{d}x \quad \text{for all } \boldsymbol{\varphi}, \boldsymbol{\psi} \in \boldsymbol{L}^2(D).$$

Moreover, for $\boldsymbol{\Phi}, \boldsymbol{\Psi} \in L^2(D)^{3\times 3}$, with $\boldsymbol{\Phi} = [\boldsymbol{\varphi}_1, \boldsymbol{\varphi}_2, \boldsymbol{\varphi}_3]$ and $\boldsymbol{\Psi} = [\boldsymbol{\psi}_1, \boldsymbol{\psi}_2, \boldsymbol{\psi}_3]$, where $\boldsymbol{\varphi}_\ell, \boldsymbol{\psi}_\ell \in \boldsymbol{L}^2(D)$ for all $\ell \in \{1,2,3\}$, we reuse the latter notation and write

$$\langle \boldsymbol{\Phi}, \boldsymbol{\Psi} \rangle_{\boldsymbol{L}^2(D)} := \sum_{\ell=1}^{3} \langle \boldsymbol{\varphi}_\ell, \boldsymbol{\psi}_\ell \rangle_{\boldsymbol{L}^2(D)}, \tag{2.1a}$$

$$\|\boldsymbol{\Phi}\|^2_{\boldsymbol{L}^2(D)} := \sum_{\ell=1}^{3} \|\boldsymbol{\varphi}_\ell\|^2_{\boldsymbol{L}^2(D)}. \tag{2.1b}$$

For $\boldsymbol{\varphi} := (\boldsymbol{\varphi}_1, \boldsymbol{\varphi}_2, \boldsymbol{\varphi}_3)^T \in \boldsymbol{W}^{k,p}(D)$, and a multi-index $\boldsymbol{\alpha} \in (\mathbb{N}_0)^d$, we interpret the weak derivative componentwise, i.e.,

$$D^{\boldsymbol{\alpha}} \boldsymbol{\varphi} := (\, D^{\boldsymbol{\alpha}} \boldsymbol{\varphi}_1, D^{\boldsymbol{\alpha}} \boldsymbol{\varphi}_2, D^{\boldsymbol{\alpha}} \boldsymbol{\varphi}_3 \,)^T \in \boldsymbol{L}^p(D).$$

Then, similarly as for $\boldsymbol{L}^p(D)$, our corresponding norm on the product space reads

$$\|\boldsymbol{\varphi}\|_{\boldsymbol{W}^{k,p}(D)} := \begin{cases} \Big(\, \sum_{|\boldsymbol{\alpha}| \le k} \|D^{\boldsymbol{\alpha}} \boldsymbol{\varphi}\|^p_{\boldsymbol{L}^p(D)} \Big)^{1/p} & \text{for } p \in [1,\infty), \\ \max_{|\boldsymbol{\alpha}| \le k} \|D^{\boldsymbol{\alpha}} \boldsymbol{\varphi}\|_{\boldsymbol{L}^\infty(D)} & \text{for } p = \infty. \end{cases}$$

Moreover, for $D \subset \mathbb{R}^3$, we extend the usual gradient notation to the Jacobian and write

$$\nabla \boldsymbol{\varphi} := \big[\, \partial_{\boldsymbol{x}_1}\boldsymbol{\varphi}, \partial_{\boldsymbol{x}_2}\boldsymbol{\varphi}, \partial_{\boldsymbol{x}_3}\boldsymbol{\varphi} \,\big] \in L^p(D)^{3\times 3}.$$

We note that $\partial_{\boldsymbol{x}_\ell}\boldsymbol{\varphi} \in \boldsymbol{L}^p(D)$ for all $\ell \in \{1,2,3\}$. Moreover, for $p = 2$ and $\boldsymbol{\varphi}, \boldsymbol{\psi} \in \boldsymbol{H}^1(D)$, the notations (2.1) then yield that

$$\begin{aligned} \langle\, \nabla\boldsymbol{\varphi}, \nabla\boldsymbol{\psi} \,\rangle_{\boldsymbol{L}^2(D)} &= \sum_{\ell=1}^{3} \langle \partial_{\boldsymbol{x}_\ell}\boldsymbol{\varphi}, \partial_{\boldsymbol{x}_\ell}\boldsymbol{\psi} \rangle_{\boldsymbol{L}^2(D)}, \\ \|\nabla\boldsymbol{\varphi}\|^2_{\boldsymbol{L}^2(D)} &= \sum_{\ell=1}^{3} \|\partial_{\boldsymbol{x}_\ell}\boldsymbol{\varphi}\|^2_{\boldsymbol{L}^2(D)}. \end{aligned}$$

Next, we extend the standard-notation for the dual space $\widetilde{H}^{-1}(D) := (\, H^1(D)\,)'$ to vector-valued spaces and write

$$\widetilde{\boldsymbol{H}}^{-1}(D) := (\, \boldsymbol{H}^1(D)\,)'.$$

Finally, for a bounded Lipschitz domain $D \subset \mathbb{R}^3$, we define $\boldsymbol{H}(\mathbf{curl}; D)$: For $\boldsymbol{\varphi} \in \boldsymbol{C}^\infty(D)$, recall the curl-operator

$$\nabla \times \boldsymbol{\varphi} := \begin{pmatrix} \partial_{\boldsymbol{x}_2}\boldsymbol{\varphi}_3 - \partial_{\boldsymbol{x}_3}\boldsymbol{\varphi}_2 \\ \partial_{\boldsymbol{x}_3}\boldsymbol{\varphi}_1 - \partial_{\boldsymbol{x}_1}\boldsymbol{\varphi}_3 \\ \partial_{\boldsymbol{x}_1}\boldsymbol{\varphi}_2 - \partial_{\boldsymbol{x}_2}\boldsymbol{\varphi}_1 \end{pmatrix} \in \boldsymbol{C}^\infty(D).$$

As for standard Sobolev spaces, $\nabla \times \boldsymbol{\varphi} \in \boldsymbol{L}^2(D)$ is understood in the sense of distributions. This leads us to the definition

$$\boldsymbol{H}(\mathbf{curl}; D) := \{\boldsymbol{\varphi} \in \boldsymbol{L}^2(D) : \nabla \times \boldsymbol{\varphi} \in \boldsymbol{L}^2(D)\}.$$

With the generic scalar product

$$\langle \boldsymbol{\varphi}, \boldsymbol{\psi} \rangle_{\boldsymbol{H}(\mathbf{curl};D)} := \langle \boldsymbol{\varphi}, \boldsymbol{\psi} \rangle_{\boldsymbol{L}^2(D)} + \langle \nabla \times \boldsymbol{\varphi}, \nabla \times \boldsymbol{\psi} \rangle_{\boldsymbol{L}^2(D)} \quad \text{for all } \boldsymbol{\varphi}, \boldsymbol{\psi} \in \boldsymbol{H}(\mathbf{curl}; D),$$

the space $\boldsymbol{H}(\mathbf{curl}; D)$ is a Hilbert space; see, e.g., [Mon03, Section 3.5.3] for details.

2.1.3. Time-dependent spaces

In the following section, we transfer the concepts and notations from Section 2.1.1 to Banach space valued functions and recall the definition of time-dependent L^p- and Sobolev spaces. We collect the basic definitions and results; see, e.g., [Edw65, Zei90, DL92, Rou05, Eva10]: To that end, let B be a real Banach space with the corresponding norm $\|\cdot\|_B$ and let $T > 0$.

- **Time-dependent L^p-spaces:** For $p \in [1,\infty]$, let $L^p(0,T;B)$ be the space of all measurable functions $\varphi : [0,T] \to B$ with $t \mapsto \|\varphi(t)\|_B \in L^p(0,T)$. Similarly to standard L^p-spaces, the functional

$$\|\varphi\|_{L^p(0,T;B)} := \begin{cases} \big(\int_0^T \|\varphi(t)\|_B^p \,\mathrm{d}t \big)^{1/p} & \text{for } p \in [1,\infty), \\ \operatorname{ess\,sup}_{t\in(0,T)} \|\varphi(t)\|_B & \text{for } p = \infty. \end{cases}$$

is a norm on the Banach space $L^p(0,T;B)$. Consequently, if B is a Hilbert space with the corresponding scalar product $\langle\cdot,\cdot\rangle_B$ and $p=2$, then $L^2(0,T;B)$ with the generic scalar product

$$\langle\varphi,\psi\rangle_{L^2(0,T;B)} := \int_0^T \langle\varphi(t),\psi(t)\rangle_B \,\mathrm{d}t \quad \text{for all } \varphi,\psi\in L^2(0,T;B)$$

is a Hilbert space. If B is separable and $1\le p<\infty$, then $L^p(0,T;B)$ is separable (see, e.g., [Zei90, Proposition 23.2(f)]). For dual spaces, the situation is similar to that of classical L^p-spaces.

Proposition 2.1.4 (Dual space of $L^p(0,T;B)$, [Edw65, Theorem 8.18.3, Theorem 8.20.5])**.** *Let B be a reflexive Banach space and let $1\le p<\infty$. Upon identification of the spaces, it holds that*

$$L^p(0,T;B)=L^{p'}(0,T;B'),\quad \textit{where}\quad \frac{1}{p}+\frac{1}{p'}=1,$$

and where we interpret $1/\infty$ as 0. □

For further details on $L^p(0,T;B)$, we refer to, e.g., [Zei90, Section 23.2ff].

- **Time-dependent Sobolev spaces:** First, we extend the classical definition of weak derivatives from $\mathbb{R}$-valued functions to B-valued functions, where we interpret all integrals in the sense of B-valued Bochner-integrals; see, e.g., [Yos95, Section V.5] for details.

Definition 2.1.5 (Weak derivative, [Eva10, p.301])**.** *Let $\varphi\in L^1(0,T;B)$. The function $v\in L^1(0,T;B)$ is the weak derivative of φ in time, if it holds that*

$$\int_0^T \varphi(t)\,\psi'(t)\,\mathrm{d}t = -\int_0^T v(t)\,\psi(t)\,\mathrm{d}t \quad \textit{for all } \psi\in C_0^\infty(0,T).$$

Then, we write $\varphi':=v$ and note that φ' is unique (see, e.g., [Zei90, Proposition 23.18]).

We further require the concept of evolution triples:

Definition 2.1.6 (Evolution triple, [Zei90, Definition 23.11])**.** *Let B be a real, separable, and reflexive Banach space. Let H be a real, separable Hilbert space with*

$$B\subset H\subset B'$$

such that the embedding from B to H is continuous, and B is dense in H. Then, we call (B',H,B) an evolution triple.

Built on an evolution triple (B',H,B), we introduce the time-dependent Sobolev space

$$W(0,T;H,B) := \{\varphi\in L^2(0,T;B) : \varphi'\in L^2(0,T;B')\}. \tag{2.2a}$$

With the norm

$$\|\varphi\|^2_{W(0,T;H,B)} := \|\varphi\|^2_{L^2(0,T;B)} + \|\varphi'\|^2_{L^2(0,T;B')} \quad \text{for all } \varphi\in W(0,T;H,B) \tag{2.2b}$$

the space $W(0,T;H,B)$ is a Banach space (see, e.g., [Zei90, Proposition 23.23(i)]). Clearly, if B is a Hilbert space with the corresponding scalar product $\langle\cdot,\cdot\rangle_B$, then $W(0,T;H,B)$ with the generic scalar product

$$\langle\varphi,\psi\rangle_{L^2(0,T;B)} := \int_0^T \langle\varphi(t),\psi(t)\rangle_B \,\mathrm{d}t + \int_0^T \langle\varphi'(t),\psi'(t)\rangle_{B'} \,\mathrm{d}t \quad \text{for all } \varphi,\psi \in W(0,T;H,B)$$

is a Hilbert space. The concept and results for $W(0,T;H,B)$ can be extended to a general Banach space X instead of B and B' in (2.2). Similarly to the scalar case, we then write

$$H^1(0,T;X) := \{\varphi \in L^2(0,T;X) : \varphi' \in L^2(0,T;X)\}.$$

For details on $W(0,T;H,B)$ and $H^1(0,T;X)$, we refer to, e.g., [Zei90, Section 23.6], [DL92, p.472ff] or [Rou05, Chapter 7]. For evolution triples, in particular, functions $\varphi \in W(0,T;H,B)$ are continuous with respect to time.

Proposition 2.1.7 ([Zei90, Proposition 23.23(ii)]). *Let (B',H,B) be an evolution triple. Let $\varphi \in W(0,T;H,B)$. Then, there exists a unique function $\widetilde{\varphi} \in C([0,T],H)$ with $\varphi = \widetilde{\varphi}$ a.e. on $[0,T]$.* □

Finally, we obtain the following useful and well-known compact embedding result.

Lemma 2.1.8 (Aubin-Lions lemma, [Rou05, Lemma 7.7]). *Let (B',H,B) be an evolution triple. Let the embedding from B to H be compact. Then, the embedding from $W(0,T;H,B)$ to $L^2(0,T;H)$ is compact.* □

2.2. The Landau–Lifshitz–Gilbert equation (LLG)

In this section, we present the precise setting of LLG (1.2) and collect general assumptions on the model. Recall the Gilbert form of the LLG equation [Gil55, LL08] from (1.2):

$$\partial_t \boldsymbol{m} = -\boldsymbol{m} \times \big(\boldsymbol{h}_{\mathrm{eff}}(\boldsymbol{m}) + \boldsymbol{\Pi}(\boldsymbol{m})\big) + \alpha\, \boldsymbol{m} \times \partial_t \boldsymbol{m} \qquad \text{in } \omega_T, \tag{2.3a}$$

$$\partial_{\mathbf{n}} \boldsymbol{m} = \boldsymbol{0} \qquad \text{on } (0,T) \times \partial\omega, \tag{2.3b}$$

$$\boldsymbol{m}(0) = \boldsymbol{m}^0 \qquad \text{in } \omega, \tag{2.3c}$$

where the effective field reads

$$\boldsymbol{h}_{\mathrm{eff}}(\boldsymbol{m}) = C_{\mathbf{ex}} \Delta \boldsymbol{m} + \boldsymbol{\pi}(\boldsymbol{m}) + \boldsymbol{f}. \tag{2.4}$$

We suppose that $\omega \subset \mathbb{R}^3$ is a bounded and polyhedral Lipschitz domain and recall the final time $T > 0$, the Gilbert damping constant $0 < \alpha \leq 1$, and the exchange constant $C_{\mathbf{ex}} > 0$. Moreover, we suppose that the initial data satisfies

$$\boldsymbol{m}^0 \in \boldsymbol{H}^1(\omega) \quad \text{and} \quad |\boldsymbol{m}^0| = 1 \quad \text{a.e. in } \omega. \tag{2.5}$$

We interpret the $\boldsymbol{m}$-dependent lower-order terms $\boldsymbol{\pi}(\boldsymbol{m}) : \omega \to \mathbb{R}^3$ as operator

$$\boldsymbol{\pi} : \boldsymbol{L}^2(\omega) \to \boldsymbol{L}^2(\omega), \tag{2.6}$$

and suppose the following assumptions **(L1)**–**(L3)**:

(L1) Linearity of $\boldsymbol{\pi}$: The operator $\boldsymbol{\pi} : \boldsymbol{L}^2(\omega) \to \boldsymbol{L}^2(\omega)$ is linear.

(L2) Boundedness of $\boldsymbol{\pi}$: There exists a constant $C_{\boldsymbol{\pi}} > 0$, such that

$$\|\boldsymbol{\pi}(\boldsymbol{\varphi})\|_{\boldsymbol{L}^2(\omega)} \leq C_{\boldsymbol{\pi}} \|\boldsymbol{\varphi}\|_{\boldsymbol{L}^2(\omega)} \quad \text{for all } \boldsymbol{\varphi} \in \boldsymbol{L}^2(\omega).$$

(L3) Self-adjointness of $\boldsymbol{\pi}$: The operator $\boldsymbol{\pi} : \boldsymbol{L}^2(\omega) \to \boldsymbol{L}^2(\omega)$ is self-adjoint.

While the results of this work are formulated for general $\boldsymbol{\pi}$, we have the following contributions in mind, which all satisfy **(L1)**–**(L3)**:

- **Uniaxial Anisotropy:** The so-called uniaxial anisotropy models the tendency of a magnetization to align in the direction of a given easy axis $\mathbf{a} \in \mathbb{R}^3$ with $|\mathbf{a}| = 1$. Given $\boldsymbol{\varphi} \in \boldsymbol{L}^2(\omega)$, it takes the mathematical form

$$\boldsymbol{\pi}(\boldsymbol{\varphi}) := (\mathbf{a} \cdot \boldsymbol{\varphi})\,\mathbf{a} \in \boldsymbol{L}^2(\omega). \tag{2.7}$$

  Note that this effect is local and does not depend on the shape of the domain ω. For details, we refer to, e.g., [HS98]. The uniaxial anisotropy satisfies the above assumptions **(L1)**–**(L3)**; see Proposition A.1.1 for the verification.

- **Stray field:** The so-called stray field (often also referred to as demagnetization field) models the influence of the magnetic field $\boldsymbol{h}_d : \mathbb{R}^3 \to \mathbb{R}^3$, which is generated by a given magnetization $\boldsymbol{\varphi} : \mathbb{R}^3 \to \mathbb{R}^3$ as the solution of the simplified Maxwell system

$$0 = \operatorname{div}(\boldsymbol{h}_\mathrm{d} + \boldsymbol{\varphi}) \quad \text{in } \mathbb{R}^3, \tag{2.8a}$$
$$\boldsymbol{0} = \nabla \times \boldsymbol{h}_\mathrm{d} \quad \text{in } \mathbb{R}^3; \tag{2.8b}$$

  cf. [HS98, Section 3.2.5] for details. The Helmholtz decomposition yields that $\boldsymbol{h}_\mathrm{d} = -\nabla u$ for some potential $u : \mathbb{R}^3 \to \mathbb{R}$. Hence, we can rewrite (2.8) as

$$0 = \operatorname{div}(-\nabla u + \boldsymbol{\varphi}) = -\Delta u + \operatorname{div} \boldsymbol{\varphi} \qquad \text{in } \mathbb{R}^3. \tag{2.9}$$

  If we interpret $\boldsymbol{\varphi} : \omega \to \mathbb{S}^2$ as a magnetization on $\mathbb{R}^3$ via zero-extension, we can translate (2.9) to the well-known transmission problem

$$\begin{aligned}
-\Delta u &= -\operatorname{div} \boldsymbol{\varphi} && \text{in } \omega,\\
-\Delta u &= 0 && \text{in } \mathbb{R}^3 \setminus \overline{\omega},\\
u^{\mathrm{ext}} - u^{\mathrm{int}} &= 0 && \text{on } \partial\omega,\\
(\nabla u^{\mathrm{ext}} - \nabla u^{\mathrm{int}}) \cdot \boldsymbol{n} &= -\boldsymbol{\varphi} \cdot \boldsymbol{n} && \text{on } \partial\omega,\\
u(\boldsymbol{x}) &= \mathcal{O}(|\boldsymbol{x}|^{-1}) && \text{as } |\boldsymbol{x}| \to \infty,
\end{aligned}$$

  where we supposed $u(\boldsymbol{x}) = \mathcal{O}(|\boldsymbol{x}|^{-1})$ as $|\boldsymbol{x}| \to \infty$ for unique solvability. With integration by parts, we rewrite the latter problem as in [Pra04, eq. (1.3)] in the weak form: Find $u \in H^1(\mathbb{R}^3)$ such that

$$\langle \nabla u, \nabla \psi \rangle_{\boldsymbol{L}^2(\omega)} = \langle \boldsymbol{\varphi}, \nabla \psi \rangle_{\boldsymbol{L}^2(\omega)} \quad \text{for all } \psi \in C_0^\infty(\mathbb{R}^3). \tag{2.10}$$

Altogether, for given $\boldsymbol{\varphi} \in \boldsymbol{L}^2(\omega)$, we define the stray field as

$$\boldsymbol{\pi}(\boldsymbol{\varphi}) := -\nabla u \in \boldsymbol{L}^2(\omega), \quad \text{where } u \text{ solves } (2.10). \tag{2.11}$$

Overall, the stray field is a non-local effect on the whole space $\mathbb{R}^3$, even though $\boldsymbol{\varphi}$ is defined on ω. The stray field satisfies the assumptions **(L1)**–**(L3)**; see Proposition A.1.2.

Next, we suppose that the applied field satisfies $\boldsymbol{f} \in C^1([0,T], \boldsymbol{L}^2(\omega))$. Finally, we interpret similarly to $\boldsymbol{\pi}$ the dissipative effects $\boldsymbol{\Pi}(\boldsymbol{m}) : \omega \to \mathbb{R}^3$ as operator

$$\boldsymbol{\Pi} : \boldsymbol{H}^1(\omega) \cap \boldsymbol{L}^\infty(\omega) \to \boldsymbol{L}^2(\omega). \tag{2.12}$$

While the results of this work are formulated for general $\boldsymbol{\Pi}$, we have the following contributions in mind:

- **Zhang–Li field:** The so-called Zhang–Li field [ZL04, TNMS05] models the effect of electron spins on the magnetization. Often, this is referred to as spin torque dynamics. For $\boldsymbol{\varphi} \in \boldsymbol{H}^1(\omega) \cap \boldsymbol{L}^\infty(\omega)$, we define

$$\boldsymbol{\Pi}(\boldsymbol{\varphi}) := \boldsymbol{\varphi} \times (\boldsymbol{u} \cdot \nabla)\, \boldsymbol{\varphi} + \beta\, (\boldsymbol{u} \cdot \nabla)\, \boldsymbol{\varphi} \in \boldsymbol{L}^2(\omega). \tag{2.13}$$

  Here, $\boldsymbol{u} \in \boldsymbol{L}^\infty(\omega)$ is the given spin velocity vector and $\beta \in [0,1]$ is the constant of non-adiabacity.

- **Slonczewski field:** The so-called Slonczewski field [Ber96, Slo96] models the effect of spin waves which are excited by an electric current in the direction $\mathbf{p} \in \mathbb{R}^3$, where $|\mathbf{p}| = 1$. For $\boldsymbol{\varphi} \in \boldsymbol{L}^2(\omega)$, we define

$$\boldsymbol{\Pi}(\boldsymbol{\varphi}) := \mathcal{G}(\boldsymbol{\varphi} \cdot \mathbf{p})\, \boldsymbol{\varphi} \times \mathbf{p} \in \boldsymbol{L}^2(\omega), \tag{2.14}$$

  where $\mathcal{G} \in C_0^1(\mathbb{R})$ is given.

With the latter framework at hand, we come to the notion of a weak solution of LLG (2.3). We extend [AS92, Definition 1.2] to our setting of LLG (2.3). Recalling from (1.4) the energy functional

$$\mathcal{E}_{\mathrm{LLG}}(\boldsymbol{m}) := \frac{C_{\mathbf{ex}}}{2} \|\nabla \boldsymbol{m}\|^2_{\boldsymbol{L}^2(\omega)} - \frac{1}{2} \langle \boldsymbol{\pi}(\boldsymbol{m}), \boldsymbol{m} \rangle_{\boldsymbol{L}^2(\omega)} - \langle \boldsymbol{f}, \boldsymbol{m} \rangle_{\boldsymbol{L}^2(\omega)}, \tag{2.15}$$

a weak solution is defined as follows:

Definition 2.2.1 (Weak solution of LLG)**.** *A function $\boldsymbol{m}$ is called a weak solution of LLG* (2.3)*, if it satisfies the following conditions* (i)–(iii)*:*

(i) $\boldsymbol{m} \in L^\infty(0,T; \boldsymbol{H}^1(\omega)) \cap \boldsymbol{H}^1(\omega_T)$ *and* $|\boldsymbol{m}| = 1$ *almost everywhere in* ω_T*.*

(ii) $\boldsymbol{m}(0) = \boldsymbol{m}^0$ *in the sense of traces.*

(iii) *For all* $\boldsymbol{\varphi} \in \boldsymbol{H}^1(\omega_T)$*, it holds that*

$$\begin{aligned}\int_0^T \langle \partial_t \boldsymbol{m}, \boldsymbol{\varphi}\rangle_{\boldsymbol{L}^2(\omega)} \,\mathrm{dt} = C_{\mathbf{ex}} \int_0^T \langle \boldsymbol{m} \times \nabla \boldsymbol{m}, \nabla \boldsymbol{\varphi}\rangle_{\boldsymbol{L}^2(\omega)} \,\mathrm{dt} - \int_0^T \langle \boldsymbol{m} \times \boldsymbol{\pi}(\boldsymbol{m}), \boldsymbol{\varphi}\rangle_{\boldsymbol{L}^2(\omega)} \,\mathrm{dt} \\ - \int_0^T \langle \boldsymbol{m} \times \boldsymbol{f}, \boldsymbol{\varphi}\rangle_{\boldsymbol{L}^2(\omega)} \,\mathrm{dt} - \int_0^T \langle \boldsymbol{m} \times \boldsymbol{\Pi}(\boldsymbol{m}), \boldsymbol{\varphi}\rangle_{\boldsymbol{L}^2(\omega)} \,\mathrm{dt} \\ + \alpha \int_0^T \langle \boldsymbol{m} \times \partial_t \boldsymbol{m}, \boldsymbol{\varphi}\rangle_{\boldsymbol{L}^2(\omega)} \,\mathrm{dt}\,. \end{aligned} \tag{2.16}$$

Moreover, $\boldsymbol{m}$ *is called a physical weak solution, if it additionally satisfies the following stronger energy estimate* (iv)*:*

(iv) *For almost all* $\tau \in (0, T)$*, it holds that*

$$\begin{aligned}&\mathcal{E}_{LLG}(\boldsymbol{m}(\tau)) + \alpha \int_0^\tau \|\partial_t \boldsymbol{m}\|^2_{\boldsymbol{L}^2(\omega)} \,\mathrm{dt} \\ &\quad + \int_0^\tau \langle \partial_t \boldsymbol{f}, \boldsymbol{m}\rangle_{\boldsymbol{L}^2(\omega)} \,\mathrm{dt} - \int_0^\tau \langle \boldsymbol{\Pi}(\boldsymbol{m}), \partial_t \boldsymbol{m}\rangle_{\boldsymbol{L}^2(\omega)} \,\mathrm{dt} \;\le\; \mathcal{E}_{LLG}(\boldsymbol{m}^0).\end{aligned} \tag{2.17}$$

2.2.1. Coupling with eddy currents (ELLG)

In this section, we introduce the coupling of LLG (2.3) with the eddy current equation and the corresponding notion of a weak solution. We follow the presentation of [DPP+17, Section 3.1]. We adopt the framework for plain LLG from Section 2.2. Let $\Omega \subset \mathbb{R}^3$ with $\omega \subset \Omega$ be another bounded and polyhedral Lipschitz domain, which represents a conducting body Ω with its ferromagnetic part ω. Then, the coupled ELLG system (cf., e.g., [LT13, LPPT15]) reads

$$\begin{aligned}
\partial_t \boldsymbol{m} &= -\boldsymbol{m} \times (\boldsymbol{h}_{\mathrm{eff}}(\boldsymbol{m}) + \boldsymbol{h}) + \alpha\, \boldsymbol{m} \times \partial_t \boldsymbol{m} && \text{in } \omega_T, && (2.18a)\\
-\mu_0\, \partial_t \boldsymbol{m} &= \mu_0\, \partial_t \boldsymbol{h} + \sigma^{-1} \nabla \times (\nabla \times \boldsymbol{h}) && \text{in } \Omega_T, && (2.18b)\\
\partial_{\mathbf{n}} \boldsymbol{m} &= \mathbf{0} && \text{on } (0,T) \times \partial\omega, && (2.18c)\\
(\nabla \times \boldsymbol{h}) \times \mathbf{n} &= \mathbf{0} && \text{on } (0,T) \times \partial\Omega, && (2.18d)\\
(\boldsymbol{m}, \boldsymbol{h})(0) &= (\boldsymbol{m}^0, \boldsymbol{h}^0) && \text{in } \omega \times \Omega. && (2.18e)
\end{aligned}$$

Here, $\mu_0 > 0$ is the vacuum permeability and $\sigma \in \boldsymbol{L}^\infty(\Omega)$ is the conductivity of the ferromagnetic domain Ω. We suppose that σ is uniformly bounded from below, i.e., there exists $\sigma_0 > 0$ such that $\sigma \ge \sigma_0 > 0$ a.e. on Ω. Moreover, we suppose that the initial condition $\boldsymbol{h}^0 \in \boldsymbol{H}(\mathbf{curl}; \Omega)$ satisfies the compatibility conditions

$$\mathrm{div}(\boldsymbol{h}^0 + \chi_\omega \boldsymbol{m}^0) = 0 \text{ in } \Omega \quad \text{and} \quad (\boldsymbol{h}^0 + \chi_\omega \boldsymbol{m}^0) \cdot \mathbf{n} = 0 \text{ on } \partial\Omega. \tag{2.19}$$

Unlike [LT13], we define the energy functional

$$\mathcal{E}_{\mathrm{ELLG}}(\boldsymbol{m}, \boldsymbol{h}) := \frac{C_{\mathbf{ex}}}{2} \|\nabla \boldsymbol{m}\|^2_{\boldsymbol{L}^2(\omega)} - \frac{1}{2} \langle \boldsymbol{\pi}(\boldsymbol{m}), \boldsymbol{m}\rangle_{\boldsymbol{L}^2(\omega)} - \langle \boldsymbol{f}, \boldsymbol{m}\rangle_{\boldsymbol{L}^2(\omega)} + \frac{1}{2} \|\boldsymbol{h}\|^2_{\boldsymbol{L}^2(\Omega)}. \tag{2.20}$$

Based on [LT13, Definition 2.1], we extend Definition 2.2.1 for plain LLG [AS92] and define a weak solution to ELLG (2.18) in the following way.

Definition 2.2.2 (Weak solution of ELLG)**.** *The pair* $(\boldsymbol{m}, \boldsymbol{h})$ *is called a weak solution of ELLG* (2.18)*, if it satisfies the following conditions* (i)–(iv)*:*

(i) $\boldsymbol{m} \in L^\infty(0, T, \boldsymbol{H}^1(\omega)) \cap \boldsymbol{H}^1(\omega_T)$ *with* $|\boldsymbol{m}| = 1$ *a.e. in* ω_T*.*

(ii) $\boldsymbol{h} \in H^1(0, T; \boldsymbol{L}^2(\Omega)) \cap L^\infty(0, T; \boldsymbol{H}(\mathbf{curl}; \Omega))$.

(iii) $\boldsymbol{m}(0) = \boldsymbol{m}^0$ *and* $\boldsymbol{h}(0) = \boldsymbol{h}^0$ *in the sense of traces.*

(iv) *For all* $\boldsymbol{\varphi} \in \boldsymbol{H}^1(\omega_T)$*, it holds that*

$$\begin{aligned}\int_0^T \langle \partial_t \boldsymbol{m}, \boldsymbol{\varphi} \rangle_{\boldsymbol{L}^2(\omega)} \, \mathrm{d}t = C_{\mathbf{ex}} \int_0^T \langle \boldsymbol{m} \times \nabla \boldsymbol{m}, \nabla \boldsymbol{\varphi} \rangle_{\boldsymbol{L}^2(\omega)} \, \mathrm{d}t - \int_0^T \langle \boldsymbol{m} \times \boldsymbol{\pi}(\boldsymbol{m}), \boldsymbol{\varphi} \rangle_{\boldsymbol{L}^2(\omega)} \, \mathrm{d}t \\ - \int_0^T \langle \boldsymbol{m} \times \boldsymbol{f}, \boldsymbol{\varphi} \rangle_{\boldsymbol{L}^2(\omega)} \, \mathrm{d}t - \int_0^T \langle \boldsymbol{m} \times \boldsymbol{h}, \boldsymbol{\varphi} \rangle_{\boldsymbol{L}^2(\omega)} \, \mathrm{d}t \\ - \int_0^T \langle \boldsymbol{m} \times \boldsymbol{\Pi}(\boldsymbol{m}), \boldsymbol{\varphi} \rangle_{\boldsymbol{L}^2(\omega)} \, \mathrm{d}t + \alpha \int_0^T \langle \boldsymbol{m} \times \partial_t \boldsymbol{m}, \boldsymbol{\varphi} \rangle_{\boldsymbol{L}^2(\omega)} \, \mathrm{d}t,\end{aligned} \tag{2.21a}$$

and for all $\boldsymbol{\zeta} \in \boldsymbol{L}^2(0, T, \boldsymbol{H}(\mathbf{curl}; \Omega))$*, it holds that*

$$- \mu_0 \int_0^T \langle \partial_t \boldsymbol{m}, \boldsymbol{\zeta} \rangle_{\boldsymbol{L}^2(\omega)} \, \mathrm{d}t = \mu_0 \int_0^T \langle \partial_t \boldsymbol{h}, \boldsymbol{\zeta} \rangle_{\boldsymbol{L}^2(\Omega)} \, \mathrm{d}t + \int_0^T \langle \sigma^{-1} \nabla \times \boldsymbol{h}, \nabla \times \boldsymbol{\zeta} \rangle_{\boldsymbol{L}^2(\Omega)} \, \mathrm{d}t \, . \tag{2.21b}$$

The pair $(\boldsymbol{m}, \boldsymbol{h})$ *is called a physical weak solution, if it additionally satisfies the following stronger energy estimate* (v)*:*

(v) *For almost all* $\tau \in (0, T)$*, it holds that*

$$\begin{aligned}\mathcal{E}_{ELLG}(\boldsymbol{m}(\tau), \boldsymbol{h}(\tau)) + \alpha \int_0^\tau \|\partial_t \boldsymbol{m}\|^2_{\boldsymbol{L}^2(\omega)} \, \mathrm{d}t + \frac{1}{\mu_0} \int_0^\tau \|\sigma^{-1/2} \nabla \times \boldsymbol{h}\|^2_{\boldsymbol{L}^2(\Omega)} \, \mathrm{d}t \\ + \int_0^\tau \langle \partial_t \boldsymbol{f}, \boldsymbol{m} \rangle_{\boldsymbol{L}^2(\omega)} \, \mathrm{d}t - \int_0^\tau \langle \boldsymbol{\Pi}(\boldsymbol{m}), \partial_t \boldsymbol{m} \rangle_{\boldsymbol{L}^2(\omega)} \, \mathrm{d}t \, \le \, \mathcal{E}_{ELLG}(\boldsymbol{m}(0), \boldsymbol{h}(0)).\end{aligned} \tag{2.22}$$

2.2.2. Coupling with spin diffusion (SDLLG)

In this section, we introduce the coupling of LLG (2.3) with the spin diffusion equation and the corresponding weak solution. To this end, we adopt the framework for plain LLG from Section 2.2, and let $\Omega \subset \mathbb{R}^3$ with $\omega \subset \Omega$ be another bounded and polyhedral Lipschitz domain. To simplify the notation, we recall for $\mathbf{a}, \mathbf{b} \in \mathbb{R}^3$, the definition of the outer product

$$\mathbf{a} \otimes \mathbf{b} := \begin{pmatrix} \mathbf{a}_1\mathbf{b}_1 & \mathbf{a}_1\mathbf{b}_2 & \mathbf{a}_1\mathbf{b}_3 \\ \mathbf{a}_2\mathbf{b}_1 & \mathbf{a}_2\mathbf{b}_2 & \mathbf{a}_2\mathbf{b}_3 \\ \mathbf{a}_3\mathbf{b}_1 & \mathbf{a}_3\mathbf{b}_2 & \mathbf{a}_3\mathbf{b}_3 \end{pmatrix} \in \mathbb{R}^{3\times 3}.$$

For the coupled SDLLG system, we adopt the setting from [AHP+14, eq.(9)], which reads

$$\begin{aligned}\partial_t \boldsymbol{m} &= -\boldsymbol{m} \times (\boldsymbol{h}_{\text{eff}}(\boldsymbol{m}) + c\boldsymbol{s}) + \alpha\, \boldsymbol{m} \times \partial_t \boldsymbol{m} && \text{in } \omega_T && (2.23a)\\ \partial_t \boldsymbol{s} &= -\operatorname{div}(\beta \boldsymbol{m} \otimes \boldsymbol{j} - D_0(\nabla \boldsymbol{s} - \beta\beta' \boldsymbol{m} \otimes ([\nabla \boldsymbol{s}]^T \boldsymbol{m}))) \\ &\quad - D_0(\boldsymbol{s} + \boldsymbol{s} \times \boldsymbol{m}) && \text{in } \Omega_T, && (2.23b)\\ \partial_{\mathbf{n}} \boldsymbol{m} &= \mathbf{0} && \text{on } (0,T) \times \partial\omega, && (2.23c)\\ \partial_{\mathbf{n}} \boldsymbol{s} &= \mathbf{0} && \text{on } (0,T) \times \partial\Omega, && (2.23d)\\ (\boldsymbol{m}, \boldsymbol{s})(0) &= (\boldsymbol{m}^0, \boldsymbol{s}^0) && \text{in } \omega \times \Omega. && (2.23e)\end{aligned}$$

Here, $c > 0$ is the coupling parameter, $\beta, \beta' \in (0,1)$ are the non-dimensional spin polarization parameters, $\boldsymbol{j} \in L^2(0,T;\boldsymbol{H}^1(\Omega))$ is the spin current, and $D_0 \in \boldsymbol{L}^\infty(\Omega)$ is the diffusion coefficient. We suppose that D_0 is uniformly bounded from below, i.e., for some $D > 0$, it holds that $D_0 \geq D > 0$ a.e. in Ω. Moreover, we suppose that $\boldsymbol{s}^0 \in \boldsymbol{L}^2(\Omega)$.

To further simplify the notation, we adopt for given $\boldsymbol{\mu} \in \boldsymbol{L}^\infty(\omega)$ the $\boldsymbol{\mu}$-dependent bilinear form $\boldsymbol{a}(\boldsymbol{\mu};\cdot,\cdot) : \boldsymbol{H}^1(\Omega) \times \boldsymbol{H}^1(\Omega) \to \mathbb{R}$ from [AHP+14, Section 2.3] and define

$$\begin{aligned}\boldsymbol{a}(\boldsymbol{\mu};\boldsymbol{\zeta}_1,\boldsymbol{\zeta}_2) :=& \langle D_0 \nabla\boldsymbol{\zeta}_1, \nabla\boldsymbol{\zeta}_2\rangle_{\boldsymbol{L}^2(\Omega)} - \beta\beta'\langle D_0 \boldsymbol{\mu} \otimes ([\nabla\boldsymbol{\zeta}_1]^T \boldsymbol{\mu}), \nabla\boldsymbol{\zeta}_2\rangle_{\boldsymbol{L}^2(\omega)} \\ &+ \langle D_0 \boldsymbol{\zeta}_1, \boldsymbol{\zeta}_2\rangle_{\boldsymbol{L}^2(\Omega)} + \langle D_0(\boldsymbol{\zeta}_1 \times \boldsymbol{\mu}), \boldsymbol{\zeta}_2\rangle_{\boldsymbol{L}^2(\omega)} \\ =& \langle D_0 \nabla\boldsymbol{\zeta}_1, \nabla\boldsymbol{\zeta}_2\rangle_{\boldsymbol{L}^2(\Omega)} - \beta\beta'\langle D_0 (\boldsymbol{\mu} \otimes \boldsymbol{\mu})\nabla\boldsymbol{\zeta}_1, \nabla\boldsymbol{\zeta}_2\rangle_{\boldsymbol{L}^2(\omega)} \\ &+ \langle D_0 \boldsymbol{\zeta}_1, \boldsymbol{\zeta}_2\rangle_{\boldsymbol{L}^2(\Omega)} + \langle D_0(\boldsymbol{\zeta}_1 \times \boldsymbol{\mu}), \boldsymbol{\zeta}_2\rangle_{\boldsymbol{L}^2(\omega)} \end{aligned} \tag{2.24}$$

for all $\boldsymbol{\zeta}_1, \boldsymbol{\zeta}_2 \in \boldsymbol{H}^1(\Omega)$. Given $\boldsymbol{\mu} \in \boldsymbol{L}^\infty(\Omega)$, the following lemma yields (uniform) continuity and ellipticity of the bilinear form $\boldsymbol{a}(\boldsymbol{\mu};\cdot,\cdot)$. We extend the statement of [AHP+14, Lemma 5] from $|\boldsymbol{\mu}| = 1$ a.e. in Ω to $\boldsymbol{\mu} \in \boldsymbol{L}^\infty(\Omega)$. The proof, however, follows the lines of [AHP+14, Lemma 5] and is therefore omitted.

Lemma 2.2.3. *Given $\boldsymbol{\mu} \in \boldsymbol{L}^\infty(\omega)$, the bilinear form $\boldsymbol{a}(\boldsymbol{\mu};\cdot,\cdot) : \boldsymbol{H}^1(\Omega) \times \boldsymbol{H}^1(\Omega) \to \mathbb{R}$ from* (2.24) *satisfies the following assertions* (i) *and* (ii)*:*

(i) $\boldsymbol{a}(\boldsymbol{\mu};\cdot,\cdot)$ *is continuous in the sense that for all $\boldsymbol{\zeta}_1, \boldsymbol{\zeta}_2 \in \boldsymbol{H}^1(\Omega)$, it holds that*

$$\boldsymbol{a}(\boldsymbol{\mu};\boldsymbol{\zeta}_1,\boldsymbol{\zeta}_2) \leq \|D_0\|_{\boldsymbol{L}^\infty(\Omega)}\big(1 + \|\boldsymbol{\mu}\|_{\boldsymbol{L}^\infty(\omega)} + \|\boldsymbol{\mu}\|^2_{\boldsymbol{L}^\infty(\omega)}\big)\|\boldsymbol{\zeta}_1\|_{\boldsymbol{H}^1(\Omega)}\|\boldsymbol{\zeta}_2\|_{\boldsymbol{H}^1(\Omega)}.$$

(ii) *If $\beta\beta'\|\boldsymbol{\mu}\|^2_{\boldsymbol{L}^\infty(\omega)} < 1$, then $\boldsymbol{a}(\boldsymbol{\mu};\cdot,\cdot)$ is positive definite in the sense that*

$$\boldsymbol{a}(\boldsymbol{\mu};\boldsymbol{\zeta},\boldsymbol{\zeta}) \geq \big(1 - \beta\beta'\|\boldsymbol{\mu}\|^2_{\boldsymbol{L}^\infty(\omega)}\big)D\|\boldsymbol{\zeta}\|^2_{\boldsymbol{H}^1(\Omega)} \quad \textit{for all } \boldsymbol{\zeta} \in \boldsymbol{H}^1(\Omega). \qquad \square$$

With the $\boldsymbol{\mu}$-dependent bilinear form $\boldsymbol{a}(\boldsymbol{\mu};\cdot,\cdot)$ at hand, we are ready to introduce the notion of a weak solution of the coupled SDLLG system: To do so, we require the corresponding energy functional. Unlike [AHP+14, Section 5], we consider the spin diffusion variable $\boldsymbol{s}$ as a dissipative effect to the model, i.e., $\boldsymbol{s}$ is not represented in our corresponding energy-functional, which still reads

$$\mathcal{E}_{\text{LLG}}(\boldsymbol{m}) \overset{(2.15)}{:=} \frac{C_{\mathbf{ex}}}{2}\|\nabla\boldsymbol{m}\|^2_{\boldsymbol{L}^2(\omega)} - \frac{1}{2}\langle\boldsymbol{\pi}(\boldsymbol{m}), \boldsymbol{m}\rangle_{\boldsymbol{L}^2(\omega)} - \langle\boldsymbol{f}, \boldsymbol{m}\rangle_{\boldsymbol{L}^2(\omega)}. \tag{2.25}$$

The following notion of a weak solution of SDLLG (2.23) goes back to [GW07, Definition 1] and extends Definition 2.2.1 for plain LLG [AS92]; see also [AHP+14, Rug16].

Definition 2.2.4 (Weak solution of SDLLG)**.** *The pair* $(\boldsymbol{m}, \boldsymbol{s})$ *is called a weak solution of SDLLG* (2.23)*, if it satisfies the following conditions* (i)–(iv)*:*

(i) $\boldsymbol{m} \in L^\infty(0,T,\boldsymbol{H}^1(\omega)) \cap \boldsymbol{H}^1(\omega_T)$ *with* $|\boldsymbol{m}| = 1$ *a.e. in* ω_T*.*

(ii) $\boldsymbol{s} \in L^\infty(0,T;\boldsymbol{L}^2(\Omega)) \cap W(0,T;\boldsymbol{L}^2(\Omega),\boldsymbol{H}^1(\Omega))$.

(iii) $\boldsymbol{m}(0) = \boldsymbol{m}^0$ *and* $\boldsymbol{s}(0) = \boldsymbol{s}^0$ *in the sense of traces.*

(iv) *For all* $\boldsymbol{\varphi} \in \boldsymbol{H}^1(\omega_T)$*, it holds that*

$$\begin{aligned}\int_0^T \langle \partial_t \boldsymbol{m}, \boldsymbol{\varphi}\rangle_{\boldsymbol{L}^2(\omega)} \,\mathrm{d}t = C_{\mathbf{ex}} \int_0^T \langle \boldsymbol{m} \times \nabla \boldsymbol{m}, \nabla\boldsymbol{\varphi}\rangle_{\boldsymbol{L}^2(\omega)} \,\mathrm{d}t - \int_0^T \langle \boldsymbol{m} \times \boldsymbol{\pi}(\boldsymbol{m}), \boldsymbol{\varphi}\rangle_{\boldsymbol{L}^2(\omega)} \,\mathrm{d}t \\ - \int_0^T \langle \boldsymbol{m} \times \boldsymbol{f}, \boldsymbol{\varphi}\rangle_{\boldsymbol{L}^2(\omega)} \,\mathrm{d}t - \int_0^T \langle \boldsymbol{m} \times \boldsymbol{\Pi}(\boldsymbol{m}), \boldsymbol{\varphi}\rangle_{\boldsymbol{L}^2(\omega)} \,\mathrm{d}t \\ - \int_0^T \langle \boldsymbol{m} \times \boldsymbol{s}, \boldsymbol{\varphi}\rangle_{\boldsymbol{L}^2(\omega)} \,\mathrm{d}t + \alpha \int_0^T \langle \boldsymbol{m} \times \partial_t \boldsymbol{m}, \boldsymbol{\varphi}\rangle_{\boldsymbol{L}^2(\omega)} \,\mathrm{d}t,\end{aligned} \tag{2.26a}$$

and for all $\boldsymbol{\zeta} \in \boldsymbol{H}^1(\Omega_T)$*, it holds that*

$$\begin{aligned}\int_0^T \langle \partial_t \boldsymbol{s}, \boldsymbol{\zeta}\rangle_{\tilde{\boldsymbol{H}}^{-1}(\Omega)\times \boldsymbol{H}^1(\Omega)} \,\mathrm{d}t + \int_0^T \boldsymbol{a}(\boldsymbol{m}; \boldsymbol{s}, \boldsymbol{\zeta}) \,\mathrm{d}t \\ = \beta \int_0^T \langle \boldsymbol{m} \otimes \boldsymbol{j}, \nabla \boldsymbol{\zeta}\rangle_{\boldsymbol{L}^2(\omega)} \,\mathrm{d}t - \beta \int_0^T \langle \boldsymbol{j}\cdot\boldsymbol{n}, \boldsymbol{m}\cdot\boldsymbol{\zeta}\rangle_{\boldsymbol{L}^2(\partial\Omega\cap\partial\omega)} \,\mathrm{d}t\,.\end{aligned} \tag{2.26b}$$

The pair $(\boldsymbol{m}, \boldsymbol{s})$ *is called a physical weak solution, if it additionally satisfies the following stronger energy estimate* (v)*:*

(v) *For almost all* $\tau \in (0,T)$*, it holds that*

$$\begin{aligned}\mathcal{E}_{LLG}(\boldsymbol{m}(\tau)) + \alpha \int_0^\tau \|\partial_t \boldsymbol{m}\|^2_{\boldsymbol{L}^2(\omega)} \,\mathrm{d}t + \int_0^\tau \langle \partial_t \boldsymbol{f}, \boldsymbol{m}\rangle_{\boldsymbol{L}^2(\omega)} \,\mathrm{d}t \\ - \int_0^\tau \langle \boldsymbol{\Pi}(\boldsymbol{m}), \partial_t \boldsymbol{m}\rangle_{\boldsymbol{L}^2(\omega)} \,\mathrm{d}t - c \int_0^\tau \langle \boldsymbol{s}, \partial_t \boldsymbol{m}\rangle_{\boldsymbol{L}^2(\omega)} \,\mathrm{d}t \,\le\, \mathcal{E}_{LLG}(\boldsymbol{m}^0).\end{aligned} \tag{2.27}$$

Remark 2.2.5. *In [GW07, AHP+14], the energy estimate* (2.27) *is not included in the definition of the weak solution. For a first-order tangent plane scheme for coupled SDLLG with* $\boldsymbol{\Pi} = \boldsymbol{0}$*, [AHP+14, Section 5] considers the alternate energy functional*

$$\widetilde{\mathcal{E}}_{SDLLG}(\boldsymbol{m}, \boldsymbol{s}) := \mathcal{E}_{LLG}(\boldsymbol{m}) - c\langle \boldsymbol{s}, \boldsymbol{m}\rangle_{\boldsymbol{L}^2(\omega)},$$

and proves that the limit $(\boldsymbol{m}, \boldsymbol{s})$ *of the approximations satisfies*

$$\begin{aligned}\widetilde{\mathcal{E}}_{SDLLG}(\boldsymbol{m}(\tau), \boldsymbol{s}(\tau)) \,+\, \alpha \int_0^\tau \|\partial_t \boldsymbol{m}\|^2_{\boldsymbol{L}^2(\omega)} \,\mathrm{d}t \\ + \int_0^\tau \langle \partial_t \boldsymbol{f}, \boldsymbol{m}\rangle_{\boldsymbol{L}^2(\omega)} \,\mathrm{d}t + c \int_0^\tau \langle \partial_t \boldsymbol{s}, \boldsymbol{m}\rangle_{\tilde{\boldsymbol{H}}^{-1}(\Omega)\times \boldsymbol{H}^1(\Omega)} \,\mathrm{d}t \,\le\, \widetilde{\mathcal{E}}_{SDLLG}(\boldsymbol{m}^0, \boldsymbol{s}^0).\end{aligned}$$

for almost all $\tau \in (0,T)$*. Upon integration by parts, this is equivalent to our* (2.27)*. Moreover, note that [Rug16, Definition 5.1.2] also uses the energy functional* (2.25)*.*

3. Discretization

In this section, the overall goal is to unify, elaborate, and extend the setting for the discretization of LLG and its coupled systems from the main sources [DPP+17, PRS18]. As for the analytical framework, we start with general definitions and results, and then fix the discrete framework. We divide this chapter into the following four parts:

- **General:** We introduce general meshes and approximation spaces; see Section 3.1.
- **Time:** We fix uniform time-stepping as discretization in time; see Section 3.2.
- **Space:** We fix the FEM-based discretization in space; see Section 3.3.
- **Model:** We introduce the discretizations of the data $\boldsymbol{m}^0$, $\boldsymbol{\pi}$, $\boldsymbol{f}$, and $\boldsymbol{\Pi}$ and collect corresponding general assumptions; see Section 3.4.

3.1. General meshes and approximation spaces

In this section, we introduce meshes and standard $H^1(D)$- and $\boldsymbol{H}(\mathbf{curl}; D)$-conforming finite element spaces, where $D \subset \mathbb{R}^3$ is a general bounded and polyhedral Lipschitz domain.

3.1.1. Meshes

We collect some standard notations and results for meshes; see, e.g., [Bra07, BS08, EG04, Mon03]. Throughout, $D \subset \mathbb{R}^3$ is a bounded and polyhedral Lipschitz domain.

Definition 3.1.1 (Mesh)**.** *We call a set $\mathcal{T}^D$ a mesh on D with the elements $K \in \mathcal{T}^D$, if it satisfies the following properties* (i)–(iv)*:*

(i) *Each element $K \in \mathcal{T}^D$ is a closed non-degenerate tetrahedron.*

(ii) *The elements $K \in \mathcal{T}^D$ cover $\overline{D}$, i.e., it holds that*

$$\overline{D} = \bigcup_{K \in \mathcal{T}^D} K.$$

In particular, $K \subset \overline{D}$ for all elements $K \in \mathcal{T}^D$.

(iii) *Two distinct elements do not overlap, i.e., for $K, \widetilde{K} \in \mathcal{T}^D$ with $K \neq \widetilde{K}$, it holds that* $\mathrm{int}(K) \cap \mathrm{int}(\widetilde{K}) = \emptyset$.

(iv) *There are no hanging-nodes, i.e., no vertex of any element $K \in \mathcal{T}^D$ lies in the interior of any face or any edge of any other element $\widetilde{K} \in \mathcal{T}^D$.*

Definition 3.1.2 (Mesh-size)**.** *Let $\mathcal{T}^D$ be a mesh on D. We call $h := \max_{K\in\mathcal{T}^D} \operatorname{diam}(K)$ the mesh-size of $\mathcal{T}^D$.*

Definition 3.1.3 ($C_{\mathbf{mesh}}$-shape-regular meshes)**.** *Let $C_{\mathbf{mesh}} > 0$. We say that a family $(\mathcal{T}_h^D)_{h>0}$ of meshes on D is $C_{\mathbf{mesh}}$-shape regular, if*

$$\frac{\operatorname{diam}(K)}{\rho_K} \leq C_{\mathbf{mesh}} \quad \textit{for all elements } K \in \mathcal{T}_h^D \textit{ and for all } h > 0,$$

where $\rho_K > 0$ is the diameter of the largest ball that can be inscribed in $K \in \mathcal{T}_h^D$.

Definition 3.1.4 ($C_{\mathbf{mesh}}$-quasi-uniform meshes)**.** *Let $C_{\mathbf{mesh}} > 0$. We say that a family $(\mathcal{T}_h^D)_{h>0}$ of meshes on D is $C_{\mathbf{mesh}}$-quasi-uniform, if it is $C_{\mathbf{mesh}}$-shape regular and if*

$$h \leq C_{\mathbf{mesh}} \operatorname{diam}(K) \quad \textit{for all elements } K \in \mathcal{T}_h^D \textit{ and for all } h > 0.$$

In order to match with subdomains $D_{\text{sub}} \subset D \subset \mathbb{R}^3$, we require the following definition:

Definition 3.1.5 (Resolved meshes)**.** *Let $D \subset \mathbb{R}^3$ be a bounded and polyhedral Lipschitz domain with a polyhedral Lipschitz subdomain $D_{sub} \subset D \subset \mathbb{R}^3$. Let $\mathcal{T}^D$ be a mesh on D. We say that $\mathcal{T}^D$ resolves D_{sub}, if for all elements $K \in \mathcal{T}^D$ with $\operatorname{int}(K) \cap D_{sub} \neq \emptyset$, it holds that $K \subset \overline{D_{sub}}$.*

Proposition 3.1.6 ($C_{\mathbf{mesh}}$-quasi-uniform sub-meshes)**.** *Let $D \subset \mathbb{R}^3$ be a bounded and polyhedral Lipschitz domain with a polyhedral Lipschitz subdomain $D_{sub} \subset D \subset \mathbb{R}^3$. Let $(\mathcal{T}_h^D)_{h>0}$ be a family of $C_{\mathbf{mesh}}$-quasi-uniform meshes on D, which, for each $h > 0$, resolves D_{sub}. Then, the family of corresponding sub-meshes*

$$\mathcal{T}_h^{D_{sub}} := \{K \in \mathcal{T}_h : K \subset \overline{D_{sub}}\}$$

is a family of $C_{\mathbf{mesh}}$-quasi-uniform meshes on D_{sub}. □

3.1.2. Standard P1-FEM

Given a bounded polyhedral Lipschitz domain $D \subset \mathbb{R}^3$ and a $C_{\mathbf{mesh}}$-quasi-uniform family of meshes $(\mathcal{T}_h^D)_{h>0}$ on D, we employ the lowest-order Courant finite element space

$$\mathcal{S}_h^D := \left\{v_h \in C(\overline{D}) : v_h|_K \in \mathcal{P}^1(K) \text{ for all } K \in \mathcal{T}_h^D\right\} \subset H^1(D),$$

which consists of piecewise affine, globally continuous functions; cf., e.g., [EG04, Bra07, BS08]. We write $\mathcal{I}_h^D : C(\overline{D}) \to \mathcal{S}_h^D$ for the corresponding nodal interpolant. We collect the following two standard FEM results.

Proposition 3.1.7 (Approximation properties of $\mathcal{I}_h^D$, [EG04, Corollary 1.109])**.** *Let $(\mathcal{T}_h^D)_{h>0}$ be a family of $C_{\mathbf{mesh}}$-quasi-uniform meshes on $D \subset \mathbb{R}^3$. Let $p \in (3/2, \infty]$. Then, there exists a constant $C > 0$, which depends only on p, D, and $C_{\mathbf{mesh}}$, such that for all $h > 0$, it holds that*

$$\|\varphi - \mathcal{I}_h^D \varphi\|_{L^p(D)} + h\, \|\nabla\varphi - \nabla\mathcal{I}_h^D \varphi\|_{L^p(D)} \leq C\, h^2\, |\varphi|_{W^{2,p}(D)} \quad \textit{for all } \varphi \in W^{2,p}(D). \qquad \square$$

Proposition 3.1.8 (Inverse estimate, [EG04, Corollary 1.141])**.** *Let $(\mathcal{T}_h^D)_{h>0}$ be a family of $C_{\mathbf{mesh}}$-quasi-uniform meshes on $D \subset \mathbb{R}^3$. Let $p \in [1, \infty]$. Then, there exists a constant $C > 0$, which depends only on p, D, and $C_{\mathbf{mesh}}$, such that, for all $h > 0$, it holds that*

$$\|\nabla\varphi_h\|_{L^p(K)} \leq C\, h^{-1} \|\varphi_h\|_{L^p(K)} \quad \textit{for all } K \in \mathcal{T}_h^D \quad \textit{and for all } \varphi_h \in \mathcal{S}_h^D. \qquad \square$$

3.1.3. Nédélec-elements of the second kind

Given a bounded and polyhedral Lipschitz domain $D \subset \mathbb{R}^3$ and a $C_{\mathbf{mesh}}$-quasi-uniform family of meshes $(\mathcal{T}_h^D)_{h>0}$ on D, we employ the Nédélec-elements [Néd86] of second kind and order one

$$\boldsymbol{\mathcal{X}}_h^D := \{\boldsymbol{\zeta}_h \in \boldsymbol{H}(\mathbf{curl}; D) : \boldsymbol{\zeta}_h|_K \in \mathcal{P}^1(K) \text{ for all elements } K \in \mathcal{T}_h^D\} \subset \boldsymbol{H}(\mathbf{curl}; D)\,;$$

see, e.g., [Mon03, Section 8.2.2]. Unlike the standard $H^1(D)$–conforming space of piecewise affine functions $\mathcal{S}_h^D$ from the latter section, the degrees of freedom of $\boldsymbol{\mathcal{X}}_h^D$ are associated with the edges. This is reflected in the following elementwise definition of the corresponding interpolation operator $\boldsymbol{\mathcal{J}}_h^D$:

Let $K \in \mathcal{T}_h$ and let $\boldsymbol{\tau_e}$ the unit tangent vector to some edge $\boldsymbol{e}$ of K. For $\boldsymbol{\varphi}_K \in \boldsymbol{H}^1(K)$, define $\boldsymbol{\mathcal{J}}_K\boldsymbol{\varphi}_K \in \mathcal{P}^1(K)$ via the relation

$$\int_{\boldsymbol{e}} \big(\boldsymbol{\varphi}_K - \boldsymbol{\mathcal{J}}_K\boldsymbol{\varphi}_K\big)\,\boldsymbol{\tau}_e\,\boldsymbol{p}\,\mathrm{d}\boldsymbol{e} = 0 \quad \text{for all } \boldsymbol{p} \in \mathcal{P}^1(\boldsymbol{e}) \text{ and for all edges } \boldsymbol{e} \text{ of } K. \tag{3.1}$$

Then, we define the interpolation operator $\boldsymbol{\mathcal{J}}_h^D : \boldsymbol{H}^1(D) \to \boldsymbol{\mathcal{X}}_h^D$ via

$$\big(\boldsymbol{\mathcal{J}}_h^D\boldsymbol{\varphi}\big)|_K := \boldsymbol{\mathcal{J}}_K(\boldsymbol{\varphi}|_K) \quad \text{ for all } \boldsymbol{\varphi} \in \boldsymbol{H}^1(D),$$

and get the following approximation properties.

Proposition 3.1.9 (Approximation properties of $\boldsymbol{\mathcal{J}}_h^D$, [Mon03, Theorem 8.15])**.** *Let $(\mathcal{T}_h^D)_{h>0}$ be a family of $C_{\mathbf{mesh}}$-quasi-uniform meshes on $D \subset \mathbb{R}^3$. Then, there exists a constant $C > 0$, which depends only on D, and $C_{\mathbf{mesh}}$, such that, for all $h > 0$, it holds that*

$$\|\boldsymbol{\varphi} - \boldsymbol{\mathcal{J}}_h^D\boldsymbol{\varphi}\|_{\boldsymbol{L}^2(D)} + h\,\|\nabla \times \big(\boldsymbol{\varphi} - \boldsymbol{\mathcal{J}}_h^D\boldsymbol{\varphi}\big)\|_{\boldsymbol{L}^2(D)} \le C\,h^2|\boldsymbol{\varphi}|_{\boldsymbol{H}^2(D)} \quad \textit{for all } \boldsymbol{\varphi} \in \boldsymbol{H}^2(D). \qquad \square$$

3.2. Time-discretization

In this section, we fix the time-discretization of the time-scale $[0, T]$ of this work. For $M \in \mathbb{N}$, we employ the uniform time-steps $t_j := jk$ for all $j = 0, \dots, M$, where

$$k := \frac{T}{M},$$

is the uniform time-step size. For a Banach space B and a finite sequence $(\varphi^i)_{i=-1}^M \subset B$, we define the mean-values $\varphi^{i+1/2} \in B$ via

$$\varphi^{i+1/2} := \frac{\varphi^{i+1} + \varphi^i}{2} \quad \text{for} \quad i = 0, \dots, M-1 \tag{3.2a}$$

and the discrete time-derivatives $\mathrm{d_t}\varphi^{i+1} \in B$ via

$$\mathrm{d_t}\boldsymbol{\varphi}^{i+1} := \frac{\varphi^{i+1} - \varphi^i}{k} \in B \quad \text{for} \quad i = 0, \dots, M-1. \tag{3.2b}$$

Moreover, we interpret sequences $(\varphi^i)_{i=-1}^M \subset B$ as functions from $[0,T]$ to B in the following way: For $t \in [t_i, t_{i+1})$ and $i = 0, \dots, M-1$, we define

$$\varphi_k^{=}(t) := \boldsymbol{\varphi}^{i-1}\ ,\ \varphi_k^{-}(t) := \boldsymbol{\varphi}^{i}\ ,\ \varphi_k^{+}(t) := \boldsymbol{\varphi}^{i+1}\ ,\ \overline{\varphi}_k(t) := \boldsymbol{\varphi}^{i+1/2}, \quad \text{and} \tag{3.3a}$$

$$\varphi_k(t) := \varphi^{i+1}\,\frac{t - t_i}{k} + \varphi^i\,\frac{t_{i+1} - t}{k}. \tag{3.3b}$$

We refer to the latter functions as the postprocessed output of the sequence $(\boldsymbol{\varphi}^i)_{i=-1}^M \in B$.

Remark 3.2.1. *Note that* $\varphi_k^{=}, \varphi_k^{-}, \varphi_k^{+}, \overline{\varphi}_k \in L^2(0,T;B)$ *as well as* $\varphi_k \in H^1(0,T;B)$ *with* $\partial_t \varphi_k(t) = \mathrm{d_t}\varphi^{i+1}$ *for* $t \in (t_i, t_{i+1})$ *and* $i = 0, \dots, M-1$.

3.3. Space-discretization

In this section, we fix the space-discretization which we will employ in the algorithms for the numerical integration of LLG and its couplings. We distinguish between space discretization for plain LLG on ω, and coupled systems on $\Omega \supset \omega$. Recalling from Section 2.2 that ω and $\Omega \supset \omega$ are bounded and polyhedral Lipschitz domains, we start with the meshes:

- **Plain LLG:** If we only consider the LLG equation on ω, we employ a family of $C_{\mathbf{mesh}}$-quasi-uniform meshes $(\mathcal{T}_h)_{h>0}$ on ω and denote the corresponding nodes by

$$\mathcal{N}_h := \{\boldsymbol{z} \in \overline{\omega} : \boldsymbol{z} \text{ is a vertex of any element } K \in \mathcal{T}_h\}. \tag{3.4}$$

  We suppose a numbering of the nodes, i.e., $\mathcal{N}_h = \{\boldsymbol{z}_1, \dots, \boldsymbol{z}_N\}$ with $N = |\mathcal{N}_h|$.

- **Couplings:** For couplings of LLG with equations on $\Omega \supset \omega$, we employ a family of $C_{\mathbf{mesh}}$-quasi-uniform meshes $(\mathcal{T}_h^\Omega)_{h>0}$ on Ω. We suppose that for all $h > 0$, the meshes $\mathcal{T}_h^\Omega$ resolve the subdomain ω. For all $h > 0$, we denote the nodes of $\mathcal{T}_h^\Omega$ by

$$\mathcal{N}_h^\Omega := \{\boldsymbol{z} \in \overline{\Omega} : \boldsymbol{z} \text{ is a vertex of any element } K \in \mathcal{T}_h^\Omega\}.$$

  Since $(\mathcal{T}_h^\Omega)_{h>0}$ is $C_{\mathbf{mesh}}$-quasi-uniform and since $\mathcal{T}_h^\Omega$ resolves the subdomain ω for all $h > 0$, Proposition 3.1.6 yields that the sub-meshes of $(\mathcal{T}_h^\Omega)_{h>0}$ on ω are $C_{\mathbf{mesh}}$-quasi-uniform on ω. This justifies that we reuse the notation from the latter point and write

$$\mathcal{T}_h := \{K \in \mathcal{T}_h^\Omega : K \subset \overline{\omega}\}$$

  in this case. Similarly, we reuse from (3.4) the notation

$$\mathcal{N}_h := \mathcal{N}_h^\Omega \cap \overline{\omega} = \{\boldsymbol{z}_1, \dots, \boldsymbol{z}_N\}.$$

Next, we introduce spaces and notations for the space discretization:

- **Plain LLG:** If we only consider the LLG equation, we build on the family of $C_{\mathbf{mesh}}$-quasi-uniform meshes $(\mathcal{T}_h)_{h>0}$, the space

$$\mathcal{S}_h := \big\{v_h \in C(\overline{\omega}) : v_h|_K \in \mathcal{P}^1(K) \text{ for all elements } K \in \mathcal{T}_h\big\} \subset H^1(\omega). \tag{3.5}$$

and denote the vector-valued version by $\boldsymbol{\mathcal{S}}_h := (\mathcal{S}_h)^3$. To mimic the modulus constraint $|\boldsymbol{m}| = 1$ a.e. in ω_T on a discrete level, we define as in, e.g., [Alo08, AKST14, BSF$^+$14], the set

$$\boldsymbol{\mathcal{M}}_h := \{\boldsymbol{\varphi}_h \in \boldsymbol{\mathcal{S}}_h : |\boldsymbol{\varphi}_h(\boldsymbol{z})| = 1 \text{ for all nodes } \boldsymbol{z} \in \mathcal{N}_h\} \subset \boldsymbol{\mathcal{S}}_h. \tag{3.6}$$

- **Couplings:** For the coupling of LLG with the spin diffusion equation (2.23) on $\Omega \supset \omega$, we employ

  $$\mathcal{S}_h^\Omega := \left\{\varphi_h \in C(\overline{\Omega}) : \varphi_h|_K \in \mathcal{P}^1(K) \text{ for all elements } K \in \mathcal{T}_h^\Omega\right\} \subset H^1(\Omega),$$

  and denote the vector-valued version with $\boldsymbol{\mathcal{S}}_h^\Omega := \left(\mathcal{S}_h^\Omega\right)^3$. According to Proposition 3.1.6, the family of sub-meshes $\left(\mathcal{T}_h\right)_{h>0}$ on ω is also $C_{\mathbf{mesh}}$-quasi-uniform. This justifies that we reuse the notation $\mathcal{S}_h$ from (3.5) and write

  $$\mathcal{S}_h := \left\{\varphi_h \in C(\overline{\omega}) : \varphi_h|_K \in \mathcal{P}^1(K) \text{ for all elements } K \in \mathcal{T}_h\right\} \subset H^1(\omega),$$

  as well as $\boldsymbol{\mathcal{S}}_h := (\mathcal{S}_h)^3$ for the corresponding vector valued version. Moreover, we reuse the notation from (3.6) and write

  $$\boldsymbol{\mathcal{M}}_h := \{\boldsymbol{v}_h \in \boldsymbol{\mathcal{S}}_h : |\boldsymbol{\varphi}_h(\boldsymbol{z})| = 1 \text{ for all nodes } \boldsymbol{z} \in \mathcal{N}_h\} \subset \boldsymbol{\mathcal{S}}_h.$$

  Finally, for the coupling of LLG with eddy currents (2.18), we employ the $\boldsymbol{H}(\mathbf{curl};\Omega)$-conforming space of Nédélec-elements of the second kind [Néd86] and define

  $$\boldsymbol{\mathcal{X}}_h := \{\boldsymbol{\zeta}_h \in \boldsymbol{H}(\mathbf{curl};\Omega) : \boldsymbol{\zeta}_h|_K \in \mathcal{P}^1(K) \text{ for all elements } K \in \mathcal{T}_h\} \subset \boldsymbol{H}(\mathbf{curl};\Omega).$$

3.3.1. Discrete tangent space

For the tangent plane schemes from Section 1.3.1, the sought $\boldsymbol{v} : \omega \to \mathbb{R}^3$ is pointwise tangential to $\boldsymbol{m} : \omega \to \mathbb{S}^2$, i.e., it holds that

$$\boldsymbol{v} \in \boldsymbol{\mathcal{K}}(\boldsymbol{m}) := \{\boldsymbol{\varphi} : \omega \to \mathbb{R}^3 : \boldsymbol{\varphi} \cdot \boldsymbol{m} = 0 \text{ a.e. in } \omega\}. \tag{3.7}$$

To mimic the latter space on a discrete level, we proceed as in, e.g., [Alo08, AKST14, BSF$^+$14], and seek $\boldsymbol{v}_h^i \approx \boldsymbol{v}(t_i)$ in the following discrete version: Given $\boldsymbol{\mu}_h \in \boldsymbol{\mathcal{M}}_h$, we define the discrete tangent space as

$$\boldsymbol{\mathcal{K}}_h(\boldsymbol{\mu}_h) := \{\boldsymbol{\varphi}_h \in \boldsymbol{\mathcal{S}}_h : \boldsymbol{\varphi}_h(\boldsymbol{z}) \cdot \boldsymbol{\mu}_h(\boldsymbol{z}) = 0 \text{ for all nodes } \boldsymbol{z} \in \mathcal{N}_h\}, \tag{3.8}$$

i.e., the tangent space constraint in (3.7) is satisfied nodewise. Figure 3.1 illustrates the $2D$ case: While the FEM space in $2D$ yields 2 degrees of freedom at each node, the nodewise tangent space yields only one. As a consequence, we get that $\dim \boldsymbol{\mathcal{K}}_h(\boldsymbol{\mu}_h) = 2N$, while $\dim(\boldsymbol{\mathcal{S}}_h) = 3N$. Moreover, these degrees of freedom vary with $\boldsymbol{\mu}_h(\boldsymbol{z})$ for all nodes $\boldsymbol{z} \in \mathcal{N}_h$.

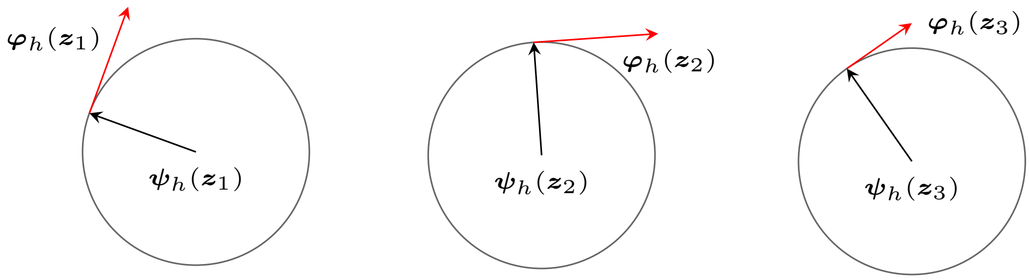

Figure 3.1.: Illustration of the nodewise tangent space in 2D for three nodes $\boldsymbol{z}_1, \boldsymbol{z}_2, \boldsymbol{z}_3$.

3.3.2. Approximate $\boldsymbol{L}^2$–scalar product

In particular for the midpoint scheme from Section 1.3.2, we require an approximate $\boldsymbol{L}^2(\omega)$-inner product, which depends only on the values at the nodes $\mathcal{N}_h$ of the (sub-)meshes $\mathcal{T}_h$ on ω. We proceed as in [BP06, BBP08, Bar15]: Let $\mathcal{I}_h$ be the nodal interpolant corresponding to $\mathcal{S}_h$. Given $\boldsymbol{\varphi}, \boldsymbol{\psi} \in \boldsymbol{C}(\overline{\omega})$, the approximate $\boldsymbol{L}^2$-scalar product employs the mass-lumping

$$\langle \boldsymbol{\varphi}, \boldsymbol{\psi} \rangle_h := \int_\omega \mathcal{I}_h(\boldsymbol{\varphi} \cdot \boldsymbol{\psi}) \, \mathrm{d}\boldsymbol{x} \approx \int_\omega \boldsymbol{\varphi} \cdot \boldsymbol{\psi} \, \mathrm{d}\boldsymbol{x} = \langle \boldsymbol{\varphi}, \boldsymbol{\psi} \rangle_{\boldsymbol{L}^2(\omega)} \tag{3.9}$$

To derive a handier representation, let $\phi_{\boldsymbol{z}} \in \mathcal{S}_h$ be the hat-functions assigned to the nodes $\boldsymbol{z} \in \mathcal{N}_h$. Then, we get that

$$\mathcal{I}_h(\boldsymbol{\varphi} \cdot \boldsymbol{\psi}) = \sum_{\boldsymbol{z} \in \mathcal{N}_h} \boldsymbol{\varphi}(\boldsymbol{z}) \cdot \boldsymbol{\psi}(\boldsymbol{z}) \, \phi_{\boldsymbol{z}}.$$

From the latter equation, we infer that the approximate $\boldsymbol{L}^2$-scalar product reads

$$\langle \boldsymbol{\varphi}, \boldsymbol{\psi} \rangle_h \overset{(3.9)}{=} \sum_{\boldsymbol{z} \in \mathcal{N}_h} \boldsymbol{\varphi}(\boldsymbol{z}) \cdot \boldsymbol{\psi}(\boldsymbol{z}) \Big(\int_\omega \phi_{\boldsymbol{z}} \, \mathrm{d}\boldsymbol{x} \Big), \quad \text{where} \Big(\int_\omega \phi_{\boldsymbol{z}} \, \mathrm{d}\boldsymbol{x} \Big) > 0. \tag{3.10}$$

Moreover, we write $\| \cdot \|_h$ for the corresponding norm. We stress that $\langle \cdot, \cdot \rangle_h$ is indeed a scalar product on $\boldsymbol{\mathcal{S}}_h \subset \boldsymbol{C}(\overline{\omega})$. The following lemma summarizes approximation properties of $\langle \cdot, \cdot \rangle_h$.

Lemma 3.3.1 ([Bar15, Lemma 3.9])**.** *Let $\langle \cdot, \cdot \rangle_h$ be the approximate $\boldsymbol{L}^2$-scalar from* (3.10) *with the corresponding norm $\| \cdot \|_h$. Then, the following two assertions* (i)–(ii) *hold true:*

(i) *It holds that*

$$\|\boldsymbol{\varphi}_h\|_{\boldsymbol{L}^2(\omega)} \leq \|\boldsymbol{\varphi}_h\|_h \leq \sqrt{5} \|\boldsymbol{\varphi}_h\|_{\boldsymbol{L}^2(\omega)} \quad \textit{for all } \boldsymbol{\varphi}_h \in \boldsymbol{\mathcal{S}}_h.$$

(ii) *There exists a constant $C > 0$, which depends only on ω and on $C_{\mathbf{mesh}}$, such that*

$$|\langle \boldsymbol{\varphi}_h, \boldsymbol{\psi}_h \rangle_h - \langle \boldsymbol{\varphi}_h, \boldsymbol{\psi}_h \rangle_{\boldsymbol{L}^2(\omega)}| \leq C \, h^2 \, \|\nabla \boldsymbol{\varphi}_h\|_{\boldsymbol{L}^2(\omega)} \, \|\nabla \boldsymbol{\psi}_h\|_{\boldsymbol{L}^2(\omega)} \quad \textit{for all } \boldsymbol{\varphi}_h, \boldsymbol{\psi}_h \in \boldsymbol{\mathcal{S}}_h.$$

□

With the definition of $\langle\cdot,\cdot\rangle_h$ at hand, we introduce the following discrete versions of the Laplacian and the $\boldsymbol{L}^2$-projection:

Discrete Laplacian: Mimicking the well-known integration by parts formula, we define the discrete Laplacian $\Delta_h : \boldsymbol{H}^1(\omega) \to \boldsymbol{\mathcal{S}}_h$ as in [BP06, eq. (2.1)] via the relation

$$\langle \Delta_h \boldsymbol{\varphi}, \boldsymbol{\psi}_h \rangle_h = -\langle \nabla\boldsymbol{\varphi}, \nabla\boldsymbol{\psi}_h \rangle_{\boldsymbol{L}^2(\omega)} \quad \text{for all } \boldsymbol{\varphi} \in \boldsymbol{H}^1(\omega) \text{ and for all } \boldsymbol{\psi}_h \in \boldsymbol{\mathcal{S}}_h. \tag{3.11}$$

Besides the obvious linearity, Δ_h is bounded in the following sense.

Lemma 3.3.2 ([BP06, Equation (2.3)])**.** *Consider the discrete Laplacian Δ_h from* (3.11)*. There exists a constant $C > 0$, which depends only on ω and on $C_{\mathbf{mesh}}$, such that*

$$\|\Delta_h \boldsymbol{\varphi}_h\|_h \leq C\, h^{-2}\, \|\boldsymbol{\varphi}_h\|_{\boldsymbol{L}^2(\omega)} \quad \textit{for all } \boldsymbol{\varphi}_h \in \boldsymbol{\mathcal{S}}_h. \qquad \square$$

Quasi-$\boldsymbol{L}^2$-projection: Similarly to Δ_h from (3.11), we mimic the $\boldsymbol{L}^2(\omega)$-projection: As in [BBP08, p. 1401], we define $\boldsymbol{\mathcal{P}}_h : \boldsymbol{L}^2(\omega) \to \boldsymbol{\mathcal{S}}_h$ via the relation

$$\langle \boldsymbol{\mathcal{P}}_h \boldsymbol{\varphi}, \boldsymbol{\psi}_h \rangle_h = \langle \boldsymbol{\varphi}, \boldsymbol{\psi}_h \rangle_{\boldsymbol{L}^2(\omega)} \quad \text{for all } \boldsymbol{\varphi} \in \boldsymbol{L}^2(\omega) \quad \text{and for all } \boldsymbol{\psi}_h \in \boldsymbol{\mathcal{S}}_h. \tag{3.12}$$

Besides the obvious linearity, $\boldsymbol{\mathcal{P}}_h$ is bounded in the following sense.

Lemma 3.3.3. *The $\boldsymbol{L}^2(\omega)$-quasi-projection $\boldsymbol{\mathcal{P}}_h$ from* (3.12) *satisfies that*

$$\|\boldsymbol{\mathcal{P}}_h \boldsymbol{\varphi}\|_h \leq \|\boldsymbol{\varphi}\|_{\boldsymbol{L}^2(\omega)} \quad \textit{for all } \boldsymbol{\varphi} \in \boldsymbol{L}^2(\omega).$$

Proof. Given $\boldsymbol{\varphi} \in \boldsymbol{L}^2(\omega)$, we test (3.12) with $\boldsymbol{\psi} := \boldsymbol{\mathcal{P}}_h \boldsymbol{\varphi} \in \boldsymbol{\mathcal{S}}_h$ and obtain that

$$\|\boldsymbol{\mathcal{P}}_h \boldsymbol{\varphi}\|_h^2 = \langle \boldsymbol{\mathcal{P}}_h \boldsymbol{\varphi}, \boldsymbol{\mathcal{P}}_h \boldsymbol{\varphi} \rangle_h \overset{(3.12)}{=} \langle \boldsymbol{\varphi}, \boldsymbol{\mathcal{P}}_h \boldsymbol{\varphi} \rangle_{\boldsymbol{L}^2(\omega)} \leq \|\boldsymbol{\varphi}\|_{\boldsymbol{L}^2(\omega)}\, \|\boldsymbol{\mathcal{P}}_h \boldsymbol{\varphi}\|_{\boldsymbol{L}^2(\omega)}.$$

Together with $\|\boldsymbol{\mathcal{P}}_h \boldsymbol{\varphi}\|_{\boldsymbol{L}^2(\omega)} \leq \|\boldsymbol{\mathcal{P}}_h \boldsymbol{\varphi}\|_h$ from Lemma 3.3.1(i), this concludes the proof. $\square$

3.4. Discretization of the data

In this section, we unify the discretization assumptions of the own works [DPP+17, PRS18] for the data $\boldsymbol{m}^0$, $\boldsymbol{\pi}$, $\boldsymbol{f}$, and $\boldsymbol{\Pi}$ of LLG (2.3) and its coupled systems. Here, we collect the assumptions, which we require to formulate the results in this work and which are independent of the specific algorithm. Note that additional assumptions, which are enforced by a specific algorithm, are made in the corresponding chapter.

3.4.1. Discretization of $\boldsymbol{m}^0$

We define the approximation to the initial condition for all $h > 0$ as

$$\boldsymbol{\mathcal{S}}_h \ni \boldsymbol{m}_h^0 \approx \boldsymbol{m}^0.$$

To formulate the theorems in this work, we require

(D1) Weak consistency of $\boldsymbol{m}_h^0$: It holds that $\boldsymbol{m}_h^0 \rightharpoonup \boldsymbol{m}^0$ in $\boldsymbol{H}^1(\omega)$ as $h \to 0$.

Moreover, we require the following stronger assumption to derive energy estimates such as Definition 2.2.1(iv):

(D1$^+$) Strong consistency of $\boldsymbol{m}_h^0$: It holds that $\boldsymbol{m}_h^0 \to \boldsymbol{m}^0$ in $\boldsymbol{H}^1(\omega)$ as $h \to 0$.

3.4.2. Discretization of $\boldsymbol{\pi}$

For the approximation of $\boldsymbol{\pi}$ from Section 2.2, we suppose operators

$$\boldsymbol{\pi}_h : \boldsymbol{\mathcal{S}}_h \to \boldsymbol{L}^2(\omega) \quad \text{for all } h > 0.$$

As in Section 2.2 for $\boldsymbol{\pi}$, the specific contributions are postponed and discussed at the end of this section. For the results in this work, we require the following general assumptions:

(D2) Linearity of $\boldsymbol{\pi}_h$: For all $h > 0$, the operators $\boldsymbol{\pi}_h : \boldsymbol{\mathcal{S}}_h \to \boldsymbol{L}^2(\omega)$ are linear.

(D3) Uniform boundedness of $\boldsymbol{\pi}_h$: There exists a constant $C_{\boldsymbol{\pi}} > 0$ such that

$$\|\boldsymbol{\pi}_h(\boldsymbol{\varphi}_h)\|_{\boldsymbol{L}^2(\omega)} \leq C_{\boldsymbol{\pi}} \|\boldsymbol{\varphi}_h\|_{\boldsymbol{L}^2(\omega)} \quad \text{for all } \boldsymbol{\varphi}_h \in \boldsymbol{\mathcal{S}}_h \quad \text{and for all } h > 0.$$

(D4) Weak consistency of $\boldsymbol{\pi}_h$: For all sequences $(\boldsymbol{\varphi}_h)_{h>0} \subset \boldsymbol{\mathcal{S}}_h$ with $\boldsymbol{\varphi}_h \to \boldsymbol{\varphi}$ in $\boldsymbol{L}^2(\omega)$ as $h \to 0$, it holds that

$$\boldsymbol{\pi}_h(\boldsymbol{\varphi}_h) \rightharpoonup \boldsymbol{\pi}(\boldsymbol{\varphi}) \quad \text{in } \boldsymbol{L}^2(\omega) \quad \text{as } h \to 0.$$

Moreover, we require the following stronger assumptions to derive stronger energy estimates such as Definition 2.2.1(iv):

(D4$^+$) Strong consistency of $\boldsymbol{\pi}_h$: For all sequences $(\boldsymbol{\varphi}_h)_{h>0} \subset \boldsymbol{\mathcal{S}}_h$ with $\boldsymbol{\varphi}_h \to \boldsymbol{\varphi}$ in $\boldsymbol{L}^2(\omega)$ as $h \to 0$, it holds that

$$\boldsymbol{\pi}_h(\boldsymbol{\varphi}_h) \to \boldsymbol{\pi}(\boldsymbol{\varphi}) \quad \text{in } \boldsymbol{L}^2(\omega) \quad \text{as } h \to 0.$$

In many works, the consistency assumptions **(D4)** and **(D4$^+$)** are formulated with convergences in $\boldsymbol{L}^2(\omega_T)$: In this case, one assumes that

$$\boldsymbol{\pi}_h(\boldsymbol{\varphi}_{hk}) \rightharpoonup \boldsymbol{\pi}(\boldsymbol{\varphi}) \quad \text{or} \quad \boldsymbol{\pi}_h(\boldsymbol{\varphi}_{hk}) \to \boldsymbol{\pi}(\boldsymbol{\varphi}) \tag{3.13}$$

for (certain) sequences $(\boldsymbol{\varphi}_{hk})_{h,k>0}$ with $\boldsymbol{\varphi}_{hk} \to \boldsymbol{\varphi}$ in $\boldsymbol{L}^2(\omega_T)$ as $h, k \to 0$; see, e.g., [Pag13, AHP$^+$14, BSF$^+$14, BPP15, LPPT15]. In contrast to these works, we deem the formulation **(D4)** and **(D4$^+$)** to be more natural. After all, this does not involve any analytical problems. In all relevant situation, we recover the required convergences (3.13) from the following lemma.

Lemma 3.4.1 (Consistency of $\boldsymbol{\pi}_h$ on $\boldsymbol{L}^2(\omega_T)$)**.** *Suppose that $\boldsymbol{\pi}$ is bounded* **(L2)**. *Let $\boldsymbol{\varphi} \in \boldsymbol{L}^\infty(0,T;\boldsymbol{L}^2(\omega))$ and let the sequence $(\boldsymbol{\varphi}_{hk})_{h,k>0} \subset L^\infty(0,T,\boldsymbol{\mathcal{S}}_h)$, satisfy*

$$\boldsymbol{\varphi}_{hk} \overset{*}{\rightharpoonup} \boldsymbol{\varphi} \qquad \textit{in } L^\infty(0,T,\boldsymbol{L}^2(\omega)), \quad \textit{and} \tag{3.14a}$$

$$\boldsymbol{\varphi}_{hk}(t) \to \boldsymbol{\varphi}(t) \qquad \textit{in } \boldsymbol{L}^2(\omega) \quad \textit{a.e. for } t \in (0,T). \tag{3.14b}$$

as $h, k \to 0$. Then, the following two assertions (i)–(ii) *hold true:*

(i) *Suppose that* $\boldsymbol{\pi}_h$ *is uniformly bounded* **(D2)** *and weakly consistent* **(D4)**. *Then, it holds that*

$$\boldsymbol{\pi}_h(\boldsymbol{\varphi}_{hk}) \rightharpoonup \boldsymbol{\pi}(\boldsymbol{\varphi}) \quad \text{in } \boldsymbol{L}^2(\omega_T) \quad \text{as } h,k \to 0.$$

(ii) *Suppose that* $\boldsymbol{\pi}_h$ *is uniformly bounded* **(D2)** *and strongly consistent* **(D4⁺)**. *Then, it holds that*

$$\boldsymbol{\pi}_h(\boldsymbol{\varphi}_{hk}) \to \boldsymbol{\pi}(\boldsymbol{\varphi}) \quad \text{in } \boldsymbol{L}^2(\omega_T) \quad \text{as } h,k \to 0.$$

Proof. As a direct consequence of the principle of uniform boundedness (see, e.g., [Yos95, Chapter II.1, Corollary 1])[1], weak* convergent sequences are bounded. With **(L2)** and **(D3)**, this yields that

$$\sup_{t\in(0,T)} \|\boldsymbol{\pi}_h(\boldsymbol{\varphi}_{hk}(t))\|_{\boldsymbol{L}^2(\omega)} + \operatorname*{ess\,sup}_{t\in(0,T)} \|\boldsymbol{\pi}(\boldsymbol{\varphi}(t))\|_{\boldsymbol{L}^2(\omega)} \overset{(3.14a)}{\lesssim} \|\boldsymbol{\varphi}\|_{\boldsymbol{L}^\infty(0,T;\boldsymbol{L}^2(\omega))} < \infty. \tag{3.15}$$

First, we prove (i): For all $\boldsymbol{\zeta} \in \boldsymbol{C}^\infty(\overline{\omega_T})$, the convergence (3.14b) proves that

$$\langle \boldsymbol{\pi}_h(\boldsymbol{\varphi}_{hk}(t)), \boldsymbol{\zeta}\rangle_{\boldsymbol{L}^2(\omega)} \overset{\textbf{(D4)}}{\to} \langle \boldsymbol{\pi}(\boldsymbol{\varphi}(t)), \boldsymbol{\zeta}\rangle_{\boldsymbol{L}^2(\omega)} \quad \text{for almost all } t \in (0,T) \quad \text{as } h,k \to 0.$$

With (3.15), we obtain an integrable majorant and the dominated convergence theorem yields that

$$\int_0^T \langle \boldsymbol{\pi}_h(\boldsymbol{\varphi}_{hk}), \boldsymbol{\zeta}\rangle_{\boldsymbol{L}^2(\omega)} \,\mathrm{d}t \to \int_0^T \langle \boldsymbol{\pi}(\boldsymbol{\varphi}), \boldsymbol{\zeta}\rangle_{\boldsymbol{L}^2(\omega)} \,\mathrm{d}t \quad \text{as } h,k \to 0.$$

With (3.15) and Lemma B.2.1, this proves (i). To prove (ii), we similarly get from the convergence (3.14b) that

$$\|\boldsymbol{\pi}_h(\boldsymbol{\varphi}_{hk}(t)) - \boldsymbol{\pi}(\boldsymbol{\varphi}(t))\|_{\boldsymbol{L}^2(\omega)} \overset{\textbf{(D4}^+\textbf{)}}{\to} 0 \quad \text{for almost all } t \in (0,T) \quad \text{as } h,k \to 0.$$

With (3.15), we obtain an integrable majorant and the dominated convergence theorem proves that

$$\|\boldsymbol{\pi}_h(\boldsymbol{\varphi}_{hk}) - \boldsymbol{\pi}(\boldsymbol{\varphi})\|^2_{\boldsymbol{L}^2(\omega_T)} = \int_0^T \|\boldsymbol{\pi}_h(\boldsymbol{\varphi}_{hk}(t)) - \boldsymbol{\pi}(\boldsymbol{\varphi}(t))\|^2_{\boldsymbol{L}^2(\omega)} \,\mathrm{d}t \to 0 \quad \text{as } h,k \to 0.$$

This proves (ii) and concludes the proof. ∎

Finally, for the approximation operators to the exemplary contributions of $\boldsymbol{\pi}$, we proceed as follows:

[1]In our reference, this theorem is called resonance theorem. However, it is also often referred to as (a corollary of the) Banach–Steinhaus theorem.

- **Approximate uniaxial anisotropy:** For the uniaxial anistropy operator $\boldsymbol{\pi}$ from (2.7), we define

$$\boldsymbol{\pi}_h(\boldsymbol{\varphi}_h) := (\mathbf{a} \cdot \boldsymbol{\varphi}_h)\,\mathbf{a} \in \boldsymbol{\mathcal{S}}_h \quad \text{for all } \boldsymbol{\varphi}_h \in \boldsymbol{\mathcal{S}}_h, \tag{3.16}$$

where $\mathbf{a} \in \mathbb{R}^3$ with $|\mathbf{a}| = 1$ is the easy axis, i.e., $\boldsymbol{\pi}_h = \boldsymbol{\pi}|_{\boldsymbol{\mathcal{S}}_h}$. The approximate uniaxial anisotropy satisfies the above assumptions **(D2)**, **(D3)**, and **(D4$^+$)**. For the verification, we refer to Proposition A.2.1.

- **Approximate stray field:** For the stray field operator from (2.11), the situation is more complicated than for uniaxial anisotropy. This is due to the fact that stray field computations are connected to the solution of the variational problem (2.10) on the whole space $\mathbb{R}^3$. We employ a variant of the well-known Fredkin–Koehler algorithm [FK90]. This involves the numerically expensive solution of a hybrid FEM-BEM-problem. For a precise formulation, we refer to Section 3.4.5 at the end of this chapter. However, we note that the approximate stray field satisfies the above assumptions **(D2)**, **(D3)**, and **(D4$^+$)**. For the verification, we refer to Proposition A.2.2.

Remark 3.4.2. *For further approaches for the approximate stray field computation, the reader is referred to [Gol12]. We note that also these approaches satisfy* **(D2)**, **(D3)**, *and* **(D4$^+$)**.

3.4.3. Discretization of $\boldsymbol{f}$

We define the approximation to the applied field $\boldsymbol{f} \in \boldsymbol{C}^1([0,T]; \boldsymbol{L}^2(\omega))$ as

$$\boldsymbol{\mathcal{S}}_h \ni \boldsymbol{f}_h^i \approx \boldsymbol{f}(t_i) \quad \text{for all } i = 0, 1, \ldots, M, \tag{3.17}$$

and require the following convergence assumption:

(D5) Weak consistency of $(\boldsymbol{f}_h^i)_{i=0}^M$: The postprocessed output $\overline{\boldsymbol{f}}_{hk} \subset \boldsymbol{L}^2(\omega_T)$ of $(\boldsymbol{f}_h^i)_{i=0}^M$ satisfies that

$$\overline{\boldsymbol{f}}_{hk} \rightharpoonup \boldsymbol{f} \quad \text{in } \boldsymbol{L}^2(\omega_T) \quad \text{as } h, k \to 0.$$

Moreover, we require the following stronger assumption to derive energy estimates such as Definition 2.2.1(iv).

(D5$^+$) Strong consistency of $(\boldsymbol{f}_h^i)_{i=0}^M$: The postprocessed output $\overline{\boldsymbol{f}}_{hk} \in \boldsymbol{L}^2(\omega_T)$ of $(\boldsymbol{f}_h^i)_{i=0}^M$ satisfies that

$$\overline{\boldsymbol{f}}_{hk} \to \boldsymbol{f} \quad \text{in } \boldsymbol{L}^2(\omega_T) \quad \text{as } h, k \to 0.$$

3.4.4. Discretization of Π

For the approximation of $\boldsymbol{\Pi}$ from Section 2.2, we suppose operators

$$\boldsymbol{\Pi}_h : \boldsymbol{\mathcal{S}}_h \to \boldsymbol{L}^2(\omega) \quad \text{for all } h > 0.$$

As in Section 2.2 for $\boldsymbol{\Pi}$, the specific contributions are postponed and discussed at the end of this section. For the results in this work, we require the following general assumptions:

(D6) Uniform boundednes of $\boldsymbol{\Pi}_h$: There exists a constant $C > 0$ such that

$$\|\boldsymbol{\Pi}_h(\boldsymbol{\varphi}_h)\|_{\boldsymbol{L}^2(\omega)} \le C\,\big(\,1 + \|\boldsymbol{\varphi}_h\|_{\boldsymbol{L}^\infty(\omega)}\,\big)\,\|\boldsymbol{\varphi}_h\|_{\boldsymbol{H}^1(\omega)} \quad \text{for all } \boldsymbol{\varphi}_h \in \boldsymbol{\mathcal{S}}_h \quad \text{and for all } h > 0.$$

(D7) Weak consistency of $\boldsymbol{\Pi}_h$: For all $\boldsymbol{\varphi} \in \boldsymbol{H}^1(\omega_T) \cap \boldsymbol{L}^\infty(\omega_T)$ and all sequences $(\boldsymbol{\varphi}_{hk})_{h,k>0} \subset \boldsymbol{L}^2(0,T;\boldsymbol{\mathcal{S}}_h)$ with

$$\boldsymbol{\varphi}_{hk} \to \boldsymbol{\varphi} \quad \text{in } \boldsymbol{L}^2(\omega_T) \quad \text{and} \quad \nabla\boldsymbol{\varphi}_{hk} \rightharpoonup \nabla\boldsymbol{\varphi} \quad \text{in } \boldsymbol{L}^2(\omega_T) \quad \text{as } h,k \to 0,$$

as well as $\|\boldsymbol{\varphi}_{hk}\|_{\boldsymbol{L}^\infty(\omega_T)} \le C$ for all $h,k > 0$ for some fixed $C > 0$, it holds that

$$\boldsymbol{\Pi}_h(\boldsymbol{\varphi}_{hk}) \rightharpoonup \boldsymbol{\Pi}(\boldsymbol{\varphi}) \quad \text{in } \boldsymbol{L}^2(\omega_T) \quad \text{as } h \to 0.$$

For energy estimates such as Definition 2.2.1(iv), we require the following stronger assumption:

(D7$^+$) Strong consistency of $\boldsymbol{\Pi}_h$: For all $\boldsymbol{\varphi} \in \boldsymbol{H}^1(\omega_T) \cap \boldsymbol{L}^\infty(\omega_T)$ and all sequences $(\boldsymbol{\varphi}_{hk})_{h,k>0} \subset \boldsymbol{L}^2(0,T;\boldsymbol{\mathcal{S}}_h)$ with

$$\boldsymbol{\varphi}_{hk} \to \boldsymbol{\varphi} \quad \text{in } \boldsymbol{L}^2(\omega_T) \quad \text{and} \quad \nabla\boldsymbol{\varphi}_{hk} \rightharpoonup \nabla\boldsymbol{\varphi} \quad \text{in } \boldsymbol{L}^2(\omega_T) \quad \text{as } h,k \to 0,$$

as well as $\|\boldsymbol{\varphi}_{hk}\|_{\boldsymbol{L}^\infty(\omega_T)} \le C$ for all $h,k > 0$ for some fixed $C > 0$, it holds that

$$\boldsymbol{\Pi}_h(\boldsymbol{\varphi}_{hk}) \to \boldsymbol{\Pi}(\boldsymbol{\varphi}) \quad \text{in } \boldsymbol{L}^2(\omega_T) \quad \text{as } h,k \to 0.$$

Finally, for the approximation operators to the exemplary contributions from Section 2.2, we proceed as follows:

- **Approximate Zhang–Li field:** For the Zhang–Li field $\boldsymbol{\Pi}$ from (2.13), we define

$$\boldsymbol{\Pi}_h(\boldsymbol{\varphi}_h) := \boldsymbol{\varphi}_h \times (\boldsymbol{u}\cdot\nabla)\,\boldsymbol{\varphi}_h + \beta\,(\boldsymbol{u}\cdot\nabla)\,\boldsymbol{\varphi}_h \in \boldsymbol{L}^2(\omega) \quad \text{for all } \boldsymbol{\varphi}_h \in \boldsymbol{\mathcal{S}}_h, \tag{3.18}$$

  where we suppose exact evaluation of the spin velocity vector $\boldsymbol{u} \in \boldsymbol{L}^\infty(\omega)$ and where $\beta \in [0,1]$ is the constant of non-adiabacity, i.e., $\boldsymbol{\Pi}_h := \boldsymbol{\Pi}|_{\boldsymbol{\mathcal{S}}_h}$. The approximate Zhang–Li field satisfies the assumptions **(D6)** and **(D7)**. For the verification, we refer to Proposition A.3.1(i).

- **Approximate Slonczewski field:** For the Slonczewski field $\boldsymbol{\Pi}$ from (2.14), we define

$$\boldsymbol{\Pi}_h(\boldsymbol{\varphi}_h) := \mathcal{G}(\boldsymbol{\varphi}_h\cdot\mathbf{p})\,\boldsymbol{\varphi}_h \times \mathbf{p} \in \boldsymbol{L}^2(\omega) \quad \text{for all } \boldsymbol{\varphi}_h \in \boldsymbol{\mathcal{S}}_h, \tag{3.19}$$

  where we recall that $\mathbf{p} \in \mathbb{R}^3$ with $|\mathbf{p}| = 1$ and $\mathcal{G} \in C^1_0(\mathbb{R})$, i.e., we set $\boldsymbol{\Pi}_h := \boldsymbol{\Pi}|_{\boldsymbol{\mathcal{S}}_h}$. The approximate Slonczewski field satisfies the assumptions **(D6)** and **(D7$^+$)**. For the verification, we refer to Proposition A.3.3(i).

3.4.5. Approximate stray field computations with Fredkin–Koehler method

In this section, we introduce an approximation operator $\boldsymbol{\pi}_h \approx \boldsymbol{\pi}$, where $\boldsymbol{\pi}$ is the stray field operator from (2.11). There, the discretization of the variational problem (2.10) for the function $u \in H^1(\mathbb{R}^3)$ (on the whole space) seems not to be easily feasible. We employ (a variant of) the well-known Fredkin–Koehler approach [FK90], which uses a superposition principle and transfers the evaluation of $\boldsymbol{\pi}$ to a problem on the domain ω. Here, we follow the presentation in [PRS18, Section 4]: First, we introduce for $u \in H^1(\omega)$ the well-known double-layer integral operator for the Laplace problem as

$$K(u|_{\partial\omega})(\boldsymbol{x}) := \frac{1}{4\pi} \int_{\partial\omega} \frac{(\boldsymbol{x}-\boldsymbol{y}) \cdot \boldsymbol{n}(\boldsymbol{y})}{|\boldsymbol{x}-\boldsymbol{y}|^3} \, u|_{\partial\omega} \, \mathrm{d}S(\boldsymbol{y}) \in L^2(\partial\omega); \tag{3.20}$$

see, e.g., [McL00, Section 6] or [SS11, Section 3.1] for details. Then, given a magnetization $\boldsymbol{\varphi} \in \boldsymbol{L}^2(\omega)$, we define $u_1 \in H^1_\star(\omega) := \{u \in H^1(\omega) : \int_\omega u \, \mathrm{d}x = 0\}$ as the unique weak solution of

$$\Delta u_1 = \operatorname{div} \boldsymbol{\varphi} \quad \text{in } \omega, \tag{3.21a}$$
$$\partial_{\boldsymbol{n}} u_1 = 0 \quad \text{on } \partial\omega. \tag{3.21b}$$

With u_1 at hand, we define $u_2 \in H^1(\omega)$ as the unique weak solution of

$$\Delta u_2 = 0 \quad \text{in } \omega, \tag{3.21c}$$
$$u_2 = \Big(K - \frac{1}{2}\Big) u_1|_{\partial\omega} \quad \text{on } \partial\omega. \tag{3.21d}$$

Finally, [FK90] yields that we can evaluate $\boldsymbol{\pi}$ with the superposition

$$\boldsymbol{\pi}(\boldsymbol{\varphi}) = -\nabla u = -\nabla u_1 - \nabla u_2 \in \boldsymbol{L}^2(\omega).$$

With the latter representation, we can employ as in, e.g., [BSF$^+$14], the following hybrid FEM-BEM approach and solve the problem from (3.21) on a discrete variational level: To that end, we define the space of piecewise affine and globally continuous functions with zero integral mean, on the boundary, and with zero trace as

$$\mathcal{S}_h^\star := \Big\{ \phi_h \in \mathcal{S}_h : \int_\omega \varphi_h \, \mathrm{d}x = 0 \Big\},$$
$$\mathcal{S}_h^{\partial\omega} := \mathcal{S}_h|_{\partial\omega}, \quad \text{and}$$
$$\mathcal{S}_h^0 := \big\{ \phi_h \in \mathcal{S}_h : \boldsymbol{\varphi}_h|_{\partial\omega} = 0 \big\},$$

respectively. Then, our algorithm reads as follows:

Algorithm 3.4.3 (Stray field computation by Fredkin–Koehler method, [FK90])**. Input:** $\boldsymbol{\mathcal{S}}_h \ni \boldsymbol{\varphi}_h \approx \boldsymbol{\varphi}$.
Perform the following four steps (a)–(d)*:*

(a) *Find* $u_{1,h} \in \mathcal{S}_h^\star$ *such that*

$$\langle \nabla u_1, \nabla \phi_h \rangle_{L^2(\omega)} = \langle \boldsymbol{\varphi}_h, \nabla \phi_h \rangle_{L^2(\omega)} \quad \textit{for all } \phi_h \in \mathcal{S}_h^\star.$$

(b) *Compute* $g_h \in \mathcal{S}_h^{\partial\omega}$ *such that*

$$\langle g_h, \phi_h \rangle_{L^2(\partial\omega)} = \langle\, [\,K - 1/2\,]\,(u_1|_{\partial\omega})\,, \phi_h \rangle_{L^2(\partial\omega)} \quad \textit{for all } \phi_h \in \mathcal{S}_h^{\partial\Omega}.$$

(c) *Compute* $u_{2,h} \in \mathcal{S}_h$ *with* $(u_{2,h})|_{\partial\omega} = g_h$ *such that*

$$\langle \nabla u_{2,h}, \nabla \phi_h \rangle_{L^2(\omega)} = 0 \quad \textit{for all } \phi_h \in \mathcal{S}_h^0.$$

(d) *Compute* $\boldsymbol{\pi}_h(\boldsymbol{\varphi}_h) := -\nabla u_1 - \nabla u_2 \in \boldsymbol{L}^2(\omega)$.

Output: *Approximate stray field* $\boldsymbol{\pi}_h(\boldsymbol{\varphi}_h) \approx \boldsymbol{\pi}(\boldsymbol{\varphi})$. □

Remark 3.4.4. *The original algorithm from [FK90] employs nodal interpolation of* $g := (K - 1/2)(u_1|_{\partial\omega})$ *to obtain* $g_h \in \mathcal{S}_h^{\partial\omega}$*, which is not stable in the sense of finite element analysis. Therefore, we discretize* g *by the* $L^2(\partial\omega)$*-orthogonal projection onto* $\mathcal{S}_h^{\partial\omega}$*. Instead, one could also employ the Scott–Zhang projection [SZ90] in step* (b) *of Algorithm 3.4.3 and not the* $L^2(\partial\omega)$*-orthogonal projection; see, e.g., [BSF*$^+$*14]. However, with the* $L^2(\partial\omega)$*-orthogonal projection, we obtained numerically more accurate results for coarse meshes on thin layers; see [PRS18, Section 4.1].*

Altogether, we define the discrete stray field operator in the following way:

$$\boldsymbol{\pi}_h : \boldsymbol{\mathcal{S}}_h \to \boldsymbol{L}^2(\omega) : \boldsymbol{\varphi}_h \mapsto \boldsymbol{\pi}_h(\boldsymbol{\varphi}_h), \quad \text{with the output of Algorithm 3.4.3.} \tag{3.22}$$

Note that $\boldsymbol{\pi}_h$ satisfies the assumptions **(D2)**, **(D3)**, and **(D4$^+$)** from Section 3.4.2. For the verification, we refer to Proposition A.2.2.

4. Implicit-explicit second-order tangent plane scheme for LLG

The following chapter is mainly based on [DPP+17], which is joint work with *Giovanni Di Fratta*[1], *Carl-Martin Pfeiler*[1], *Dirk Praetorius*[1], and *Michele Ruggeri*[2]. In parts, these findings are also elaborated in the co-supervised master thesis [Pfe17]. Moreover, we incorporate ideas of [KPP+18], which is ongoing joint work with *Johannes Kraus*[3], *Carl-Martin Pfeiler*[1], *Dirk Praetorius*[1], and *Michele Ruggeri*[2].

4.1. Introduction

Based on the preliminary works [AJ06, BKP08], the work [Alo08] is the first milestone in the development of today's tangent plane schemes in computational micromagnetism. The overall benefit of the method is that—despite the non-linear nature of LLG (2.3)—only one linear system has to be solved per time-step. The basic idea from [Alo08] can be summarized as follows:

For a smooth solution $\boldsymbol{m}$, LLG (2.3a) allows for an equivalent reformulation, which reads

$$\alpha\,\partial_t\boldsymbol{m} + \boldsymbol{m}\times\partial_t\boldsymbol{m} = \big[\,\boldsymbol{h}_{\mathrm{eff}}(\boldsymbol{m}) + \boldsymbol{\Pi}(\boldsymbol{m})\,\big] - \big(\boldsymbol{h}_{\mathrm{eff}}(\boldsymbol{m})\cdot\boldsymbol{m}\big)\boldsymbol{m} - \big(\boldsymbol{\Pi}(\boldsymbol{m})\cdot\boldsymbol{m}\big)\boldsymbol{m}. \tag{4.1}$$

In particular, (4.1) is linear in $\boldsymbol{v}(t) := \partial_t\boldsymbol{m}(t) \in \boldsymbol{\mathcal{K}}(\boldsymbol{m}(t))$. Upon adding a stabilization term, this gives rise to a variational problem for $\boldsymbol{v}(t)$ in the tangent space $\boldsymbol{\mathcal{K}}(\boldsymbol{m}(t))$. The scheme then employs the uniform time-stepping from Section 3.2 and the lowest-order Courant-type FEM space $\boldsymbol{\mathcal{S}}_h$ from Section 3.3 in space. Then, at at each time-step t_i and for given $\boldsymbol{\mathcal{M}}_h \ni \boldsymbol{m}_h^i \approx \boldsymbol{m}(t_i)$, one solves the corresponding discrete variational problem in the discrete tangent space $\boldsymbol{\mathcal{K}}_h(\boldsymbol{m}_h^i) \subsetneqq \boldsymbol{\mathcal{S}}_h$ for $\boldsymbol{\mathcal{K}}_h(\boldsymbol{m}_h^i) \ni \boldsymbol{v}_h^i \approx \boldsymbol{v}(t_i)$. With $\boldsymbol{v}_h^i \approx \boldsymbol{v}(t_i)$ at hand, one computes the approximation $\boldsymbol{\mathcal{M}}_h \ni \boldsymbol{m}_h^{i+1} \approx \boldsymbol{m}(t_{i+1})$ via the update formula

$$\boldsymbol{m}_h^{i+1}(\boldsymbol{z}) := \frac{\boldsymbol{m}_h^{i+1}(\boldsymbol{z}) + k\,\boldsymbol{v}_h^i(\boldsymbol{z})}{|\boldsymbol{m}_h^{i+1}(\boldsymbol{z}) + k\,\boldsymbol{v}_h^i(\boldsymbol{z})|} \quad \text{for all nodes } \boldsymbol{z} \in \mathcal{N}_h. \tag{4.2}$$

i.e., the modulus constraint (1.1) is enforced nodewise.

Since the reformulation (4.1) is linear in $\boldsymbol{v}$ and despite the non-linear nature of LLG (2.3), the tangent plane scheme requires only the solution of *one* linear system in the discrete tangent space $\boldsymbol{\mathcal{K}}_h(\boldsymbol{m}_h^i) \subsetneqq \boldsymbol{\mathcal{S}}_h$. The resulting numerical integrator is formally first-order in time.

[1]TU Wien
[2]Universität Wien
[3]University of Duisburg-Essen

In [Alo08], the tangent plane scheme is formulated and analyzed for $\boldsymbol{h}_{\text{eff}}(\boldsymbol{m}) := \Delta \boldsymbol{m}$ and $\boldsymbol{\Pi}(\boldsymbol{m}) = \boldsymbol{0}$ and proved to be unconditionally convergent in the sense of Convention 1.3.1. With its (relatively) low complexity, it has attracted scientific interest in the computational micromagnetics community. In particular, [Alo08] was extended to lower-order contributions [AKT12, Gol12, Pag13, BSF$^+$14], the coupling with eddy currents/the full Maxwell system [LPPT15, LT13, Pag13, BPP15], the coupling with the spin diffusion equation [AHP$^+$14, ARB$^+$15, Rug16], and the coupling with magnetostriction [Pag13, BPPR14]. Moreover, [GLT16] and [AdBH14] (semi-discrete) even takes into account stochastic effects. As a by-product, [AHP$^+$14, Rug16] prove that the normalization in the update (4.2) can be omitted. All the latter extensions are again formally first-order in time, however, without normalization and given a smooth enough (and thus unique [DS14]) strong solution to LLG (2.3), the recent work [FT17] even proves an a-priori estimate, which is first-order in time and space.

Curiously, the tangent plane scheme allows for a slight modification, which yields the (almost) second-order in-time numerical integrator of [AKST14]. This is based on the following key observation, which was already noted in [AKT12, Section 4]: Let $\mathbb{P}_{\boldsymbol{m}(t)}$ be the pointwise orthogonal projection onto $\boldsymbol{m}(t)^\perp := \text{span}\{\boldsymbol{m}(t)\}^\perp$. With the smarter choice of the sought unknown

$$\boldsymbol{v}(t) := \partial_t \boldsymbol{m}(t) + \frac{k}{2}\, \mathbb{P}_{\boldsymbol{m}(t)} \partial_{tt} \boldsymbol{m}(t) \in \boldsymbol{\mathcal{K}}(\boldsymbol{m}(t)). \tag{4.3}$$

we formally get from [AKST14, p.413] that

$$\frac{\boldsymbol{m}(t) + k\boldsymbol{v}(t)}{|\boldsymbol{m}(t) + k\boldsymbol{v}(t)|} = \boldsymbol{m}(t+k) + \mathcal{O}(k^3), \tag{4.4}$$

i.e., the normalized update is a second-order in time approximation of the update $\boldsymbol{m}(t+k)$. Then, [AKST14, Section 6] formally derives from (4.1) a linear variational formulation for the new $\boldsymbol{v}$ from (4.3) in the tangent space $\boldsymbol{\mathcal{K}}(\boldsymbol{m}(t))$. As for the classical first-order tangent plane scheme, [AKST14] employs the uniform time-stepping from Section 3.2 and the FEM-space $\boldsymbol{\mathcal{S}}_h$ from Section 3.3 for space-discretization and solves *one* linear system for

$$\boldsymbol{\mathcal{K}}_h(\boldsymbol{m}_h^i) \ni \boldsymbol{v}_h^i \approx \boldsymbol{v}(t_i) \overset{(4.3)}{=} \partial_t \boldsymbol{m}(t) + \frac{k}{2}\, \mathbb{P}_{\boldsymbol{m}(t)} \partial_{tt} \boldsymbol{m}(t) \in \boldsymbol{\mathcal{K}}(\boldsymbol{m}(t)). \tag{4.5}$$

Upon a stabilization, the resulting scheme of [AKST14] is unconditionally convergent in the sense of Convention 1.3.1. The stabilization, however, slightly perturbs the formal convergence order in the sense that one may only expect order $\mathcal{O}(k^{2-\varepsilon})$ in time, for all $\varepsilon > 0$. Omitting the stabilization yields full second-order in time convergence, but comes at the cost of the mild CFL-type condition $k = \mathbf{o}(h)$ for convergence towards a weak solution of LLG. While superior to the classical tangent plane scheme [Alo08] in terms of convergence order, the original algorithm from [AKST14] suffers, in particular, from the following issues:

- In [AKST14], the external field is assumed to be constant in time. Moreover, $\boldsymbol{f}$ and $\boldsymbol{\pi}$ are not approximated, but assumed to be available exactly.

- Dissipative effects are not covered in [AKST14], i.e., $\mathbf{\Pi} = \mathbf{0}$.
- The integrator of [AKST14] involves the (possibly) computationally costly evaluation of $\boldsymbol{\pi}_h(\boldsymbol{v}_h^i)$. Since $\boldsymbol{v}_h^i$ is the sought unknown, this term contributes to the bilinear form of the discrete variational formulation. For example for stray field computations, the corresponding system matrix is fully-populated and often not explicitly available.
- Shipping around the latter issue with an explicit Euler approach for the $\boldsymbol{\pi}$-contribution [AKT12, BSF$^+$14], reduces the convergence from (almost) second-order to first-order in time, i.e., we are reduced to the accuracy of the classical first-order tangent plane scheme.

4.1.1. Contributions

Based on the own work [DPP$^+$17], we make the following contributions:

- We extend the algorithm and its formal justification from [AKST14] to dissipative effects $\mathbf{\Pi}$ and to non-constant external fields, i.e., $\mathbf{\Pi} \neq \mathbf{0}$ and $\partial_t \boldsymbol{f} \neq \mathbf{0}$. This yields a (formally) second-order in time extension of the algorithm of [AKST14] to a broader class of model problems.
- We introduce a second-order in time explicit approach for $\boldsymbol{\pi}$ and $\mathbf{\Pi}$ and provide a formal justification. This approach goes back to the own work [PRS18] for the midpoint scheme (see Chapter 6) and avoids the numerically expensive implicit treatment of $\boldsymbol{\pi}$ and $\mathbf{\Pi}$.
- Our analysis allows for approximations $\boldsymbol{\pi}_h \approx \boldsymbol{\pi}$, $\boldsymbol{f}_h^i \approx \boldsymbol{f}(t_i)$, and $\mathbf{\Pi}_h \approx \mathbf{\Pi}$, where we adapt techniques of [AKT12, BSF$^+$14] as well as the own work [PRS18] for the midpoint scheme (see Chapter 6).
- We confirm the formal convergence order of our algorithm with a numerical experiment; see Section 4.4. For a qualitative experiment with a physically relevant example, we refer to the later Section 6.4, where we also make a comparison with our extension of the midpoint scheme from Chapter 6.
- We prove unconditional convergence of our extended algorithm in the sense of Convention 1.3.1; see Section 4.5.
- In order to avoid the (eventually) fully-populated system matrix from the implicit treatment of $\boldsymbol{\pi}$ and $\mathbf{\Pi}$, we introduce a fixed-point scheme for the solution of the linear system and prove its convergence; see Section 4.6.1.
- We sketch an approach for the (non-trivial) solution of the discrete variational problem in the discrete subspace $\boldsymbol{\mathcal{K}}_h(\boldsymbol{m}_h^i) \subsetneqq \boldsymbol{\mathcal{S}}_h$ on a linear algebra level; see Section 4.6.2. For details, we refer to [Rug16, KPP$^+$18].

Note that for $\mathbf{\Pi} = \mathbf{0}$ and $\partial_t \boldsymbol{f} = \mathbf{0}$, the contributions of this section are also elaborated in the master thesis [Pfe17], which was co-supervised by the author and which is also based on [DPP$^+$17].

4.2. Algorithm

In this section, we extend [AKST14, Algorithm 2] to our setting of LLG (2.3) and formulate our algorithm as in [DPP+17, Section 2.4]. In order to employ approximations $\boldsymbol{\pi}_h \approx \boldsymbol{\pi}$, $\boldsymbol{f}_h^i \approx \boldsymbol{f}(t_i)$, and $\boldsymbol{\Pi}_h \approx \boldsymbol{\Pi}$, we adapt the techniques of [AKT12, BSF+14] as well as the own work [PRS18] for the midpoint scheme (see Chapter 6): To this end, we need to extend our notations. First, we define the stabilization

$$G : \mathbb{R}_{>0} \to \mathbb{R}_{>0} \quad \text{with } \lim_{s\to 0} G(s) = \infty \quad \text{and} \quad \lim_{s\to 0} G(s)s = 0, \tag{4.6a}$$

and, morally, the reciprocal stabilization

$$\rho : \mathbb{R}_{>0} \to \mathbb{R}_{>0} \quad \text{with } \lim_{s\to 0} \rho(s) = 0 \quad \text{and} \quad \lim_{s\to 0} \rho(s)\, s^{-1} = \infty. \tag{4.6b}$$

Moreover, as in [AKST14, p.415], we define the weight-function

$$\mathcal{W}_{G(k)}(s) := \begin{cases} \alpha + \frac{k}{2}\min\{s, G(k)\} & \text{for } s \geq 0, \\ \alpha\left(1 + \frac{k}{2\alpha}\min\{-s, G(k)\}\right)^{-1} & \text{for } s < 0, \end{cases} \tag{4.6c}$$

and note that $G(k) \geq \alpha/2$ for sufficiently small k. Throughout this chapter, we wrap $\partial_t[\boldsymbol{\Pi}(\boldsymbol{m})]$ in the formal derivation operator

$$\boldsymbol{D}(\boldsymbol{m}, \partial_t \boldsymbol{m}) := \partial_t[\boldsymbol{\Pi}(\boldsymbol{m})], \tag{4.7a}$$

and note that $\boldsymbol{D}$ is linear in the second argument. Moreover, we consider a corresponding approximation $\boldsymbol{D}_h \approx \boldsymbol{D}$, where

$$\boldsymbol{D}_h : \boldsymbol{\mathcal{S}}_h \times \boldsymbol{\mathcal{S}}_h \to \boldsymbol{L}^2(\omega). \tag{4.7b}$$

For the exemplary contributions of $\boldsymbol{\Pi}$ from Section 2.2 and their discretizations from Section 3.4.4, we refer to Section 4.2.1 below for the precise definition of the corresponding operators $\boldsymbol{D}$ and $\boldsymbol{D}_h$. Then, we employ a general time-stepping approach for the discretization of $\boldsymbol{\pi}$ and $\boldsymbol{\Pi}$, which, in particular, covers implicit-explicit approaches. With $(\boldsymbol{m}_h^i)_{i=0}^M$ and $(\boldsymbol{v}_h^i)_{i=0}^M$ being the sequence of sought approximations to $\boldsymbol{m}(t_i)$ and $\boldsymbol{v}(t_i)$ with $\boldsymbol{v}$ from (4.3), respectively, we define

$$\boldsymbol{\pi}_h^{\boldsymbol{D}}(\boldsymbol{v}_h^i; \boldsymbol{m}_h^i, \boldsymbol{m}_h^{i-1}) \approx \boldsymbol{\pi}(\boldsymbol{m}(t_i + k/2)) \quad \text{and} \quad \boldsymbol{\Pi}_h^{\boldsymbol{D}}(\boldsymbol{v}_h^i; \boldsymbol{m}_h^i, \boldsymbol{m}_h^{i-1}) \approx \boldsymbol{\Pi}(\boldsymbol{m}(t_i + k/2))$$

with one of the following three approaches **(A1)**–**(A3)** below and refer to Section 4.3 for a formal justification. We allow

(A1) the implicit second-order in time approach from [AKST14, Algorithm 2]

$$\boldsymbol{\pi}_h^{\boldsymbol{D}}(\boldsymbol{v}_h^i; \boldsymbol{m}_h^i, \boldsymbol{m}_h^{i-1}) := \boldsymbol{\pi}_h(\boldsymbol{m}_h^i) + \frac{k}{2}\,\boldsymbol{\pi}_h(\boldsymbol{v}_h^i), \quad \text{and}$$
$$\boldsymbol{\Pi}_h^{\boldsymbol{D}}(\boldsymbol{v}_h^i; \boldsymbol{m}_h^i, \boldsymbol{m}_h^{i-1}) := \boldsymbol{\Pi}_h(\boldsymbol{m}_h^i) + \frac{k}{2}\,\boldsymbol{D}_h(\boldsymbol{m}_h^i, \boldsymbol{v}_h^i);$$

(A2) the explicit second-order in time Adams–Bashforth-type approach

$$\boldsymbol{\pi}_h^{\boldsymbol{D}}(\boldsymbol{v}_h^i; \boldsymbol{m}_h^i, \boldsymbol{m}_h^{i-1}) := \begin{cases} \boldsymbol{\pi}_h(\boldsymbol{m}_h^i) + k\boldsymbol{\pi}_h(\boldsymbol{v}_h^i) & \text{for } i = 0, \\ \frac{3}{2}\boldsymbol{\pi}_h(\boldsymbol{m}_h^i) - \frac{1}{2}\boldsymbol{\pi}_h(\boldsymbol{m}_h^{i-1}) & \text{else,} \end{cases}$$

and

$$\boldsymbol{\Pi}_h^{\boldsymbol{D}}(\boldsymbol{v}_h^i; \boldsymbol{m}_h^i, \boldsymbol{m}_h^{i-1}) := \begin{cases} \boldsymbol{\Pi}_h(\boldsymbol{m}_h^i) + k\boldsymbol{D}_h(\boldsymbol{m}_h^i, \boldsymbol{v}_h^i) & \text{for } i = 0, \\ \boldsymbol{\Pi}_h(\boldsymbol{m}_h^i) + \frac{1}{2}\boldsymbol{D}_h(\boldsymbol{m}_h^i, \boldsymbol{m}_h^i) - \frac{1}{2}\boldsymbol{D}_h(\boldsymbol{m}_h^i, \boldsymbol{m}_h^{i-1}) & \text{else;} \end{cases}$$

(A3) the first-order in time explicit Euler approach from [AKT12, BSF⁺14]

$$\boldsymbol{\pi}_h^{\boldsymbol{D}}(\boldsymbol{v}_h^i; \boldsymbol{m}_h^i, \boldsymbol{m}_h^{i-1}) := \boldsymbol{\pi}_h(\boldsymbol{m}_h^i) \quad \text{and} \quad \boldsymbol{\Pi}_h^{\boldsymbol{D}}(\boldsymbol{v}_h^i; \boldsymbol{m}_h^i, \boldsymbol{m}_h^{i-1}) := \boldsymbol{\Pi}_h(\boldsymbol{m}_h^i).$$

With these preparations, we have everything together to formulate our algorithm.

Algorithm 4.2.1 (IMEX TPS2, [DPP⁺17, Algorithm 2])**. Input:** *Approximation* $\boldsymbol{m}_h^{-1} := \boldsymbol{m}_h^0 \in \boldsymbol{\mathcal{M}}_h$ *of initial magnetization.*
Loop: *For* $i = 0, \dots, M-1$*, iterate the following steps* (a)–(c)*:*

(a) *Compute the discrete function*

$$\lambda_h^i := -C_{\mathbf{ex}} \, |\nabla \boldsymbol{m}_h^i|^2 + \big(\boldsymbol{f}_h^i + \boldsymbol{\pi}_h(\boldsymbol{m}_h^i) + \boldsymbol{\Pi}_h(\boldsymbol{m}_h^i)\big) \cdot \boldsymbol{m}_h^i. \tag{4.8}$$

(b) *Find* $\boldsymbol{v}_h^i \in \boldsymbol{\mathcal{K}}_h(\boldsymbol{m}_h^i)$ *such that, for all* $\boldsymbol{\varphi}_h \in \boldsymbol{\mathcal{K}}_h(\boldsymbol{m}_h^i)$*, it holds that*

$$\begin{aligned} &\langle \mathcal{W}_{G(k)}(\lambda_h^i)\, \boldsymbol{v}_h^i, \boldsymbol{\varphi}_h \rangle_{\boldsymbol{L}^2(\omega)} + \langle \boldsymbol{m}_h^i \times \boldsymbol{v}_h^i, \boldsymbol{\varphi}_h \rangle_{\boldsymbol{L}^2(\omega)} + \frac{C_{\mathbf{ex}}}{2}\, k\,(1+\rho(k))\, \langle \nabla \boldsymbol{v}_h^i, \nabla \boldsymbol{\varphi}_h \rangle_{\boldsymbol{L}^2(\omega)} \\ &= -C_{\mathbf{ex}}\, \langle \nabla \boldsymbol{m}_h^i, \nabla \boldsymbol{\varphi}_h \rangle_{\boldsymbol{L}^2(\omega)} + \langle \boldsymbol{\pi}_h^{\boldsymbol{D}}(\boldsymbol{v}_h^i; \boldsymbol{m}_h^i, \boldsymbol{m}_h^{i-1}), \boldsymbol{\varphi}_h \rangle_{\boldsymbol{L}^2(\omega)} + \langle \boldsymbol{f}_h^{i+1/2}, \boldsymbol{\varphi}_h \rangle_{\boldsymbol{L}^2(\omega)} \\ &\quad + \langle \boldsymbol{\Pi}_h^{\boldsymbol{D}}(\boldsymbol{v}_h^i; \boldsymbol{m}_h^i, \boldsymbol{m}_h^{i-1}), \boldsymbol{\varphi}_h \rangle_{\boldsymbol{L}^2(\omega)}. \end{aligned} \tag{4.9}$$

(c) *Define* $\boldsymbol{m}_h^{i+1} \in \boldsymbol{\mathcal{M}}_h$ *by*

$$\boldsymbol{m}_h^{i+1}(\boldsymbol{z}) := \frac{\boldsymbol{m}_h^i(\boldsymbol{z}) + k\boldsymbol{v}_h^i(\boldsymbol{z})}{|\boldsymbol{m}_h^i(\boldsymbol{z}) + k\boldsymbol{v}_h^i(\boldsymbol{z})|} \quad \textit{for all nodes } \boldsymbol{z} \in \mathcal{N}_h. \tag{4.10}$$

Output: *Approximations* $\boldsymbol{m}_h^i \approx \boldsymbol{m}(t_i)$*.* □

Remark 4.2.2. (i) *If we suppose linearity of* $\boldsymbol{\pi}_h$ *and linearity in the second argument of* $\boldsymbol{D}_h$*, all general time-stepping approaches* **(A1)**–**(A3)** *are affine in* $\boldsymbol{v}_h^i$*. Then, the discrete variational formulation* (4.9) *gives rise to a linear system for* $\boldsymbol{v}_h^i$*. We refer to Section 4.6 for details on how to solve this system.*

(ii) *The implicit approaches* **(A1)** *and* **(A2)** *with* $i = 0$ *depend on* $\boldsymbol{\pi}_h(\boldsymbol{v}_h^i)$ *and* $\boldsymbol{D}_h(\boldsymbol{m}_h^i, \boldsymbol{v}_h^i)$*. In practice, however, we then may require a numerically expensive fixed-point iteration to solve* (4.9)*, even though this is a linear system for* $\boldsymbol{v}_h^i$*; see Section 4.6.1 for details.*

(iii) *In contrast to* (ii)*, the Adams–Bashforth-type approach* **(A2)** *for* $i > 0$ *and the explicit Euler approach* **(A3)** *avoid the implicit evaluation of* $\boldsymbol{\pi}_h(\boldsymbol{v}_h^i)$ *and* $\boldsymbol{D}_h(\boldsymbol{m}_h^i, \boldsymbol{v}_h^i)$*. The explicit Euler approach* **(A3)** *is formally first-order in time. It will generically reduce the convergence order of the scheme and is only analyzed for comparison. However, the Adams–Bashforth-type approach* **(A2)** *avoids the evaluation of* $\boldsymbol{\pi}_h(\boldsymbol{v}_h^i)$ *and* $\boldsymbol{D}_h(\boldsymbol{m}_h^i, \boldsymbol{v}_h^i)$ *at least from the second time-step on and is formally second-order in time. It is thus our preferred choice.*

(iv) *For all approaches* **(A1)**–**(A3)***, the discrete variational problem* (4.9) *generally gives rise to a linear system, which has to be solved in the time-dependent discrete subspace* $\boldsymbol{\mathcal{K}}_h(\boldsymbol{m}_h^i) \subsetneqq \boldsymbol{\mathcal{S}}_h$*. We refer to Section 4.6.2 for a strategy on a linear algebra level.*

(v) *The update* (4.10) *is well-defined for any* $\boldsymbol{v}_h^i \in \boldsymbol{\mathcal{K}}_h(\boldsymbol{m}_h^i)$*: To see this, note that the nodewise definition* (3.8) *of the discrete tangent space* $\boldsymbol{\mathcal{K}}_h(\boldsymbol{m}_h^i)$ *yields that*

$$\boldsymbol{v}_h^i(\boldsymbol{z}) \cdot \boldsymbol{m}_h^i(\boldsymbol{z}) = 0 \quad \textit{for all nodes} \quad \boldsymbol{z} \in \mathcal{N}_h. \tag{4.11}$$

Recalling that $\boldsymbol{m}_h^i \in \boldsymbol{\mathcal{M}}_h$*, we get for all nodes* $\boldsymbol{z} \in \mathcal{N}_h$ *that*

$$|\boldsymbol{m}_h^i(\boldsymbol{z}) + k\boldsymbol{v}_h^i(\boldsymbol{z})|^2 = |\boldsymbol{m}_h^i(\boldsymbol{z})|^2 + 2k\,\boldsymbol{m}_h^i(\boldsymbol{z}) \cdot \boldsymbol{v}_h^i(\boldsymbol{z}) + |\boldsymbol{v}_h^i(\boldsymbol{z})|^2 \overset{(4.11)}{=} 1 + |\boldsymbol{v}_h^i(\boldsymbol{z})|^2 \geq 1,$$

i.e., the denominator in the update (4.10) *is always positive.*

(vi) *The standard choices for the stabilization functions are* $\rho(k) := |\log(k)k|$ *and* $G(k) := \rho(k)^{-1}$*. Note that these fit into the setting of* (4.6)*, while* $\rho(k) = 0$ *does not satisfy* (4.6b)*.*

(vii) *With the second-order approaches* **(A1)** *and* **(A2)***, Proposition 4.3.2 yields the formal convergence order* $\mathcal{O}(k^2 + \rho(k)k)$ *of Algorithm 4.2.1. With* ρ *from* (vi)*, we obtain the formal convergence order* $\mathcal{O}(k^{2-\varepsilon})$ *for all* $\varepsilon > 0$*, i.e., almost second-order in time. The choice* $\rho = 0$ *comes at the cost of the CFL-condition* $k = \mathbf{o}(h)$ *for convergence of the postprocessed output of Algorithm 4.2.1 towards a weak solution of LLG* (2.3)*.*

(viii) *With* $\mathcal{W}_{G(k)} = \alpha$ *and* $\rho = 0$*, Algorithm 4.2.1 degenerates to the classical first-order tangent plane scheme of [Alo08, AKT12, BSF⁺14].*

4.2.1. Formal derivation of exemplary $\boldsymbol{\Pi}$-contributions

In this section, we derive the formal derivative $\boldsymbol{D}$ for the exemplary contributions to $\boldsymbol{\Pi}$ from Section 2.2. To this end, recall that $\boldsymbol{D}$ was defined in (4.7a) via the relation

$$\boldsymbol{D}(\boldsymbol{m}, \partial_t \boldsymbol{m}) := \partial_t \big[\, \boldsymbol{\Pi}(\boldsymbol{m}) \,\big]$$

Moreover, we introduce corresponding approximations $\boldsymbol{D}_h \approx \boldsymbol{D}$.

- **Zhang–Li field:** For the Zhang–Li field [ZL04, TNMS05] from (2.13), we get with formal derivation as in [DPP⁺17, Section 7.2.2] that

$$\partial_t \big[\, \boldsymbol{\Pi}(\boldsymbol{m}) \,\big] \overset{(2.13)}{=} \partial_t \boldsymbol{m} \times (\boldsymbol{u} \cdot \nabla)\, \boldsymbol{m} + \boldsymbol{m} \times (\boldsymbol{u} \cdot \nabla)\, \partial_t \boldsymbol{m} + \beta(\boldsymbol{u} \cdot \nabla)\, \partial_t \boldsymbol{m} =: \boldsymbol{D}(\boldsymbol{m}, \partial_t \boldsymbol{m}),$$

where $\boldsymbol{u} \in \boldsymbol{L}^\infty(\omega_T)$ and $\beta \in [0,1]$. Then, we define the corresponding approximation operator $\boldsymbol{D}_h \approx \boldsymbol{D}$ as

$$\boldsymbol{D}_h(\boldsymbol{\varphi}_h, \boldsymbol{\psi}_h) := \boldsymbol{\psi}_h \times (\boldsymbol{u} \cdot \nabla)\, \boldsymbol{\varphi}_h + \boldsymbol{\varphi}_h \times (\boldsymbol{u} \cdot \nabla)\, \boldsymbol{\psi}_h + \beta\, (\boldsymbol{u} \cdot \nabla)\, \boldsymbol{\psi}_h \in \boldsymbol{L}^2(\omega), \quad (4.12)$$

for all $\boldsymbol{\varphi}_h, \boldsymbol{\psi}_h \in \boldsymbol{\mathcal{S}}_h$, i.e., $\boldsymbol{D}_h := \boldsymbol{D}|_{\boldsymbol{\mathcal{S}}_h \times \boldsymbol{\mathcal{S}}_h}$.

- **Slonczewski field:** For the Slonczewski field [Ber96, Slo96] from (2.14), we get with formal derivation as in [DPP+17, Section 7.2.1] that

$$\partial_t \big[\, \boldsymbol{\Pi}(\boldsymbol{m}) \,\big] \overset{(2.14)}{=} \big[\, \mathcal{G}'(\boldsymbol{m} \cdot \mathbf{p})\, \partial_t \boldsymbol{m} \cdot \mathbf{p} \,\big] \boldsymbol{m} \times \mathbf{p} + \mathcal{G}(\boldsymbol{m} \cdot \mathbf{p})\, \partial_t \boldsymbol{m} \times \mathbf{p} =: \boldsymbol{D}(\boldsymbol{m}, \partial_t \boldsymbol{m}),$$

where $\mathcal{G} \in C_0^1(\mathbb{R})$ and $\mathbf{p} \in \mathbb{R}^3$ with $|\mathbf{p}| = 1$. Then, we define the corresponding approximation operator $\boldsymbol{D}_h \approx \boldsymbol{D}$ as

$$\boldsymbol{D}_h(\boldsymbol{\varphi}_h, \boldsymbol{\psi}_h) := \big[\, \mathcal{G}'(\boldsymbol{\varphi}_h \cdot \mathbf{p})\, \boldsymbol{\psi}_h \cdot \mathbf{p} \,\big] \boldsymbol{\varphi}_h \times \mathbf{p} + \mathcal{G}(\boldsymbol{\varphi}_h \cdot \mathbf{p})\, \boldsymbol{\psi}_h \times \mathbf{p} \in \boldsymbol{L}^2(\omega), \quad (4.13)$$

for all $\boldsymbol{\varphi}_h, \boldsymbol{\psi}_h \in \boldsymbol{\mathcal{S}}_h$, i.e., $\boldsymbol{D}_h := \boldsymbol{D}|_{\boldsymbol{\mathcal{S}}_h \times \boldsymbol{\mathcal{S}}_h}$.

4.3. Formal justification of Algorithm 4.2.1

In this section, we extend the formal justification of the (almost) second-order tangent plane scheme from [AKST14, Section 6] to our setting of LLG (2.3), i.e., we cover $\partial_t \boldsymbol{f} \neq \boldsymbol{0}$ and $\boldsymbol{\Pi} \neq \boldsymbol{0}$ in general, and IMEX approaches for $\boldsymbol{\pi}$ and $\boldsymbol{\Pi}$, in particular. First, we elaborate the key-idea of [AKST14] behind the definition of $\boldsymbol{v}$ from (4.4).

Lemma 4.3.1 ([AKST14, p. 413])**.** *For $\boldsymbol{m} \in \boldsymbol{C}^\infty(\overline{\omega_T})$ with $|\boldsymbol{m}| = 1$, it holds that*

$$\frac{\boldsymbol{m}(t) + k\boldsymbol{v}(t)}{|\boldsymbol{m}(t) + k\boldsymbol{v}(t)|} = \boldsymbol{m}(t+k) + \mathcal{O}(k^3), \quad \textit{where} \quad \boldsymbol{v}(t) := \partial_t \boldsymbol{m}(t) + \frac{k}{2}\, \mathbb{P}_{\boldsymbol{m}(t)}(\partial_{tt} \boldsymbol{m}(t)) \quad (4.14)$$

for all $t \in [0, T-k]$. □

Recall the pointwise orthogonal projection $\mathbb{P}_{\boldsymbol{m}(t)}$ onto $\boldsymbol{m}(t)^\perp$. For $|\boldsymbol{m}| = 1$ in ω_T, we obtain the representation

$$\mathbb{P}_{\boldsymbol{m}(t)}(\boldsymbol{\psi}) := \boldsymbol{\psi} - (\boldsymbol{\psi} \cdot \boldsymbol{m}(t))\, \boldsymbol{m}(t) \quad \text{for all } \boldsymbol{\psi} \in \boldsymbol{C}(\overline{\omega}). \quad (4.15)$$

Note that, here, we elaborate [DPP+17, Proposition 13]. Then, the following proposition clarifies on a continuous-in-space-level why Algorithm 4.2.1 is expected to be of (almost) second-order in time.

Proposition 4.3.2 (Formal justification of IMEX TPS2, [DPP+17, Proposition 13])**.** *Let $\boldsymbol{m} \in \boldsymbol{C}^\infty(\overline{\omega_T})$ be a strong solution of LLG (2.3) and suppose that*

$$\lambda(\boldsymbol{m}) := \big(\, \boldsymbol{h}_{\mathrm{eff}}(\boldsymbol{m}) + \boldsymbol{\Pi}(\boldsymbol{m}) \,\big) \cdot \boldsymbol{m} \quad \textit{satisfies} \quad B := \|\lambda(\boldsymbol{m})\|_{\boldsymbol{L}^\infty(\omega)} \leq G(k) < \infty. \quad (4.16)$$

For $\boldsymbol{\psi}, \boldsymbol{\varphi} \in \boldsymbol{H}^1(\omega_T)$, define the bilinear form

$$\boldsymbol{B}_{\boldsymbol{m}}(\boldsymbol{\psi}, \boldsymbol{\varphi}) := \langle \mathcal{W}_{G(k)}\big(\lambda(\boldsymbol{m})\big)\boldsymbol{\psi}, \boldsymbol{\varphi} \rangle_{\boldsymbol{L}^2(\omega)} + \langle \boldsymbol{m} \times \boldsymbol{\psi}, \boldsymbol{\varphi} \rangle_{\boldsymbol{L}^2(\omega)} + \frac{C_{\mathbf{ex}}}{2}\, k\, (1 + \rho(k))\, \langle \nabla \boldsymbol{\psi}, \nabla \boldsymbol{\varphi} \rangle_{\boldsymbol{L}^2(\omega)}.$$

For $\boldsymbol{\varphi} \in \boldsymbol{H}^1(\omega_T)$*, define the linear form*

$$\boldsymbol{L}_{\Delta,\boldsymbol{f}}(\boldsymbol{\varphi}) := -C_{\mathbf{ex}}\langle \nabla \boldsymbol{m}(t), \nabla \boldsymbol{\varphi}\rangle_{\boldsymbol{L}^2(\omega)} + \Big\langle \boldsymbol{f}\big(t + \frac{k}{2}\big), \boldsymbol{\varphi} \Big\rangle_{\boldsymbol{L}^2(\omega)}.$$

Let $\mathbb{P}_{\boldsymbol{m}(t)}$ *be the pointwise orthogonal projection onto* $\boldsymbol{m}(t)^\perp$ *from* (4.15)*. Then,*

$$\boldsymbol{v}(t) := \partial_t \boldsymbol{m}(t) + \frac{k}{2}\,\mathbb{P}_{\boldsymbol{m}(t)}\partial_{tt}\boldsymbol{m}(t) \in \boldsymbol{\mathcal{K}}(\boldsymbol{m}(t)) \cap \boldsymbol{C}^\infty(\overline{\omega}) \tag{4.17}$$

satisfies the following two assertions (i)–(ii)*:*

(i) *Let* $t \in [0, T-k]$*. There exists* $\boldsymbol{R}_1 = \mathcal{O}(k^2 + k\rho(k))$ *such that*

$$\begin{aligned} &\boldsymbol{B}_{\boldsymbol{m}}(\boldsymbol{v}(t), \boldsymbol{\varphi}) - \frac{k}{2}\langle \boldsymbol{\pi}(\boldsymbol{v}(t)), \boldsymbol{\varphi}\rangle_{\boldsymbol{L}^2(\omega)} - \frac{k}{2}\langle \boldsymbol{D}(\boldsymbol{m}(t), \boldsymbol{v}(t)), \boldsymbol{\varphi}\rangle_{\boldsymbol{L}^2(\omega)} \\ &\quad = \boldsymbol{L}_{\Delta,\boldsymbol{f}}(\boldsymbol{\varphi}) + \langle \boldsymbol{\pi}(\boldsymbol{m}(t)), \boldsymbol{\varphi}\rangle_{\boldsymbol{L}^2(\omega)} + \langle \boldsymbol{\Pi}(\boldsymbol{m}(t)), \boldsymbol{\varphi}\rangle_{\boldsymbol{L}^2(\omega)} + \langle \boldsymbol{R}_1, \boldsymbol{\varphi}\rangle_{\boldsymbol{L}^2(\omega)} \end{aligned} \tag{4.18a}$$

for all $\boldsymbol{\varphi} \in \boldsymbol{\mathcal{K}}(\boldsymbol{m}) \cap \boldsymbol{C}^\infty(\overline{\omega})$*.*

(ii) *Let* $t \in [k, T-k]$*. There exists* $\boldsymbol{R}_2 = \mathcal{O}(k^2 + k\rho(k))$ *such that*

$$\begin{aligned} \boldsymbol{B}_{\boldsymbol{m}}(\boldsymbol{v}(t), \boldsymbol{\varphi}) &= \boldsymbol{L}_{\Delta,\boldsymbol{f}}(\boldsymbol{\varphi}) + \frac{3}{2}\langle \boldsymbol{\pi}(\boldsymbol{m}(t)), \boldsymbol{\varphi}\rangle_{\boldsymbol{L}^2(\omega)} - \frac{1}{2}\langle \boldsymbol{\pi}(\boldsymbol{m}(t-k)), \boldsymbol{\varphi}\rangle_{\boldsymbol{L}^2(\omega)} \\ &\quad + \langle \boldsymbol{\Pi}(\boldsymbol{m}(t)), \boldsymbol{\varphi}\rangle_{\boldsymbol{L}^2(\omega)} + \frac{1}{2}\langle \boldsymbol{D}(\boldsymbol{m}(t), \boldsymbol{m}(t)), \boldsymbol{\varphi}\rangle_{\boldsymbol{L}^2(\omega)} \\ &\quad - \frac{1}{2}\langle \boldsymbol{D}(\boldsymbol{m}(t), \boldsymbol{m}(t-k)), \boldsymbol{\varphi}\rangle_{\boldsymbol{L}^2(\omega)} + \langle \boldsymbol{R}_2, \boldsymbol{\varphi}\rangle_{\boldsymbol{L}^2(\omega)} \end{aligned} \tag{4.18b}$$

for all $\boldsymbol{\varphi} \in \boldsymbol{\mathcal{K}}(\boldsymbol{m}) \cap \boldsymbol{C}^\infty(\overline{\omega})$*.*

The proof of Proposition 4.3.2 requires the following elementary lemma, which is already implicitly stated (without a proof) in [AKST14]. For a proof, we refer to [DPP+17, Lemma 12].

Lemma 4.3.3 (Weight function properties, [DPP+17, Lemma 12])**.** *Let* $\mathcal{W}_{G(k)}(s)$ *be the weight function from* (4.6c)*. Then, the following assertions* (i)–(iii) *hold true:*

(i) *There exists* $k_0 > 0$*, which depends only on* α *and* G*, such that*

$$\mathcal{W}_{G(k)}(s) > \frac{\alpha}{2} \quad \text{for all } s \in \mathbb{R}.$$

(ii) *It holds that*

$$|\alpha - \mathcal{W}_{G(k)}(s)| \le \frac{G(k)k}{2} \quad \text{for all } s \in \mathbb{R}.$$

(iii) *For* $G(k) \ge B > 0$ *and* $k < \alpha/B$*, it holds that*

$$|\alpha + \frac{k}{2}s - \mathcal{W}_{G(k)}(s)| \le \frac{B^2}{2\alpha}k^2 \quad \text{for all } s \in [-B, B]. \qquad \square$$

Proof of Proposition 4.3.2. We follow the arguments of [AKST14, Section 6] for

$$\boldsymbol{\mathcal{H}}(\boldsymbol{m}) := \boldsymbol{h}_{\mathrm{eff}}(\boldsymbol{m}) + \boldsymbol{\Pi}(\boldsymbol{m}). \tag{4.19}$$

The proof is split into the following seven steps.

Step 1. We prove (i). To that end, we make auxiliary definitions and steps: Recall that $\boldsymbol{D}$ from (4.7a) stems from the formal differentiation $\boldsymbol{D}(\boldsymbol{m}, \partial_t \boldsymbol{m}) := \partial_t\big[\boldsymbol{\Pi}(\boldsymbol{m})\big]$. Together with the differentiation of (4.19) with respect to t, this yields that

$$\begin{aligned}
\partial_t\big[\boldsymbol{\mathcal{H}}(\boldsymbol{m})\big] &= \partial_t\big[\boldsymbol{h}_{\mathrm{eff}}(\boldsymbol{m})\big] + \partial_t\big[\boldsymbol{\Pi}(\boldsymbol{m})\big] \\
&\overset{(2.4)}{=} C_{\mathbf{ex}}\, \Delta \partial_t \boldsymbol{m} + \partial_t\big[\boldsymbol{\pi}(\boldsymbol{m})\big] + \partial_t \boldsymbol{f} + \partial_t\big[\boldsymbol{\Pi}(\boldsymbol{m})\big] \\
&\overset{(\mathbf{L1})}{=} C_{\mathbf{ex}}\, \Delta \partial_t \boldsymbol{m} + \boldsymbol{\pi}(\partial_t \boldsymbol{m}) + \partial_t \boldsymbol{f} + \partial_t\big[\boldsymbol{\Pi}(\boldsymbol{m})\big] \\
&= C_{\mathbf{ex}}\, \Delta \partial_t \boldsymbol{m} + \boldsymbol{\pi}(\partial_t \boldsymbol{m}) + \partial_t \boldsymbol{f} + \boldsymbol{D}(\boldsymbol{m}, \partial_t \boldsymbol{m}).
\end{aligned} \tag{4.20}$$

Moreover, the equivalent formulation (4.1) of LLG (2.3a) becomes

$$\alpha\, \partial_t \boldsymbol{m} + \boldsymbol{m} \times \partial_t \boldsymbol{m} \overset{(4.19)}{=} \boldsymbol{\mathcal{H}}(\boldsymbol{m}) - \big(\boldsymbol{\mathcal{H}}(\boldsymbol{m}) \cdot \boldsymbol{m}\big)\boldsymbol{m}. \tag{4.21}$$

We test the latter equation with $\boldsymbol{\varphi} \in \boldsymbol{\mathcal{K}}(\boldsymbol{m}(t)) \cap \boldsymbol{C}^\infty(\overline{\omega})$, and recall that $\boldsymbol{m} \cdot \boldsymbol{\varphi} = 0$. This yields that

$$\alpha\, \langle \partial_t \boldsymbol{m}, \boldsymbol{\varphi} \rangle_{\boldsymbol{L}^2(\omega)} + \langle \boldsymbol{m} \times \partial_t \boldsymbol{m}, \boldsymbol{\varphi} \rangle_{\boldsymbol{L}^2(\omega)} = \langle \boldsymbol{\mathcal{H}}(\boldsymbol{m}), \boldsymbol{\varphi} \rangle_{\boldsymbol{L}^2(\omega)} \tag{4.22}$$

for all $\boldsymbol{\varphi} \in \boldsymbol{\mathcal{K}}(\boldsymbol{m}(t)) \cap \boldsymbol{C}^\infty(\overline{\omega})$.

Step 2. We derive a variational formulation for $\boldsymbol{v}$: To that end, formal differentiation of (4.21) with respect to time yields that

$$\begin{aligned}
\alpha\, \partial_{tt} \boldsymbol{m} + \boldsymbol{m} \times \partial_{tt} \boldsymbol{m} = \partial_t\big[\boldsymbol{\mathcal{H}}(\boldsymbol{m})\big] - \big(\partial_t\big[\boldsymbol{\mathcal{H}}(\boldsymbol{m})\big] \cdot \boldsymbol{m}\big)\boldsymbol{m} \\
- \big(\boldsymbol{\mathcal{H}}(\boldsymbol{m}) \cdot \partial_t \boldsymbol{m}\big)\boldsymbol{m} - \big(\boldsymbol{\mathcal{H}}(\boldsymbol{m}) \cdot \boldsymbol{m}\big)\partial_t \boldsymbol{m}.
\end{aligned} \tag{4.23}$$

For the next steps, recall from (4.15) that

$$\boldsymbol{\psi} = \mathbb{P}_{\boldsymbol{m}(t)} \boldsymbol{\psi} + (\boldsymbol{\psi} \cdot \boldsymbol{m}(t))\, \boldsymbol{m}(t) \quad \text{for all } \boldsymbol{\psi} \in \boldsymbol{C}(\overline{\omega}).$$

In particular, we get that $\mathbb{P}_{\boldsymbol{m}(t)} \boldsymbol{m} = \boldsymbol{0}$. Moreover, $\mathbf{a} \times \mathbf{a} = \mathbf{0}$ and $(\mathbf{a} \times \mathbf{b}) \cdot \mathbf{b} = \mathbf{0}$ for vectors $\mathbf{a}, \mathbf{b} \in \mathbb{R}^3$ yields that

$$\begin{aligned}
\mathbb{P}_{\boldsymbol{m}(t)}\big[\, \boldsymbol{m} \times \partial_{tt} \boldsymbol{m}\, \big] &= \boldsymbol{m} \times \partial_{tt} \boldsymbol{m} - \big[\big(\, \boldsymbol{m} \times \partial_{tt} \boldsymbol{m}\, \big) \cdot \partial_{tt} \boldsymbol{m}\big]\boldsymbol{m} = \boldsymbol{m} \times \partial_{tt} \boldsymbol{m} \\
&= \boldsymbol{m} \times \big[\mathbb{P}_{\boldsymbol{m}(t)} \partial_{tt} \boldsymbol{m}\big] + \boldsymbol{m} \times \big[\big(\, \partial_{tt} \boldsymbol{m} \cdot \boldsymbol{m}\, \big)\boldsymbol{m}\big] = \boldsymbol{m} \times \big[\, \mathbb{P}_{\boldsymbol{m}(t)} \partial_{tt} \boldsymbol{m}\, \big].
\end{aligned}$$

Then, we apply $\mathbb{P}_{\boldsymbol{m}(t)}$ to (4.23) and obtain with the latter equation that

$$\alpha\, \big[\mathbb{P}_{\boldsymbol{m}(t)} \partial_{tt} \boldsymbol{m}\big] + \boldsymbol{m} \times \big[\, \mathbb{P}_{\boldsymbol{m}(t)} \partial_{tt} \boldsymbol{m}\, \big] = \mathbb{P}_{\boldsymbol{m}(t)} \partial_t\big[\boldsymbol{\mathcal{H}}(\boldsymbol{m})\big] - \big(\boldsymbol{\mathcal{H}}(\boldsymbol{m}) \cdot \boldsymbol{m}\big)\big[\mathbb{P}_{\boldsymbol{m}(t)} \partial_t \boldsymbol{m}\big]. \tag{4.24}$$

Finally, we note that for any $\boldsymbol{\psi} \in \boldsymbol{C}(\overline{\omega})$, it holds that

$$\big[\, \mathbb{P}_{\boldsymbol{m}(t)} \boldsymbol{\psi}\, \big] \cdot \boldsymbol{\varphi} \;=\; \boldsymbol{\psi} \cdot \boldsymbol{\varphi} \quad \text{for all } \boldsymbol{\varphi} \in \boldsymbol{\mathcal{K}}(\boldsymbol{m}(t)) \cap \boldsymbol{C}^\infty(\overline{\omega}). \tag{4.25}$$

With these preliminary steps, we test (4.24) with $\boldsymbol{\varphi} \in \boldsymbol{\mathcal{K}}(\boldsymbol{m}(t)) \cap \boldsymbol{C}^\infty(\overline{\omega})$ and obtain that

$$\begin{aligned}
&\alpha \left\langle \mathbb{P}_{\boldsymbol{m}(t)} \partial_{tt} \boldsymbol{m}, \boldsymbol{\varphi} \right\rangle_{\boldsymbol{L}^2(\omega)} + \left\langle \boldsymbol{m} \times \mathbb{P}_{\boldsymbol{m}(t)} \partial_{tt} \boldsymbol{m}, \boldsymbol{\varphi} \right\rangle_{\boldsymbol{L}^2(\omega)} \\
&\overset{(4.24)}{=} \langle \mathbb{P}_{\boldsymbol{m}(t)} \partial_t \big[\boldsymbol{\mathcal{H}}(\boldsymbol{m}) \big], \boldsymbol{\varphi} \rangle_{\boldsymbol{L}^2(\omega)} - \langle \big(\boldsymbol{\mathcal{H}}(\boldsymbol{m}) \cdot \boldsymbol{m} \big) \mathbb{P}_{\boldsymbol{m}(t)} \partial_t \boldsymbol{m}, \boldsymbol{\varphi} \rangle_{\boldsymbol{L}^2(\omega)} \qquad (4.26) \\
&\overset{(4.25)}{=} \langle \partial_t \big[\boldsymbol{\mathcal{H}}(\boldsymbol{m}) \big], \boldsymbol{\varphi} \rangle_{\boldsymbol{L}^2(\omega)} - \langle \big(\boldsymbol{\mathcal{H}}(\boldsymbol{m}) \cdot \boldsymbol{m} \big) \partial_t \boldsymbol{m}, \boldsymbol{\varphi} \rangle_{\boldsymbol{L}^2(\omega)}.
\end{aligned}$$

In a first step towards the variational formulation (4.18a), we add (4.22) and (4.26). With the definition (4.17) of $\boldsymbol{v}$, we obtain for all $\boldsymbol{\varphi} \in \boldsymbol{\mathcal{K}}(\boldsymbol{m}(t)) \cap \boldsymbol{C}^\infty(\overline{\omega})$ that

$$\begin{aligned}
T_1 + T_2 &:= \alpha \left\langle \boldsymbol{v}, \boldsymbol{\varphi} \right\rangle_{\boldsymbol{L}^2(\omega)} + \left\langle \boldsymbol{m} \times \boldsymbol{v}, \boldsymbol{\varphi} \right\rangle_{\boldsymbol{L}^2(\omega)} \\
&= \langle \boldsymbol{\mathcal{H}}(\boldsymbol{m}), \boldsymbol{\varphi} \rangle_{\boldsymbol{L}^2(\omega)} + \frac{k}{2} \langle \partial_t \big[\boldsymbol{\mathcal{H}}(\boldsymbol{m}) \big], \boldsymbol{\varphi} \rangle_{\boldsymbol{L}^2(\omega)} - \frac{k}{2} \langle \big(\boldsymbol{\mathcal{H}}(\boldsymbol{m}) \cdot \boldsymbol{m} \big) \partial_t \boldsymbol{m}, \boldsymbol{\varphi} \rangle_{\boldsymbol{L}^2(\omega)} \\
&= \langle \boldsymbol{\mathcal{H}}(\boldsymbol{m}), \boldsymbol{\varphi} \rangle_{\boldsymbol{L}^2(\omega)} + \frac{k}{2} \langle \partial_t \big[\boldsymbol{\mathcal{H}}(\boldsymbol{m}) \big], \boldsymbol{\varphi} \rangle_{\boldsymbol{L}^2(\omega)} \\
&\qquad - \frac{k}{2} \langle \big(\boldsymbol{\mathcal{H}}(\boldsymbol{m}) \cdot \boldsymbol{m} \big) \boldsymbol{v}, \boldsymbol{\varphi} \rangle_{\boldsymbol{L}^2(\omega)} + \frac{k^2}{4} \langle \big(\boldsymbol{\mathcal{H}}(\boldsymbol{m}) \cdot \boldsymbol{m} \big) \mathbb{P}_{\boldsymbol{m}(t)} \partial_{tt} \boldsymbol{m}, \boldsymbol{\varphi} \rangle_{\boldsymbol{L}^2(\omega)} \\
&=: T_3 + \frac{k}{2} T_4 - \frac{k}{2} T_5 + \frac{k^2}{4} T_6. \qquad (4.27)
\end{aligned}$$

In the remainder of the proof, we generate from the terms $T_1, \ldots, T_6$, the terms from the variational formulation (4.18a).

Step 3. We generate the first term in $\boldsymbol{B}_{\boldsymbol{m}}$ from $T_1 + (k/2)T_5$. With the definition $\lambda(\boldsymbol{m}) = \boldsymbol{\mathcal{H}}(\boldsymbol{m}) \cdot \boldsymbol{m}$ and the assumption (4.16), we apply Lemma 4.3.3(iii). This yields that

$$\alpha + \frac{k}{2} \big(\boldsymbol{\mathcal{H}}(\boldsymbol{m}) \cdot \boldsymbol{m} \big) = \mathcal{W}_{G(k)} \big(\lambda(\boldsymbol{m}) \big) \boldsymbol{v} + \mathcal{O}(k^2).$$

From this, we obtain that

$$T_1 + \frac{k}{2} T_5 \overset{(4.27)}{=} \alpha \left\langle \boldsymbol{v}, \boldsymbol{\varphi} \right\rangle_{\boldsymbol{L}^2(\omega)} + \frac{k}{2} \langle \big(\boldsymbol{\mathcal{H}}(\boldsymbol{m}) \cdot \boldsymbol{m} \big) \boldsymbol{v}, \boldsymbol{\varphi} \rangle_{\boldsymbol{L}^2(\omega)} = \langle \mathcal{W}_{G(k)} \big(\lambda(\boldsymbol{m}) \big) \boldsymbol{v}, \boldsymbol{\varphi} \rangle_{\boldsymbol{L}^2(\omega)} + \mathcal{O}(k^2).$$

Step 4. We transform T_3: Integration by parts yields that

$$\begin{aligned}
T_3 \overset{(4.27)}{=} \langle \boldsymbol{\mathcal{H}}(\boldsymbol{m}), \boldsymbol{\varphi} \rangle_{\boldsymbol{L}^2(\omega)} &\overset{(2.3b)}{=} - C_{\mathbf{ex}} \langle \nabla \boldsymbol{m}, \nabla \boldsymbol{\varphi} \rangle_{\boldsymbol{L}^2(\omega)} + \langle \boldsymbol{\pi}(\boldsymbol{m}), \boldsymbol{\varphi} \rangle_{\boldsymbol{L}^2(\omega)} \\
&\qquad + \langle \boldsymbol{f}(t), \boldsymbol{\varphi} \rangle_{\boldsymbol{L}^2(\omega)} + \langle \boldsymbol{\Pi}(\boldsymbol{m}), \boldsymbol{\varphi} \rangle_{\boldsymbol{L}^2(\omega)}.
\end{aligned}$$

Step 5. We transform T_4: Recalling from (4.17) that $\boldsymbol{v} = \partial_t \boldsymbol{m} + \mathcal{O}(k)$, linearity **(L1)** of $\boldsymbol{\pi}$ and linearity of $\boldsymbol{D}$ in the second argument yield that

$$\begin{aligned}
T_4 &\overset{(4.20)}{=} C_{\mathbf{ex}} \langle \Delta \partial_t \boldsymbol{m}, \boldsymbol{\varphi} \rangle_{\boldsymbol{L}^2(\omega)} + \langle \boldsymbol{\pi}(\partial_t \boldsymbol{m}), \boldsymbol{\varphi} \rangle_{\boldsymbol{L}^2(\omega)} + \langle \partial_t \boldsymbol{f}(t), \boldsymbol{\varphi} \rangle_{\boldsymbol{L}^2(\omega)} + \langle \boldsymbol{D}(\boldsymbol{m}, \partial_t \boldsymbol{m}), \boldsymbol{\varphi} \rangle_{\boldsymbol{L}^2(\omega)} \\
&\overset{(4.17)}{=} C_{\mathbf{ex}} \langle \Delta \boldsymbol{v}, \boldsymbol{\varphi} \rangle_{\boldsymbol{L}^2(\omega)} + \langle \boldsymbol{\pi}(\boldsymbol{v}), \boldsymbol{\varphi} \rangle_{\boldsymbol{L}^2(\omega)} + \langle \partial_t \boldsymbol{f}(t), \boldsymbol{\varphi} \rangle_{\boldsymbol{L}^2(\omega)} + \langle \boldsymbol{D}(\boldsymbol{m}, \boldsymbol{v}), \boldsymbol{\varphi} \rangle_{\boldsymbol{L}^2(\omega)} + \mathcal{O}(k).
\end{aligned}$$

Then, we add $\rho(k)$ in the first term and obtain that

$$\begin{aligned}
T_4 &\overset{(4.17)}{=} C_{\mathbf{ex}} \left(1 + \rho(k) \right) \left\langle \Delta \boldsymbol{v}, \boldsymbol{\varphi} \right\rangle_{\boldsymbol{L}^2(\omega)} + \left\langle \boldsymbol{\pi}(\boldsymbol{v}), \boldsymbol{\varphi} \right\rangle_{\boldsymbol{L}^2(\omega)} \\
&\qquad + \langle \partial_t \boldsymbol{f}(t), \boldsymbol{\varphi} \rangle_{\boldsymbol{L}^2(\omega)} + \langle \boldsymbol{D}(\boldsymbol{m}, \boldsymbol{v}), \boldsymbol{\varphi} \rangle_{\boldsymbol{L}^2(\omega)} + \mathcal{O}(k) + \mathcal{O}(\rho(k)).
\end{aligned}$$

To generate corresponding terms in the variational formulation (4.18a) from the latter equation, we note that

$$\partial_{\boldsymbol{n}}\boldsymbol{v}(t) \overset{(4.17)}{=} \partial_{\boldsymbol{n}}\boldsymbol{m}(t) + \frac{k}{2}\partial_{\boldsymbol{n}}\mathbb{P}_{\boldsymbol{m}(t)}\partial_{tt}\boldsymbol{m}(t) \overset{(2.3b)}{=} \frac{k}{2}\partial_{\boldsymbol{n}}\mathbb{P}_{\boldsymbol{m}(t)}\partial_{tt}\boldsymbol{m}(t) = \mathcal{O}(k). \tag{4.28}$$

With integration by parts, we obtain that

$$\begin{aligned} T_4 &\overset{(4.17)}{=} -C_{\mathbf{ex}}\,(1+\rho(k))\,\langle\nabla\boldsymbol{v},\nabla\boldsymbol{\varphi}\rangle_{\boldsymbol{L}^2(\omega)} + \langle\boldsymbol{\pi}(\boldsymbol{v}),\boldsymbol{\varphi}\rangle_{\boldsymbol{L}^2(\omega)} \\ &\quad + \langle\partial_t\boldsymbol{f}(t),\boldsymbol{\varphi}\rangle_{\boldsymbol{L}^2(\omega)} + \langle\boldsymbol{D}(\boldsymbol{m},\boldsymbol{v}),\boldsymbol{\varphi}\rangle_{\boldsymbol{L}^2(\omega)} + \mathcal{O}(k) + \mathcal{O}(\rho(k)). \end{aligned}$$

Step 6. We combine **Step 1**–**Step 5** to conclude (i): For the $\boldsymbol{f}$-contributions in T_3 and T_4, we recover from

$$\boldsymbol{f}(t) + \frac{k}{2}\partial_t\boldsymbol{f}(t) = \boldsymbol{f}\big(t+\frac{k}{2}\big) + \mathcal{O}(k^2) \quad \text{for } t\in[0,T-k),$$

the corresponding term in the variational formulation (4.18a) via

$$\langle\boldsymbol{f}(t),\boldsymbol{\varphi}\rangle_{\boldsymbol{L}^2(\omega)} + \frac{k}{2}\langle\partial_t\boldsymbol{f}(t),\boldsymbol{\varphi}\rangle_{\boldsymbol{L}^2(\omega)} = \big\langle\boldsymbol{f}\big(t+\frac{k}{2}\big),\boldsymbol{\varphi}\big\rangle_{\boldsymbol{L}^2(\omega)} + \mathcal{O}(k^2).$$

Moreover, for the remaining term T_6 from (4.27), we obtain that

$$T_6 \overset{(4.27)}{=} \frac{k^2}{4}\big\langle\big(\boldsymbol{\mathcal{H}}(\boldsymbol{m})\cdot\boldsymbol{m}\big)\mathbb{P}_{\boldsymbol{m}(t)}\partial_{tt}\boldsymbol{m},\boldsymbol{\varphi}\big\rangle_{\boldsymbol{L}^2(\omega)} = \mathcal{O}(k^2).$$

Overall, we conclude (i) from **Step 3**–**Step 5** and the latter two equations.

Step 7. We prove (ii): To that end, note that for $t\in[k,T-k]$, it holds that

$$k^{-1}\big(\boldsymbol{m}(t)-\boldsymbol{m}(t-k)\big) = \partial_t\boldsymbol{m}(t) + \mathcal{O}(k) \overset{(4.17)}{=} \boldsymbol{v}(t) + \mathcal{O}(k).$$

With the linearity of $\boldsymbol{\pi}$ and of $\boldsymbol{D}$ in the second argument, this yields that

$$\begin{aligned} &\frac{k}{2}\langle\boldsymbol{\pi}(\boldsymbol{v}(t)),\boldsymbol{\varphi}\rangle_{\boldsymbol{L}^2(\omega)} + \frac{k}{2}\langle\boldsymbol{D}(\boldsymbol{m}(t),\boldsymbol{v}(t)),\boldsymbol{\varphi}\rangle_{\boldsymbol{L}^2(\omega)} \\ &= \frac{1}{2}\langle\boldsymbol{\pi}(\boldsymbol{m}(t)),\boldsymbol{\varphi}\rangle_{\boldsymbol{L}^2(\omega)} - \frac{1}{2}\langle\boldsymbol{\pi}(\boldsymbol{m}(t-k)),\boldsymbol{\varphi}\rangle_{\boldsymbol{L}^2(\omega)} \\ &\quad + \frac{1}{2}\langle\boldsymbol{D}(\boldsymbol{m}(t),\boldsymbol{m}(t)),\boldsymbol{\varphi}\rangle_{\boldsymbol{L}^2(\omega)} - \frac{1}{2}\langle\boldsymbol{D}(\boldsymbol{m}(t),\boldsymbol{m}(t-k)),\boldsymbol{\varphi}\rangle_{\boldsymbol{L}^2(\omega)} + \mathcal{O}(k^2). \end{aligned}$$

Replacing the corresponding terms in the left-hand side of (4.18a), we prove (ii). Altogether, this concludes the proof. □

Remark 4.3.4. (i) *Proposition 4.3.2*(i) *and* (ii) *correspond to Algorithm 4.2.1 with the general time-stepping approaches* **(A1)** *and* **(A2)***, respectively.*

(ii) *In* **Step 3** *of the proof of Proposition 4.3.2, the replacement of*

$$\big\langle\,\alpha + \frac{k}{2}\big(\boldsymbol{h}_{\mathrm{eff}}(\boldsymbol{m}) + \boldsymbol{\Pi}(\boldsymbol{m})\big)\cdot\boldsymbol{v}\,\big\rangle_{\boldsymbol{L}^2(\omega)} \quad \textit{with} \quad \langle\mathcal{W}_{G(k)}\big(\lambda(\boldsymbol{m})\big)\boldsymbol{\psi},\boldsymbol{\varphi}\rangle_{\boldsymbol{L}^2(\omega)}$$

illustrates the idea of [AKST14] behind the weight-function $\mathcal{W}_{G(k)}$: On the one hand, the replacement results in a second-order in time error, on the other hand it ensures for sufficiently small $k>0$ ellipticity of the bilinear form $\boldsymbol{B}_{\boldsymbol{m}}(\cdot,\cdot)$; see Lemma 4.3.3(i).

(iii) *In* **Step 5** *of the proof of Proposition 4.3.2, we can choose* $\rho = 0$*. Then, we require the mild CFL-type condition* $k = \mathbf{o}(h)$ *for convergence of Algorithm 4.2.1. However, with* ρ *as in* (4.6b)*, this convergence is unconditional in the sense of Convention 1.3.1. In* (4.6b)*, the generic choice is* $\rho(k) := \log(k)k$*. This results in a formal convergence order* $\mathcal{O}(k^2\log(k)) \leq \mathcal{O}(k^{2-\varepsilon})$ *for all* $\varepsilon > 0$*, i.e., almost second-order in time.*

4.4. Experimental convergence order

In this section, we illustrate the accuracy and computational costs of different variants of Algorithm 4.2.1 with a numerical experiment. To this end, we use our `Python`-based extension of `NGS/Py` [ngs], which was mainly developed by *Carl-Martin Pfeiler*[4]. Note that the numerical experiment of the own work [DPP$^+$17, Section 7.1] already confirms the formal convergence order from Remark 4.2.2 and that these results were also reported in the co-supervised master-thesis [Pfe17, Section 4.4.3]. However, this experiment neglects dissipative effects, i.e., $\mathbf{\Pi}(\boldsymbol{m}) = \mathbf{0}$. In contrast to that, we additionally include the Slonczewski-field [Ber96, Slo96] in the form

$$\mathbf{\Pi}(\boldsymbol{\varphi}) := \mathcal{G}(\boldsymbol{\varphi}\cdot\mathbf{p})\,\boldsymbol{\varphi}\times\mathbf{p}, \quad \text{with} \quad \mathcal{G}(x) := \left[\frac{(1+P)^3(3+x)}{4P^{3/2}} - 4\right]^{-1} \quad \text{for } x\in[-1,1],$$

where $\mathbf{p} = (1,0,0)^T$ and $P = 0.8$. Besides that, we slightly adapt [DPP$^+$17, Section 7.1]: The lower-order $\boldsymbol{m}$-dependent energy terms $\boldsymbol{\pi}(\boldsymbol{m})$ consist always of the stray field, i.e., one evaluation of the corresponding approximation $\boldsymbol{\pi}_h$ employs the Fredkin–Koehler algorithm [FK90] in the variant of Algorithm 3.4.3. We always employ the standard choices $\rho(k) := |\log(k)k|$ and $G(k) := \rho(k)^{-1}$ from Remark 4.2.2(vi) and compare the performance of the different approaches to $\boldsymbol{\pi}_h^{\boldsymbol{D}}$ and $\mathbf{\Pi}_h^{\boldsymbol{D}}$ with the following five variants of Algorithm 4.2.1:

- `TPS2`**:** We employ the implicit second-order approach **(A1)**. For all $i = 0,\dots,M-1$, we perform (inexact) time-steps with Algorithm 4.6.1 below, with the iteration tolerance $\varepsilon = 10^{-10}$ for the underlying fixed-point iteration.
- `TPS2+AB`**:** We employ the explicit second-order Adams–Bashforth-type approach **(A2)**. For the first time-step, we use `TPS2`. For all other time-steps, the right-hand side of the discrete variational formulation (4.9) is independent of $\boldsymbol{v}_h^i$, and we solve the arising linear system in $\boldsymbol{\mathcal{K}}_h(\boldsymbol{m}_h^i)$ with the approach from Section 4.6.2.
- `TPS2+EE`**:** We employ the first-order explicit Euler approach **(A3)**. For all time-steps, the right-hand side of the discrete variational formulation (4.9) is independent of $\boldsymbol{v}_h^i$, and we solve the arising linear system in $\boldsymbol{\mathcal{K}}_h(\boldsymbol{m}_h^i)$ with the approach from Section 4.6.2.
- `TPS1+AB`**:** We combine the classical first-order tangent plane scheme [Alo08, AKT12, BSF$^+$14] with the implicit second-order approach **(A2)**. Essentially, this is `TPS2+AB` with $\mathcal{W}_{G(k)} = \alpha$ and $\rho = 0$.

[4] TU Wien

- **TPS1+EE:** We employ the classical first-order tangent plane scheme [Alo08, AKT12, BSF+14]. Essentially, this is TPS2+EE with $\mathcal{W}_{G(k)} = \alpha$ and $\rho = 0$.

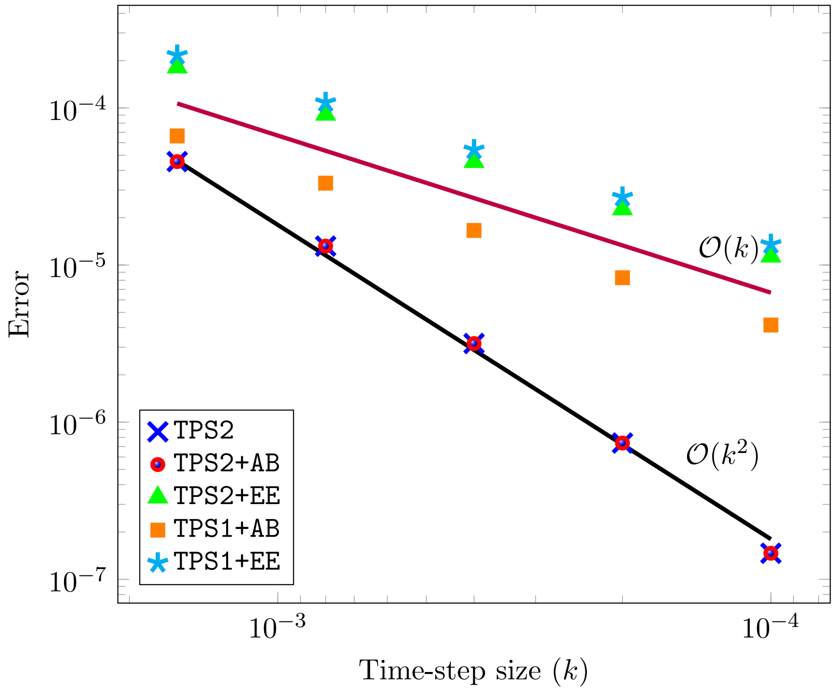

Figure 4.1.: Experiment of Section 4.4: Reference error $\max_i(\|\boldsymbol{m}_{hk_{\rm ref}}(t_i) - \boldsymbol{m}_{hk}(t_i)\|_{\boldsymbol{H}^1(\omega)})$ for $k = 2^\ell\, k_{\rm ref}$ with $\ell \in \{1,2,3,4,5\}$ and $k_{\rm ref} = 5 \cdot 10^{-5}$.

For all these variants, we choose the final time $T = 7$, the domain $\omega = (0,1)^3$, the Gilbert-damping parameter $\alpha = 1$, the exchange constant $C_{\mathbf{ex}} = 1$, the external field $\boldsymbol{f} = (0,1,0)^T$, and the initial value $\boldsymbol{m}^0 = \boldsymbol{m}_h^0 = (1,0,0)^T$.

For space discretization, we employ the triangulation $\mathcal{T}_h$ obtained from the NGS/Py-embedded Netgen [ngs] with the mesh-size $h = 0.125$, which corresponds to 3939 elements and 917 nodes. We note that we checked the corresponding stiffness matrix to verify the angle condition **(T1)**. Having fixed the space discretization, we perform the latter variants with varying time-step size. Since the exact solution is unknown, we employ TPS2+AB to compute a reference solution $\boldsymbol{m}_{hk_{\rm ref}}$, where the reference time $k_{\rm ref} := 5 \cdot 10^{-5}$ is a fine time-step size.

In Figure 4.1, we illustrate the experimental convergence order of our variants. For our setting, the plot confirms the predictions of Remark 4.2.2: For TPS2 and TPS2+AB, we obtain the convergence order

$$\mathcal{O}(k^2\rho(k)) = \mathcal{O}(k^2|\log(k)|) \le \mathcal{O}(k^{2-\varepsilon}) \quad \text{for all } \varepsilon > 0.$$

For TPS2+EE, TPS1+AB and TPS1+EE, we obtain the reduced convergence order $\mathcal{O}(k)$.

In Table 4.1, we illustrate the computational costs of our variants. As expected, TPS2 with its fixed-point iteration is by far the most expensive method. The methods TPS2+AB and

	TPS2 absolute	TPS2 relative	TPS2+AB relative	TPS2+EE relative	TPS1+AB relative	TPS1+EE relative
$k = 0.0016$	1.44	100%	38.15%	33.13%	31.46%	26.63%
$k = 0.0008$	1.48	100%	37.74%	32.96%	31.21%	26.75%
$k = 0.0004$	1.53	100%	37.27%	32.48%	31.12%	26.62%
$k = 0.0002$	1.44	100%	40.23%	35.39%	33.75%	28.95%
$k = 0.0001$	1.33	100%	44.30%	38.86%	37.32%	31.91%

Table 4.1.: Experiment of Section 4.4: Average absolute time (in s) of TPS2 and relative times of all variants.

TPS2+EE are slightly costlier than their counterparts TPS1+AB and TPS1+EE, respectively. This is due to the fact that the mass-term $\langle \mathcal{W}_{G(k)}(\lambda_h^i)\, \boldsymbol{v}_h^i, \boldsymbol{\varphi}_h \rangle_{\boldsymbol{L}^2(\omega)}$ in the discrete variational formulation (4.9) depends on the time-step for TPS2+AB and TPS2+EE. In contrast to TPS1+AB and TPS1+EE where $\mathcal{W}_{G(k)} = \alpha$, we thus have to reassemble the corresponding system matrix at each time-step. Similarly, the Adams–Bashforth-type methods TPS2+AB and TPS1+AB are slightly costlier than their explicit Euler counterparts TPS2+EE and TPS1+EE, respectively. This is due to the fact that for TPS2+AB and TPS1+AB, the Slonczewski-field from (4.13) additionally gives rise to four additional $\boldsymbol{D}_h$-terms in the right-hand side of the discrete variational formulation (4.9), which we have to reassemble at each time-step. In [DPP+17, Table 1], we have $\boldsymbol{\Pi}(\boldsymbol{m}) = \boldsymbol{0}$ and this effect (almost) disappears.

In conclusion, TPS2+AB is the method of choice. It is the only method that benefits (at least from the second time-step on) from the IMEX approach and conserves the (almost) second-order in time convergence. Compared to TPS2+EE and TPS1+EE, the higher computational costs are justified with the (almost) doubled convergence rate. Moreover, the Crank–Nicholson type approach of TPS1+AB is not enough to obtain (almost) second-order in time.

4.5. Main result

In this section, we formulate and prove the main result of this chapter. We extend [AKST14, Theorem 2] to the setting of our implicit-explicit (almost) second-order tangent plane scheme and prove unconditional convergence in the sense of Convention 1.3.1. Note that this result is based on the own work [DPP+17, Theorem 4] and stands in line with corresponding results for the first-order tangent plane scheme; see, e.g., [Alo08, AKT12, BSF+14]. To formulate the main result, we additionally require the following assumptions:

(T1) Angle condition of $\mathcal{T}_h$: For all $h > 0$, the nodal hat functions $\varphi_{\boldsymbol{z}} \in \mathcal{S}_h$, where $\boldsymbol{z} \in \mathcal{N}_h$, satisfy that

$$\int_\omega \nabla \varphi_{\boldsymbol{z}}\, \nabla \varphi_{\boldsymbol{z}'}\, \mathrm{d}\boldsymbol{x} \;\le\; 0 \quad \text{for all nodes } \boldsymbol{z} \neq \boldsymbol{z}'.$$

(T2) Nodewise normalized $\boldsymbol{m}_h^0$: It holds that $\boldsymbol{m}_h^0 \in \boldsymbol{\mathcal{M}}_h$ for all $h > 0$.

(T3) Linearity of $\boldsymbol{D}_h$: For all $h > 0$, the operators $\boldsymbol{D}_h$ are linear in the second argument.

(T4) Uniform boundedness of $\boldsymbol{D}_h$: There exists a constant $C_{\boldsymbol{D}} > 0$ such that, for all $h > 0$, it holds that

$$\langle \boldsymbol{D}_h(\boldsymbol{\varphi}_h, \boldsymbol{\psi}_h), \boldsymbol{\psi}_h \rangle_{\boldsymbol{L}^2(\omega)} \leq C_{\boldsymbol{D}} \, \|\boldsymbol{\psi}_h\|_{\boldsymbol{L}^2(\omega)} \, \|\boldsymbol{\psi}_h\|_{\boldsymbol{H}^1(\omega)} \text{ for all } \boldsymbol{\varphi}_h \in \boldsymbol{\mathcal{M}}_h \text{ and all } \boldsymbol{\psi}_h \in \boldsymbol{\mathcal{S}}_h$$

as well as

$$\|\boldsymbol{D}_h(\boldsymbol{\varphi}_h, \widetilde{\boldsymbol{\varphi}}_h)\|_{\boldsymbol{L}^2(\omega)} \leq C_{\boldsymbol{D}} \left(\|\boldsymbol{\varphi}_h\|_{\boldsymbol{H}^1(\omega)} + \|\widetilde{\boldsymbol{\varphi}}_h\|_{\boldsymbol{H}^1(\omega)} \right) \quad \text{for all } \boldsymbol{\varphi}_h, \widetilde{\boldsymbol{\varphi}}_h \in \boldsymbol{\mathcal{M}}_h.$$

(T5) Weak consistency of $\boldsymbol{D}_h$: For all sequences $(\boldsymbol{\varphi}_{hk})_{h,k>0} \subset L^2(0,T;\boldsymbol{\mathcal{S}}_h)$ which satisfy $\|\boldsymbol{\varphi}_{hk}\|_{\boldsymbol{L}^\infty(\omega_T)} \leq C$ for all $h, k > 0$ and some fixed $C > 0$, and for all sequences $(\boldsymbol{\psi}_{hk})_{h,k>0} \subset L^2(0,T;\boldsymbol{\mathcal{S}}_h)$ with $\boldsymbol{\psi}_{hk} \to \boldsymbol{0}$ in $\boldsymbol{L}^2(\omega_T)$, it holds that

$$\boldsymbol{D}_h(\boldsymbol{\varphi}_{hk}, \boldsymbol{\psi}_{hk}) \rightharpoonup \boldsymbol{0} \quad \text{in } \boldsymbol{L}^2(\omega_T) \quad \text{as } h \to 0.$$

For the additional stronger statement (c) from Theorem 4.5.1 below, we require the following additional assumptions:

(T5$^+$) Strong consistency of $\boldsymbol{D}_h$: For all sequences $(\boldsymbol{\varphi}_{hk})_{h,k>0} \subset L^2(0,T;\boldsymbol{\mathcal{S}}_h)$ which satisfy $\|\boldsymbol{\varphi}_{hk}\|_{\boldsymbol{L}^\infty(\omega_T)} \leq C$ for all $h, k > 0$ and some fixed $C > 0$, and for all sequences $(\boldsymbol{\psi}_{hk})_{h,k>0} \subset \boldsymbol{L}^2(\omega_T)$ with $\boldsymbol{\psi}_{hk} \to \boldsymbol{0}$ in $\boldsymbol{L}^2(\omega_T)$, it holds that

$$\boldsymbol{D}_h(\boldsymbol{\varphi}_{hk}, \boldsymbol{\psi}_{hk}) \to \boldsymbol{0} \quad \text{in } \boldsymbol{L}^2(\omega_T) \quad \text{as } h \to 0.$$

(T6) $\boldsymbol{L}^3$-stability of $\boldsymbol{\pi}$: There exists a constant $C'_{\boldsymbol{\pi}} > 0$ such that

$$\|\boldsymbol{\pi}(\boldsymbol{\varphi})\|_{\boldsymbol{L}^3(\omega)} \leq C'_{\boldsymbol{\pi}} \, \|\boldsymbol{\varphi}\|_{\boldsymbol{L}^3(\omega)} \quad \text{for all } \boldsymbol{\varphi} \in \boldsymbol{L}^2(\omega).$$

(T7) Additional regularity of $\boldsymbol{f}$: It holds that $\boldsymbol{f} \in \boldsymbol{C}^1([0,T];\boldsymbol{L}^2(\omega)) \cap \boldsymbol{C}([0,T];\boldsymbol{L}^3(\omega))$.

With these preparation, we are ready to formulate the main result of this chapter.

Theorem 4.5.1 (Convergence of IMEX TPS2 for LLG, [DPP+17, Theorem 4])**.** *Consider Algorithm 4.2.1 for the discretization of LLG* (2.3)*. Then, the following three assertions* (a)–(c) *hold true:*

(a) *Suppose linearity and uniform boundedness of $\boldsymbol{\pi}_h$ and $\boldsymbol{D}_h$, i.e., there hold* **(D2)**–**(D3)** *and* **(T3)**–**(T4)***. Then, there exists $k_0 > 0$, which depends only on $\boldsymbol{m}^0$, $C_{\mathbf{ex}}$, α, $\boldsymbol{\pi}(\cdot)$, $\boldsymbol{\Pi}(\cdot)$, and $C_{\mathbf{mesh}}$ such that, for all $k < k_0$, the discrete variational problem* (4.9) *is uniquely solvable. Then, in particular, Algorithm 4.2.1 is well-defined.*

(b) *Suppose that*

- *the meshes $\mathcal{T}_h$ satisfy the angle condition* **(T1)***;*
- *the approximations $\boldsymbol{m}_h^0$ satisfy* **(D1)** *and* **(T2)***;*

- *the approximation operators* $\boldsymbol{\pi}_h$ *satisfy* **(D2)**–**(D4)***;*
- *the approximations* $(\boldsymbol{f}_h^i)_{i=0}^M$ *are weakly consistent* **(D5)***;*
- *the approximation operators* $\boldsymbol{\Pi}_h$ *satisfy* **(D6)**–**(D7)***;*
- *the approximation operators* $\boldsymbol{D}_h$ *satisfy* **(T3)**–**(T5)***;*
- *the general time-stepping approaches* $\boldsymbol{\pi}_h^{\boldsymbol{D}}$ *and* $\boldsymbol{\Pi}_h^{\boldsymbol{D}}$ *are defined by one of the three options* **(A1)**–**(A3)***.*

Then, there exists a subsequence of the postprocessed output $\boldsymbol{m}_{hk}$ *from Algorithm 4.2.1, and a weak solution*

$$\boldsymbol{m} \in L^\infty(0,T;\boldsymbol{H}^1(\Omega)) \cap \boldsymbol{H}^1(\omega_T)$$

of LLG (2.3) *in the sense of Definition 2.2.1*(i)–(iii)*, such that*

$$\boldsymbol{m}_{hk} \rightharpoonup \boldsymbol{m} \quad \text{in } \boldsymbol{H}^1(\omega_T) \quad \text{as } h,k \to 0.$$

(c) *Additionally to the assumptions from* (b)*, suppose that*

- *the operator* $\boldsymbol{\pi}$ *is* $\boldsymbol{L}^3$*-stable* **(T6)***;*
- *the applied field* $\boldsymbol{f}$ *satisfies the additional regularity assumption* **(T7)***;*
- *the approximations* $\boldsymbol{m}_h^0$ *are strongly consistent* **(D1$^+$)***;*
- *the approximation operators* $\boldsymbol{\pi}_h$ *are strongly consistent* **(D4$^+$)***;*
- *the approximations* $(\boldsymbol{f}_h^i)_{i=0}^M$ *are strongly consistent* **(D5$^+$)***;*
- *the approximations operators* $\boldsymbol{\Pi}_h$ *are strongly consistent* **(D7$^+$)***;*
- *the approximations operators* $\boldsymbol{D}_h$ *are strongly consistent* **(T5$^+$)***.*

Then, the weak solution $\boldsymbol{m}$ *from* (b) *is a physical weak solution in the sense of Definition 2.2.1*(i)–(iv)*, i.e., it additionally satisfies the stronger energy estimate* (2.17)*.*

Remark 4.5.2. (i) *The angle condition* **(T1)** *means that the off-diagonal entries of the corresponding stiffness matrices are non-positive. In particular,* **(T1)** *is satisfied, if for all* $h > 0$*, the dihedral angles of all elements* $K \in \mathcal{T}_h$ *have an angle less or equal* $\pi/2$*; cf., e.g., [Bar05, Remark 3.3(ii)].*

(ii) *As in [AKST14], Theorem 4.5.1 holds also with* $\rho \equiv \mathbf{0}$*, provided the mild CFL-type condition* $k = \mathbf{o}(h)$*. The proof follows the same lines, except for the proof of the convergence property in Lemma 4.5.4*(viii)*, which is established in Remark 4.5.5 instead.*

(iii) *Theorem 4.5.1*(a) *implies only unique solvability of the discrete variational formulation* (4.9)*. In practice, we employ the fixed-point iteration from Algorithm 4.6.1 for the implicit approaches. To prove the corresponding convergence result in Proposition 4.6.3, we will additionally require the stronger assumption* **(T4$^+$)** *below.*

(iv) *Uniaxial anisotropy and stray field and the corresponding approximations satisfy the assumptions of Theorem 4.5.1*(c) *to* $\boldsymbol{\pi}$ *and* $\boldsymbol{\pi}_h$*, respectively. We refer to Appendix A for the verification.*

(v) *For the Zhang–Li field [ZL04, TNMS05], the corresponding approximation operators* $\boldsymbol{\Pi}_h$ *and* $\boldsymbol{D}_h$ *satisfy all assumptions of Theorem 4.5.1*(b)*, except weak consistency* **(T5)** *of* $\boldsymbol{D}_h$*; see Proposition A.3.1 for the verification. However, the statement remains valid and Remark 4.5.8 bypasses the corresponding gap in the proof. This extends [DPP+17, Section 7.2.2], where the statement was only valid for*

$$\|\nabla \boldsymbol{m}_h^0\|_{\boldsymbol{L}^\infty(\omega)} \lesssim 1 \qquad \textit{and} \qquad \textit{the Adams–Bashforth-type approach } (\mathbf{A2}) \tag{4.29}$$

or the explicit Euler approach **(A3)**. *However, the practical solution of the discrete variational formulation* (4.9) *for the implicit approaches requires a fixed-point iteration; see also* (iii). *Only in the setting of* (4.29)*, we obtain the required convergence of the fixed-point iteration in the first time-step. We refer to Remark 4.6.4 for details.*

(vi) *For the Slonczewski field [Ber96, Slo96], the corresponding approximation operators* $\boldsymbol{\Pi}_h$ *and* $\boldsymbol{D}_h$ *satisfy the assumptions from Theorem 4.5.1*(c) *and even the stronger assumption* **(T4$^+$)** *below; see Proposition A.3.3 for the verification.*

(vii) *In the main source [DPP+17], we made assumptions directly to* $\boldsymbol{\pi}_h^{\boldsymbol{D}}$ *and* $\boldsymbol{\Pi}_h^{\boldsymbol{D}}$*, while here we differentiate between assumptions to* $\boldsymbol{\pi}_h$*,* $\boldsymbol{\Pi}_h$*, and* $\boldsymbol{D}_h$*, respectively.*

We split the proof of Theorem 4.5.1 into the following subsections. In Section 4.5.1, we prove well-posednes (a). For the proof of (b), we follow a standard energy argument (see, e.g., [Eva10]), which consists of the following three steps:

- We derive a discrete energy bound; see Section 4.5.2.
- We extract weakly convergent subsequences and identify the limits; see Section 4.5.3.
- We verify that the limit $\boldsymbol{m}$ is a weak solution of LLG in the sense of Definition 2.2.1(i)–(iii) and thus conclude the proof of (b); see Section 4.5.4.

In Section 4.5.5, we prove (c).

4.5.1. Well-posedness

Proof of Theorem 4.5.1(a). Since for given $\boldsymbol{m}_h^i \in \boldsymbol{\mathcal{M}}_h$ the update from (4.10) is well-defined for any $\boldsymbol{v}_h^i \in \boldsymbol{\mathcal{K}}_h(\boldsymbol{m}_h^i)$ (see Remark 4.2.2(v) for details), we only have to prove that the discrete variational formulation (4.9) is uniquely solvable for sufficiently small $k > 0$. To this end, note that with linearity **(D2)** and **(T2)** of $\boldsymbol{\pi}_h$ and $\boldsymbol{D}_h$, respectively, the right-hand side of the discrete variational formulation (4.9) is affine on $\boldsymbol{v}_h^i$. Hence, for all approaches **(A1)**–**(A3)**, we can reorganize the terms to the classical setting with a bilinear forms on the left-hand side and a linear form on the right-hand side. In particular, for the explicit Euler approach **(A3)**, and the explicit Adams–Bashforth-type approach **(A2)** with $i > 0$, the corresponding bilinear form of the discrete variational formulation (4.9) reads

$$\begin{aligned}\boldsymbol{B}_h^i(\boldsymbol{\psi}_h, \boldsymbol{\varphi}_h) := \langle \mathcal{W}_{G(k)}(\lambda_h^i)\,\boldsymbol{\psi}_h, \boldsymbol{\varphi}_h\rangle_{\boldsymbol{L}^2(\omega)} + \langle \boldsymbol{m}_h^i \times \boldsymbol{\psi}_h, \boldsymbol{\varphi}_h\rangle_{\boldsymbol{L}^2(\omega)} \\ + \frac{C_{\mathbf{ex}}}{2}\, k\,(1+\rho(k))\,\langle \nabla\boldsymbol{\psi}_h, \nabla\boldsymbol{\varphi}_h\rangle_{\boldsymbol{L}^2(\omega)} \quad \text{for all } \boldsymbol{\psi}_h, \boldsymbol{\varphi}_h \in \boldsymbol{\mathcal{K}}_h(\boldsymbol{m}_h^i).\end{aligned} \tag{4.30a}$$

In the implicit case of approach **(A1)** and **(A2)** for $i = 0$, the corresponding bilinear form reads

$$\widetilde{\boldsymbol{B}}_h^i(\boldsymbol{\psi}_h, \boldsymbol{\varphi}_h) := \boldsymbol{B}_h^i(\boldsymbol{\psi}_h, \boldsymbol{\varphi}_h) - \frac{k}{2}\,\langle \boldsymbol{\pi}_h(\boldsymbol{\psi}_h), \boldsymbol{\varphi}_h\rangle_{\boldsymbol{L}^2(\omega)} - \frac{k}{2}\,\langle \boldsymbol{D}_h(\boldsymbol{m}_h^i, \boldsymbol{\psi}_h), \boldsymbol{\varphi}_h\rangle_{\boldsymbol{L}^2(\omega)}. \tag{4.30b}$$

for all $\boldsymbol{\psi}_h, \boldsymbol{\varphi}_h \in \boldsymbol{\mathcal{K}}_h(\boldsymbol{m}_h^i)$. With the Lax–Milgram theorem (see Theorem B.2.4), we thus only have to prove that, for sufficiently small $k > 0$, the corresponding bilinear forms are positive definite on $\boldsymbol{\mathcal{K}}_h(\boldsymbol{m}_h^i)$. This is done in the following two steps.

Step 1. We show that $\boldsymbol{B}_h^i$ from (4.30a) is positive definite: Since $(\mathbf{a} \times \mathbf{b}) \cdot \mathbf{a} = 0$ for $\mathbf{a}, \mathbf{b} \in \mathbb{R}^3$, Lemma 4.3.3(i) yields for sufficiently small $k > 0$ that

$$\begin{aligned}\boldsymbol{B}_h^i(\boldsymbol{\psi}_h, \boldsymbol{\psi}_h) &\overset{(4.30a)}{=} \langle \mathcal{W}_{G(k)}(\lambda_h^i)\,\boldsymbol{\psi}_h, \boldsymbol{\psi}_h\rangle_{\boldsymbol{L}^2(\omega)} + \frac{C_{\mathbf{ex}}}{2}\, k\,(1+\rho(k))\,\langle \nabla\boldsymbol{\psi}_h, \nabla\boldsymbol{\psi}_h\rangle_{\boldsymbol{L}^2(\omega)} \\ &\overset{(4.6)}{\geq} \frac{\alpha}{2}\|\boldsymbol{\psi}_h\|^2_{\boldsymbol{L}^2(\omega)} + \frac{C_{\mathbf{ex}}}{2}\, k\,\|\nabla\boldsymbol{\psi}_h\|^2_{\boldsymbol{L}^2(\omega)} \quad \text{for all } \boldsymbol{\psi}_h \in \boldsymbol{\mathcal{K}}_h(\boldsymbol{m}_h^i).\end{aligned}$$

Step 2. We show that $\widetilde{\boldsymbol{B}}_h^i$ from (4.30b) is positive definite: To this end, the latter equation and uniform boundedness **(D3)** of $\boldsymbol{\pi}_h$ and **(T4)** of $\boldsymbol{D}_h$ yield for sufficiently small $k > 0$ that

$$\begin{aligned}\widetilde{\boldsymbol{B}}_h^i(\boldsymbol{\psi}_h, \boldsymbol{\psi}_h) &\overset{(4.30b)}{\geq} \frac{\alpha}{2}\|\boldsymbol{\psi}_h\|^2_{\boldsymbol{L}^2(\omega)} + \frac{C_{\mathbf{ex}}}{2}\, k\,\|\nabla\boldsymbol{\psi}_h\|^2_{\boldsymbol{L}^2(\omega)} \\ &\quad - (\,C_{\boldsymbol{\pi}} + C_{\boldsymbol{D}}\,)\,\frac{k}{2}\,\|\boldsymbol{\psi}_h\|^2_{\boldsymbol{L}^2(\omega)} - C_{\boldsymbol{D}}\,\frac{k}{2}\,\|\boldsymbol{\psi}_h\|_{\boldsymbol{L}^2(\omega)}\|\nabla\boldsymbol{\psi}_h\|_{\boldsymbol{L}^2(\omega)}.\end{aligned}$$

With the Young inequality, this yields for arbitrary $\delta > 0$ that

$$\begin{aligned}\widetilde{\boldsymbol{B}}_h^i(\boldsymbol{\psi}_h, \boldsymbol{\psi}_h) &\geq \frac{1}{2}\Big(\alpha - \big[\,C_{\boldsymbol{\pi}} + C_{\boldsymbol{D}}\,\big]\,k - \frac{C_{\boldsymbol{D}}}{2\delta}\,k\Big)\,\|\boldsymbol{\psi}_h\|^2_{\boldsymbol{L}^2(\omega)} \\ &\quad + \frac{1}{2}\Big(C_{\mathbf{ex}} - \frac{C_{\boldsymbol{D}}}{2}\delta\Big)\,k\|\nabla\boldsymbol{\psi}_h\|^2_{\boldsymbol{L}^2(\omega)} \quad \text{for all } \boldsymbol{\psi}_h \in \boldsymbol{\mathcal{K}}_h(\boldsymbol{m}_h^i).\end{aligned}$$

With the choice $\delta = C_{\mathbf{ex}}/C_{\boldsymbol{D}}$ and sufficiently small $k > 0$, the factors on the right-hand side of the latter estimate are positive.

Hence, for all approaches **(A1)**–**(A3)** the corresponding bilinear form is positive definite. Altogether, this concludes the proof. □

4.5.2. Discrete energy bound

In this section, we derive a discrete energy bound, which represents the mathematical core of the proof of Theorem 4.5.1(b). Note that the used techniques go back to [Alo08], where a corresponding result was proved for the first-order tangent plane scheme for $\boldsymbol{h}_{\rm eff}(\boldsymbol{m}) := \Delta\boldsymbol{m}$ and $\boldsymbol{\Pi}(\boldsymbol{m}) = \boldsymbol{0}$. For the second-order tangent plane scheme, [AKST14, Section 6] essentially adapts [Alo08, AKT12, BSF+14] but covers only implicit treatment of $\boldsymbol{\pi}(\boldsymbol{m})$ and $\boldsymbol{\Pi}(\boldsymbol{m}) = 0$. Here, we extend [AKST14, Section 6] to the setting of Algorithm 4.2.1. To this end, we elaborate the own work [DPP+17, Lemma 15].

Lemma 4.5.3 (Discrete energy bound, [DPP+17, Lemma 15])**.** *Let the assumptions of Theorem 4.5.1*(b) *be satisfied and let $k > 0$ be sufficiently small. Then, the following assertions* (i)–(ii) *hold true:*

(i) *For all $i = 0, \dots, M-1$, it holds that*

$$\frac{C_{\mathbf{ex}}}{2}\,\mathrm{d_t}\,\|\nabla\boldsymbol{m}_h^{i+1}\|^2_{\boldsymbol{L}^2(\omega)} + \langle\mathcal{W}_{G(k)}(\lambda_h^i)\,\boldsymbol{v}_h^i, \boldsymbol{v}_h^i\rangle_{\boldsymbol{L}^2(\omega)} + \frac{C_{\mathbf{ex}}}{2}k\rho(k)\|\nabla\boldsymbol{v}_h^i\|^2_{\boldsymbol{L}^2(\omega)}$$
$$\leq \langle\boldsymbol{\pi}_h^{\boldsymbol{D}}(\boldsymbol{v}_h^i;\boldsymbol{m}_h^i,\boldsymbol{m}_h^{i-1}),\boldsymbol{v}_h^i\rangle_{\boldsymbol{L}^2(\omega)} + \langle\boldsymbol{f}_h^{i+1/2},\boldsymbol{v}_h^i\rangle_{\boldsymbol{L}^2(\omega)} + \langle\boldsymbol{\Pi}_h^{\boldsymbol{D}}(\boldsymbol{v}_h^i;\boldsymbol{m}_h^i,\boldsymbol{m}_h^{i-1}),\boldsymbol{v}_h^i\rangle_{\boldsymbol{L}^2(\omega)}.$$

(ii) *There exists a constant $C > 0$ which depends only on T, ω, $\boldsymbol{m}^0$, α, $C_{\mathbf{ex}}$, $\boldsymbol{\pi}(\cdot)$, $\boldsymbol{f}$, $\boldsymbol{\Pi}(\cdot)$, and $C_{\mathbf{mesh}}$ such that, for all $j = 0, \dots, M$, it holds that*

$$\|\nabla\boldsymbol{m}_h^j\|^2_{\boldsymbol{L}^2(\omega)} + k\sum_{i=0}^{j-1}\|\boldsymbol{v}_h^i\|^2_{\boldsymbol{L}^2(\omega)} + k^2\rho(k)\sum_{i=0}^{j-1}\|\nabla\boldsymbol{v}_h^i\|^2_{\boldsymbol{L}^2(\omega)} \leq C < \infty.$$

Proof. For the proof of (i), we test the discrete variational formulation (4.9) with $\boldsymbol{v}_h^i \in \boldsymbol{\mathcal{K}}_h(\boldsymbol{m}_h^i)$. Since $(\mathbf{b}\times\mathbf{a})\cdot\mathbf{a} = 0$ for $\mathbf{a},\mathbf{b}\in\mathbb{R}^3$, we get that

$$\begin{aligned}
&\langle\mathcal{W}_{G(k)}(\lambda_h^i)\,\boldsymbol{v}_h^i, \boldsymbol{v}_h^i\rangle_{\boldsymbol{L}^2(\omega)} + \frac{C_{\mathbf{ex}}}{2}\,k\,(1+\rho(k))\,\langle\nabla\boldsymbol{v}_h^i,\nabla\boldsymbol{v}_h^i\rangle_{\boldsymbol{L}^2(\omega)}\\
&= -C_{\mathbf{ex}}\,\langle\nabla\boldsymbol{m}_h^i,\nabla\boldsymbol{v}_h^i\rangle_{\boldsymbol{L}^2(\omega)} + \langle\boldsymbol{\pi}_h^{\boldsymbol{D}}(\boldsymbol{v}_h^i;\boldsymbol{m}_h^i,\boldsymbol{m}_h^{i-1}),\boldsymbol{v}_h^i\rangle_{\boldsymbol{L}^2(\omega)} + \langle\boldsymbol{f}_h^{i+1/2},\boldsymbol{v}_h^i\rangle_{\boldsymbol{L}^2(\omega)}\\
&\quad + \langle\boldsymbol{\Pi}_h^{\boldsymbol{D}}(\boldsymbol{v}_h^i;\boldsymbol{m}_h^i,\boldsymbol{m}_h^{i-1}),\boldsymbol{v}_h^i\rangle_{\boldsymbol{L}^2(\omega)}\,.
\end{aligned} \tag{4.31}$$

In the following, we generate as in [Alo08] from the first term on the right-hand side of (4.31) the missing terms on the left-hand side of (i). To this end, let $\boldsymbol{\mathcal{I}}_h$ be the nodal interpolant corresponding to $\boldsymbol{\mathcal{S}}_h$. Moreover, note that, since $\boldsymbol{v}_h^i \in \boldsymbol{\mathcal{K}}_h(\boldsymbol{m}_h^i)$, we get that $\boldsymbol{m}_h^i(\boldsymbol{z})\cdot\boldsymbol{v}_h^i(\boldsymbol{z}) = 0$ for all nodes $\boldsymbol{z}\in\mathcal{N}_h$. Recalling that $\boldsymbol{m}_h^i \in \boldsymbol{\mathcal{M}}_h$, we get that

$$\big|\,\boldsymbol{m}_h^i(\boldsymbol{z}) + k\boldsymbol{v}_h^i(\boldsymbol{z})\,\big|^2 = |\boldsymbol{m}_h^i(\boldsymbol{z})|^2 + k^2|\boldsymbol{v}_h^i(\boldsymbol{z})|^2 = 1 + k^2|\boldsymbol{v}_h^i(\boldsymbol{z})|^2 \geq 1,$$

for all nodes $\boldsymbol{z}\in\mathcal{N}_h$. Since $\mathcal{T}_h$ satisfies the angle condition **(T1)**, Lemma B.1.1 then yields for $\boldsymbol{\varphi}_h = \boldsymbol{m}_h^i + k\boldsymbol{v}_h^i \in \boldsymbol{\mathcal{S}}_h$ that

$$\begin{aligned}
\|\nabla\boldsymbol{m}_h^{i+1}\|^2_{\boldsymbol{L}^2(\omega)} &\overset{(4.10)}{=} \Big\|\,\nabla\boldsymbol{\mathcal{I}}_h\Big(\frac{\boldsymbol{m}_h^i + k\boldsymbol{v}_h^i}{|\boldsymbol{m}_h^i + k\boldsymbol{v}_h^i|}\Big)\,\Big\|^2_{\boldsymbol{L}^2(\omega)} \leq \|\nabla(\boldsymbol{m}_h^i + k\boldsymbol{v}_h^i)\|^2_{\boldsymbol{L}^2(\omega)}\\
&= \|\nabla\boldsymbol{m}_h^i\|^2_{\boldsymbol{L}^2(\omega)} + 2k\,\langle\nabla\boldsymbol{m}_h^i,\nabla\boldsymbol{v}_h^i\rangle_{\boldsymbol{L}^2(\omega)} + k^2\,\|\nabla\boldsymbol{v}_h^i\|^2_{\boldsymbol{L}^2(\omega)}.
\end{aligned}$$

Reorganizing the terms in the latter estimate, we infer that

$$\frac{C_{\mathbf{ex}}}{2}\,\mathrm{d_t}\,\|\boldsymbol{m}_h^{i+1}\|^2_{\boldsymbol{L}^2(\omega)} - \frac{C_{\mathbf{ex}}}{2}k\|\nabla\boldsymbol{v}_h^i\|^2_{\boldsymbol{L}^2(\omega)} \leq C_{\mathbf{ex}}\,\langle\nabla\boldsymbol{m}_h^i,\nabla\boldsymbol{v}_h^i\rangle_{\boldsymbol{L}^2(\omega)}. \tag{4.32}$$

Then, the combination of (4.31) and (4.32) proves (i). Next, we show (ii) and split the proof into the following six steps.

Step 1. We derive a preliminary estimate: To that end, note that Lemma 4.3.3(i), yields for sufficiently small $k > 0$, that

$$\frac{\alpha}{2}\,\|\boldsymbol{v}_h^i\|^2_{\boldsymbol{L}^2(\omega)} \;\leq\; \langle\mathcal{W}_{G(k)}(\lambda_h^i)\,\boldsymbol{v}_h^i,\boldsymbol{v}_h^i\rangle_{\boldsymbol{L}^2(\omega)}. \tag{4.33}$$

Then, we sum (i) over $i = 0,\dots,j-1$ and exploit the telescopic sum property. This way, we obtain that

$$\begin{aligned}
\chi^{(j)} \quad &:= \quad \frac{C_{\mathbf{ex}}}{2}\,\|\nabla\boldsymbol{m}_h^j\|^2_{\boldsymbol{L}^2(\omega)} + \frac{\alpha}{2}\,k\sum_{i=0}^{j-1}\|\boldsymbol{v}_h^i\|^2_{\boldsymbol{L}^2(\omega)} + \frac{C_{\mathbf{ex}}}{2}\,\rho(k)\,k^2\sum_{i=0}^{j-1}\|\nabla\boldsymbol{v}_h^i\|^2_{\boldsymbol{L}^2(\omega)}\\
&\overset{(4.33)}{\leq} \quad \frac{C_{\mathbf{ex}}}{2}\,\|\nabla\boldsymbol{m}_h^j\|^2_{\boldsymbol{L}^2(\omega)} + \langle\mathcal{W}_{G(k)}(\lambda_h^i)\,\boldsymbol{v}_h^i,\boldsymbol{v}_h^i\rangle_{\boldsymbol{L}^2(\omega)} + \frac{C_{\mathbf{ex}}}{2}\,\rho(k)\,k^2\sum_{i=0}^{j-1}\|\nabla\boldsymbol{v}_h^i\|^2_{\boldsymbol{L}^2(\omega)}\\
&\overset{\text{(i)}}{\leq} \quad \frac{C_{\mathbf{ex}}}{2}\,\|\nabla\boldsymbol{m}_h^0\|^2_{\boldsymbol{L}^2(\omega)} + k\sum_{i=0}^{j-1}\langle\boldsymbol{\pi}_h^{\boldsymbol{D}}(\boldsymbol{v}_h^i;\boldsymbol{m}_h^i,\boldsymbol{m}_h^{i-1}),\boldsymbol{v}_h^i\rangle_{\boldsymbol{L}^2(\omega)} + k\sum_{i=0}^{j-1}\langle\boldsymbol{f}_h^{i+1/2},\boldsymbol{v}_h^i\rangle_{\boldsymbol{L}^2(\omega)}\\
&\qquad + k\sum_{i=0}^{j-1}\langle\boldsymbol{\Pi}_h^{\boldsymbol{D}}(\boldsymbol{v}_h^i;\boldsymbol{m}_h^i,\boldsymbol{m}_h^{i-1}),\boldsymbol{v}_h^i\rangle_{\boldsymbol{L}^2(\omega)} =: S_1 + S_2 + S_3 + S_4.
\end{aligned} \tag{4.34}$$

In the following, we estimate $S_1,\dots,S_4$. Then, our goal is to absorb as many terms as possible to $\chi^{(j)}$ and to apply the discrete Gronwall lemma afterwards.

Step 2. We estimate S_1: We get that

$$S_1 \overset{(4.34)}{=} \frac{C_{\mathbf{ex}}}{2}\,\|\nabla\boldsymbol{m}_h^0\|^2_{\boldsymbol{L}^2(\omega)} \overset{\textbf{(D1)}}{\lesssim} 1.$$

Step 3. We estimate S_2: For all approaches **(A1)**–**(A3)**, we get that

$$\begin{aligned}
&\langle\boldsymbol{\pi}_h^{\boldsymbol{D}}(\boldsymbol{v}_h^i;\boldsymbol{m}_h^i,\boldsymbol{m}_h^{i-1}),\boldsymbol{v}_h^i\rangle_{\boldsymbol{L}^2(\omega)}\\
&\quad\lesssim\; k\,\|\boldsymbol{\pi}_h(\boldsymbol{v}_h^i)\|_{\boldsymbol{L}^2(\omega)}\|\boldsymbol{v}_h^i\|_{\boldsymbol{L}^2(\omega)} + \|\boldsymbol{\pi}_h(\boldsymbol{m}_h^i)\|_{\boldsymbol{L}^2(\omega)}\|\boldsymbol{v}_h^i\|_{\boldsymbol{L}^2(\omega)} + \|\boldsymbol{\pi}_h(\boldsymbol{m}_h^{i-1})\|_{\boldsymbol{L}^2(\omega)}\|\boldsymbol{v}_h^i\|_{\boldsymbol{L}^2(\omega)}\\
&\quad\overset{\textbf{(D3)}}{\lesssim}\; k\,\|\boldsymbol{v}_h^i\|^2_{\boldsymbol{L}^2(\omega)} + \|\boldsymbol{m}_h^i\|_{\boldsymbol{L}^2(\omega)}\|\boldsymbol{v}_h^i\|_{\boldsymbol{L}^2(\omega)} + \|\boldsymbol{m}_h^{i-1}\|_{\boldsymbol{L}^2(\omega)}\|\boldsymbol{v}_h^i\|_{\boldsymbol{L}^2(\omega)}.
\end{aligned}$$

Recall that $\boldsymbol{m}_h^i,\boldsymbol{m}_h^{i-1} \in \boldsymbol{\mathcal{M}}_h$. With the Young inequality, we conclude from the latter estimate for arbitrary $\delta > 0$ that

$$\begin{aligned} S_2 &\overset{(4.34)}{=} k \sum_{i=0}^{j-1} \langle \boldsymbol{\pi}_h^{\boldsymbol{D}}(\boldsymbol{v}_h^i; \boldsymbol{m}_h^i, \boldsymbol{m}_h^{i-1}), \boldsymbol{v}_h^i \rangle_{\boldsymbol{L}^2(\omega)} \\ &\lesssim k^2 \sum_{i=0}^{j-1} \|\boldsymbol{v}_h^i\|_{\boldsymbol{L}^2(\omega)}^2 + \frac{k}{\delta} \sum_{i=0}^{j-1} \|\boldsymbol{m}_h^i\|_{\boldsymbol{L}^2(\omega)}^2 + \delta k \sum_{i=0}^{j-1} \|\boldsymbol{v}_h^i\|_{\boldsymbol{L}^2(\omega)}^2 \\ &\lesssim \frac{1}{\delta} + (k+\delta)\, k \sum_{i=0}^{j-1} \|\boldsymbol{v}_h^i\|_{\boldsymbol{L}^2(\omega)}^2. \end{aligned}$$

Step 4. We estimate S_3: The Young inequality yields for arbitrary $\delta > 0$ that

$$\begin{aligned} S_3 \overset{(4.34)}{=} k \sum_{i=0}^{j-1} \langle \boldsymbol{f}_h^{i+1/2}, \boldsymbol{v}_h^i \rangle_{\boldsymbol{L}^2(\omega)} &\lesssim \frac{k}{\delta} \sum_{i=0}^{j-1} \|\boldsymbol{f}_h^{i+1/2}\|_{\boldsymbol{L}^2(\omega)}^2 + \delta k \sum_{i=0}^{j-1} \|\boldsymbol{v}_h^i\|_{\boldsymbol{L}^2(\omega)}^2 \\ &\overset{\textbf{(D5)}}{\lesssim} \frac{1}{\delta} + \delta k \sum_{i=0}^{j-1} \|\boldsymbol{v}_h^i\|_{\boldsymbol{L}^2(\omega)}^2. \end{aligned}$$

Step 5. We estimate S_4: To that end, recall that $\boldsymbol{m}_h^i, \boldsymbol{m}_h^{i-1} \in \boldsymbol{\mathcal{M}}_h$. We deal with the different approaches **(A1)**–**(A3)** one after the other. For the implicit approach **(A1)** and the explicit Adams–Bashforth-type approach **(A2)** with $i = 0$, we obtain that

$$\begin{aligned} \langle \boldsymbol{\Pi}_h^{\boldsymbol{D}}(\boldsymbol{v}_h^i; \boldsymbol{m}_h^i, \boldsymbol{m}_h^{i-1}), \boldsymbol{v}_h^i \rangle_{\boldsymbol{L}^2(\omega)} &= \langle \boldsymbol{\Pi}_h(\boldsymbol{m}_h^i), \boldsymbol{v}_h^i \rangle_{\boldsymbol{L}^2(\omega)} + k \, \langle \boldsymbol{D}_h(\boldsymbol{m}_h^i, \boldsymbol{v}_h^i), \boldsymbol{v}_h^i \rangle_{\boldsymbol{L}^2(\omega)} \\ &\overset{\text{(T4)}}{\lesssim} \|\boldsymbol{\Pi}_h(\boldsymbol{m}_h^i)\|_{\boldsymbol{L}^2(\omega)} \|\boldsymbol{v}_h^i\|_{\boldsymbol{L}^2(\omega)} + k \, \|\boldsymbol{v}_h^i\|_{\boldsymbol{L}^2(\omega)} \|\boldsymbol{v}_h^i\|_{\boldsymbol{H}^1(\omega)} \\ &=: T_1 + T_2. \end{aligned}$$

For T_1, the Young inequality yields for arbitrary $\delta > 0$ that

$$\begin{aligned} T_1 &\overset{\textbf{(D6)}}{\lesssim} \|\boldsymbol{m}_h^i\|_{\boldsymbol{H}^1(\omega)} \|\boldsymbol{v}_h^i\|_{\boldsymbol{L}^2(\omega)} \lesssim \frac{1}{\delta} \|\boldsymbol{m}_h^i\|_{\boldsymbol{H}^1(\omega)}^2 + \delta \, \|\boldsymbol{v}_h^i\|_{\boldsymbol{L}^2(\omega)}^2 \\ &\lesssim \frac{1}{\delta} + \frac{1}{\delta} \|\nabla \boldsymbol{m}_h^i\|_{\boldsymbol{L}^2(\omega)}^2 + \delta \, \|\boldsymbol{v}_h^i\|_{\boldsymbol{L}^2(\omega)}^2. \end{aligned}$$

For T_2, we insert $\rho(k)$ in order to match with the third term in the definition (4.34) of $\chi^{(j)}$. With the Young inequality, we get for arbitrary $\delta > 0$ that

$$T_2 \lesssim \delta k \rho(k) \, \|\nabla \boldsymbol{v}_h^i\|_{\boldsymbol{L}^2(\omega)}^2 + \big(k + \frac{k}{\delta \rho(k)} \big) \, \|\boldsymbol{v}_h^i\|_{\boldsymbol{L}^2(\omega)}^2.$$

For the explicit Adams–Bashforth-type approach **(A2)** with $i > 0$, we obtain with similar steps as for T_1 for arbitrary $\delta > 0$ that

$$\begin{aligned}
&\langle \boldsymbol{\Pi}_h^{\boldsymbol{D}}(\boldsymbol{v}_h^i; \boldsymbol{m}_h^i, \boldsymbol{m}_h^{i-1}), \boldsymbol{v}_h^i \rangle_{\boldsymbol{L}^2(\omega)} \\
&\quad = \langle \boldsymbol{\Pi}_h(\boldsymbol{m}_h^i), \boldsymbol{v}_h^i \rangle_{\boldsymbol{L}^2(\omega)} + \frac{1}{2} \langle \boldsymbol{D}_h(\boldsymbol{m}_h^i, \boldsymbol{m}_h^i), \boldsymbol{v}_h^i \rangle_{\boldsymbol{L}^2(\omega)} - \frac{1}{2} \langle \boldsymbol{D}_h(\boldsymbol{m}_h^i, \boldsymbol{m}_h^{i-1}), \boldsymbol{v}_h^i \rangle_{\boldsymbol{L}^2(\omega)} \\
&\quad \overset{(\mathrm{T}\mathbf{4})}{\lesssim} \|\boldsymbol{\Pi}_h(\boldsymbol{m}_h^i)\|_{\boldsymbol{L}^2(\omega)} \|\boldsymbol{v}_h^i\|_{\boldsymbol{L}^2(\omega)} + \|\boldsymbol{v}_h^i\|_{\boldsymbol{L}^2(\omega)} \Big(\|\boldsymbol{m}_h^i\|_{\boldsymbol{H}^1(\omega)} + \|\boldsymbol{m}_h^{i-1}\|_{\boldsymbol{H}^1(\omega)} \Big) \\
&\quad \overset{(\mathbf{D6})}{\lesssim} \frac{1}{\delta} + \frac{1}{\delta} \|\nabla \boldsymbol{m}_h^i\|^2_{\boldsymbol{L}^2(\omega)} + \frac{1}{\delta} \|\nabla \boldsymbol{m}_h^{i-1}\|^2_{\boldsymbol{L}^2(\omega)} + \delta \|\boldsymbol{v}_h^i\|^2_{\boldsymbol{L}^2(\omega)}.
\end{aligned}$$

For the explicit Euler approach **(A3)**, we omit in the latter arguments the $\boldsymbol{D}_h$ contribution and obtain that

$$\langle \boldsymbol{\Pi}_h^{\boldsymbol{D}}(\boldsymbol{v}_h^i; \boldsymbol{m}_h^i, \boldsymbol{m}_h^{i-1}), \boldsymbol{v}_h^i \rangle_{\boldsymbol{L}^2(\omega)} \lesssim \frac{1}{\delta} + \frac{1}{\delta} \|\nabla \boldsymbol{m}_h^i\|^2_{\boldsymbol{L}^2(\omega)} + \delta \|\boldsymbol{v}_h^i\|^2_{\boldsymbol{L}^2(\omega)}.$$

Altogether, we infer for all approaches **(A1)**–**(A3)** that

$$\begin{aligned}
S_4 &\overset{(4.34)}{=} k \sum_{i=0}^{j-1} \langle \boldsymbol{\Pi}_h^{\boldsymbol{D}}(\boldsymbol{v}_h^i; \boldsymbol{m}_h^i, \boldsymbol{m}_h^{i-1}), \boldsymbol{v}_h^i \rangle_{\boldsymbol{L}^2(\omega)} \\
&\lesssim \frac{1}{\delta} + \frac{k}{\delta} \sum_{i=0}^{j-1} \|\nabla \boldsymbol{m}_h^i\|^2_{\boldsymbol{L}^2(\omega)} + \Big(k + \delta + \frac{k}{\delta \rho(k)} \Big) k \sum_{i=0}^{j-1} \|\boldsymbol{v}_h^i\|^2_{\boldsymbol{L}^2(\omega)} + \delta k^2 \rho(k) \sum_{i=0}^{j-1} \|\nabla \boldsymbol{v}_h^i\|^2_{\boldsymbol{L}^2(\omega)}.
\end{aligned}$$

Step 6. We combine **Step 1**–**Step 5**: We arrive for arbitrary $\delta > 0$ at

$$\begin{aligned}
\chi^{(j)} &\lesssim 1 + \frac{1}{\delta} + \frac{k}{\delta} \sum_{i=0}^{j-1} \|\nabla \boldsymbol{m}_h^i\|^2_{\boldsymbol{L}^2(\omega)} \\
&\qquad + \Big(k + \delta + \frac{k}{\delta \rho(k)} \Big) k \sum_{i=0}^{j-1} \|\boldsymbol{v}_h^i\|^2_{\boldsymbol{L}^2(\omega)} + \delta k^2 \rho(k) \sum_{i=0}^{j-1} \|\nabla \boldsymbol{v}_h^i\|^2_{\boldsymbol{L}^2(\omega)}.
\end{aligned} \tag{4.35}$$

First, we choose a $\delta > 0$ small enough such that we can absorb the terms

$$\delta k \sum_{i=0}^{j-1} \|\boldsymbol{v}_h^i\|^2_{\boldsymbol{L}^2(\omega)} \quad \text{and} \quad \delta k^2 \rho(k) \sum_{i=0}^{j-1} \|\nabla \boldsymbol{v}_h^i\|^2_{\boldsymbol{L}^2(\omega)}$$

into $\chi^{(j)}$. Next, recall from (4.6b) that $k\rho(k)^{-1} \to 0$ as $k \to 0$. In particular, for sufficiently small $k > 0$, we can absorb the terms

$$k^2 \sum_{i=0}^{j-1} \|\boldsymbol{v}_h^i\|^2_{\boldsymbol{L}^2(\omega)} \quad \text{and} \quad \frac{k^2}{\delta \rho(k)} \sum_{i=0}^{j-1} \|\boldsymbol{v}_h^i\|^2_{\boldsymbol{L}^2(\omega)}$$

into $\chi^{(j)}$. With the definition of $\chi^{(j)}$ from (4.34), we then get for all $j = 1, \dots, M$ that

$$\chi^{(j)} \lesssim 1 + k \sum_{i=0}^{j-1} \|\nabla \boldsymbol{m}_h^i\|^2_{\boldsymbol{L}^2(\omega)} \lesssim 1 + k \sum_{i=0}^{j-1} \chi^{(i)}. \tag{4.36a}$$

Moreover, it holds that

$$\chi^{(0)} \overset{(4.34)}{=} \|\nabla \boldsymbol{m}_h^0\|_{\boldsymbol{L}^2(\omega)} \overset{(\mathbf{D1})}{\lesssim} 1. \tag{4.36b}$$

Note that (4.36) fits in the setting of the discrete Gronwall lemma (see Lemma B.3.1). This yields that

$$\chi^{(j)} \lesssim \exp\Big(\sum_{i=0}^{j-1} k\Big) \lesssim \exp(T) < \infty, \quad \text{for all } j = 1, \dots, M.$$

Altogether, this shows (ii) and concludes the proof. □

4.5.3. Extraction of weakly convergent subsequences

In this section, we exploit the discrete energy bound from Lemma 4.5.3 and extract weakly convergent subsequences of the postprocessed output of Algorithm 4.2.1. The specific adaptation of these standard techniques to the tangent plane scheme goes back to [Alo08, AKT12, BSF$^+$14] for the classical first-order variant and was extended to the second-order variant in [AKST14]. Here, we elaborate the corresponding [DPP$^+$17, Lemma 16].

Lemma 4.5.4 (Convergence properties, [DPP$^+$17, Lemma 16])**.** *Let the assumptions of Theorem 4.5.1*(b) *be satisfied. Then, there exists subsequences of the postprocessed output*

$$\boldsymbol{m}_{hk}^\star \in \{\boldsymbol{m}_{hk}^+, \boldsymbol{m}_{hk}^-, \boldsymbol{m}_{hk}^=, \boldsymbol{m}_{hk}\} \quad \textit{and} \quad \boldsymbol{v}_{hk}^-,$$

of Algorithm 4.2.1 and a function

$$\boldsymbol{m} \in L^\infty(0,T;\boldsymbol{H}^1(\omega)) \cap \boldsymbol{H}^1(\omega_T)$$

such that the following convergence properties hold true simultaneously for the same subsequence as $h, k \to 0$:

(i) $\boldsymbol{m}_{hk} \rightharpoonup \boldsymbol{m}$ *in* $\boldsymbol{H}^1(\omega_T)$.

(ii) $\boldsymbol{m}_{hk}^\star \overset{*}{\rightharpoonup} \boldsymbol{m}$ *in* $L^\infty(0,T;\boldsymbol{H}^1(\omega))$.

(iii) $\boldsymbol{m}_{hk}^\star \rightharpoonup \boldsymbol{m}$ *in* $L^2(0,T;\boldsymbol{H}^1(\omega))$.

(iv) $\boldsymbol{m}_{hk}^\star \to \boldsymbol{m}$ *in* $\boldsymbol{L}^2(\omega_T)$.

(v) $\boldsymbol{m}_{hk}^\star(t) \to \boldsymbol{m}(t)$ *in* $\boldsymbol{L}^2(\omega)$ *a.e. for* $t \in [0,T)$.

(vi) $\boldsymbol{m}_{hk}^\star \to \boldsymbol{m}$ *pointwise a.e. in* ω_T.

(vii) $\boldsymbol{v}_{hk} \rightharpoonup \partial_t \boldsymbol{m}$ *in* $\boldsymbol{L}^2(\omega_T)$.

(viii) $k\nabla \boldsymbol{v}_{hk} \to \boldsymbol{0}$ *in* $\boldsymbol{L}^2(\omega_T)$.

Proof. For the proof of (i)–(vi), we follow [Alo08, BSF+14]: We infer from Lemma B.1.4(ii) that

$$\| \mathrm{d_t} \boldsymbol{m}_h^{i+1} \|_{\boldsymbol{L}^2(\omega)} \lesssim \| \boldsymbol{v}_h^i \|_{\boldsymbol{L}^2(\omega)} \quad \text{for all } i = 0, 1, \dots, M-1.$$

With Lemma 4.5.3(ii), the definition (3.3) of the postprocessed output yields that

$$\| \partial_t \boldsymbol{m}_{hk} \|_{\boldsymbol{L}^2(\omega)} \lesssim \| \boldsymbol{v}_{hk}^- \|_{\boldsymbol{L}^2(\omega)} \lesssim 1. \tag{4.37}$$

Moreover, since $\boldsymbol{m}_h^i \in \boldsymbol{\mathcal{M}}_h$ for all $i = 0, \dots, M$, it holds that $\| \boldsymbol{m}_{hk}^\star \|_{\boldsymbol{L}^\infty(\omega_T)} = 1$. With Lemma 4.5.3(ii), we altogether get that

$$\| \boldsymbol{m}_{hk} \|_{\boldsymbol{H}^1(\omega_T)} + \| \boldsymbol{m}_{hk}^\star \|_{L^\infty(0,T;\boldsymbol{H}^1(\omega))} \lesssim 1. \tag{4.38}$$

With the Eberlein–Šmulian theorem (see Theorem B.2.2), we can successively extract weakly convergent subsequences of $\boldsymbol{m}_{hk}^\star$ with corresponding limits

$$\boldsymbol{m}^\star \in \{ \boldsymbol{m}^+, \boldsymbol{m}^-, \boldsymbol{m}^=, \boldsymbol{m} \} \quad \text{where } \boldsymbol{m}^\star \in L^2(0,T;\boldsymbol{H}^1(\omega)) \quad \text{and} \quad \boldsymbol{m} \in \boldsymbol{H}^1(\omega_T) \tag{4.39}$$

such that there hold the convergence properties

$$\boldsymbol{m}_{hk} \rightharpoonup \boldsymbol{m} \quad \text{in } \boldsymbol{H}^1(\omega_T), \quad \text{and} \quad \boldsymbol{m}_{hk}^\star \rightharpoonup \boldsymbol{m}^\star \quad \text{in } L^2(0,T;\boldsymbol{H}^1(\omega)) \quad \text{as } h, k \to 0.$$

With the Rellich–Kondrachov theorem (see Theorem 2.1.2), this proves (i) and (iv) for $\boldsymbol{m}_{hk}$. Moreover, it is a direct consequence of the definitions of the postprocessed output and the discrete time-derivative, that

$$\| \boldsymbol{m}_{hk}^\star - \boldsymbol{m}_{hk} \|_{\boldsymbol{L}^2(\omega_T)} \lesssim k \, \| \partial_t \boldsymbol{m}_{hk} \|_{\boldsymbol{L}^2(\omega)} \overset{(4.37)}{\lesssim} k \to 0 \quad \text{as } h, k \to 0,$$

and altogether, we obtain that

$$\| \boldsymbol{m} - \boldsymbol{m}_{hk}^* \|_{\boldsymbol{L}^2(\omega_T)} \lesssim \| \boldsymbol{m} - \boldsymbol{m}_{hk} \|_{\boldsymbol{L}^2(\omega_T)} + \| \boldsymbol{m}_{hk} - \boldsymbol{m}_{hk}^* \|_{\boldsymbol{L}^2(\omega_T)} \to 0 \quad \text{as } h, k \to 0.$$

Hence, we can identify all limits from (4.39) and conclude (i) as well as (iii)–(iv). Next, we show (ii). Upon further extraction of subsequences, the Alaoglu theorem (see Theorem B.2.3) yields subsequences of $\boldsymbol{m}_{hk}^\star$, which are weak* convergent in $L^\infty(0,T;\boldsymbol{H}^1(\omega))$. Since weak* convergence in $L^\infty(0,T;\boldsymbol{H}^1(\omega))$ implies weak convergence in $\boldsymbol{L}^2(\omega_T)$, this yields the common limit $\boldsymbol{m}$ and we conclude (ii). Moreover, further successive extraction of subsequences proves (v)–(vi). For the proof of (vii), we follow [BSF+14, Lemma 3.8]: Boundedness of $\| \boldsymbol{v}_{hk}^- \|_{\boldsymbol{L}^2(\omega)}$ from (4.37) and the Eberlein–Šmulian theorem (see Theorem B.2.2) yield upon extraction of another subsequence a function $\boldsymbol{v} \in \boldsymbol{L}^2(\omega_T)$ such that

$$\boldsymbol{v}_{hk}^- \rightharpoonup \boldsymbol{v} \quad \text{in } \boldsymbol{L}^2(\omega_T) \quad \text{as } h, k \to 0.$$

In order to get $\boldsymbol{v} = \partial_t \boldsymbol{m}$, Lemma B.1.4(ii) with $p = 1$ yields that

$$\begin{aligned} \| \boldsymbol{v}_{hk}^- - \partial_t \boldsymbol{m}_{hk} \|_{\boldsymbol{L}^1(\omega_T)} &= k \sum_{i=0}^{M-1} \| \boldsymbol{v}_h^i - \mathrm{d_t} \boldsymbol{m}_h^{i+1} \|_{\boldsymbol{L}^1(\omega)} \lesssim k^2 \sum_{i=0}^{M-1} \| \boldsymbol{v}_h^i \|_{\boldsymbol{L}^2(\omega)}^2 \\ &= k \, \| \boldsymbol{v}_{hk}^- \|_{\boldsymbol{L}^2(\omega_T)}^2 \lesssim k \to 0 \quad \text{as } h, k \to 0. \end{aligned}$$

Since $\|\cdot\|_{\boldsymbol{L}^1(\omega_T)}$ is lower-semicontinuous on $\boldsymbol{L}^2(\omega_T)$, the latter equation yields that

$$\|\boldsymbol{v} - \partial_t \boldsymbol{m}\|_{\boldsymbol{L}^1(\omega_T)} \leq \liminf_{h,k\to 0} \|\boldsymbol{v}_{hk}^- - \partial_t \boldsymbol{m}_{hk}\|_{\boldsymbol{L}^1(\omega_T)} = 0,$$

and hence $\boldsymbol{v} = \partial_t \boldsymbol{m}$. For the proof of (viii), we follow [AKST14, p.420]: With Lemma 4.5.3(ii), the definition (3.3) of the postprocessed output yields that

$$\begin{aligned} k^2 \|\nabla \boldsymbol{v}_{hk}^-\|_{\boldsymbol{L}^2(\omega_T)}^2 &= k^3 \sum_{i=0}^{M-1} \|\nabla \boldsymbol{v}_h^i\|_{\boldsymbol{L}^2(\omega)}^2 = \big[\, k\rho(k)^{-1} \,\big]\, \rho(k)\, k^2 \sum_{i=0}^{M-1} \|\nabla \boldsymbol{v}_h^i\|_{\boldsymbol{L}^2(\omega)}^2 \\ &\lesssim k\rho(k)^{-1} \overset{(4.6b)}{\to} 0 \quad \text{as } h,k \to 0. \end{aligned} \tag{4.40}$$

This proves (viii) and altogether concludes the proof. □

Remark 4.5.5. *If $\rho \equiv 0$, then we cannot proceed as in* (4.40) *to prove Lemma 4.5.4*(vii)*. Instead, we get as in [AKST14, p.420] with the uniform boundedness statement from Lemma 4.5.3*(ii) *and an inverse estimate that*

$$k^2 \|\nabla \boldsymbol{v}_{hk}^-\|_{\boldsymbol{L}^2(\omega_T)}^2 = k^3 \sum_{i=0}^{M-1} \|\nabla \boldsymbol{v}_h^i\|_{\boldsymbol{L}^2(\omega)}^2 \lesssim h^{-2} k^3 \sum_{i=0}^{M-1} \|\boldsymbol{v}_h^i\|_{\boldsymbol{L}^2(\omega)}^2 \lesssim h^{-2} k^2.$$

Hence, with the mild CFL-type condition $k = \mathbf{o}(h)$, Lemma 4.5.4 still holds.

Moreover, we note a direct consequence of the latter convergence properties, which already anticipates the verification of Definition 2.2.1(i) for the proof of Theorem 4.5.1(b).

Lemma 4.5.6 ($|\boldsymbol{m}| = 1$ a.e. in ω_T)**.** *Let the assumptions of Theorem 4.5.1*(b) *be satisfied. Then, $\boldsymbol{m} \in L^\infty(0,T;\boldsymbol{H}^1(\omega)) \cap \boldsymbol{H}^1(\omega_T)$ from Lemma 4.5.4 satisfies $|\boldsymbol{m}| = 1$ a.e. in ω_T.*

Proof. We follow [Alo08, BSF⁺14]. First, we estimate

$$\begin{aligned} \|1 - |\boldsymbol{m}|\|_{L^2(\omega_T)} &\leq \|1 - |\boldsymbol{m}_{hk}^-|\|_{L^2(\omega_T)} + \||\boldsymbol{m}_{hk}^-| - |\boldsymbol{m}|\|_{L^2(\omega_T)} \\ &\leq \|1 - |\boldsymbol{m}_{hk}^-|\|_{L^2(\omega_T)} + \|\boldsymbol{m}_{hk}^- - \boldsymbol{m}\|_{\boldsymbol{L}^2(\omega_T)} =: T_1 + T_2. \end{aligned} \tag{4.41}$$

Note that with the convergence property of Lemma 4.5.4(iv), we get that $T_2 \to 0$ as $h,k \to 0$, i.e., we only have to deal with T_1. To this end, fix $t \in [0,T)$ and $\boldsymbol{x} \in \omega$. Let $i \in \{0,1,\dots,M-1\}$ such that $t \in [t_i, t_{i+1})$ and $K \in \mathcal{T}_h$ such that $\mathbf{x} \in \overline{K}$. Since $\nabla \boldsymbol{m}_h^i$ is constant elementwise and since $\boldsymbol{m}_h^i \in \boldsymbol{\mathcal{M}}_h$, it holds for all nodes $\boldsymbol{z} \in \overline{K}$ with the definition of the postprocessed output that

$$\begin{aligned} \big|\, 1 - |\boldsymbol{m}_{hk}^-(t,\boldsymbol{x})| \,\big| &= \big|\, 1 - |\boldsymbol{m}_h^i(\boldsymbol{x})| \,\big| = \big|\, |\boldsymbol{m}_h^i(\boldsymbol{z})| - |\boldsymbol{m}_h^i(\boldsymbol{x})| \,\big| \leq \big|\, \boldsymbol{m}_h^i(\boldsymbol{z}) - \boldsymbol{m}_h^i(\boldsymbol{x}) \,\big| \\ &\lesssim |\boldsymbol{z} - \boldsymbol{x}| \, \big|\nabla \boldsymbol{m}_h^i(\boldsymbol{x})|_K\big| \leq h \, \big|\nabla \boldsymbol{m}_h^i(\boldsymbol{x})|_K\big| = h \, \big|\nabla \boldsymbol{m}_{hk}^-(t,\boldsymbol{x})|_K\big|. \end{aligned}$$

Since $t \in [0,T)$ and $\boldsymbol{x} \in \omega$ were arbitrary, we can integrate in the latter estimate over ω_T, and obtain that

$$T_1 \overset{(4.41)}{=} \|1 - |\boldsymbol{m}_{hk}^-|\|_{L^2(\omega_T)} \lesssim h \, \|\nabla \boldsymbol{m}_{hk}^-\|_{\boldsymbol{L}^2(\omega_T)} \lesssim h \to 0 \quad \text{as } h,k \to 0.$$

Altogether, this yields that $|\boldsymbol{m}| = 1$ a.e. in ω_T. □

4.5.4. Convergence to weak solution

In this section, we prove Theorem 4.5.1(b). To this end, we first prove a weak consistency property of the general time-stepping approaches **(A1)**–**(A3)** in $\boldsymbol{L}^2(\omega_T)$.

Lemma 4.5.7 (Weak consistency of $\boldsymbol{\pi}_h^{\boldsymbol{D}}$ and $\boldsymbol{\Pi}_h^{\boldsymbol{D}}$)**.** *Let the assumptions of Theorem 4.5.1*(b) *be satisfied. Consider the general time-stepping approaches* **(A1)**–**(A3)**. *Then, the following two convergence properties* (i)–(ii) *hold true as* $h, k \to 0$*:*

(i) $\boldsymbol{\pi}_h^{\boldsymbol{D}}(\boldsymbol{v}_{hk}^-; \boldsymbol{m}_{hk}^-, \boldsymbol{m}_{hk}^=) \rightharpoonup \boldsymbol{\pi}(\boldsymbol{m})$ *in* $\boldsymbol{L}^2(\omega_T)$.

(ii) $\boldsymbol{\Pi}_h^{\boldsymbol{D}}(\boldsymbol{v}_{hk}^-; \boldsymbol{m}_{hk}^-, \boldsymbol{m}_{hk}^=) \rightharpoonup \boldsymbol{\Pi}(\boldsymbol{m})$ *in* $\boldsymbol{L}^2(\omega_T)$.

Proof. First, we prove (i): With the convergence properties from Lemma 4.5.4 and with Lemma 3.4.1, we get that

$$\boldsymbol{\pi}_h(\boldsymbol{m}_{hk}^-) \overset{\textbf{(D4)}}{\rightharpoonup} \boldsymbol{\pi}(\boldsymbol{m}) \quad \text{and} \quad \boldsymbol{\pi}_h(\boldsymbol{m}_{hk}^=) \overset{\textbf{(D4)}}{\rightharpoonup} \boldsymbol{\pi}(\boldsymbol{m}) \quad \text{in } \boldsymbol{L}^2(\omega_T) \quad \text{as } h, k \to 0. \tag{4.42a}$$

Moreover, we get with the convergence property from Lemma 4.5.4(vii) that

$$k\,\|\boldsymbol{\pi}_h(\boldsymbol{v}_{hk}^-)\|_{\boldsymbol{L}^2(\omega_T)} \overset{\textbf{(D3)}}{\lesssim} k\,\|\boldsymbol{v}_{hk}^-\|_{\boldsymbol{L}^2(\omega_T)} \lesssim k \to 0 \quad \text{as } h, k \to 0, \tag{4.42b}$$

i.e., $k\,\boldsymbol{\pi}_h(\boldsymbol{v}_{hk}^-) \to \boldsymbol{0}$ in $\boldsymbol{L}^2(\omega_T)$ as $h, k \to 0$. This yields that

$$\boldsymbol{\pi}_h(\boldsymbol{m}_{hk}^-) + \frac{k}{2}\,\boldsymbol{\pi}_h(\boldsymbol{v}_{hk}^-) \overset{(4.42a)}{\rightharpoonup} \boldsymbol{\pi}(\boldsymbol{m}) \quad \text{in } \boldsymbol{L}^2(\omega_T) \quad \text{as } h, k \to 0. \tag{4.42c}$$

Then, (i) is a direct consequence of the convergence properties (4.42), where for the Adams–Bashforth-type approach **(A2)** we use (4.42c) for $[0, k]$ and (4.42a) for $[k, T]$. Next, we show (ii). With Lemma 4.5.6, we get that $\boldsymbol{m} \in \boldsymbol{H}^1(\omega_T) \cap \boldsymbol{L}^\infty(\omega_T)$. Hence, $\boldsymbol{\Pi}(\boldsymbol{m}) \in \boldsymbol{L}^2(\omega_T)$ is well-defined. Then, the convergence properties from Lemma 4.5.4 yield that

$$\boldsymbol{\Pi}_h(\boldsymbol{m}_{hk}^-) \overset{\textbf{(D7)}}{\rightharpoonup} \boldsymbol{\Pi}(\boldsymbol{m}) \quad \text{in } \boldsymbol{L}^2(\omega_T) \quad \text{as } h, k \to 0. \tag{4.43a}$$

Together with weak consistency **(T5)** of $\boldsymbol{D}_h$, this yields that

$$\begin{aligned} &\boldsymbol{\Pi}_h(\boldsymbol{m}_{hk}^-) + \frac{k}{2}\,\boldsymbol{D}_h(\boldsymbol{m}_{hk}^-, \boldsymbol{v}_{hk}^-) \\ &\quad \overset{\text{(T3)}}{=} \boldsymbol{\Pi}_h(\boldsymbol{m}_{hk}^-) + \boldsymbol{D}_h\big(\boldsymbol{m}_{hk}^-, \frac{k}{2}\,\boldsymbol{v}_{hk}^-\big) \overset{(4.42b)}{\rightharpoonup} \boldsymbol{\Pi}(\boldsymbol{m}) \quad \text{in } \boldsymbol{L}^2(\omega_T) \quad \text{as } h, k \to 0. \end{aligned} \tag{4.43b}$$

Moreover, we infer from the convergence property from Lemma 4.5.4(iv) that

$$\begin{aligned} &\boldsymbol{\Pi}_h(\boldsymbol{m}_{hk}^-) + \frac{1}{2}\,\boldsymbol{D}_h(\boldsymbol{m}_{hk}^-, \boldsymbol{m}_{hk}^-) - \frac{1}{2}\,\boldsymbol{D}_h(\boldsymbol{m}_{hk}^-, \boldsymbol{m}_{hk}^=) \\ &\quad \overset{\text{(T3)}}{=} \boldsymbol{\Pi}_h(\boldsymbol{m}_{hk}^-) + \boldsymbol{D}_h\big(\boldsymbol{m}_{hk}^-,\, \frac{1}{2}(\boldsymbol{m}_{hk}^- - \boldsymbol{m}_{hk}^=)\big) \rightharpoonup \boldsymbol{\Pi}(\boldsymbol{m}), \quad \text{in } \boldsymbol{L}^2(\omega_T) \end{aligned} \tag{4.43c}$$

as $h, k \to 0$. Then, the convergences (4.43) cover all approaches **(A1)**–**(A3)**, where for **(A2)** we deal with $[0, k]$ and $[k, T]$ separately. This shows (ii) and concludes the proof. □

We come to the actual proof of Theorem 4.5.1(b): The used techniques go back to [Alo08], where a corresponding result was proved for the first-order tangent plane scheme with $\boldsymbol{h}_{\text{eff}}(\boldsymbol{m}) = \Delta\boldsymbol{m}$ and $\boldsymbol{\Pi}(\boldsymbol{m}) = \boldsymbol{0}$. These techniques were extended to implicit-explicit lower-order term contributions in [AKT12, BSF⁺14] and adapted in [AKST14] to the (almost) second-order tangent plane scheme. However, only $\boldsymbol{\Pi}(\boldsymbol{m}) = \boldsymbol{0}$, $\partial_t \boldsymbol{f} = \boldsymbol{0}$, and the implicit approach **(A1)** were covered in [AKST14]. For the explicit approaches **(A2)** and **(A3)**, a corresponding result for the midpoint scheme was proved in the own work [PRS18]; see Section 6 below. Here, we combine the ideas from [AKST14] and [PRS18] for the setting of Algorithm 4.2.1 and elaborate the proof of the own work [DPP⁺17, Theorem 4(ii)].

Proof of Theorem 4.5.1(b). We show that the limit from Lemma 4.5.4

$$\boldsymbol{m} \in L^\infty(0,T;\boldsymbol{H}^1(\omega)) \cap \boldsymbol{H}^1(\omega_T) \tag{4.44}$$

is a weak solution in the sense of Definition 2.2.1. In Lemma 4.5.6, we have already verified Definition 2.2.1(i). We split the remaining verifications into the following eight steps.

Step 1. We verify Definition 2.2.1(ii), i.e., $\boldsymbol{m}(0) = \boldsymbol{m}^0$ in the sense of traces: To this end, note that consistency **(D1)** yields that $\boldsymbol{m}_h^0 \rightharpoonup \boldsymbol{m}^0$ in $\boldsymbol{H}^1(\omega)$ as $h, k \to 0$. Recall that $\boldsymbol{m}(0)$ is understood in the sense of traces. Moreover, recall that the trace operator is continuous from $\boldsymbol{H}^1(\omega_T)$ to $\boldsymbol{L}^2(\omega)$. Since continuous mappings conserve weak convergence, the convergence property from Lemma 4.5.4(i) yields that $\boldsymbol{m}_h^0 = \boldsymbol{m}_{hk}(0) \rightharpoonup \boldsymbol{m}(0)$ in $\boldsymbol{L}^2(\omega)$ as $h, k \to 0$. Since weak limits are unique, we altogether get that $\boldsymbol{m}^0 = \boldsymbol{m}(0)$.

Step 2. We verify Definition 2.2.1(iii), i.e., $\boldsymbol{m}$ satisfies the variational formulation (2.16). To this end, we denote with $\boldsymbol{\mathcal{I}}_h$ the vector-valued nodal interpolant on $\boldsymbol{\mathcal{S}}_h$ and let $\boldsymbol{\varphi} \in \boldsymbol{C}^\infty(\overline{\omega_T})$. Since $(\mathbf{a} \times \mathbf{b}) \cdot \mathbf{a} = \mathbf{0}$ for $\mathbf{a}, \mathbf{b} \in \mathbb{R}^3$, we get that

$$\boldsymbol{\mathcal{I}}_h\big(\boldsymbol{m}_h^i \times \boldsymbol{\varphi}(t)\big) \in \boldsymbol{\mathcal{K}}_h(\boldsymbol{m}_h^i) \quad \text{for } t \in [t_i, t_{i+1}) \text{ and } i \in \{0, 1, \dots, M-1\}.$$

For each interval $[t_i, t_{i+1})$, we test the corresponding discrete variational formulation (4.9) with $\boldsymbol{\mathcal{I}}_h(\boldsymbol{m}_h^i \times \boldsymbol{\varphi}(t))$ and integrate over $[0, T]$. Then, we plug in the definition (3.3) of the postprocessed output. Altogether, we obtain that

$$\begin{aligned}
&I_{hk}^1 + I_{hk}^2 + I_{hk}^3 := \\
&\int_0^T \langle \mathcal{W}_{G(k)}(\lambda_{hk}^-)\boldsymbol{v}_{hk}^-, \boldsymbol{\mathcal{I}}_h(\boldsymbol{m}_{hk}^- \times \boldsymbol{\varphi})\rangle_{\boldsymbol{L}^2(\omega)}\,\mathrm{d}t + \int_0^T \langle \boldsymbol{m}_{hk}^- \times \boldsymbol{v}_{hk}^-, \boldsymbol{\mathcal{I}}_h(\boldsymbol{m}_{hk}^- \times \boldsymbol{\varphi})\rangle_{\boldsymbol{L}^2(\omega)}\,\mathrm{d}t \\
&\quad + \frac{C_{\mathbf{ex}}}{2} k(1+\rho(k)) \int_0^T \langle \nabla \boldsymbol{v}_{hk}^-, \nabla \boldsymbol{\mathcal{I}}_h(\boldsymbol{m}_{hk}^- \times \boldsymbol{\varphi})\rangle_{\boldsymbol{L}^2(\omega)}\,\mathrm{d}t \\
&\overset{(4.9)}{=} -C_{\mathbf{ex}} \int_0^T \langle \nabla \boldsymbol{m}_{hk}^-, \nabla \boldsymbol{\mathcal{I}}_h(\boldsymbol{m}_{hk}^- \times \boldsymbol{\varphi})\rangle_{\boldsymbol{L}^2(\omega)}\mathrm{d}t + \int_0^T \langle \boldsymbol{\pi}_h^{\boldsymbol{D}}(\boldsymbol{v}_{hk}^-; \boldsymbol{m}_{hk}^-, \boldsymbol{m}_{hk}^{=}), \boldsymbol{\mathcal{I}}_h(\boldsymbol{m}_{hk}^- \times \boldsymbol{\varphi})\rangle_{\boldsymbol{L}^2(\omega)}\mathrm{d}t \\
&\quad + \int_0^T \langle \overline{\boldsymbol{f}}_{hk}, \boldsymbol{\mathcal{I}}_h(\boldsymbol{m}_{hk}^- \times \boldsymbol{\varphi})\rangle_{\boldsymbol{L}^2(\omega)}\,\mathrm{d}t + \int_0^T \langle \boldsymbol{\Pi}_h^{\boldsymbol{D}}(\boldsymbol{v}_{hk}^-; \boldsymbol{m}_{hk}^-, \boldsymbol{m}_{hk}^{=}), \boldsymbol{\mathcal{I}}_h(\boldsymbol{m}_{hk}^- \times \boldsymbol{\varphi})\rangle_{\boldsymbol{L}^2(\omega)}\,\mathrm{d}t \\
&=: -C_{\mathbf{ex}} I_{hk}^4 + I_{hk}^5 + I_{hk}^6 + I_{hk}^7.
\end{aligned} \tag{4.45}$$

In the following, we show convergence of the integrals $I_{hk}^1, \dots, I_{hk}^7$ and obtain the variational formulation (2.16) from the limits.

Step 3. Similarly to [Alo08, p.193], we derive the auxiliary convergence results

$$\mathcal{I}_h(\boldsymbol{m}_{hk}^- \times \boldsymbol{\varphi}) \to \boldsymbol{m} \times \boldsymbol{\varphi} \quad \text{in } \boldsymbol{L}^2(\omega_T) \quad \text{as } h,k \to 0, \quad \text{and} \tag{4.46a}$$

$$\nabla\mathcal{I}_h(\boldsymbol{m}_{hk}^- \times \boldsymbol{\varphi}) - \nabla(\boldsymbol{m}_{hk}^- \times \boldsymbol{\varphi}) \to \boldsymbol{0} \quad \text{in } \boldsymbol{L}^2(\omega_T) \quad \text{as } h,k \to 0. \tag{4.46b}$$

To this end, recall that $\boldsymbol{m}_{hk}^-(t)$ is piecewise affine for $t \in [0,T)$ a.e.. This yields that

$$D^2\, \boldsymbol{m}_{hk}^-(t)|_K = \boldsymbol{0} \quad \text{for all elements } K \in \mathcal{T}_h \quad \text{and } t \in [0,T) \text{ a.e.} \tag{4.47}$$

Then, the approximation properties of the nodal interpolant $\mathcal{I}_h$ (see Proposition 3.1.7) together with the convergence properties from Lemma 4.5.4 yield that

$$\begin{aligned}
&\|\mathcal{I}_h(\boldsymbol{m}_{hk}^- \times \boldsymbol{\varphi}) - \boldsymbol{m}_{hk}^- \times \boldsymbol{\varphi}\|_{\boldsymbol{L}^2(\omega_T)} + \|\nabla\mathcal{I}_h(\boldsymbol{m}_{hk}^- \times \boldsymbol{\varphi}) - \nabla(\boldsymbol{m}_{hk}^- \times \boldsymbol{\varphi})\|_{\boldsymbol{L}^2(\omega_T)} \\
&\lesssim h \Big(\sum_{K \in \mathcal{T}_h} \int_0^T |\boldsymbol{m}_{hk}^- \times \boldsymbol{\varphi}|_{\boldsymbol{H}^2(K)}^2 \, \mathrm{d}t \Big)^{1/2} \\
&\overset{(4.47)}{\lesssim} h\, \|\boldsymbol{\varphi}\|_{L^2(0,T,\boldsymbol{W}^{2,\infty}(\omega))} \|\boldsymbol{m}_{hk}^-\|_{L^2(0,T,\boldsymbol{H}^1(\omega))} \\
&\lesssim h\, \|\boldsymbol{m}_{hk}^-\|_{L^2(0,T,\boldsymbol{H}^1(\omega))} \to 0 \quad \text{as } h,k \to 0.
\end{aligned} \tag{4.48}$$

This already verifies (4.46b), and with the convergence property from Lemma 4.5.4(iv), we further get that

$$\begin{aligned}
&\|\mathcal{I}_h(\boldsymbol{m}_{hk}^- \times \boldsymbol{\varphi}) - \boldsymbol{m} \times \boldsymbol{\varphi}\|_{\boldsymbol{L}^2(\omega_T)} \\
&\quad \lesssim \|\mathcal{I}_h(\boldsymbol{m}_{hk}^- \times \boldsymbol{\varphi}) - \boldsymbol{m}_{hk}^- \times \boldsymbol{\varphi}\|_{\boldsymbol{L}^2(\omega_T)} + \|(\boldsymbol{m}_{hk}^- - \boldsymbol{m}) \times \boldsymbol{\varphi}\|_{\boldsymbol{L}^2(\omega_T)} \\
&\quad \overset{(4.48)}{\lesssim} h\, \|\boldsymbol{m}_{hk}^-\|_{L^2(0,T,\boldsymbol{H}^1(\omega))} + \|\boldsymbol{m}_{hk}^- - \boldsymbol{m}\|_{\boldsymbol{L}^2(\omega_T)} \to 0 \quad \text{as } h,k \to 0,
\end{aligned}$$

which also verifies (4.46a).

Step 4. We deal with I_{hk}^1 as in [AKST14, p.422f]: From Lemma 4.3.3(ii), we get that

$$\mathcal{W}_{G(k)}(\lambda_{hk}^-) \overset{(4.6a)}{\to} \alpha \quad \text{in } L^\infty(\omega_T) \quad \text{as } h,k \to 0.$$

Together with the convergence property from Lemma 4.5.4(vii), we infer that

$$\mathcal{W}_{G(k)}(\lambda_{hk}^-)\, \boldsymbol{v}_{hk}^- \rightharpoonup \alpha\, \partial_t \boldsymbol{m} \quad \text{in } \boldsymbol{L}^2(\omega_T) \quad \text{as } h,k \to 0.$$

Then, the auxiliary result (4.46a) yields that

$$I_{hk}^1 \overset{(4.45)}{=} \int_0^T \langle \mathcal{W}_{G(k)}(\lambda_{hk}^-)\boldsymbol{v}_{hk}^-, \mathcal{I}_h(\boldsymbol{m}_{hk}^- \times \boldsymbol{\varphi}) \rangle_{\boldsymbol{L}^2(\omega)} \, \mathrm{d}t \to \alpha \int_0^T \langle \partial_t \boldsymbol{m}, \boldsymbol{m} \times \boldsymbol{\varphi} \rangle_{\boldsymbol{L}^2(\omega)} \, \mathrm{d}t,$$

as $h,k \to 0$.

Step 5. We deal with I_{hk}^2 and elaborate the corresponding arguments of [Alo08, BSF$^+$14]. First, we show that

$$\boldsymbol{m}_{hk}^- \times \boldsymbol{v}_{hk}^- \rightharpoonup \boldsymbol{m} \times \partial_t \boldsymbol{m} \quad \text{in } \boldsymbol{L}^2(\omega_T) \quad \text{as } h,k \to 0. \tag{4.49}$$

To this end, recall that $\|\boldsymbol{m}_{hk}^-\|_{\boldsymbol{L}^\infty(\omega_T)} = 1$. Then, the convergence properties from Lemma 4.5.4 yield that $\|\boldsymbol{m}_{hk}^- \times \boldsymbol{v}_{hk}^-\|_{\boldsymbol{L}^2(\omega_T)} \lesssim 1$. Moreover, we get for all $\boldsymbol{\zeta} \in \boldsymbol{C}^\infty(\overline{\omega_T})$ that

$$\begin{aligned}\int_0^T \langle \boldsymbol{m}_{hk}^- \times \boldsymbol{v}_{hk}^-, \boldsymbol{\zeta}\rangle_{\boldsymbol{L}^2(\omega)}\,\mathrm{d}t &= -\int_0^T \langle \boldsymbol{v}_{hk}^-, \boldsymbol{m}_{hk}^- \times \boldsymbol{\zeta}\rangle_{\boldsymbol{L}^2(\omega)}\,\mathrm{d}t \to -\int_0^T \langle \partial_t\boldsymbol{m}, \boldsymbol{m} \times \boldsymbol{\zeta}\rangle_{\boldsymbol{L}^2(\omega)}\,\mathrm{d}t \\ &= \int_0^T \langle \boldsymbol{m} \times \partial_t\boldsymbol{m}, \boldsymbol{\zeta}\rangle_{\boldsymbol{L}^2(\omega)}\,\mathrm{d}t \quad \text{as } h,k \to 0.\end{aligned}$$

Hence, Lemma B.2.1 implies the convergence (4.49) and as a consequence, we obtain that

$$I_{hk}^2 \overset{(4.45)}{=} \int_0^T \langle \boldsymbol{m}_{hk}^- \times \boldsymbol{v}_{hk}^-, \boldsymbol{\mathcal{I}}_h(\boldsymbol{m}_{hk}^- \times \boldsymbol{\varphi})\rangle_{\boldsymbol{L}^2(\omega)}\,\mathrm{d}t \overset{(4.46a)}{\to} \int_0^T \langle \boldsymbol{m} \times \partial_t\boldsymbol{m}, \boldsymbol{m} \times \boldsymbol{\varphi}\rangle_{\boldsymbol{L}^2(\omega)}\,\mathrm{d}t,$$

as $h,k \to 0$. With Lagrange's identity, the integrand becomes

$$(\boldsymbol{m} \times \partial_t\boldsymbol{m}) \cdot (\boldsymbol{m} \times \boldsymbol{\varphi}) = |\boldsymbol{m}|^2\,\partial_t\boldsymbol{m} \cdot \boldsymbol{\varphi} - (\boldsymbol{m} \cdot \boldsymbol{\varphi})(\partial_t\boldsymbol{m} \cdot \boldsymbol{m}) \quad \text{a.e. on } \omega_T. \tag{4.50}$$

With Lemma 4.5.6 and the product rule, we further get that

$$|\boldsymbol{m}| = 1 \quad \text{and} \quad 0 = \frac{1}{2}\,\partial_t|\boldsymbol{m}|^2 = \partial_t\boldsymbol{m} \cdot \boldsymbol{m} \quad \text{a.e. in } \omega_T.$$

Hence, the combination of the latter three equations yields that

$$I_{hk}^2 \to \int_0^T \langle \partial_t\boldsymbol{m}, \boldsymbol{\varphi}\rangle_{\boldsymbol{L}^2(\omega)}\,\mathrm{d}t \quad \text{as } h,k \to 0.$$

Step 6. We deal with I_{hk}^3: To this end, we elaborate the corresponding arguments in [Alo08, AKST14]. First, the convergence properties of Lemma 4.5.4 yield that

$$\begin{aligned}\|\nabla\boldsymbol{\mathcal{I}}_h(\boldsymbol{m}_{hk}^- \times \boldsymbol{\varphi})\|_{\boldsymbol{L}^2(\omega_T)} &\le \|\nabla(\boldsymbol{m}_{hk}^- \times \boldsymbol{\varphi})\|_{\boldsymbol{L}^2(\omega_T)} + \|\nabla\boldsymbol{\mathcal{I}}_h(\boldsymbol{m}_{hk}^- \times \boldsymbol{\varphi}) - \nabla(\boldsymbol{m}_{hk}^- \times \boldsymbol{\varphi})\|_{\boldsymbol{L}^2(\omega_T)} \\ &\lesssim \|\boldsymbol{m}_{hk}^-\|_{L^2(0,T;\boldsymbol{H}^1(\omega))}\,\|\boldsymbol{\varphi}\|_{L^2(0,T;\boldsymbol{W}^{1,\infty}(\omega))} \\ &\qquad + \|\nabla\boldsymbol{\mathcal{I}}_h(\boldsymbol{m}_{hk}^- \times \boldsymbol{\varphi}) - \nabla(\boldsymbol{m}_{hk}^- \times \boldsymbol{\varphi})\|_{\boldsymbol{L}^2(\omega_T)} \overset{(4.46b)}{\lesssim} 1.\end{aligned} \tag{4.51}$$

Then, the convergence property from Lemma 4.5.4(viii) yields that

$$\begin{aligned}|I_{hk}^3| &\overset{(4.45)}{=} \left|\frac{C_{\mathbf{ex}}}{2}k(1+\rho(k))\int_0^T \langle \nabla\boldsymbol{v}_{hk}^-, \nabla\boldsymbol{\mathcal{I}}_h(\boldsymbol{m}_{hk}^- \times \boldsymbol{\varphi})\rangle_{\boldsymbol{L}^2(\omega)}\,\mathrm{d}t\right| \\ &\overset{(4.6b)}{\lesssim} k\,\|\nabla\boldsymbol{v}_{hk}^-\|_{\boldsymbol{L}^2(\omega_T)}\,\|\nabla\boldsymbol{\mathcal{I}}_h(\boldsymbol{m}_{hk}^- \times \boldsymbol{\varphi})\|_{\boldsymbol{L}^2(\omega_T)} \lesssim k\,\|\nabla\boldsymbol{v}_{hk}^-\|_{\boldsymbol{L}^2(\omega_T)} \to 0 \quad \text{as } h,k \to 0,\end{aligned}$$

i.e., we get that $I_{hk}^3 \to 0$ as $h,k \to 0$.

Step 7. We deal with I_{hk}^4 as in [Alo08, BSF+14]: We get that

$$\begin{aligned}I_{hk}^4 &= \int_0^T \langle \nabla\boldsymbol{m}_{hk}^-, \nabla\boldsymbol{\mathcal{I}}_h(\boldsymbol{m}_{hk}^- \times \boldsymbol{\varphi})\rangle_{\boldsymbol{L}^2(\omega)}\,\mathrm{d}t \\ &= \int_0^T \langle \nabla\boldsymbol{m}_{hk}^-, \nabla(\boldsymbol{m}_{hk}^- \times \boldsymbol{\varphi})\rangle_{\boldsymbol{L}^2(\omega)}\,\mathrm{d}t \\ &\qquad + \int_0^T \langle \nabla\boldsymbol{m}_{hk}^-, \nabla\boldsymbol{\mathcal{I}}_h(\boldsymbol{m}_{hk}^- \times \boldsymbol{\varphi}) - \nabla(\boldsymbol{m}_{hk}^- \times \boldsymbol{\varphi})\rangle_{\boldsymbol{L}^2(\omega)}\,\mathrm{d}t =: I_{hk}^{4,A} + I_{hk}^{4,B}.\end{aligned}$$

The product rule and the convergence properties from Lemma 4.5.4 yield that

$$\begin{aligned} I_{hk}^{4,A} &= \int_0^T \langle \nabla \boldsymbol{m}_{hk}^-, \nabla \boldsymbol{m}_{hk}^- \times \boldsymbol{\varphi} \rangle_{\boldsymbol{L}^2(\omega)} \,\mathrm{d}t + \int_0^T \langle \nabla \boldsymbol{m}_{hk}^-, \boldsymbol{m}_{hk}^- \times \nabla \boldsymbol{\varphi} \rangle_{\boldsymbol{L}^2(\omega)} \,\mathrm{d}t \\ &= \int_0^T \langle \nabla \boldsymbol{m}_{hk}^-, \boldsymbol{m}_{hk}^- \times \nabla \boldsymbol{\varphi} \rangle_{\boldsymbol{L}^2(\omega)} \,\mathrm{d}t \to \int_0^T \langle \nabla \boldsymbol{m}, \boldsymbol{m} \times \nabla \boldsymbol{\varphi} \rangle_{\boldsymbol{L}^2(\omega)} \,\mathrm{d}t \end{aligned}$$

as $h, k \to 0$. Moreover, we get from (4.46b) that $I_{hk}^{4,B} \to 0$ as $h, k \to 0$. Altogether, we conclude that

$$I_{hk}^4 \to \int_0^T \langle \nabla \boldsymbol{m}, \boldsymbol{m} \times \nabla \boldsymbol{\varphi}) \rangle_{\boldsymbol{L}^2(\omega)} \,\mathrm{d}t = - \int_0^T \langle \boldsymbol{m} \times \nabla \boldsymbol{m}, \nabla \boldsymbol{\varphi} \rangle_{\boldsymbol{L}^2(\omega)} \,\mathrm{d}t \quad \text{as } h, k \to 0.$$

Step 8. We deal with $I_{hk}^5, I_{hk}^6, I_{hk}^7$: To this end, we extend the arguments of [AKST14, BSF⁺14]. With the convergence properties from (4.46a) and Lemma 4.5.7, we derive that

$$\begin{aligned} I_{hk}^5 &= \int_0^T \langle \boldsymbol{\pi}_h^{\boldsymbol{D}}(\boldsymbol{v}_{hk}^-; \boldsymbol{m}_{hk}^-, \boldsymbol{m}_{hk}^{=}), \boldsymbol{\mathcal{I}}_h(\boldsymbol{m}_{hk}^- \times \boldsymbol{\varphi}) \rangle_{\boldsymbol{L}^2(\omega)} \,\mathrm{d}t \to \int_0^T \langle \boldsymbol{\pi}(\boldsymbol{m}), \boldsymbol{m} \times \boldsymbol{\varphi} \rangle_{\boldsymbol{L}^2(\omega)} \,\mathrm{d}t, \\ I_{hk}^6 &= \int_0^T \langle \overline{\boldsymbol{f}}_{hk}, \boldsymbol{\mathcal{I}}_h(\boldsymbol{m}_{hk}^- \times \boldsymbol{\varphi}) \rangle_{\boldsymbol{L}^2(\omega)} \,\mathrm{d}t \overset{\textbf{(D5)}}{\to} \int_0^T \langle \boldsymbol{f}, \boldsymbol{m} \times \boldsymbol{\varphi} \rangle_{\boldsymbol{L}^2(\omega)} \,\mathrm{d}t, \quad \text{and} \\ I_{hk}^7 &= \int_0^T \langle \boldsymbol{\Pi}_h^{\boldsymbol{D}}(\boldsymbol{v}_{hk}^-; \boldsymbol{m}_{hk}^-, \boldsymbol{m}_{hk}^{=}), \boldsymbol{\mathcal{I}}_h(\boldsymbol{m}_{hk}^- \times \boldsymbol{\varphi}) \rangle_{\boldsymbol{L}^2(\omega)} \,\mathrm{d}t \to \int_0^T \langle \boldsymbol{\Pi}(\boldsymbol{m}), \boldsymbol{m} \times \boldsymbol{\varphi} \rangle_{\boldsymbol{L}^2(\omega)} \,\mathrm{d}t, \end{aligned} \tag{4.52}$$

as $h, k \to 0$. Then, the combination of **Step 1**–**Step 8** concludes the proof. □

Remark 4.5.8. *For the Zhang–Li field, the corresponding contributions to $\boldsymbol{\Pi}_h$ and $\boldsymbol{D}_h$ satisfy all assumptions from Theorem 4.5.1*(b)*, except weak consistency* **(T5)** *of $\boldsymbol{D}_h$. Note that* **(T5)** *is only required to establish the convergence in* (4.52)*. However, even without* **(T5)***, Lemma 4.5.4 still holds. Instead of* **(T5)***, Proposition A.3.2 then proves the weaker convergences*

$$\begin{aligned} \int_0^T \langle \boldsymbol{D}_h(\boldsymbol{m}_{hk}^-, k\boldsymbol{v}_{hk}^-), \boldsymbol{\mathcal{I}}_h(\boldsymbol{m}_{hk}^- \times \boldsymbol{\varphi}) \rangle_{\boldsymbol{L}^2(\omega)} \,\mathrm{d}t \to 0, &\quad \textit{and} \\ \int_0^T \langle \boldsymbol{D}_h(\boldsymbol{m}_{hk}^-, \boldsymbol{m}_{hk}^- - \boldsymbol{m}_{hk}^{=}), \boldsymbol{\mathcal{I}}_h(\boldsymbol{m}_{hk}^- \times \boldsymbol{\varphi}) \rangle_{\boldsymbol{L}^2(\omega)} \,\mathrm{d}t \to 0, &\quad \textit{as } h, k \to 0. \end{aligned}$$

Recalling the definitions of the general time-stepping approaches **(A1)**–**(A3)** *and with the weak consistency* **(D7)** *for $\boldsymbol{\Pi}_h$ at hand (see Proposition A.3.1*(i)*), this proves the convergence* (4.52)*.*

4.5.5. Stronger energy estimate

In this section, we prove Theorem 4.5.1(c), i.e., under stronger assumptions, the solution $\boldsymbol{m}$ from (b) is a physical weak solution in the sense of Definition 2.2.1(i)–(iv). To this end, we first prove a strong consistency property of the general time-stepping approaches **(A1)**–**(A3)** in $\boldsymbol{L}^2(\omega_T)$.

Lemma 4.5.9 (Strong consistency of $\boldsymbol{\pi}_h^{\boldsymbol{D}}$ and $\boldsymbol{\Pi}_h^{\boldsymbol{D}}$)**.** *Let the assumptions of Theorem 4.5.1*(c) *be satisfied. Consider the general time-stepping approaches* **(A1)**–**(A3)***. Then, the following two convergence properties* (i)–(ii) *hold true as* $h, k \to 0$*:*

(i) $\boldsymbol{\pi}_h^{\boldsymbol{D}}(\boldsymbol{v}_{hk}^-; \boldsymbol{m}_{hk}^-, \boldsymbol{m}_{hk}^=) \to \boldsymbol{\pi}(\boldsymbol{m})$ *in* $\boldsymbol{L}^2(\omega_T)$.

(ii) $\boldsymbol{\Pi}_h^{\boldsymbol{D}}(\boldsymbol{v}_{hk}^-; \boldsymbol{m}_{hk}^-, \boldsymbol{m}_{hk}^=) \to \boldsymbol{\Pi}(\boldsymbol{m})$ *in* $\boldsymbol{L}^2(\omega_T)$.

Proof. First, we show (i): For all approaches **(A1)**–**(A3)**, we get from Lemma 4.5.4 that

$$k\,\|\boldsymbol{\pi}_h(\boldsymbol{v}_{hk}^-)\|_{\boldsymbol{L}^2(\omega_T)} \overset{\textbf{(D3)}}{\lesssim} k\,\|\boldsymbol{v}_{hk}^-\|_{\boldsymbol{L}^2(\omega_T)} \lesssim k \to 0 \quad \text{as } h, k \to 0. \tag{4.53a}$$

Moreover, we get from the stronger consistency assumption **(D4$^+$)** with Lemma 3.4.1 that

$$\boldsymbol{\pi}_h(\boldsymbol{m}_{hk}^=), \boldsymbol{\pi}_h(\boldsymbol{m}_{hk}^-), \boldsymbol{\pi}_h(\boldsymbol{m}_{hk}^+) \to \boldsymbol{\pi}(\boldsymbol{m}) \quad \text{in } \boldsymbol{L}^2(\omega_T) \quad \text{as } h, k \to 0. \tag{4.53b}$$

Then, (i) is a direct consequence of the convergences (4.53). Next, we show (ii): With Lemma 4.5.6, we get that $\boldsymbol{m} \in \boldsymbol{H}^1(\omega_T) \cap \boldsymbol{L}^\infty(\omega_T)$. Hence, $\boldsymbol{\Pi}(\boldsymbol{m}) \in \boldsymbol{L}^2(\omega_T)$ is well-defined. With the stronger consistency assumptions **(D7$^+$)** for $\boldsymbol{\Pi}_h$ and **(T5$^+$)** for the corresponding $\boldsymbol{D}_h$, we get for all approaches **(A1)**–**(A3)** that

$$\begin{aligned}
&\|\boldsymbol{\Pi}_h^{\boldsymbol{D}}(\boldsymbol{v}_{hk}^-; \boldsymbol{m}_{hk}^-, \boldsymbol{m}_{hk}^=) - \boldsymbol{\Pi}(\boldsymbol{m})\|_{\boldsymbol{L}^2(\omega_T)} \\
&\lesssim \|\boldsymbol{\Pi}_h(\boldsymbol{m}_{hk}^-) - \boldsymbol{\Pi}(\boldsymbol{m})\|_{\boldsymbol{L}^2(\omega_T)} + \|k\boldsymbol{D}_h(\boldsymbol{m}_{hk}^-, \boldsymbol{v}_{hk}^-)\|_{\boldsymbol{L}^2(\omega_T)} \\
&\quad + \|\boldsymbol{D}_h(\boldsymbol{m}_{hk}^-, \boldsymbol{m}_{hk}^-) - \boldsymbol{D}_h(\boldsymbol{m}_{hk}^-, \boldsymbol{m}_{hk}^=)\|_{\boldsymbol{L}^2(\omega_T)} \\
&\overset{\textbf{(T3)}}{=} \|\boldsymbol{\Pi}_h(\boldsymbol{m}_{hk}^-) - \boldsymbol{\Pi}(\boldsymbol{m})\|_{\boldsymbol{L}^2(\omega_T)} + \|\boldsymbol{D}_h(\boldsymbol{m}_{hk}^-, k\boldsymbol{v}_{hk}^-)\|_{\boldsymbol{L}^2(\omega_T)} \\
&\quad + \|\boldsymbol{D}_h(\boldsymbol{m}_{hk}^-, \boldsymbol{m}_{hk}^- - \boldsymbol{m}_{hk}^=)\|_{\boldsymbol{L}^2(\omega_T)} \overset{(4.53)}{\to} 0 \quad \text{as } h, k \to 0.
\end{aligned}$$

Altogether, this concludes the proof. □

We come to the actual proof of Theorem 4.5.1(c). To this end, we extend the techniques from [BSF$^+$14, Appendix A] for the first-order tangent plane scheme and from [AKST14, p.424f] for the (almost) second-order tangent plane scheme to the extended setting of Theorem 4.5.1(c). Here, we elaborate the proof of the own work [DPP$^+$17, Theorem 4(iii)].

Proof of Theorem 4.5.1(c)*.* Since the assumptions from (c) are stronger than those of (b), we only have to verify, that $\boldsymbol{m}$ from (b) satisfies the energy estimate (2.17). To this end, recall from (2.15) the notion of the energy functional

$$\mathcal{E}_{\text{LLG}}(\boldsymbol{m}) := \frac{C_{\mathbf{ex}}}{2}\|\nabla \boldsymbol{m}\|_{\boldsymbol{L}^2(\omega)}^2 - \frac{1}{2}\langle \boldsymbol{\pi}(\boldsymbol{m}), \boldsymbol{m}\rangle_{\boldsymbol{L}^2(\omega)} - \langle \boldsymbol{f}, \boldsymbol{m}\rangle_{\boldsymbol{L}^2(\omega)}. \tag{4.54}$$

Let $\tau \in [0, T)$ be arbitrary and let $j \in \{1 \ldots, M\}$ such that $\tau \in [t_{j-1}, t_j)$. Since we supposed $\boldsymbol{f} \in C^1([0, T; \boldsymbol{L}^2(\omega))$, we can define $\boldsymbol{f}^i := \boldsymbol{f}(t_i)$ for all $i \in \{0, \ldots, M\}$. Then, we split the proof into the following five steps.

Step 1. We exploit the discrete energy estimate from Lemma 4.5.3 (i): For all $i \in \{0, \ldots, j-1\}$, we get that

$$
\begin{aligned}
&\mathcal{E}_{\mathrm{LLG}}(\boldsymbol{m}_h^{i+1}) - \mathcal{E}_{\mathrm{LLG}}(\boldsymbol{m}_h^i) \\
&\overset{(4.54)}{=} \frac{C_{\mathbf{ex}}}{2}\, k\, \mathrm{d_t}\, \|\nabla \boldsymbol{m}_h^{i+1}\|^2_{\boldsymbol{L}^2(\omega)} - \frac{1}{2}\langle \boldsymbol{\pi}(\boldsymbol{m}_h^{i+1}), \boldsymbol{m}_h^{i+1}\rangle_{\boldsymbol{L}^2(\omega)} + \frac{1}{2}\langle \boldsymbol{\pi}(\boldsymbol{m}_h^{i}), \boldsymbol{m}_h^{i}\rangle_{\boldsymbol{L}^2(\omega)} \\
&\qquad - \langle \boldsymbol{f}^{i+1}, \boldsymbol{m}_h^{i+1}\rangle_{\boldsymbol{L}^2(\omega)} + \langle \boldsymbol{f}^{i}, \boldsymbol{m}_h^{i}\rangle_{\boldsymbol{L}^2(\omega)} \\
&\leq\ -k\langle \mathcal{W}_{G(k)}(\lambda_{hk}^-)\boldsymbol{v}_h^i, \boldsymbol{v}_h^i\rangle_{\boldsymbol{L}^2(\omega)} - \frac{C_{\mathbf{ex}}}{2} k^2 \rho(k) \|\nabla \boldsymbol{v}_h^i\|^2_{\boldsymbol{L}^2(\omega)} \\
&\qquad + k\langle \boldsymbol{\pi}_h^{\boldsymbol{D}}(\boldsymbol{v}_h^i; \boldsymbol{m}_h^i, \boldsymbol{m}_h^{i-1}), \boldsymbol{v}_h^i\rangle_{\boldsymbol{L}^2(\omega)} - \frac{1}{2}\langle \boldsymbol{\pi}(\boldsymbol{m}_h^{i+1}), \boldsymbol{m}_h^{i+1}\rangle_{\boldsymbol{L}^2(\omega)} + \frac{1}{2}\langle \boldsymbol{\pi}(\boldsymbol{m}_h^{i}), \boldsymbol{m}_h^{i}\rangle_{\boldsymbol{L}^2(\omega)} \\
&\qquad + k\langle \boldsymbol{f}_h^{i+1/2}, \boldsymbol{v}_h^i\rangle_{\boldsymbol{L}^2(\omega)} - \langle \boldsymbol{f}^{i+1}, \boldsymbol{m}_h^{i+1}\rangle_{\boldsymbol{L}^2(\omega)} + \langle \boldsymbol{f}^{i}, \boldsymbol{m}_h^{i}\rangle_{\boldsymbol{L}^2(\omega)} \\
&\qquad + k\langle \boldsymbol{\Pi}_h^{\boldsymbol{D}}(\boldsymbol{v}_h^i; \boldsymbol{m}_h^i, \boldsymbol{m}_h^{i-1}), \boldsymbol{v}_h^i\rangle_{\boldsymbol{L}^2(\omega)} \\
&=:\ -k\langle \mathcal{W}_{G(k)}(\lambda_{hk}^-)\boldsymbol{v}_h^i, \boldsymbol{v}_h^i\rangle_{\boldsymbol{L}^2(\omega)} - \frac{C_{\mathbf{ex}}}{2}\, k^2 \rho(k) \|\nabla \boldsymbol{v}_h^i\|^2_{\boldsymbol{L}^2(\omega)} + \sum_{\ell=1}^{3} T_{\boldsymbol{\pi}}^{(\ell)} + \sum_{\ell=1}^{3} T_{\boldsymbol{f}}^{(\ell)} \\
&\qquad + k\langle \boldsymbol{\Pi}_h^{\boldsymbol{D}}(\boldsymbol{v}_h^i; \boldsymbol{m}_h^i, \boldsymbol{m}_h^{i-1}), \boldsymbol{v}_h^i\rangle_{\boldsymbol{L}^2(\omega)}.
\end{aligned}
\tag{4.55}
$$

Step 2. We transform $\sum_{\ell=1}^3 T_{\boldsymbol{\pi}}^{(\ell)}$: With linearity **(L1)** and self-adjointness **(L3)** of $\boldsymbol{\pi}$, we get that

$$
\begin{aligned}
\sum_{\ell=1}^{3} T_{\boldsymbol{\pi}}^{(\ell)} &\overset{(4.55)}{=} k\,\langle \boldsymbol{\pi}_h^{\boldsymbol{D}}(\boldsymbol{v}_h^i; \boldsymbol{m}_h^i, \boldsymbol{m}_h^{i-1}), \boldsymbol{v}_h^i\rangle_{\boldsymbol{L}^2(\omega)} - \frac{1}{2}\langle \boldsymbol{\pi}(\boldsymbol{m}_h^{i+1}), \boldsymbol{m}_h^{i+1}\rangle_{\boldsymbol{L}^2(\omega)} + \frac{1}{2}\langle \boldsymbol{\pi}(\boldsymbol{m}_h^{i}), \boldsymbol{m}_h^{i}\rangle_{\boldsymbol{L}^2(\omega)} \\
&= k\,\langle \boldsymbol{\pi}_h^{\boldsymbol{D}}(\boldsymbol{v}_h^i; \boldsymbol{m}_h^i, \boldsymbol{m}_h^{i-1}), \boldsymbol{v}_h^i\rangle_{\boldsymbol{L}^2(\omega)} - k\,\langle \boldsymbol{\pi}(\boldsymbol{m}_h^i), \boldsymbol{v}_h^i\rangle_{\boldsymbol{L}^2(\omega)} + k\,\langle \boldsymbol{\pi}(\boldsymbol{m}_h^i), \boldsymbol{v}_h^i\rangle_{\boldsymbol{L}^2(\omega)} \\
&\quad + \langle \boldsymbol{\pi}(\boldsymbol{m}_h^i), \boldsymbol{m}_h^i\rangle_{\boldsymbol{L}^2(\omega)} - \langle \boldsymbol{\pi}(\boldsymbol{m}_h^i), \boldsymbol{m}_h^{i+1}\rangle_{\boldsymbol{L}^2(\omega)} + \langle \boldsymbol{\pi}(\boldsymbol{m}_h^i), \boldsymbol{m}_h^{i+1}\rangle_{\boldsymbol{L}^2(\omega)} \\
&\quad - \frac{1}{2}\langle \boldsymbol{\pi}(\boldsymbol{m}_h^{i+1}), \boldsymbol{m}_h^{i+1}\rangle_{\boldsymbol{L}^2(\omega)} - \frac{1}{2}\langle \boldsymbol{\pi}(\boldsymbol{m}_h^{i}), \boldsymbol{m}_h^{i}\rangle_{\boldsymbol{L}^2(\omega)} \\
&= k\,\langle \boldsymbol{\pi}_h^{\boldsymbol{D}}(\boldsymbol{v}_h^i; \boldsymbol{m}_h^i, \boldsymbol{m}_h^{i-1}) - \boldsymbol{\pi}(\boldsymbol{m}_h^i), \boldsymbol{v}_h^i\rangle_{\boldsymbol{L}^2(\omega)} - \langle \boldsymbol{\pi}(\boldsymbol{m}_h^i), \boldsymbol{m}_h^{i+1} - \boldsymbol{m}_h^i - k\,\boldsymbol{v}_h^i\rangle_{\boldsymbol{L}^2(\omega)} \\
&\quad - \frac{1}{2}\langle \boldsymbol{\pi}(\boldsymbol{m}_h^{i+1} - \boldsymbol{m}_h^i), \boldsymbol{m}_h^{i+1} - \boldsymbol{m}_h^i\rangle_{\boldsymbol{L}^2(\omega)}.
\end{aligned}
\tag{4.56}
$$

For the second term on the right-hand side of (4.56), Lemma B.1.4(ii) does not provide a suitable estimate for $\boldsymbol{m}_h^{i+1} - \boldsymbol{m}_h^i - k\boldsymbol{v}_h^i$ in the $\boldsymbol{L}^2$-norm. However, the Hölder inequality and $\boldsymbol{m}_h^i \in \boldsymbol{\mathcal{M}}_h$ yield that

$$
\begin{aligned}
\langle \boldsymbol{\pi}(\boldsymbol{m}_h^i), \boldsymbol{m}_h^{i+1} - \boldsymbol{m}_h^i - k\boldsymbol{v}_h^i\rangle_{\boldsymbol{L}^2(\omega)} &\leq \|\boldsymbol{\pi}(\boldsymbol{m}_h^i)\|_{\boldsymbol{L}^3(\omega)}\, \|\boldsymbol{m}_h^{i+1} - \boldsymbol{m}_h^i - k\,\boldsymbol{v}_h^i\|_{\boldsymbol{L}^{3/2}(\omega)} \\
&\overset{\textbf{(T6)}}{\lesssim} \|\boldsymbol{m}_h^i\|_{\boldsymbol{L}^3(\omega)}\, \|\boldsymbol{m}_h^{i+1} - \boldsymbol{m}_h^i - k\,\boldsymbol{v}_h^i\|_{\boldsymbol{L}^{3/2}(\omega)} \\
&\lesssim \|\boldsymbol{m}_h^{i+1} - \boldsymbol{m}_h^i - k\boldsymbol{v}_h^i\|_{\boldsymbol{L}^{3/2}(\omega)}.
\end{aligned}
$$

With Lemma B.1.4(ii) for $p = 3/2$, we get that

$$\|\boldsymbol{m}_h^{i+1} - \boldsymbol{m}_h^i - k\,\boldsymbol{v}_h^i\|_{\boldsymbol{L}^{3/2}(\omega)} \lesssim k^2\,\|\boldsymbol{v}_h^i\|_{\boldsymbol{L}^3(\omega)}^2. \tag{4.57a}$$

Then, an interpolation estimate (see Proposition 2.1.1 with $p = 2$, $q = 3$, $r = 6$, and $\theta = 1/2$) and the Sobolev embedding $\boldsymbol{H}^1(\omega) \subset \boldsymbol{L}^6(\omega)$ (see Theorem 2.1.3) further yield that

$$\begin{aligned} k^2\,\|\boldsymbol{v}_h^i\|_{\boldsymbol{L}^3(\omega)}^2 &\le k^2\,\|\boldsymbol{v}_h^i\|_{\boldsymbol{L}^2(\omega)}\,\|\boldsymbol{v}_h^i\|_{\boldsymbol{L}^6(\omega)} \le k^2\,\|\boldsymbol{v}_h^i\|_{\boldsymbol{L}^2(\omega)}\,\|\boldsymbol{v}_h^i\|_{\boldsymbol{H}^1(\omega)} \\ &\lesssim k^2\,\|\boldsymbol{v}_h^i\|_{\boldsymbol{L}^2(\omega)}^2 + k^2\,\|\boldsymbol{v}_h^i\|_{\boldsymbol{L}^2(\omega)}\,\|\nabla\boldsymbol{v}_h^i\|_{\boldsymbol{L}^2(\omega)}. \end{aligned} \tag{4.57b}$$

For the third term on the right-hand side of (4.56), Lemma B.1.4(ii) yields that

$$\Big|\,\frac{1}{2}\langle\boldsymbol{\pi}(\boldsymbol{m}_h^{i+1} - \boldsymbol{m}_h^i), \boldsymbol{m}_h^{i+1} - \boldsymbol{m}_h^i\rangle_{\boldsymbol{L}^2(\omega)}\Big| \overset{\textbf{(L2)}}{\lesssim} \|\boldsymbol{m}_h^{i+1} - \boldsymbol{m}_h^i\|_{\boldsymbol{L}^2(\omega)}^2 \lesssim k^2\,\|\boldsymbol{v}_h^i\|_{\boldsymbol{L}^2(\omega)}^2.$$

Altogether, the combination of the latter steps yields that

$$\begin{aligned} \sum_{\ell=1}^{3} T_{\boldsymbol{\pi}}^{(\ell)} \lesssim k\,\Big|\,\langle\boldsymbol{\pi}_h^{\boldsymbol{D}}(\boldsymbol{v}_h^i;\boldsymbol{m}_h^i,\boldsymbol{m}_h^{i-1}) - \boldsymbol{\pi}(\boldsymbol{m}_h^i), \boldsymbol{v}_h^i\rangle_{\boldsymbol{L}^2(\omega)}\Big| \\ + k^2\,\|\boldsymbol{v}_h^i\|_{\boldsymbol{L}^2(\omega)}^2 + k^2\,\|\boldsymbol{v}_h^i\|_{\boldsymbol{L}^2(\omega)}\,\|\nabla\boldsymbol{v}_h^i\|_{\boldsymbol{L}^2(\omega)}. \end{aligned}$$

Step 3. We deal with $\sum_{\ell=1}^3 T_{\boldsymbol{f}}^{(\ell)}$: We get that

$$\begin{aligned} \sum_{\ell=1}^{3} T_{\boldsymbol{f}}^{(\ell)} &\overset{(4.55)}{=} k\langle\boldsymbol{f}_h^{i+1/2}, \boldsymbol{v}_h^i\rangle_{\boldsymbol{L}^2(\omega)} - \langle\boldsymbol{f}^{i+1}, \boldsymbol{m}_h^{i+1}\rangle_{\boldsymbol{L}^2(\omega)} + \langle\boldsymbol{f}^i, \boldsymbol{m}_h^i\rangle_{\boldsymbol{L}^2(\omega)} \\ &= k\langle\boldsymbol{f}_h^{i+1/2}, \boldsymbol{v}_h^i\rangle_{\boldsymbol{L}^2(\omega)} - k\langle\boldsymbol{f}^{i+1}, \boldsymbol{v}_h^i\rangle_{\boldsymbol{L}^2(\omega)} + k\langle\boldsymbol{f}^{i+1}, \boldsymbol{v}_h^i\rangle_{\boldsymbol{L}^2(\omega)} \\ &\quad - \langle\boldsymbol{f}^{i+1}, \boldsymbol{m}_h^{i+1}\rangle_{\boldsymbol{L}^2(\omega)} + \langle\boldsymbol{f}^{i+1}, \boldsymbol{m}_h^i\rangle_{\boldsymbol{L}^2(\omega)} - \langle\boldsymbol{f}^{i+1}, \boldsymbol{m}_h^i\rangle_{\boldsymbol{L}^2(\omega)} \\ &\quad + \langle\boldsymbol{f}^i, \boldsymbol{m}_h^i\rangle_{\boldsymbol{L}^2(\omega)} \\ &= k\,\langle\boldsymbol{f}_h^{i+1/2} - \boldsymbol{f}^{i+1}, \boldsymbol{v}_h^i\rangle_{\boldsymbol{L}^2(\omega)} - \langle\boldsymbol{f}^{i+1}, \boldsymbol{m}_h^{i+1} - \boldsymbol{m}_h^i - k\boldsymbol{v}_h^i\rangle_{\boldsymbol{L}^2(\omega)} \\ &\quad - k\,\langle\mathrm{d_t}\boldsymbol{f}^{i+1}, \boldsymbol{m}_h^i\rangle_{\boldsymbol{L}^2(\omega)}. \end{aligned}$$

In order to estimate the second term in the latter equation, we argue as in **Step 2**. With the estimates from (4.57), the Hölder inequality yields that

$$\begin{aligned} \Big|\,\langle\boldsymbol{f}^{i+1}, \boldsymbol{m}_h^{i+1} - \boldsymbol{m}_h^i - k\boldsymbol{v}_h^i\rangle_{\boldsymbol{L}^2(\omega)}\Big| &\le \|\boldsymbol{f}^{i+1}\|_{\boldsymbol{L}^3(\omega)}\,\|\boldsymbol{m}_h^{i+1} - \boldsymbol{m}_h^i - k\boldsymbol{v}_h^i\|_{\boldsymbol{L}^{3/2}(\omega)} \\ &\overset{\textbf{(T7)}}{\lesssim} \|\boldsymbol{m}_h^{i+1} - \boldsymbol{m}_h^i - k\boldsymbol{v}_h^i\|_{\boldsymbol{L}^{3/2}(\omega)} \lesssim k^2\,\|\boldsymbol{v}_h^i\|_{\boldsymbol{L}^2(\omega)}^2 + k^2\,\|\boldsymbol{v}_h^i\|_{\boldsymbol{L}^2(\omega)}\,\|\nabla\boldsymbol{v}_h^i\|_{\boldsymbol{L}^2(\omega)}. \end{aligned}$$

Then, the combination of the latter steps yields that

$$\begin{aligned} \sum_{\ell=1}^{3} T_{\boldsymbol{f}}^{(\ell)} + k\,\langle\mathrm{d_t}\boldsymbol{f}^{i+1}, \boldsymbol{m}_h^i\rangle_{\boldsymbol{L}^2(\omega)} \lesssim k\Big|\,\langle\boldsymbol{f}_h^{i+1/2} - \boldsymbol{f}^{i+1}, \boldsymbol{v}_h^i\rangle_{\boldsymbol{L}^2(\omega)}\Big| \\ + k^2\,\|\boldsymbol{v}_h^i\|_{\boldsymbol{L}^2(\omega)}^2 + k^2\,\|\boldsymbol{v}_h^i\|_{\boldsymbol{L}^2(\omega)}\,\|\nabla\boldsymbol{v}_h^i\|_{\boldsymbol{L}^2(\omega)}. \end{aligned}$$

Step 4. We combine **Step 1**–**Step 3**. Since $\rho(k) \geq 0$, we can omit $(C_{\mathbf{ex}}/2)\,\rho(k)k\|\nabla \boldsymbol{v}_h^i\|^2_{\boldsymbol{L}^2(\omega)}$ in (4.55). We obtain that

$$
\begin{aligned}
&\mathcal{E}_{\mathrm{LLG}}(\boldsymbol{m}_h^{i+1}) - \mathcal{E}_{\mathrm{LLG}}(\boldsymbol{m}_h^i) + k\langle \mathcal{W}_{G(k)}(\lambda_{hk}^-)\boldsymbol{v}_h^i, \boldsymbol{v}_h^i\rangle_{\boldsymbol{L}^2(\omega)} \\
&\quad + k\langle \mathrm{d_t}\boldsymbol{f}^{i+1}, \boldsymbol{m}_h^i\rangle_{\boldsymbol{L}^2(\omega)} - k\,\langle \boldsymbol{\Pi}_h^{\boldsymbol{D}}(\boldsymbol{v}_h^i; \boldsymbol{m}_h^i, \boldsymbol{m}_h^{i-1}), \boldsymbol{v}_h^i\rangle_{\boldsymbol{L}^2(\omega)} \\
&\overset{(4.55)}{\lesssim} k\,\Big|\,\langle \boldsymbol{\pi}_h^{\boldsymbol{D}}(\boldsymbol{v}_h^i; \boldsymbol{m}_h^i, \boldsymbol{m}_h^{i-1}) - \boldsymbol{\pi}(\boldsymbol{m}_h^i), \boldsymbol{v}_h^i\rangle_{\boldsymbol{L}^2(\omega)}\Big| + k\,\Big|\,\langle \boldsymbol{f}_h^{i+1/2} - \boldsymbol{f}^{i+1}, \boldsymbol{v}_h^i\rangle_{\boldsymbol{L}^2(\omega)}\Big| \\
&\quad + k^2\,\|\boldsymbol{v}_h^i\|^2_{\boldsymbol{L}^2(\omega)} + k^2\,\|\boldsymbol{v}_h^i\|_{\boldsymbol{L}^2(\omega)}\,\|\nabla \boldsymbol{v}_h^i\|_{\boldsymbol{L}^2(\omega)}.
\end{aligned}
$$

We sum in the latter estimate over $i = 0, \dots, j-1$. With the telescopic sum property, we obtain that

$$
\begin{aligned}
&\mathcal{E}_{\mathrm{LLG}}(\boldsymbol{m}_h^j) - \mathcal{E}_{\mathrm{LLG}}(\boldsymbol{m}_h^0) + k\sum_{i=0}^{j-1} \langle \mathcal{W}_{G(k)}(\lambda_{hk}^-)\boldsymbol{v}_h^i, \boldsymbol{v}_h^i\rangle_{\boldsymbol{L}^2(\omega)} \\
&\quad + k\sum_{i=0}^{j-1} \langle \mathrm{d_t}\boldsymbol{f}^{i+1}, \boldsymbol{m}_h^i\rangle_{\boldsymbol{L}^2(\omega)} - k\sum_{i=0}^{j-1} \langle \boldsymbol{\Pi}_h^{\boldsymbol{D}}(\boldsymbol{v}_h^i; \boldsymbol{m}_h^i, \boldsymbol{m}_h^{i-1}), \boldsymbol{v}_h^i\rangle_{\boldsymbol{L}^2(\omega)} \\
&\lesssim k\sum_{i=0}^{j-1} \Big|\,\langle \boldsymbol{\pi}_h^{\boldsymbol{D}}(\boldsymbol{v}_h^i; \boldsymbol{m}_h^i, \boldsymbol{m}_h^{i-1}) - \boldsymbol{\pi}(\boldsymbol{m}_h^i), \boldsymbol{v}_h^i\rangle_{\boldsymbol{L}^2(\omega)}\Big| + k\sum_{i=0}^{j-1} \Big|\,\langle \boldsymbol{f}_h^{i+1/2} - \boldsymbol{f}^{i+1}, \boldsymbol{v}_h^i\rangle_{\boldsymbol{L}^2(\omega)}\Big| \\
&\quad + k^2\sum_{i=0}^{j-1} \|\boldsymbol{v}_h^i\|^2_{\boldsymbol{L}^2(\omega)} + k^2\sum_{i=0}^{j-1} \|\boldsymbol{v}_h^i\|_{\boldsymbol{L}^2(\omega)}\,\|\nabla \boldsymbol{v}_h^i\|_{\boldsymbol{L}^2(\omega)}.
\end{aligned}
$$

With the definition (3.3) of the postprocessed output, we rewrite the latter estimate as

$$
\begin{aligned}
&\mathcal{E}_{\mathrm{LLG}}(\boldsymbol{m}_{hk}^+(\tau)) - \mathcal{E}_{\mathrm{LLG}}(\boldsymbol{m}_h^0) + \int_0^{t_j} \langle \mathcal{W}_{G(k)}(\lambda_{hk}^-)\boldsymbol{v}_{hk}^-, \boldsymbol{v}_{hk}^-\rangle_{\boldsymbol{L}^2(\omega)}\,\mathrm{d}t \\
&\quad + \int_0^{t_j} \langle \partial_t \boldsymbol{f}_k, \boldsymbol{m}_{hk}^-\rangle_{\boldsymbol{L}^2(\omega)}\,\mathrm{d}t - \int_0^{t_j} \langle \boldsymbol{\Pi}_h^{\boldsymbol{D}}(\boldsymbol{v}_{hk}^-; \boldsymbol{m}_{hk}^-, \boldsymbol{m}_{hk}^{=}), \boldsymbol{v}_{hk}^-\rangle_{\boldsymbol{L}^2(\omega)}\,\mathrm{d}t \\
&\lesssim \int_0^{t_j} \Big|\,\langle \boldsymbol{\pi}_h^{\boldsymbol{D}}(\boldsymbol{v}_{hk}^-; \boldsymbol{m}_{hk}^-, \boldsymbol{m}_{hk}^{=}) - \boldsymbol{\pi}(\boldsymbol{m}_{hk}^-), \boldsymbol{v}_{hk}^-\rangle_{\boldsymbol{L}^2(\omega)}\Big|\,\mathrm{d}t + \int_0^{t_j} \Big|\,\langle \overline{\boldsymbol{f}}_{hk} - \boldsymbol{f}_k, \boldsymbol{v}_{hk}^-\rangle_{\boldsymbol{L}^2(\omega)}\Big|\,\mathrm{d}t \\
&\quad + k\int_0^{t_j} \|\boldsymbol{v}_{hk}^-\|^2_{\boldsymbol{L}^2(\omega)}\,\mathrm{d}t + k\int_0^{t_j} \|\nabla \boldsymbol{v}_{hk}^-\|_{\boldsymbol{L}^2(\omega)}\|\boldsymbol{v}_{hk}^-\|_{\boldsymbol{L}^2(\omega)}\,\mathrm{d}t\,.
\end{aligned}
\tag{4.58}
$$

Step 5. We conclude the proof with standard lower semi-continuity arguments: To this end, we require the strong consistencies **(D4⁺)**, **(D7⁺)** and **(T5⁺)** of $\boldsymbol{\pi}_h$, $\boldsymbol{\Pi}_h$ and $\boldsymbol{D}_h$, respectively, for the convergence properties from Lemma 4.5.9. Together with linearity **(L1)** as well as boundedness **(L2)** of $\boldsymbol{\pi}$, we then get that

$$
\begin{aligned}
&\int_0^{t_j} \Big|\,\langle \boldsymbol{\pi}_h^{\boldsymbol{D}}(\boldsymbol{v}_{hk}^-; \boldsymbol{m}_{hk}^-, \boldsymbol{m}_{hk}^{=}) - \boldsymbol{\pi}(\boldsymbol{m}_{hk}^-), \boldsymbol{v}_{hk}^-\rangle_{\boldsymbol{L}^2(\omega)}\Big|\,\mathrm{d}t \to 0, \quad \text{and} \\
&\qquad\qquad \int_0^{t_j} \langle \boldsymbol{\Pi}_h^{\boldsymbol{D}}(\boldsymbol{v}_{hk}^-; \boldsymbol{m}_{hk}^-, \boldsymbol{m}_{hk}^{=}), \boldsymbol{v}_{hk}^-\rangle_{\boldsymbol{L}^2(\omega)}\,\mathrm{d}t \to \int_0^{\tau} \langle \boldsymbol{\Pi}(\boldsymbol{m}), \partial_t \boldsymbol{m}\rangle_{\boldsymbol{L}^2(\omega)}\,\mathrm{d}t
\end{aligned}
$$

as $h, k \to 0$. Together with the consistency **(D5$^+$)** of $(\boldsymbol{f}_h^i)_{i=0}^M$, the right-hand side of (4.58) vanishes as $h, k \to 0$. Moreover, the no-concentration of Lebesgue functions yields that

$$\int_0^{t_j} \langle \partial_t \boldsymbol{f}_k, \boldsymbol{m}_{hk}^- \rangle_{\boldsymbol{L}^2(\omega)} \,\mathrm{d}t \overset{\textbf{(D5}^+\textbf{)}}{\to} \int_0^{\tau} \langle \partial_t \boldsymbol{f}, \boldsymbol{m} \rangle_{\boldsymbol{L}^2(\omega)} \,\mathrm{d}t \quad \text{as } h, k \to 0.$$

Next, we get that

$$\mathcal{E}_{\mathrm{LLG}}(\boldsymbol{m}_h^0) \overset{\textbf{(D1}^+\textbf{)}}{\to} \mathcal{E}_{\mathrm{LLG}}(\boldsymbol{m}^0) \quad \text{as } h, k \to 0.$$

With Lemma 4.3.3(ii) and the convergence properties from Lemma 4.5.4, standard lower semi-continuity arguments yield for arbitrary intervals $I \subset [0, T]$ that

$$\begin{aligned}
&\int_I \bigg(\mathcal{E}_{\mathrm{LLG}}(\boldsymbol{m}(\tau)) + \alpha \int_0^{\tau} \|\partial_t \boldsymbol{m}\|_{\boldsymbol{L}^2(\omega)}^2 \,\mathrm{d}t \bigg) \,\mathrm{d}\tau \\
&\quad \le \liminf_{h,k \to 0} \int_I \bigg(\mathcal{E}_{\mathrm{LLG}}(\boldsymbol{m}_{hk}^+(\tau)) + \inf_{x \in \omega} |\mathcal{W}_{G(k)}(x)| \int_0^{\tau} \|\boldsymbol{v}_{hk}^-\|_{\boldsymbol{L}^2(\omega)}^2 \,\mathrm{d}t \bigg) \,\mathrm{d}\tau \\
&\quad \le \liminf_{h,k \to 0} \int_I \bigg(\mathcal{E}_{\mathrm{LLG}}(\boldsymbol{m}_{hk}^+(\tau)) + \int_0^{\tau} \langle \mathcal{W}_{G(k)}(\lambda_{hk}^-) \boldsymbol{v}_{hk}^-, \boldsymbol{v}_{hk}^- \rangle_{\boldsymbol{L}^2(\omega)} \,\mathrm{d}t \bigg) \,\mathrm{d}\tau \,.
\end{aligned}$$

Altogether, we obtain that

$$\begin{aligned}
&\int_I \bigg(\mathcal{E}_{\mathrm{LLG}}(\boldsymbol{m}(\tau)) + \alpha \int_0^{\tau} \|\partial_t \boldsymbol{m}\|_{\boldsymbol{L}^2(\omega)}^2 \,\mathrm{d}t \bigg) \,\mathrm{d}\tau \\
&\quad + \int_I \bigg(\int_0^{\tau} \langle \partial_t \boldsymbol{f}, \boldsymbol{m} \rangle_{\boldsymbol{L}^2(\omega)} \,\mathrm{d}t - \int_0^{\tau} \langle \boldsymbol{\Pi}(\boldsymbol{m}), \partial_t \boldsymbol{m} \rangle_{\boldsymbol{L}^2(\omega)} \,\mathrm{d}t \bigg) \,\mathrm{d}\tau \overset{(4.58)}{\le} \int_I \mathcal{E}_{\mathrm{LLG}}(\boldsymbol{m}^0) \,\mathrm{d}\tau \,.
\end{aligned}$$

Since the interval $I \subset [0, T]$ was arbitrary, the latter estimate also holds pointwise a.e. in $(0, T)$. This concludes the proof. □

4.6. How to solve the discrete variational formulation

Given a time-step $\boldsymbol{m}_h^i \in \boldsymbol{\mathcal{M}}_h$, this section focuses on how to solve the discrete variational problem (4.9). Here, we face two main issues:

- While the discrete variational formulation (4.9) in general gives rise to a linear system for $\boldsymbol{v}_h^i$, the corresponding system matrix for the implicit approaches may be fully populated or not even explicitly available. Then, the remedy is a fixed-point iteration; see Section 4.6.1, which is based on the own work [DPP+17].

- The discrete variational formulation (4.9) gives rise to a variational problem, which has to solved in the time-dependent subspace $\boldsymbol{\mathcal{K}}_h(\boldsymbol{m}_h^i) \subsetneqq \boldsymbol{\mathcal{S}}_h$. In Section 4.6.2, we present a strategy, which, on a linear algebra level, allows us to solve a corresponding $2N$-dimensional problem. This section is based on [KPP+18, Section 3] and a corresponding (and very similar) approach for the first-order tangent-plane scheme is also contained in [Rug16, Section 6.1.2].

Related to both problems and throughout this section, we define for $\boldsymbol{\psi}_h, \boldsymbol{\varphi}_h \in \boldsymbol{\mathcal{K}}_h(\boldsymbol{m}_h^i)$ the bilinear form

$$
\begin{aligned}
\boldsymbol{B}_h^i(\boldsymbol{\psi}_h, \boldsymbol{\varphi}_h) := \langle \mathcal{W}_{G(k)}(\lambda_h^i)\, \boldsymbol{\psi}_h, \boldsymbol{\varphi}_h \rangle_{\boldsymbol{L}^2(\omega)} + \langle \boldsymbol{m}_h^i \times \boldsymbol{\psi}_h, \boldsymbol{\varphi}_h \rangle_{\boldsymbol{L}^2(\omega)} \\
+ \frac{C_{\mathbf{ex}}}{2}\, k\,(1+\rho(k))\, \langle \nabla \boldsymbol{\psi}_h, \nabla \boldsymbol{\varphi}_h \rangle_{\boldsymbol{L}^2(\omega)}
\end{aligned}
\tag{4.59a}
$$

as well as the linear functional

$$
\boldsymbol{R}_h^i(\boldsymbol{\varphi}_h) := -C_{\mathbf{ex}}\, \langle \nabla \boldsymbol{m}_h^i, \nabla \boldsymbol{\varphi}_h \rangle_{\boldsymbol{L}^2(\omega)} + \langle \boldsymbol{\pi}_h(\boldsymbol{m}_h^i), \boldsymbol{\varphi}_h \rangle_{\boldsymbol{L}^2(\omega)} + \langle \boldsymbol{f}_h^{i+1/2}, \boldsymbol{\varphi}_h \rangle_{\omega}. \tag{4.59b}
$$

4.6.1. Fixed-point iteration for the implicit approach

Consider the implicit approach **(A1)** and the Adams–Bashforth-type approach **(A2)** with $i = 0$. Suppose linearity **(D2)** of $\boldsymbol{\pi}_h$ and linearity in the second argument **(T3)**. Then, to solve discrete variational formulation (4.9), one has to find $\boldsymbol{v}_h^i \in \boldsymbol{\mathcal{K}}_h(\boldsymbol{m}_h^i)$ such that

$$
\boldsymbol{B}_h^i(\boldsymbol{v}_h^i, \boldsymbol{\varphi}_h) - \frac{k}{2}\, \langle \boldsymbol{\pi}_h(\boldsymbol{v}_h^i), \boldsymbol{\varphi}_h \rangle_{\boldsymbol{L}^2(\omega)} - \frac{k}{2}\, \langle \boldsymbol{D}_h(\boldsymbol{v}_h^i, \boldsymbol{\psi}_h), \boldsymbol{\varphi}_h \rangle_{\boldsymbol{L}^2(\omega)} = \boldsymbol{R}_h^i(\boldsymbol{\varphi}_h),
$$

for all $\boldsymbol{\varphi}_h \in \boldsymbol{\mathcal{K}}_h(\boldsymbol{m}_h^i)$. Here, the terms

$$
\frac{k}{2}\, \langle \boldsymbol{\pi}_h(\boldsymbol{v}_h^i), \boldsymbol{\varphi}_h \rangle_{\boldsymbol{L}^2(\omega)} \quad \text{and} \quad \frac{k}{2}\, \langle \boldsymbol{D}_h(\boldsymbol{v}_h^i, \boldsymbol{\psi}_h), \boldsymbol{\varphi}_h \rangle_{\boldsymbol{L}^2(\omega)}. \tag{4.60}
$$

are of particular interest. If, for example, (non-local) approximate stray field computations with the Fredkin–Koehler method [FK90] (see Section 3.4.5) contribute to the operator $\boldsymbol{\pi}_h$, the corresponding matrix is fully-populated and/or can only be assembled with sufficient accuracy at high computational costs; cf. [DPP⁺17, Remark 3(i)]. To ship around this issue, we proceed as in the own work [DPP⁺17]: We incorporate the terms from (4.60) in the right-hand side and solve the resulting system by a fixed-point iteration. Given $\boldsymbol{m}_h^i \in \boldsymbol{\mathcal{M}}_h$, the following algorithm then performs one (inexact) time-step with Algorithm 4.2.1. It is implicitly contained in [DPP⁺17, p.15f].

Algorithm 4.6.1 (Inexact implicit TPS 2.0, one time-step, [DPP⁺17, p.15f])**. Input:** $\boldsymbol{m}_h^i \in \boldsymbol{\mathcal{M}}_h$, *initial guess* $\boldsymbol{u}_h^{(0)} := \mathbf{0} \in \boldsymbol{\mathcal{K}}_h(\boldsymbol{m}_h^i)$, *iteration tolerance* $\varepsilon > 0$. *Iterate the following steps* (a)–(b).

(a) **Loop:** *For* $\ell = 1, 2, \dots,$ *and until*

$$
\|\boldsymbol{u}_h^{(\ell+1)} - \boldsymbol{u}_h^{(\ell)}\|_{\boldsymbol{L}^2(\omega)} \le \varepsilon
$$

find $\boldsymbol{u}_h^{(\ell+1)} \in \boldsymbol{\mathcal{K}}_h(\boldsymbol{m}_h^i)$ *such that*

$$
\boldsymbol{B}_h^i(\boldsymbol{u}_h^{(\ell+1)}, \boldsymbol{\varphi}_h) = \boldsymbol{R}_h^i(\boldsymbol{\varphi}_h) + \frac{k}{2}\langle \boldsymbol{\pi}_h(\boldsymbol{u}_h^{(\ell)}), \boldsymbol{\varphi}_h \rangle_{\boldsymbol{L}^2(\omega)} + \frac{k}{2}\langle \boldsymbol{D}_h(\boldsymbol{m}_h^i, \boldsymbol{u}_h^{(\ell)}), \boldsymbol{\varphi}_h \rangle_{\boldsymbol{L}^2(\omega)} \tag{4.61}
$$

for all $\boldsymbol{\varphi}_h \in \boldsymbol{\mathcal{K}}_h(\boldsymbol{m}_h^i)$, *where* $\boldsymbol{B}_h^i(\cdot,\cdot)$ *and* $\boldsymbol{R}_h^i(\cdot)$ *stem from* (4.59).

(b) *Define* $\boldsymbol{m}_h^{i+1} \in \boldsymbol{\mathcal{M}}_h$ *by*

$$\boldsymbol{m}_h^{i+1}(\boldsymbol{z}) := \frac{\boldsymbol{m}_h^i(\boldsymbol{z}) + k\,\boldsymbol{u}_h^{(\ell+1)}(\boldsymbol{z})}{|\boldsymbol{m}_h^i(\boldsymbol{z}) + k\,\boldsymbol{u}_h^{(\ell+1)}(\boldsymbol{z})|} \quad \textit{for all nodes } \boldsymbol{z} \in \mathcal{N}_h. \tag{4.62}$$

Output: *Approximation* $\boldsymbol{m}_h^{i+1} \approx \boldsymbol{m}(t_{i+1})$. □

Remark 4.6.2. *Since* $\boldsymbol{u}_h^{(\ell+1)} \in \boldsymbol{\mathcal{K}}_h(\boldsymbol{m}_h^i)$*, we conclude as in Remark 4.2.2*(v) *that the update* (4.62) *is well-defined.*

For sufficiently small $k > 0$, the following proposition proves convergence of $\boldsymbol{u}_h^{(\ell)}$ towards the sought $\boldsymbol{v}_h^i \in \boldsymbol{\mathcal{K}}_h(\boldsymbol{m}_h^i)$ as $\ell \to 0$. To this end, we require the following stronger version of the assumption **(T4)** to $\boldsymbol{D}_h$:

(T4$^+$) Strong uniform boundedness of $\boldsymbol{D}_h$: There exists a constant $C_{\boldsymbol{D}} > 0$ such that, for all $h > 0$, it holds that

$$\|\boldsymbol{D}_h(\boldsymbol{\varphi}_h, \boldsymbol{\psi}_h)\|_{\boldsymbol{L}^2(\omega)} \le C_{\boldsymbol{D}}\, \|\boldsymbol{\psi}_h\|_{\boldsymbol{H}^1(\omega)} \quad \text{for all } \boldsymbol{\varphi}_h \in \boldsymbol{\mathcal{M}}_h \text{ and all } \boldsymbol{\psi}_h \in \boldsymbol{\mathcal{S}}_h.$$

Implicitly, the following convergence result of the fixed-point iteration in Algorithm 4.6.1(a) is contained in the proof of [DPP$^+$17, Theorem 4(i)].

Proposition 4.6.3 (Convergence of fixed-point iteration, [DPP$^+$17, p.15f])**.** *Consider the fixed-point iteration from Algorithm 4.6.1. Suppose linearity* **(D2)** *and uniform boundedness* **(D3)** *of* $\boldsymbol{\pi}_h$*. Suppose linearity in the second-argument* **(T2)** *and strong uniform boundedness* **(T4$^+$)** *of* $\boldsymbol{D}_h$*. Then, the fixed-point iterates* $\boldsymbol{u}_h^{(\ell)}$ *from* (4.61) *are well-defined. For sufficiently small* $k > 0$*, it holds that*

$$\boldsymbol{u}_h^{(\ell)} \to \boldsymbol{v}_h^i \quad \textit{in } \boldsymbol{L}^2(\omega) \quad \textit{as } \ell \to \infty,$$

where $\boldsymbol{v}_h^i \in \boldsymbol{\mathcal{K}}_h(\boldsymbol{m}_h^i)$ *is the unique solution* $\boldsymbol{v}_h^i$ *of the discrete variational problem* (4.9)*.*

Proof. For $\boldsymbol{\varphi}_h \in \boldsymbol{\mathcal{K}}_h(\boldsymbol{m}_h^i)$, we define the energy norm

$$|\!|\!|\boldsymbol{\varphi}_h|\!|\!|^2 := \frac{\alpha}{2}\|\boldsymbol{\varphi}_h\|_{\boldsymbol{L}^2(\omega)}^2 + \frac{C_{\mathbf{ex}}}{2} k\,\|\nabla\boldsymbol{\varphi}_h\|_{\boldsymbol{L}^2(\omega)}^2. \tag{4.63}$$

For sufficiently small $k > 0$, we get from Lemma 4.3.3(i) that

$$\boldsymbol{B}_h^i(\boldsymbol{\varphi}_h, \boldsymbol{\varphi}_h) \ge |\!|\!|\boldsymbol{\varphi}_h|\!|\!|^2 \quad \text{for all } \boldsymbol{\varphi}_h \in \boldsymbol{\mathcal{K}}_h(\boldsymbol{m}_h^i). \tag{4.64}$$

i.e., $\boldsymbol{B}_h^i$ is positive definite with respect to $|\!|\!| \cdot |\!|\!|$. As a consequence, the Lax–Milgram theorem (see Theorem B.2.4) yields existence and uniqueness of the fixed-point iterates $\boldsymbol{u}_h^{(\ell)} \in \boldsymbol{\mathcal{K}}_h(\boldsymbol{m}_h^i)$. Moreover, linearity **(D2)** and **(T3)** of $\boldsymbol{\pi}_h$ and $\boldsymbol{D}_h$, respectively, yield for all $\ell \in \mathbb{N}_0$ and all $\boldsymbol{\varphi}_h \in \boldsymbol{\mathcal{K}}_h(\boldsymbol{m}_h^i)$ that

$$\begin{aligned}
&\boldsymbol{B}_h^i(\boldsymbol{u}_h^{(\ell+1)} - \boldsymbol{u}_h^{(\ell)}, \boldsymbol{\varphi}_h) \\
&\overset{(4.61)}{=} \frac{k}{2}\,\langle \boldsymbol{\pi}_h(\boldsymbol{u}_h^{(\ell)}), \boldsymbol{\varphi}_h\rangle_{\boldsymbol{L}^2(\omega)} + \frac{k}{2}\,\langle \boldsymbol{D}_h(\boldsymbol{m}_h^i, \boldsymbol{u}_h^{(\ell)}), \boldsymbol{\varphi}_h\rangle_{\boldsymbol{L}^2(\omega)} \\
&\qquad - \frac{k}{2}\,\langle \boldsymbol{\pi}_h(\boldsymbol{u}_h^{(\ell-1)}), \boldsymbol{\varphi}_h\rangle_{\boldsymbol{L}^2(\omega)} - \frac{k}{2}\,\langle \boldsymbol{D}_h(\boldsymbol{m}_h^i, \boldsymbol{u}_h^{(\ell-1)}), \boldsymbol{\varphi}_h\rangle_{\boldsymbol{L}^2(\omega)} \\
&= \frac{k}{2}\,\langle \boldsymbol{\pi}_h(\boldsymbol{u}_h^{(\ell)} - \boldsymbol{u}_h^{(\ell-1)}), \boldsymbol{\varphi}_h\rangle_{\boldsymbol{L}^2(\omega)} + \frac{k}{2}\,\langle \boldsymbol{D}_h(\boldsymbol{m}_h^i, \boldsymbol{u}_h^{(\ell)} - \boldsymbol{u}_h^{(\ell-1)}), \boldsymbol{\varphi}_h\rangle_{\boldsymbol{L}^2(\omega)}.
\end{aligned}$$

Testing the latter equation with $\boldsymbol{\varphi}_h := \boldsymbol{u}_h^{(\ell+1)} - \boldsymbol{u}_h^{(\ell)}$, we infer from uniform boundedness **(D3)** of $\boldsymbol{\pi}_h$ and stronger uniform boundedness **(T4$^+$)** of $\boldsymbol{D}_h$ that

$$\begin{aligned}
&|||\boldsymbol{u}_h^{(\ell+1)} - \boldsymbol{u}_h^{(\ell)}|||^2 \overset{(4.64)}{\leq} \boldsymbol{B}_h^i(\boldsymbol{u}_h^{(\ell+1)} - \boldsymbol{u}_h^{(\ell)}, \boldsymbol{u}_h^{(\ell+1)} - \boldsymbol{u}_h^{(\ell)}) \\
&= \frac{k}{2}\,\langle \boldsymbol{\pi}_h(\boldsymbol{u}_h^{(\ell)} - \boldsymbol{u}_h^{(\ell-1)}), \boldsymbol{u}_h^{(\ell+1)} - \boldsymbol{u}_h^{(\ell)}\rangle_{\boldsymbol{L}^2(\omega)} + \frac{k}{2}\,\langle \boldsymbol{D}_h(\boldsymbol{m}_h^i, \boldsymbol{u}_h^{(\ell)} - \boldsymbol{u}_h^{(\ell-1)}), \boldsymbol{u}_h^{(\ell+1)} - \boldsymbol{u}_h^{(\ell)}\rangle_{\boldsymbol{L}^2(\omega)} \\
&\leq C_{\boldsymbol{\pi}}\,\frac{k}{2}\,\|\boldsymbol{u}_h^{(\ell)} - \boldsymbol{u}_h^{(\ell-1)}\|_{\boldsymbol{L}^2(\omega)}\,\|\boldsymbol{u}_h^{(\ell+1)} - \boldsymbol{u}_h^{(\ell)}\|_{\boldsymbol{L}^2(\omega)} \\
&\qquad + C_{\boldsymbol{D}}\,\frac{k}{2}\,\|\boldsymbol{u}_h^{(\ell)} - \boldsymbol{u}_h^{(\ell-1)}\|_{\boldsymbol{H}^1(\omega)}\,\|\boldsymbol{u}_h^{(\ell+1)} - \boldsymbol{u}_h^{(\ell)}\|_{\boldsymbol{L}^2(\omega)} &&(4.65)\\
&\leq \big[\, C_{\boldsymbol{\pi}} + C_{\boldsymbol{D}} \,\big]\,\frac{k}{2}\,\|\boldsymbol{u}_h^{(\ell)} - \boldsymbol{u}_h^{(\ell-1)}\|_{\boldsymbol{L}^2(\omega)}\,\|\boldsymbol{u}_h^{(\ell+1)} - \boldsymbol{u}_h^{(\ell)}\|_{\boldsymbol{L}^2(\omega)} \\
&\qquad + C_{\boldsymbol{D}}\,\frac{k}{2}\,\|\nabla\boldsymbol{u}_h^{(\ell)} - \nabla\boldsymbol{u}_h^{(\ell-1)}\|_{\boldsymbol{L}^2(\omega)}\,\|\boldsymbol{u}_h^{(\ell+1)} - \boldsymbol{u}_h^{(\ell)}\|_{\boldsymbol{L}^2(\omega)}. &&(4.66)
\end{aligned}$$

With the Young inequality, we get for arbitrary $\delta > 0$, that

$$\begin{aligned}
&|||\boldsymbol{u}_h^{(\ell+1)} - \boldsymbol{u}_h^{(\ell)}|||^2 \\
&\quad \overset{(4.63)}{\lesssim} \frac{k}{\delta}\,\|\boldsymbol{u}_h^{(\ell+1)} - \boldsymbol{u}_h^{(\ell)}\|^2_{\boldsymbol{L}^2(\omega)} + \delta k\,\|\boldsymbol{u}_h^{(\ell)} - \boldsymbol{u}_h^{(\ell-1)}\|^2_{\boldsymbol{L}^2(\omega)} + \delta k\,\|\nabla\boldsymbol{u}_h^{(\ell)} - \nabla\boldsymbol{u}_h^{(\ell-1)}\|^2_{\boldsymbol{L}^2(\omega)} \\
&\quad \lesssim \frac{k}{\delta}\,|||\boldsymbol{u}_h^{(\ell+1)} - \boldsymbol{u}_h^{(\ell)}|||^2 + \delta\,|||\boldsymbol{u}_h^{(\ell)} - \boldsymbol{u}_h^{(\ell-1)}|||^2,
\end{aligned}$$

i.e., there exists a constant $C > 0$ which depends only on α, $C_{\mathbf{ex}}$, $C_{\boldsymbol{\pi}}$, and $C_{\boldsymbol{\Pi}}$ such that, for arbitrary $\delta > 0$, it holds that

$$|||\boldsymbol{u}_h^{(\ell+1)} - \boldsymbol{u}_h^{(\ell)}|||^2 \leq C\,\frac{k}{\delta}\,|||\boldsymbol{u}_h^{(\ell+1)} - \boldsymbol{u}_h^{(\ell)}|||^2 + C\,\delta\,|||\boldsymbol{u}_h^{(\ell)} - \boldsymbol{u}_h^{(\ell-1)}|||^2$$

With $\delta = 1/(2C)$ and $k \leq 1/(8C^2) := k_0$, we arrive at

$$|||\boldsymbol{u}_h^{(\ell+1)} - \boldsymbol{u}_h^{(\ell)}|||^2 \leq \frac{1}{4}\,|||\boldsymbol{u}_h^{(\ell+1)} - \boldsymbol{u}_h^{(\ell)}|||^2 + \frac{1}{2}\,|||\boldsymbol{u}_h^{(\ell)} - \boldsymbol{u}_h^{(\ell-1)}|||^2.$$

If we absorb the first term on the right-hand side of the latter equation, this yields that

$$|||\boldsymbol{u}_h^{(\ell+1)} - \boldsymbol{u}_h^{(\ell)}|||^2 \leq \frac{2}{3}\,|||\boldsymbol{u}_h^{(\ell)} - \boldsymbol{u}_h^{(\ell-1)}|||^2 \quad \text{for all } \ell \in \mathbb{N},$$

i.e., the sequence $(\boldsymbol{u}_h^{(\ell)})_{\ell=0}^{\infty}$ is a contraction with respect to the energy norm $|||\cdot|||$. Hence, the Banach fixed-point theorem (see Theorem B.2.6) yields convergence to a (unique) fixed-point $\boldsymbol{u}_h^{(\infty)} \in \boldsymbol{\mathcal{K}}_h(\boldsymbol{m}_h^i)$ of (4.61). Since any fixed-point of (4.61) solves the discrete variational formulation (4.9), we conclude from the uniqueness of solutions in Theorem 4.5.1(a) that $\boldsymbol{u}_h^{(\infty)} = \boldsymbol{v}_h^i$. □

Remark 4.6.4. (i) *Compared to Theorem 4.5.1*(a)*, Proposition 4.6.3 additionally requires the stronger uniform boundedness* **(T4$^+$)** *of* $\boldsymbol{D}_h$.

(ii) *The approximate uniaxial anisotropy and the approximate stray field as well as the approximate Slonczewksi field and the corresponding approximate derivation* $\boldsymbol{D}_h$ *satisfy all assumption of Proposition 4.6.3 to* $\boldsymbol{\pi}_h$, $\boldsymbol{\Pi}_h$ *and* $\boldsymbol{D}_h$*, respectively.*

(iii) *The approximate Zhang–Li field* $\boldsymbol{\Pi}_h$ *and the corresponding approximate derivation* $\boldsymbol{D}_h$ *satisfy all assumptions of Proposition 4.6.3, except the additional stronger uniform boundedness* **(T4⁺)** *of* $\boldsymbol{D}_h$*. In the proof, however, the assumption* **(T4⁺)** *is only needed to establish* (4.65)*. In particular, in the setting*

$$\|\nabla \boldsymbol{m}_h^0\|_{\boldsymbol{L}^\infty(\omega)} \lesssim 1 \qquad \text{and} \qquad \text{the Adams–Bashforth-type approach } (\mathbf{A2}) \tag{4.67}$$

we employ the fixed-point iteration only in the first time-step. This lets us bypass (4.65) *in our specific situation in the following way: For* $\boldsymbol{\psi}_h \in \boldsymbol{\mathcal{S}}_h$*, we estimate*

$$\begin{aligned}
&\|\boldsymbol{D}_h(\boldsymbol{m}_h^0, \boldsymbol{\psi}_h)\|_{\boldsymbol{L}^2(\omega)} \\
&\overset{(4.12)}{\leq} \|\boldsymbol{\psi}_h \times (\boldsymbol{u}\cdot\nabla)\,\boldsymbol{m}_h^0\|_{\boldsymbol{L}^2(\omega)} + \|\boldsymbol{m}_h^0 \times (\boldsymbol{u}\cdot\nabla)\,\boldsymbol{\psi}_h\|_{\boldsymbol{L}^2(\omega)} + \|\beta\,(\boldsymbol{u}\cdot\nabla)\,\boldsymbol{\psi}_h\|_{\boldsymbol{L}^2(\omega)} \\
&\lesssim \|\boldsymbol{\psi}_h\|_{\boldsymbol{L}^2(\omega)}\,\|\boldsymbol{u}\|_{\boldsymbol{L}^\infty(\omega)}\,\|\nabla \boldsymbol{m}_h^0\|_{\boldsymbol{L}^\infty(\omega)} + \big(\,\|\boldsymbol{m}_h^0\|_{\boldsymbol{L}^\infty(\omega)} + \beta\,\big)\,\|\boldsymbol{u}\|_{\boldsymbol{L}^\infty(\omega)}\,\|\nabla\boldsymbol{\psi}_h\|_{\boldsymbol{L}^2(\omega)} \\
&\overset{(4.67)}{\lesssim} \|\boldsymbol{\psi}_h\|_{\boldsymbol{H}^1(\omega)}.
\end{aligned}$$

Hence, in the setting of (4.67)*, the fixed-point iteration of the first time-step still converges towards* $\boldsymbol{v}_h^i$*.*

4.6.2. Solve the tangent space system

The discrete variational formulation (4.9) in the explicit cases as well as the subsequent discrete variational formulation (4.61) of the fixed-point iteration in the implicit cases give rise to the following variational problem: Find $\boldsymbol{\mu}_h \in \boldsymbol{\mathcal{K}}_h(\boldsymbol{m}_h^i)$ such that

$$\boldsymbol{B}_h^i(\boldsymbol{\mu}_h, \boldsymbol{\varphi}_h) = \widetilde{\boldsymbol{R}}_h^i(\boldsymbol{\varphi}_h) \quad \text{for all } \boldsymbol{\varphi}_h \in \boldsymbol{\mathcal{K}}_h(\boldsymbol{m}_h^i), \tag{4.68}$$

where the linear form $\widetilde{\boldsymbol{R}}_h^i(\cdot)$ depends on the choice of the general time-stepping approaches **(A1)**–**(A3)**. On a linear algebra level, problems arise, in particular, from the fact that $\boldsymbol{\mathcal{K}}_h(\boldsymbol{m}_h^i) \subsetneqq \boldsymbol{\mathcal{S}}_h$ and $\dim(\boldsymbol{\mathcal{K}}_h(\boldsymbol{m}_h^i)) = 2N$, while $\dim(\boldsymbol{\mathcal{S}}_h) = 3N$. Moreover, note that $\boldsymbol{\mathcal{K}}_h(\boldsymbol{m}_h^i)$ depends on the time-step $\boldsymbol{m}_h^i$. In the ongoing cooperation [KPP⁺18], we investigate solution techniques to solve (4.68) on a linear algebra level and to develop corresponding preconditioning techniques for the application of iterative methods (see, e.g.,[Saa03]). A closer look on these results, however, is beyond the scope of this work. We only state here the specific technique, which we use for our numerical computations. Note that for the first-order tangent plane scheme, the linear algebra techniques are also included in parts in [Rug16, Section 6.1].

We transfer (4.68) to a system in $2N = \dim(\boldsymbol{\mathcal{K}}_h(\boldsymbol{m}_h^i))$ dimensions; see also [Rug16, Section 6.1.2] and [KPP⁺18, Section 3]. Here, we follow the presentation of [KPP⁺18, Section 3]: Let $\varphi_j \in \mathcal{S}_h$ be the nodal hat function associated with $\boldsymbol{z}_j$, i.e., $\varphi_j(\boldsymbol{z}_k) = \delta_{jk}$ with Kronecker's delta. As basis of $\boldsymbol{\mathcal{S}}_h$, we define

$$\boldsymbol{\phi}_{3(j-1)+\ell} := \varphi_j\,\boldsymbol{e}_\ell \quad \text{for all } j = 1,\dots,N \text{ and all } \ell = 1,2,3,$$

i.e., for fixed $j \in \{1, \dots, N\}$ the three consecutive basis vectors obtained from $\ell \in \{1, 2, 3\}$ belong to the node $\boldsymbol{z}_j$. Then, define the matrix $\mathbf{A}(\boldsymbol{m}_h^i) \in \mathbb{R}^{3N \times 3N}$ via

$$\big[\,\mathbf{A}(\boldsymbol{m}_h^i)\,\big]_{jk} := \boldsymbol{B}_h^i(\boldsymbol{\phi}_k, \boldsymbol{\phi}_j) \quad \text{for all} \quad j, k \in \{1, \dots, 3N\},$$

and note that for k small enough $\mathbf{A}(\boldsymbol{m}_h^i)$ is positive definite; cf. Lemma 4.3.3(i). Moreover, define $\mathbf{r}(\boldsymbol{m}_h^i) \in \mathbb{R}^{3N}$ via

$$\big[\,\mathbf{r}(\boldsymbol{m}_h^i)\,\big]_j := \widetilde{\boldsymbol{R}}_h^i(\boldsymbol{\phi}_j) \quad \text{for all} \quad j \in \{1, \dots, 3N\}.$$

To map $\mathbb{R}^{2N}$ to $\boldsymbol{\mathcal{K}}_h(\boldsymbol{m}_h^i)$ on a coordinate level, we proceed as follows: Given $\mathbf{m} \in \mathbb{R}^3$ with $|\boldsymbol{m}| = 1$, the matrix

$$\mathbb{R}^{3\times 3} \ni \widetilde{\mathbf{H}}(\mathbf{m}) := \begin{cases} \mathbf{I} - 2\mathbf{w}\mathbf{w}^T, & \text{where} \quad \mathbf{w} := \frac{\mathbf{m}+\mathbf{e}_3}{|\mathbf{m}+\mathbf{e}_3|} \quad \text{for } \mathbf{m} \neq -\mathbf{e}_3, \\ \big[\,\mathbf{e}_1, \mathbf{e}_2, -\mathbf{e}_3\,\big] & \qquad\qquad\qquad\qquad\quad \text{for } \mathbf{m} = -\mathbf{e}_3. \end{cases}$$

has orthonormal columns and maps $\mathbf{e}_3$ to $\mathbf{m}$, i.e.,

$$\mathbf{H}(\mathbf{m}) := \big[\,\widetilde{\mathbf{H}}(\mathbf{m})\mathbf{e}_1, \widetilde{\mathbf{H}}(\mathbf{m})\mathbf{e}_2\,\big] \in \mathbb{R}^{3\times 2},$$

in `Matlab` notation satisfies span$(\mathbf{H}(\mathbf{m}))\perp\mathbf{m}$. Hence, the block-diagonal matrix

$$\mathbf{Q}(\boldsymbol{m}_h^i) := \begin{pmatrix} \mathbf{H}\big(\boldsymbol{m}_h^i(\boldsymbol{z}_1)\big) & \mathbf{0} & \cdots & \mathbf{0} \\ \mathbf{0} & \mathbf{H}\big(\boldsymbol{m}_h^i(\boldsymbol{z}_2)\big) & \ddots & \vdots \\ \vdots & \ddots & \ddots & \mathbf{0} \\ \mathbf{0} & \cdots & \mathbf{0} & \mathbf{H}\big(\boldsymbol{m}_h^i(\boldsymbol{z}_N)\big) \end{pmatrix} \in \mathbb{R}^{3N\times 2N}$$

mimics $\boldsymbol{\mathcal{K}}_h(\boldsymbol{m}_h^i)$ nodewise in each diagonal block. Then, [KPP+18, Theorem 3] proves that the reduced system

$$\big[\,\mathbf{Q}(\boldsymbol{m}_h^i)^T\mathbf{A}(\boldsymbol{m}_h^i)\mathbf{Q}(\boldsymbol{m}_h^i)\,\big]\,\mathbf{x} = \mathbf{Q}(\boldsymbol{m}_h^i)^T\mathbf{r}(\boldsymbol{m}_h^i)$$

admits a unique solution $\mathbf{x} \in \mathbb{R}^{2N}$ and that we can recover the sought solution $\boldsymbol{\mu}_h \in \boldsymbol{\mathcal{K}}_h(\boldsymbol{m}_h^i)$ to the discrete variational problem (4.68) from

$$\boldsymbol{\mu}_h = \sum_{j=1}^{3N} \big[\mathbf{Q}(\boldsymbol{m}_h^i)\,\mathbf{x}\,\big]_j \boldsymbol{\phi}_j \in \boldsymbol{\mathcal{K}}_h(\boldsymbol{m}_h^i).$$

5. Decoupled second-order tangent plane scheme for ELLG

The following chapter is based on [DPP+17], which is joint work with *Giovanni Di Fratta*[1], *Carl-Martin Pfeiler*[1], *Dirk Praetorius*[1], and *Michele Ruggeri*[2].

5.1. Introduction

In the chapter, we extend the effective (almost) second-order tangent plane scheme from Chaper 5 to the ELLG system (2.18).

For the coupled ELLG system (2.18) and the related coupling with the full Maxwell system, the works [LT13, Pag13, BPP15, LPPT15, FT17] formulate extensions of the (formally) first-order tangent plane scheme. There, [LT13, Pag13, LPPT15, BPP15] extend the techniques of [Alo08] and prove unconditional convergence in the sense of Convention 1.3.1. Moreover, [FT17] even proves a first-order in time and space a-priori estimate for a tangent plane scheme for ELLG in the spirit of [AHP+14, Rug16]. Moreover, [LPPT15, Pag13, BPP15, FT17] employ an explicit Euler approach on the coupling term, which decouples the computation of $\boldsymbol{m}_h^{i+1} \approx \boldsymbol{m}(t_{i+1})$ and the magnetic field $\boldsymbol{h}_h^{i+1} \approx \boldsymbol{h}(t_{i+1})$ from the eddy current equation.

For higher-order in time integration of the coupled ELLG system (2.18), only the work [BBP08] considers the related coupling with the full Maxwell system of the (formally) second-order in time midpoint scheme. There, one non-linear fully coupled system has to be solved per time-step. An extension of the (almost) second-order tangent plane scheme [AKST14] from plain LLG to ELLG is an obvious idea, however, we identify the following issues:

- The formulation of an (almost) second-order tangent plane scheme for the coupled ELLG system (2.18) is not straightforward. This is due to the fact that $\partial_t \boldsymbol{m}$ is represented in the eddy current part (2.18b) and, in contrast to the first-order tangent plane scheme, $\boldsymbol{v}$ is defined as in (4.3) and thus $\boldsymbol{v} \neq \partial_t \boldsymbol{m}$.

- In order to decouple the computations of $\boldsymbol{m}_h^{i+1} \approx \boldsymbol{m}(t_{i+1})$ and $\boldsymbol{h}_h^{i+1} \approx \boldsymbol{h}(t_{i+1})$, the explicit Euler approach of [Pag13, BPP15, LPPT15, FT17] for the coupling term reduces the convergence order down to (formal) first-order in time convergence of the overall numerical integrator.

[1]TU Wien
[2]Universität Wien

5.1.1. Contributions

Based on the own work [DPP+17], we make the following contributions:

- We extend the (almost) second-order in time tangent plane scheme from [AKST14] and Chapter 4 to a formally (almost) second-order in time numerical integrator for ELLG (2.18); see Section 5.2.
- We adopt the second-order implicit-explicit approach for the lower-order terms $\boldsymbol{\pi}_h$ and $\boldsymbol{\Pi}_h$ to the coupling term. From the second time-step on, this decouples the computation of $\boldsymbol{m}_h^{i+1} \approx \boldsymbol{m}(t_{i+1})$ and $\boldsymbol{h}_h^{i+1} \approx \boldsymbol{h}(t_{i+1})$. In particular, only two linear systems have to be solved sequentially at each time-step; see Section 5.2.1.
- We confirm the formal convergence order of our algorithm with a numerical experiment; see Section 5.3;
- We prove well-posedness and unconditional convergence of our algorithm towards a weak solution in the sense of Definition 2.2.2(i)–(iv).
- Provided the CFL-type condition $k = \mathbf{o}(h^{3/2})$, we prove convergence of our algorithm towards a weak solution in the sense of Definition 2.2.2(i)–(v), i.e., there even holds the stronger energy estimate (2.22).

5.2. Algorithm

Based on the own work [DPP+17, Algorithm 7], we formulate in this section an (almost) second-order extension of Algorithm 4.2.1 for plain LLG to ELLG (2.18), which computes approximations

$$\boldsymbol{\mathcal{S}}_h \ni \boldsymbol{m}_h^i \approx \boldsymbol{m}(t_i) \quad \text{and} \quad \boldsymbol{\mathcal{X}}_h \ni \boldsymbol{h}_h^i \approx \boldsymbol{h}(t_i), \quad \text{for all } i = 0, \dots, M.$$

Roughly, we proceed as follows: For the LLG part (2.18a), we adopt Algorithm 4.2.1, which improves the (almost) second-order tangent plane scheme from [AKST14]. For the ELLG part (2.18b), we adopt the implicit midpoint approach from [BPP15, Algorithm 4.1] (full Maxwell-LLG) and [LT13, Algorithm 2.1]. To formulate our algorithm, we recall the notations from the (almost) second-order tangent plane scheme for plain LLG (2.3) from Chapter 4 and recall, in particular, the implicit-explicit approaches

$$\boldsymbol{\pi}_h^{\boldsymbol{D}}(\boldsymbol{v}_h^i, \boldsymbol{m}_h^i, \boldsymbol{m}_h^{i-1}) \approx \boldsymbol{\pi}(\boldsymbol{m}(t_i + k/2)) \quad \text{and} \quad \boldsymbol{\Pi}_h^{\boldsymbol{D}}(\boldsymbol{v}_h^i, \boldsymbol{m}_h^i, \boldsymbol{m}_h^{i-1}) \approx \boldsymbol{\Pi}(\boldsymbol{m}(t_i + k/2)),$$

which were defined by one of the three options **(A1)**–**(A3)**. Accordingly, we define the coupling term $\boldsymbol{h}_h^{i,\boldsymbol{\Theta}} \approx \boldsymbol{h}(t_i)$ with one of the following three options:

(C1) The implicit and formally second-order in time midpoint approach [LT13, Pag13, BPP15]

$$\boldsymbol{h}_h^{i,\boldsymbol{\Theta}} := \boldsymbol{h}_h^{i+1/2} \in \boldsymbol{\mathcal{X}}_h.$$

(C2) The explicit and formally second-order in time Adams–Bashforth-type approach

$$\boldsymbol{\mathcal{X}}_h \ni \boldsymbol{h}_h^{i,\boldsymbol{\Theta}} := \begin{cases} \boldsymbol{h}_h^{i+1/2} & \text{for } i = 0, \\ \frac{3}{2}\,\boldsymbol{h}_h^i - \frac{1}{2}\,\boldsymbol{h}_h^{i-1} & \text{else.} \end{cases}$$

(C3) The explicit and formally first-order in time Euler approach [Pag13, LPPT15, BPP15, FT17]

$$\boldsymbol{h}_h^{i,\boldsymbol{\Theta}} := \boldsymbol{h}_h^i \in \boldsymbol{\mathcal{X}}_h.$$

With these preparations, we are ready to formulate our algorithm.

Algorithm 5.2.1 (TPS2 for ELLG, [DPP+17, Algorithm 7])**. Input:** *Approximations* $\boldsymbol{m}_h^{-1} := \boldsymbol{m}_h^0 \in \boldsymbol{\mathcal{M}}_h$ *and* $\boldsymbol{h}_h^{-1} := \boldsymbol{h}_h^0 \in \boldsymbol{\mathcal{X}}_h$.
Loop: *For* $i = 0, \ldots, M-1$, *iterate the following steps* (a)–(b)*:*

(a) *Compute the discrete function*

$$\lambda_h^i := -C_{\mathbf{ex}}\,|\nabla \boldsymbol{m}_h^i|^2 + \big(\boldsymbol{f}_h^i + \boldsymbol{\pi}_h(\boldsymbol{m}_h^i) + \boldsymbol{h}_h^i + \boldsymbol{\Pi}_h(\boldsymbol{m}_h^i)\big) \cdot \boldsymbol{m}_h^i. \tag{5.1}$$

(b) *Find* $\boldsymbol{v}_h^i \in \boldsymbol{\mathcal{K}}_h(\boldsymbol{m}_h^i)$ *and* $\boldsymbol{h}_h^{i+1} \in \boldsymbol{\mathcal{X}}_h$ *such that, for all* $\boldsymbol{\varphi}_h \in \boldsymbol{\mathcal{K}}_h(\boldsymbol{m}_h^i)$, *it holds that*

$$\begin{aligned} &\langle \mathcal{W}_{G(k)}(\lambda_h^i)\,\boldsymbol{v}_h^i, \boldsymbol{\varphi}_h\rangle_{\boldsymbol{L}^2(\omega)} + \langle \boldsymbol{m}_h^i \times \boldsymbol{v}_h^i, \boldsymbol{\varphi}_h\rangle_{\boldsymbol{L}^2(\omega)} + \frac{C_{\mathbf{ex}}}{2}\,k\,(1+\rho(k))\,\langle \nabla \boldsymbol{v}_h^i, \nabla \boldsymbol{\varphi}_h\rangle_{\boldsymbol{L}^2(\omega)} \\ &= -C_{\mathbf{ex}}\,\langle \nabla \boldsymbol{m}_h^i, \nabla \boldsymbol{\varphi}_h\rangle_{\boldsymbol{L}^2(\omega)} + \langle \boldsymbol{\pi}_h^{\boldsymbol{D}}(\boldsymbol{v}_h^i; \boldsymbol{m}_h^i, \boldsymbol{m}_h^{i-1}), \boldsymbol{\varphi}_h\rangle_{\boldsymbol{L}^2(\omega)} + \langle \boldsymbol{f}_h^{i+1/2}, \boldsymbol{\varphi}_h\rangle_{\boldsymbol{L}^2(\omega)} \\ &\quad + \langle \boldsymbol{h}_h^{i,\boldsymbol{\Theta}}, \boldsymbol{\varphi}_h\rangle_{\boldsymbol{L}^2(\omega)} + \langle \boldsymbol{\Pi}_h^{\boldsymbol{D}}(\boldsymbol{v}_h^i; \boldsymbol{m}_h^i, \boldsymbol{m}_h^{i-1}), \boldsymbol{\varphi}_h\rangle_{\boldsymbol{L}^2(\omega)}, \end{aligned} \tag{5.2a}$$

and for all $\boldsymbol{\zeta}_h \in \boldsymbol{\mathcal{X}}_h$, *it holds that*

$$-\mu_0\langle \mathrm{d_t}\boldsymbol{m}_h^{i+1}, \boldsymbol{\zeta}_h\rangle_{\boldsymbol{L}^2(\omega)} = \mu_0\langle \mathrm{d_t}\boldsymbol{h}_h^{i+1}, \boldsymbol{\zeta}_h\rangle_{\boldsymbol{L}^2(\Omega)} + \langle \sigma^{-1}\nabla \times \boldsymbol{h}_h^{i+1/2}, \nabla \times \boldsymbol{\zeta}_h\rangle_{\boldsymbol{L}^2(\Omega)}, \tag{5.2b}$$

where $\boldsymbol{m}_h^{i+1} \in \boldsymbol{\mathcal{M}}_h$ *is defined by*

$$\boldsymbol{m}_h^{i+1}(\boldsymbol{z}) := \frac{\boldsymbol{m}_h^i(\boldsymbol{z}) + k\boldsymbol{v}_h^i(\boldsymbol{z})}{|\boldsymbol{m}_h^i(\boldsymbol{z}) + k\boldsymbol{v}_h^i(\boldsymbol{z})|} \quad \text{for all nodes } \boldsymbol{z} \in \mathcal{N}_h. \tag{5.2c}$$

Output: *Approximations* $\boldsymbol{m}_h^i \approx \boldsymbol{m}(t_i)$ *and* $\boldsymbol{h}_h^i \approx \boldsymbol{h}(t_i)$ □

Remark 5.2.2. (i) *With* $\boldsymbol{h}_h^{i,\boldsymbol{\Theta}} = \boldsymbol{h}_h^{i+1/2}$ *from the implicit approach, the system* (5.2) *is fully coupled. The resulting algorithm is formally (almost) second-order in time. Moreover, note that* $\langle \mathrm{d_t}\boldsymbol{m}_h^{i+1}, \boldsymbol{\zeta}_h\rangle_{\boldsymbol{L}^2(\omega)}$ *in* (5.2b) *non-linearly depends on the sought* $\boldsymbol{v}_h^i$ *via* (5.2c). *This results in a non-linear fully coupled system* (5.2).

(ii) *To solve the non-linear system from* (i), *we employ a fixed-point iteration; see Algorithm 5.2.5. Clearly, this is computationally costly. Moreover, it prevents the general advantage of the tangent plane scheme, that only one (potentially coupled) linear system has to be solved per step; cf., e.g., [LT13, Pag13, BPP15, LPPT15].*

(iii) *Our preferred choice for the coupling term* $\boldsymbol{h}_h^{i,\boldsymbol{\Theta}}$ *is the second-order Adams–Bashforth-type approach* **(C2)**. *The resulting algorithm is formally (almost) second-order in time. For* $i > 0$ *and provided that* $\boldsymbol{\pi}_h^{\boldsymbol{D}}$ *and* $\boldsymbol{\Pi}_h^{\boldsymbol{D}}$ *are affine in* $\boldsymbol{v}_h^i$, *we can sequentially solve two linear systems for* $\boldsymbol{v}_h^{i+1}$ *and* $\boldsymbol{h}_h^{i+1}$, *respectively; see the decoupled Algorithm 5.2.3. Only for* $i = 0$, *the system* (5.2) *is fully coupled and non-linear; see* (i) *for details.*

(iv) *As for the Adams–Bashforth-type approach* **(C2)**, *the explicit Euler approach* **(C3)** *allows for the sequential computation of* $\boldsymbol{v}_h^{i+1}$ *and* $\boldsymbol{h}_h^{i+1}$, *but the resulting algorithm is (formally) only first-order in time. We analyze this approach only for comparison.*

(v) *Following [LT13, Pag13, LPPT15, BPP15], we can replace in* (5.2b) *the term*

$$\langle \mathrm{d_t}\boldsymbol{m}_h^{i+1}, \boldsymbol{\zeta}_h\rangle_{\boldsymbol{L}^2(\omega)} \quad \text{by} \quad \langle \boldsymbol{v}_h^i, \boldsymbol{\zeta}_h\rangle_{\boldsymbol{L}^2(\omega)}. \tag{5.3}$$

Provided that $\boldsymbol{\pi}_h^{\boldsymbol{D}}$ *and* $\boldsymbol{\Pi}_h^{\boldsymbol{D}}$ *are affine in* $\boldsymbol{v}_h^i$, *the overall system* (5.2) *is then linear for* $\boldsymbol{v}_h^i$ *and* $\boldsymbol{h}_h^{i+1}$ *even for the implicit approach* $\boldsymbol{h}_h^{i,\boldsymbol{\Theta}} = \boldsymbol{h}_h^{i+1/2}$. *However, note that Lemma 4.3.1 yields* $\partial_t \boldsymbol{m} = \boldsymbol{v} + \mathcal{O}(k)$, *i.e., the replacement* (5.3) *formally results in a first-order in time error. Thus, we may only expect first-order in time convergence of the overall integrator.*

(vi) *In practice, we solve the eddy current part* (5.2b) *for the unknown* $\boldsymbol{g}_h := \boldsymbol{h}_h^{i+1/2} \in \boldsymbol{\mathcal{X}}_h$, *i.e., we compute the unique* $\boldsymbol{g}_h \in \boldsymbol{\mathcal{X}}_h$ *such that, for all* $\boldsymbol{\zeta}_h \in \boldsymbol{\mathcal{X}}_h$, *it holds that*

$$\begin{aligned} 2\mu_0 \langle \boldsymbol{g}_h, \boldsymbol{\zeta}_h\rangle_{\boldsymbol{L}^2(\Omega)} &+ k\,\langle \sigma^{-1}\nabla\times\boldsymbol{g}_h, \nabla\times\boldsymbol{\zeta}_h\rangle_{\boldsymbol{L}^2(\Omega)} \\ &= -\mu_0 k\,\langle \mathrm{d_t}\boldsymbol{m}_h^{i+1}, \boldsymbol{\zeta}_h\rangle_{\boldsymbol{L}^2(\omega)} + 2\mu_0\,\langle \boldsymbol{h}_h^i, \boldsymbol{\zeta}_h\rangle_{\boldsymbol{L}^2(\Omega)}. \end{aligned} \tag{5.4}$$

Then, $\boldsymbol{h}_h^{i+1} := 2\,\boldsymbol{g}_h - \boldsymbol{h}_h^i$ *solves the eddy current equation* (5.2b).

(vii) *For the sake of readability, we suppose exact evaluation of* $\sigma \in L^\infty(\omega)$.

In the following two subsections, we take a closer look at one time-step of Algorithm 5.2.1 and elaborate two particular variants. We cover:

- **The ideal case:** We employ for $i > 0$ the explicit second-order in time Adams–Bashforth-type approaches **(A2)** for $\boldsymbol{\pi}_h^{\boldsymbol{D}}$ and $\boldsymbol{\Pi}_h^{\boldsymbol{D}}$ as well as **(C2)** for $\boldsymbol{h}_h^{i,\boldsymbol{\Theta}}$ and decouple the time-stepping; see Section 5.2.1.
- **The worst-case:** We employ the implicit approaches **(A1)** for $\boldsymbol{\pi}_h^{\boldsymbol{D}}$ and $\boldsymbol{\Pi}_h^{\boldsymbol{D}}$ as well as **(C1)** for $\boldsymbol{h}_h^{i,\boldsymbol{\Theta}}$ and present a fixed-point scheme for the solution of the resulting non-linear system; see Section 5.2.2.

Throughout, we recall from Section 4.6 for $\boldsymbol{\psi}_h, \boldsymbol{\varphi}_h \in \boldsymbol{\mathcal{K}}_h(\boldsymbol{m}_h^i)$ the bilinear form

$$\begin{aligned} \boldsymbol{B}_h^i(\boldsymbol{\psi}_h, \boldsymbol{\varphi}_h) := \langle \mathcal{W}_{G(k)}(\lambda_h^i)\,\boldsymbol{\psi}_h, \boldsymbol{\varphi}_h\rangle_{\boldsymbol{L}^2(\omega)} &+ \langle \boldsymbol{m}_h^i \times \boldsymbol{\psi}_h, \boldsymbol{\varphi}_h\rangle_{\boldsymbol{L}^2(\omega)} \\ &+ \frac{C_{\mathbf{ex}}}{2}\,k\,(1+\rho(k))\,\langle \nabla\boldsymbol{\psi}_h, \nabla\boldsymbol{\varphi}_h\rangle_{\boldsymbol{L}^2(\omega)}. \end{aligned} \tag{5.5}$$

5.2.1. One decoupled (almost) second-order time-step

In this section, we present one time-step of Algorithm 5.2.1 in its ideal form. We exploit for $i > 0$ the advantages of the explicit second-order in time approaches and employ the explicit second-order Adams–Bashforth-type approach

$$\boldsymbol{h}_h^{i,\boldsymbol{\Theta}} = \frac{3}{2}\,\boldsymbol{h}_h^i - \frac{1}{2}\,\boldsymbol{h}_h^i, \tag{5.6}$$

from **(C2)** for the coupling term as well as the explicit second-order approaches

$$\boldsymbol{\pi}_h^{\boldsymbol{D}}(\boldsymbol{v}_h^i;\boldsymbol{m}_h^i,\boldsymbol{m}_h^{i-1}) = \frac{3}{2}\,\boldsymbol{\pi}_h(\boldsymbol{m}_h^i) - \frac{1}{2}\,\boldsymbol{\pi}_h(\boldsymbol{m}_h^{i-1}), \quad \text{and} \tag{5.7a}$$

$$\boldsymbol{\Pi}_h^{\boldsymbol{D}}(\boldsymbol{v}_h^i;\boldsymbol{m}_h^i,\boldsymbol{m}_h^{i-1}) = \boldsymbol{\Pi}_h(\boldsymbol{m}_h^i) + \frac{1}{2}\,\boldsymbol{D}_h(\boldsymbol{m}_h^i,\boldsymbol{m}_h^i) - \frac{1}{2}\,\boldsymbol{D}_h(\boldsymbol{m}_h^i,\boldsymbol{m}_h^{i-1}), \tag{5.7b}$$

from **(A2)** for the lower-order terms. Moreover, we follow Remark 5.2.2(vi) and solve the eddy current part (5.2b) for $\boldsymbol{g}_h := \boldsymbol{h}_h^{i+1/2}$.

Algorithm 5.2.3 (Decoupled TPS 2, one time-step with **(A2)** and **(C2)**, $i > 0$)**. Input:** *$i > 0$ with approximations $\boldsymbol{\mathcal{M}}_h \ni \boldsymbol{m}_h^i \approx \boldsymbol{m}(t_i)$, $\boldsymbol{\mathcal{M}}_h \ni \boldsymbol{m}_h^{i-1} \approx \boldsymbol{m}(t_{i-1})$, $\boldsymbol{\mathcal{X}}_h \ni \boldsymbol{h}_h^i \approx \boldsymbol{h}(t_i)$, and $\boldsymbol{\mathcal{X}}_h \ni \boldsymbol{h}_h^{i-1} \approx \boldsymbol{h}(t_{i-1})$. Iterate the following steps* (a)–(d)*:*

(a) *Find $\boldsymbol{v}_h^i \in \boldsymbol{\mathcal{K}}_h(\boldsymbol{m}_h^i)$ such that, for all $\boldsymbol{\varphi}_h \in \boldsymbol{\mathcal{K}}_h(\boldsymbol{m}_h^i)$, it holds that*

$$\begin{aligned}
&\boldsymbol{B}_h^i(\boldsymbol{v}_h^i,\boldsymbol{\varphi}_h)\\
&= -\,C_{\mathbf{ex}}\langle\nabla\boldsymbol{m}_h^i,\nabla\boldsymbol{\varphi}_h\rangle_{\boldsymbol{L}^2(\omega)} + \frac{3}{2}\,\langle\boldsymbol{\pi}_h(\boldsymbol{m}_h^i),\boldsymbol{\varphi}_h\rangle_{\boldsymbol{L}^2(\omega)} - \frac{1}{2}\,\langle\boldsymbol{\pi}_h(\boldsymbol{m}_h^{i-1}),\boldsymbol{\varphi}_h\rangle_{\boldsymbol{L}^2(\omega)}\\
&\quad + \langle\boldsymbol{f}_h^{i+1/2},\boldsymbol{\varphi}_h\rangle_{\boldsymbol{L}^2(\omega)} + \frac{3}{2}\,\langle\boldsymbol{h}_h^i,\boldsymbol{\varphi}_h\rangle_{\boldsymbol{L}^2(\omega)} - \frac{1}{2}\,\langle\boldsymbol{h}_h^{i-1},\boldsymbol{\varphi}_h\rangle_{\boldsymbol{L}^2(\omega)}\\
&\quad + \langle\boldsymbol{\Pi}_h(\boldsymbol{m}_h^i),\boldsymbol{\varphi}_h\rangle_{\boldsymbol{L}^2(\omega)} + \frac{1}{2}\,\langle\boldsymbol{D}_h(\boldsymbol{m}_h^i,\boldsymbol{m}_h^i),\boldsymbol{\varphi}_h\rangle_{\boldsymbol{L}^2(\omega)} - \frac{1}{2}\,\langle\boldsymbol{D}_h(\boldsymbol{m}_h^i,\boldsymbol{m}_h^{i-1}),\boldsymbol{\varphi}_h\rangle_{\boldsymbol{L}^2(\omega)}.
\end{aligned}$$

(b) *Define $\boldsymbol{m}_h^{i+1} \in \boldsymbol{\mathcal{M}}_h$ by*

$$\boldsymbol{m}_h^{i+1}(\boldsymbol{z}) := \frac{\boldsymbol{m}_h^i(\boldsymbol{z}) + k\,\boldsymbol{v}_h^i(\boldsymbol{z})}{|\boldsymbol{m}_h^i(\boldsymbol{z}) + k\,\boldsymbol{v}_h^i(\boldsymbol{z})|} \qquad \textit{for all nodes } \boldsymbol{z} \in \mathcal{N}_h.$$

(c) *Find $\boldsymbol{g}_h \in \boldsymbol{\mathcal{X}}_h$ such that, for all $\boldsymbol{\zeta}_h \in \boldsymbol{\mathcal{X}}_h$, it holds that*

$$\begin{aligned}
&2\mu_0\,\langle\boldsymbol{g}_h,\boldsymbol{\zeta}_h\rangle_{\boldsymbol{L}^2(\Omega)} + k\,\langle\sigma^{-1}\nabla\times\boldsymbol{g}_h,\nabla\times\boldsymbol{\zeta}_h\rangle_{\boldsymbol{L}^2(\Omega)}\\
&\quad = -\mu_0 k\,\langle \mathrm{d_t}\boldsymbol{m}_h^{i+1},\boldsymbol{\zeta}_h\rangle_{\boldsymbol{L}^2(\omega)} + 2\mu_0\,\langle\boldsymbol{h}_h^i,\boldsymbol{\zeta}_h\rangle_{\boldsymbol{L}^2(\Omega)}.
\end{aligned}$$

(d) *Compute $\boldsymbol{h}_h^{i+1} \in \boldsymbol{\mathcal{X}}_h$ by $\boldsymbol{h}_h^{i+1} := 2\boldsymbol{g}_h - \boldsymbol{h}_h^i$.*

Output: *Approximations $\boldsymbol{\mathcal{M}}_h \ni \boldsymbol{m}_h^{i+1} \approx \boldsymbol{m}(t_{i+1})$ and $\boldsymbol{\mathcal{X}}_h \ni \boldsymbol{h}_h^{i+1} \approx \boldsymbol{h}(t_{i+1})$.* □

Remark 5.2.4. (i) *With the Lax–Milgram theorem (see Theorem B.2.4), the linear systems in* (a) *and* (c) *are uniquely solvable. As in Remark 4.2.2*(vii) *for plain LLG, we conlcude that the update in* (b) *is well-defined. Altogether, Algorithm 5.2.1 is well-posed.*

(ii) *For the explicit Euler approaches* **(A3)** *for* $\boldsymbol{\pi}_h^{\boldsymbol{D}}$ *and* $\boldsymbol{\Pi}_h^{\boldsymbol{D}}$ *as well as* **(C3)** *for* $\boldsymbol{h}_h^{i,\boldsymbol{\Theta}}$, *we only have to change the right-hand side of* (a) *accordingly, i.e., the resulting algorithm is well-posed.*

5.2.2. One coupled time-step with fixed-point iteration

In this section, we deal with one time-step of Algorithm 5.2.1 in a worst-case scenario: We employ the implicit approaches

$$\boldsymbol{h}_h^{i,\boldsymbol{\Theta}} = \boldsymbol{h}_h^{i+1/2}, \tag{5.8}$$

from **(C1)**–**(C2)** for the coupling term as well as

$$\boldsymbol{\pi}_h^{\boldsymbol{D}}(\boldsymbol{v}_h^i; \boldsymbol{m}_h^i, \boldsymbol{m}_h^{i-1}) = \boldsymbol{\pi}_h(\boldsymbol{m}_h^i) + \frac{k}{2}\, \boldsymbol{\pi}_h(\boldsymbol{v}_h^i), \quad \text{and} \tag{5.9a}$$

$$\boldsymbol{\Pi}_h^{\boldsymbol{D}}(\boldsymbol{v}_h^i; \boldsymbol{m}_h^i, \boldsymbol{m}_h^{i-1}) = \boldsymbol{\Pi}_h(\boldsymbol{m}_h^i) + \frac{k}{2}\, \boldsymbol{D}_h(\boldsymbol{m}_h^i; \boldsymbol{v}_h^i), \tag{5.9b}$$

from **(A1)**–**(A2)** for the lower-order terms. With the choice (5.8), the discrete variational formulation (5.2) is a fully-coupled non-linear problem. To this end, we employ a fixed-point iteration which builds on the corresponding Algorithm 4.6.1 for plain LLG. Note that this scheme is implicitly contained in the proof of the own work [DPP⁺17, Theorem 9].

Algorithm 5.2.5 (Inexact implicit TPS2, one time-step, [DPP⁺17, p.21f])**. Input:** *Approximations* $\boldsymbol{\mathcal{M}}_h \ni \boldsymbol{m}_h^i \approx \boldsymbol{m}(t_i)$, *and* $\boldsymbol{\mathcal{X}}_h \ni \boldsymbol{h}_h^i \approx \boldsymbol{h}(t_i)$, *initial guesses* $\boldsymbol{u}_h^{(0)} := \boldsymbol{0} \in \boldsymbol{\mathcal{K}}_h(\boldsymbol{m}_h^i)$ *and* $\boldsymbol{g}_h^{(0)} := \boldsymbol{h}_h^i \in \boldsymbol{\mathcal{X}}_h$, *iteration tolerance* $\varepsilon > 0$. *Iterate the following steps* (a)–(c)*:*

(a) **Loop.** *For* $\ell = 1, 2, \dots,$ *and until*

$$\Big(\|\boldsymbol{\mu}_h^{(\ell+1)} - \boldsymbol{u}_h^{(\ell)}\|_{\boldsymbol{L}^2(\omega)}^2 + \|\boldsymbol{g}_h^{(\ell+1)} - \boldsymbol{g}_h^{(\ell)}\|_{\boldsymbol{L}^2(\Omega)}^2 \Big)^{1/2} \leq \varepsilon$$

perform the following steps (a-i)–(a-iii)*:*

(a-i) *Find* $\boldsymbol{u}_h^{(\ell+1)} \in \boldsymbol{\mathcal{K}}_h(\boldsymbol{m}_h^i)$ *such that, for all* $\boldsymbol{\varphi}_h \in \boldsymbol{\mathcal{K}}_h(\boldsymbol{m}_h^i)$, *it holds that*

$$\begin{aligned} \boldsymbol{B}_h^i(\boldsymbol{u}_h^{(\ell+1)}, \boldsymbol{\varphi}_h) = {} & -C_{\mathbf{ex}} \langle \nabla \boldsymbol{m}_h^i, \nabla \boldsymbol{\varphi}_h \rangle_{\boldsymbol{L}^2(\omega)} + \langle \boldsymbol{\pi}_h(\boldsymbol{m}_h^i), \boldsymbol{\varphi}_h \rangle_{\boldsymbol{L}^2(\omega)} + \frac{k}{2} \langle \boldsymbol{\pi}_h(\boldsymbol{u}_h^{(\ell)}), \boldsymbol{\varphi}_h \rangle_{\boldsymbol{L}^2(\omega)} \\ & + \langle \boldsymbol{f}_h^{i+1/2}, \boldsymbol{\varphi}_h \rangle_{\boldsymbol{L}^2(\omega)} + \langle \boldsymbol{g}_h^{(\ell)}, \boldsymbol{\varphi}_h \rangle_{\boldsymbol{L}^2(\omega)} \\ & + \langle \boldsymbol{\Pi}_h(\boldsymbol{m}_h^i), \boldsymbol{\varphi}_h \rangle_{\boldsymbol{L}^2(\omega)} + \frac{k}{2} \langle \boldsymbol{D}_h(\boldsymbol{m}_h^i, \boldsymbol{u}_h^{(\ell)})), \boldsymbol{\varphi}_h \rangle_{\boldsymbol{L}^2(\omega)}. \end{aligned} \tag{5.10}$$

(a-ii) *Define* $\boldsymbol{d}_h^{(\ell+1)} \in \boldsymbol{\mathcal{S}}_h$ *by*

$$\boldsymbol{d}_h^{(\ell+1)}(\boldsymbol{z}) := \frac{1}{k}\left(\frac{\boldsymbol{m}_h^i(\boldsymbol{z}) + k\,\boldsymbol{u}_h^{(\ell+1)}(\boldsymbol{z})}{|\boldsymbol{m}_h^i(\boldsymbol{z}) + k\,\boldsymbol{u}_h^{(\ell+1)}(\boldsymbol{z})|} - \boldsymbol{m}_h^i(\boldsymbol{z})\right) \text{ for all nodes } \boldsymbol{z} \in \mathcal{N}_h. \quad (5.11)$$

(a-iii) *Find* $\boldsymbol{g}_h^{(\ell+1)} \in \boldsymbol{\mathcal{X}}_h$ *such that, for all* $\boldsymbol{\zeta}_h \in \boldsymbol{\mathcal{X}}_h$*, it holds that*

$$\begin{aligned} 2\mu_0 \langle \boldsymbol{g}_h^{(\ell+1)}, \boldsymbol{\zeta}_h \rangle_{\boldsymbol{L}^2(\omega)} + k \langle \sigma^{-1}\nabla \times \boldsymbol{g}_h^{(\ell+1)}, \nabla \times \boldsymbol{\zeta}_h \rangle_{\boldsymbol{L}^2(\omega)} \\ = -\mu_0 k \langle \boldsymbol{d}_h^{(\ell+1)}, \boldsymbol{\zeta}_h \rangle_{\boldsymbol{L}^2(\omega)} + 2\mu_0 \langle \boldsymbol{h}_h^i, \boldsymbol{\zeta}_h \rangle_{\boldsymbol{L}^2(\omega)}. \end{aligned} \quad (5.12)$$

(b) *Define* $\boldsymbol{m}_h^{i+1} \in \boldsymbol{\mathcal{M}}_h$ *by*

$$\boldsymbol{m}_h^{i+1} := \frac{\boldsymbol{m}_h^i(\boldsymbol{z}) + k\,\boldsymbol{u}_h^{(\ell+1)}(\boldsymbol{z})}{|\boldsymbol{m}_h^i(\boldsymbol{z}) + k\,\boldsymbol{u}_h^{(\ell+1)}(\boldsymbol{z})|} \quad \text{for all nodes } \boldsymbol{z} \in \mathcal{N}_h.$$

(c) *Compute* $\boldsymbol{h}_h^{i+1} := 2\boldsymbol{g}_h^{(\ell+1)} - \boldsymbol{h}_h^i \in \boldsymbol{\mathcal{X}}_h$.

Output: *Approximations* $\boldsymbol{\mathcal{M}}_h \ni \boldsymbol{m}_h^{i+1} \approx \boldsymbol{m}(t_{i+1})$ *and* $\boldsymbol{\mathcal{X}}_h \ni \boldsymbol{h}_h^{i+1} \approx \boldsymbol{h}(t_{i+1})$. □

Remark 5.2.6. *In step* (a-ii) *of Algorithm 5.2.5,* $\boldsymbol{d}_h^{(\ell+1)} \in \boldsymbol{\mathcal{S}}_h$ *mimics* $\mathrm{d_t}\boldsymbol{m}_h^{i+1}$.

In the following proposition, we prove a convergence result for the fixed-point iterates of Algorithm 5.2.5. To this end, we follow the proof of [DPP$^+$17, Theorem 9(i)]. In analogy to Proposition 4.6.3 for plain LLG, we require the stronger assumption **(T4$^+$)** to $\boldsymbol{D}_h$ instead of **(T4)**, which we recall from Section 4.6.1.

(T4$^+$) **Strong uniform boundedness of $\boldsymbol{D}_h$:** There exists a constant $C_{\boldsymbol{D}} > 0$ such that, for all $h > 0$, it holds that

$$\|\boldsymbol{D}_h(\boldsymbol{\varphi}_h, \boldsymbol{\psi}_h)\|_{\boldsymbol{L}^2(\omega)} \leq C_{\boldsymbol{D}} \|\boldsymbol{\psi}_h\|_{\boldsymbol{H}^1(\omega)} \quad \text{for all } \boldsymbol{\varphi}_h \in \boldsymbol{\mathcal{M}}_h \text{ and all } \boldsymbol{\psi}_h \in \boldsymbol{\mathcal{S}}_h.$$

Proposition 5.2.7 (Convergence of fixed-point iteration, [DPP$^+$17, p.21f])**.** *Consider the fixed-point iteration from Algorithm 5.2.5. Suppose linearity* **(D2)** *and uniform boundedness* **(D3)** *of* $\boldsymbol{\pi}_h$*. Suppose linearity in the second-argument* **(T2)** *and strong uniform boundedness* **(T4$^+$)** *of* $\boldsymbol{D}_h$*. Then, the fixed-point iterates* $\boldsymbol{u}_h^{(\ell)} \in \boldsymbol{\mathcal{K}}_h(\boldsymbol{m}_h^i)$ *and* $\boldsymbol{g}_h^{(\ell)} \in \boldsymbol{\mathcal{X}}_h$ *are well-defined. For sufficiently small* $k > 0$*, there exists a unique solution* $(\boldsymbol{v}_h^i, \boldsymbol{h}_h^{i+1/2}) \in \boldsymbol{\mathcal{K}}_h(\boldsymbol{m}_h^i) \times \boldsymbol{\mathcal{X}}_h$ *of the discrete variational formulation* (5.2) *and it holds that*

$$\boldsymbol{u}_h^{(\ell)} \to \boldsymbol{v}_h^i \quad \text{in } \boldsymbol{L}^2(\omega) \quad \text{as well as} \quad \boldsymbol{g}_h^{(\ell)} \to \boldsymbol{h}_h^{i+1/2} \quad \text{in } \boldsymbol{L}^2(\Omega), \quad \text{as } \ell \to \infty. \quad (5.13)$$

Proof. The well-definedness of the fixed-point iterates follows from the ellipticity of the bilinear form $\boldsymbol{B}_h^i$ from the LLG part and of the corresponding bilinear form from the eddy current part as in Remark 5.2.4(i). To show the convergence (5.13), we proceed as follows: We recall from (4.63) for $\varphi_h \in \mathcal{K}_h(\boldsymbol{m}_h^i)$ the energy norm

$$|||\varphi_h|||^2 := \frac{\alpha}{2}\|\varphi_h\|^2_{\boldsymbol{L}^2(\omega)} + \frac{C_{\mathbf{ex}}}{2} k\,\|\nabla\varphi_h\|^2_{\boldsymbol{L}^2(\omega)}, \tag{5.14}$$

As in the proof of Theorem 4.5.1(a) for plain LLG, the bilinear form $\boldsymbol{B}_h^i$ from the variational formulation (5.10) is elliptic with respect to $|||\cdot|||$ for $k > 0$ small enough, i.e., it holds that

$$\boldsymbol{B}_h^i(\varphi_h, \varphi_h) \geq |||\varphi_h|||^2 \quad \text{for all } \varphi_h \in \mathcal{K}_h(\boldsymbol{m}_h^i). \tag{5.15}$$

We endow the product space $\mathcal{K}_h(\boldsymbol{m}_h^i) \times \boldsymbol{\mathcal{X}}_h$, with the norm

$$|||(\varphi_h, \zeta_h)|||_*^2 := |||\varphi_h|||^2 + \|\zeta_h\|^2_{\boldsymbol{L}^2(\Omega)} \quad \text{for all } \varphi_h \in \mathcal{K}_h(\boldsymbol{m}_h^i) \quad \text{and all } \zeta_h \in \boldsymbol{\mathcal{X}}_h. \tag{5.16}$$

In the following three steps, we show that the sequence $(\boldsymbol{u}_h^{(\ell)}, \boldsymbol{g}_h^{(\ell)})_{\ell\in\mathbb{N}_0}$ is a contraction in the product space with respect to the product norm $|||\cdot|||_*$ and then apply the Banach fixed-point theorem (see Theorem B.2.6).

Step 1. We estimate $|||\boldsymbol{u}_h^{(\ell+1)} - \boldsymbol{u}_h^{(\ell)}|||^2$. Using the assumptions **(D2)**–**(D3)**, **(T2)** and **(T4$^+$)**, we get as in the proof of Proposition 4.6.3 and with the additional term $\langle \boldsymbol{g}_h^{(\ell)}, \varphi_h\rangle_{\boldsymbol{L}^2(\omega)}$ in (5.10) for all $\ell \in \mathbb{N}$ that

$$\begin{aligned}
|||\boldsymbol{u}_h^{(\ell+1)} - \boldsymbol{u}_h^{(\ell)}|||^2 &\overset{(5.15)}{\leq} \boldsymbol{B}_h^i(\boldsymbol{u}_h^{(\ell+1)} - \boldsymbol{u}_h^{(\ell)}, \boldsymbol{u}_h^{(\ell+1)} - \boldsymbol{u}_h^{(\ell)}) \\
&\overset{(5.10)}{\leq} \big[\, C_{\boldsymbol{\pi}} + C_{\boldsymbol{D}}\,\big]\, \frac{k}{2}\, \|\boldsymbol{u}_h^{(\ell)} - \boldsymbol{u}_h^{(\ell-1)}\|_{\boldsymbol{L}^2(\omega)}\, \|\boldsymbol{u}_h^{(\ell+1)} - \boldsymbol{u}_h^{(\ell)}\|_{\boldsymbol{L}^2(\omega)} \\
&\quad + C_{\boldsymbol{D}}\, \frac{k}{2}\, \|\nabla\boldsymbol{u}_h^{(\ell)} - \nabla\boldsymbol{u}_h^{(\ell-1)}\|_{\boldsymbol{L}^2(\omega)}\, \|\boldsymbol{u}_h^{(\ell+1)} - \boldsymbol{u}_h^{(\ell)}\|_{\boldsymbol{L}^2(\omega)} \\
&\quad + \|\boldsymbol{g}_h^{(\ell)} - \boldsymbol{g}_h^{(\ell-1)}\|_{\boldsymbol{L}^2(\Omega)}\, \|\boldsymbol{u}_h^{(\ell+1)} - \boldsymbol{u}_h^{(\ell)}\|_{\boldsymbol{L}^2(\omega)}.
\end{aligned} \tag{5.17}$$

Step 2. We estimate $\|\boldsymbol{g}_h^{(\ell+1)} - \boldsymbol{g}_h^{(\ell)}\|_{\boldsymbol{L}^2(\Omega)}$. For all $\ell \in \mathbb{N}_0$, we get that

$$\begin{aligned}
&2\mu_0\, \langle \boldsymbol{g}_h^{(\ell+1)} - \boldsymbol{g}_h^{(\ell)}, \zeta_h\rangle_{\boldsymbol{L}^2(\Omega)} + k\, \langle \sigma^{-1}\nabla\times\boldsymbol{g}_h^{(\ell+1)} - \sigma^{-1}\nabla\times\boldsymbol{g}_h^{(\ell)}, \nabla\times\zeta_h\rangle_{\boldsymbol{L}^2(\Omega)} \\
&\qquad = -\mu_0 k\, \langle \boldsymbol{d}_h^{(\ell+1)} - \boldsymbol{d}_h^{(\ell)}, \zeta_h\rangle_{\boldsymbol{L}^2(\omega)} \quad \text{for all } \zeta_h \in \boldsymbol{\mathcal{X}}_h.
\end{aligned}$$

Testing the latter equation with $\zeta_h := \boldsymbol{g}_h^{(\ell+1)} - \boldsymbol{g}_h^{(\ell)} \in \boldsymbol{\mathcal{X}}_h$, we obtain that

$$\|\boldsymbol{g}_h^{(\ell+1)} - \boldsymbol{g}_h^{(\ell)}\|^2_{\boldsymbol{L}^2(\Omega)} \leq \frac{k}{2}\, \|\boldsymbol{d}_h^{(\ell+1)} - \boldsymbol{d}_h^{(\ell)}\|_{\boldsymbol{L}^2(\omega)}\, \|\boldsymbol{g}_h^{(\ell+1)} - \boldsymbol{g}_h^{(\ell)}\|_{\boldsymbol{L}^2(\Omega)} \quad \text{for all } \ell \in \mathbb{N}_0. \tag{5.18}$$

Next, we estimate the right-hand side of the latter estimate. To this end, elementary calculations show that

$$\Big|\, \frac{\mathbf{x}}{|\mathbf{x}|} - \frac{\mathbf{y}}{|\mathbf{y}|} \Big| \leq 2\,|\mathbf{x} - \mathbf{y}| \quad \text{for all } \mathbf{x} \in \mathbb{R}^3 \quad \text{with } |\mathbf{x}| \geq 1 \quad \text{and all } \mathbf{y} \in \mathbb{R}^3 \setminus \{\mathbf{0}\}. \tag{5.19}$$

With $\boldsymbol{\mathcal{I}}_h$ being the nodal interpolant corresponding to $\boldsymbol{\mathcal{S}}_h$, we get from the definition (5.11) of $\boldsymbol{d}_h^\ell \in \boldsymbol{\mathcal{S}}_h$ that

$$\boldsymbol{d}_h^{(\ell+1)} - \boldsymbol{d}_h^{(\ell)} = \frac{1}{k}\,\boldsymbol{\mathcal{I}}_h\bigg(\frac{\boldsymbol{m}_h^i + k\,\boldsymbol{u}_h^{(\ell+1)}}{|\boldsymbol{m}_h^i + k\,\boldsymbol{u}_h^{(\ell+1)}|}\bigg) - \frac{1}{k}\,\boldsymbol{\mathcal{I}}_h\bigg(\frac{\boldsymbol{m}_h^i + k\,\boldsymbol{u}_h^{(\ell)}}{|\boldsymbol{m}_h^i + k\,\boldsymbol{u}_h^{(\ell)}|}\bigg) \tag{5.20}$$

Moreover, we conclude as in Remark 4.2.2(i), that

$$|\boldsymbol{m}_h^i(\boldsymbol{z}) + k\,\boldsymbol{u}_h^{(\ell+1)}(\boldsymbol{z})| \geq 1 \quad \text{and} \quad |\boldsymbol{m}_h^i(\boldsymbol{z}) + k\,\boldsymbol{u}_h^{(\ell)}(\boldsymbol{z})| \geq 1 \quad \text{for all nodes } \boldsymbol{z} \in \mathcal{N}_h,$$

i.e., nodewise we are in the situation of (5.19). Together with the norm equivalence $\|\cdot\|_h \simeq \|\cdot\|_{\boldsymbol{L}^2(\omega)}$ of the approximate $\boldsymbol{L}^2$-norm from Lemma 3.3.1, this yields that

$$\begin{aligned}
&\|\boldsymbol{d}_h^{(\ell+1)} - \boldsymbol{d}_h^{(\ell)}\|_{\boldsymbol{L}^2(\omega)} \\
&\quad\leq \|\boldsymbol{d}_h^{(\ell+1)} - \boldsymbol{d}_h^{(\ell)}\|_h \overset{(5.20)}{=} \frac{1}{k}\bigg\|\boldsymbol{\mathcal{I}}_h\bigg(\frac{\boldsymbol{m}_h^i + k\,\boldsymbol{u}_h^{(\ell+1)}}{|\boldsymbol{m}_h^i + k\,\boldsymbol{u}_h^{(\ell+1)}|}\bigg) - \boldsymbol{\mathcal{I}}_h\bigg(\frac{\boldsymbol{m}_h^i + k\,\boldsymbol{u}_h^{(\ell)}}{|\boldsymbol{m}_h^i + k\,\boldsymbol{u}_h^{(\ell)}|}\bigg)\bigg\|_h \\
&\quad\overset{(5.19)}{\leq} 2\,\|\boldsymbol{u}_h^{(\ell+1)} - \boldsymbol{u}_h^{(\ell)}\|_h \leq 2\sqrt{5}\,\|\boldsymbol{u}_h^{(\ell+1)} - \boldsymbol{u}_h^{(\ell)}\|_{\boldsymbol{L}^2(\omega)}.
\end{aligned}$$

Altogether, we arrive at

$$\|\boldsymbol{g}_h^{(\ell+1)} - \boldsymbol{g}_h^{(\ell)}\|_{\boldsymbol{L}^2(\Omega)} \overset{(5.18)}{\leq} \sqrt{5}\,k\,\|\boldsymbol{u}_h^{(\ell+1)} - \boldsymbol{u}_h^{(\ell)}\|_{\boldsymbol{L}^2(\omega)} \quad \text{for all } \ell \in \mathbb{N}_0. \tag{5.21}$$

Step 3. We combine **Step 1** and **Step 2**. For all $\ell \in \mathbb{N}$, this yields that

$$\begin{aligned}
|||\boldsymbol{u}_h^{(\ell+1)} - \boldsymbol{u}_h^{(\ell)}|||^2 &\leq \big[\,C_{\boldsymbol{\pi}} + C_{\boldsymbol{D}} + 2\sqrt{5}\,\big]\,\frac{k}{2}\,\|\boldsymbol{u}_h^{(\ell)} - \boldsymbol{u}_h^{(\ell-1)}\|_{\boldsymbol{L}^2(\omega)}\,\|\boldsymbol{u}_h^{(\ell+1)} - \boldsymbol{u}_h^{(\ell)}\|_{\boldsymbol{L}^2(\omega)} \\
&\quad + C_{\boldsymbol{D}}\,\frac{k}{2}\,\|\nabla\boldsymbol{u}_h^{(\ell)} - \nabla\boldsymbol{u}_h^{(\ell-1)}\|_{\boldsymbol{L}^2(\omega)}\,\|\boldsymbol{u}_h^{(\ell+1)} - \boldsymbol{u}_h^{(\ell)}\|_{\boldsymbol{L}^2(\omega)},
\end{aligned}$$

The remainder of the proof follows the lines of the proof of Proposition 4.6.3 for plain LLG. With the Young inequality, we get for arbitrary $\delta > 0$ that

$$|||\boldsymbol{u}_h^{(\ell+1)} - \boldsymbol{u}_h^{(\ell)}|||^2 \lesssim \frac{k}{\delta}\,|||\boldsymbol{u}_h^{(\ell+1)} - \boldsymbol{u}_h^{(\ell)}|||^2 + \delta\,|||\boldsymbol{u}_h^{(\ell)} - \boldsymbol{u}_h^{(\ell-1)}|||^2 \quad \text{for all } \ell \in \mathbb{N}.$$

Choosing $\delta > 0$ small enough, we get from the latter estimate for $k > 0$ small enough that

$$|||\boldsymbol{u}_h^{(\ell+1)} - \boldsymbol{u}_h^{(\ell)}|||^2 \leq \frac{2}{3}\,|||\boldsymbol{u}_h^{(\ell)} - \boldsymbol{u}_h^{(\ell-1)}|||^2 \quad \text{for all } \ell \in \mathbb{N}. \tag{5.22}$$

For the sequence $(\boldsymbol{u}_h^{(\ell)}, \boldsymbol{g}_h^{(\ell)})_{\ell\in\mathbb{N}_0}$, we further get for sufficiently small $k > 0$ that

$$\begin{aligned}
|||(\boldsymbol{u}_h^{(\ell+1)} - \boldsymbol{u}_h^{(\ell)}, \boldsymbol{g}_h^{(\ell+1)} - \boldsymbol{g}_h^{(\ell)})|||_*^2 &\overset{(5.16)}{=} |||\boldsymbol{u}_h^{(\ell+1)} - \boldsymbol{u}_h^{(\ell)}|||^2 + \|\boldsymbol{g}_h^{(\ell+1)} - \boldsymbol{g}_h^{(\ell)}\|_{\boldsymbol{L}^2(\Omega)}^2 \\
&\overset{(5.21)}{\leq} \Big(1 + \frac{10}{\alpha}\,k^2\Big)\,|||\boldsymbol{u}_h^{(\ell+1)} - \boldsymbol{u}_h^{(\ell)}|||^2 \\
&\overset{(5.22)}{\leq} \frac{2}{3}\Big(1 + \frac{10}{\alpha}\,k^2\Big)\,|||\boldsymbol{u}_h^{(\ell)} - \boldsymbol{u}_h^{(\ell-1)}|||^2 \\
&\overset{(5.16)}{\leq} \frac{3}{4}\,|||(\boldsymbol{u}_h^{(\ell)} - \boldsymbol{u}_h^{(\ell-1)}, \boldsymbol{g}_h^{(\ell)} - \boldsymbol{g}_h^{(\ell-1)})|||_*^2
\end{aligned}$$

for all $\ell \in \mathbb{N}$. Hence, the sequence $(\boldsymbol{u}_h^{(\ell)}, \boldsymbol{g}_h^{(\ell)})_{\ell\in\mathbb{N}_0}$ is a contraction in the product space with respect to the product norm $\|\!| \cdot |\!\|_*$. With the Banach fixed-point theorem (see Theorem B.2.6), there exists a unique fixed point $(\boldsymbol{\mu}_h, \boldsymbol{\nu}_h) \in \boldsymbol{\mathcal{K}}_h(\boldsymbol{m}_h^i) \times \boldsymbol{\mathcal{X}}_h$ of the iteration, and the sequence $(\boldsymbol{u}_h^{(\ell)}, \boldsymbol{g}_h^{(\ell)})_{\ell\in\mathbb{N}_0}$ converges to $(\boldsymbol{\mu}_h, \boldsymbol{\nu}_h)$, with respect to $\|\!| \cdot |\!\|_*$. By construction, there holds $(\boldsymbol{\mu}_h, \boldsymbol{\nu}_h) = (\boldsymbol{v}_h^i, \boldsymbol{h}_h^{i+1/2})$. Altogether, this concludes the proof. ☐

Remark 5.2.8. (i) *For the validity of the assumptions from Proposition 5.2.7 for exemplary contributions to $\boldsymbol{\pi}_h$, $\boldsymbol{\Pi}_h$, and $\boldsymbol{D}_h$, the situation is precisely the same as in Remark 4.6.4*(ii)–(iii) *for plain LLG.*

(ii) *The statement of Proposition 5.2.7 remains valid for the explicit choices from* **(A2)**–**(A3)** *for $\boldsymbol{\pi}_h^{\boldsymbol{D}}$ and $\boldsymbol{\Pi}_h^{\boldsymbol{D}}$ instead of the implicit choices from* (5.9) *even if the assumptions* **(D2)**–**(D3)**, **(T2)**, *and* **(T4⁺)** *fail to hold. Since the terms on the right-hand side of* (5.17) *stem from the implicit approaches to $\boldsymbol{\pi}_h^{\boldsymbol{D}}$, $\boldsymbol{\Pi}_h^{\boldsymbol{D}}$, and $\boldsymbol{h}_h^{i,\boldsymbol{\Theta}}$,* **Step 1** *of the proof in this case simply becomes*

$$\|\!|\boldsymbol{u}_h^{(\ell+1)} - \boldsymbol{u}_h^{(\ell)}|\!\|^2 \leq \|\boldsymbol{g}_h^{(\ell)} - \boldsymbol{g}_h^{(\ell-1)}\|_{\boldsymbol{L}^2(\Omega)} \, \|\boldsymbol{u}_h^{(\ell)} - \boldsymbol{u}_h^{(\ell-1)}\|_{\boldsymbol{L}^2(\omega)} \quad \text{for all } \ell \in \mathbb{N}.$$

The remainder of the proof follows the same lines.

5.3. Experimental convergence order

In this section, we illustrate the accuracy and computational costs of different variants of Algorithm 5.2.1 with a numerical experiment. To this end, we use our `Python`-based extension of `NGS/Py` [ngs], which was mainly developed by *Carl-Martin Pfeiler*[3], and slightly adapt the numerical experiment from the own work [DPP⁺17, Section 7.3]: We lay our focus on the performance of different approaches of the coupling term $\boldsymbol{h}_h^{i,\boldsymbol{\Theta}}$ and neglect the $\boldsymbol{m}$-dependent energy contributions to the effective field as well as any further dissipative effects, i.e.,

$$\boldsymbol{\pi} = \boldsymbol{\pi}_h = \boldsymbol{0} \quad \text{and} \quad \boldsymbol{\Pi} = \boldsymbol{\Pi}_h = \boldsymbol{D}_h = \boldsymbol{0}.$$

We always employ the standard choices $\rho(k) := |\log(k)k|$ and $G(k) := \rho(k)^{-1}$ from Remark 4.2.2(vi) and compare the following four variants of Algorithm 5.2.1:

- `FC`: We employ the fully-coupled second-order approach **(C1)**, i.e., the coupling term reads $\boldsymbol{h}_h^{i,\boldsymbol{\Theta}} = \boldsymbol{h}_h^{i+1/2}$ for all $i = 0, \dots, M-1$ and the discrete variational formulation gives rise to a fully-coupled non-linear system. At each time-step, we perform Algorithm 5.2.5 for an (inexact) time-step and perform the underlying fixed-point iteration with tolerance $\varepsilon = 10^{-10}$.

- `DC-2`: We employ the second-order explicit Adams–Bashforth-type approach **(C2)**. For the first time-step, this is `FC` from the latter point. From the second time-step on, we have

$$\boldsymbol{h}_h^{i,\boldsymbol{\Theta}} = \frac{3}{2}\boldsymbol{h}_h^i - \frac{1}{2}\boldsymbol{h}_h^{i-1},$$

[3]TU Wien

and we employ the decoupled Algorithm 5.2.3.

- `DC-1`: We employ the first-order explicit Euler approach **(C3)**, i.e., the coupling term reads $\boldsymbol{h}_h^{i,\boldsymbol{\Theta}} = \boldsymbol{h}_h^i$ for all $i = 0, \dots, M-1$. For all time-steps, we perform the decoupled Algorithm 5.2.3, where we replace the terms

$$\frac{3}{2}\,\langle \boldsymbol{h}_h^i, \boldsymbol{\varphi}_h \rangle_{\boldsymbol{L}^2(\omega)} - \frac{1}{2}\,\langle \boldsymbol{h}_h^{i-1}, \boldsymbol{\varphi}_h \rangle_{\boldsymbol{L}^2(\omega)} \quad \text{by} \quad \langle \boldsymbol{h}_h^i, \boldsymbol{\varphi}_h \rangle_{\boldsymbol{L}^2(\omega)}\,.$$

- `SF`: We employ the explicit second-order Adams–Bashforth-type approach **(C2)** and make the simplification from Remark 5.2.2(v). Essentially, this is `DC-2` with

$$\langle \mathrm{d_t} \boldsymbol{m}_h^{i+1}, \boldsymbol{\zeta}_h \rangle_{\boldsymbol{L}^2(\omega)} \quad \text{replaced by} \quad \langle \boldsymbol{v}_h^i, \boldsymbol{\zeta}_h \rangle_{\boldsymbol{L}^2(\omega)}$$

in the eddy current part (5.2b).

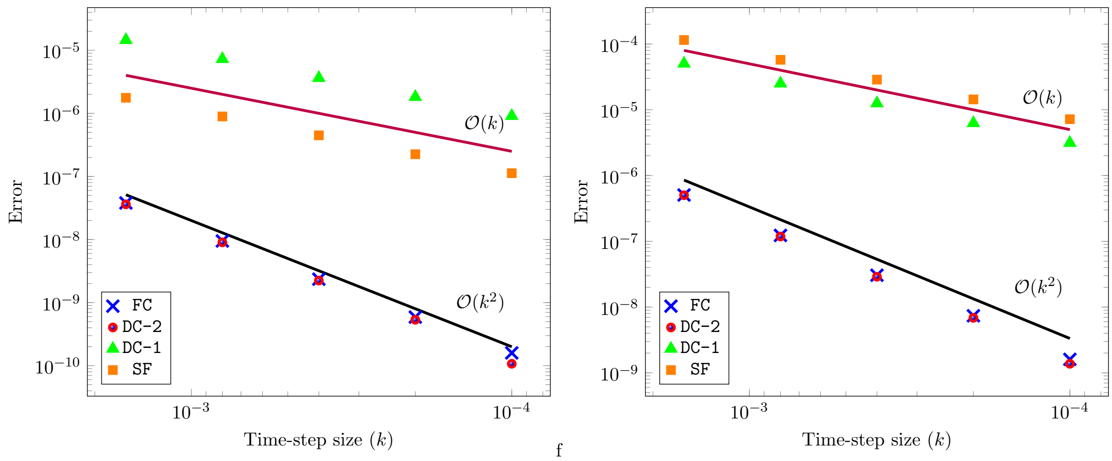

Figure 5.1.: Experiment of Section 5.3: Reference error $\max_i(\|\boldsymbol{m}_{hk_{\mathrm{ref}}}(t_i) - \boldsymbol{m}_{hk}(t_i)\|_{\boldsymbol{H}^1(\omega)})$ (left) and $\max_i(\|\boldsymbol{h}_{hk_{\mathrm{ref}}}(t_i) - \boldsymbol{h}_{hk}(t_i)\|_{\boldsymbol{H}(\mathbf{curl};\Omega)})$ (right) for $k = 2^\ell\, k_{\mathrm{ref}}$ with $\ell \in \{1,2,3,4,5\}$ and $k_{\mathrm{ref}} = 5 \cdot 10^{-5}$.

For all these variants, we choose the final time $T = 7$, the Gilbert-damping parameter $\alpha = 1$, the inner domain $\omega = (-1/8, 1/8)^3$, and the overall domain $\Omega = (-1,1)^3$. In the LLG part (2.18a), we choose $C_{\mathbf{ex}} = 1$ and $\boldsymbol{f} := (f_1, 0, 0)^T \in \boldsymbol{C}^\infty([0,T])$, where, in contrast to [DPP+17, Section 7.3], we set $f_1(t, \boldsymbol{x}) := \sin(\pi t)$. In the eddy current part (2.18a), we choose $\mu_0 = 1$ and define $\sigma \in L^\infty(\Omega)$ via

$$\sigma(\boldsymbol{x}) = \begin{cases} 100 & \text{in } \omega, \\ 1 & \text{in } \Omega \setminus \overline{\omega}. \end{cases}$$

For space-discretization, we employ the triangulation $\mathcal{T}_h^\Omega$ obtained from the `NGS/Py`-embedded `Netgen` [ngs], where we choose the maximal mesh-size 0.03 in the sub-domain ω and 1/8 in the outer domain $\Omega \setminus \omega$. The resulting mesh resolves ω, the sub-mesh $\mathcal{T}_h$

	FC absolute	FC relative	DC-2 relative	DC-1 relative	SF relative
$k = 0.0016$	2.97	100%	26.08%	25.52%	24.44%
$k = 0.0008$	2.97	100%	26.20%	25.61%	24.43%
$k = 0.0004$	2.98	100%	26.23%	25.59%	24.52%
$k = 0.0002$	2.79	100%	28.20%	27.64%	26.40%
$k = 0.0001$	2.45	100%	32.46%	31.78%	30.54%

Table 5.1.: Experiment of Section 5.3: Average absolute time (in s) of FC and relative times of all variants.

on ω consists of 2388 elements and 665 nodes, and the overall mesh $\mathcal{T}_h^\Omega$ consists of 22381 elements and 4383 nodes. We note that we checked the corresponding stiffness matrix to verify that the sub-mesh $\mathcal{T}_h$ satisfies, in fact, the angle condition **(T1)**.

Having fixed the space discretization, we perform the latter variants with varying time-step size. Since the exact solution is unknown, we employ DC-2 to compute a reference solution $\boldsymbol{m}_{hk_{\mathrm{ref}}}$, where the reference time $k_{\mathrm{ref}} := 5 \cdot 10^{-5}$ is a fine time-step size. The initial values of our simulations are the result of the following relaxation process: We start with the nodal interpolant of

$$\boldsymbol{m}^0 := -\frac{1}{\sqrt{3}} \begin{pmatrix} 1 \\ 1 \\ 1 \end{pmatrix}, \qquad \text{and} \qquad \boldsymbol{h}^0 := \begin{cases} -\boldsymbol{m}^0 & \text{on } \omega \\ \mathbf{0} & \text{on } \overline{\Omega} \setminus \overline{\omega}, \end{cases}$$

adopt the above setting, but let $\boldsymbol{f} = \mathbf{0}$. Then, we simulate with DC-2 and the reference time k_{ref} for 1s. As a result, we obtain an energy equilibrium, which represents the actual initial values for our simulations.

In Figure 5.1, we illustrate the experimental convergence order of our variants. For our setting, the plot confirms the predictions of Remark 5.2.2: For FC and DC-2, we obtain the convergence order

$$\mathcal{O}(k^2 \rho(k)) = \mathcal{O}(k^2 |\log(k)|) \leq \mathcal{O}(k^{2-\varepsilon}) \quad \text{for all } \varepsilon > 0.$$

For DC-1 and SF, we obtain the reduced convergence order $\mathcal{O}(k)$.

In Table 5.1, we illustrate the computational costs of our variants. Recall that DC-2 requires the solution of a fully-coupled non-linear system and therefore is (by far) the most expensive method. All other methods successively employ an explicit approach to the coupling term $\boldsymbol{h}_h^{i,\boldsymbol{\Theta}}$ and consequently only require the computationally cheaper solution of two linear systems for $\boldsymbol{m}_h^{i+1}$ and $\boldsymbol{h}_h^{i+1}$.

In conclusion, DC-2 is the method of choice. It is the only method that benefits (at least from the second time-step on) from the IMEX approach and conserves the (almost) second-order in time convergence. Hence, the computationally more expensive (almost) second-order in time method FC does not pay off. Moreover, the simplification from Remark 5.2.2(v) in SF comes at the prize of a reduced convergence order in time.

5.4. Main result

In this section, we formulate and prove a convergence result for our (almost) second-order tangent plane scheme for ELLG. Recall that for plain LLG, we extended in Chapter 4 the convergence result from [AKST14, Theorem 2] to an extended setting of LLG. For ELLG (and the full Maxwell-LLG system), similar results for the first-order tangent plane schemes are proved in [LT13, Pag13, BPP15, LPPT15]. Based on the own work [DPP+17, Theorem 9], our convergence result combines and extends all the latter findings and requires the following assumptions for the eddy current part of Algorithm 5.2.1:

(E1) Weak consistency of $\boldsymbol{h}_h^0$: It holds that $\boldsymbol{h}_h^0 \rightharpoonup \boldsymbol{h}^0$ in $\boldsymbol{L}^2(\Omega)$ as $h \to 0$.

(E2) Uniform boundedness of $\nabla \times \boldsymbol{h}_h^0$: There exists a constant $C_0 > 0$ such that

$$\|\nabla \times \boldsymbol{h}_h^0\|_{\boldsymbol{L}^2(\Omega)} \le C_0 \quad \text{for all } h > 0.$$

For the stronger statement from Theorem 5.4.1(c) below, we also require the following assumptions:

(E1$^+$) Strong consistency of $\boldsymbol{h}_h^0$: It holds that $\boldsymbol{h}_h^0 \to \boldsymbol{h}^0$ in $\boldsymbol{L}^2(\Omega)$ as $h \to 0$.

(CFL) CFL-type condition: It holds that $k = \mathbf{o}(h^{3/2})$.

With these preparations, we are ready to formulate our main result.

Theorem 5.4.1 (Convergence of TPS2 for ELLG, [DPP+17, Theorem 9])**.** *Consider Algorithm 5.2.1 for the discretization of ELLG* (2.18)*. Then, the following three assertions* (a)–(c) *hold true:*

(a) *Let the assumptions of Theorem 4.5.1*(a) *for plain LLG be satisfied. Then, there exists $k_0 > 0$, which depends only on $\boldsymbol{m}^0$, $C_{\mathbf{ex}}$, α, $\boldsymbol{\pi}(\cdot)$, $\boldsymbol{\Pi}(\cdot)$, μ_0, σ, and $C_{\mathbf{mesh}}$ such that for all $k < k_0$, the discrete variational problem* (5.2) *admits a unique solution. In particular, Algorithm 5.2.1 is well-defined.*

(b) *Let the assumptions of Theorem 4.5.1*(b) *for plain LLG be satisfied and suppose that*
- *the approximations $\boldsymbol{h}_h^0$ satisfy* **(E1)** *and* **(E2)***;*
- *the coupling approach $\boldsymbol{h}_h^{i,\boldsymbol{\Theta}}$ is defined by one of the three options* **(C1)**–**(C3)**.

Then, there exists a subsequence of the postprocessed output $\boldsymbol{m}_{hk}$ and $\boldsymbol{h}_{hk}$ of Algorithm 5.2.1 as well as a weak solution

$$\boldsymbol{m} \in L^\infty(0,T;\boldsymbol{H}^1(\omega)) \cap \boldsymbol{H}^1(\omega_T) \quad \textit{and}$$
$$\boldsymbol{h} \in L^\infty(0,T;\boldsymbol{H}(\mathbf{curl};\Omega)) \cap H^1(0,T;\boldsymbol{L}^2(\Omega))$$

of ELLG (2.18) *in the sense of Definition 2.2.2*(i)–(iv) *such that*

$$\boldsymbol{m}_{hk} \rightharpoonup \boldsymbol{m} \quad \textit{in } \boldsymbol{H}^1(\omega_T) \quad \textit{and} \quad \boldsymbol{h}_{hk} \rightharpoonup \boldsymbol{h} \quad \textit{in } \boldsymbol{L}^2(\Omega_T) \quad \textit{as } h,k \to 0.$$

(c) *Let the assumptions of Theorem 4.5.1*(c) *for plain LLG be satisfied and suppose that*

- *the approximations* $\boldsymbol{h}_h^0$ *satisfy* **(E1⁺)** *and* **(E2)***;*
- *the coupling approach* $\boldsymbol{h}_h^{i,\boldsymbol{\Theta}}$ *is defined by one of the three options* **(C1)**–**(C3)***;*
- *there holds the CFL-type condition* $k = \mathbf{o}(h^{3/2})$ *from* **(CFL)***.*

Then, $(\boldsymbol{m}, \boldsymbol{h})$ *from* (b) *is a physical weak solution in the sense of Definition 2.2.2*(i)–(v)*, i.e., it additionally satisfies the stronger energy estimate* (2.22)*.*

Remark 5.4.2. (i) *In contrast to the unconditional convergence results from [LT13, Pag13, BPP15, LPPT15] for the first-order tangent plane scheme for ELLG (and the full Maxwell-LLG system), we require the CFL-type condition* $k = \mathbf{o}(h^{3/2})$ *to prove* (c)*. We note that this refines the original [DPP⁺17, Theorem 9(iii)], where we supposed the stronger* $k = \mathbf{o}(h^2)$*. We refer to Section 5.4.5 for details.*

(ii) *As for plain LLG, Theorem 5.4.1 holds for* $\rho \equiv 0$ *under the mild CFL-type condition* $k = \mathbf{o}(h)$*; see Remark 4.5.2*(iii) *for details. Note that for* (c)*, we required the even stronger* $k = \mathbf{o}(h^{3/2})$*.*

(iii) *For the validity of the assumptions for our exemplary contributions to* $\boldsymbol{\pi}_h$*,* $\boldsymbol{\Pi}_h$*, and* $\boldsymbol{D}_h$*, the situation is precisely the same as in Remark 4.5.2*(iii)–(vi) *for plain LLG.*

We split the proof of Theorem 5.4.1 into the following subsections. In Section 5.4.1, we prove well-posedness (a). To prove (b), we use a standard energy argument (see, e.g., [Eva10]), which consists of the following three steps:

- We derive a discrete energy bound for the output of Algorithm 5.2.1; see Section 5.4.2.
- We extract weakly convergent subsequences and identify the limits; see Section 5.4.3.
- We verify that the limit $(\boldsymbol{m}, \boldsymbol{h})$ is a weak solution of ELLG in the sense of Definition 2.2.2(i)–(iv) and thus conclude the proof of (b); see Section 5.4.4.

In Section 5.4.5, we prove (c). To this end, we extend the concept of the postprocessed output to the coupling term $\boldsymbol{h}_h^{i,\boldsymbol{\Theta}}$ and write

$$\boldsymbol{h}_{hk}^{\boldsymbol{\Theta}}(t) := \boldsymbol{h}_h^{i,\boldsymbol{\Theta}} \quad \text{for } t \in [t_i, t_{i+1}), \quad \text{where} \quad i \in \{0, 1, \ldots, M-1\}. \tag{5.23}$$

5.4.1. Well-posedness

Proof of Theorem 5.4.1(a). At first, we show that one time-step of Algorithm 5.2.1 is well-defined, i.e., we fix $i \in \{0, \ldots, M-1\}$. Then, we conclude the proof with an induction argument for $i = 0, \ldots, M-1$.

The explicit approaches from **(C2)** and **(C3)** for $\boldsymbol{h}_h^{i,\boldsymbol{\Theta}}$ decouple the time-stepping. There, the corresponding $\boldsymbol{h}_h^i$- and $\boldsymbol{h}_h^{i-1}$-terms only contribute to the right-hand side of the linear system of the LLG part and unique solvability for all choices **(A1)**–**(A3)** for $\boldsymbol{\pi}_h^{\boldsymbol{D}}$ and $\boldsymbol{\Pi}_h^{\boldsymbol{D}}$ follows as in Theorem 4.5.1(a) for the LLG part (5.2a) for sufficiently small $k > 0$ and with the ellipticity of the bilinear form in the eddy current part (5.2b).

For the implicit approach $\boldsymbol{h}_h^{i,\boldsymbol{\Theta}} = \boldsymbol{h}_h^{i+1/2}$ from **(C1)** and **(C2)** and the explicit approaches for $\boldsymbol{\pi}_h^{\boldsymbol{D}}$ and $\boldsymbol{\Pi}_h^{\boldsymbol{D}}$ from **(A2)** and **(A3)**, Remark 5.2.8(ii) implicitly yields well-definedness for sufficiently small $k > 0$ even without the assumptions **(D2)**–**(D3)**, **(T2)** and **(T4)**.

Consequently, the only left case is the combination of the implicit approach

$$\boldsymbol{h}_h^{i,\boldsymbol{\Theta}} = \boldsymbol{h}_h^{i+1/2} \tag{5.24a}$$

from **(C1)** and **(C2)** for the coupling term and the implicit approaches

$$\boldsymbol{\pi}_h^{\boldsymbol{D}}(\boldsymbol{v}_h^i; \boldsymbol{m}_h^i, \boldsymbol{m}_h^{i-1}) = \boldsymbol{\pi}_h(\boldsymbol{m}_h^i) + \frac{k}{2}\,\boldsymbol{\pi}_h(\boldsymbol{v}_h^i), \quad \text{and} \tag{5.24b}$$

$$\boldsymbol{\Pi}_h^{\boldsymbol{D}}(\boldsymbol{v}_h^i; \boldsymbol{m}_h^i, \boldsymbol{m}_h^{i-1}) = \boldsymbol{\Pi}_h(\boldsymbol{m}_h^i) + \frac{k}{2}\,\boldsymbol{D}_h(\boldsymbol{m}_h^i; \boldsymbol{v}_h^i), \tag{5.24c}$$

from **(A1)** and **(A2)** for the lower-order terms. Since we supposed only the weaker **(T4)** instead of **(T4$^+$)**, this case is not covered by Proposition 5.2.7. As a remedy, we introduce an alternate (and artificial) fixed-point iteration, which computes iterates $\boldsymbol{u}_h^{(\ell)} \approx \boldsymbol{v}_h^i$ and $\boldsymbol{g}_h^{(\ell)} \approx \boldsymbol{h}_h^{i+1/2}$ (not relabeled), and prove convergence with the Banach-fixed point theorem towards a unique solution of the discrete variational problem (5.2) with our weaker assumptions. To this end, recall from (5.5) the bilinear form

$$\begin{aligned}\boldsymbol{B}_h^i(\boldsymbol{\psi}_h, \boldsymbol{\varphi}_h) := {}& \langle \mathcal{W}_{G(k)}(\lambda_h^i)\,\boldsymbol{\psi}_h, \boldsymbol{\varphi}_h\rangle_{\boldsymbol{L}^2(\omega)} + \langle \boldsymbol{m}_h^i \times \boldsymbol{\psi}_h, \boldsymbol{\varphi}_h\rangle_{\boldsymbol{L}^2(\omega)} \\ & + \frac{C_{\mathbf{ex}}}{2}\,k\,(1+\rho(k))\,\langle \nabla\boldsymbol{\psi}_h, \nabla\boldsymbol{\varphi}_h\rangle_{\boldsymbol{L}^2(\omega)} \quad \text{for all } \boldsymbol{\psi}_h, \boldsymbol{\varphi}_h \in \boldsymbol{\mathcal{K}}_h(\boldsymbol{m}_h^i).\end{aligned}$$

We note that the corresponding bilinear form for the LLG part (5.2a) then reads

$$\widetilde{\boldsymbol{B}}_h^i(\boldsymbol{\psi}_h, \boldsymbol{\varphi}_h) := \boldsymbol{B}_h^i(\boldsymbol{\psi}_h, \boldsymbol{\varphi}_h) - \frac{k}{2}\,\langle \boldsymbol{\pi}_h(\boldsymbol{\psi}_h), \boldsymbol{\varphi}_h\rangle_{\boldsymbol{L}^2(\omega)} - \frac{k}{2}\,\langle \boldsymbol{D}_h(\boldsymbol{m}_h^i, \boldsymbol{\psi}_h), \boldsymbol{\varphi}_h\rangle_{\boldsymbol{L}^2(\omega)}. \tag{5.25a}$$

for all $\boldsymbol{\psi}_h, \boldsymbol{\varphi}_h \in \boldsymbol{\mathcal{K}}_h(\boldsymbol{m}_h^i)$ and that the corresponding linear form reads

$$\begin{aligned}\boldsymbol{R}_h^i(\boldsymbol{\varphi}_h) := {}& -C_{\mathbf{ex}}\,\langle \nabla\boldsymbol{m}_h^i, \nabla\boldsymbol{\varphi}_h\rangle_{\boldsymbol{L}^2(\omega)} + \langle \boldsymbol{\pi}_h(\boldsymbol{m}_h^i), \boldsymbol{\varphi}_h\rangle_{\boldsymbol{L}^2(\omega)} + \langle \boldsymbol{f}_h^{i+1/2}, \boldsymbol{\varphi}_h\rangle_{\boldsymbol{L}^2(\omega)} \\ & + \langle \boldsymbol{\Pi}_h(\boldsymbol{m}_h^i), \boldsymbol{\varphi}_h\rangle_{\boldsymbol{L}^2(\omega)} + \langle \boldsymbol{h}_h^{i+1/2}, \boldsymbol{\varphi}_h\rangle_{\boldsymbol{L}^2(\omega)} \\ =: {}& \widetilde{\boldsymbol{R}}_h^i(\boldsymbol{\varphi}_h) + \langle \boldsymbol{h}_h^{i+1/2}, \boldsymbol{\varphi}_h\rangle_{\boldsymbol{L}^2(\omega)} \quad \text{for all } \boldsymbol{\varphi}_h \in \boldsymbol{\mathcal{K}}_h(\boldsymbol{m}_h^i).\end{aligned} \tag{5.25b}$$

Our alternate fixed-point iteration then follows the one in Algorithm 5.2.5(a), but, instead of Algorithm 5.2.5(a-i), computes $\boldsymbol{u}_h^{(\ell+1)} \in \boldsymbol{\mathcal{K}}_h(\boldsymbol{m}_h^i)$ as solution of

$$\widetilde{\boldsymbol{B}}_h^i(\boldsymbol{u}_h^{(\ell+1)}, \boldsymbol{\varphi}_h) = \boldsymbol{R}_h^i(\boldsymbol{\varphi}_h) \stackrel{(5.25b)}{=} \widetilde{\boldsymbol{R}}_h^i(\boldsymbol{\varphi}_h) + \langle \boldsymbol{g}_h^{(\ell)}, \boldsymbol{\varphi}_h\rangle_{\boldsymbol{L}^2(\omega)} \quad \text{for all } \boldsymbol{\varphi}_h \in \boldsymbol{\mathcal{K}}_h(\boldsymbol{m}_h^i). \tag{5.25c}$$

Hence, compared to Algorithm 5.2.5, the only difference of our alternate fixed-point iteration is that we incorporate the implicit contributions of $\boldsymbol{\pi}_h$ and $\boldsymbol{D}_h$ in (5.25b) into the bilinear form of the LLG part.

For well-definedness and convergence of the iterates $(\boldsymbol{u}_h^{(\ell)}, \boldsymbol{g}_h^{(\ell)})_{\ell=0}^\infty$, we follow the proof of Proposition 5.2.7. To this end, we denote the energy norm by

$$\|\!|\boldsymbol{\varphi}_h\|\!|^2 := \frac{\alpha}{2}\|\boldsymbol{\varphi}_h\|_{\boldsymbol{L}^2(\omega)}^2 + \frac{C_{\mathbf{ex}}}{2}k\,\|\nabla\boldsymbol{\varphi}_h\|_{\boldsymbol{L}^2(\omega)}^2 \quad \text{for all } \boldsymbol{\varphi}_h \in \boldsymbol{\mathcal{K}}_h(\boldsymbol{m}_h^i) \tag{5.26}$$

and endow the product space $\boldsymbol{\mathcal{K}}_h(\boldsymbol{m}_h^i) \times \boldsymbol{\mathcal{X}}_h$, with the norm

$$\|\!|(\boldsymbol{\varphi}_h, \boldsymbol{\zeta}_h)\|\!|_*^2 := \|\!|\boldsymbol{\varphi}_h\|\!|^2 + \|\boldsymbol{\zeta}_h\|_{\boldsymbol{L}^2(\Omega)}^2 \quad \text{for all } \boldsymbol{\varphi}_h \in \boldsymbol{\mathcal{K}}_h(\boldsymbol{m}_h^i) \quad \text{and all } \boldsymbol{\zeta}_h \in \boldsymbol{\mathcal{X}}_h. \tag{5.27}$$

With our assumptions **(D2)**–**(D3)**, **(T2)** and **(T4)**, we get for sufficiently small $k > 0$ as in **Step 2** of the proof of Theorem 4.5.1(a) for plain LLG that

$$\widetilde{\boldsymbol{B}}_h^i(\boldsymbol{\varphi}_h, \boldsymbol{\varphi}_h) \gtrsim \|\!|\boldsymbol{\varphi}_h\|\!|^2 \quad \text{for all } \boldsymbol{\varphi}_h \in \boldsymbol{\mathcal{K}}_h(\boldsymbol{m}_h^i), \tag{5.28}$$

i.e., ellipticity of $\widetilde{\boldsymbol{B}}_h^i$ with respect to $\|\!|\cdot\|\!|$. Moreover, we note that the bilinear form of the eddy current part (5.12) is elliptic with respect to $\|\cdot\|_{\boldsymbol{L}^2(\Omega)}$. The Lax–Milgram theorem (see Theorem B.2.4) then yields well-definedness of the iterates $(\boldsymbol{u}_h^{(\ell)}, \boldsymbol{g}_h^{(\ell)})_{\ell=0}^\infty$ and we obtain that

$$\begin{aligned}\|\!|\boldsymbol{u}_h^{(\ell+1)} - \boldsymbol{u}_h^{(\ell)}\|\!|^2 &\overset{(5.28)}{\lesssim} \widetilde{\boldsymbol{B}}_h^i(\boldsymbol{u}_h^{(\ell+1)} - \boldsymbol{u}_h^{(\ell)}, \boldsymbol{u}_h^{(\ell+1)} - \boldsymbol{u}_h^{(\ell)}) \\ &\overset{(5.25)}{\leq} \langle \boldsymbol{g}_h^{(\ell)} - \boldsymbol{g}_h^{(\ell-1)}, \boldsymbol{u}_h^{(\ell+1)} - \boldsymbol{u}_h^{(\ell)}\rangle_{\boldsymbol{L}^2(\omega)} \leq \|\boldsymbol{g}_h^{(\ell)} - \boldsymbol{g}_h^{(\ell-1)}\|_{\boldsymbol{L}^2(\Omega)}\,\|\boldsymbol{u}_h^{(\ell+1)} - \boldsymbol{u}_h^{(\ell)}\|_{\boldsymbol{L}^2(\omega)}.\end{aligned}$$

Following the lines of **Step 2** of the proof of Proposition 5.2.7, we further obtain that

$$\|\boldsymbol{g}_h^{(\ell+1)} - \boldsymbol{g}_h^{(\ell)}\|_{\boldsymbol{L}^2(\Omega)} \overset{(5.18)}{\leq} \sqrt{5}k\,\|\boldsymbol{u}_h^{(\ell+1)} - \boldsymbol{u}_h^{(\ell)}\|_{\boldsymbol{L}^2(\omega)} \quad \text{for all } \ell \in \mathbb{N}_0.$$

The combination of the latter two equations then yields that

$$\|\!|\boldsymbol{u}_h^{(\ell+1)} - \boldsymbol{u}_h^{(\ell)}\|\!| \lesssim k\,\|\boldsymbol{u}_h^{(\ell)} - \boldsymbol{u}_h^{(\ell-1)}\|_{\boldsymbol{L}^2(\omega)} \quad \text{for all } \ell \in \mathbb{N}.$$

and altogether, we infer that

$$\begin{aligned}\|\!|(\boldsymbol{u}_h^{(\ell+1)} - \boldsymbol{u}_h^{(\ell)}, \boldsymbol{g}_h^{(\ell+1)} - \boldsymbol{g}_h^{(\ell)})\|\!|_* &\overset{(5.27)}{\lesssim} k\,\|\boldsymbol{u}_h^{(\ell)} - \boldsymbol{u}_h^{(\ell-1)}\|_{\boldsymbol{L}^2(\omega)} \\ &\overset{(5.27)}{\lesssim} k\,\|\!|(\boldsymbol{u}_h^{(\ell)} - \boldsymbol{u}_h^{(\ell-1)}, \boldsymbol{g}_h^{(\ell)} - \boldsymbol{g}_h^{(\ell-1)})\|\!|_* \quad \text{for all } \ell \in \mathbb{N}.\end{aligned}$$

Hence, for sufficiently small $k > 0$, the sequence $(\boldsymbol{u}_h^{(\ell)}, \boldsymbol{g}_h^{(\ell)})_{\ell=0}^\infty$ from our artificial fixed-point iteration is a contraction with respect to $\|\!|\cdot\|\!|_*$. With the Banach fixed-point theorem (see Theorem B.2.6), this yields, in particular, convergence in $\boldsymbol{L}^2(\omega)\times\boldsymbol{L}^2(\Omega)$ towards the unique solution $(\boldsymbol{v}_h^i, \boldsymbol{h}_h^{i+1/2}) \in \boldsymbol{\mathcal{K}}_h(\boldsymbol{m}_h^i) \times \boldsymbol{\mathcal{X}}_h$ of the discrete variational formulation (5.2). Hence, our assumptions also cover the setting of (5.24). Altogether, this concludes the proof. □

5.4.2. Discrete energy bound

In this section, we derive a discrete energy bound, which represents the mathematical core of the proof of Theorem 5.4.1(b). For plain LLG, recall that Lemma 4.5.3 extends the techniques of [Alo08, AKT12, AKST14, BSF$^+$14]. For the ELLG setting of Algorithm 5.2.1, we combine these techniques with extensions of [LT13, Pag13, BPP15, LPPT15] for the eddy current part (2.18b). Here, we elaborate the own work [DPP$^+$17, Lemma 18].

Lemma 5.4.3 (Discrete energy bound, [DPP$^+$17, Lemma 18])**.** *Let the assumptions of Theorem 5.4.1*(b) *be satisfied and let $k > 0$ be small enough. Then, the following assertions* (i)–(iii) *hold true:*

(i) *For all $i = 0, \dots, M-1$, it holds that*

$$\begin{aligned}
&\frac{C_{\mathbf{ex}}}{2}\,\mathrm{d_t}\,\|\nabla \boldsymbol{m}_h^{i+1}\|^2_{\boldsymbol{L}^2(\omega)} + \langle \mathcal{W}_{G(k)}(\lambda_h^i)\,\boldsymbol{v}_h^i, \boldsymbol{v}_h^i\rangle_{\boldsymbol{L}^2(\omega)} + \frac{C_{\mathbf{ex}}}{2} k\rho(k)\|\nabla \boldsymbol{v}_h^i\|^2_{\boldsymbol{L}^2(\omega)}\\
&\qquad + \frac{1}{2}\,\mathrm{d_t}\,\|\boldsymbol{h}_h^{i+1}\|^2_{\boldsymbol{L}^2(\Omega)} + \frac{1}{\mu_0}\,\|\sigma^{-1}\nabla\times \boldsymbol{h}_h^{i+1/2}\|^2_{\boldsymbol{L}^2(\Omega)}\\
&\le \langle \boldsymbol{\pi}_h^{\boldsymbol{D}}(\boldsymbol{v}_h^i; \boldsymbol{m}_h^i, \boldsymbol{m}_h^{i-1}), \boldsymbol{v}_h^i\rangle_{\boldsymbol{L}^2(\omega)} + \langle \boldsymbol{f}_h^{i+1/2}, \boldsymbol{v}_h^i\rangle_{\boldsymbol{L}^2(\omega)} + \langle \boldsymbol{\Pi}_h^{\boldsymbol{D}}(\boldsymbol{v}_h^i; \boldsymbol{m}_h^i, \boldsymbol{m}_h^{i-1}), \boldsymbol{v}_h^i\rangle_{\boldsymbol{L}^2(\omega)}\\
&\qquad + \langle \boldsymbol{h}_h^{i+1/2}, \boldsymbol{v}_h^i - \mathrm{d_t}\boldsymbol{m}_h^{i+1}\rangle_{\boldsymbol{L}^2(\omega)} + \langle \boldsymbol{h}_h^{i,\boldsymbol{\Theta}} - \boldsymbol{h}_h^{i+1/2}, \boldsymbol{v}_h^i\rangle_{\boldsymbol{L}^2(\omega)}.
\end{aligned}$$

(ii) *For all $i = 0, \dots, M-1$, it holds that*

$$\mu_0\,\|\,\mathrm{d_t}\boldsymbol{h}_h^{i+1}\|^2_{\boldsymbol{L}^2(\Omega)} + \mathrm{d_t}\,\|\sigma^{-1/2}\nabla\times \boldsymbol{h}^{i+1}\|^2_{\boldsymbol{L}^2(\Omega)} \;\le\; \mu_0\,\|\,\mathrm{d_t}\boldsymbol{m}_h^{i+1}\|^2_{\boldsymbol{L}^2(\omega)}.$$

(iii) *There exists a constant $C > 0$, which depends only on T, ω, Ω, $\boldsymbol{m}^0$, α, $C_{\mathbf{ex}}$, $\boldsymbol{\pi}(\cdot)$, $\boldsymbol{f}$, $\boldsymbol{\Pi}(\cdot)$, $\boldsymbol{h}^0$, μ_0, σ, and $C_{\mathbf{mesh}}$, such that, for all $j = 0, \dots, M$, it holds that*

$$\begin{aligned}
&\|\nabla \boldsymbol{m}_h^j\|^2_{\boldsymbol{L}^2(\omega)} + k\sum_{i=0}^{j-1}\|\boldsymbol{v}_h^i\|^2_{\boldsymbol{L}^2(\omega)} + k^2\rho(k)\sum_{i=0}^{j-1}\|\nabla \boldsymbol{v}_h^i\|^2_{\boldsymbol{L}^2(\omega)}\\
&\qquad + \|\boldsymbol{h}_h^j\|^2_{\boldsymbol{L}^2(\Omega)} + \|\nabla\times \boldsymbol{h}_h^j\|^2_{\boldsymbol{L}^2(\Omega)} + k\sum_{i=0}^{j-1}\|\,\mathrm{d_t}\boldsymbol{h}_h^{i+1}\|^2_{\boldsymbol{L}^2(\Omega)} \le C < \infty.
\end{aligned}$$

Proof. We split the proof into the following seven steps.

Step 1. We prove (i). Following the lines of the proof of Lemma 4.5.3(i), we infer from the LLG part (5.2a) that

$$\begin{aligned}
&\frac{C_{\mathbf{ex}}}{2}\,\mathrm{d_t}\,\|\nabla \boldsymbol{m}_h^{i+1}\|^2_{\boldsymbol{L}^2(\omega)} + \langle \mathcal{W}_{M(k)}(\lambda_h^i)\boldsymbol{v}_h^i, \boldsymbol{v}_h^i\rangle_{\boldsymbol{L}^2(\omega)} + \frac{C_{\mathbf{ex}}}{2}\,k\rho(k)\,\|\nabla \boldsymbol{v}_h^i\|^2_{\boldsymbol{L}^2(\Omega)}\\
&\le \langle \boldsymbol{\pi}_h^{\boldsymbol{D}}(\boldsymbol{v}_h^i; \boldsymbol{m}_h^i, \boldsymbol{m}_h^{i-1}), \boldsymbol{v}_h^i\rangle_{\boldsymbol{L}^2(\omega)} + \langle \boldsymbol{f}_h^{i+1/2}, \boldsymbol{v}_h^i\rangle_{\boldsymbol{L}^2(\omega)}\\
&\qquad + \langle \boldsymbol{h}_h^{i,\boldsymbol{\Theta}}, \boldsymbol{v}_h^i\rangle_{\boldsymbol{L}^2(\omega)} + \langle \boldsymbol{\Pi}_h^{\boldsymbol{D}}(\boldsymbol{v}_h^i; \boldsymbol{m}_h^i, \boldsymbol{m}_h^{i-1}), \boldsymbol{v}_h^i\rangle_{\boldsymbol{L}^2(\omega)}.
\end{aligned} \tag{5.29}$$

Next, we test the eddy current part (5.2b) with $\boldsymbol{\zeta}_h := -(1/\mu_0)\,\boldsymbol{h}_h^{i+1/2}$ and obtain that

$$\begin{aligned}\langle \mathrm{d_t}\boldsymbol{m}_h^{i+1}, \boldsymbol{h}_h^{i+1/2}\rangle_{\boldsymbol{L}^2(\omega)} &\overset{(5.2b)}{=} -\langle \mathrm{d_t}\boldsymbol{h}_h^{i+1}, \boldsymbol{h}_h^{i+1/2}\rangle_{\boldsymbol{L}^2(\Omega)} - \frac{1}{\mu_0}\|\sigma^{-1/2}\nabla\times\boldsymbol{h}_h^{i+1/2}\|^2_{\boldsymbol{L}^2(\Omega)}\\ &= -\frac{1}{2}\,\mathrm{d_t}\,\|\boldsymbol{h}_h^{i+1}\|^2_{\boldsymbol{L}^2(\Omega)} - \frac{1}{\mu_0}\|\sigma^{-1/2}\nabla\times\boldsymbol{h}_h^{i+1/2}\|^2_{\boldsymbol{L}^2(\Omega)}.\end{aligned}$$

We insert $\boldsymbol{h}_h^{i,\boldsymbol{\Theta}}$ and $\boldsymbol{v}_h^i$ in the latter equation and derive that

$$\begin{aligned}\langle \boldsymbol{v}_h^i, \boldsymbol{h}_h^{i,\boldsymbol{\Theta}}\rangle_{\boldsymbol{L}^2(\omega)} = \langle \boldsymbol{v}_h^i, \boldsymbol{h}_h^{i,\boldsymbol{\Theta}} - \boldsymbol{h}_h^{i+1/2}\rangle_{\boldsymbol{L}^2(\omega)} + \langle \boldsymbol{v}_h^i - \mathrm{d_t}\boldsymbol{m}_h^{i+1}, \boldsymbol{h}_h^{i+1/2}\rangle_{\boldsymbol{L}^2(\omega)}\\ - \frac{1}{2}\,\mathrm{d_t}\,\|\boldsymbol{h}_h^{i+1}\|^2_{\boldsymbol{L}^2(\Omega)} - \frac{1}{\mu_0}\|\sigma^{-1/2}\nabla\times\boldsymbol{h}_h^{i+1/2}\|^2_{\boldsymbol{L}^2(\Omega)}.\end{aligned} \tag{5.30}$$

Finally, the combination of (5.29) and (5.30) proves (i).

Step 2. We prove (ii). We test (5.2b) with $\boldsymbol{\zeta}_h := \mathrm{d_t}\boldsymbol{h}_h^{i+1} \in \boldsymbol{\mathcal{X}}_h$. With the Young inequality, we obtain that

$$\begin{aligned}\mu_0\|\,\mathrm{d_t}\boldsymbol{h}_h^{i+1}\|^2_{\boldsymbol{L}^2(\Omega)} + \frac{1}{2}\,\mathrm{d_t}\,\|\sigma^{-1/2}\nabla\times\boldsymbol{h}_h^{i+1}\|^2_{\boldsymbol{L}^2(\Omega)} = -\mu_0\langle \mathrm{d_t}\boldsymbol{m}_h^{i+1}, \mathrm{d_t}\boldsymbol{h}_h^{i+1}\rangle_{\boldsymbol{L}^2(\omega)}\\ \le \frac{\mu_0}{2}\,\|\,\mathrm{d_t}\boldsymbol{m}_h^{i+1}\|^2_{\boldsymbol{L}^2(\omega)} + \frac{\mu_0}{2}\,\|\,\mathrm{d_t}\boldsymbol{h}_h^{i+1}\|^2_{\boldsymbol{L}^2(\Omega)}.\end{aligned}$$

Absorbing $(\mu_0/2)\,\|\,\mathrm{d_t}\boldsymbol{h}_h^{i+1}\|^2_{\boldsymbol{L}^2(\Omega)}$ in the latter estimate to the left-hand side, we conclude (ii).

Step 3. We prove (iii). To this end, we recall from (4.33) that

$$\frac{\alpha}{2}\,\|\boldsymbol{v}_h^i\|^2_{\boldsymbol{L}^2(\omega)} \;\le\; \langle \mathcal{W}_{G(k)}(\lambda_h^i)\,\boldsymbol{v}_h^i, \boldsymbol{v}_h^i\rangle_{\boldsymbol{L}^2(\omega)} \tag{5.31}$$

for sufficiently small $k > 0$. We sum (i) over $i = 0, \dots, j-1$ and exploit the telescopic sum property. This yields that

$$\begin{aligned}
\chi^{(j)} \quad &:= \quad \frac{C_{\mathbf{ex}}}{2}\,\|\nabla \boldsymbol{m}_h^j\|^2_{\boldsymbol{L}^2(\omega)} + \frac{\alpha}{2}\,k\sum_{i=0}^{j-1}\|\boldsymbol{v}_h^i\|^2_{\boldsymbol{L}^2(\omega)} + \frac{C_{\mathbf{ex}}}{2}\,\rho(k)\,k^2\sum_{i=0}^{j-1}\|\nabla \boldsymbol{v}_h^i\|^2_{\boldsymbol{L}^2(\omega)} \\
&\quad + \frac{1}{2}\,\|\boldsymbol{h}_h^j\|^2_{\boldsymbol{L}^2(\Omega)} + \frac{k}{\mu_0}\sum_{i=0}^{j-1}\|\sigma^{-1}\nabla\times\boldsymbol{h}_h^{i+1/2}\|^2_{\boldsymbol{L}^2(\Omega)} \\
&\overset{(5.31)}{\leq} \quad \frac{C_{\mathbf{ex}}}{2}\,\|\nabla \boldsymbol{m}_h^j\|^2_{\boldsymbol{L}^2(\omega)} + k\sum_{i=0}^{j-1}\langle \mathcal{W}_{G(k)}(\lambda_h^i)\,\boldsymbol{v}_h^i, \boldsymbol{v}_h^i\rangle_{\boldsymbol{L}^2(\omega)} + \frac{C_{\mathbf{ex}}}{2}\,\rho(k)\,k^2\sum_{i=0}^{j-1}\|\nabla \boldsymbol{v}_h^i\|^2_{\boldsymbol{L}^2(\omega)} \\
&\quad + \frac{1}{2}\,\|\boldsymbol{h}_h^j\|^2_{\boldsymbol{L}^2(\Omega)} + \frac{k}{\mu_0}\sum_{i=0}^{j-1}\|\sigma^{-1}\nabla\times\boldsymbol{h}_h^{i+1/2}\|^2_{\boldsymbol{L}^2(\Omega)} \\
&\overset{\text{(i)}}{\leq} \quad \frac{C_{\mathbf{ex}}}{2}\,\|\nabla \boldsymbol{m}_h^0\|^2_{\boldsymbol{L}^2(\omega)} + \frac{1}{2}\,\|\boldsymbol{h}_h^0\|^2_{\boldsymbol{L}^2(\Omega)} + k\sum_{i=0}^{j-1}\langle \boldsymbol{\pi}_h^{\boldsymbol{D}}(\boldsymbol{v}_h^i;\boldsymbol{m}_h^i,\boldsymbol{m}_h^{i-1}), \boldsymbol{v}_h^i\rangle_{\boldsymbol{L}^2(\omega)} \\
&\quad + k\sum_{i=0}^{j-1}\langle \boldsymbol{f}_h^{i+1/2}, \boldsymbol{v}_h^i\rangle_{\boldsymbol{L}^2(\omega)} + k\sum_{i=0}^{j-1}\langle \boldsymbol{\Pi}_h^{\boldsymbol{D}}(\boldsymbol{v}_h^i;\boldsymbol{m}_h^i,\boldsymbol{m}_h^{i-1}), \boldsymbol{v}_h^i\rangle_{\boldsymbol{L}^2(\omega)} \\
&\quad + k\sum_{i=0}^{j-1}\langle \boldsymbol{h}_h^{i+1/2}, \boldsymbol{v}_h^i - \mathrm{d_t}\boldsymbol{m}_h^{i+1}\rangle_{\boldsymbol{L}^2(\omega)} + k\sum_{i=0}^{j-1}\langle \boldsymbol{h}_h^{i,\boldsymbol{\Theta}} - \boldsymbol{h}_h^{i+1/2}, \boldsymbol{v}_h^i\rangle_{\boldsymbol{L}^2(\omega)} \\
&=: \quad S_1+S_2+S_3+S_4+S_5+S_6+S_7.
\end{aligned} \tag{5.32}$$

Note that $\chi^{(j)}$ includes all terms in (iii), but

$$\|\nabla\times\boldsymbol{h}_h^j\|^2_{\boldsymbol{L}^2(\Omega)} \quad \text{and} \quad k\sum_{i=0}^{j-1}\|\,\mathrm{d_t}\boldsymbol{h}_h^{i+1}\|^2_{\boldsymbol{L}^2(\Omega)}.$$

In a first step, we bound $\chi^{(j)}$. To this end, we first estimate $S_1,\dots,S_7$. Then, we absorb as many terms as possible to $\chi^{(j)}$ and apply the discrete Gronwall lemma afterwards.

Step 4. We deal with $S_1,\dots,S_5$. First, we note that

$$S_2 \overset{(5.32)}{:=} \frac{1}{2}\,\|\boldsymbol{h}_h^0\|^2_{\boldsymbol{L}^2(\Omega)} \overset{\textbf{(E1)}}{\lesssim} 1.$$

Following the lines of **Step 2**–**Step 5** in the proof of Lemma 4.5.3(ii) for plain LLG, we obtain together with the latter estimate for arbitrary $\delta > 0$ that

$$\begin{aligned}
\sum_{\ell=1}^{5}|S_\ell| &\lesssim 1 + \frac{1}{\delta} + \frac{k}{\delta}\sum_{i=0}^{j-1}\|\nabla \boldsymbol{m}_h^i\|^2_{\boldsymbol{L}^2(\omega)} \\
&\quad + \Big(k+\delta+\frac{k}{\delta\rho(k)}\Big)\,k\sum_{i=0}^{j-1}\|\boldsymbol{v}_h^i\|^2_{\boldsymbol{L}^2(\omega)} + \delta k^2\rho(k)\sum_{i=0}^{j-1}\|\nabla \boldsymbol{v}_h^i\|^2_{\boldsymbol{L}^2(\omega)};
\end{aligned}$$

see (4.35) for the corresponding estimate for plain LLG.

Step 5. We deal with S_6 and S_7. To this end, we get from Lemma B.1.4(ii) that

$$\|\,\mathrm{d_t}\boldsymbol{m}_h^{i+1}\|_{\boldsymbol{L}^2(\omega)} \lesssim \|\boldsymbol{v}_h^i\|_{\boldsymbol{L}^2(\omega)} \tag{5.33}$$

For all approaches **(C1)**–**(C3)**, the Young inequality yields for arbitrary $\delta > 0$ that

$$\begin{aligned}
|S_6| + |S_7| &\overset{(5.32)}{\leq} k \sum_{i=0}^{j-1} \Big| \langle \boldsymbol{h}_h^{i+1/2}, \boldsymbol{v}_h^i - \mathrm{d_t}\boldsymbol{m}_h^{i+1} \rangle_{\boldsymbol{L}^2(\omega)} \Big| + k \sum_{i=0}^{j-1} \Big| \langle \boldsymbol{h}_h^{i,\boldsymbol{\Theta}} - \boldsymbol{h}_h^{i+1/2}, \boldsymbol{v}_h^i \rangle_{\boldsymbol{L}^2(\omega)} \Big| \\
&\lesssim \frac{k}{\delta} \sum_{i=0}^{j-1} \|\boldsymbol{h}_h^{i+1/2}\|^2_{\boldsymbol{L}^2(\Omega)} + \delta k \sum_{i=0}^{j-1} \|\boldsymbol{v}_h^i - \mathrm{d_t}\boldsymbol{m}_h^{i+1}\|^2_{\boldsymbol{L}^2(\omega)} \\
&\quad + \frac{k}{\delta} \sum_{i=0}^{j-1} \|\boldsymbol{h}_h^{i,\boldsymbol{\Theta}} - \boldsymbol{h}_h^{i+1/2}\|^2_{\boldsymbol{L}^2(\Omega)} + \delta k \sum_{i=0}^{j-1} \|\boldsymbol{v}_h^i\|^2_{\boldsymbol{L}^2(\omega)} \\
&\lesssim \frac{k}{\delta} \sum_{i=0}^{j} \|\boldsymbol{h}_h^i\|^2_{\boldsymbol{L}^2(\Omega)} + \delta k \sum_{i=0}^{j-1} \|\boldsymbol{v}_h^i\|^2_{\boldsymbol{L}^2(\omega)} + \delta k \sum_{i=0}^{j-1} \|\,\mathrm{d_t}\boldsymbol{m}_h^{i+1}\|^2_{\boldsymbol{L}^2(\omega)} \\
&\overset{(5.33)}{\lesssim} \frac{k}{\delta} \sum_{i=0}^{j} \|\boldsymbol{h}_h^i\|^2_{\boldsymbol{L}^2(\Omega)} + \delta k \sum_{i=0}^{j-1} \|\boldsymbol{v}_h^i\|^2_{\boldsymbol{L}^2(\omega)}.
\end{aligned}$$

Step 6. We combine **Step 2**–**Step 5**. This yields for all $j = 1, \dots, M$ the estimate

$$\begin{aligned}
\chi^{(j)} &\lesssim 1 + \frac{1}{\delta} + \frac{k}{\delta} \sum_{i=0}^{j-1} \|\nabla \boldsymbol{m}_h^i\|^2_{\boldsymbol{L}^2(\omega)} + \Big(k + \delta + \frac{k}{\delta\rho(k)} \Big) k \sum_{i=0}^{j-1} \|\boldsymbol{v}_h^i\|^2_{\boldsymbol{L}^2(\omega)} \\
&\quad + \delta k^2 \rho(k) \sum_{i=0}^{j-1} \|\nabla \boldsymbol{v}_h^i\|^2_{\boldsymbol{L}^2(\omega)} + \frac{k}{\delta} \sum_{i=0}^{j} \|\boldsymbol{h}_h^i\|^2_{\boldsymbol{L}^2(\Omega)}.
\end{aligned}$$

We proceed as in **Step 6** of the proof of Lemma 4.5.3(ii) and choose $\delta > 0$ small enough to absorb the terms

$$\delta k \sum_{i=0}^{j-1} \|\boldsymbol{v}_h^i\|^2_{\boldsymbol{L}^2(\omega)} \quad \text{and} \quad \delta k^2 \rho(k) \sum_{i=0}^{j-1} \|\nabla \boldsymbol{v}_h^i\|^2_{\boldsymbol{L}^2(\omega)}$$

into $\chi^{(j)}$. With $k\rho(k)^{-1} \to 0$ from (4.6b) as $k \to 0$, we further absorb for sufficiently small $k > 0$ the terms

$$k^2 \sum_{i=0}^{j-1} \|\boldsymbol{v}_h^i\|^2_{\boldsymbol{L}^2(\omega)} \quad \text{and} \quad \frac{k^2}{\delta\rho(k)} \sum_{i=0}^{j-1} \|\boldsymbol{v}_h^i\|^2_{\boldsymbol{L}^2(\omega)} \quad \text{and} \quad k\,\|\boldsymbol{h}_h^j\|^2_{\boldsymbol{L}^2(\Omega)}$$

into $\chi^{(j)}$. Altogether, this yields for all $j = 1, \dots, M$ that

$$\chi^{(j)} \lesssim 1 + k \sum_{i=0}^{j-1} \|\nabla \boldsymbol{m}_h^i\|^2_{\boldsymbol{L}^2(\omega)} + k \sum_{i=0}^{j-1} \|\boldsymbol{h}_h^i\|^2_{\boldsymbol{L}^2(\omega)} \overset{(5.32)}{\lesssim} 1 + k \sum_{i=0}^{j-1} \chi^{(i)}. \tag{5.34a}$$

Moreover, we get with the assumptions **(D1)** for $\boldsymbol{m}_h^0$ and **(E2)** for $\boldsymbol{h}_h^0$ that

$$\chi^{(0)} \overset{(5.32)}{=} \frac{C_{\mathbf{ex}}}{2} \|\nabla \boldsymbol{m}_h^0\|^2_{\boldsymbol{L}^2(\omega)} + \frac{1}{2} \|\boldsymbol{h}_h^0\|^2_{\boldsymbol{L}^2(\Omega)} \lesssim 1. \tag{5.34b}$$

Observe that (5.34) fits in the setting of the discrete Gronwall lemma (see Lemma B.3.1), which yields that

$$\chi^{(j)} \lesssim \exp\Big(\sum_{i=0}^{j-1} k\Big) \lesssim \exp(T) < \infty \quad \text{for all } j = 1, \dots, M. \tag{5.35}$$

Step 7. We estimate the remaining $\|\nabla \times \boldsymbol{h}_h^j\|^2_{\boldsymbol{L}^2(\Omega)}$ and $k \sum_{i=0}^{j-1} \| \mathrm{d_t} \boldsymbol{h}_h^{i+1}\|^2_{\boldsymbol{L}^2(\Omega)}$. To this end, we sum (ii) over $i = 0, \dots, j-1$. The telescopic sum property yields that

$$\begin{aligned} &\mu_0 \, k \sum_{i=0}^{j-1} \| \mathrm{d_t} \boldsymbol{h}_h^{i+1}\|^2_{\boldsymbol{L}^2(\Omega)} + \|\sigma^{-1/2} \nabla \times \boldsymbol{h}^j\|^2_{\boldsymbol{L}^2(\Omega)} \\ &\leq \; \|\sigma^{-1/2} \nabla \times \boldsymbol{h}^0\|^2_{\boldsymbol{L}^2(\Omega)} + \mu_0 \, k \sum_{i=0}^{j-1} \| \mathrm{d_t} \boldsymbol{m}_h^{i+1}\|^2_{\boldsymbol{L}^2(\omega)} \\ &\overset{(5.32)}{\leq} \; \|\sigma^{-1/2} \nabla \times \boldsymbol{h}^0\|^2_{\boldsymbol{L}^2(\Omega)} + \chi^{(j)} \overset{\mathbf{(E2)}}{\leq} 1 + \chi^{(j)} \overset{(5.35)}{\lesssim} 1. \end{aligned}$$

Together with $\sigma \geq \sigma_0 > 0$ in ELLG (2.18), this concludes the proof. ☐

5.4.3. Extraction of weakly convergent subsequences

In this section, we exploit the discrete energy bound from Lemma 5.4.3 and extract weakly convergent subsequences of the postprocessed output of Algorithm 5.2.1. Note that corresponding results are proved in, e.g., [Alo08, AKT12, AKST14, BSF+14] and Lemma 4.5.4 for plain LLG and in, e.g., [LT13, Pag13, BPP15, LPPT15] for ELLG (and full Maxwell-LLG). Here, we elaborate [DPP+17, Lemma 19].

Lemma 5.4.4 (Convergence properties, [DPP+17, Lemma 19])**.** *Let the assumptions of Theorem 5.4.1*(b) *be satisfied. Then, there exist subsequences of the postprocessed output*

$$\begin{aligned} \boldsymbol{m}_{hk}^\star &\in \{\boldsymbol{m}_{hk}^=, \boldsymbol{m}_{hk}^-, \boldsymbol{m}_{hk}^+, \overline{\boldsymbol{m}}_{hk}, \boldsymbol{m}_{hk}\}, \quad \textit{and} \\ \boldsymbol{h}_{hk}^\star &\in \{\boldsymbol{h}_{hk}^=, \boldsymbol{h}_{hk}^-, \boldsymbol{h}_{hk}^+, \overline{\boldsymbol{h}}_{hk}, \boldsymbol{h}_{hk}, \boldsymbol{h}_{hk}^{\boldsymbol{\Theta}}\}, \end{aligned}$$

as well as functions

$$\begin{aligned} \boldsymbol{m} &\in L^\infty(0,T; \boldsymbol{H}^1(\omega)) \cap \boldsymbol{H}^1(\omega_T), \quad \textit{and} \\ \boldsymbol{h} &\in L^\infty(0,T; \boldsymbol{H}\,(\mathbf{curl}; \Omega)) \cap H^1(0,T; \boldsymbol{L}^2(\Omega)) \end{aligned}$$

such that the following convergence properties (i)–(xii) *hold true simultaneously for the same subsequence as $h, k \to 0$:*

(i) $\boldsymbol{m}_{hk} \rightharpoonup \boldsymbol{m}$ *in* $\boldsymbol{H}^1(\omega_T)$.

(ii) $\boldsymbol{m}_{hk}^{\star} \overset{*}{\rightharpoonup} \boldsymbol{m}$ *in* $L^{\infty}(0,T;\boldsymbol{H}^1(\omega))$.

(iii) $\boldsymbol{m}_{hk}^{\star} \rightharpoonup \boldsymbol{m}$ *in* $L^2(0,T;\boldsymbol{H}^1(\omega))$.

(iv) $\boldsymbol{m}_{hk}^{\star} \to \boldsymbol{m}$ *in* $\boldsymbol{L}^2(\omega_T)$.

(v) $\boldsymbol{m}_{hk}^{\star}(t) \to \boldsymbol{m}(t)$ *in* $\boldsymbol{L}^2(\omega)$ *a.e. for* $t \in (0,T)$.

(vi) $\boldsymbol{m}_{hk}^{\star} \to \boldsymbol{m}$ *pointwise a.e. in* ω_T.

(vii) $\boldsymbol{v}_{hk}^{-} \rightharpoonup \partial_t \boldsymbol{m}$ *in* $\boldsymbol{L}^2(\omega_T)$.

(viii) $k\,\nabla \boldsymbol{v}_{hk}^{-} \to \boldsymbol{0}$ *in* $\boldsymbol{L}^2(\omega_T)$.

(ix) $\boldsymbol{h}_{hk} \rightharpoonup \boldsymbol{h}$ *in* $H^1(0,T;\boldsymbol{L}^2(\Omega))$.

(x) $\boldsymbol{h}_{hk}^{\star} \overset{*}{\rightharpoonup} \boldsymbol{h}$ *in* $L^{\infty}(0,T;\boldsymbol{H}(\mathrm{curl},\Omega))$.

(xi) $\boldsymbol{h}_{hk}^{\star} \rightharpoonup \boldsymbol{h}$ *in* $L^2(0,T;\boldsymbol{H}(\mathrm{curl},\Omega))$.

(xii) $\boldsymbol{h}_{hk}^{\star} - \boldsymbol{h}_{hk} \to \boldsymbol{0}$ *in* $\boldsymbol{L}^2(\Omega_T)$.

Proof. (i)–(viii) follow as for plain LLG; see Lemma 4.5.4. To prove (ix)–(xii), we proceed as in [LT13, Pag13, BPP15, LPPT15] and retrieve from Lemma 5.4.3(iii) that

$$\|\boldsymbol{h}_{hk}\|_{H^1(0,T;\boldsymbol{L}^2(\Omega))} + \|\boldsymbol{h}_{hk}^{\star}\|_{L^{\infty}(0,T;\boldsymbol{H}(\mathbf{curl};\Omega))} \lesssim 1. \tag{5.36}$$

With the Eberlein–Šmulian theorem (see Theorem B.2.2), we can successively extract weakly convergent subsequences of $\boldsymbol{h}_{hk}^{\star}$ with corresponding limits

$$\boldsymbol{h}^{\star} \in \{\boldsymbol{h}^{=}, \boldsymbol{h}^{-}, \boldsymbol{h}^{+}, \overline{\boldsymbol{h}}, \boldsymbol{h}, \boldsymbol{h}^{\boldsymbol{\Theta}}\} \tag{5.37}$$

such that there hold the convergence properties

$$\boldsymbol{h}_{hk}^{\star} \rightharpoonup \boldsymbol{h}^{\star} \quad \text{in } \boldsymbol{L}^2(0,T,\boldsymbol{H}\,(\mathbf{curl};\Omega)) \quad \text{and} \quad \boldsymbol{h}_{hk} \rightharpoonup \boldsymbol{h} \quad \text{in } H^1(0,T;\boldsymbol{L}^2(\Omega))$$

as $h,k \to 0$. Moreover, it is a direct consequence of the definitions of the postprocessed output and the discrete time-derivative, that

$$\|\boldsymbol{h}_{hk}^{\star} - \boldsymbol{h}_{hk}\|_{\boldsymbol{L}^2(\Omega_T)} \lesssim k\,\|\partial_t \boldsymbol{h}_{hk}\|_{\boldsymbol{L}^2(\Omega_T)} \overset{(5.36)}{\lesssim} k \to 0 \quad \text{as } h,k \to 0.$$

This lets us identify all limits $\boldsymbol{h}^{\star}$ in (5.37) and proves (ix), and (xi)–(xii). Finally, we prove (x). With (5.36), the Banach-Alaoglu theorem (see Theorem B.2.3) lets us successively extract further subsequences of $\boldsymbol{h}_{hk}^{\star}$, which converge in $L^{\infty}(0,T;\boldsymbol{H}\,(\mathbf{curl};\Omega))$. Since weak* convergence in $L^{\infty}(0,T;\boldsymbol{H}\,(\mathbf{curl};\Omega))$ implies weak convergence in $L^2(0,T;\boldsymbol{H}\,(\mathbf{curl};\Omega))$, we can identify these limits with $\boldsymbol{h}$ and conclude (xi). Altogether, this concludes the proof. □

As for plain LLG, we note a direct consequence of the latter convergence properties for $\boldsymbol{m}_{hk}^{*}$ and anticipate the verification of Definition 2.2.2(i) for the proof of Theorem 5.4.1(b). The proof follows the lines of Lemma 4.5.4 for plain LLG.

Lemma 5.4.5 ($|\boldsymbol{m}| = 1$ a.e. in ω_T)**.** *Let the assumptions of Theorem 5.4.1*(b) *be satisfied. Then,* $\boldsymbol{m} \in L^{\infty}(0,T;\boldsymbol{H}^1(\omega)) \cap \boldsymbol{H}^1(\omega_T)$ *from Lemma 5.4.4 satisfies* $|\boldsymbol{m}| = 1$ *a.e. in* ω_T. □

5.4.4. Convergence to weak solution

In this section, we prove Theorem 5.4.1(b). For plain LLG, recall that in Section 4.5.4, we extended the techniques of [Alo08, AKT12, AKST14, BSF$^+$14]. For ELLG (and full Maxwell-LLG), note that [LT13, Pag13, BPP15, LPPT15] prove similar results for the first-order tangent plane scheme. For our (almost) second-order in time setting of Algorithm 5.2.1 for ELLG, we proceed as in Section 4.5.4 for the LLG part (2.18a) and extend [LT13, Pag13, BPP15, LPPT15] for the eddy current part (2.18b). Here, we elaborate the proof of the own work [DPP$^+$17, Theorem 9(ii)].

Proof of Theorem 5.4.1(b). We show that

$$\boldsymbol{m} \in L^\infty(0,T;\boldsymbol{H}^1(\omega)) \cap \boldsymbol{H}^1(\omega_T) \quad \text{and} \tag{5.38a}$$

$$\boldsymbol{h} \in L^\infty(0,T;\boldsymbol{H}(\mathbf{curl};\Omega)) \cap H^1(0,T;\boldsymbol{L}^2(\omega)), \tag{5.38b}$$

from Lemma 5.4.4 are a weak solution of ELLG in the sense of Definition 2.2.2(i)–(iv). The combination of (5.38) and Lemma 5.4.5 already yields Definition 2.2.2(i) and (ii), and we split the remaining verifications into the following four steps.

Step 1. We verify Definition 2.2.2(iii), i.e., $\boldsymbol{m}(0) = \boldsymbol{m}^0$ and $\boldsymbol{h}(0) = \boldsymbol{h}^0$ in the sense of traces. For $\boldsymbol{m}$, this follows as in **Step 2** of the proof of Theorem 4.5.1(b) for plain LLG. For $\boldsymbol{h}$, we proceed as in [LT13, Pag13, BPP15, LPPT15]: On the one hand, note that

$$\boldsymbol{h}_{hk}(0) = \boldsymbol{h}_h^0 \overset{\textbf{(E1)}}{\rightharpoonup} \boldsymbol{h}^0 \quad \text{in } \boldsymbol{L}^2(\Omega) \quad \text{as } h,k \to 0.$$

On the other hand, the continuous trace mapping conserves weak convergence and we get from Lemma 5.4.4(ix) that

$$\boldsymbol{h}_{hk}(0) \rightharpoonup \boldsymbol{h}(0) \quad \text{in } \boldsymbol{L}^2(\Omega) \quad \text{as } h,k \to 0.$$

Since weak limits are unique, this verifies $\boldsymbol{h}(0) = \boldsymbol{h}^0$ in the sense of the traces.

Step 2. We verify Definition 2.2.2(iv), i.e., $(\boldsymbol{m}, \boldsymbol{h})$ satisfies the variational formulation (2.21). To this end, let $\boldsymbol{\mathcal{I}}_h$ the nodal interpolation operator associated to $\boldsymbol{\mathcal{S}}_h$. Moreover, let $\boldsymbol{\mathcal{J}}_h : \boldsymbol{C}(\overline{\Omega_T}) \to \boldsymbol{\mathcal{X}}_h$ be the interpolation operator corresponding to the Nédélec-elements of the second kind [Néd86]. Then, let $\boldsymbol{\varphi} \in \boldsymbol{C}^\infty(\overline{\omega_T})$ and $\boldsymbol{\zeta} \in \boldsymbol{C}^\infty(\overline{\Omega_T})$. Since $(\mathbf{a} \times \mathbf{b}) \cdot \mathbf{b} = \mathbf{0}$ for $\mathbf{a}, \mathbf{b} \in \mathbb{R}^3$, we get that

$$\boldsymbol{\mathcal{I}}_h\big(\boldsymbol{m}_h^i \times \boldsymbol{\varphi}(t)\big) \in \boldsymbol{\mathcal{K}}_h(\boldsymbol{m}_h^i) \quad \text{and} \quad \boldsymbol{\mathcal{J}}_h(\boldsymbol{\zeta}(t)) \in \boldsymbol{\mathcal{X}}_h$$

for $t \in [t_i, t_{i+1})$ and $i \in \{0, 1, \dots, M-1\}$. Then, we test the LLG part (5.2a) and the eddy current part (5.2a) of the discrete variational formulation with $\boldsymbol{\mathcal{I}}_h(\boldsymbol{m}_h^i \times \boldsymbol{\varphi}(t))$ and $\boldsymbol{\mathcal{J}}_h(\boldsymbol{\zeta}(t))$, respectively, and integrate over $[0,T]$. Plugging in the definition of the postprocessed output, we get the LLG part

$$
\begin{aligned}
& I_{hk}^1 + I_{hk}^2 + \frac{C_{\mathbf{ex}}}{2}\, I_{hk}^3 := \\
& \int_0^T \langle \mathcal{W}_{G(k)}(\lambda_{hk}^-)\boldsymbol{v}_{hk}^-, \boldsymbol{\mathcal{I}}_h(\boldsymbol{m}_{hk}^- \times \boldsymbol{\varphi})\rangle_{\boldsymbol{L}^2(\omega)}\,\mathrm{d}t + \int_0^T \langle \boldsymbol{m}_{hk}^- \times \boldsymbol{v}_{hk}^-, \boldsymbol{\mathcal{I}}_h(\boldsymbol{m}_{hk}^- \times \boldsymbol{\varphi})\rangle_{\boldsymbol{L}^2(\omega)}\,\mathrm{d}t \\
& \quad + \frac{C_{\mathbf{ex}}}{2}\, k(1+\rho(k)) \int_0^T \langle \nabla \boldsymbol{v}_{hk}^-, \nabla \boldsymbol{\mathcal{I}}_h(\boldsymbol{m}_{hk}^- \times \boldsymbol{\varphi})\rangle_{\boldsymbol{L}^2(\omega)}\,\mathrm{d}t \\
& \overset{(5.2a)}{=} -C_{\mathbf{ex}} \int_0^T \langle \nabla \boldsymbol{m}_{hk}^-, \nabla \boldsymbol{\mathcal{I}}_h(\boldsymbol{m}_{hk}^- \times \boldsymbol{\varphi})\rangle_{\boldsymbol{L}^2(\omega)}\,\mathrm{d}t + \int_0^T \langle \boldsymbol{\pi}_h^{\boldsymbol{D}}(\boldsymbol{v}_{hk}^-; \boldsymbol{m}_{hk}^-, \boldsymbol{m}_{hk}^{=}), \boldsymbol{\mathcal{I}}_h(\boldsymbol{m}_{hk}^- \times \boldsymbol{\varphi})\rangle_{\boldsymbol{L}^2(\omega)}\,\mathrm{d}t \\
& \quad + \int_0^T \langle \overline{\boldsymbol{f}}_{hk}, \boldsymbol{\mathcal{I}}_h(\boldsymbol{m}_{hk}^- \times \boldsymbol{\varphi})\rangle_{\boldsymbol{L}^2(\omega)}\,\mathrm{d}t + \int_0^T \langle \boldsymbol{h}_{hk}^{\boldsymbol{\Theta}}, \boldsymbol{\mathcal{I}}_h(\boldsymbol{m}_{hk}^- \times \boldsymbol{\varphi})\rangle_{\boldsymbol{L}^2(\omega)}\,\mathrm{d}t \\
& \quad + \int_0^T \langle \boldsymbol{\Pi}_h^{\boldsymbol{D}}(\boldsymbol{v}_{hk}^-; \boldsymbol{m}_{hk}^-, \boldsymbol{m}_{hk}^{=}), \boldsymbol{\mathcal{I}}_h(\boldsymbol{m}_{hk}^- \times \boldsymbol{\varphi})\rangle_{\boldsymbol{L}^2(\omega)}\,\mathrm{d}t \\
& =: \; -C_{\mathbf{ex}} I_{hk}^4 + I_{hk}^5 + I_{hk}^6 + I_{hk}^7 + I_{hk}^8
\end{aligned}
\tag{5.39a}
$$

as well as the eddy current part

$$
\begin{aligned}
& -\mu_0\, I_{hk}^9 := -\mu_0 \int_0^T \langle \partial_t \boldsymbol{m}_{hk}, \boldsymbol{\mathcal{J}}_h \boldsymbol{\zeta}\rangle_{\boldsymbol{L}^2(\omega)}\,\mathrm{d}t \\
& \overset{(5.2b)}{=} \mu_0 \int_0^T \langle \partial_t \boldsymbol{h}_{hk}, \boldsymbol{\mathcal{J}}_h \boldsymbol{\zeta}\rangle_{\boldsymbol{L}^2(\Omega)}\,\mathrm{d}t + \int_0^T \langle \sigma^{-1} \nabla \times \overline{\boldsymbol{h}}_{hk}, \nabla \times (\boldsymbol{\mathcal{J}}_h \boldsymbol{\zeta})\rangle_{\boldsymbol{L}^2(\Omega)}\,\mathrm{d}t \\
& =: \; \mu_0 I_{hk}^{10} + I_{hk}^{11}.
\end{aligned}
\tag{5.39b}
$$

In the following, we prove convergence of the integrals $I_{hk}^1,\dots,I_{hk}^{11}$ and obtain the variational formulation (2.16) from the limits.

Step 3. We deal with the LLG part (5.39a). We start with the coupling term I_{hk}^7. From **Step 4** of the proof of Theorem 4.5.1(b) for plain LLG, we recall the auxiliary convergence

$$
\boldsymbol{\mathcal{I}}_h(\boldsymbol{m}_{hk}^- \times \boldsymbol{\varphi}) \to \boldsymbol{m} \times \boldsymbol{\varphi} \quad \text{in } \boldsymbol{L}^2(\omega_T) \quad \text{as } h,k \to 0.
$$

Together with the convergence property from Lemma 5.4.4(xi), this yields that

$$
I_{hk}^7 \overset{(5.39a)}{=} \int_0^T \langle \boldsymbol{h}_{hk}^{\boldsymbol{\Theta}}, \boldsymbol{\mathcal{I}}_h(\boldsymbol{m}_{hk}^- \times \boldsymbol{\varphi})\rangle_{\boldsymbol{L}^2(\omega)}\,\mathrm{d}t \to \int_0^T \langle \boldsymbol{h}, \boldsymbol{m} \times \boldsymbol{\varphi}\rangle_{\boldsymbol{L}^2(\omega)}\,\mathrm{d}t, \quad \text{as } h,k \to 0.
$$

For $I_{hk}^1,\dots,I_{hk}^6$ and I_{hk}^8, we follow the lines of the proof of Theorem 4.5.1(b) for plain LLG.

We obtain that

$$
\begin{aligned}
I_{hk}^1 &\overset{(5.39a)}{=} \int_0^T \langle \mathcal{W}_{G(k)}(\lambda_{hk}^-)\boldsymbol{v}_{hk}^-, \boldsymbol{\mathcal{I}}_h(\boldsymbol{m}_{hk}^- \times \boldsymbol{\varphi})\rangle_{\boldsymbol{L}^2(\omega)}\,\mathrm{d}t \to \alpha \int_0^T \langle \partial_t \boldsymbol{m}, \boldsymbol{m}\times\boldsymbol{\varphi}\rangle_{\boldsymbol{L}^2(\omega)}\,\mathrm{d}t,\\
I_{hk}^2 &\overset{(5.39a)}{=} \int_0^T \langle \boldsymbol{m}_{hk}^- \times \boldsymbol{v}_{hk}^-, \boldsymbol{\mathcal{I}}_h(\boldsymbol{m}_{hk}^- \times \boldsymbol{\varphi})\rangle_{\boldsymbol{L}^2(\omega)}\,\mathrm{d}t \to \int_0^T \langle \partial_t \boldsymbol{m}, \boldsymbol{\varphi}\rangle_{\boldsymbol{L}^2(\omega)}\,\mathrm{d}t,\\
I_{hk}^3 &\overset{(5.39a)}{=} k(1+\rho(k)) \int_0^T \langle \nabla \boldsymbol{v}_{hk}^-, \nabla\boldsymbol{\mathcal{I}}_h(\boldsymbol{m}_{hk}^- \times \boldsymbol{\varphi})\rangle_{\boldsymbol{L}^2(\omega)}\,\mathrm{d}t \to 0,\\
I_{hk}^4 &\overset{(5.39a)}{=} \int_0^T \langle \nabla \boldsymbol{m}_{hk}^-, \nabla\boldsymbol{\mathcal{I}}_h(\boldsymbol{m}_{hk}^- \times \boldsymbol{\varphi})\rangle_{\boldsymbol{L}^2(\omega)}\,\mathrm{d}t \to -\int_0^T \langle \boldsymbol{m}\times\nabla\boldsymbol{m}, \nabla\boldsymbol{\varphi}\rangle_{\boldsymbol{L}^2(\omega)}\,\mathrm{d}t, \quad \text{and}\\
I_{hk}^6 &\overset{(5.39a)}{=} \int_0^T \langle \overline{\boldsymbol{f}}_{hk}, \boldsymbol{\mathcal{I}}_h(\boldsymbol{m}_{hk}^- \times \boldsymbol{\varphi})\rangle_{\boldsymbol{L}^2(\omega)}\,\mathrm{d}t \to \int_0^T \langle \boldsymbol{f}, \boldsymbol{m}\times\boldsymbol{\varphi}\rangle_{\boldsymbol{L}^2(\omega)}\,\mathrm{d}t\,.
\end{aligned}
$$

as $h,k \to 0$. For I_{hk}^5 and I_{hk}^8, recall from plain LLG that we required the convergence properties from Lemma 4.5.4 and the weak consistencies **(D4)**, **(D7)** and **(T5)** for $\boldsymbol{\pi}_h$, $\boldsymbol{\Pi}_h$, and $\boldsymbol{D}_h$, respectively, to derive the weak consistencies from Lemma 4.5.7 for $\boldsymbol{\pi}_h^{\boldsymbol{D}}$ and $\boldsymbol{\Pi}_h^{\boldsymbol{D}}$. Hence, with Lemma 5.4.4 (i)–(viii), we get in the same way that

$$
\begin{aligned}
I_{hk}^5 &\overset{(5.39a)}{=} \int_0^T \langle \boldsymbol{\pi}_h^{\boldsymbol{D}}(\boldsymbol{v}_{hk}^-; \boldsymbol{m}_{hk}^-, \boldsymbol{m}_{hk}^{=}), \boldsymbol{\mathcal{I}}_h(\boldsymbol{m}_{hk}^- \times \boldsymbol{\varphi})\rangle_{\boldsymbol{L}^2(\omega)}\,\mathrm{d}t \to \int_0^T \langle \boldsymbol{\pi}(\boldsymbol{m}), \boldsymbol{m}\times\boldsymbol{\varphi}\rangle_{\boldsymbol{L}^2(\omega)}\,\mathrm{d}t,\\
I_{hk}^8 &\overset{(5.39a)}{=} \int_0^T \langle \boldsymbol{\Pi}_h^{\boldsymbol{D}}(\boldsymbol{v}_{hk}^-; \boldsymbol{m}_{hk}^-, \boldsymbol{m}_{hk}^{=}), \boldsymbol{\mathcal{I}}_h(\boldsymbol{m}_{hk}^- \times \boldsymbol{\varphi})\rangle_{\boldsymbol{L}^2(\omega)}\,\mathrm{d}t \to \int_0^T \langle \boldsymbol{\Pi}(\boldsymbol{m}), \boldsymbol{m}\times\boldsymbol{\varphi}\rangle_{\boldsymbol{L}^2(\omega)}\,\mathrm{d}t,
\end{aligned}
$$

as $h,k \to 0$.

Step 4. We deal with the eddy current part (5.39b) as in [LT13, Pag13, BPP15, LPPT15]: To this end, the convergence properties of the interpolant $\boldsymbol{\mathcal{J}}_h$ (see Proposition 3.1.9) yield that

$$
\boldsymbol{\mathcal{J}}_h\boldsymbol{\zeta} \to \boldsymbol{\zeta} \quad \text{in } L^2(0,T;\boldsymbol{H}(\mathbf{curl};\Omega)) \quad \text{as } h,k\to 0. \tag{5.40}
$$

Together with the convergence properties from Lemma 5.4.4, we obtain that

$$
\begin{aligned}
I_{hk}^9 &\overset{(5.39b)}{=} \int_0^T \langle \partial_t \boldsymbol{m}_{hk}, \boldsymbol{\mathcal{J}}_h\boldsymbol{\zeta}\rangle_{\boldsymbol{L}^2(\omega)}\,\mathrm{d}t \to \int_0^T \langle \partial_t\boldsymbol{m}, \boldsymbol{\zeta}\rangle_{\boldsymbol{L}^2(\omega)}\,\mathrm{d}t,\\
I_{hk}^{10} &\overset{(5.39b)}{=} \int_0^T \langle \partial_t \boldsymbol{h}_{hk}, \boldsymbol{\mathcal{J}}_h\boldsymbol{\zeta}\rangle_{\boldsymbol{L}^2(\Omega)}\,\mathrm{d}t \to \int_0^T \langle \partial_t\boldsymbol{h}, \boldsymbol{\zeta}\rangle_{\boldsymbol{L}^2(\Omega)}\,\mathrm{d}t, \quad \text{and}\\
I_{hk}^{11} &\overset{(5.39b)}{=} \int_0^T \langle \sigma^{-1}\nabla\times\overline{\boldsymbol{h}}_{hk}, \nabla\times(\boldsymbol{\mathcal{J}}_h\boldsymbol{\zeta})\rangle_{\boldsymbol{L}^2(\Omega)}\,\mathrm{d}t \to \int_0^T \langle \sigma^{-1}\nabla\times\boldsymbol{h}, \nabla\times\boldsymbol{\zeta}\rangle_{\boldsymbol{L}^2(\Omega)}\,\mathrm{d}t,
\end{aligned}
$$

as $h,k \to 0$. Altogether, this concludes the proof. □

5.4.5. Stronger energy estimate

In this section, we prove Theorem 5.4.1(c), i.e., under stronger assumptions, the solution $(\boldsymbol{m},\boldsymbol{h})$ from (b) also satisfies the stronger energy estimate (2.22). To this end, recall that in Section 4.5.5, we extended the techniques of [AKST14, BSF$^+$14] and proved a corresponding result for LLG. For ELLG and full Maxwell-LLG, [LT13, BPP15, LPPT15] state and [Pag13] proves similar results for the classical first-order tangent plane scheme. Based on the proof of the own work [DPP$^+$17, Theorem 9(iii)], we combine the latter findings to prove Theorem 5.4.1(c). However, we face the following problem: Compared to the classical first-order tangent plane schemes for ELLG (and full Maxwell-LLG) in [LT13, Pag13, BPP15, LPPT15], the first term in the eddy current part (5.2b) reads

$$\langle \mathrm{d_t} \boldsymbol{m}_h^{i+1}, \boldsymbol{\zeta}_h \rangle_{\boldsymbol{L}^2(\omega)} \quad \text{instead of} \quad \langle \boldsymbol{v}_h^i, \boldsymbol{\zeta}_h \rangle_{\boldsymbol{L}^2(\omega)}. \tag{5.41}$$

However, the replacement (5.41) is essential to establish (almost) second-order in time convergence; see Remark 5.2.2(v). Yet, throughout the verification of the stronger energy estimate (2.22), the replacement (5.41) gives rise to the additional error term

$$\int_0^{t_j} \langle \overline{\boldsymbol{h}}_{hk}, \boldsymbol{v}_{hk}^- - \partial_t \boldsymbol{m}_{hk} \rangle_{\boldsymbol{L}^2(\omega)} \,\mathrm{d}t, \tag{5.42}$$

which must converge to 0 as $h, k \to 0$. To this end, we require the additional convergence property of the following lemma, where the

$$\text{CFL-type condition} \quad k = \mathbf{o}(h^{3/2}).$$

from **(CFL)** comes into play.

Lemma 5.4.6 (Additional convergence property, [DPP$^+$17, p.27])**.** *Let the assumptions of Theorem 5.4.1*(b) *and the CFL-condition* **(CFL)** *be satisfied. Then, it holds that*

$$\boldsymbol{v}_{hk}^- - \partial_t \boldsymbol{m}_{hk} \to \boldsymbol{0} \quad \text{in } L^1(0,T;\boldsymbol{L}^2(\omega)) \quad \text{as } h, k \to 0.$$

Proof. With Lemma B.1.4(ii), we get that

$$\begin{aligned} \|\boldsymbol{v}_{hk}^- - \partial_t \boldsymbol{m}_{hk}\|_{L^1(0,T;\boldsymbol{L}^2(\omega))} &= \int_0^T \|\boldsymbol{v}_{hk}^- - \partial_t \boldsymbol{m}_{hk}\|_{\boldsymbol{L}^2(\omega)} \,\mathrm{d}t \\ &= k \sum_{i=0}^{M-1} \|\boldsymbol{v}_h^j - \mathrm{d_t}\boldsymbol{m}_h^{i+1}\|_{\boldsymbol{L}^2(\omega)} \lesssim k^2 \sum_{i=0}^{M-1} \|\boldsymbol{v}_h^i\|_{\boldsymbol{L}^4(\omega)}^2. \end{aligned}$$

With the interpolation estimate (see Proposition 2.1.1 with $p = 2$, $q = 4$, $r = 6$, and $\theta = 1/4$), and since the Sobolev-embedding $\boldsymbol{H}^1(\omega) \hookrightarrow \boldsymbol{L}^6(\omega)$ is continuous, we obtain that

$$\|\boldsymbol{v}_h^i\|_{\boldsymbol{L}^4(\omega)} \lesssim \|\boldsymbol{v}_h^i\|_{\boldsymbol{L}^2(\omega)}^{1/4} \|\boldsymbol{v}_h^i\|_{\boldsymbol{L}^6(\omega)}^{3/4} \lesssim \|\boldsymbol{v}_h^i\|_{\boldsymbol{L}^2(\omega)}^{1/4} \|\boldsymbol{v}_h^i\|_{\boldsymbol{H}^1(\omega)}^{3/4}. \tag{5.43}$$

We combine the latter two equations. An inverse estimate (see Proposition 3.1.8) and the convergence property from Lemma 5.4.4(vii) then yield that

$$\begin{aligned} \|\boldsymbol{v}_{hk}^- - \partial_t \boldsymbol{m}_{hk}\|_{L^1(0,T;\boldsymbol{L}^2(\omega))} &\lesssim k^2 \sum_{i=0}^{M-1} \|\boldsymbol{v}_h^i\|_{\boldsymbol{L}^2(\omega)}^{1/2} \|\boldsymbol{v}_h^i\|_{\boldsymbol{H}^1(\omega)}^{3/2} \\ &\lesssim k^2 h^{-3/2} \sum_{i=0}^{M-1} \|\boldsymbol{v}_h^i\|_{\boldsymbol{L}^2(\omega)}^2 = k h^{-3/2} \|\boldsymbol{v}_{hk}^-\|_{\boldsymbol{L}^2(\omega_T)}^2 \lesssim k h^{-3/2} \overset{\textbf{(CFL)}}{\to} 0 \quad \text{as } h, k \to 0. \end{aligned}$$

This concludes the proof. ∎

Remark 5.4.7. *Our formulation of Lemma 5.4.6 improves [DPP⁺17], in the sense that we only require* $k = \mathbf{o}(h^{3/2})$ *instead of the stronger CFL-type condition* $k = \mathbf{o}(h^2)$*.*

We have everything together for the proof of Theorem 5.4.1(c).

Proof of Theorem 5.4.1(c). Since the assumptions from (c) are stronger than those of (b), we only have to verify, that $(\boldsymbol{m}, \boldsymbol{h})$ from (b) satisfies the energy estimate (2.22). To this end, recall the notion of the energy functional from (2.20)

$$\mathcal{E}_{\mathrm{ELLG}}(\boldsymbol{m}, \boldsymbol{h}) := \frac{C_{\mathbf{ex}}}{2} \|\nabla \boldsymbol{m}\|^2_{\boldsymbol{L}^2(\omega)} - \frac{1}{2} \langle \boldsymbol{\pi}(\boldsymbol{m}), \boldsymbol{m} \rangle_{\boldsymbol{L}^2(\omega)} - \langle \boldsymbol{f}, \boldsymbol{m} \rangle_{\boldsymbol{L}^2(\omega)} + \frac{1}{2} \|\boldsymbol{h}\|^2_{\boldsymbol{L}^2(\Omega)}. \tag{5.44}$$

Then, let $\tau \in [0, T)$ be arbitrary and let $j \in \{1 \ldots, M\}$ such that $\tau \in [t_{j-1}, t_j)$. Since we supposed $\boldsymbol{f} \in C^1([0, T; \boldsymbol{L}^2(\omega))$, we can define $\boldsymbol{f}^i := \boldsymbol{f}(t_i)$ for all $i \in \{0, \ldots, M\}$. With the discrete energy estimate from Lemma 5.4.3(i), we get for all $i \in \{0, \ldots, j-1\}$ that

$$\begin{aligned}
&\mathcal{E}_{\mathrm{ELLG}}(\boldsymbol{m}_h^{i+1}, \boldsymbol{h}_h^{i+1}) - \mathcal{E}_{\mathrm{ELLG}}(\boldsymbol{m}_h^{i}, \boldsymbol{h}_h^{i}) \\
&\overset{(5.44)}{=} \frac{C_{\mathbf{ex}}}{2} k \, \mathrm{d_t} \|\nabla \boldsymbol{m}_h^{i+1}\|^2_{\boldsymbol{L}^2(\omega)} - \frac{1}{2} \langle \boldsymbol{\pi}(\boldsymbol{m}_h^{i+1}), \boldsymbol{m}_h^{i+1} \rangle_{\boldsymbol{L}^2(\omega)} + \frac{1}{2} \langle \boldsymbol{\pi}(\boldsymbol{m}_h^{i}), \boldsymbol{m}_h^{i} \rangle_{\boldsymbol{L}^2(\omega)} \\
&\qquad - \langle \boldsymbol{f}^{i+1}, \boldsymbol{m}_h^{i+1} \rangle_{\boldsymbol{L}^2(\omega)} + \langle \boldsymbol{f}^{i}, \boldsymbol{m}_h^{i} \rangle_{\boldsymbol{L}^2(\omega)} + \frac{1}{2} \mathrm{d_t} \|\boldsymbol{h}_h^{i+1}\|^2_{\boldsymbol{L}^2(\Omega)} \\
&\leq \; -k \langle \mathcal{W}_{G(k)}(\lambda_h^i) \boldsymbol{v}_h^i, \boldsymbol{v}_h^i \rangle_{\boldsymbol{L}^2(\omega)} - \frac{C_{\mathbf{ex}}}{2} k^2 \rho(k) \|\nabla \boldsymbol{v}_h^i\|^2_{\boldsymbol{L}^2(\omega)} - \frac{k}{\mu_0} \|\sigma^{-1} \nabla \times \boldsymbol{h}_h^{i+1/2}\|^2_{\boldsymbol{L}^2(\Omega)} \\
&\qquad + k \langle \boldsymbol{\pi}_h^{\boldsymbol{D}}(\boldsymbol{v}_h^i; \boldsymbol{m}_h^i, \boldsymbol{m}_h^{i-1}), \boldsymbol{v}_h^i \rangle_{\boldsymbol{L}^2(\omega)} - \frac{1}{2} \langle \boldsymbol{\pi}(\boldsymbol{m}_h^{i+1}), \boldsymbol{m}_h^{i+1} \rangle_{\boldsymbol{L}^2(\omega)} + \frac{1}{2} \langle \boldsymbol{\pi}(\boldsymbol{m}_h^{i}), \boldsymbol{m}_h^{i} \rangle_{\boldsymbol{L}^2(\omega)} \\
&\qquad + k \langle \boldsymbol{f}_h^{i+1/2}, \boldsymbol{v}_h^i \rangle_{\boldsymbol{L}^2(\omega)} - \langle \boldsymbol{f}^{i+1}, \boldsymbol{m}_h^{i+1} \rangle_{\boldsymbol{L}^2(\omega)} + \langle \boldsymbol{f}^{i}, \boldsymbol{m}_h^{i} \rangle_{\boldsymbol{L}^2(\omega)} \\
&\qquad + k \langle \boldsymbol{\Pi}_h^{\boldsymbol{D}}(\boldsymbol{v}_h^i; \boldsymbol{m}_h^i, \boldsymbol{m}_h^{i-1}), \boldsymbol{v}_h^i \rangle_{\boldsymbol{L}^2(\omega)} + k \langle \boldsymbol{h}_h^{i+1/2}, \boldsymbol{v}_h^i - \mathrm{d_t} \boldsymbol{m}_h^{i+1} \rangle_{\boldsymbol{L}^2(\omega)} \\
&\qquad + k \langle \boldsymbol{h}_h^{i,\boldsymbol{\Theta}} - \boldsymbol{h}_h^{i+1/2}, \boldsymbol{v}_h^i \rangle_{\boldsymbol{L}^2(\omega)} \\
&=: \; -k \langle \mathcal{W}_{G(k)}(\lambda_h^i) \boldsymbol{v}_h^i, \boldsymbol{v}_h^i \rangle_{\boldsymbol{L}^2(\omega)} - \frac{C_{\mathbf{ex}}}{2} k^2 \rho(k) \|\nabla \boldsymbol{v}_h^i\|^2_{\boldsymbol{L}^2(\omega)} - \frac{k}{\mu_0} \|\sigma^{-1} \nabla \times \boldsymbol{h}_h^{i+1/2}\|^2_{\boldsymbol{L}^2(\Omega)} \\
&\qquad + \sum_{\ell=1}^{3} T_{\boldsymbol{\pi}}^{(\ell)} + \sum_{\ell=1}^{3} T_{\boldsymbol{f}}^{(\ell)} + k \langle \boldsymbol{\Pi}_h^{\boldsymbol{D}}(\boldsymbol{v}_h^i; \boldsymbol{m}_h^i, \boldsymbol{m}_h^{i-1}), \boldsymbol{v}_h^i \rangle_{\boldsymbol{L}^2(\omega)} + k \langle \boldsymbol{h}_h^{i+1/2}, \boldsymbol{v}_h^i - \mathrm{d_t} \boldsymbol{m}_h^{i+1} \rangle_{\boldsymbol{L}^2(\omega)} \\
&\qquad + k \langle \boldsymbol{h}_h^{i,\boldsymbol{\Theta}} - \boldsymbol{h}_h^{i+1/2}, \boldsymbol{v}_h^i \rangle_{\boldsymbol{L}^2(\omega)}.
\end{aligned} \tag{5.45a}$$

Following the lines of **Step 2** and **Step 3** in the proof of Theorem 4.5.1(c) for plain LLG, we get that

$$\begin{aligned}
\sum_{\ell=1}^{3} T_{\boldsymbol{\pi}}^{(\ell)} \lesssim k \, \Big| \langle \boldsymbol{\pi}_h^{\boldsymbol{D}}(\boldsymbol{v}_h^i; \boldsymbol{m}_h^i, \boldsymbol{m}_h^{i-1}) - \boldsymbol{\pi}(\boldsymbol{m}_h^i), \boldsymbol{v}_h^i \rangle_{\boldsymbol{L}^2(\omega)} \Big| \\
+ k^2 \|\boldsymbol{v}_h^i\|^2_{\boldsymbol{L}^2(\omega)} + k^2 \|\boldsymbol{v}_h^i\|_{\boldsymbol{L}^2(\omega)} \|\nabla \boldsymbol{v}_h^i\|_{\boldsymbol{L}^2(\omega)}
\end{aligned} \tag{5.45b}$$

as well as

$$\sum_{\ell=1}^{3} T_{\boldsymbol{f}}^{(\ell)} + k\,\langle \mathrm{d_t}\boldsymbol{f}^{i+1}, \boldsymbol{m}_h^i\rangle_{\boldsymbol{L}^2(\omega)} \lesssim k \left| \langle \boldsymbol{f}_h^{i+1/2} - \boldsymbol{f}^{i+1}, \boldsymbol{v}_h^i\rangle_{\boldsymbol{L}^2(\omega)} \right| + k^2\,\|\boldsymbol{v}_h^i\|_{\boldsymbol{L}^2(\omega)}^2 + k^2\,\|\boldsymbol{v}_h^i\|_{\boldsymbol{L}^2(\omega)}\,\|\nabla\boldsymbol{v}_h^i\|_{\boldsymbol{L}^2(\omega)}. \tag{5.45c}$$

Since $\rho(k) \geq 0$, we can omit $(C_{\mathbf{ex}}/2)k^2\rho(k)\|\nabla\boldsymbol{v}_h^i\|_{\boldsymbol{L}^2(\omega)}^2$ in (5.45a) and obtain that

$$\begin{aligned}
&\mathcal{E}_{\mathrm{ELLG}}(\boldsymbol{m}_h^{i+1}, \boldsymbol{h}_h^{i+1}) - \mathcal{E}_{\mathrm{ELLG}}(\boldsymbol{m}_h^i, \boldsymbol{h}_h^i) + k\langle \mathcal{W}_{G(k)}(\lambda_h^i)\boldsymbol{v}_h^i, \boldsymbol{v}_h^i\rangle_{\boldsymbol{L}^2(\omega)} + k\,\langle \mathrm{d_t}\boldsymbol{f}^{i+1}, \boldsymbol{m}_h^i\rangle_{\boldsymbol{L}^2(\omega)} \\
&\quad + \frac{k}{\mu_0}\,\|\sigma^{-1}\nabla\times\boldsymbol{h}_h^{i+1/2}\|_{\boldsymbol{L}^2(\Omega)}^2 - k\langle \boldsymbol{\Pi}_h^{\boldsymbol{D}}(\boldsymbol{v}_h^i; \boldsymbol{m}_h^i, \boldsymbol{m}_h^{i-1}), \boldsymbol{v}_h^i\rangle_{\boldsymbol{L}^2(\omega)} \\
&\overset{(5.45)}{\lesssim} k\left| \langle \boldsymbol{\pi}_h^{\boldsymbol{D}}(\boldsymbol{v}_h^i; \boldsymbol{m}_h^i, \boldsymbol{m}_h^{i-1}) - \boldsymbol{\pi}(\boldsymbol{m}_h^i), \boldsymbol{v}_h^i\rangle_{\boldsymbol{L}^2(\omega)} \right| + k\left| \langle \boldsymbol{f}_h^{i+1/2} - \boldsymbol{f}^{i+1}, \boldsymbol{v}_h^i\rangle_{\boldsymbol{L}^2(\omega)} \right| \\
&\quad + k^2\,\|\boldsymbol{v}_h^i\|_{\boldsymbol{L}^2(\omega)}^2 + k^2\,\|\boldsymbol{v}_h^i\|_{\boldsymbol{L}^2(\omega)}\,\|\nabla\boldsymbol{v}_h^i\|_{\boldsymbol{L}^2(\omega)} + k\left| \langle \boldsymbol{h}_h^{i+1/2}, \boldsymbol{v}_h^i - \mathrm{d_t}\boldsymbol{m}_h^{i+1}\rangle_{\boldsymbol{L}^2(\omega)} \right| \\
&\quad + k\left| \langle \boldsymbol{h}_h^{i,\boldsymbol{\Theta}} - \boldsymbol{h}_h^{i+1/2}, \boldsymbol{v}_h^i\rangle_{\boldsymbol{L}^2(\omega)} \right|.
\end{aligned}$$

Summing in the latter estimate over $i = 0, \dots, j-1$, we get that

$$\begin{aligned}
&\mathcal{E}_{\mathrm{ELLG}}(\boldsymbol{m}_h^j, \boldsymbol{h}_h^j) - \mathcal{E}_{\mathrm{ELLG}}(\boldsymbol{m}_h^0, \boldsymbol{h}_h^0) + k\sum_{i=0}^{j-1} \langle \mathcal{W}_{G(k)}(\lambda_h^i)\boldsymbol{v}_h^i, \boldsymbol{v}_h^i\rangle_{\boldsymbol{L}^2(\omega)} + k\sum_{i=0}^{j-1} \langle \mathrm{d_t}\boldsymbol{f}^{i+1}, \boldsymbol{m}_h^i\rangle_{\boldsymbol{L}^2(\omega)} \\
&\quad + \frac{k}{\mu_0}\sum_{i=0}^{j-1} \|\sigma^{-1}\nabla\times\boldsymbol{h}_h^{i+1/2}\|_{\boldsymbol{L}^2(\Omega)}^2 - k\sum_{i=0}^{j-1} \langle \boldsymbol{\Pi}_h^{\boldsymbol{D}}(\boldsymbol{v}_h^i; \boldsymbol{m}_h^i, \boldsymbol{m}_h^{i-1}), \boldsymbol{v}_h^i\rangle_{\boldsymbol{L}^2(\omega)} \\
&\lesssim k\sum_{i=0}^{j-1} \left| \langle \boldsymbol{\pi}_h^{\boldsymbol{D}}(\boldsymbol{v}_h^i; \boldsymbol{m}_h^i, \boldsymbol{m}_h^{i-1}) - \boldsymbol{\pi}(\boldsymbol{m}_h^i), \boldsymbol{v}_h^i\rangle_{\boldsymbol{L}^2(\omega)} \right| + k\sum_{i=0}^{j-1} \left| \langle \boldsymbol{f}_h^{i+1/2} - \boldsymbol{f}^{i+1}, \boldsymbol{v}_h^i\rangle_{\boldsymbol{L}^2(\omega)} \right| \\
&\quad + k^2\sum_{i=0}^{j-1} \|\boldsymbol{v}_h^i\|_{\boldsymbol{L}^2(\omega)}^2 + k^2\sum_{i=0}^{j-1} \|\boldsymbol{v}_h^i\|_{\boldsymbol{L}^2(\omega)}\,\|\nabla\boldsymbol{v}_h^i\|_{\boldsymbol{L}^2(\omega)} + k\sum_{i=0}^{j-1} \left| \langle \boldsymbol{h}_h^{i+1/2}, \boldsymbol{v}_h^i - \mathrm{d_t}\boldsymbol{m}_h^{i+1}\rangle_{\boldsymbol{L}^2(\omega)} \right| \\
&\quad + k\sum_{i=0}^{j-1} \left| \langle \boldsymbol{h}_h^{i,\boldsymbol{\Theta}} - \boldsymbol{h}_h^{i+1/2}, \boldsymbol{v}_h^i\rangle_{\boldsymbol{L}^2(\omega)} \right|.
\end{aligned}$$

With the definition of the postprocessed output, we rewrite the latter estimate as

$$
\begin{aligned}
&\mathcal{E}_{\mathrm{ELLG}}(\boldsymbol{m}_{hk}^{+}(\tau), \boldsymbol{h}_{hk}^{+}(\tau)) - \mathcal{E}_{\mathrm{ELLG}}(\boldsymbol{m}_h^0, \boldsymbol{h}_h^0) \\
&\quad + \int_0^{t_j} \langle \mathcal{W}_{G(k)}(\lambda_{hk}^{-}) \boldsymbol{v}_{hk}^{-}, \boldsymbol{v}_{hk}^{-} \rangle_{\boldsymbol{L}^2(\omega)} \,\mathrm{d}t + \int_0^{t_j} \langle \partial_t \boldsymbol{f}_k, \boldsymbol{m}_{hk}^{-} \rangle_{\boldsymbol{L}^2(\omega)} \,\mathrm{d}t \\
&\quad + \frac{1}{\mu_0} \int_0^{t_j} \|\sigma^{-1} \nabla \times \overline{\boldsymbol{h}}_{hk}\|_{\boldsymbol{L}^2(\Omega)}^2 \,\mathrm{d}t - \int_0^{t_j} \langle \boldsymbol{\Pi}_h^{\boldsymbol{D}}(\boldsymbol{v}_{hk}^{-}; \boldsymbol{m}_{hk}^{-}, \boldsymbol{m}_{hk}^{=}), \boldsymbol{v}_{hk}^{-} \rangle_{\boldsymbol{L}^2(\omega)} \,\mathrm{d}t \\
&\lesssim \int_0^{t_j} \Big| \langle \boldsymbol{\pi}_h^{\boldsymbol{D}}(\boldsymbol{v}_{hk}^{-}; \boldsymbol{m}_{hk}^{-}, \boldsymbol{m}_{hk}^{=}) - \boldsymbol{\pi}(\boldsymbol{m}_{hk}^{-}), \boldsymbol{v}_{hk}^{-} \rangle_{\boldsymbol{L}^2(\omega)} \Big| \,\mathrm{d}t + \int_0^{t_j} \Big| \langle \overline{\boldsymbol{f}}_{hk} - \boldsymbol{f}_k^{+}, \boldsymbol{v}_{hk}^{-} \rangle_{\boldsymbol{L}^2(\omega)} \Big| \,\mathrm{d}t \\
&\quad + k \int_0^{t_j} \|\boldsymbol{v}_{hk}^{-}\|_{\boldsymbol{L}^2(\omega)}^2 \,\mathrm{d}t + k \int_0^{t_j} \|\boldsymbol{v}_{hk}^{-}\|_{\boldsymbol{L}^2(\omega)} \|\nabla \boldsymbol{v}_{hk}^{-}\|_{\boldsymbol{L}^2(\omega)} \,\mathrm{d}t + \int_0^{t_j} \Big| \langle \overline{\boldsymbol{h}}_{hk}, \boldsymbol{v}_{hk}^{-} - \partial_t \boldsymbol{m}_{hk} \rangle_{\boldsymbol{L}^2(\omega)} \Big| \,\mathrm{d}t \\
&\quad + \int_0^{t_j} \Big| \langle \boldsymbol{h}_{hk}^{\boldsymbol{\Theta}} - \overline{\boldsymbol{h}}_{hk}, \boldsymbol{v}_{hk}^{-} \rangle_{\boldsymbol{L}^2(\omega)} \Big| \,\mathrm{d}t \,.
\end{aligned}
\tag{5.46}
$$

For the terms with $\boldsymbol{\pi}_h^{\boldsymbol{D}}$ and $\boldsymbol{\Pi}_h^{\boldsymbol{D}}$, recall from plain LLG that we required the convergence properties from Lemma 6.5.5 and the strong consistencies **(D4$^+$)**, **(D7$^+$)** and **(T5$^+$)** for $\boldsymbol{\pi}_h$, $\boldsymbol{\Pi}_h$, and $\boldsymbol{D}_h$, respectively, to derive the strong consistencies from Lemma 4.5.9. Hence, with Lemma 5.4.4 (i)–(viii), we get in the same way that

$$
\begin{aligned}
&\int_0^{t_j} \Big| \langle \boldsymbol{\pi}_h^{\boldsymbol{D}}(\boldsymbol{v}_{hk}^{-}; \boldsymbol{m}_{hk}^{-}, \boldsymbol{m}_{hk}^{=}) - \boldsymbol{\pi}(\boldsymbol{m}_{hk}^{-}), \boldsymbol{v}_{hk}^{-} \rangle_{\boldsymbol{L}^2(\omega)} \Big| \,\mathrm{d}t \to 0, \quad \text{and} \\
&\qquad \int_0^{t_j} \langle \boldsymbol{\Pi}_h^{\boldsymbol{D}}(\boldsymbol{v}_{hk}^{-}; \boldsymbol{m}_{hk}^{-}, \boldsymbol{m}_{hk}^{=}), \boldsymbol{v}_{hk}^{-} \rangle_{\boldsymbol{L}^2(\omega)} \,\mathrm{d}t \to \int_0^{\tau} \langle \boldsymbol{\Pi}(\boldsymbol{m}), \partial_t \boldsymbol{m} \rangle_{\boldsymbol{L}^2(\omega)} \,\mathrm{d}t
\end{aligned}
$$

as $h, k \to 0$.

On the right-hand side of (5.46), only the last but one term is new. However, Lemma 5.4.6 proves that

$$
\begin{aligned}
\int_0^{t_j} \Big| \langle \overline{\boldsymbol{h}}_{hk}, \boldsymbol{v}_{hk}^{-} - \partial_t \boldsymbol{m}_{hk} \rangle_{\boldsymbol{L}^2(\omega)} \Big| \,\mathrm{d}t &\lesssim \|\overline{\boldsymbol{h}}_{hk}\|_{L^\infty(0,T;\boldsymbol{L}^2(\Omega))} \|\boldsymbol{v}_{hk}^{-} - \partial_t \boldsymbol{m}_{hk}\|_{L^1(0,T;\boldsymbol{L}^2(\omega))} \\
&\lesssim \|\boldsymbol{v}_{hk}^{-} - \partial_t \boldsymbol{m}_{hk}\|_{L^1(0,T;\boldsymbol{L}^2(\omega))} \to 0 \quad \text{as } h, k \to 0.
\end{aligned}
$$

As in the proof of Theorem 4.5.1(c) for plain LLG, the remaining terms on the right-hand side of (5.46) vanish as $h, k \to 0$.

On the left hand side, note that we require strong consistency **(E1$^+$)** of $\boldsymbol{h}_h^0$ to show that

$$
\mathcal{E}_{\mathrm{ELLG}}(\boldsymbol{m}_h^0, \boldsymbol{h}_h^0) \to \mathcal{E}_{\mathrm{ELLG}}(\boldsymbol{m}^0, \boldsymbol{h}^0) \quad \text{as } h, k \to 0.
$$

The remainder of the proof employs standard lower semi-continuity arguments and follows the lines of **Step 5** of the proof of the corresponding Theorem 4.5.1(c) for plain LLG. □

6. Implicit-explicit midpoint scheme for LLG

The following chapter is mainly based on [PRS18], which is joint work with *Dirk Praetorius*[1] and *Michele Ruggeri*[2]. Moreover, we present some new ideas, which are not part of [PRS18].

6.1. Introduction

The midpoint scheme was first-analyzed in [BP06] for $\boldsymbol{h}_{\text{eff}} = \Delta \boldsymbol{m}$ and $\boldsymbol{\Pi} = \boldsymbol{0}$. The basic idea can be summarized as follows: Based on the Gilbert form of LLG (2.3a), we employ

- an implicit midpoint rule in time;
- FEM for space discretization;
- a mass-lumping for modulus conservation over time.

In contrast to the tangent plane scheme, one *non-linear* system has to solved at each time-step. However, since the mass-lumping yields modulus conservation over time in each node, no pointwise normalization is required. In addition, the symplectic nature of the implicit midpoint rule yields a discrete energy equality, i.e., there is no artificial damping. The resulting numerical integrator is (formally) second-order in time and [BP06] proves unconditional convergence in the sense of Convention 1.3.1. Closely related to LLG, discrete energy inequalities and modulus conservation through mass-lamping are also of great interest in the development of algorithms for the related (p-)harmonic map heat flow: In [BP07, BP08], corresponding adaptations of the midpoint scheme were formulated and analyzed. Moreover, [BBP08] extends the algorithm and convergence results of [BP06] to the coupling of LLG with the Maxwell equation.

In [Cim09], the midpoint scheme was formulated for the equivalent Landau–Lifshitz form of LLG, which reads

$$\partial_t \boldsymbol{m} = -\boldsymbol{m} \times \boldsymbol{h}_{\text{eff}}(\boldsymbol{m}) - \alpha\, \boldsymbol{m} \times (\boldsymbol{m} \times \boldsymbol{h}_{\text{eff}}(\boldsymbol{m})). \tag{6.1}$$

There, again $\boldsymbol{h}_{\text{eff}}(\boldsymbol{m}) = \Delta \boldsymbol{m}$ and $\boldsymbol{\Pi}(\boldsymbol{m}) = \boldsymbol{0}$ and the resulting integrator has the same basic properties as the classical midpoint scheme from [BP06]: Unconditional convergence, (formal) second-order in time convergence, modulus conservation, and a discrete energy equality [Cim09]. Moreover, based on (6.1), the works [BBP13, BBNP14] introduce and analyze a midpoint scheme, which additionally takes into account stochastic effects.

The midpoint schemes of [BP06, Cim09] were adapted to an unconditionally convergent numerical integrator for LLG in thermally assisted recording [BPS09, BPS12]. There,

[1] TU Wien
[2] Universität Wien

an additional PDE-inherent mass term adapts the modulus of the magnetization to a phenomenological temperature-modulus law. Due to the mass-lumping, the algorithms preserves this modulus constraint also on the discrete level.

The usual approach for the solution of the non-linear system is a fixed-point iteration; see, e.g., [Bar06, BP06, BBP08, BPS09, Cim09, BPS12]. For the convergence of the fixed-point iteration, one usually requires the CFL-type condition $k = \mathbf{o}(h^2)$. Moreover, [Bar06, Cim09] analyze the effect of the inexact solution of the non-linear system.

For the midpoint scheme for plain LLG, we identify, in particular, the following issues:

- While [BBP08, BPS09, BPS12] hint the extension of the midpoint scheme to lower-order terms, the corresponding rigorous extension of the analysis seems to be missing.
- The extension of the midpoint scheme to dissipative effects $\mathbf{\Pi}$ seems to be missing.
- While the naive extension of the midpoint scheme to lower-order terms seems to be straightforward, the implicit treatment of $\boldsymbol{\pi}$ and $\mathbf{\Pi}$ requires one evaluation of $\boldsymbol{\pi}_h \approx \boldsymbol{\pi}$ and $\mathbf{\Pi}_h \approx \mathbf{\Pi}$ at each step of the fixed-point iteration at each time-step. For stray field computations, for example, the evaluation of $\boldsymbol{\pi}_h$ then involves the solution of a computationally expensive problem.
- To circumvent the latter issue, an explicit Euler approach is unfavourable since it reduces the (formal) convergence order in time from second to first-order.
- The midpoint scheme is well-defined, however, uniqueness of the discrete solution is a by-product of the convergence result of the fixed-point iterations, which requires the CFL-type condition $k = \mathbf{o}(h^2)$; see, e.g., [Bar06, BP06, BBP08, BPS09].
- At each fixed-point iteration, a FEM-type problem has to be solved. However, none of the latter works provides a solution strategy on a linear algebra level.

6.1.1. Contributions

Based on the own work [PRS18], we make the following contributions:

- We formulate an extended midpoint scheme, which takes into account the lower-order terms $\boldsymbol{\pi}$, $\boldsymbol{f}$, and, in particular, $\mathbf{\Pi}$. To this end, we transfer techniques for the tangent plane scheme [AKT12, BSF$^+$14] to the midpoint scheme. This makes the midpoint scheme applicable to a broader class of model problems.
- For $\boldsymbol{\pi}$ and $\mathbf{\Pi}$, we employ an explicit second-order in time approach so that the overall numerical integrator is (formally) second-order in time. This way, we only require one evaluation of the numerically expensive operators $\boldsymbol{\pi}_h$ and $\mathbf{\Pi}_h$ per time-step.
- We confirm the formal convergence order of our algorithm with a numerical experiment; see Section 6.3. Moreover, we confirm in Section 6.4 the applicability of our algorithm with a physically relevant example, where we also make a comparison with our extension of the (almost) second-order tangent plane scheme from Chapter 4.

- We prove well-posedness and unconditional convergence of our extended algorithm in the sense of Convention 1.3.1; see Section 6.5.

Note that the (more recent) own work [DPP$^+$17] makes corresponding contributions for the (almost) second-order tangent plane scheme; see Chapter 4. Moreover, note that the master thesis [Kem14] already deals with the latter points, but considers only $\boldsymbol{\Pi} = \mathbf{0}$ and a formally first-order in-time explicit Euler approach for the discretization of (a possible non-linear) $\boldsymbol{\pi}$.

In addition to the latter points, we present the following new ideas:

- We provide a solution strategy for the variational problems which arise from the fixed-point iteration. Moreover, we prove that–despite the FEM-nature of the problem–the fixed-point iterates can be computed nodewise, greatly reducing the computational complexity of the method; see Section 6.6.3.
- Under the assumption that there is no finite time-blow up, we prove that, the uniqueness of discrete solutions follows already from the weaker CFL-type condition $k = \mathbf{o}(h)$ (instead of $k = \mathbf{o}(h^2)$ in, e.g., [Bar06, BP06, BBP08, BPS09]); see Section 6.7.

6.2. Algorithm

In this section, we formulate the extended midpoint scheme as in the own work [PRS18, Algorithm 2]. Morally, we start with with [BP06, Algorithm 1.1], where $\boldsymbol{h}_{\text{eff}}(\boldsymbol{m}) := \Delta \boldsymbol{m}$ and $\boldsymbol{\Pi} = \mathbf{0}$. Then, we adapt and extend the techniques for lower-order terms for the tangent plane scheme from [AKT12, BSF$^+$14]. We employ a general time-stepping approach for the discretization of $\boldsymbol{\pi}$ and $\boldsymbol{\Pi}$, which, in particular, covers implicit-explicit approaches. With $(\boldsymbol{m}_h^i)_{i=0}^M$ being the sequence of sought approximations to $\boldsymbol{m}(t_i)$, we define

$$\boldsymbol{\pi}_h^{\boldsymbol{\Theta}}(\boldsymbol{m}_h^{i+1}, \boldsymbol{m}_h^i, \boldsymbol{m}_h^{i-1}) \approx \boldsymbol{\pi}(\boldsymbol{m}(t_i + k/2)) \quad \text{and} \quad \boldsymbol{\Pi}_h^{\boldsymbol{\Theta}}(\boldsymbol{m}_h^{i+1}, \boldsymbol{m}_h^i, \boldsymbol{m}_h^{i-1}) \approx \boldsymbol{\Pi}(\boldsymbol{m}(t_i + k/2))$$

with one of the following three options **(A1)**–**(A3)**:

(A1) The implicit second-order in time midpoint approach [BBP08, BPS09, BPS12]

$$\begin{aligned}\boldsymbol{\pi}_h^{\boldsymbol{\Theta}}(\boldsymbol{m}_h^{i+1}, \boldsymbol{m}_h^i, \boldsymbol{m}_h^{i-1}) &:= \boldsymbol{\pi}_h\Big(\frac{\boldsymbol{m}_h^{i+1} + \boldsymbol{m}_h^i}{2}\Big) \quad \text{and} \\ \boldsymbol{\Pi}_h^{\boldsymbol{\Theta}}(\boldsymbol{m}_h^{i+1}, \boldsymbol{m}_h^i, \boldsymbol{m}_h^{i-1}) &:= \boldsymbol{\Pi}_h\Big(\frac{\boldsymbol{m}_h^{i+1} + \boldsymbol{m}_h^i}{2}\Big).\end{aligned}$$

(A2) The explicit second-order in time Adams–Bashforth approach

$$\boldsymbol{\pi}_h^{\boldsymbol{\Theta}}(\boldsymbol{m}_h^{i+1}, \boldsymbol{m}_h^i, \boldsymbol{m}_h^{i-1}) := \begin{cases} \boldsymbol{\pi}_h\Big(\frac{\boldsymbol{m}_h^{i+1} + \boldsymbol{m}_h^i}{2}\Big) & \text{for } i = 0, \\ \frac{3}{2}\,\boldsymbol{\pi}_h(\boldsymbol{m}_h^i) - \frac{1}{2}\,\boldsymbol{\pi}_h(\boldsymbol{m}_h^{i-1}) & \text{else,} \end{cases}$$

and

$$\boldsymbol{\Pi}_h^{\boldsymbol{\Theta}}(\boldsymbol{m}_h^{i+1}, \boldsymbol{m}_h^i, \boldsymbol{m}_h^{i-1}) := \begin{cases} \boldsymbol{\Pi}_h\Big(\frac{\boldsymbol{m}_h^{i+1} + \boldsymbol{m}_h^i}{2}\Big) & \text{for } i = 0, \\ \frac{3}{2}\,\boldsymbol{\Pi}_h(\boldsymbol{m}_h^i) - \frac{1}{2}\,\boldsymbol{\Pi}_h(\boldsymbol{m}_h^{i-1}) & \text{else.} \end{cases}$$

(A3) The first-order in time explicit Euler approach from [AKT12, BSF+14, Kem14]

$$\boldsymbol{\pi}_h^{\boldsymbol{\Theta}}(\boldsymbol{m}_h^{i+1}, \boldsymbol{m}_h^{i}, \boldsymbol{m}_h^{i-1}) := \boldsymbol{\pi}_h(\boldsymbol{m}_h^{i}), \quad \text{and} \quad \boldsymbol{\Pi}_h^{\boldsymbol{\Theta}}(\boldsymbol{m}_h^{i+1}, \boldsymbol{m}_h^{i}, \boldsymbol{m}_h^{i-1}) := \boldsymbol{\Pi}_h(\boldsymbol{m}_h^{i}).$$

Based on [PRS18, Algorithm 2], we are now ready to formulate our IMEX midpoint scheme. To this end, we recall, in particular, the approximate $\boldsymbol{L}^2$-product $\langle\cdot,\cdot\rangle_h$, the discrete Laplacian Δ_h, and the quasi-$\boldsymbol{L}^2$ projection $\boldsymbol{\mathcal{P}}_h$ from Section 3.3.2.

Algorithm 6.2.1 (IMEX MPS, [PRS18, Algorithm 2])**. Input:** *Approximation* $\boldsymbol{m}_h^{-1} := \boldsymbol{m}_h^0 \in \boldsymbol{\mathcal{S}}_h$ *of initial magnetization.*
Loop: *For* $0 \le i \le M-1$*, find* $\boldsymbol{m}_h^{i+1} \in \boldsymbol{\mathcal{S}}_h$ *such that, for all* $\boldsymbol{\varphi}_h \in \boldsymbol{\mathcal{S}}_h$*, it holds that*

$$\begin{aligned}
&\langle \mathrm{d_t}\boldsymbol{m}_h^{i+1}, \boldsymbol{\varphi}_h\rangle_h = \\
&\quad - C_{\mathbf{ex}}\langle \boldsymbol{m}_h^{i+1/2} \times \Delta_h \boldsymbol{m}_h^{i+1/2}, \boldsymbol{\varphi}_h\rangle_h - \langle \boldsymbol{m}_h^{i+1/2} \times \boldsymbol{\mathcal{P}}_h \boldsymbol{\pi}_h^{\boldsymbol{\Theta}}(\boldsymbol{m}_h^{i+1}, \boldsymbol{m}_h^{i}, \boldsymbol{m}_h^{i-1}), \boldsymbol{\varphi}_h\rangle_h \\
&\quad - \langle \boldsymbol{m}_h^{i+1/2} \times \boldsymbol{\mathcal{P}}_h \boldsymbol{\Pi}_h^{\boldsymbol{\Theta}}(\boldsymbol{m}_h^{i+1}, \boldsymbol{m}_h^{i}, \boldsymbol{m}_h^{i-1}), \boldsymbol{\varphi}_h\rangle_h - \langle \boldsymbol{m}_h^{i+1/2} \times \boldsymbol{\mathcal{P}}_h \boldsymbol{f}_h^{i+1/2}, \boldsymbol{\varphi}_h\rangle_h \\
&\quad + \alpha\langle \boldsymbol{m}_h^{i+1/2} \times \mathrm{d_t}\boldsymbol{m}_h^{i+1}, \boldsymbol{\varphi}_h\rangle_h.
\end{aligned} \tag{6.2}$$

Output: *Approximations* $\boldsymbol{m}_h^i \approx \boldsymbol{m}(t_i)$. □

Remark 6.2.2. (i) *Given* $\boldsymbol{m}_h^i \in \boldsymbol{\mathcal{S}}_h$*, the discrete variational formulation* (6.2) *gives rise to a non-linear system for* $\boldsymbol{m}_h^{i+1} \in \boldsymbol{\mathcal{S}}_h$*, which admits a solution; see Theorem 6.5.1*(a)*. For uniqueness, we require additional assumptions; see Section 6.7 for details.*

(ii) *The non-linear system* (6.2) *can be (approximately) solved by a fixed-point iteration; see Section 6.6 for details.*

(iii) *The fixed-point iteration for the solution of the non-linear system* (6.2) *with the implicit second-order in time approaches* **(A1)** *and* **(A2)** *for* $i = 0$ *involve the numerically expensive evaluation of* $\boldsymbol{\pi}_h$ *and* $\boldsymbol{\Pi}_h$ *at each iteration at each time-step.*

(iv) *In contrast to* (iii)*, the explicit Euler approach* **(A3)***, requires only one evaluation of* $\boldsymbol{\pi}_h$ *and* $\boldsymbol{\Pi}_h$ *per time-step, but it generically reduces the convergence order from second to first-order in time. We analyze this approach only for comparison. At least from the second time-step on, the Adams–Bashforth approach* **(A2)***, however, still requires only one evaluation of* $\boldsymbol{\pi}_h$ *and* $\boldsymbol{\Pi}_h$ *per time-step, but is formally second-order in time. It is thus our preferred choice.*

(v) *The approximate* $\boldsymbol{L}^2$*-product* $\langle\cdot,\cdot\rangle_h$ *ensures the nodewise modulus conservation (and thus uniform boundedness); see Proposition 6.5.3. Moreover, we can compute the fixed-point iterates by the nodewise solution of* 3×3 *systems, which can even be done in parallel; see Section 6.6.3 for details.*

(vi) *In [PRS18], the operators* $\boldsymbol{\pi}$ *and* $\boldsymbol{\Pi}$ *as well as their discretizations* $\boldsymbol{\pi}_h$ *and* $\boldsymbol{\Pi}_h$ *are summarized in the single operator* $\boldsymbol{\pi}$ *with the discretization* $\boldsymbol{\pi}_h$*.*

6.3. Experimental convergence order

In this section, we illustrate the accuracy and computational costs of different variants of Algorithm 6.2.1 with a numerical experiment. To this end, we use our `C++`-based extension of `NGS/Py` [ngs], which was mainly developed by the author. Note that the numerical experiment of the own work [PRS18, Section 6.1] confirms the formal convergence orders from Remark 6.2.2. However, this experiment neglects dissipative effects and considers only $\boldsymbol{\Pi}(\boldsymbol{m}) = \mathbf{0}$. In contrast to that, we slightly adapt [PRS18, Section 6.1] and, most importantly, additionally cover the Slonczewski-field [Ber96, Slo96] in the form

$$\boldsymbol{\Pi}(\boldsymbol{\varphi}) := \mathcal{G}(\boldsymbol{\varphi} \cdot \mathbf{p})\, \boldsymbol{\varphi} \times \mathbf{p}, \quad \text{with} \quad \mathcal{G}(x) := \left[\frac{(1+P)^3(3+x)}{4P^{3/2}} - 4 \right]^{-1} \quad \text{for } x \in [-1, 1],$$

where $\mathbf{p} = (1,0,0)^T$ and $P = 0.8$. Note that this repeats the numerical experiment from Section 4.4 for the (almost) second-order tangent plane with our midpoint scheme. The lower-order $\boldsymbol{m}$-dependent energy term $\boldsymbol{\pi}(\boldsymbol{m})$ always consists of the stray field, i.e., one evaluation of the corresponding approximation $\boldsymbol{\pi}_h$ employs the Fredkin–Koehler algorithm [FK90] in the variant of Algorithm 3.4.3. Then, we compare the performance of the different approaches to $\boldsymbol{\pi}_h^{\boldsymbol{\Theta}}$ and $\boldsymbol{\Pi}_h^{\boldsymbol{\Theta}}$ with the following three variants of Algorithm 6.2.1:

- `MPS+MP`: We employ the implicit second-order midpoint approach **(A1)**.
- `MPS+AB`: We employ the explicit second-order Adams–Bashforth approach **(A2)**.
- `MPS+EE`: We employ the explicit first-order explicit Euler approach **(A3)**.

For the solution of the non-linear system, we always employ the fixed-point iteration with the nodewise approach from Algorithm 6.6.8 below with the iteration tolerance $\varepsilon = 10^{-10}$; see Section 6.6 for details.

For all our variants, we choose the final time $T = 7$, the domain $\omega = (0,1)^3$, the Gilbert damping constant $\alpha = 1$, the exchange constant $C_{\mathbf{ex}} = 1$, the constant external field $\boldsymbol{f} = (0,1,0)^T$, and the constant initial value $\boldsymbol{m}^0 = \boldsymbol{m}_h^0 = (1,0,0)^T$.

For space discretization, we employ a uniform triangulation $\mathcal{T}_h$ with 8 elements per edge. This corresponds to 3072 elements, 729 nodes, and a mesh-size $h = 0.125$. Having fixed the space discretization, we perform our variants with varying time-step size. Since the exact solution is unknown, we use `MPS+AB` to compute a reference solution $\boldsymbol{m}_{hk_{\mathrm{ref}}}$, where the reference time $k_{\mathrm{ref}} := 5 \cdot 10^{-5}$ is a fine time-step size.

In Figure 6.1, we illustrate the experimental convergence order of our variants. For our setting, the plot confirms the predictions of Remark 6.2.2: For `MPS+MP` and `MPS+AB`, we observe second-order convergence in time. For `MPS+EE`, the explicit Euler approach to $\boldsymbol{\pi}_h$ and $\boldsymbol{\Pi}_h$ reduces the convergence order to one.

In Table 6.1 and Table 6.2, we illustrate the computational costs of our variants. In Table 6.1, we observe that all variants require for all time-step sizes roughly the same number of fixed-point iterations for the approximate solution of the discrete variational formulation (6.2). However, Table 6.1 shows that `MPS+MP` is (by far) the most expensive method, and `MPS+AB` and `MPS+EE` are much cheaper and essentially of the same cost. This is due to the fact that MPS+MP requires one evaluation of $\boldsymbol{\pi}_h$ and $\boldsymbol{\Pi}_h$ per iteration per time-step, while MPS+AB and MPS+EE require only one evaluation per time-step. In the present setting, the evaluation of our $\boldsymbol{\Pi}_h$ is cheap, whereas the evaluation of $\boldsymbol{\pi}_h$ employs the Fredkin–Koehler algorithm [FK90] in the variant of Algorithm 3.4.3.

In conclusion, MPS+AB is the method of choice. It is the only method that benefits from the IMEX approach and conserves the second-order convergence in time.

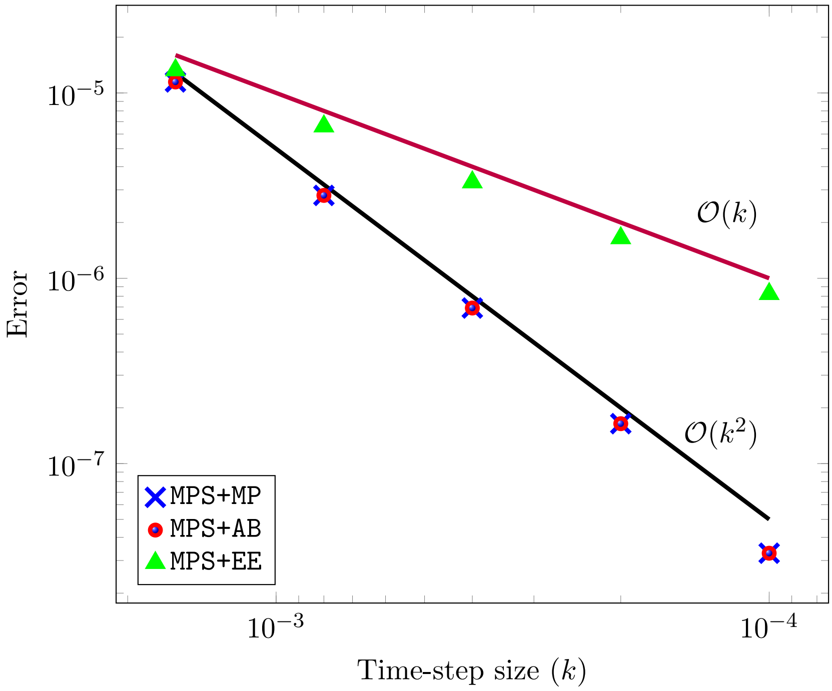

Figure 6.1.: Experiment of Section 6.3: Reference error $\max_i(\|\boldsymbol{m}_{hk_{\mathrm{ref}}}(t_i) - \boldsymbol{m}_{hk}(t_i)\|_{\boldsymbol{H}^1(\omega)})$ for $k = 2^\ell\, k_{\mathrm{ref}}$ with $\ell \in \{1, 2, 3, 4, 5\}$ and $k_{\mathrm{ref}} := 5 \cdot 10^{-5}$.

	MPS+MP absolute	MPS+MP relative	MPS+AB relative	MPS+EE relative
$k = 0.0016$	19.33	100%	99.99%	106.92%
$k = 0.0008$	7.75	100%	100.00%	106.78%
$k = 0.0004$	5.30	100%	100.00%	104.47%
$k = 0.0002$	3.96	100%	100.00%	108.65%
$k = 0.0001$	3.36	100%	100.00%	104.70%

Table 6.1.: Experiment of Section 6.3: Average iteration numbers of MPS+MP per time-step and relative iterations numbers of all variants.

	MPS+MP absolute	MPS+MP relative	MPS+AB relative	MPS+EE relative
$k = 0.0016$	0.67	100%	7.10%	7.14%
$k = 0.0008$	0.27	100%	15.79%	15.91%
$k = 0.0004$	0.21	100%	20.87%	20.94%
$k = 0.0002$	0.16	100%	26.27%	27.06%
$k = 0.0001$	0.14	100%	29.31%	30.05%

Table 6.2.: Experiment of Section 6.3: Average time (in s) of MPS+MP per time-step and relative times of all variants.

6.4. Qualitative comparison

In the section, we consider the physically relevant μ-MAG standard problem #5 [mum] for a qualitative test of the midpoint scheme from Algorithm 6.2.1 vs. the (almost) second-order tangent plane scheme from Algorithm 4.2.1; see Chapter 4 for details. Note that this section essentially repeats the corresponding experiments from the own works [PRS18, Section 6.2] and [DPP+17, Section 7.2.2]. For the μ-MAG standard problem #5 [mum], we employ the domain $\omega := (-50\text{nm}, 50\text{nm}) \times (-50\text{nm}, 50\text{nm}) \times (-5\text{nm}, 5\text{nm})$, which represents a permalloy film. We have

$$\alpha = 0.1, \quad C_{\mathbf{ex}} = \frac{2A}{\mu_0 {M_s}^2 L^2}, \quad \text{and} \quad \boldsymbol{f} = \mathbf{0},$$

where $\mu_0 = 4\pi \cdot 10^{-7}\text{N/A}^2$ is the magnetic permeability, $A = 1.3 \cdot 10^{-11}\text{J/m}$ is the physical exchange constant, $M_s = 8.0 \cdot 10^5\text{A/m}$ is the saturation magnetization, and $L = 10^{-9}$ is the spatial scaling parameter. The operator $\boldsymbol{\pi}$ consists of the stray field, and the dissipative effects $\mathbf{\Pi}$ consist of the Zhang–Li field [ZL04, TNMS05], which reads

$$\mathbf{\Pi}(\boldsymbol{\varphi}) := \boldsymbol{\varphi} \times (\boldsymbol{u} \cdot \nabla)\, \boldsymbol{\varphi} + \beta\, (\boldsymbol{u} \cdot \nabla)\, \boldsymbol{\varphi} \tag{6.3a}$$

with $\boldsymbol{u} \in \boldsymbol{L}^\infty(\omega)$ being the spin velocity vector and $\beta \in [0, 1]$ the constant of non-adiabacity. Here, we have $\beta = 0.05$ and our (already rescaled) velocity vector reads

$$\boldsymbol{u} := \frac{1}{\gamma_0 M_s L} \begin{pmatrix} 72.17 \\ 0 \\ 0 \end{pmatrix}, \tag{6.3b}$$

where $\gamma_0 = 2.21 \cdot 10^5\text{m/(As)}$ is the gyromagnetic ratio. Then, we consider the following three algorithms:

- MPS+AB: We employ the second-order midpoint scheme from Algorithm 6.2.1 with the explicit Adams–Bashforth approach **(A2)** for $\boldsymbol{\pi}_h^{\boldsymbol{\Theta}}$ and $\mathbf{\Pi}_h^{\boldsymbol{\Theta}}$ and the time-step size $k = 0.05$ps. For space discretization, we employ a triangulation $\mathcal{T}_h$ obtained from the NGS/Py-embedded Netgen [ngs] with 25666 elements and 5915 nodes. We solve the underlying non-linear system (6.2) with the fixed-point iteration from Algorithm 6.6.1, where we use the iteration tolerance $\varepsilon = 10^{-6}$; see Section 6.6 for details.

We perform these computations with our C++-based extension of NGS/Py [ngs], which was mainly developed by the author.

- TPS2+AB: We employ the (almost) second-order tangent plane scheme from Algorithm 4.2.1 with the explicit Adams–Bashforth–type approach **(A2)** for $\boldsymbol{\pi}_h^{\boldsymbol{D}}$ and $\boldsymbol{\Pi}_h^{\boldsymbol{D}}$, where we use the same time-step size and mesh as for MPS+AB. We note that we checked the corresponding stiffness matrix to verify the angle condition **(T1)**. We perform these computations with our Python-based extension of NGS/Py [ngs], which was mainly developed by *Carl-Martin Pfeiler*[3].

- OOMMF: The OOMMF-software package [DP99] employs a finite difference method with an adaptive time-step size. For our particular setting, the results are available on the μ-MAG homepage [mum].

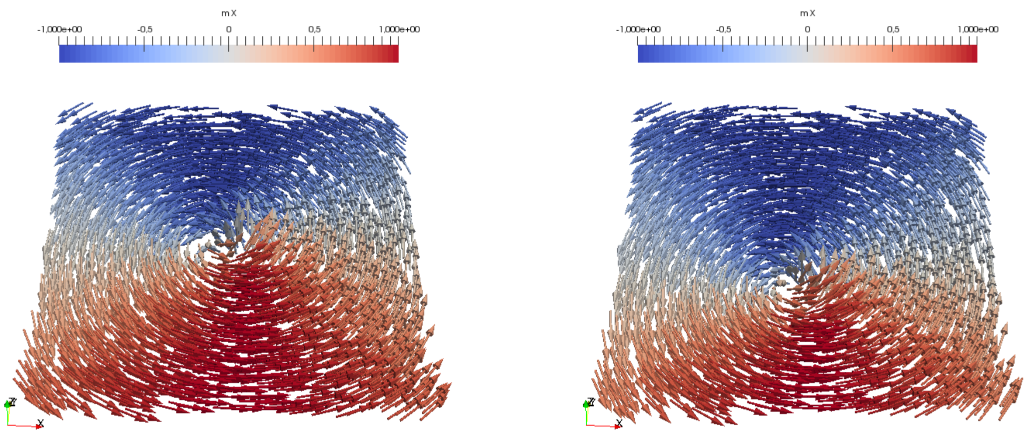

(a) Initial state, $t = 0$ns.

(b) Equilibrium state, $t = 8$ns.

Figure 6.2.: Experiment of Section 6.4: The initial vortex (left) and the equilibrium vortex (right) computed with MPS+AB. The visualization was done with ParaView [AGL05].

In all cases, the initial value is obtained from the relaxation of the nodal interpolant of

$$\boldsymbol{m}^0(\boldsymbol{x}) = \frac{1}{({\boldsymbol{x}_1}^2 + {\boldsymbol{x}_2}^2 + R^2)^{1/2}} \begin{pmatrix} -\boldsymbol{x}_2 \\ \boldsymbol{x}_1 \\ R \end{pmatrix}, \quad \text{where} \quad R = 10\text{nm}$$

and $\boldsymbol{\Pi} = \boldsymbol{0}$, which yields the initial vortex from Figure 6.2a; cf., the relaxation in the numerical experiment in Section 5.3. Then, one applies the Zhang–Li field from (6.3). This induces a wandering of the vortex towards the new equilibrium from Figure 6.2b, where we

[3]TU Wien

stop our simulation at the final time $T = 8$ns. We monitor the wandering with the nodal averages

$$\langle \boldsymbol{m}_x \rangle := \frac{1}{N} \sum_{\boldsymbol{z} \in \mathcal{N}_h} \big(\boldsymbol{m}_{hk}(\boldsymbol{z})\big)_1, \quad \text{and} \quad \langle \boldsymbol{m}_y \rangle := \frac{1}{N} \sum_{\boldsymbol{z} \in \mathcal{N}_h} \big(\boldsymbol{m}_{hk}(\boldsymbol{z})\big)_2,$$

in the sense that, roughly, the vortex center follows the path $(\langle \boldsymbol{m}_x \rangle, \langle \boldsymbol{m}_y \rangle, 0)^T$ when looking at ω from above.

In Figure 6.3, we plot the dynamics of $\langle \boldsymbol{m}_x \rangle$ and $\langle \boldsymbol{m}_y \rangle$. Note that the results differ slightly and that `TPS2+AB` is slightly phase-shifted. However, we observe that all three method show the same qualitative behavior.

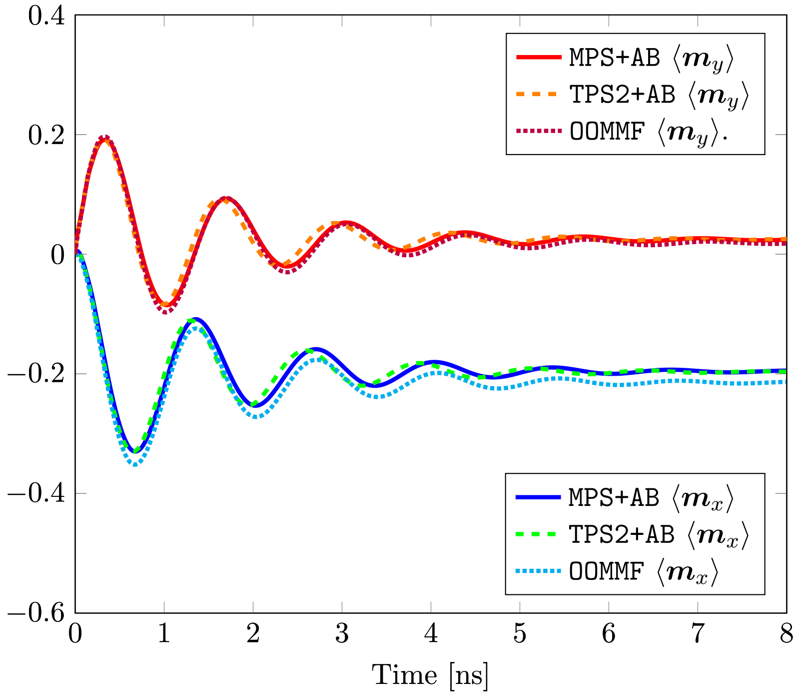

Figure 6.3.: Experiment of Section 6.4: Development of $\langle \boldsymbol{m}_x \rangle$ and $\langle \boldsymbol{m}_y \rangle$ over time.

6.5. Main result

In this section, we formulate and prove the main result of this chapter. We extend [BP06, Thereom 3.1] from $\boldsymbol{h}_{\text{eff}}(\boldsymbol{m}) = \Delta \boldsymbol{m}$ and $\boldsymbol{\Pi}(\boldsymbol{m}) = \boldsymbol{0}$ to the setting of Algorithm 6.2.1 and prove unconditional convergence of the postprocessed output in the sense of Convention 1.3.1. Note that corresponding results are proved, e.g., in [BPS09, Cim09] and that our main result is based on the own works [PRS18, Proposition 3] for (a) and on [PRS18, Theorem 4] for (b) and (c). In addition to the assumptions from the setting of LLG from Section 2.2 and the general discretization from Section 3.2–3.4, we require the following assumptions:

(M1) Uniform boundedness of $\boldsymbol{m}_h^0$: There exists a constant $C_0 > 0$ such that

$$\|\boldsymbol{m}_h^0\|_{\boldsymbol{L}^\infty(\omega)} \leq C_0 \quad \text{for all } h > 0.$$

(M2) Lipschitz-type condition for $\boldsymbol{\Pi}_h$: There exists a constant $C > 0$ such that, for all $h > 0$, it holds that

$$\|\boldsymbol{\Pi}_h(\boldsymbol{\varphi}_h) - \boldsymbol{\Pi}_h(\boldsymbol{\psi}_h)\|_{\boldsymbol{L}^2(\omega)} \leq C\, h^{-1} \left[\, 1 + \|\boldsymbol{\varphi}_h\|_{\boldsymbol{L}^\infty(\omega)} + \|\boldsymbol{\psi}_h\|_{\boldsymbol{L}^\infty(\omega)} \,\right] \|\boldsymbol{\varphi}_h - \boldsymbol{\psi}_h\|_{\boldsymbol{L}^2(\omega)}$$

for all $\boldsymbol{\varphi}_h, \boldsymbol{\psi}_h \in \boldsymbol{\mathcal{S}}_h$.

With these preparations, we are ready to formulate our convergence theorem.

Theorem 6.5.1 (Convergence of IMEX MPS, [PRS18, Proposition 3, Theorem 4])**.** *Consider Algorithm 6.2.1 for the discretization of LLG* (2.3)*. Then, the following three assertions* (a)–(c) *hold true:*

(a) *Suppose that*

- *the approximation operators $\boldsymbol{\pi}_h$ are linear* **(D2)***;*
- *the approximation operators $\boldsymbol{\Pi}_h$ satisfy the Lipschitz-type condition* **(M2)***.*

Then, Algorithm 6.2.1 is well-posed, and for all $i \in \{0, \dots, M\}$, it holds that

$$|\boldsymbol{m}_h^i(\boldsymbol{z})| = |\boldsymbol{m}_h^0(\boldsymbol{z})| \quad \textit{for all nodes } \boldsymbol{z} \in \mathcal{N}_h.$$

In particular, it holds that $\|\boldsymbol{m}_h^i\|_h = \|\boldsymbol{m}_h^0\|_h$ and $\|\boldsymbol{m}_h^i\|_{\boldsymbol{L}^\infty(\omega)} = \|\boldsymbol{m}_h^0\|_{\boldsymbol{L}^\infty(\omega)}$ for all $i \in \{0, \dots, M\}$.

(b) *Suppose that*

- *the approximations $\boldsymbol{m}_h^0$ satisfy* **(D1)** *and* **(M1)***;*
- *the approximation operators $\boldsymbol{\pi}_h$ satisfy* **(D2)**–**(D4)***;*
- *the approximations $(\boldsymbol{f}_h^i)_{i=0}^M$ satisfy* **(D5)***;*
- *the approximation operators $\boldsymbol{\Pi}_h$ satisfy* **(D6)**–**(D7)** *and* **(M2)***;*
- *the general time-stepping approaches $\boldsymbol{\pi}_h^{\boldsymbol{\Theta}}$ and $\boldsymbol{\Pi}_h^{\boldsymbol{\Theta}}$ are defined by one of the three options* **(A1)**–**(A3)***.*

Then, there exists a subsequence of the postprocessed output $\boldsymbol{m}_{hk}$ of Algorithm 6.2.1 as well as a weak solution

$$\boldsymbol{m} \in L^\infty(0,T;\boldsymbol{H}^1(\Omega)) \cap \boldsymbol{H}^1(\omega_T)$$

of LLG (2.3) *in the sense of Definition 2.2.1*(i)–(iii) *such that*

$$\boldsymbol{m}_{hk} \rightharpoonup \boldsymbol{m} \quad \textit{in } \boldsymbol{H}^1(\omega_T) \quad \textit{as } h,k \to 0.$$

(c) *Additionally to the assumptions from* (b)*, suppose that*

- *the approximations* $\boldsymbol{m}_h^0$ *are strongly consistent* **(D1⁺)**;
- *the approximation operators* $\boldsymbol{\pi}_h$ *are strongly consistent* **(D4⁺)**;
- *the approximations* $(\boldsymbol{f}_h^{i+1/2})_{i=0}^M$ *are strongly consistent* **(D5⁺)**;
- *the approximation operators* $\boldsymbol{\Pi}_h$ *are strongly consistent* **(D7⁺)**.

Then, the weak solution $\boldsymbol{m}$ *from* (b) *is a physical weak solution in the sense of Definition 2.2.1*(i)–(iv)*, i.e., it additionally satisfies the stronger energy estimate* (2.17).

Remark 6.5.2. (i) *Theorem 6.5.1 supposes the exact solution of the non-linear variational problem* (6.2) *and the convergence is unconditional in the sense of Convention 1.3.1. In contrast to that, Theorem 6.6.12 below takes into account the effect of the inexact solution of* (6.2) *by a fixed-point iteration. This requires the CFL-type condition* $k = \mathbf{o}(h^2)$ *for convergence.*

(ii) *Uniaxial anistropy, stray field and the corresponding approximations, satisfy the assumptions from Theorem 6.5.1*(c) *to* $\boldsymbol{\pi}$ *and* $\boldsymbol{\pi}_h$*, respectively. We refer to Appendix A for the verification.*

(iii) *For the Zhang–Li field [ZL04, TNMS05], the corresponding approximation operator* $\boldsymbol{\Pi}_h$ *satisfies the assumptions from Theorem 6.5.1*(b)*. We refer to Proposition A.3.1 for the verification.*

(iv) *For the Slonczewski field [Ber96, Slo96], the corresponding approximation operator* $\boldsymbol{\Pi}_h$ *satisfies the assumptions from Theorem 6.5.1*(c)*. We refer to Proposition A.3.3 for the verification.*

We split the proof of Theorem 6.5.1 into the following subsections. In Section 6.5.1, we prove well-posedness (a). For the proof of (b), we follow a standard energy argument (see, e.g., [Eva10]), which consists of the following three steps:

- We derive a discrete energy bound; see Section 6.5.2.
- We extract weakly convergent subsequences and identify the limits; see Section 6.5.3.
- We verify that the limit $\boldsymbol{m}$ is a weak solution of LLG in the sense of Definition 2.2.1(i)–(iii) and thus conclude the proof of (b); see Section 6.5.4.

In Section 6.5.5, we prove (c).

6.5.1. Well-posedness

The well-posedness of Algorithm 6.2.1 follows from the following proposition, which considers one isolated time-step. We adapt the techniques of [BPS09, Lemma 5.1] to the setting of Algorithm 6.2.1 and elaborate [PRS18, Proposition 3].

Proposition 6.5.3 (Well-posedness of IMEX MPS, one time-step, [PRS18, Proposition 3])**.** *Suppose linearity* **(D2)** *of* $\boldsymbol{\pi}_h$ *as well as the Lipschitz-type continuity* **(M2)** *of* $\boldsymbol{\Pi}_h$*. For* $i \in \{0, 1, \ldots, M-1\}$ *and given* $\boldsymbol{m}_h^i, \boldsymbol{m}_h^{i-1} \in \boldsymbol{\mathcal{S}}_h$*, the discrete variational formulation* (6.2) *admits a solution* $\boldsymbol{m}_h^{i+1} \in \boldsymbol{\mathcal{S}}_h$*, which satisfies*

$$|\boldsymbol{m}_h^{i+1}(\boldsymbol{z})| = |\boldsymbol{m}_h^i(\boldsymbol{z})| \quad \textit{for all nodes } \boldsymbol{z} \in \mathcal{N}_h.$$

In particular, it holds that $\|\boldsymbol{m}_h^{i+1}\|_h = \|\boldsymbol{m}_h^i\|_h$ *as well as* $\|\boldsymbol{m}_h^{i+1}\|_{\boldsymbol{L}^\infty(\omega)} = \|\boldsymbol{m}_h^i\|_{\boldsymbol{L}^\infty(\omega)}$.

Proof. Given $\boldsymbol{m}_h^i \in \boldsymbol{\mathcal{S}}_h$, we split the proof into the following three steps.

Step 1. We define an auxiliary mapping $\boldsymbol{\mathcal{F}} : \boldsymbol{\mathcal{S}}_h \to \boldsymbol{\mathcal{S}}_h$: To that end, let $\boldsymbol{\mathcal{I}}_h$ be the nodal interpolant corresponding to $\boldsymbol{\mathcal{S}}_h$. We define the mapping $\boldsymbol{\mathcal{F}} : \boldsymbol{\mathcal{S}}_h \to \boldsymbol{\mathcal{S}}_h$ by

$$\boldsymbol{\mathcal{F}}(\boldsymbol{\varphi}_h) := \frac{2}{k}(\boldsymbol{\varphi}_h - \boldsymbol{m}_h^i) + \boldsymbol{\mathcal{I}}_h\Big(\boldsymbol{\varphi}_h \times \boldsymbol{\mathcal{R}}_h^i(\boldsymbol{\varphi}_h)\Big) \text{ for all } \boldsymbol{\varphi}_h \in \boldsymbol{\mathcal{S}}_h, \tag{6.4}$$

where the residual term is defined as

$$\begin{aligned}\boldsymbol{\mathcal{R}}_h^i(\boldsymbol{\varphi}_h) &:= C_{\mathbf{ex}}\Delta_h\boldsymbol{\varphi}_h + \boldsymbol{\mathcal{P}}_h\boldsymbol{\pi}_h^{\boldsymbol{\Theta}}(2\boldsymbol{\varphi}_h - \boldsymbol{m}_h^i, \boldsymbol{m}_h^i, \boldsymbol{m}_h^{i-1}) \\ &\quad + \boldsymbol{\mathcal{P}}_h\boldsymbol{f}_h^{i+1/2} + \boldsymbol{\mathcal{P}}_h\boldsymbol{\Pi}_h^{\boldsymbol{\Theta}}(2\boldsymbol{\varphi}_h - \boldsymbol{m}_h^i, \boldsymbol{m}_h^i, \boldsymbol{m}_h^{i-1}) - \frac{2\alpha}{k}(\boldsymbol{\varphi}_h - \boldsymbol{m}_h^i) \in \boldsymbol{\mathcal{S}}_h.\end{aligned}$$

With linearity **(D2)** of $\boldsymbol{\pi}_h$ as well as the Lipschitz-type continuity **(M2)** of $\boldsymbol{\Pi}_h$, the auxiliary mapping $\boldsymbol{\mathcal{F}} : \boldsymbol{\mathcal{S}}_h \to \boldsymbol{\mathcal{S}}_h$ is continuous for all general time-stepping approaches **(A1)**–**(A3)**.

Step 2. We analyse $\boldsymbol{\mathcal{F}}$: Let $\boldsymbol{\psi}_h \in \boldsymbol{\mathcal{S}}_h$ and suppose that $\boldsymbol{\mathcal{F}}(\boldsymbol{\psi}_h) = \mathbf{0}$. Then, direct calculations show that $\boldsymbol{m}_h^{i+1} := 2\boldsymbol{\psi}_h - \boldsymbol{m}_h^i \in \boldsymbol{\mathcal{S}}_h$ solves the discrete variational formulation (6.2). Moreover, we get that $|\boldsymbol{m}_h^i(\boldsymbol{z})| = |\boldsymbol{m}_h^{i+1}(\boldsymbol{z})|$ for all nodes $\boldsymbol{z} \in \mathcal{N}_h$: To see this, let $\phi_{\boldsymbol{z}}$ be the nodal basis function corresponding to some node $\boldsymbol{z} \in \mathcal{N}_h$. From the definition (3.10) of $\langle \cdot, \cdot \rangle_h$ and with $\boldsymbol{\psi}_h = (\boldsymbol{m}_h^{i+1} + \boldsymbol{m}_h^i)/2$, we get that

$$\begin{aligned} 0 &= \langle \boldsymbol{\mathcal{F}}(\boldsymbol{\psi}_h), \boldsymbol{\psi}_h(\boldsymbol{z})\phi_{\boldsymbol{z}} \rangle_h \\ &\overset{(6.4)}{=} \frac{2}{k}\Big(\int_\omega \phi_{\boldsymbol{z}} \,\mathrm{d}\boldsymbol{x}\Big)\big(\boldsymbol{\psi}_h(\boldsymbol{z}) - \boldsymbol{m}_h^i(\boldsymbol{z})\big) \cdot \boldsymbol{\psi}_h(\boldsymbol{z}) \\ &= \frac{1}{2k}\Big(\int_\omega \phi_{\boldsymbol{z}} \,\mathrm{d}\boldsymbol{x}\Big)\big(\boldsymbol{m}_h^{i+1}(\boldsymbol{z}) - \boldsymbol{m}_h^i(\boldsymbol{z})\big) \cdot \big(\boldsymbol{m}_h^{i+1}(\boldsymbol{z}) + \boldsymbol{m}_h^i(\boldsymbol{z})\big) \\ &= \frac{1}{2k}\Big(\int_\omega \phi_{\boldsymbol{z}} \,\mathrm{d}\boldsymbol{x}\Big)\big(|\boldsymbol{m}_h^{i+1}(\boldsymbol{z})|^2 - |\boldsymbol{m}_h^i(\boldsymbol{z})|^2\big). \end{aligned}$$

Since $\int_\omega \phi_{\boldsymbol{z}} \,\mathrm{d}\boldsymbol{x} > 0$, this yields that $|\boldsymbol{m}_h^{i+1}(\boldsymbol{z})| = |\boldsymbol{m}_h^i(\boldsymbol{z})|$ for all nodes $\boldsymbol{z} \in \mathcal{N}_h$.

Step 3. We show that there exists such a $\boldsymbol{\psi}_h \in \boldsymbol{\mathcal{S}}_h$ with $\boldsymbol{\mathcal{F}}(\boldsymbol{\psi}_h) = \mathbf{0}$: To that end, note that for all $\boldsymbol{\varphi}_h \in \boldsymbol{\mathcal{S}}_h$, it holds that

$$\langle \boldsymbol{\mathcal{F}}(\boldsymbol{\varphi}_h), \boldsymbol{\varphi}_h \rangle_h = \frac{2}{k}\big(\|\boldsymbol{\varphi}_h\|_h^2 - \langle \boldsymbol{m}_h^i, \boldsymbol{\varphi}_h \rangle_h\big) \geq \frac{2}{k}\|\boldsymbol{\varphi}_h\|_h\big(\|\boldsymbol{\varphi}_h\|_h - \|\boldsymbol{m}_h^i\|_h\big). \tag{6.5}$$

If we choose $r > 0$ such that $r \geq \|\boldsymbol{m}_h^i\|_h$, it holds that

$$\langle \boldsymbol{\mathcal{F}}(\boldsymbol{\varphi}_h), \boldsymbol{\varphi}_h \rangle_h \overset{(6.5)}{\geq} 0 \quad \text{for all} \quad \boldsymbol{\varphi}_h \in \boldsymbol{\mathcal{S}}_h \quad \text{with} \quad \|\boldsymbol{\varphi}_h\|_h = r.$$

Then, the Brouwer fixed-point theorem (see Theorem B.2.5) yields the existence of $\boldsymbol{\psi}_h \in \boldsymbol{\mathcal{S}}_h$ with $\|\boldsymbol{\psi}_h\|_h < r$ and $\boldsymbol{\mathcal{F}}(\boldsymbol{\psi}_h) = \mathbf{0}$.

Step 4. We combine **Step 1**–**Step 3** and conclude existence of a solution $\boldsymbol{m}_h^{i+1}$ to the variational formulation (6.2), which satisfies $|\boldsymbol{m}_h^i(\boldsymbol{z})| = |\boldsymbol{m}_h^{i+1}(\boldsymbol{z})|$ for all nodes $\boldsymbol{z} \in \mathcal{N}_h$. In particular, the definition (3.10) of the approximate $\boldsymbol{L}^2$-product $\langle \cdot, \cdot \rangle_h$ yields that $\|\boldsymbol{m}_h^{i+1}\|_h = \|\boldsymbol{m}_h^i\|_h$. Moreover, since affine functions attain their maximal modulus in one of the nodes $\boldsymbol{z} \in \mathcal{N}_h$, we get that $\|\boldsymbol{m}_h^{i+1}\|_{\boldsymbol{L}^\infty(\omega)} = \|\boldsymbol{m}_h^i\|_{\boldsymbol{L}^\infty(\omega)}$. This concludes the proof. □

Proof of Theorem 6.5.1(a). Proposition 6.5.3 yields well-posedness for given $\boldsymbol{m}_h^i \in \boldsymbol{\mathcal{S}}_h$ and induction on $i = 0, 1, \ldots, M-1$ proves that

$$|\boldsymbol{m}_h^{i+1}(z)| = |\boldsymbol{m}_h^0(z)| \quad \text{for all nodes } \boldsymbol{z} \in \mathcal{N}_h.$$

Therefore,

$$\|\boldsymbol{m}_h^{i+1}\|_h = \|\boldsymbol{m}_h^0\|_h \quad \text{and} \quad \|\boldsymbol{m}_h^{i+1}\|_{\boldsymbol{L}^\infty(\omega)} = \|\boldsymbol{m}_h^0\|_{\boldsymbol{L}^\infty(\omega)}.$$

This concludes the proof. □

6.5.2. Discrete energy bound

In this section, we derive a discrete energy bound, which represents the mathematical core of the remainder of the proof of Theorem 6.5.1(b)–(c). Note that [BP06, Lemma 3.1(i)] proves the statement for $\boldsymbol{h}_{\text{eff}}(\boldsymbol{m}) = \Delta \boldsymbol{m}$ and $\boldsymbol{\Pi}(\boldsymbol{m}) = \mathbf{0}$. For extensions of the midpoint scheme, corresponding results are proved in, e.g., [BBP08, BPS09, BPS12]. Moreover, note that [AKT12, BSF$^+$14] provide corresponding results for the tangent plane scheme with lower-order terms. In the own work [PRS18, Lemma 9] and [PRS18, Lemma 10], the corresponding ideas of [BSF$^+$14] are exploited to extend [BP06, Lemma 3.1] to the setting of Algorithm 6.2.1. The following lemma elaborates [PRS18, Lemma 9] and [PRS18, Lemma 10].

Lemma 6.5.4 (Discrete energy bound, [PRS18, Lemma 9, Lemma 10])**.** *Let the assumptions of Theorem 6.5.1*(b) *be satisfied and let $k > 0$ be sufficiently small. Then, the following assertions* (i)–(ii) *hold true:*

(i) *For all $i = 0, \ldots, M-1$, it holds that*

$$\begin{aligned}
&\frac{C_{\mathbf{ex}}}{2} \, \mathrm{d_t} \, \|\nabla \boldsymbol{m}_h^{i+1}\|_{\boldsymbol{L}^2(\omega)}^2 + \alpha \| \, \mathrm{d_t} \boldsymbol{m}_h^{i+1}\|_h^2 \\
&\quad = \langle \mathrm{d_t} \boldsymbol{m}_h^{i+1}, \boldsymbol{\pi}_h^{\boldsymbol{\Theta}}(\boldsymbol{m}_h^{i+1}, \boldsymbol{m}_h^i, \boldsymbol{m}_h^{i-1}) \rangle_{\boldsymbol{L}^2(\omega)} + \langle \mathrm{d_t} \boldsymbol{m}_h^{i+1}, \boldsymbol{f}_h^{i+1/2} \rangle_{\boldsymbol{L}^2(\omega)} \\
&\qquad + \langle \mathrm{d_t} \boldsymbol{m}_h^{i+1}, \boldsymbol{\Pi}_h^{\boldsymbol{\Theta}}(\boldsymbol{m}_h^{i+1}, \boldsymbol{m}_h^i, \boldsymbol{m}_h^{i-1}) \rangle_{\boldsymbol{L}^2(\omega)}.
\end{aligned}$$

(ii) *There exists a constant $C > 0$ which depends only on T, ω, $\boldsymbol{m}^0$, α, $C_{\mathbf{ex}}$, $\boldsymbol{\pi}(\cdot)$, $\boldsymbol{f}$, $\boldsymbol{\Pi}(\cdot)$, and $C_{\mathbf{mesh}}$, such that, for all $j = 0, \ldots, M$, it holds that*

$$\|\nabla \boldsymbol{m}_h^j\|_{\boldsymbol{L}^2(\omega)}^2 + k \sum_{i=0}^{j-1} \| \, \mathrm{d_t} \boldsymbol{m}_h^{i+1}\|_{\boldsymbol{L}^2(\omega)}^2 \le C < \infty.$$

Proof. First, we prove (i). To this end, we define the approximate effective field and dissipative effects as

$$\begin{aligned}\boldsymbol{\mathcal{H}}_h^{i+\frac{1}{2}} &:= C_{\mathbf{ex}}\Delta_h \boldsymbol{m}_h^{i+1/2} + \boldsymbol{\mathcal{P}}_h \boldsymbol{\pi}_h^{\boldsymbol{\Theta}}(\boldsymbol{m}_h^{i+1}, \boldsymbol{m}_h^{i}, \boldsymbol{m}_h^{i-1}) \\ &\quad + \boldsymbol{\mathcal{P}}_h \boldsymbol{f}_h^{i+1/2} + \boldsymbol{\mathcal{P}}_h \boldsymbol{\Pi}_h^{\boldsymbol{\Theta}}(\boldsymbol{m}_h^{i+1}, \boldsymbol{m}_h^{i}, \boldsymbol{m}_h^{i-1}) \in \boldsymbol{\mathcal{S}}_h. \qquad (6.6)\end{aligned}$$

With this notation, we rewrite the discrete variational formulation (6.2) and, for all $\boldsymbol{\varphi}_h \in \boldsymbol{\mathcal{S}}_h$, we obtain that

$$\langle \mathrm{d_t}\boldsymbol{m}_h^{i+1}, \boldsymbol{\varphi}_h\rangle_h \overset{(6.2)}{=} -\langle \boldsymbol{m}_h^{i+1/2} \times \boldsymbol{\mathcal{H}}_h^{i+\frac{1}{2}}, \boldsymbol{\varphi}_h\rangle_h + \alpha\langle \boldsymbol{m}_h^{i+1/2} \times \mathrm{d_t}\boldsymbol{m}_h^{i+1}, \boldsymbol{\varphi}_h\rangle_h. \qquad (6.7)$$

We test the latter equation with $\boldsymbol{\varphi}_h := \alpha\, \mathrm{d_t}\boldsymbol{m}_h^{i+1} \in \boldsymbol{\mathcal{S}}_h$. Since $(\mathbf{a} \times \mathbf{b}) \cdot \mathbf{b} = \mathbf{0}$ for all $\mathbf{a}, \mathbf{b} \in \mathbb{R}^3$, we obtain that

$$\alpha \,\|\, \mathrm{d_t}\boldsymbol{m}_h^{i+1}\|_h^2 = -\alpha\, \langle \boldsymbol{m}_h^{i+1/2} \times \boldsymbol{\mathcal{H}}_h^{i+\frac{1}{2}}, \mathrm{d_t}\boldsymbol{m}_h^{i+1}\rangle_h = \alpha\langle \boldsymbol{m}_h^{i+1/2} \times \mathrm{d_t}\boldsymbol{m}_h^{i+1}, \boldsymbol{\mathcal{H}}_h^{i+\frac{1}{2}}\rangle_h.$$

Next, we test (6.7) with $\boldsymbol{\varphi}_h := \boldsymbol{\mathcal{H}}_h^{i+\frac{1}{2}} \in \boldsymbol{\mathcal{S}}_h$ and obtain that

$$\langle \mathrm{d_t}\boldsymbol{m}_h^{i+1}, \boldsymbol{\mathcal{H}}_h^{i+\frac{1}{2}}\rangle_h \overset{(6.7)}{=} \alpha\langle \boldsymbol{m}_h^{i+1/2} \times \mathrm{d_t}\boldsymbol{m}_h^{i+1}, \boldsymbol{\mathcal{H}}_h^{i+\frac{1}{2}}\rangle_h.$$

With the definition (3.12) of the quasi-$\boldsymbol{L}^2$ projection $\boldsymbol{\mathcal{P}}_h$, the combination of the latter two equations yields that

$$\begin{aligned}\alpha\|\, \mathrm{d_t}\boldsymbol{m}_h^{i+1}\|_h^2 &= \langle \mathrm{d_t}\boldsymbol{m}_h^{i+1}, \boldsymbol{\mathcal{H}}_h^{i+\frac{1}{2}}\rangle_h \\ &\overset{(6.6)}{=} C_{\mathbf{ex}}\langle \mathrm{d_t}\boldsymbol{m}_h^{i+1}, \Delta_h\boldsymbol{m}_h^{i+1/2}\rangle_h + \langle \mathrm{d_t}\boldsymbol{m}_h^{i+1}, \boldsymbol{\mathcal{P}}_h\boldsymbol{\pi}_h^{\boldsymbol{\Theta}}(\boldsymbol{m}_h^{i+1}, \boldsymbol{m}_h^{i}, \boldsymbol{m}_h^{i-1})\rangle_h \\ &\quad + \langle \mathrm{d_t}\boldsymbol{m}_h^{i+1}, \boldsymbol{\mathcal{P}}_h\boldsymbol{f}_h^{i+1/2}\rangle_h + \langle \mathrm{d_t}\boldsymbol{m}_h^{i+1}, \boldsymbol{\mathcal{P}}_h\boldsymbol{\Pi}_h^{\boldsymbol{\Theta}}(\boldsymbol{m}_h^{i+1}, \boldsymbol{m}_h^{i}, \boldsymbol{m}_h^{i-1})\rangle_h \\ &= C_{\mathbf{ex}}\langle \mathrm{d_t}\boldsymbol{m}_h^{i+1}, \Delta_h\boldsymbol{m}_h^{i+1/2}\rangle_h + \langle \mathrm{d_t}\boldsymbol{m}_h^{i+1}, \boldsymbol{\pi}_h^{\boldsymbol{\Theta}}(\boldsymbol{m}_h^{i+1}, \boldsymbol{m}_h^{i}, \boldsymbol{m}_h^{i-1})\rangle_{\boldsymbol{L}^2(\omega)} \\ &\quad + \langle \mathrm{d_t}\boldsymbol{m}_h^{i+1}, \boldsymbol{f}_h^{i+1/2}\rangle_{\boldsymbol{L}^2(\omega)} + \langle \mathrm{d_t}\boldsymbol{m}_h^{i+1}, \boldsymbol{\Pi}_h^{\boldsymbol{\Theta}}(\boldsymbol{m}_h^{i+1}, \boldsymbol{m}_h^{i}, \boldsymbol{m}_h^{i-1})\rangle_{\boldsymbol{L}^2(\omega)}.\end{aligned}$$

For the first term on the right-hand side, the definition (3.11) of the discrete Laplacian Δ_h yields that

$$\langle \mathrm{d_t}\boldsymbol{m}_h^{i+1}, \Delta_h\boldsymbol{m}_h^{i+1/2}\rangle_h = -\langle \nabla\, \mathrm{d_t}\boldsymbol{m}_h^{i+1}, \nabla\boldsymbol{m}_h^{i+1/2}\rangle_{\boldsymbol{L}^2(\omega)} = -\frac{1}{2}\, \mathrm{d_t}\, \|\nabla\boldsymbol{m}_h^{i+1}\|_{\boldsymbol{L}^2(\omega)}^2.$$

Then, the combination of the latter two equations proves (i). We split the proof of (ii) into the following seven steps.

Step 1. We sum (i) over $i = 0, \ldots, j-1$: Together with the telescopic sum property, we obtain that

$$\begin{aligned}\chi^{(j)} &:= \frac{C_{\mathbf{ex}}}{2}\|\nabla \boldsymbol{m}_h^j\|_{\boldsymbol{L}^2(\omega)}^2 + \alpha k \sum_{i=0}^{j-1} \|\,\mathrm{d_t}\boldsymbol{m}_h^{i+1}\|_h^2 \\ &\overset{\text{(i)}}{=} \frac{C_{\mathbf{ex}}}{2}\|\nabla \boldsymbol{m}_h^0\|_{\boldsymbol{L}^2(\omega)}^2 + k\sum_{i=0}^{j-1}\langle \mathrm{d_t}\boldsymbol{m}_h^{i+1}, \boldsymbol{\pi}_h^{\boldsymbol{\Theta}}(\boldsymbol{m}_h^{i+1}, \boldsymbol{m}_h^i, \boldsymbol{m}_h^{i-1})\rangle_{\boldsymbol{L}^2(\omega)} \\ &\quad + k\sum_{i=0}^{j-1}\langle \mathrm{d_t}\boldsymbol{m}_h^{i+1}, \boldsymbol{f}_h^{i+1/2}\rangle_{\boldsymbol{L}^2(\omega)} + k\sum_{i=0}^{j-1}\langle \mathrm{d_t}\boldsymbol{m}_h^{i+1}, \boldsymbol{\Pi}_h^{\boldsymbol{\Theta}}(\boldsymbol{m}_h^{i+1}, \boldsymbol{m}_h^i, \boldsymbol{m}_h^{i-1})\rangle_{\boldsymbol{L}^2(\omega)} \\ &=: S_1 + \cdots + S_4. \end{aligned} \tag{6.8}$$

In the following steps, we estimate $S_1, \dots, S_4$. Then, our goal is to absorb as many terms as possible to $\chi^{(j)}$ and to apply the discrete Gronwall lemma afterwards.

Step 2. We estimate S_1: We obtain that

$$S_1 = \frac{C_{\mathbf{ex}}}{2}\|\nabla \boldsymbol{m}_h^0\|_{\boldsymbol{L}^2(\omega)}^2 \overset{\textbf{(D1)}}{\lesssim} 1. \tag{6.9}$$

Step 3. We estimate S_2: To this end, we note that

$$\max_{i=0,\dots,M}\|\boldsymbol{m}_h^i\|_{\boldsymbol{L}^\infty(\omega)} \overset{\text{(a)}}{=} \|\boldsymbol{m}_h^0\|_{\boldsymbol{L}^\infty(\omega)} \overset{\textbf{(M1)}}{\lesssim} 1. \tag{6.10}$$

For all approaches **(A1)**–**(A3)**, this yields that that

$$\|\boldsymbol{\pi}_h^{\boldsymbol{\Theta}}(\boldsymbol{m}_h^{i+1}, \boldsymbol{m}_h^i, \boldsymbol{m}_h^{i-1})\|_{\boldsymbol{L}^2(\omega)} \overset{\textbf{(D3)}}{\lesssim} \|\boldsymbol{m}_h^{i+1/2}\|_{\boldsymbol{L}^2(\omega)} + \sum_{\ell=i-1}^{i+1}\|\boldsymbol{m}_h^\ell\|_{\boldsymbol{L}^2(\omega)} \overset{(6.10)}{\lesssim} 1. \tag{6.11}$$

Then, the Young inequality yields for arbitrary $\delta > 0$ that

$$\begin{aligned} S_2 &\overset{(6.8)}{=} k\sum_{i=0}^{j-1}\langle \mathrm{d_t}\boldsymbol{m}_h^{i+1}, \boldsymbol{\pi}_h^{\boldsymbol{\Theta}}(\boldsymbol{m}_h^{i+1}, \boldsymbol{m}_h^i, \boldsymbol{m}_h^{i-1})\rangle_{\boldsymbol{L}^2(\omega)} \\ &\lesssim \delta k\sum_{i=0}^{j-1}\|\,\mathrm{d_t}\boldsymbol{m}_h^{i+1}\|_{\boldsymbol{L}^2(\omega)}^2 + \frac{k}{\delta}\sum_{i=0}^{j-1}\|\boldsymbol{\pi}_h^{\boldsymbol{\Theta}}(\boldsymbol{m}_h^{i+1}, \boldsymbol{m}_h^i, \boldsymbol{m}_h^{i-1})\|_{\boldsymbol{L}^2(\omega)}^2 \\ &\overset{(6.11)}{\lesssim} \delta k\sum_{i=0}^{j-1}\|\,\mathrm{d_t}\boldsymbol{m}_h^{i+1}\|_{\boldsymbol{L}^2(\omega)}^2 + \frac{1}{\delta}. \end{aligned}$$

Step 4. We estimate S_3: The Young inequality yields for arbitrary $\delta > 0$ that

$$\begin{aligned} S_3 \overset{(6.8)}{=} k\sum_{i=0}^{j-1}\langle \mathrm{d_t}\boldsymbol{m}_h^{i+1}, \boldsymbol{f}_h^{i+1/2}\rangle_{\boldsymbol{L}^2(\omega)} &\lesssim \delta k\sum_{i=0}^{j-1}\|\,\mathrm{d_t}\boldsymbol{m}_h^{i+1}\|_{\boldsymbol{L}^2(\omega)}^2 + \frac{k}{\delta}\sum_{i=0}^{j-1}\|\boldsymbol{f}_h^{i+1/2}\|_{\boldsymbol{L}^2(\omega)}^2 \\ &\overset{\textbf{(D5)}}{\lesssim} \delta k\sum_{i=0}^{j-1}\|\,\mathrm{d_t}\boldsymbol{m}_h^{i+1}\|_{\boldsymbol{L}^2(\omega)}^2 + \frac{1}{\delta}. \end{aligned}$$

Step 5. We estimate S_4: For all approaches **(A1)**–**(A3)**, it holds that

$$\begin{aligned}
\|\boldsymbol{\Pi}_h^{\boldsymbol{\Theta}}(\boldsymbol{m}_h^{i+1}, \boldsymbol{m}_h^{i}, \boldsymbol{m}_h^{i-1})\|_{\boldsymbol{L}^2(\omega)} &\lesssim \|\boldsymbol{\Pi}_h(\boldsymbol{m}_h^{i+1/2})\|_{\boldsymbol{L}^2(\omega)} + \sum_{j=i-1}^{i+1} \|\boldsymbol{\Pi}_h(\boldsymbol{m}_h^{j})\|_{\boldsymbol{L}^2(\omega)} \\
&\overset{\textbf{(D6)}}{\lesssim} \big(1 + \|\boldsymbol{m}_h^{i+1/2}\|_{\boldsymbol{L}^\infty(\omega)}\big)\, \|\boldsymbol{m}_h^{i+1/2}\|_{\boldsymbol{H}^1(\omega)} + \sum_{\ell=i-1}^{i+1} \big(1 + \|\boldsymbol{m}_h^{\ell}\|_{\boldsymbol{L}^\infty(\omega)}\big)\, \|\boldsymbol{m}_h^{\ell}\|_{\boldsymbol{H}^1(\omega)} \\
&\overset{(6.10)}{\lesssim} 1 + \sum_{\ell=i-1}^{i+1} \|\nabla \boldsymbol{m}_h^{\ell}\|_{\boldsymbol{L}^2(\omega)}.
\end{aligned} \tag{6.12}$$

Then, the Young inequality yields for arbitrary $\delta > 0$ that

$$\begin{aligned}
S_4 &\overset{(6.8)}{=} k \sum_{i=0}^{j-1} \langle \mathrm{d}_t \boldsymbol{m}_h^{i+1}, \boldsymbol{\Pi}_h^{\boldsymbol{\Theta}}(\boldsymbol{m}_h^{i+1}, \boldsymbol{m}_h^{i}, \boldsymbol{m}_h^{i-1}) \rangle_{\boldsymbol{L}^2(\omega)} \\
&\lesssim \delta k \sum_{i=0}^{j-1} \|\, \mathrm{d}_t \boldsymbol{m}_h^{i+1}\|_{\boldsymbol{L}^2(\omega)}^2 + \frac{k}{\delta} \sum_{i=0}^{j-1} \|\boldsymbol{\Pi}_h^{\boldsymbol{\Theta}}(\boldsymbol{m}_h^{i+1}, \boldsymbol{m}_h^{i}, \boldsymbol{m}_h^{i-1})\|_{\boldsymbol{L}^2(\omega)}^2 \\
&\overset{(6.12)}{\lesssim} \delta k \sum_{i=0}^{j-1} \|\, \mathrm{d}_t \boldsymbol{m}_h^{i+1}\|_{\boldsymbol{L}^2(\omega)}^2 + \frac{1}{\delta} + \frac{k}{\delta} \sum_{i=0}^{j} \|\nabla \boldsymbol{m}_h^{i}\|_{\boldsymbol{L}^2(\omega)}^2.
\end{aligned}$$

Step 6. We combine **Step 1**–**Step 5** and get for arbitrary $\delta > 0$ that

$$\begin{aligned}
\chi^{(j)} &\overset{(6.8)}{=} \frac{C_{\mathbf{ex}}}{2} \|\nabla \boldsymbol{m}_h^{j}\|_{\boldsymbol{L}^2(\omega)}^2 + \alpha k \sum_{i=0}^{j-1} \|\, \mathrm{d}_t \boldsymbol{m}_h^{i+1}\|_h^2 \\
&\lesssim 1 + \frac{1}{\delta} + \delta k \sum_{i=0}^{j-1} \|\, \mathrm{d}_t \boldsymbol{m}_h^{i+1}\|_{\boldsymbol{L}^2(\omega)}^2 + \frac{k}{\delta} \sum_{i=0}^{j} \|\nabla \boldsymbol{m}_h^{i}\|_{\boldsymbol{L}^2(\omega)}^2.
\end{aligned}$$

If we choose $\delta > 0$ small enough, we can absorb $\delta k \sum_{i=0}^{j-1} \|\, \mathrm{d}_t \boldsymbol{m}_h^{i+1}\|_{\boldsymbol{L}^2(\omega)}^2$ from the right-hand side into $\chi^{(j)}$. Moreover, for sufficiently small $k > 0$, we can absorb $k/\delta \|\nabla \boldsymbol{m}_h^{i}\|_{\boldsymbol{L}^2(\omega)}^2$ from the last term into $\chi^{(j)}$. Altogether, this results in

$$\chi^{(j)} \lesssim 1 + k \sum_{i=0}^{j-1} \|\nabla \boldsymbol{m}_h^{i}\|_{\boldsymbol{L}^2(\omega)}^2 \overset{(6.8)}{\leq} 1 + k \sum_{i=0}^{j-1} \chi^{(i)} \quad \text{for all } j = 1, \dots, M. \tag{6.13a}$$

Moreover, it holds that

$$\chi^{(0)} \overset{(6.8)}{=} \frac{C_{\mathbf{ex}}}{2} \|\nabla \boldsymbol{m}_h^{0}\|_{\boldsymbol{L}^2(\omega)}^2 \overset{\textbf{(D1)}}{\lesssim} 1. \tag{6.13b}$$

Altogether, (6.13) fits in the setting of the discrete Gronwall lemma (see Lemma B.3.1), which yields that

$$\chi^{(j)} \lesssim \exp\Big(\sum_{i=0}^{j-1} k \Big) \leq \exp(T) < \infty, \quad \text{for all } j = 1, \dots, M.$$

With Proposition 3.3.1(i), we can replace the $\|\cdot\|_h$-norm by the $\|\cdot\|_{\boldsymbol{L}^2(\omega)}$-norm in $\chi^{(i)}$. This proves (ii), and concludes the proof. □

6.5.3. Extraction of weakly convergent subsequences

In this section, we exploit the discrete energy bound from Lemma 6.5.4 and extract weakly convergent subsequences of the postprocessed output of Algorithm 6.2.1. Corresponding results are obtained in, e.g., [BP06, BBP08, BPS09]. The following lemma is based on [PRS18, Lemma 11].

Lemma 6.5.5 (Convergence properties, [PRS18, Lemma 11])**.** *Let the assumptions of Theorem 6.5.1*(b) *be satisfied. Then, there exist subsequences of the postprocessed output*

$$\boldsymbol{m}_{hk}^{\star} \in \{\boldsymbol{m}_{hk}, \boldsymbol{m}_{hk}^{+}, \boldsymbol{m}_{hk}^{-}, \overline{\boldsymbol{m}}_{hk}, \boldsymbol{m}_{hk}^{=}\},$$

of Algorithm 6.2.1 and a function

$$\boldsymbol{m} \in L^{\infty}(0,T;\boldsymbol{H}^1(\omega)) \cap \boldsymbol{H}^1(\omega_T)$$

such that the following convergence properties (i)–(vi) *hold true simultaneously for the same subsequence as $h,k \to 0$:*

(i) $\boldsymbol{m}_{hk} \rightharpoonup \boldsymbol{m}$ *in* $\boldsymbol{H}^1(\omega_T)$.

(ii) $\boldsymbol{m}_{hk}^{\star} \overset{*}{\rightharpoonup} \boldsymbol{m}$ *in* $L^{\infty}(0,T;\boldsymbol{H}^1(\omega))$.

(iii) $\boldsymbol{m}_{hk}^{\star} \rightharpoonup \boldsymbol{m}$ *in* $L^2(0,T;\boldsymbol{H}^1(\omega))$.

(iv) $\boldsymbol{m}_{hk}^{\star} \to \boldsymbol{m}$ *in* $\boldsymbol{L}^2(\omega_T)$.

(v) $\boldsymbol{m}_{hk}^{\star}(t) \to \boldsymbol{m}(t)$ *in* $\boldsymbol{L}^2(\omega)$ *a.e. for* $t \in [0,T)$.

(vi) $\boldsymbol{m}_{hk}^{\star} \to \boldsymbol{m}$ *pointwise a.e. in* ω_T.

Proof. From the definition of the postprocessed output, we get that

$$\|\boldsymbol{m}_{hk}^{\star}\|_{\boldsymbol{L}^{\infty}(\omega_T)} \lesssim \max_{i=0,\dots,M} \|\boldsymbol{m}_h^i\|_{\boldsymbol{L}^{\infty}(\omega)} \overset{\text{(a)}}{=} \|\boldsymbol{m}_h^0\|_{\boldsymbol{L}^{\infty}(\omega)} \overset{\textbf{(L2)}}{\lesssim} 1 \quad \text{and thus} \quad \|\boldsymbol{m}_{hk}^{\star}\|_{\boldsymbol{L}^2(\omega_T)} \lesssim 1.$$

Together with the discrete energy bound from Lemma 6.5.4(ii), this yields that

$$\|\boldsymbol{m}_{hk}\|_{\boldsymbol{H}^1(\omega_T)} + \|\boldsymbol{m}_{hk}^{\star}\|_{L^{\infty}(0,T;\boldsymbol{H}^1(\omega))} \lesssim 1. \tag{6.14}$$

With the Eberlein–Šmulian theorem (see Theorem B.2.2), we can successively extract weakly convergent subsequences of $\boldsymbol{m}_{hk}^{\star}$ with the corresponding limits

$$\boldsymbol{m}^{\star} \in \{\boldsymbol{m}, \boldsymbol{m}^{+}, \boldsymbol{m}^{-}, \overline{\boldsymbol{m}}, \boldsymbol{m}^{=}\}, \quad \text{where} \quad \boldsymbol{m}^{\star} \in \boldsymbol{L}^2(0,T;\boldsymbol{H}^1(\omega)) \quad \text{and} \quad \boldsymbol{m} \in \boldsymbol{H}^1(\omega_T),$$

and the convergence properties

$$\boldsymbol{m}_{hk}^{\star} \rightharpoonup \boldsymbol{m}^{\star} \quad \text{in } \boldsymbol{L}^2(0,T;\boldsymbol{H}^1(\omega)) \quad \text{as well as} \quad \boldsymbol{m}_{hk} \rightharpoonup \boldsymbol{m} \quad \text{in } \boldsymbol{H}^1(\omega_T).$$

With the Rellich–Kondrachov theorem (see Theorem 2.1.2), the latter equation implies that $\boldsymbol{m}_{hk} \to \boldsymbol{m}$ in $\boldsymbol{L}^2(\omega_T)$ as $h,k \to 0$ and this proves (i) and (iii)–(iv) for $\boldsymbol{m}_{hk}$. For the remaining $\boldsymbol{m}_{hk}^{\star}$, we need to identify all corresponding limits $\boldsymbol{m}^{\star}$. To this end, the definitions of the postprocessed output and the discrete time-derivative directly yields that

$$\|\boldsymbol{m}_{hk} - \boldsymbol{m}_{hk}^{\star}\|_{\boldsymbol{L}^2(\omega_T)} \leq k\,\|\partial_t \boldsymbol{m}_{hk}\|_{\boldsymbol{L}^2(\omega_T)} \overset{(6.14)}{\lesssim} k \to 0 \quad \text{as } h,k \to 0.$$

Since (iv) holds already for $\boldsymbol{m}_{hk}$, we altogether get that

$$\|\boldsymbol{m} - \boldsymbol{m}_{hk}^{\star}\|_{\boldsymbol{L}^2(\omega_T)} \lesssim \|\boldsymbol{m} - \boldsymbol{m}_{hk}\|_{\boldsymbol{L}^2(\omega_T)} + \|\boldsymbol{m}_{hk} - \boldsymbol{m}_{hk}^{\star}\|_{\boldsymbol{L}^2(\omega_T)} \to 0 \quad \text{as } h,k \to 0,$$

i.e., $\boldsymbol{m}^{\star} = \boldsymbol{m}$. This proves (i) as well as (iii)–(iv). To prove (ii), we use (6.14) and the Alaoglu theorem (see Theorem B.2.3) for further successive extraction of subsequences which are weak* convergent in $L^{\infty}(0,T,\boldsymbol{H}^1(\omega))$. Since weak* convergence in $L^{\infty}(0,T,\boldsymbol{H}^1(\omega))$ implies weak convergence in $L^2(0,T,\boldsymbol{H}^1(\omega))$, this identifies the latter limits with $\boldsymbol{m}$ and thus proves (ii). Upon successive extraction of further subsequences, (v) and (vi) are direct consequences of (iv). Altogether, this concludes the proof. □

Moreover, we note a direct consequence of the latter convergence properties, which already anticipates the verification of Definition 6.5.1(b) for the proof of Theorem 4.5.1(b).

Lemma 6.5.6 ($|\boldsymbol{m}| = 1$ a.e. in ω_T)**.** *Let the assumptions of Theorem 6.5.1*(b) *be satisfied. Then,* $\boldsymbol{m} \in L^{\infty}(0,T;\boldsymbol{H}^1(\omega)) \cap \boldsymbol{H}^1(\omega_T)$ *from Lemma 6.5.5 satisfies* $|\boldsymbol{m}| = 1$ *a.e. in* ω_T.

Proof. We extend the corresponding technique of [BP06] and estimate

$$\begin{aligned}\|1 - |\boldsymbol{m}|\|_{L^2(\omega_T)} &\leq \|1 - |\boldsymbol{m}_{hk}^{-}|\|_{L^2(\omega_T)} + \||\boldsymbol{m}_{hk}^{-}| - |\boldsymbol{m}|\|_{L^2(\omega_T)} \\ &\leq \|1 - |\boldsymbol{m}_{hk}^{-}|\|_{L^2(\omega_T)} + \|\boldsymbol{m}_{hk}^{-} - \boldsymbol{m}\|_{\boldsymbol{L}^2(\omega_T)} =: T_1 + T_2.\end{aligned} \tag{6.15}$$

With the convergence property of Lemma 6.5.5(iv), we get that $T_2 \to 0$ as $h,k \to 0$, i.e., we only have to deal with T_1: To this end, fix $t \in [0,T)$ and $\boldsymbol{x} \in \omega$. Let $i \in \{0,1,\dots,M-1\}$ such that $t \in [t_i, t_{i+1})$ and $K \in \mathcal{T}_h$ such that $\boldsymbol{x} \in \overline{K}$. For all nodes $\boldsymbol{z} \in \overline{K}$, it holds that $|\boldsymbol{m}_h^i(\boldsymbol{z})| = |\boldsymbol{m}_h^0(\boldsymbol{z})|$ and with the definition of the postprocessed output, we get that

$$\begin{aligned}\big|1 - |\boldsymbol{m}_{hk}^{-}(t,\boldsymbol{x})|\big| &= \big|1 - |\boldsymbol{m}_h^i(\boldsymbol{x})|\big| \leq \big|1 - |\boldsymbol{m}_h^i(\boldsymbol{z})|\big| + \big||\boldsymbol{m}_h^i(\boldsymbol{z})| - |\boldsymbol{m}_h^i(\boldsymbol{x})|\big| \\ &= \big|1 - |\boldsymbol{m}_h^0(\boldsymbol{z})|\big| + \big||\boldsymbol{m}_h^i(\boldsymbol{z})| - |\boldsymbol{m}_h^i(\boldsymbol{x})|\big| =: T_1^A + T_1^B.\end{aligned}$$

Since we supposed in (2.5) that $|\boldsymbol{m}^0| = 1$ a.e. in ω and since $\nabla \boldsymbol{m}_h^0$ is elementwise constant, we obtain that

$$\begin{aligned}T_1^A &\leq \big|1 - |\boldsymbol{m}_h^0(\boldsymbol{x})|\big| + \big||\boldsymbol{m}_h^0(\boldsymbol{x})| - |\boldsymbol{m}_h^0(\boldsymbol{z})|\big| = \big||\boldsymbol{m}^0(\boldsymbol{x})| - |\boldsymbol{m}_h^0(\boldsymbol{x})|\big| + \big||\boldsymbol{m}_h^0(\boldsymbol{x})| - |\boldsymbol{m}_h^0(\boldsymbol{z})|\big| \\ &\leq \big|\boldsymbol{m}^0(\boldsymbol{x}) - \boldsymbol{m}_h^0(\boldsymbol{x})\big| + \big|\boldsymbol{m}_h^0(\boldsymbol{x}) - \boldsymbol{m}_h^0(\boldsymbol{z})\big| \leq \big|\boldsymbol{m}^0(\boldsymbol{x}) - \boldsymbol{m}_h^0(\boldsymbol{x})\big| + \big|\nabla \boldsymbol{m}_h^0|_K\big|\,|\boldsymbol{x} - \boldsymbol{z}|.\end{aligned}$$

Similarly, since $\nabla \boldsymbol{m}_h^i$ is elementwise constant, we get that

$$T_1^B \leq |\boldsymbol{m}_h^i(\boldsymbol{z}) - \boldsymbol{m}_h^i(\boldsymbol{x})| \leq \big|\nabla \boldsymbol{m}_h^i|_K\big|\,|\boldsymbol{x} - \boldsymbol{z}| = \big|\nabla \boldsymbol{m}_{hk}^{-}|_K\big|\,|\boldsymbol{x} - \boldsymbol{z}|.$$

Combining the latter three equations, we obtain that

$$\big|\,1 - |\boldsymbol{m}_{hk}^{-}(t,\boldsymbol{x})|\,\big| \leq \big|\,\boldsymbol{m}^0(\boldsymbol{x}) - \boldsymbol{m}_h^0(\boldsymbol{x})\,\big| + \big|\nabla \boldsymbol{m}_h^0|_K\big|\,|\boldsymbol{x} - \boldsymbol{z}| + \big|\nabla \boldsymbol{m}_{hk}^{-}|_K\big|\,|\boldsymbol{x} - \boldsymbol{z}|.$$

We integrate in the latter estimate over ω_T and arrive at

$$T_1 \overset{(6.15)}{=} \| 1 - |\boldsymbol{m}_{hk}^-| \, \|_{L^2(\omega_T)} \lesssim \|\boldsymbol{m}_h^0 - \boldsymbol{m}^0\|_{\boldsymbol{L}^2(\omega)} + h\, \|\nabla \boldsymbol{m}_h^0\|_{\boldsymbol{L}^2(\omega)} + h\, \|\nabla \boldsymbol{m}_{hk}^-\|_{\boldsymbol{L}^2(\omega_T)}.$$

For the first two terms, we infer from **(D1)** that

$$\|\nabla \boldsymbol{m}_h^0\|_{\boldsymbol{L}^2(\omega_T)} \lesssim 1 \quad \text{and} \quad \boldsymbol{m}_h^0 \to \boldsymbol{m}^0 \quad \text{in } \boldsymbol{L}^2(\omega) \quad \text{as } h, k \to 0,$$

where the convergence property holds with the Rellich–Kondrachov theorem (see Proposition 2.1.2). Together with the convergence properties of Lemma 6.5.5, this yields that $T_1 \to 0$ as $h, k \to 0$. Altogether, this concludes the proof. ☐

6.5.4. Convergence to weak solution

In this section, we prove Theorem 6.5.1(b). To this end, we first prove a weak consistency property of the general time-stepping approaches **(A1)**–**(A3)** on $\boldsymbol{L}^2(\omega_T)$.

Lemma 6.5.7 (Weak consistency of $\boldsymbol{\pi}_h^{\boldsymbol{\Theta}}$ and $\boldsymbol{\Pi}_h^{\boldsymbol{\Theta}}$)**.** *Let the assumptions of Theorem 6.5.1*(b) *be satisfied. Consider the general time-stepping approaches* **(A1)**–**(A3)***. Then, the following two convergence properties* (i)–(ii) *hold true as* $h, k \to 0$*:*

(i) $\boldsymbol{\pi}_h^{\boldsymbol{\Theta}}(\boldsymbol{m}_{hk}^+, \boldsymbol{m}_{hk}^-, \boldsymbol{m}_{hk}^=) \rightharpoonup \boldsymbol{\pi}(\boldsymbol{m})$ *in* $\boldsymbol{L}^2(\omega_T)$.

(ii) $\boldsymbol{\Pi}_h^{\boldsymbol{\Theta}}(\boldsymbol{m}_{hk}^+, \boldsymbol{m}_{hk}^-, \boldsymbol{m}_{hk}^=) \rightharpoonup \boldsymbol{\Pi}(\boldsymbol{m})$ *in* $\boldsymbol{L}^2(\omega_T)$.

Proof. First, we show (i): With the convergence properties from Lemma 6.5.5, and uniform boundedness **(D3)** as well as weak-consistency **(D4)** of $\boldsymbol{\pi}_h$, we can apply Lemma 3.4.1. This yields that

$$\boldsymbol{\pi}_h(\boldsymbol{m}_{hk}^-),\ \boldsymbol{\pi}_h(\boldsymbol{m}_{hk}^=),\ \boldsymbol{\pi}_h(\overline{\boldsymbol{m}}_{hk}) \rightharpoonup \boldsymbol{\pi}(\boldsymbol{m}) \quad \text{in } \boldsymbol{L}^2(\omega_T) \quad \text{as } h, k \to 0.$$

Then, (i) is a direct consequence of the latter convergence properties, where for the Adams–Bashforth approach **(A2)** we deal differently with $[0, k]$ and $[k, T]$, respectively. To show (ii), we get with Lemma 6.5.6 that $\boldsymbol{m} \in \boldsymbol{H}^1(\omega_T) \cap \boldsymbol{L}^\infty(\omega)$ and thus $\boldsymbol{\Pi}(\boldsymbol{m}) \in \boldsymbol{L}^2(\omega)$ is well defined. Then, (ii) is a direct consequence of the convergence properties from Lemma 6.5.5 and the weak consistency property **(D7)** of $\boldsymbol{\Pi}_h$. This concludes the proof. ☐

We come to the actual proof of Theorem 6.5.1(b). In [BP06], the result is proved for the basic configuration $\boldsymbol{h}_{\text{eff}}(\boldsymbol{m}) = \Delta \boldsymbol{m}$ and $\boldsymbol{\Pi}(\boldsymbol{m}) = \boldsymbol{0}$. Moreover, [AKT12, BSF$^+$14] prove corresponding results for the tangent plane scheme with lower-order terms similar to our setting of LLG (2.3). We combine and extend the ideas of [BP06, AKT12, BSF$^+$14] and base the following proof on the own work [PRS18, Section 3.3–3.4].

Proof of Theorem 6.5.1(b)*.* We show that

$$\boldsymbol{m} \in L^\infty(0, T; \boldsymbol{H}^1(\omega)) \cap \boldsymbol{H}^1(\omega_T) \tag{6.16}$$

from Lemma 6.5.5 is a weak solution of LLG in the sense of Definition 2.2.1(i)–(iii). Together with (6.16), Definition 2.2.1(i) is a direct consequence of Lemma 6.5.6 and we split the remaining verifications into the following seven steps.

Step 1. We verify Definition 2.2.1(ii), i.e., $\boldsymbol{m}(0) = \boldsymbol{m}^0$ in the sense of traces: To that end, note that $\boldsymbol{m}_{hk}(0) = \boldsymbol{m}_h^0 \rightharpoonup \boldsymbol{m}^0$ in $\boldsymbol{H}^1(\omega)$ as $h, k \to 0$. Moreover, boundedness of the trace operator from $\boldsymbol{H}^1(\omega_T)$ to $\boldsymbol{L}^2(\omega)$ implies that $\boldsymbol{m}_{hk}(0) \rightharpoonup \boldsymbol{m}(0)$ in $\boldsymbol{L}^2(\omega)$ as $h, k \to 0$. Since weak limits are unique, we get that $\boldsymbol{m}^0 = \boldsymbol{m}(0)$. Thus, $\boldsymbol{m}$ satisfies Definition 2.2.1(ii).

Step 2. We verify Definition 2.2.1(iii), i.e., $\boldsymbol{m}$ satisfies the variational formulation (2.16): To this end, let $\boldsymbol{\varphi} \in \boldsymbol{C}^\infty(\overline{\omega_T})$. Let $\boldsymbol{\mathcal{I}}_h$ be the nodal interpolant corresponding to $\boldsymbol{\mathcal{S}}_h$ and define

$$\boldsymbol{\varphi}_h(t) := \boldsymbol{\mathcal{I}}_h(\boldsymbol{\varphi}(t)) \in \boldsymbol{\mathcal{S}}_h. \tag{6.17}$$

For each interval $[t_i, t_{i+1})$ with $i \in \{0, 1 \ldots, M-1\}$, we test the corresponding discrete variational formulation (6.2) with $\boldsymbol{\varphi}_h(t)$ and integrate over $[0, T]$. The definition of the postprocessed output, yields that

$$\begin{aligned} I_{hk}^1 &:= \int_0^T \langle \partial_t \boldsymbol{m}_{hk}, \boldsymbol{\varphi}_h \rangle_h \,\mathrm{d}t \\ &\overset{(6.2)}{=} -C_{\mathbf{ex}} \int_0^T \langle \overline{\boldsymbol{m}}_{hk} \times \Delta_h \overline{\boldsymbol{m}}_{hk}, \boldsymbol{\varphi}_h \rangle_h \,\mathrm{d}t - \int_0^T \langle \overline{\boldsymbol{m}}_{hk} \times \boldsymbol{\mathcal{P}}_h \boldsymbol{\pi}_h^{\boldsymbol{\Theta}}(\boldsymbol{m}_{hk}^+, \boldsymbol{m}_{hk}^-, \boldsymbol{m}_{hk}^=), \boldsymbol{\varphi}_h \rangle_h \,\mathrm{d}t \\ &\quad - \int_0^T \langle \overline{\boldsymbol{m}}_{hk} \times \boldsymbol{\mathcal{P}}_h \overline{\boldsymbol{f}}_{hk}, \boldsymbol{\varphi}_h \rangle_h \,\mathrm{d}t - \int_0^T \langle \overline{\boldsymbol{m}}_{hk} \times \boldsymbol{\mathcal{P}}_h \boldsymbol{\Pi}_h^{\boldsymbol{\Theta}}(\boldsymbol{m}_{hk}^+, \boldsymbol{m}_{hk}^-, \boldsymbol{m}_{hk}^=), \boldsymbol{\varphi}_h \rangle_h \,\mathrm{d}t \\ &\quad + \alpha \int_0^T \langle \overline{\boldsymbol{m}}_{hk} \times \partial_t \boldsymbol{m}_{hk}, \boldsymbol{\varphi}_h \rangle_h \,\mathrm{d}t \;=:\; -C_{\mathbf{ex}} I_{hk}^2 - I_{hk}^3 - I_{hk}^4 - I_{hk}^5 + \alpha I_{hk}^6. \end{aligned} \tag{6.18}$$

In the following, we prove convergence of the integrals $I_{hk}^1, \ldots, I_{hk}^6$ towards their continuous counterparts in the variational formulation (2.16).

Step 3. We collect auxiliary convergence results: Note that similar results are implicitly contained in, e.g., [BP06, BPS09]. Here, we elaborate the corresponding arguments. For $p \in (3/2, \infty]$ and $q \in [1, \infty]$, we show that

$$\boldsymbol{\varphi}_h \to \boldsymbol{\varphi} \quad \text{in } L^q(0,T; \boldsymbol{W}^{1,p}(\omega)), \tag{6.19a}$$

$$\boldsymbol{\mathcal{I}}_h(\overline{\boldsymbol{m}}_{hk} \times \boldsymbol{\varphi}_h) \to \boldsymbol{m} \times \boldsymbol{\varphi} \quad \text{in } \boldsymbol{L}^2(\omega_T), \tag{6.19b}$$

$$\nabla(\overline{\boldsymbol{m}}_{hk} \times \boldsymbol{\varphi}_h) - \nabla \boldsymbol{\mathcal{I}}_h(\overline{\boldsymbol{m}}_{hk} \times \boldsymbol{\varphi}_h) \to \boldsymbol{0} \quad \text{in } \boldsymbol{L}^2(\omega_T), \quad \text{and} \tag{6.19c}$$

$$\overline{\boldsymbol{m}}_{hk} \times \nabla \boldsymbol{\varphi}_h \to \boldsymbol{m} \times \nabla \boldsymbol{\varphi} \quad \text{in } \boldsymbol{L}^2(\omega_T), \tag{6.19d}$$

as $h, k \to 0$. First, the convergence (6.19a) is a direct consequence of the definition (6.17) of $\boldsymbol{\varphi}_h$ and the approximation properties of the nodal interpolant $\boldsymbol{\mathcal{I}}_h$ (see Proposition 3.1.7). To show (6.19b) and (6.19c), we first note that $D^2\, \overline{\boldsymbol{m}}_{hk}|_K = \boldsymbol{0}$ for all elements $K \in \mathcal{T}_h$. This implies that

$$|\overline{\boldsymbol{m}}_{hk} \times \boldsymbol{\varphi}_h|_{\boldsymbol{H}^2(K)} \lesssim \|\nabla \overline{\boldsymbol{m}}_{hk}\|_{\boldsymbol{L}^2(K)} \, \|\nabla \boldsymbol{\varphi}_h\|_{\boldsymbol{L}^\infty(K)} \quad \text{for all elements } K \in \mathcal{T}_h.$$

With approximation properties of the nodal interpolant $\boldsymbol{\mathcal{I}}_h$ (see Proposition 3.1.7) and the convergence properties of Lemma 6.5.5, we then obtain that

$$\begin{aligned}
&\|\overline{\boldsymbol{m}}_{hk} \times \boldsymbol{\varphi}_h - \boldsymbol{\mathcal{I}}_h(\overline{\boldsymbol{m}}_{hk} \times \boldsymbol{\varphi}_h)\|_{\boldsymbol{L}^2(\omega_T)} + \|\nabla(\overline{\boldsymbol{m}}_{hk} \times \boldsymbol{\varphi}_h) - \nabla\boldsymbol{\mathcal{I}}_h(\overline{\boldsymbol{m}}_{hk} \times \boldsymbol{\varphi}_h)\|_{\boldsymbol{L}^2(\omega_T)} \\
&\quad\lesssim h\bigg(\sum_{K\in\mathcal{T}_h}\int_0^T |\overline{\boldsymbol{m}}_{hk} \times \boldsymbol{\varphi}_h|^2_{\boldsymbol{H}^2(K)}\,\mathrm{d}t\bigg)^{1/2} \\
&\quad\lesssim h\bigg(\sum_{K\in\mathcal{T}_h}\int_0^T \|\nabla\overline{\boldsymbol{m}}_{hk}(t)\|^2_{\mathbf{L}^2(K)}\|\nabla\boldsymbol{\varphi}_h(t)\|^2_{\mathbf{L}^\infty(K)}\,\mathrm{d}t\bigg)^{1/2} \\
&\quad\lesssim h\,\|\nabla\overline{\boldsymbol{m}}_{hk}\|_{\boldsymbol{L}^2(\omega_T)}\,\|\nabla\boldsymbol{\varphi}_h\|_{\boldsymbol{L}^\infty(\omega_T)} \overset{(6.19a)}{\lesssim} h \to 0 \quad \text{as } h,k\to 0,
\end{aligned}$$

This already verifies (6.19c). With $|\boldsymbol{m}| = 1$ a.e. in ω_T from Lemma 6.5.6, we further get that

$$\begin{aligned}
&\|\boldsymbol{m}\times\boldsymbol{\varphi} - \overline{\boldsymbol{m}}_{hk}\times\boldsymbol{\varphi}_h\|_{\boldsymbol{L}^2(\omega_T)} \\
&\qquad\lesssim \|\boldsymbol{m}\times(\boldsymbol{\varphi}-\boldsymbol{\varphi}_h)\|_{\boldsymbol{L}^2(\omega_T)} + \|(\boldsymbol{m}-\overline{\boldsymbol{m}}_{hk})\times\boldsymbol{\varphi}_h\|_{\boldsymbol{L}^2(\omega_T)} \\
&\qquad\lesssim \|\boldsymbol{m}\|_{\boldsymbol{L}^\infty(\omega_T)}\|\boldsymbol{\varphi}-\boldsymbol{\varphi}_h\|_{\boldsymbol{L}^2(\omega_T)} + \|\boldsymbol{m}-\overline{\boldsymbol{m}}_{hk}\|_{\boldsymbol{L}^2(\omega_T)}\,\|\boldsymbol{\varphi}_h\|_{\boldsymbol{L}^\infty(\omega_T)} \\
&\qquad\overset{(6.19a)}{\lesssim} \|\boldsymbol{\varphi}-\boldsymbol{\varphi}_h\|_{\boldsymbol{L}^2(\omega_T)} + \|\boldsymbol{m}-\overline{\boldsymbol{m}}_{hk}\|_{\boldsymbol{L}^2(\omega_T)} \overset{(6.19a)}{\to} 0 \quad \text{as } h,k\to 0.
\end{aligned}$$

The combination of the latter two estimates proves (6.19b). Replacing $\boldsymbol{\varphi}$ and $\boldsymbol{\varphi}_h$ with $\nabla\boldsymbol{\varphi}$ and $\nabla\boldsymbol{\varphi}_h$, respectively, in the latter estimate, we conclude (6.19d).

Step 4. We deal with I^1_{hk} as in [BP06, Section 3]: We derive that

$$\begin{aligned}
I^1_{hk} &\overset{(6.18)}{=} \int_0^T \langle\partial_t\boldsymbol{m}_{hk},\boldsymbol{\varphi}_h\rangle_h\,\mathrm{d}t \\
&= \int_0^T \langle\partial_t\boldsymbol{m}_{hk},\boldsymbol{\varphi}_h\rangle_{\boldsymbol{L}^2(\omega)}\,\mathrm{d}t + \int_0^T \langle\partial_t\boldsymbol{m}_{hk},\boldsymbol{\varphi}_h\rangle_h - \langle\partial_t\boldsymbol{m}_{hk},\boldsymbol{\varphi}_h\rangle_{\boldsymbol{L}^2(\omega)}\,\mathrm{d}t := I^{1,A}_{hk} + I^{1,B}_{hk}.
\end{aligned}$$

With the convergence property of Lemma 6.5.5(i), we get that

$$I^{1,A}_{hk} \overset{(6.18)}{=} \int_0^T \langle\partial_t\boldsymbol{m}_{hk},\boldsymbol{\varphi}_h\rangle_{\boldsymbol{L}^2(\omega)}\,\mathrm{d}t \overset{(6.19a)}{\to} \int_0^T \langle\partial_t\boldsymbol{m},\boldsymbol{\varphi}\rangle_{\boldsymbol{L}^2(\omega)}\,\mathrm{d}t \quad \text{as } h,k\to 0.$$

For $I^{1,B}_{hk}$, we recall from Lemma 6.5.5(i) that $\|\partial_t\boldsymbol{m}_{hk}\|_{\boldsymbol{L}^2(\omega_T)} \lesssim 1$. With Lemma 3.3.1(ii) and an inverse estimate (see Proposition 3.1.8), we then get that

$$\begin{aligned}
|\,I^{1,B}_{hk}\,| &\lesssim h^2\|\nabla\partial_t\boldsymbol{m}_{hk}\|_{\boldsymbol{L}^2(\omega_T)}\,\|\nabla\boldsymbol{\varphi}_h\|_{\boldsymbol{L}^2(\omega_T)} \\
&\lesssim h\,\|\partial_t\boldsymbol{m}_{hk}\|_{\boldsymbol{L}^2(\omega_T)}\,\|\nabla\boldsymbol{\varphi}_h\|_{\boldsymbol{L}^2(\omega_T)} \overset{(6.19a)}{\lesssim} h\to 0 \quad \text{as } h,k\to 0.
\end{aligned} \tag{6.20}$$

The combination of the latter three equations yields that

$$I^1_{hk} \to \int_0^T \langle\partial_t\boldsymbol{m},\boldsymbol{\varphi}\rangle_{\boldsymbol{L}^2(\omega)}\,\mathrm{d}t \quad \text{as } h,k\to 0.$$

Step 5. We deal with I_{hk}^2 as in [BP06, Section 3]: To this end, recall from the definition (3.10) that the approximate $\boldsymbol{L}^2$-product $\langle \cdot, \cdot \rangle_h$ depends only on the nodal values of the arguments. Together with the definition (3.11) of the discrete Laplacian Δ_h, we obtain that

$$
\begin{aligned}
I_{hk}^2 &\overset{(6.18)}{=} \int_0^T \langle \overline{\boldsymbol{m}}_{hk} \times \Delta_h \overline{\boldsymbol{m}}_{hk}, \boldsymbol{\varphi}_h \rangle_h \, \mathrm{d}t = - \int_0^T \langle \Delta_h \overline{\boldsymbol{m}}_{hk}, \overline{\boldsymbol{m}}_{hk} \times \boldsymbol{\varphi}_h \rangle_h \, \mathrm{d}t \\
&= - \int_0^T \langle \Delta_h \overline{\boldsymbol{m}}_{hk}, \boldsymbol{\mathcal{I}}_h (\overline{\boldsymbol{m}}_{hk} \times \boldsymbol{\varphi}_h) \rangle_h \, \mathrm{d}t = \int_0^T \langle \nabla \overline{\boldsymbol{m}}_{hk}, \nabla \boldsymbol{\mathcal{I}}_h (\overline{\boldsymbol{m}}_{hk} \times \boldsymbol{\varphi}_h) \rangle_{\boldsymbol{L}^2(\omega)} \, \mathrm{d}t \\
&= \int_0^T \langle \nabla \overline{\boldsymbol{m}}_{hk}, \nabla \boldsymbol{\mathcal{I}}_h (\overline{\boldsymbol{m}}_{hk} \times \boldsymbol{\varphi}_h) - \nabla \left(\overline{\boldsymbol{m}}_{hk} \times \boldsymbol{\varphi}_h \right) \rangle_{\boldsymbol{L}^2(\omega)} \, \mathrm{d}t \\
&\quad + \int_0^T \langle \nabla \overline{\boldsymbol{m}}_{hk}, \nabla \left(\overline{\boldsymbol{m}}_{hk} \times \boldsymbol{\varphi}_h \right) \rangle_{\boldsymbol{L}^2(\omega)} \, \mathrm{d}t =: I_{hk}^{2,A} + I_{hk}^{2,B}.
\end{aligned}
$$

For $I_{hk}^{2,A}$, the convergence properties from Lemma 6.5.5 and (6.19c) yield that $I_{hk}^{2,A} \to 0$ as $h, k \to 0$. For $I_{hk}^{2,B}$, recall that for $\mathbf{a}, \mathbf{b} \in \mathbb{R}^3$, it holds that $(\mathbf{a} \times \mathbf{b}) \cdot \mathbf{a} = 0$. Together with the convergence properties of Lemma 6.5.5, the product rule yields that

$$
\begin{aligned}
I_{hk}^{2,B} &= \int_0^T \langle \nabla \overline{\boldsymbol{m}}_{hk}, \nabla \overline{\boldsymbol{m}}_{hk} \times \boldsymbol{\varphi}_h \rangle_{\boldsymbol{L}^2(\omega)} \, \mathrm{d}t + \int_0^T \langle \nabla \overline{\boldsymbol{m}}_{hk}, \overline{\boldsymbol{m}}_{hk} \times \nabla \boldsymbol{\varphi}_h \rangle_{\boldsymbol{L}^2(\omega)} \, \mathrm{d}t \\
&= \int_0^T \langle \nabla \overline{\boldsymbol{m}}_{hk}, \overline{\boldsymbol{m}}_{hk} \times \nabla \boldsymbol{\varphi}_h \rangle_{\boldsymbol{L}^2(\omega)} \, \mathrm{d}t \overset{(6.19\mathrm{d})}{\to} \int_0^T \langle \nabla \boldsymbol{m}, \boldsymbol{m} \times \nabla \boldsymbol{\varphi} \rangle_{\boldsymbol{L}^2(\omega)} \, \mathrm{d}t \\
&= - \int_0^T \langle \boldsymbol{m} \times \nabla \boldsymbol{m}, \nabla \boldsymbol{\varphi} \rangle_{\boldsymbol{L}^2(\omega)} \, \mathrm{d}t \quad \text{as } h, k \to 0.
\end{aligned}
$$

Altogether, we obtain that

$$
I_{hk}^2 \to - \int_0^T \langle \boldsymbol{m} \times \nabla \boldsymbol{m}, \nabla \boldsymbol{\varphi} \rangle_{\boldsymbol{L}^2(\omega)} \, \mathrm{d}t \quad \text{as } h, k \to 0.
$$

Step 6. We deal with I_{hk}^3, I_{hk}^4, and I_{hk}^5: Since we can apply the nodal interpolant $\boldsymbol{\mathcal{I}}_h$ to the arguments of $\langle \cdot, \cdot \rangle_h$, we get for I_{hk}^3 from the definition (3.12) of the quasi-$\boldsymbol{L}^2$ projection $\boldsymbol{\mathcal{P}}_h$ that

$$
\begin{aligned}
I_{hk}^3 &\overset{(6.18)}{=} \int_0^T \langle \overline{\boldsymbol{m}}_{hk} \times \boldsymbol{\mathcal{P}}_h \boldsymbol{\pi}_h^{\boldsymbol{\Theta}} (\boldsymbol{m}_{hk}^+, \boldsymbol{m}_{hk}^-, \boldsymbol{m}_{hk}^=), \boldsymbol{\varphi}_h \rangle_h \, \mathrm{d}t \\
&= - \int_0^T \langle \boldsymbol{\mathcal{P}}_h \boldsymbol{\pi}_h^{\boldsymbol{\Theta}} (\boldsymbol{m}_{hk}^+, \boldsymbol{m}_{hk}^-, \boldsymbol{m}_{hk}^=), \boldsymbol{\mathcal{I}}_h (\overline{\boldsymbol{m}}_{hk} \times \boldsymbol{\varphi}_h) \rangle_h \, \mathrm{d}t \\
&\overset{(3.12)}{=} - \int_0^T \langle \boldsymbol{\pi}_h^{\boldsymbol{\Theta}} (\boldsymbol{m}_{hk}^+, \boldsymbol{m}_{hk}^-, \boldsymbol{m}_{hk}^=), \boldsymbol{\mathcal{I}}_h (\overline{\boldsymbol{m}}_{hk} \times \boldsymbol{\varphi}_h) \rangle_{\boldsymbol{L}^2(\omega)} \, \mathrm{d}t
\end{aligned}
$$

With the convergence properties from Lemma 6.5.7(i), we infer that

$$
I_{hk}^3 \overset{(6.19\mathrm{b})}{\to} - \int_0^T \langle \boldsymbol{\pi}(\boldsymbol{m}), \boldsymbol{m} \times \boldsymbol{\varphi} \rangle_{\boldsymbol{L}^2(\omega)} \, \mathrm{d}t = \int_0^T \langle \boldsymbol{m} \times \boldsymbol{\pi}(\boldsymbol{m}), \boldsymbol{\varphi} \rangle_{\boldsymbol{L}^2(\omega)} \, \mathrm{d}t \quad \text{as } h, k \to 0. \tag{6.21}
$$

If we replace in the latter two equations $\boldsymbol{\pi}_h$ by $\overline{\boldsymbol{f}}_{hk}$ or $\boldsymbol{\Pi}_h$, the convergence properties from assumption **(D5)** for $\overline{\boldsymbol{f}}_{hk}$ and Lemma 6.5.7(ii) for $\boldsymbol{\Pi}_h$ similarly yield that

$$I_{hk}^4 \overset{(6.19b)}{\rightarrow} \int_0^T \langle \boldsymbol{m} \times \boldsymbol{f}, \boldsymbol{\varphi} \rangle_{\boldsymbol{L}^2(\omega)} \, \mathrm{d}t \qquad \text{as } h, k \to 0, \quad \text{and}$$
$$I_{hk}^5 \overset{(6.19b)}{\rightarrow} \int_0^T \langle \boldsymbol{m} \times \boldsymbol{\Pi}(\boldsymbol{m}), \boldsymbol{\varphi} \rangle_{\boldsymbol{L}^2(\omega)} \, \mathrm{d}t \quad \text{as } h, k \to 0.$$

Step 7. We deal with I_{hk}^6 as in [BP06, Section 3]: Similarly as in **Step 4**, we exploit the nodewise definition (3.10) of the approximate $\boldsymbol{L}^2$-product $\langle \cdot, \cdot \rangle_h$ and apply the nodal interpolant $\boldsymbol{\mathcal{I}}_h$ to the arguments. Then, we derive that

$$\begin{aligned} I_{hk}^6 &\overset{(6.18)}{=} \int_0^T \langle \overline{\boldsymbol{m}}_{hk} \times \partial_t \boldsymbol{m}_{hk}, \boldsymbol{\varphi}_h \rangle_h \, \mathrm{d}t = - \int_0^T \langle \partial_t \boldsymbol{m}_{hk}, \boldsymbol{\mathcal{I}}_h(\overline{\boldsymbol{m}}_{hk} \times \boldsymbol{\varphi}_h) \rangle_h \, \mathrm{d}t \\ &= - \int_0^T \langle \partial_t \boldsymbol{m}_{hk}, \boldsymbol{\mathcal{I}}_h(\overline{\boldsymbol{m}}_{hk} \times \boldsymbol{\varphi}_h) \rangle_{\boldsymbol{L}^2(\omega)} \, \mathrm{d}t \\ &\quad - \int_0^T \langle \partial_t \boldsymbol{m}_{hk}, \boldsymbol{\mathcal{I}}_h(\overline{\boldsymbol{m}}_{hk} \times \boldsymbol{\varphi}_h) \rangle_h - \langle \partial_t \boldsymbol{m}_{hk}, \boldsymbol{\mathcal{I}}_h(\overline{\boldsymbol{m}}_{hk} \times \boldsymbol{\varphi}_h) \rangle_{\boldsymbol{L}^2(\omega)} \, \mathrm{d}t =: -I_{hk}^{6,A} - I_{hk}^{6,B}. \end{aligned}$$

With the convergence properties from Lemma 6.5.5, we get that

$$I_{hk}^{6,A} \overset{(6.19b)}{\rightarrow} \int_0^T \langle \partial_t \boldsymbol{m}, \boldsymbol{m} \times \boldsymbol{\varphi} \rangle_{\boldsymbol{L}^2(\omega)} \, \mathrm{d}t \quad \text{as } h, k \to 0.$$

For $I_{hk}^{6,B}$, we recall from Lemma 6.5.5(i) that $\|\partial_t \boldsymbol{m}_{hk}\|_{\boldsymbol{L}^2(\omega_T)} \lesssim 1$. With Lemma 3.3.1(ii) and an inverse estimate (see Proposition 3.1.8), we get that

$$\begin{aligned} \left| I_{hk}^{6,B} \right| &\lesssim h^2 \, \|\nabla \partial_t \boldsymbol{m}_{hk}\|_{\boldsymbol{L}^2(\omega_T)} \, \|\nabla \boldsymbol{\mathcal{I}}_h(\overline{\boldsymbol{m}}_{hk} \times \boldsymbol{\varphi}_h)\|_{\boldsymbol{L}^2(\omega_T)} \\ &\lesssim h \, \|\partial_t \boldsymbol{m}_{hk}\|_{\boldsymbol{L}^2(\omega_T)} \, \|\nabla \boldsymbol{\mathcal{I}}_h(\overline{\boldsymbol{m}}_{hk} \times \boldsymbol{\varphi}_h)\|_{\boldsymbol{L}^2(\omega_T)} \\ &\lesssim h \, \|\nabla \boldsymbol{\mathcal{I}}_h(\overline{\boldsymbol{m}}_{hk} \times \boldsymbol{\varphi}_h)\|_{\boldsymbol{L}^2(\omega_T)} \\ &\leq h \, \|\nabla(\overline{\boldsymbol{m}}_{hk} \times \boldsymbol{\varphi}_h)\|_{\boldsymbol{L}^2(\omega_T)} + h \, \|\nabla(\overline{\boldsymbol{m}}_{hk} \times \boldsymbol{\varphi}_h) - \nabla \boldsymbol{\mathcal{I}}_h(\overline{\boldsymbol{m}}_{hk} \times \boldsymbol{\varphi}_h)\|_{\boldsymbol{L}^2(\omega_T)} \\ &\overset{(6.19c)}{\lesssim} h \left(\|\nabla(\overline{\boldsymbol{m}}_{hk} \times \boldsymbol{\varphi}_h)\|_{\boldsymbol{L}^2(\omega_T)} + 1 \right) \\ &\lesssim h \left(\|\boldsymbol{m}_{hk}\|_{L^2(0,T;\boldsymbol{H}^1(\omega))} \, \|\boldsymbol{\varphi}_h\|_{L^\infty(0,T;\boldsymbol{W}^{1,\infty}(\omega))} + 1 \right) \overset{(6.19a)}{\lesssim} h \to 0 \quad \text{as } h, k \to 0, \end{aligned}$$

i.e., $I_{hk}^{6,B} \to 0$ as $h, k \to 0$. Altogether, the latter three equations yield that

$$I_{hk}^6 \to - \int_0^T \langle \partial_t \boldsymbol{m}, \boldsymbol{m} \times \boldsymbol{\varphi} \rangle_{\boldsymbol{L}^2(\omega)} \, \mathrm{d}t = \int_0^T \langle \boldsymbol{m} \times \partial_t \boldsymbol{m}, \boldsymbol{\varphi} \rangle_{\boldsymbol{L}^2(\omega)} \, \mathrm{d}t \quad \text{as } h, k \to 0.$$

The combination of **Step 1**–**Step 7** concludes the proof. □

6.5.5. Stronger energy estimate

In this section, we prove Theorem 6.5.1(c), i.e., under stronger assumptions, the solution $\boldsymbol{m}$ from (b) is a physical weak solution in the sense of Definition 2.2.1(i)–(iv). To this end, we first prove a strong consistency property of the general time-stepping approaches **(A1)**–**(A3)** on $\boldsymbol{L}^2(\omega_T)$.

Lemma 6.5.8 (Strong consistency of $\boldsymbol{\pi}_h^{\boldsymbol{\Theta}}$ and $\boldsymbol{\Pi}_h^{\boldsymbol{\Theta}}$)**.** *Let the assumptions of Theorem 6.5.1*(c) *be satisfied. Consider the general time-stepping approaches* **(A1)**–**(A3)***. Then, the following two convergence properties* (i)–(ii) *hold true as* $h, k \to 0$*:*

(i) $\boldsymbol{\pi}_h^{\boldsymbol{\Theta}}(\boldsymbol{m}_{hk}^{+}, \boldsymbol{m}_{hk}^{-}, \boldsymbol{m}_{hk}^{=}) \to \boldsymbol{\pi}(\boldsymbol{m})$ *in* $\boldsymbol{L}^2(\omega_T)$.

(ii) $\boldsymbol{\Pi}_h^{\boldsymbol{\Theta}}(\boldsymbol{m}_{hk}^{+}, \boldsymbol{m}_{hk}^{-}, \boldsymbol{m}_{hk}^{=}) \to \boldsymbol{\Pi}(\boldsymbol{m})$ *in* $\boldsymbol{L}^2(\omega_T)$.

Proof. First, we show (i): With the convergence properties from Lemma 6.5.5, uniform boundedness **(D3)** and strong consistency **(D4$^+$)** of $\boldsymbol{\pi}_h$, we can apply Lemma 3.4.1. For all approaches **(A1)** and **(A3)** this yields that

$$\begin{aligned}
&\|\boldsymbol{\pi}_h^{\boldsymbol{\Theta}}(\boldsymbol{m}_{hk}^{+}, \boldsymbol{m}_{hk}^{-}, \boldsymbol{m}_{hk}^{=}) - \boldsymbol{\pi}(\boldsymbol{m})\|_{\boldsymbol{L}^2(\omega_T)} \\
&\lesssim \|\boldsymbol{\pi}_h(\overline{\boldsymbol{m}}_{hk}) - \boldsymbol{\pi}(\boldsymbol{m})\|_{\boldsymbol{L}^2(\omega_T)} + \|\boldsymbol{\pi}_h(\boldsymbol{m}_{hk}^{-}) - \boldsymbol{\pi}(\boldsymbol{m})\|_{\boldsymbol{L}^2(\omega_T)} \\
&\quad + \|\boldsymbol{\pi}_h(\boldsymbol{m}_{hk}^{=}) - \boldsymbol{\pi}(\boldsymbol{m})\|_{\boldsymbol{L}^2(\omega_T)} \to 0 \quad \text{as } h, k \to 0,
\end{aligned}$$

which proves (i). To prove (ii), the detour of Lemma 3.4.1 is not required. We recall from Lemma 6.5.6 that $\boldsymbol{m} \in \boldsymbol{L}^\infty(\omega_T) \cap \boldsymbol{H}^1(\omega_T)$ and thus $\boldsymbol{\Pi}(\boldsymbol{m}) \in \boldsymbol{L}^2(\omega_T)$ is well-defined. Then, (ii) is a direct consequence of the strong consistency **(D7$^+$)** of $\boldsymbol{\Pi}_h$. □

We come to the actual proof of Theorem 6.5.1(c). In [BP06], the result is proved for $\boldsymbol{h}_{\mathrm{eff}}(\boldsymbol{m}) := \Delta \boldsymbol{m}$ and $\boldsymbol{\Pi}(\boldsymbol{m}) = \boldsymbol{0}$. In [BSF$^+$14, Appendix A], a corresponding result was proved for the tangent plane scheme. Here, we elaborate the own work [PRS18, Section 3.5] and transfer the techniques of [BSF$^+$14] to the setting of Algorithm 6.2.1. In addition to [PRS18], we cover dissipative effects, i.e., $\boldsymbol{\Pi}(\boldsymbol{m}) \neq \boldsymbol{0}$.

Proof of Theorem 6.5.1(c). Since the assumptions of (c) are stronger than those of (b), we only have to verify that $\boldsymbol{m}$ from (b) satisfies the energy estimate (2.17). To that end, recall from (2.15) the notion of the energy functional

$$\mathcal{E}_{\mathrm{LLG}}(\boldsymbol{m}) := \frac{C_{\mathbf{ex}}}{2} \|\nabla \boldsymbol{m}\|_{\boldsymbol{L}^2(\omega)}^2 - \frac{1}{2} \langle \boldsymbol{\pi}(\boldsymbol{m}), \boldsymbol{m} \rangle_{\boldsymbol{L}^2(\omega)} - \langle \boldsymbol{f}, \boldsymbol{m} \rangle_{\boldsymbol{L}^2(\omega)}. \tag{6.22}$$

Then, let $\tau \in (0, T)$ and define $j \in \{1, \ldots, M\}$ such that $\tau \in [t_{j-1}, t_j)$. Since we supposed in Section 2.2 that $\boldsymbol{f} \in C^1([0,T], \boldsymbol{L}^2(\omega))$, we can define $\boldsymbol{f}^i := \boldsymbol{f}(t_i)$ for $i \in \{0, \ldots, M\}$. Then, we split the proof into the following five steps.

Step 1. We exploit the discrete energy equality from Lemma 6.5.4(i): For any $i \in \{0, 1, \ldots, j-1\}$, we get that

$$\begin{aligned}
&\mathcal{E}_{\mathrm{LLG}}(\boldsymbol{m}_h^{i+1}) - \mathcal{E}_{\mathrm{LLG}}(\boldsymbol{m}_h^i) \\
&\overset{(6.22)}{=} \frac{C_{\mathbf{ex}} k}{2}\, \mathrm{d_t}\, \|\nabla \boldsymbol{m}_h^{i+1}\|^2_{\boldsymbol{L}^2(\omega)} - \frac{1}{2}\langle \boldsymbol{\pi}(\boldsymbol{m}_h^{i+1}), \boldsymbol{m}_h^{i+1}\rangle_{\boldsymbol{L}^2(\omega)} + \frac{1}{2}\langle \boldsymbol{\pi}(\boldsymbol{m}_h^{i}), \boldsymbol{m}_h^{i}\rangle_{\boldsymbol{L}^2(\omega)} \\
&\quad - \langle \boldsymbol{f}^{i+1}, \boldsymbol{m}_h^{i+1}\rangle_{\boldsymbol{L}^2(\omega)} + \langle \boldsymbol{f}^{i}, \boldsymbol{m}_h^{i}\rangle_{\boldsymbol{L}^2(\omega)} \\
&= \; -\alpha k \,\| \,\mathrm{d_t} \boldsymbol{m}_h^{i+1}\|_h^2 - \frac{1}{2}\langle \boldsymbol{\pi}(\boldsymbol{m}_h^{i+1}), \boldsymbol{m}_h^{i+1}\rangle_{\boldsymbol{L}^2(\omega)} + \frac{1}{2}\langle \boldsymbol{\pi}(\boldsymbol{m}_h^{i}), \boldsymbol{m}_h^{i}\rangle_{\boldsymbol{L}^2(\omega)} \\
&\quad + k\,\langle \mathrm{d_t}\boldsymbol{m}_h^{i+1}, \boldsymbol{\pi}_h^{\boldsymbol{\Theta}}(\boldsymbol{m}_h^{i+1}, \boldsymbol{m}_h^{i}, \boldsymbol{m}_h^{i-1})\rangle_{\boldsymbol{L}^2(\omega)} - \langle \boldsymbol{f}^{i+1}, \boldsymbol{m}_h^{i+1}\rangle_{\boldsymbol{L}^2(\omega)} + \langle \boldsymbol{f}^{i}, \boldsymbol{m}_h^{i}\rangle_{\boldsymbol{L}^2(\omega)} \\
&\quad + k\,\langle \mathrm{d_t}\boldsymbol{m}_h^{i+1}, \boldsymbol{f}_h^{i+1/2}\rangle_{\boldsymbol{L}^2(\omega)} + k\,\langle \mathrm{d_t}\boldsymbol{m}_h^{i+1}, \boldsymbol{\Pi}_h^{\boldsymbol{\Theta}}(\boldsymbol{m}_h^{i+1}, \boldsymbol{m}_h^{i}, \boldsymbol{m}_h^{i-1})\rangle_{\boldsymbol{L}^2(\omega)} \\
&=: \; -\alpha k \,\| \,\mathrm{d_t} \boldsymbol{m}_h^{i+1}\|_h^2 + \sum_{\ell=1}^{3} T_{\boldsymbol{\pi}}^{(\ell)} + \sum_{\ell=1}^{3} T_{\boldsymbol{f}}^{(\ell)} + k\,\langle \boldsymbol{\Pi}_h^{\boldsymbol{\Theta}}(\boldsymbol{m}_h^{i+1}, \boldsymbol{m}_h^{i}, \boldsymbol{m}_h^{i-1}), \mathrm{d_t}\boldsymbol{m}_h^{i+1}\rangle_{\boldsymbol{L}^2(\omega)}.
\end{aligned} \tag{6.23}$$

Step 2. We show that

$$\sum_{\ell=1}^{3} T_{\boldsymbol{\pi}}^{(\ell)} = k\,\langle \mathrm{d_t}\boldsymbol{m}_h^{i+1}, \boldsymbol{\pi}_h^{\boldsymbol{\Theta}}(\boldsymbol{m}_h^{i+1}, \boldsymbol{m}_h^{i}, \boldsymbol{m}_h^{i-1}) - \boldsymbol{\pi}(\boldsymbol{m}_h^{i+1/2})\rangle_{\boldsymbol{L}^2(\omega)}. \tag{6.24}$$

To this end, we rewrite

$$\begin{aligned}
T_{\boldsymbol{\pi}}^{(1)} + T_{\boldsymbol{\pi}}^{(2)} &\overset{(6.23)}{=} -\frac{1}{2}\langle \boldsymbol{\pi}(\boldsymbol{m}_h^{i+1}), \boldsymbol{m}_h^{i+1}\rangle_{\boldsymbol{L}^2(\omega)} + \frac{1}{2}\langle \boldsymbol{\pi}(\boldsymbol{m}_h^{i}), \boldsymbol{m}_h^{i}\rangle_{\boldsymbol{L}^2(\omega)} \\
&= -\frac{1}{2}\langle \boldsymbol{\pi}(\boldsymbol{m}_h^{i+1}), \boldsymbol{m}_h^{i+1}\rangle_{\boldsymbol{L}^2(\omega)} - \frac{1}{2}\langle \boldsymbol{\pi}(\boldsymbol{m}_h^{i+1}), \boldsymbol{m}_h^{i}\rangle_{\boldsymbol{L}^2(\omega)} \\
&\quad + \frac{1}{2}\langle \boldsymbol{\pi}(\boldsymbol{m}_h^{i+1}), \boldsymbol{m}_h^{i}\rangle_{\boldsymbol{L}^2(\omega)} + \frac{1}{2}\langle \boldsymbol{\pi}(\boldsymbol{m}_h^{i}), \boldsymbol{m}_h^{i}\rangle_{\boldsymbol{L}^2(\omega)} \\
&\overset{\textbf{(L1)}}{=} -\langle \boldsymbol{\pi}(\boldsymbol{m}_h^{i+1}), \boldsymbol{m}_h^{i+1/2}\rangle_{\boldsymbol{L}^2(\omega)} + \langle \boldsymbol{\pi}(\boldsymbol{m}_h^{i+1/2}), \boldsymbol{m}_h^{i}\rangle_{\boldsymbol{L}^2(\omega)} \\
&\overset{\textbf{(L3)}}{=} -k\langle \boldsymbol{\pi}(\boldsymbol{m}_h^{i+1/2}), \mathrm{d_t}\boldsymbol{m}_h^{i+1}\rangle_{\boldsymbol{L}^2(\omega)}.
\end{aligned}$$

With the definition of $T_{\boldsymbol{\pi}}^{(3)}$, this shows (6.24).

Step 3. We show that

$$\sum_{\ell=1}^{3} T_{\boldsymbol{f}}^{(\ell)} = k\,\langle \mathrm{d_t}\boldsymbol{m}_h^{i+1}, \boldsymbol{f}_h^{i+1/2} - \boldsymbol{f}^{i+1/2}\rangle_{\boldsymbol{L}^2(\omega)} - k\,\langle \mathrm{d_t}\boldsymbol{f}^{i+1}, \boldsymbol{m}_h^{i+1/2}\rangle_{\boldsymbol{L}^2(\omega)}. \tag{6.25}$$

To this end, we rewrite

$$\begin{aligned}
\sum_{\ell=1}^{3} T_{\boldsymbol{f}}^{(\ell)} &\overset{(6.23)}{=} -\langle \boldsymbol{f}^{i+1}, \boldsymbol{m}_h^{i+1}\rangle_{\boldsymbol{L}^2(\omega)} + \langle \boldsymbol{f}^{i}, \boldsymbol{m}_h^{i}\rangle_{\boldsymbol{L}^2(\omega)} + k\,\langle \mathrm{d_t}\boldsymbol{m}_h^{i+1}, \boldsymbol{f}_h^{i+1/2}\rangle_{\boldsymbol{L}^2(\omega)} \\
&= \; k\,\langle \mathrm{d_t}\boldsymbol{m}_h^{i+1}, \boldsymbol{f}_h^{i+1/2} - \boldsymbol{f}^{i+1/2}\rangle_{\boldsymbol{L}^2(\omega)} + k\,\langle \mathrm{d_t}\boldsymbol{m}_h^{i+1}, \boldsymbol{f}^{i+1/2}\rangle_{\boldsymbol{L}^2(\omega)} \\
&\quad - \langle \boldsymbol{f}^{i+1}, \boldsymbol{m}_h^{i+1}\rangle_{\boldsymbol{L}^2(\omega)} + \langle \boldsymbol{f}^{i}, \boldsymbol{m}_h^{i}\rangle_{\boldsymbol{L}^2(\omega)}.
\end{aligned}$$

For the last three terms in the latter equation, we expand the first term and compute

$$
\begin{aligned}
&k\,\langle \mathrm{d_t}\boldsymbol{m}_h^{i+1}, \boldsymbol{f}^{i+1/2}\rangle_{\boldsymbol{L}^2(\omega)} - \langle \boldsymbol{f}^{i+1}, \boldsymbol{m}_h^{i+1}\rangle_{\boldsymbol{L}^2(\omega)} + \langle \boldsymbol{f}^{i}, \boldsymbol{m}_h^{i}\rangle_{\boldsymbol{L}^2(\omega)} \\
&\quad = \frac{1}{2}\langle \boldsymbol{m}_h^{i+1}, \boldsymbol{f}^{i+1}\rangle_{\boldsymbol{L}^2(\omega)} - \frac{1}{2}\langle \boldsymbol{m}_h^{i}, \boldsymbol{f}^{i+1}\rangle_{\boldsymbol{L}^2(\omega)} + \frac{1}{2}\langle \boldsymbol{m}_h^{i+1}, \boldsymbol{f}^{i}\rangle_{\boldsymbol{L}^2(\omega)} - \frac{1}{2}\langle \boldsymbol{m}_h^{i}, \boldsymbol{f}^{i}\rangle_{\boldsymbol{L}^2(\omega)} \\
&\qquad - \langle \boldsymbol{f}^{i+1}, \boldsymbol{m}_h^{i+1}\rangle_{\boldsymbol{L}^2(\omega)} + \langle \boldsymbol{f}^{i}, \boldsymbol{m}_h^{i}\rangle_{\boldsymbol{L}^2(\omega)} \\
&\quad = -\frac{1}{2}\langle \boldsymbol{m}_h^{i+1}, \boldsymbol{f}^{i+1}\rangle_{\boldsymbol{L}^2(\omega)} - \frac{1}{2}\langle \boldsymbol{m}_h^{i}, \boldsymbol{f}^{i+1}\rangle_{\boldsymbol{L}^2(\omega)} + \frac{1}{2}\langle \boldsymbol{m}_h^{i+1}, \boldsymbol{f}^{i}\rangle_{\boldsymbol{L}^2(\omega)} + \frac{1}{2}\langle \boldsymbol{m}_h^{i}, \boldsymbol{f}^{i}\rangle_{\boldsymbol{L}^2(\omega)} \\
&\quad = -\langle \boldsymbol{m}_h^{i+1/2}, \boldsymbol{f}^{i+1}\rangle_{\boldsymbol{L}^2(\omega)} + \langle \boldsymbol{m}_h^{i+1/2}, \boldsymbol{f}^{i}\rangle_{\boldsymbol{L}^2(\omega)} \\
&\quad = -k\,\langle \boldsymbol{m}_h^{i+1/2}, \mathrm{d_t}\boldsymbol{f}^{i+1}\rangle_{\boldsymbol{L}^2(\omega)}.
\end{aligned}
$$

The combination of the latter two equations proves (6.25).

Step 4. We combine **Step 1**–**Step 3** and obtain that

$$
\begin{aligned}
&\mathcal{E}_{\mathrm{LLG}}(\boldsymbol{m}_h^{i+1}) - \mathcal{E}_{\mathrm{LLG}}(\boldsymbol{m}_h^{i}) + \alpha k \|\,\mathrm{d_t}\boldsymbol{m}_h^{i+1}\|_h^2 \\
&= k\,\langle \mathrm{d_t}\boldsymbol{m}_h^{i+1}, \boldsymbol{\pi}_h^{\boldsymbol{\Theta}}(\boldsymbol{m}_h^{i+1}, \boldsymbol{m}_h^{i}, \boldsymbol{m}_h^{i-1}) - \boldsymbol{\pi}(\boldsymbol{m}_h^{i+1/2})\rangle_{\boldsymbol{L}^2(\omega)} + k\,\langle \mathrm{d_t}\boldsymbol{m}_h^{i+1}, \boldsymbol{f}_h^{i+1/2} - \boldsymbol{f}^{i+1/2}\rangle_{\boldsymbol{L}^2(\omega)} \\
&\quad - k\,\langle \mathrm{d_t}\boldsymbol{f}^{i+1}, \boldsymbol{m}_h^{i+1/2}\rangle_{\boldsymbol{L}^2(\omega)} + k\,\langle \mathrm{d_t}\boldsymbol{m}_h^{i+1}, \boldsymbol{\Pi}_h^{\boldsymbol{\Theta}}(\boldsymbol{m}_h^{i+1}, \boldsymbol{m}_h^{i}, \boldsymbol{m}_h^{i-1})\rangle_{\boldsymbol{L}^2(\omega)}.
\end{aligned}
$$

We sum the latter equation over $i = 0, \dots, j-1$ and exploit the telescopic sum property. This yields that

$$
\begin{aligned}
&\mathcal{E}_{\mathrm{LLG}}(\boldsymbol{m}_h^{j}) + \alpha k \sum_{i=0}^{j-1} \|\,\mathrm{d_t}\boldsymbol{m}_h^{i+1}\|_h^2 + k \sum_{i=0}^{j-1} \langle \mathrm{d_t}\boldsymbol{f}^{i+1}, \boldsymbol{m}_h^{i+1/2}\rangle_{\boldsymbol{L}^2(\omega)} \\
&\quad - k \sum_{i=0}^{j-1} \langle \boldsymbol{\Pi}_h^{\boldsymbol{\Theta}}(\boldsymbol{m}_h^{i+1}, \boldsymbol{m}_h^{i}, \boldsymbol{m}_h^{i-1}), \mathrm{d_t}\boldsymbol{m}_h^{i+1}\rangle_{\boldsymbol{L}^2(\omega)} \\
&= \mathcal{E}_{\mathrm{LLG}}(\boldsymbol{m}_h^{0}) + k \sum_{i=0}^{j-1} \langle \mathrm{d_t}\boldsymbol{m}_h^{i+1}, \boldsymbol{\pi}_h^{\boldsymbol{\Theta}}(\boldsymbol{m}_h^{i+1}, \boldsymbol{m}_h^{i}, \boldsymbol{m}_h^{i-1}) - \boldsymbol{\pi}(\boldsymbol{m}_h^{i+1/2})\rangle_{\boldsymbol{L}^2(\omega)} \\
&\quad + k \sum_{i=0}^{j-1} \langle \mathrm{d_t}\boldsymbol{m}_h^{i+1}, \boldsymbol{f}_h^{i+1/2} - \boldsymbol{f}^{i+1/2}\rangle_{\boldsymbol{L}^2(\omega)}.
\end{aligned}
$$

Moreover, the norm equivalence relation $\|\cdot\|_{\boldsymbol{L}^2(\omega)} \le \|\cdot\|_h$ from Lemma 3.3.1(i) yields that

$$
\begin{aligned}
&\mathcal{E}_{\mathrm{LLG}}(\boldsymbol{m}_{hk}^{+}(\tau)) + \alpha \int_0^{t_j} \|\partial_t \boldsymbol{m}_{hk}\|_{\boldsymbol{L}^2(\omega)}^2 \,\mathrm{d}t + \int_0^{t_j} \langle \partial_t \boldsymbol{f}_k, \overline{\boldsymbol{m}}_{hk}\rangle_{\boldsymbol{L}^2(\omega)} \,\mathrm{d}t \\
&\quad - \int_0^{t_j} \langle \boldsymbol{\Pi}_h^{\boldsymbol{\Theta}}(\boldsymbol{m}_{hk}^{+}, \boldsymbol{m}_{hk}^{-}, \boldsymbol{m}_{hk}^{=}), \partial_t \boldsymbol{m}_{hk}\rangle_{\boldsymbol{L}^2(\omega)} \,\mathrm{d}t \\
&\le \mathcal{E}_{\mathrm{LLG}}(\boldsymbol{m}_h^{0}) + \int_0^{t_j} \langle \partial_t \boldsymbol{m}_{hk}, \boldsymbol{\pi}_h^{\boldsymbol{\Theta}}(\boldsymbol{m}_{hk}^{+}, \boldsymbol{m}_{hk}^{-}, \boldsymbol{m}_{hk}^{=}) - \boldsymbol{\pi}(\overline{\boldsymbol{m}}_{hk})\rangle_{\boldsymbol{L}^2(\omega)} \,\mathrm{d}t \\
&\quad + \int_0^{t_j} \langle \partial_t \boldsymbol{m}_{hk}, \overline{\boldsymbol{f}}_{hk} - \overline{\boldsymbol{f}}_{k}\rangle_{\boldsymbol{L}^2(\omega)} \,\mathrm{d}t\,. \qquad (6.26)
\end{aligned}
$$

Step 5. We conclude the proof with standard lower semi-continuity arguments: To this end, we require the strong consistencies **(D4$^+$)** and **(D7$^+$)** of $\boldsymbol{\pi}_h$ and $\boldsymbol{\Pi}_h$, respectively, for the convergence properties from Lemma 6.5.8, which yield that

$$\int_0^{t_j} \langle \partial_t \boldsymbol{m}_{hk}, \boldsymbol{\pi}_h^{\boldsymbol{\Theta}}(\boldsymbol{m}_{hk}^+, \boldsymbol{m}_{hk}^-, \boldsymbol{m}_{hk}^=) - \boldsymbol{\pi}(\overline{\boldsymbol{m}}_{hk}) \rangle_{\boldsymbol{L}^2(\omega)} \, \mathrm{d}t \to 0$$

$$\int_0^{t_j} \langle \boldsymbol{\Pi}_h^{\boldsymbol{\Theta}}(\boldsymbol{m}_{hk}^+, \boldsymbol{m}_{hk}^-, \boldsymbol{m}_{hk}^=), \partial_t \boldsymbol{m}_{hk} \rangle_{\boldsymbol{L}^2(\omega)} \, \mathrm{d}t \to \int_0^{\tau} \langle \boldsymbol{\Pi}(\boldsymbol{m}), \partial_t \boldsymbol{m} \rangle_{\boldsymbol{L}^2(\omega)} \, \mathrm{d}t$$

as $h, k \to 0$. Together with the consistency **(D5$^+$)** of $(\boldsymbol{f}_h^i)_{i=0}^M$, the right-hand side of (6.26) vanishes as $h, k \to 0$. Moreover, the no-concentration of Lebesgue functions yields that

$$\int_0^{t_j} \langle \partial_t \boldsymbol{f}_k, \overline{\boldsymbol{m}}_{hk} \rangle_{\boldsymbol{L}^2(\omega)} \, \mathrm{d}t \overset{\textbf{(D5}^+\textbf{)}}{\to} \int_0^{\tau} \langle \partial_t \boldsymbol{f}, \boldsymbol{m} \rangle_{\boldsymbol{L}^2(\omega)} \, \mathrm{d}t \quad \text{as } h, k \to 0.$$

Next, we get that

$$\mathcal{E}_{\mathrm{LLG}}(\boldsymbol{m}_h^0) \overset{\textbf{(D1}^+\textbf{)}}{\to} \mathcal{E}_{\mathrm{LLG}}(\boldsymbol{m}^0) \quad \text{as } h, k \to 0.$$

With the convergence properties from Lemma 6.5.5, and standard lower semi-continuity arguments, we get for arbitrary intervals $I \subset [0, T]$ that

$$\begin{aligned} &\int_I \left(\mathcal{E}_{\mathrm{LLG}}(\boldsymbol{m}(\tau)) \, + \, \alpha \int_0^{\tau} \|\partial_t \boldsymbol{m}\|_{\boldsymbol{L}^2(\omega)}^2 \, \mathrm{d}t \right) \mathrm{d}\tau \\ &\quad \le \liminf_{h,k \to 0} \int_I \left(\mathcal{E}_{\mathrm{LLG}}(\boldsymbol{m}_{hk}^+(\tau)) \, + \, \alpha \int_0^{\tau} \|\partial_t \boldsymbol{m}_{hk}\|_{\boldsymbol{L}^2(\omega)}^2 \, \mathrm{d}t \right) \mathrm{d}\tau \, . \end{aligned}$$

Altogether, we obtain that

$$\begin{aligned} &\int_I \left(\mathcal{E}_{\mathrm{LLG}}(\boldsymbol{m}(\tau)) \, + \, \alpha \int_0^{\tau} \|\partial_t \boldsymbol{m}\|_{\boldsymbol{L}^2(\omega)}^2 \, \mathrm{d}t \right) \mathrm{d}\tau \\ &\quad + \int_I \left(\int_0^{\tau} \langle \partial_t \boldsymbol{f}, \boldsymbol{m} \rangle_{\boldsymbol{L}^2(\omega)} \, \mathrm{d}t - \int_0^{\tau} \langle \boldsymbol{\Pi}(\boldsymbol{m}), \partial_t \boldsymbol{m} \rangle_{\boldsymbol{L}^2(\omega)} \, \mathrm{d}t \right) \mathrm{d}\tau \overset{(4.58)}{\le} \int_I \mathcal{E}_{\mathrm{LLG}}(\boldsymbol{m}^0) \, \mathrm{d}\tau \, . \end{aligned}$$

Since the interval $I \subset [0, T]$ was arbitrary, the latter estimate also holds pointwise a.e. in $(0, T)$. This concludes the proof. □

6.6. Fixed-point iteration

This section is based on the own work [PRS18, Section 5]. However, we present a few extensions. For the solution of the non-linear problem (6.2), we employ a fixed-point iteration, cf., e.g., [Bar06, BP06, BBP08, BPS09, Cim09, BPS12] for various adaptations and extension of the midpoint scheme. Here, we deal with the following aspects of this method:

- We extend the fixed-point iteration for the solution of the non-linear problem (6.2) and the corresponding convergence analysis to our extended setting of LLG (2.3), i.e., we also include lower-order terms. Our goal is an algorithm for one (inexact) time-step with our IMEX midpoint scheme; see Section 6.6.1. This section elaborates the own work [PRS18, Section 5].
- For given $\boldsymbol{\psi}_h \in \boldsymbol{\mathcal{S}}_h$, we state how to compute the discrete Laplacian $\Delta_h \boldsymbol{\psi}_h$ and the quasi-$\boldsymbol{L}^2$-projection $\boldsymbol{\mathcal{P}}_h \boldsymbol{\psi}_h$; see Section 6.6.2.
- We present a strategy for the solution of the linear variational problem at each fixed-point iteration on a linear algebra level. In particular, only nodewise 3×3 systems have to be solved; see Section 6.6.3.
- We collect the knowledge from the latter three points and formulate an efficient inexact midpoint scheme for the full time-stepping. Moreover, we prove convergence under the CFL-type condition $k = \mathbf{o}(h^2)$ towards a weak solution of LLG; see Section 6.6.4. This extends [PRS18, Theorem 15].

6.6.1. One inexact time-step

In this section, we consider one isolated time-step of our IMEX midpoint scheme in Algorithm 6.2.1 and formulate an algorithm, where the non-linear system (6.2) is solved inexactly by a fixed-point iteration. We prove well-definedness and —provided a CFL-type condition— also convergence of the fixed-point iteration.

First, we formulate our algorithm. While [BP06] seeks in the discrete variational formulation (6.2) the unknown $\boldsymbol{m}_h^{i+1}$, we proceed like in [Bar06, BBP08, BPS09, Cim09, BPS12] and, given $\boldsymbol{m}_h^i \in \boldsymbol{\mathcal{S}}_h$, seek the unknown

$$\boldsymbol{\mu}_h := \boldsymbol{m}_h^{i+1/2}.$$

To this end, we first rewrite (6.2): Since $\mathbf{a} \times \mathbf{a} = \mathbf{0}$ for vectors $\mathbf{a} \in \mathbb{R}^3$, we get that

$$\boldsymbol{m}_h^{i+1/2} \times \mathrm{d_t} \boldsymbol{m}_h^{i+1} = \frac{2}{k}\, \boldsymbol{\mu}_h \times (\boldsymbol{\mu}_h - \boldsymbol{m}_h^i) = -\frac{2}{k}\, \boldsymbol{\mu}_h \times \boldsymbol{m}_h^i. \tag{6.27}$$

We define the approximation to the effective field and the dissipative effects as functional

$$\begin{aligned} \boldsymbol{\mathcal{H}}_h^i(\boldsymbol{\mu}_h) := C_{\mathbf{ex}} \Delta_h \boldsymbol{\mu}_h + \boldsymbol{\mathcal{P}}_h \boldsymbol{\pi}_h^{\boldsymbol{\Theta}}(2\boldsymbol{\mu}_h - \boldsymbol{m}_h^i, \boldsymbol{m}_h^i, \boldsymbol{m}_h^{i-1}) \\ + \boldsymbol{\mathcal{P}}_h \boldsymbol{f}_h^{i+1/2} + \boldsymbol{\mathcal{P}}_h \boldsymbol{\Pi}_h^{\boldsymbol{\Theta}}(2\boldsymbol{\mu}_h - \boldsymbol{m}_h^i, \boldsymbol{m}_h^i, \boldsymbol{m}_h^{i-1}) \in \boldsymbol{\mathcal{S}}_h. \end{aligned} \tag{6.28a}$$

With the latter two equations, the discrete variational formulation (6.2) reads as follows: Find $\boldsymbol{\mu}_h \in \boldsymbol{\mathcal{S}}_h$ such that

$$\frac{2}{k}\, \langle \boldsymbol{\mu}_h, \boldsymbol{\varphi}_h \rangle_h + \langle \boldsymbol{\mu}_h \times \boldsymbol{\mathcal{H}}_h^i(\boldsymbol{\mu}_h), \boldsymbol{\varphi}_h \rangle_h + \frac{2\alpha}{k}\, \langle \boldsymbol{\mu}_h \times \boldsymbol{m}_h^i, \boldsymbol{\varphi}_h \rangle_h = \frac{2}{k}\, \langle \boldsymbol{m}_h^i, \boldsymbol{\varphi}_h \rangle_h \tag{6.28b}$$

for all $\boldsymbol{\varphi}_h \in \boldsymbol{\mathcal{S}}_h$. With these preparations and based on [PRS18, Algorithm 13], we formulate an algorithm, which —given the previous time-step $\boldsymbol{m}_h^i$ and based on the rewritten variational formulation (6.28)— performs one (inexact) time-step of our IMEX midpoint scheme.

Algorithm 6.6.1 (Inexact IMEX MPS, one time-step). **Input.** *Previous time-step* $\boldsymbol{m}_h^i \in \boldsymbol{\mathcal{S}}_h$*, initial guess* $\boldsymbol{\mu}_h^{(0)} := \boldsymbol{m}_h^i \in \boldsymbol{\mathcal{S}}_h$*, iteration tolerance* $\varepsilon > 0$*. Perform the steps* (a)–(c)*:*

(a) *Compute* $\boldsymbol{\mathcal{H}}_h^i(\boldsymbol{\mu}_h^{(0)}) \in \boldsymbol{\mathcal{S}}_h$*; see Section 6.6.2 for details.*

(b) **Loop.** *For* $\ell = 1, 2, \dots,$ *repeat the following steps* (b-i)–(b-ii) *until*

$$\|\boldsymbol{\mathcal{H}}_h^i(\boldsymbol{\mu}_h^{(\ell+1)}) - \boldsymbol{\mathcal{H}}_h^i(\boldsymbol{\mu}_h^{(\ell)})\|_h < \varepsilon : \tag{6.29}$$

(b-i) *Find* $\boldsymbol{\mu}_h^{(\ell+1)} \in \boldsymbol{\mathcal{S}}_h$ *such that*

$$\begin{aligned}\frac{2}{k}\,\langle \boldsymbol{\mu}_h^{(\ell+1)}, \boldsymbol{\varphi}_h\rangle_h + \langle \boldsymbol{\mu}_h^{(\ell+1)} \times \boldsymbol{\mathcal{H}}_h^i(\boldsymbol{\mu}_h^{(\ell)}), \boldsymbol{\varphi}_h\rangle_h + \frac{2\alpha}{k}\,\langle \boldsymbol{\mu}_h^{(\ell+1)} \times \boldsymbol{m}_h^i, \boldsymbol{\varphi}_h\rangle_h \\ = \frac{2}{k}\,\langle \boldsymbol{m}_h^i, \boldsymbol{\varphi}_h\rangle_h \quad \text{for all } \boldsymbol{\varphi}_h \in \boldsymbol{\mathcal{S}}_h;\end{aligned} \tag{6.30}$$

see Section 6.6.3 for details.

(b-ii) *Compute* $\boldsymbol{\mathcal{H}}_h^i(\boldsymbol{\mu}_h^{(\ell+1)}) \in \boldsymbol{\mathcal{S}}_h$*; see Section 6.6.2 for details.*

(c) *Set* $\boldsymbol{m}_h^{i+1} := 2\boldsymbol{\mu}_h^{(\ell+1)} - \boldsymbol{m}_h^i \in \boldsymbol{\mathcal{S}}_h$.

Output. *Approximation* $\boldsymbol{m}_h^{i+1} \approx \boldsymbol{m}(t_{i+1})$. □

The following proposition proves that the iteration in the latter algorithm is well-defined and states general beneficial properties of the iterates. Essentially, these findings are independent of the precise definition of $\boldsymbol{h}_{\mathrm{eff}}(\boldsymbol{m})$ and $\boldsymbol{\Pi}(\boldsymbol{m})$. Based on [PRS18, Remark 14(i)–(ii)], we collect and elaborate results from, e.g., [Bar06, BBP08, BPS09]. In particular, (ii) extends [Bar06, Theorem 3.1] to our setting of LLG (2.3).

Proposition 6.6.2 (Fixed point iterates, [PRS18, Remark 14(i)–(ii)]). *Consider the fixed-point iteration from Algorithm 6.6.1*(b)*. Then, the following two assertions* (i)–(ii) *hold true:*

(i) *The iterates* $(\boldsymbol{\mu}_h^{(\ell)})_{\ell=0}^{\infty} \in \boldsymbol{\mathcal{S}}_h$ *are uniquely defined. It holds that*

$$\|\boldsymbol{\mu}_h^{(\ell)}\|_{\boldsymbol{L}^\infty(\omega)} \le \|\boldsymbol{m}_h^i\|_{\boldsymbol{L}^\infty(\omega)} \quad \text{for all } \ell \in \mathbb{N}_0.$$

(ii) *For all* $\ell \in \mathbb{N}$*, the update* $\boldsymbol{m}_h^{i+1} := 2\boldsymbol{\mu}_h^{\ell+1} - \boldsymbol{m}_h^i \in \boldsymbol{\mathcal{S}}_h$ *satisfies the perturbed discrete variational formulation*

$$\begin{aligned}\langle \mathrm{d_t}\boldsymbol{m}_h^{i+1}, \boldsymbol{\varphi}_h\rangle_h = -\langle \boldsymbol{m}_h^{i+1/2} \times \boldsymbol{\mathcal{H}}_h^i(\boldsymbol{m}_h^{i+1/2}), \boldsymbol{\varphi}_h\rangle_h + \alpha\langle \boldsymbol{m}_h^{i+1/2} \times \mathrm{d_t}\boldsymbol{m}_h^{i+1}, \boldsymbol{\varphi}_h\rangle_h \\ + \langle \boldsymbol{m}_h^{i+1/2} \times \boldsymbol{r}_h^{\ell}, \boldsymbol{\varphi}_h\rangle_h \quad \text{for all } \boldsymbol{\varphi}_h \in \boldsymbol{\mathcal{S}}_h,\end{aligned} \tag{6.31}$$

where $\boldsymbol{r}_h^{(\ell)} := \boldsymbol{\mathcal{H}}_h^i(\boldsymbol{\mu}_h^{(\ell+1)}) - \boldsymbol{\mathcal{H}}_h^i(\boldsymbol{\mu}_h^{(\ell)}) \in \boldsymbol{\mathcal{S}}_h$*. The update* $\boldsymbol{m}_h^{i+1}$ *satisfies*

$$|\boldsymbol{m}_h^{i+1}(\boldsymbol{z})| = |\boldsymbol{m}_h^i(\boldsymbol{z})| \quad \text{for all nodes } \boldsymbol{z} \in \mathcal{N}_h,$$

and, in particular, $\|\boldsymbol{m}_h^{i+1}\|_h = \|\boldsymbol{m}_h^i\|_h$ *as well as* $\|\boldsymbol{m}_h^{i+1}\|_{\boldsymbol{L}^\infty(\omega)} = \|\boldsymbol{m}_h^i\|_{\boldsymbol{L}^\infty(\omega)}$.

Proof. For the proof of (i), we follow, e.g., [BPS09, Lemma 6.1]. Given an iteration $\boldsymbol{\mu}_h^{(\ell)} \in \boldsymbol{\mathcal{S}}_h$, we define for $\boldsymbol{\psi}_h, \boldsymbol{\varphi}_h \in \boldsymbol{\mathcal{S}}_h$ the bilinear form

$$\boldsymbol{B}^{(\ell)}(\boldsymbol{\psi}_h, \boldsymbol{\varphi}_h) := \frac{2}{k}\langle \boldsymbol{\psi}_h, \boldsymbol{\varphi}_h \rangle_h + \langle \boldsymbol{\psi}_h \times \boldsymbol{\mathcal{H}}_h^i(\boldsymbol{\mu}_h^{(\ell)}), \boldsymbol{\varphi}_h \rangle_h + \frac{2\alpha}{k}\langle \boldsymbol{\psi}_h \times \boldsymbol{m}_h^i, \boldsymbol{\varphi}_h \rangle_h. \tag{6.32a}$$

With this definition, $\boldsymbol{\mu}_h^{(\ell+1)} \in \boldsymbol{\mathcal{S}}_h$ is uniquely defined by

$$\boldsymbol{B}^{(\ell)}(\boldsymbol{\mu}_h^{(\ell+1)}, \boldsymbol{\varphi}_h) \overset{(6.30)}{=} \frac{2}{k}\langle \boldsymbol{m}_h^i, \boldsymbol{\varphi}_h \rangle_h \quad \text{for all } \boldsymbol{\varphi}_h \in \boldsymbol{\mathcal{S}}_h. \tag{6.32b}$$

For all approaches **(A1)**–**(A3)**, we infer from $(\mathbf{a} \times \mathbf{b}) \times \mathbf{a} = \mathbf{0}$ for $\mathbf{a}, \mathbf{b} \in \mathbb{R}^3$ that

$$\boldsymbol{B}^{(\ell)}(\boldsymbol{\psi}_h, \boldsymbol{\psi}_h) = \frac{2}{k}\,\|\boldsymbol{\psi}_h\|_h^2 \quad \text{for all } \boldsymbol{\psi}_h \in \boldsymbol{\mathcal{S}}_h,$$

i.e., $\boldsymbol{B}^{(\ell)}(\cdot,\cdot)$ is elliptic with respect to $\|\cdot\|_h$. Hence, the Lax–Milgram theorem (see Theorem B.2.4) proves existence and uniqueness of the iterate $\boldsymbol{\mu}_h^{(\ell+1)} \in \boldsymbol{\mathcal{S}}_h$. Thus, the sequence $(\boldsymbol{\mu}_h^{(\ell)})_{\ell=0}^{\infty} \in \boldsymbol{\mathcal{S}}_h$ is uniquely defined. To show the boundedness statement, let $\boldsymbol{z} \in \mathcal{N}_h$ and denote with $\phi_{\boldsymbol{z}}$ the associated nodal basis function. Then, we test (6.32) with $\boldsymbol{\varphi}_h := \boldsymbol{\mu}_h^{(\ell+1)}(\boldsymbol{z})\,\phi_{\boldsymbol{z}} \in \boldsymbol{\mathcal{S}}_h$. Recalling that $(\mathbf{a} \times \mathbf{b}) \cdot \mathbf{a} = \mathbf{0}$ for all vectors $\mathbf{a}, \mathbf{b} \in \mathbb{R}^3$, the nodewise definition (3.10) of the approximate $\boldsymbol{L}^2$-product $\langle \cdot, \cdot \rangle_h$ cancels out the last two terms in (6.32a), and we obtain that

$$\frac{2}{k}\,|\boldsymbol{\mu}_h^{(\ell+1)}(\boldsymbol{z})|^2 \overset{(6.32)}{=} \frac{2}{k}\,\boldsymbol{m}_h^i(\boldsymbol{z}) \cdot \boldsymbol{\mu}_h^{(\ell+1)}(\boldsymbol{z}) \leq \frac{2}{k}\,|\boldsymbol{m}_h^i(\boldsymbol{z})|\,|\boldsymbol{\mu}_h^{(\ell+1)}(\boldsymbol{z})| \quad \text{for all nodes } \boldsymbol{z} \in \mathcal{N}_h.$$

Since functions in $\boldsymbol{\mathcal{S}}_h$ attain their maximal modulus at some node, this proves (i).

For the proof of (ii), we fix $\ell \in \mathbb{N}$ and write $\boldsymbol{m}_h^{i+1} := 2\boldsymbol{\mu}_h^{(\ell+1)} - \boldsymbol{m}_h^i$. From the definitions (3.2) of the mean-value and the discrete time-derivative, this yields that

$$\boldsymbol{\mu}_h^{(\ell+1)} = \boldsymbol{m}_h^{i+1/2} \quad \text{and} \quad \mathrm{d}_t \boldsymbol{m}_h^{i+1} = 2\,(\,\boldsymbol{\mu}_h^{(\ell+1)} - \boldsymbol{m}_h^i\,).$$

The perturbed variational formulation (6.31) is a direct consequence of (6.30) and (6.27). Finally, thinking of $\boldsymbol{r}_h^{(\ell)} \in \boldsymbol{\mathcal{S}}_h$ as an additional contribution to $\boldsymbol{\mathcal{H}}_h^i(\boldsymbol{m}_h^{i+1/2})$, we infer the nodewise modulus equality in the same way as in Proposition 6.5.3 for the (exactly solved) IMEX midpoint scheme. Altogether, this concludes the proof. □

Finally, we deal with the convergence of the iteration in Algorithm 6.6.1(b) and extend the convergence result of, e.g., [Bar06, BBP08, BPS09], and additionally cover lower-order terms.

Proposition 6.6.3 (Convergence of fixed-point iteration). *Consider the fixed-point iteration from Algorithm 6.6.1*(b). *Suppose linearity* **(D2)** *and boundedness* **(D3)** *for* $\boldsymbol{\pi}_h$ *as well as the Lipschitz-type condition* **(M2)** *for* $\boldsymbol{\Pi}_h$. *Then, the following two assertions* (i)–(ii) *hold true for all approaches* **(A1)**–**(A3)** *for* $\boldsymbol{\pi}_h^{\boldsymbol{\Theta}}$ *and* $\boldsymbol{\Pi}_h^{\boldsymbol{\Theta}}$.

(i) *There exists a constant $C > 0$, which depends only on $C_{\mathbf{ex}}$, $C_{\mathbf{mesh}}$, $\boldsymbol{\pi}(\cdot)$, and $\boldsymbol{\Pi}(\cdot)$ such that, for all $h, k > 0$, which satisfy the CFL-type condition*

$$\big(1 + \|\boldsymbol{m}_h^i\|^2_{\boldsymbol{L}^\infty(\omega)}\big)\, k\, h^{-2} \, < \, C, \tag{6.33}$$

the sequence of iterates $(\boldsymbol{\mu}_h^{(\ell)})_{\ell=0}^\infty$ is a contraction in $\boldsymbol{L}^2(\omega)$. Then, there exists a unique $\boldsymbol{\mu}_h \in \boldsymbol{\mathcal{S}}_h$ such that

$$\boldsymbol{\mu}_h^{(\ell)} \to \boldsymbol{\mu}_h \quad \text{in } \boldsymbol{L}^2(\omega) \quad \text{as } \ell \to \infty.$$

In particular, $\boldsymbol{\mu}_h$ and $\boldsymbol{m}_h^{i+1} := 2\boldsymbol{\mu}_h - \boldsymbol{m}_h^i$ are unique solutions of the discrete variational formulation (6.28) *and* (6.2)*, respectively.*

(ii) *Under the CFL-type condition* (6.33)*, the stopping criterion* (6.29) *is met after finitely many iterations.*

Remark 6.6.4. (i) *The appearance of $\|\boldsymbol{m}_h^i\|_{\boldsymbol{L}^\infty(\omega)}$ in the CFL-type condition* (6.33) *reflects that $\boldsymbol{m}_h^i$ is the input for one time-step in Algorithm 6.6.1. However, this is not a restriction for the full time-stepping: With Proposition 6.6.2*(ii)*, uniform boundedness* **(M1)** *of $\boldsymbol{m}_h^0$ yields that*

$$\|\boldsymbol{m}_h^i\|_{\boldsymbol{L}^\infty(\omega)} = \|\boldsymbol{m}_h^0\|_{\boldsymbol{L}^\infty(\omega)} \lesssim 1 \quad \text{for all } i = 0, \dots, M.$$

In particular, the latter holds regardless of the indices at which the subsequent iterations are stopped.

(ii) *In contrast to the stopping criterion* (6.29) *in Algorithm 6.6.1 and, e.g., [Bar06, BBP08], the works [BP06, BPS09, BPS12] employ the stropping criterion*

$$\|\boldsymbol{\mu}_h^{(\ell+1)} - \boldsymbol{\mu}_h^{(\ell)}\|_h < \varepsilon. \tag{6.34}$$

Together with the assumption **(M1)***, Lemma 6.6.5 below yields that*

$$\begin{aligned} \|\boldsymbol{\mathcal{H}}_h^i(\boldsymbol{\mu}_h^{(\ell+1)}) - \boldsymbol{\mathcal{H}}_h^i(\boldsymbol{\mu}_h^{(\ell)})\|_h &\lesssim h^{-2}\,(1 + \|\boldsymbol{m}_h^i\|^2_{\boldsymbol{L}^\infty(\omega)})\, \|\boldsymbol{\mu}_h^{(\ell+1)} - \boldsymbol{\mu}_h^{(\ell)}\|_h \\ &\overset{\text{(i)}}{=} h^{-2}\,(1 + \|\boldsymbol{m}_h^0\|^2_{\boldsymbol{L}^\infty(\omega)})\, \|\boldsymbol{\mu}_h^{(\ell+1)} - \boldsymbol{\mu}_h^{(\ell)}\|_h \overset{\textbf{(M1)}}{\lesssim} h^{-2}\, \|\boldsymbol{\mu}_h^{(\ell+1)} - \boldsymbol{\mu}_h^{(\ell)}\|_h. \end{aligned}$$

Hence, the stopping criterion (6.29) *generally yields less iterations than that in* (6.34)*.*

(iii) *For the explicit approaches* **(A2)** *for $i > 0$ and* **(A3)***, the $\boldsymbol{\pi}_h^{\boldsymbol{\Theta}}$ and $\boldsymbol{\Pi}_h^{\boldsymbol{\Theta}}$-contributions do not depend on $\boldsymbol{\mu}_h$. In this case, we obtain already from the boundedness statement for Δ_h from Lemma 3.3.2 and $\|\cdot\|_{\boldsymbol{L}^2(\omega)} \simeq \|\cdot\|_h$ from Lemma 3.3.1*(i) *that*

$$\begin{aligned} \|\boldsymbol{\mathcal{H}}_h^i(\boldsymbol{\varphi}_h) - \boldsymbol{\mathcal{H}}_h^i(\boldsymbol{\psi}_h)\|_h &\overset{(6.28a)}{=} \|C_{\mathbf{ex}}\,\Delta_h\boldsymbol{\varphi}_h - C_{\mathbf{ex}}\,\Delta_h\boldsymbol{\psi}_h\|_h \\ &\lesssim h^{-2}\,\|\boldsymbol{\varphi}_h - \boldsymbol{\psi}_h\|_{\boldsymbol{L}^2(\omega)} \lesssim h^{-2}\,\|\boldsymbol{\varphi}_h - \boldsymbol{\psi}_h\|_h, \end{aligned}$$

and the statement of Proposition 6.6.3 is valid without the assumptions to $\boldsymbol{\pi}_h$ and $\boldsymbol{\Pi}_h$.

We postpone the proof of Proposition 6.6.3 to the end of this section. In the following auxiliary Lemma 6.6.5, we establish a Lipschitz-type condition for $\boldsymbol{\mathcal{H}}_h^i(\cdot)$.

Lemma 6.6.5 (Lipschitz continuity of $\boldsymbol{\mathcal{H}}_h^i(\cdot)$)**.** *Consider the approximate effective field and dissipative effects $\boldsymbol{\mathcal{H}}_h^i(\cdot)$ from (6.28a) defined by any approach* **(A1)**–**(A3)** *for $\boldsymbol{\pi}_h^{\boldsymbol{\Theta}}$ and $\boldsymbol{\Pi}_h^{\boldsymbol{\Theta}}$. Suppose linearity* **(D2)** *and boundedness* **(D3)** *for $\boldsymbol{\pi}_h$ as well as the Lipschitz-type condition* **(M2)** *for $\boldsymbol{\Pi}_h$. Then, there exists a constant $C > 0$, which depends only on $C_{\mathbf{ex}}$, $C_{\mathbf{mesh}}$, $\boldsymbol{\pi}(\cdot)$, and $\boldsymbol{\Pi}(\cdot)$ such that*

$$\|\boldsymbol{\mathcal{H}}_h^i(\boldsymbol{\varphi}_h) - \boldsymbol{\mathcal{H}}_h^i(\boldsymbol{\psi}_h)\|_h \leq C\, h^{-2} \left[1 + \|\boldsymbol{\varphi}_h\|_{\boldsymbol{L}^\infty(\omega)} + \|\boldsymbol{\psi}_h\|_{\boldsymbol{L}^\infty(\omega)} \right] \|\boldsymbol{\varphi}_h - \boldsymbol{\psi}_h\|_h$$

for all $\boldsymbol{\varphi}_h, \boldsymbol{\psi}_h \in \boldsymbol{\mathcal{S}}_h$.

Proof. For $\boldsymbol{\varphi}_h, \boldsymbol{\psi}_h \in \boldsymbol{\mathcal{S}}_h$, it holds that

$$\begin{aligned}
&\|\boldsymbol{\mathcal{H}}_h^i(\boldsymbol{\varphi}_h) - \boldsymbol{\mathcal{H}}_h^i(\boldsymbol{\psi}_h)\|_h \\
&\overset{(6.28a)}{\lesssim} \|\Delta_h \boldsymbol{\varphi}_h - \Delta_h \boldsymbol{\psi}_h\|_h + \|\boldsymbol{\mathcal{P}}_h \boldsymbol{\pi}_h^{\boldsymbol{\Theta}}(2\boldsymbol{\varphi}_h - \boldsymbol{m}_h^i, \boldsymbol{m}_h^i, \boldsymbol{m}_h^{i-1}) - \boldsymbol{\mathcal{P}}_h \boldsymbol{\pi}_h^{\boldsymbol{\Theta}}(2\boldsymbol{\psi}_h - \boldsymbol{m}_h^i, \boldsymbol{m}_h^i, \boldsymbol{m}_h^{i-1})\|_h \\
&\quad + \|\boldsymbol{\mathcal{P}}_h \boldsymbol{\Pi}_h^{\boldsymbol{\Theta}}(2\boldsymbol{\varphi}_h - \boldsymbol{m}_h^i, \boldsymbol{m}_h^i, \boldsymbol{m}_h^{i-1}) - \boldsymbol{\mathcal{P}}_h \boldsymbol{\Pi}_h^{\boldsymbol{\Theta}}(2\boldsymbol{\psi}_h - \boldsymbol{m}_h^i, \boldsymbol{m}_h^i, \boldsymbol{m}_h^{i-1})\|_h.
\end{aligned}$$

For the explicit approaches **(A2)** with $i > 0$ and **(A3)**, the general time-stepping approaches $\boldsymbol{\pi}_h^{\boldsymbol{\Theta}}$ and $\boldsymbol{\Pi}_h^{\boldsymbol{\Theta}}$ depend only on $\boldsymbol{m}_h^i$ and $\boldsymbol{m}_h^{i-1}$. Hence, the last two terms in the latter estimate vanish in this case. For the implicit approaches **(A1)** and **(A2)** with $i = 0$, we obtain that

$$\boldsymbol{\pi}_h^{\boldsymbol{\Theta}}(2\boldsymbol{\varphi}_h - \boldsymbol{m}_h^i, \boldsymbol{m}_h^i, \boldsymbol{m}_h^{i-1}) = \boldsymbol{\pi}_h(\boldsymbol{\varphi}_h) \quad \text{as well as} \quad \boldsymbol{\Pi}_h^{\boldsymbol{\Theta}}(2\boldsymbol{\psi}_h - \boldsymbol{m}_h^i, \boldsymbol{m}_h^i, \boldsymbol{m}_h^{i-1}) = \boldsymbol{\Pi}_h(\boldsymbol{\psi}_h).$$

We thus obtain for all approaches **(A1)**–**(A3)** that

$$\begin{aligned}
\|\boldsymbol{\mathcal{H}}_h^i(\boldsymbol{\varphi}_h) - \boldsymbol{\mathcal{H}}_h^i(\boldsymbol{\psi}_h)\|_h &\lesssim \|\Delta_h \boldsymbol{\varphi}_h - \Delta_h \boldsymbol{\psi}_h\|_h + \|\boldsymbol{\mathcal{P}}_h \boldsymbol{\pi}_h(\boldsymbol{\varphi}_h) - \boldsymbol{\mathcal{P}}_h \boldsymbol{\pi}_h(\boldsymbol{\psi}_h)\|_h \\
&\quad + \|\boldsymbol{\mathcal{P}}_h \boldsymbol{\Pi}_h(\boldsymbol{\varphi}_h) - \boldsymbol{\mathcal{P}}_h \boldsymbol{\Pi}_h(\boldsymbol{\psi}_h)\|_h.
\end{aligned}$$

With the boundedness statement for Δ_h from Lemma 3.3.2, we estimate that

$$\|\Delta_h \boldsymbol{\varphi}_h - \Delta_h \boldsymbol{\psi}_h\|_h = \|\Delta_h(\boldsymbol{\varphi}_h - \boldsymbol{\psi}_h)\|_h \lesssim h^{-2} \|\boldsymbol{\varphi}_h - \boldsymbol{\psi}_h\|_{\boldsymbol{L}^2(\omega)}.$$

With the boundedness statement for $\boldsymbol{\mathcal{P}}_h$ from Lemma 3.3.3, we estimate that

$$\|\boldsymbol{\mathcal{P}}_h \boldsymbol{\pi}_h(\boldsymbol{\varphi}_h) - \boldsymbol{\mathcal{P}}_h \boldsymbol{\pi}_h(\boldsymbol{\psi}_h)\|_h \overset{\textbf{(D2)}}{\lesssim} \|\boldsymbol{\pi}_h\big(\boldsymbol{\varphi}_h - \boldsymbol{\psi}_h \big)\|_{\boldsymbol{L}^2(\omega)} \overset{\textbf{(D3)}}{\lesssim} \|\boldsymbol{\varphi}_h - \boldsymbol{\psi}_h\|_{\boldsymbol{L}^2(\omega)},$$

as well as

$$\begin{aligned}
\|\boldsymbol{\mathcal{P}}_h \boldsymbol{\Pi}_h(\boldsymbol{\varphi}_h) - \boldsymbol{\mathcal{P}}_h \boldsymbol{\Pi}_h(\boldsymbol{\psi}_h)\|_h &\lesssim \|\boldsymbol{\Pi}_h(\boldsymbol{\varphi}_h) - \boldsymbol{\Pi}_h(\boldsymbol{\psi}_h)\|_{\boldsymbol{L}^2(\omega)} \\
&\overset{\textbf{(M2)}}{\lesssim} h^{-1} \left[1 + \|\boldsymbol{\varphi}_h\|_{\boldsymbol{L}^\infty(\omega)} + \|\boldsymbol{\psi}_h\|_{\boldsymbol{L}^\infty(\omega)} \right] \|\boldsymbol{\varphi}_h - \boldsymbol{\psi}_h\|_{\boldsymbol{L}^2(\omega)}.
\end{aligned}$$

Together with $\|\cdot\|_{\boldsymbol{L}^2(\omega)} \simeq \|\cdot\|_h$ from Lemma 3.3.1(i), the combination of the latter three equations concludes the proof. □

We have everything together for the proof of Proposition 6.6.3.

Proof of Proposition 6.6.3. We adapt the corresponding technique of, e.g., [BPS09, Lemma 6.1] to our setting:

To prove (i), we estimate $\|\boldsymbol{\mu}_h^{(\ell+1)} - \boldsymbol{\mu}_h^{(\ell)}\|_h$. For all $\ell \in \mathbb{N}$, we get that

$$\begin{aligned}
\frac{2}{k}\,\langle \boldsymbol{\mu}_h^{(\ell+1)} - \boldsymbol{\mu}_h^{(\ell)}, \boldsymbol{\varphi}_h\rangle_h \overset{(6.30)}{=} & -\langle \boldsymbol{\mu}_h^{(\ell+1)} \times \boldsymbol{\mathcal{H}}_h^i(\boldsymbol{\mu}_h^{(\ell)}) - \boldsymbol{\mu}_h^{(\ell)} \times \boldsymbol{\mathcal{H}}_h^i(\boldsymbol{\mu}_h^{(\ell-1)}), \boldsymbol{\varphi}_h\rangle_h \\
& - \frac{2\alpha}{k}\,\langle(\boldsymbol{\mu}_h^{(\ell+1)} - \boldsymbol{\mu}_h^{(\ell)}) \times \boldsymbol{m}_h^i, \boldsymbol{\varphi}_h\rangle_h \\
= & -\langle \boldsymbol{\mu}_h^{(\ell+1)} \times \big[\,\boldsymbol{\mathcal{H}}_h^i(\boldsymbol{\mu}_h^{(\ell)}) - \boldsymbol{\mathcal{H}}_h^i(\boldsymbol{\mu}_h^{(\ell-1)})\,\big], \boldsymbol{\varphi}_h\rangle_h \\
& - \langle(\boldsymbol{\mu}_h^{(\ell+1)} - \boldsymbol{\mu}_h^{(\ell)}) \times \boldsymbol{\mathcal{H}}_h^i(\boldsymbol{\mu}_h^{(\ell-1)}), \boldsymbol{\varphi}_h\rangle_h \\
& - \frac{2\alpha}{k}\,\langle(\boldsymbol{\mu}_h^{(\ell+1)} - \boldsymbol{\mu}_h^{(\ell)}) \times \boldsymbol{m}_h^i, \boldsymbol{\varphi}_h\rangle_h \quad \text{for all } \boldsymbol{\varphi}_h \in \boldsymbol{\mathcal{S}}_h.
\end{aligned}$$

We test the latter equation with $\boldsymbol{\varphi}_h := \boldsymbol{\mu}_h^{(\ell+1)} - \boldsymbol{\mu}_h^{(\ell)} \in \boldsymbol{\mathcal{S}}_h$. Since $(\mathbf{a}\times\mathbf{b})\cdot\mathbf{a} = \mathbf{0}$ for vectors $\mathbf{a}, \mathbf{b} \in \mathbb{R}^3$, we obtain that

$$\begin{aligned}
\frac{2}{k}\,\|\boldsymbol{\mu}_h^{(\ell+1)} - \boldsymbol{\mu}_h^{(\ell)}\|_h^2 &= -\langle \boldsymbol{\mu}_h^{(\ell+1)} \times \big[\,\boldsymbol{\mathcal{H}}_h^i(\boldsymbol{\mu}_h^{(\ell)}) - \boldsymbol{\mathcal{H}}_h^i(\boldsymbol{\mu}_h^{(\ell-1)})\,\big], \boldsymbol{\mu}_h^{(\ell+1)} - \boldsymbol{\mu}_h^{(\ell)}\rangle_h \\
&\le \|\boldsymbol{\mu}_h^{(\ell+1)}\|_{\boldsymbol{L}^\infty(\omega)}\,\|\boldsymbol{\mathcal{H}}_h^i(\boldsymbol{\mu}_h^{(\ell)}) - \boldsymbol{\mathcal{H}}_h^i(\boldsymbol{\mu}_h^{(\ell-1)})\|_h\,\|\boldsymbol{\mu}_h^{(\ell+1)} - \boldsymbol{\mu}_h^{(\ell)}\|_h
\end{aligned}$$

for all $\ell \in \mathbb{N}$. Recall the modulus estimate

$$\|\boldsymbol{\mu}_h^{(\ell)}\|_{\boldsymbol{L}^\infty(\omega)} \;\le\; \|\boldsymbol{m}_h^i\|_{\boldsymbol{L}^\infty(\omega)} \quad \text{for all } \ell \in \mathbb{N} \tag{6.35}$$

of the iterates from Proposition 6.6.2(i). With the assumptions to $\boldsymbol{\pi}_h$ and $\boldsymbol{\Pi}_h$, we obtain from Lemma 6.6.5 that

$$\begin{aligned}
\|\boldsymbol{\mathcal{H}}_h^i(\boldsymbol{\mu}_h^{(\ell)}) - \boldsymbol{\mathcal{H}}_h^i(\boldsymbol{\mu}_h^{(\ell-1)})\|_h &\lesssim h^{-2}\,\big[\,1 + \|\boldsymbol{\mu}_h^{(\ell)}\|_{\boldsymbol{L}^\infty(\omega)} + \|\boldsymbol{\mu}_h^{(\ell-1)}\|_{\boldsymbol{L}^\infty(\omega)}\,\big]\,\|\boldsymbol{\mu}_h^{(\ell)} - \boldsymbol{\mu}_h^{(\ell-1)}\|_h \\
&\overset{(6.35)}{\lesssim} h^{-2}\,\big[\,1 + \|\boldsymbol{m}_h^i\|_{\boldsymbol{L}^\infty(\omega)}\,\big]\,\|\boldsymbol{\mu}_h^{(\ell)} - \boldsymbol{\mu}_h^{(\ell-1)}\|_h.
\end{aligned}$$

The combination of the latter three equations yields that

$$\begin{aligned}
\|\boldsymbol{\mu}_h^{(\ell+1)} - \boldsymbol{\mu}_h^{(\ell)}\|_h &\lesssim kh^{-2}\,\|\boldsymbol{m}_h^i\|_{\boldsymbol{L}^\infty(\omega)}\big[\,1 + \|\boldsymbol{m}_h^i\|_{\boldsymbol{L}^\infty(\omega)}\,\big]\,\|\boldsymbol{\mu}_h^{(\ell)} - \boldsymbol{\mu}_h^{(\ell-1)}\|_h \\
&\lesssim kh^{-2}\,\big[\,1 + \|\boldsymbol{m}_h^i\|_{\boldsymbol{L}^\infty(\omega)}^2\,\big]\,\|\boldsymbol{\mu}_h^{(\ell)} - \boldsymbol{\mu}_h^{(\ell-1)}\|_h \quad \text{for all } \ell \in \mathbb{N}.
\end{aligned}$$

Under the assumption (6.33), the sequence $(\boldsymbol{\mu}_h^{(\ell)})_{\ell=0}^\infty$ is thus a contraction. With the Banach fixed-point theorem (see Theorem B.2.6), this concludes the proof of (i). Finally, (ii) is a direct consequence of (i) and the latter estimate. □

6.6.2. Evaluation of Δ_h and $\mathcal{P}_h$

In this section, we discuss, how to evaluate, for given $\boldsymbol{\psi}_h \in \boldsymbol{\mathcal{S}}_h$, the discrete Laplacian $\Delta_h \boldsymbol{\psi}_h$ and the quasi-$\boldsymbol{L}^2$ projection $\boldsymbol{\mathcal{P}}_h \boldsymbol{\psi}_h$. To this end, let $\varphi_j \in V_h$ be the nodal hat function associated with $\boldsymbol{z}_j$, i.e., $\varphi_j(\boldsymbol{z}_k) = \delta_{jk}$ with Kronecker's delta. As basis of $\boldsymbol{\mathcal{S}}_h$, we employ

$$\boldsymbol{\phi}_{3(j-1)+\ell} := \varphi_j \, \boldsymbol{e}_\ell \quad \text{for all } j = 1, \dots, N \text{ and all } \ell = 1, 2, 3,$$

i.e., for fixed $j \in \{1, \dots, N\}$ the three consecutive basis vectors obtained from $\ell \in \{1, 2, 3\}$ in the latter definition belong to the node $\boldsymbol{z}_j$. Moreover, we define the well-known mass-matrix and stiffness-matrix $\mathbf{M} \in \mathbb{R}^{3N \times 3N}$ and $\mathbf{L} \in \mathbb{R}^{3N \times 3N}$ via

$$\mathbf{M}_{jk} := \langle \boldsymbol{\phi}_j, \boldsymbol{\phi}_k \rangle_{\boldsymbol{L}^2(\omega)} \quad \text{and} \quad \mathbf{L}_{jk} := \langle \nabla \boldsymbol{\phi}_j, \nabla \boldsymbol{\phi}_k \rangle_{\boldsymbol{L}^2(\omega)} \quad \text{for all} \quad j, k \in \{1, \dots, 3N\}. \tag{6.36}$$

Clearly, $\mathbf{M}$ is symmetric and positive definite and $\mathbf{L}$ is symmetric and positive semi-definite. Finally, we define the mass-lumped mass-matrix $\mathbf{M}_h \in \mathbb{R}^{3N \times 3N}$ via

$$\big[\, \mathbf{M}_h \,\big]_{jk} := \langle \boldsymbol{\phi}_j, \boldsymbol{\phi}_k \rangle_h \quad \text{for all} \quad j, k \in \{1, \dots, 3N\}.$$

Note that $\mathbf{M}_h$ is diagonal and positive definite. With the latter notation, we can formulate the following proposition.

Proposition 6.6.6 (Evaluation of Δ_h and $\boldsymbol{\mathcal{P}}_h$)**.** *Let $\boldsymbol{\psi}_h \in \boldsymbol{\mathcal{S}}_h$ and $\mathbf{y}, \mathbf{y}_\Delta, \mathbf{y}_\mathcal{P} \in \mathbb{R}^{3N}$ such that*

$$\boldsymbol{\psi}_h = \sum_{j=0}^{3N} \mathbf{y}_j \boldsymbol{\phi}_j, \quad \Delta_h \boldsymbol{\psi}_h = \sum_{j=0}^{3N} (\mathbf{y}_\Delta)_j \boldsymbol{\phi}_j, \quad \text{and} \quad \boldsymbol{\mathcal{P}}_h \boldsymbol{\psi}_h = \sum_{j=0}^{3N} (\mathbf{y}_\mathcal{P})_j \boldsymbol{\phi}_j.$$

Then, it holds that

$$\mathbf{y}_\Delta = -(\mathbf{M}_h)^{-1} \, \mathbf{L} \, \mathbf{y} \quad \text{and} \quad \mathbf{y}_\mathcal{P} = (\mathbf{M}_h)^{-1} \, \mathbf{M} \, \mathbf{y}. \tag{6.37}$$

Moreover, the approximate $\boldsymbol{L}^2$-scalar product $\langle \cdot, \cdot \rangle_h$ gives rise to a diagonal mass matrix $\mathbf{M}_h$. In particular, its inverse $(\mathbf{M}_h)^{-1}$ can be evaluated exactly at linear cost $\mathcal{O}(N)$.

Proof. The assertion is a direct consequence of the definition (3.11) of the discrete Laplacian Δ_h, the definition (3.12) of the quasi-$\boldsymbol{L}^2$ projection $\boldsymbol{\mathcal{P}}_h$, and of the definition (3.10) of the approximate $\boldsymbol{L}^2$-scalar product $\langle \cdot, \cdot \rangle_h$. □

6.6.3. Nodewise systems

In this section, we simplify Algorithm 6.6.1. Essentially, we can compute the fixed-point iterate with the parallel solution of nodewise 3×3 systems. This is a direct consequence of the following proposition, which requires the following standard notation: For given $\mathbf{a} \in \mathbb{R}^3$, we define the matrix

$$\big[\, \mathbf{a} \,\big]_\times := \begin{pmatrix} 0 & -\mathbf{a}_3 & \mathbf{a}_2 \\ \mathbf{a}_3 & 0 & -\mathbf{a}_1 \\ -\mathbf{a}_2 & \mathbf{a}_1 & 0 \end{pmatrix} \in \mathbb{R}^{3 \times 3}. \tag{6.38}$$

We note that $\big[\mathbf{a}\big]_\times$ is skew-symmetric satisfies that

$$\big[\,\mathbf{a}\,\big]_\times \mathbf{b} = \mathbf{a} \times \mathbf{b} \quad \text{for all vectors } \mathbf{a}, \mathbf{b} \in \mathbb{R}^3. \tag{6.39}$$

Proposition 6.6.7 (Nodewise systems)**.** *Consider the fixed-point iteration from Algorithm 6.6.1*(b)*. Let $\ell \in \mathbb{N}$ and suppose that $\boldsymbol{\mu}_h^\ell$ as well as $\boldsymbol{m}_h^i$ are known. Then, the nodewise defined matrices*

$$\mathbf{A}_j^{(\ell)} := \mathbf{I} - \frac{k}{2}\big[\big(\boldsymbol{\mathcal{H}}_h^i(\boldsymbol{\mu}_h^{(\ell)})\big)(\boldsymbol{z}_j)\big]_\times - \frac{\alpha k}{2}\big[\,\boldsymbol{m}_h^i(\boldsymbol{z}_j)\big]_\times \in \mathbb{R}^{3\times 3} \quad \textit{for all } j \in \{1, \dots, N\} \tag{6.40}$$

are positive definite. Hence, there exist unique solutions $\mathbf{y}_j \in \mathbb{R}^3$ to

$$\mathbf{A}_j^{(\ell)}\,\mathbf{y}_j = \boldsymbol{m}_h^i(\boldsymbol{z}_j). \tag{6.41}$$

Moreover, the next iterate $\boldsymbol{\mu}_h^{(\ell+1)} \in \boldsymbol{\mathcal{S}}_h$ satisfies $\boldsymbol{\mu}_h^{(\ell+1)}(\boldsymbol{z}_j) = \mathbf{y}_j$ for all $j \in \{1, \dots, N\}$.

Proof. Since for given $\mathbf{a} \in \mathbb{R}^3$, the matrix $[\mathbf{a}]_\times$ from (6.38) is skew-symmetric, we get that

$$\mathbf{A}_j^{(\ell)}\mathbf{x} \cdot \mathbf{x} \overset{(6.40)}{=} |\mathbf{x}|^2, \quad \text{for all } j \in \{1, \dots, N\}$$

i.e., the matrices $\mathbf{A}_j^{(\ell)}$ are positive definite and the nodwise systems (6.41) admit unique solutions. For the representation formula, note that the approximate $\boldsymbol{L}^2$-scalar product $\langle\cdot,\cdot\rangle_h$ depends only on the nodal values of the arguments. In particular, the next iterate $\boldsymbol{\mu}_h^{(\ell+1)} \in \boldsymbol{\mathcal{S}}_h$ satisfies that

$$\boldsymbol{\mu}_h^{(\ell+1)}(\boldsymbol{z}_j) + \frac{k}{2}\boldsymbol{\mu}_h^{(\ell+1)}(\boldsymbol{z}_j) \times \big(\boldsymbol{\mathcal{H}}_h^i(\boldsymbol{\mu}_h^{(\ell)})\big)(\boldsymbol{z}_j) + \frac{\alpha k}{2}\boldsymbol{\mu}_h^{(\ell+1)}(\boldsymbol{z}_j) \times \big[\boldsymbol{\mathcal{H}}_h^i(\boldsymbol{\mu}_h^{(\ell)})\big](\boldsymbol{z}_j) = \boldsymbol{m}_h^i(\boldsymbol{z}_j),$$

for all $j \in \{1, \dots, N\}$. Hence, with the defining property of $[\mathbf{a}]_\times \in \mathbb{R}^{3\times 3}$ for a vector $\mathbf{a} \in \mathbb{R}^3$ from (6.39), we get from the latter equation that $\boldsymbol{\mu}_h^{(\ell+1)}(\boldsymbol{z}_j) \in \mathbb{R}^3$ are the unique solutions of the nodewise systems in (6.41) for all nodes $\boldsymbol{z}_j$. Since functions in $\boldsymbol{\mathcal{S}}_h$ are uniquely defined by their nodal values, this concludes the proof. ☐

The latter proposition cumulates in a simplified version of Algorithm 6.6.1, where we replace the underlying variational formulation (6.30) by the nodewise 3×3 systems from the latter proposition.

Algorithm 6.6.8 (Inexact IMEX MPS, one time-step, nodewise systems)**. Input.** *Previous time-step $\boldsymbol{m}_h^i \in \boldsymbol{\mathcal{S}}_h$, initial guess $\boldsymbol{\mu}_h^{(0)} := \boldsymbol{m}_h^i \in \boldsymbol{\mathcal{S}}_h$, iteration tolerance $\varepsilon > 0$. Perform the steps* (a)–(c)*:*

(a) *Compute $\boldsymbol{\mathcal{H}}_h^i(\boldsymbol{\mu}_h^{(0)}) \in \boldsymbol{\mathcal{S}}_h$; see Lemma 6.6.6.*

(b) **Loop.** *For $\ell = 1, 2, \dots,$ repeat the following steps* (b-i)–(b-ii) *until*

$$\|\boldsymbol{\mathcal{H}}_h^i(\boldsymbol{\mu}_h^{(\ell+1)}) - \boldsymbol{\mathcal{H}}_h^i(\boldsymbol{\mu}_h^{(\ell)})\|_h < \varepsilon :$$

(b-i) *Compute* $\boldsymbol{\mu}_h^{(\ell+1)} \in \boldsymbol{\mathcal{S}}_h$ *by solving the nodewise systems*

$$\mathbf{A}_j^{(\ell)} \left[\boldsymbol{\mu}_h^{(\ell+1)}(\boldsymbol{z}_j)\right] = \boldsymbol{m}_h^i(\boldsymbol{z}_j) \quad \text{for all } j = 1, \dots, N,$$

where $\mathbf{A}_j^{(\ell)} \in \mathbb{R}^{3\times 3}$ *are defined by*

$$\mathbf{A}_j^{(\ell)} := \mathbf{I} - \frac{k}{2}\big[\big(\boldsymbol{\mathcal{H}}_h^i(\boldsymbol{\mu}_h^{(\ell)})\big)(\boldsymbol{z}_j)\big]_\times - \frac{\alpha k}{2}\big[\,\boldsymbol{m}_h^i(\boldsymbol{z}_j)\big]_\times.$$

(b-ii) *Compute* $\boldsymbol{\mathcal{H}}_h^i(\boldsymbol{\mu}_h^{(\ell+1)}) \in \boldsymbol{\mathcal{S}}_h$*; see Lemma 6.6.6.*

(c) *Set* $\boldsymbol{m}_h^{i+1} := 2\boldsymbol{\mu}_h^{(\ell+1)} - \boldsymbol{m}_h^i \in \boldsymbol{\mathcal{S}}_h$.

Output. *Approximation* $\boldsymbol{m}_h^{i+1} \approx \boldsymbol{m}(t_{i+1})$. □

Remark 6.6.9. (i) *With Proposition 6.6.7, the nodewise system are a smarter way to solve the discrete variational formulation* (6.30)*, i.e., the outputs of Algorithm 6.6.8 and Algorithm 6.6.1 are identical.*

(ii) *With the results from Section 6.6.2, the functional* $\boldsymbol{\mathcal{H}}_h^i(\cdot)$ *from* (6.28a) *can be evaluated exactly and at linear cost. Moreover, we get from Lemma 6.6.6 that* $\boldsymbol{\mathcal{H}}_h^i(\cdot)$ *requires only the assembly of the mass and stiffness matrix from* (6.36)*. However, this is independent of the time-step and has to be done only once at the beginning of the time-stepping.*

(iii) *The nodewise systems can be solved exactly and in parallel, and require no preconditioning. Together with* (ii)*, one iteration can be performed at linear cost.*

6.6.4. Convergence of the inexact midpoint scheme

In this section, we bring together all the findings of Section 6.6.1–6.6.3 and formulate an efficient algorithm for the full inexact time-stepping of Algorithm 6.6.1. Then, we prove convergence towards a weak solution of LLG. At first, we extend the inexact IMEX midpoint scheme with the nodewise systems from the latter section to a full time-stepping.

Algorithm 6.6.10 (Inexact IMEX MPS, full time-stepping)**. Input.** *Approximation* $\boldsymbol{m}_h^{-1} := \boldsymbol{m}_h^0 \in \boldsymbol{\mathcal{S}}_h$ *of initial magnetization, iteration tolerance* $\varepsilon > 0$.
Loop. *For* $i = 0, \dots, M-1$ *iterate the following steps* (a)–(c)*:*

(a) *Set* $\boldsymbol{\mu}_h^{(i,0)} := \boldsymbol{m}_h^i$ *and compute* $\boldsymbol{\mathcal{H}}_h^i(\boldsymbol{\mu}_h^{(i,0)}) \in \boldsymbol{\mathcal{S}}_h$*; see Lemma 6.6.6.*

(b) **Loop.** *For* $\ell = 1, 2, \dots,$ *repeat the following steps* (b-i)–(b-ii) *until*

$$\|\boldsymbol{\mathcal{H}}_h^i(\boldsymbol{\mu}_h^{(i,\ell+1)}) - \boldsymbol{\mathcal{H}}_h^i(\boldsymbol{\mu}_h^{(i,\ell)})\|_h < \varepsilon : \tag{6.42}$$

(b-i) *Compute* $\boldsymbol{\mu}_h^{(i,\ell+1)} \in \boldsymbol{\mathcal{S}}_h$ *via*

$$\mathbf{A}_j^{(i,\ell)} \big[\boldsymbol{\mu}_h^{(i,\ell+1)}(\boldsymbol{z}_j)\big] = \boldsymbol{m}_h^i(\boldsymbol{z}_j) \quad \textit{for all } j = 1, \dots, N,$$

where $\mathbf{A}_j^{(i,\ell)} \in \mathbb{R}^{3\times 3}$ *are defined by*

$$\mathbf{A}_j^{(i,\ell)} := \mathbf{I} - \frac{k}{2}\big[\big(\boldsymbol{\mathcal{H}}_h^i(\boldsymbol{\mu}_h^{(i,\ell)})\big)(\boldsymbol{z}_j)\big]_\times - \frac{\alpha k}{2}\big[\,\boldsymbol{m}_h^i(\boldsymbol{z}_j)\big]_\times.$$

(b-ii) *Compute* $\boldsymbol{\mathcal{H}}_h^i(\boldsymbol{\mu}_h^{(i,\ell+1)}) \in \boldsymbol{\mathcal{S}}_h$*; see Lemma 6.6.6.*

(c) *Set* $\boldsymbol{m}_h^{i+1} := 2\boldsymbol{\mu}_h^{(i,\ell+1)} - \boldsymbol{m}_h^i \in \boldsymbol{\mathcal{S}}_h$.

Output. *Approximations* $\boldsymbol{m}_h^i \approx \boldsymbol{m}(t_i)$. □

Remark 6.6.11. *When the iteration in the latter algorithm is stopped, the update formula of* (c) *yields that* $\boldsymbol{m}_h^{i+1/2} = \boldsymbol{\mu}_h^{(i,\ell+1)}$. *However, since the functional* $\boldsymbol{\mathcal{H}}_h^i(\cdot)$ *from* (6.28a) *is not necessarily linear, possibly*

$$\boldsymbol{\mathcal{H}}_h^i(\boldsymbol{m}_h^{i+1}) \neq 2\,\boldsymbol{\mathcal{H}}_h^i(\boldsymbol{\mu}_h^{(i,\ell+1)}) - \boldsymbol{\mathcal{H}}_h^i(\boldsymbol{m}_h^i).$$

Hence, in general one cannot recycle $\boldsymbol{\mathcal{H}}_h^i(\boldsymbol{\mu}_h^{(i,\ell+1)})$ *for the next time-step.*

Finally, we formulate our convergence theorem, which, in contrast to our basic convergence result from Theorem 6.5.1, takes into account the inexact solution of the discrete variational formulation (6.2). So far, this was considered only by [Bar06, Cim09] for $\boldsymbol{h}_{\text{eff}}(\boldsymbol{m}) := \Delta\boldsymbol{m}$ and $\boldsymbol{\Pi}(\boldsymbol{m}) = \boldsymbol{0}$. In particular, [Cim09] proves convergence towards a weak solution under the CFL-type condition $k = \mathbf{o}(h^2)$, but its algorithm is based on the equivalent Landau–Lifshitz form (6.1). For the Gilbert form (2.3a), [Bar06] proves convergence under the additional assumption $\varepsilon = \mathbf{o}(h^2)$. Our result builds on [Bar06] but requires no coupling $\varepsilon = \mathbf{o}(h^2)$ and additionally considers lower-order terms. Here, we elaborate the own work [PRS18, Theorem 15].

Theorem 6.6.12 (Convergence of inexact IMEX MPS, [PRS18, Theorem 15])**.** *Consider Algorithm 6.6.10 for the discretization of LLG* (2.3). *Then, the following three assertions* (a)–(c) *hold true:*

(a) *Suppose that*

- *the approximations* $\boldsymbol{m}_h^0$ *are uniformly bounded* **(M1)***;*
- *the approximation operators* $\boldsymbol{\pi}_h$ *are linear* **(D2)** *and uniformly bounded* **(D3)***;*
- *the approximation operators* $\boldsymbol{\Pi}_h$ *satisfy the Lipschitz-type condition* **(M2)***;*
- *there holds the CFL-type condition*

$$k = \mathbf{o}(h^2). \tag{6.43}$$

Then, there exists $k_0 > 0$, which depends only on $C_{\mathbf{ex}}$, $C_{\mathbf{mesh}}$, $\boldsymbol{\pi}(\cdot)$, $\mathbf{\Pi}(\cdot)$, and $\boldsymbol{m}^0$ such that Algorithm 6.6.10 is well-posed for all $k < k_0$ and all $\varepsilon > 0$. In particular, the underlying fixed-point iterations are contractions and converge in $\boldsymbol{L}^2(\omega)$ towards the unique solutions of the discrete variational formulations (6.2) *as $\varepsilon \to 0$.*

(b) *Suppose the assumptions from Theorem 6.5.1*(b)*, and the CFL-type condition* (6.43)*. For $\varepsilon > 0$, denote the postprocessed output of Algorithm 6.6.10 with $\boldsymbol{m}_{\varepsilon hk}$. Then, there exists a subsequence of $\boldsymbol{m}_{\varepsilon hk}$, and a weak solution*

$$\boldsymbol{m} \in \boldsymbol{H}^1(\omega_T) \cap L^\infty(0, T; \boldsymbol{H}^1(\Omega))$$

of LLG (2.3) *in the sense of Definition 2.2.1*(i)–(iii) *such that*

$$\boldsymbol{m}_{\varepsilon hk} \rightharpoonup \boldsymbol{m} \quad \text{in } \boldsymbol{H}^1(\omega_T) \quad \text{as } \varepsilon, h, k \to 0.$$

(c) *Suppose the assumptions from Theorem 6.5.1*(c)*, and the CFL-type condition* (6.43)*. Then, $\boldsymbol{m}$ from* (b) *is a physical weak solution in the sense of Definition 2.2.1*(i)–(iv).

Proof of Theorem 6.6.12. According to Proposition 6.6.7, Algorithm 6.6.10 successively performs time-steps with the inexact midpoint scheme from Algorithm 6.6.1. At the i-th time-step, Proposition 6.6.2 yields that the iterates are well-defined and that

$$\|\boldsymbol{m}_h^i\|_{\boldsymbol{L}^\infty(\omega)} = \|\boldsymbol{m}_h^0\|_{\boldsymbol{L}^\infty(\omega)} \overset{\textbf{(M1)}}{\lesssim} 1 \quad \text{for all } i \in \{0, \dots, M-1\}, \tag{6.44}$$

regardless of when the iteration is stopped. With Proposition 6.6.3(i), the sequence of iterates is a contraction for small enough

$$\big(1 + \|\boldsymbol{m}_h^i\|_{\boldsymbol{L}^\infty(\omega)}^2\big)\, k\, h^{-2} \overset{(6.44)}{\simeq} k\, h^{-2}.$$

Hence, we conclude (a) with the CFL-type condition (6.43).

To show (b)–(c), we require an operator $\widetilde{\boldsymbol{\mathcal{P}}}_h : \boldsymbol{\mathcal{S}}_h \to \boldsymbol{\mathcal{S}}_h$, which is defined by

$$\langle \widetilde{\boldsymbol{\mathcal{P}}}_h \boldsymbol{\varphi}_h, \boldsymbol{\psi}_h \rangle_{\boldsymbol{L}^2(\omega)} = \langle \boldsymbol{\varphi}_h, \boldsymbol{\psi}_h \rangle_h \quad \text{for all } \boldsymbol{\varphi}_h, \boldsymbol{\psi}_h \in \boldsymbol{\mathcal{S}}_h. \tag{6.45}$$

With the latter definition, we obtain that

$$\langle \boldsymbol{\mathcal{P}}_h \widetilde{\boldsymbol{\mathcal{P}}}_h \boldsymbol{\varphi}_h, \boldsymbol{\psi}_h \rangle_h \overset{(3.12)}{=} \langle \widetilde{\boldsymbol{\mathcal{P}}}_h \boldsymbol{\varphi}_h, \boldsymbol{\psi}_h \rangle_{\boldsymbol{L}^2(\omega)} = \langle \boldsymbol{\varphi}_h, \boldsymbol{\psi}_h \rangle_h \quad \text{for all } \boldsymbol{\psi}_h \in \boldsymbol{\mathcal{S}}_h,$$

i.e., $\widetilde{\boldsymbol{\mathcal{P}}}_h$ is the inverse of the quasi-$\boldsymbol{L}^2$-projection $\boldsymbol{\mathcal{P}}_h$ in $\boldsymbol{\mathcal{S}}_h$. Moreover, there holds a uniform boundedness property of $\widetilde{\boldsymbol{\mathcal{P}}}_h$ in $\boldsymbol{L}^2(\omega)$. To see this, let $\boldsymbol{\varphi}_h \in \boldsymbol{\mathcal{S}}_h$. With the norm equivalence $\|\cdot\|_{\boldsymbol{L}^2(\omega)} \simeq \|\cdot\|_h$ from Lemma 3.3.1(i), we obtain that

$$\begin{aligned} \|\widetilde{\boldsymbol{\mathcal{P}}}_h \boldsymbol{\varphi}_h\|_{\boldsymbol{L}^2(\omega)}^2 &= \langle \widetilde{\boldsymbol{\mathcal{P}}}_h \boldsymbol{\varphi}_h, \widetilde{\boldsymbol{\mathcal{P}}}_h \boldsymbol{\varphi}_h \rangle_{\boldsymbol{L}^2(\omega)} \overset{(6.45)}{=} \langle \boldsymbol{\varphi}_h, \widetilde{\boldsymbol{\mathcal{P}}}_h \boldsymbol{\varphi}_h \rangle_h \\ &\le \|\boldsymbol{\varphi}_h\|_h \, \|\widetilde{\boldsymbol{\mathcal{P}}}_h \boldsymbol{\varphi}_h\|_h \lesssim \|\boldsymbol{\varphi}_h\|_{\boldsymbol{L}^2(\omega)} \, \|\widetilde{\boldsymbol{\mathcal{P}}}_h \boldsymbol{\varphi}_h\|_{\boldsymbol{L}^2(\omega)}, \end{aligned}$$

i.e., it holds that

$$\|\widetilde{\boldsymbol{\mathcal{P}}}_h \boldsymbol{\varphi}_h\|_{\boldsymbol{L}^2(\omega)} \lesssim \|\boldsymbol{\varphi}_h\|_{\boldsymbol{L}^2(\omega)} \quad \text{for all } \boldsymbol{\varphi}_h \in \boldsymbol{\mathcal{S}}_h. \tag{6.46}$$

Then, we note that Proposition 6.6.3(ii) yields for given $\varepsilon > 0$ an index $\ell_\varepsilon \in \mathbb{N}$ at which the stopping criterion (6.42) is met. This lets us define

$$\overline{\boldsymbol{g}}_{\varepsilon h}^i := \boldsymbol{f}_h^{i+1/2} - \widetilde{\boldsymbol{\mathcal{P}}}_h\big[\,\boldsymbol{\mathcal{H}}_h^i(\boldsymbol{\mu}_h^{(i,\ell_\varepsilon+1)}) - \boldsymbol{\mathcal{H}}_h^i(\boldsymbol{\mu}_h^{(i,\ell_\varepsilon)})\,\big] \in \boldsymbol{\mathcal{S}}_h \text{ for all } i \in \{0,\dots,M-1\} \tag{6.47}$$

as well as the corresponding $\overline{\boldsymbol{g}}_{hk}^{(\varepsilon)} \in \boldsymbol{L}^2(\omega_T)$ via

$$\overline{\boldsymbol{g}}_{\varepsilon hk}(t) := \overline{\boldsymbol{g}}_{\varepsilon h}^i \quad \text{for all } t \in [t_i, t_{i+1}) \quad \text{and} \quad i \in \{0,\dots,M-1\}.$$

In particular, the norm equivalence $\|\cdot\|_{\boldsymbol{L}^2(\omega)} \simeq \|\cdot\|_h$ from Lemma 3.3.1(i) yields that

$$\begin{aligned}\|\overline{\boldsymbol{g}}_{\varepsilon hk} - \overline{\boldsymbol{f}}_{hk}\|_{\boldsymbol{L}^2(\omega_T)}^2 &\overset{(6.47)}{\leq} k \sum_{i=1}^{M-1} \|\widetilde{\boldsymbol{\mathcal{P}}}_h\big[\,\boldsymbol{\mathcal{H}}_h^i(\boldsymbol{\mu}_h^{(i,\ell_\varepsilon+1)}) - \boldsymbol{\mathcal{H}}_h^i(\boldsymbol{\mu}_h^{(i,\ell_\varepsilon)})\,\big]\|_{\boldsymbol{L}^2(\omega)}^2 \\ &\overset{(6.46)}{\lesssim} k \sum_{i=1}^{M-1} \|\boldsymbol{\mathcal{H}}_h^i(\boldsymbol{\mu}_h^{(i,\ell_\varepsilon+1)}) - \boldsymbol{\mathcal{H}}_h^i(\boldsymbol{\mu}_h^{(i,\ell_\varepsilon)})\|_{\boldsymbol{L}^2(\omega)}^2 \overset{(6.42)}{\lesssim} \varepsilon^2 \to 0 \quad \text{as } \varepsilon, h, k \to 0.\end{aligned}$$

Hence, the consistency properties **(D5)** and **(D5$^+$)** of $(\boldsymbol{f}_h^i)_{i=0}^M$ yield the corresponding

$$\begin{aligned}\overline{\boldsymbol{g}}_{\varepsilon hk} &\rightharpoonup \boldsymbol{f} \quad \text{in } \boldsymbol{L}^2(\omega_T) \quad \text{as } \varepsilon, h, k \to 0, \quad \text{and} \\ \overline{\boldsymbol{g}}_{\varepsilon hk} &\to \boldsymbol{f} \quad \text{in } \boldsymbol{L}^2(\omega_T) \quad \text{as } \varepsilon, h, k \to 0,\end{aligned}$$

respectively. Together with the perturbed discrete variational formulation (6.31) from Proposition 6.6.2(ii), the actual proof of (b)–(c) then follows along the lines of the proof of Theorem 6.5.1(b)–(c) for the (exactly solved) IMEX midpoint scheme with $\overline{\boldsymbol{g}}_{\varepsilon h}^i$ and $\overline{\boldsymbol{g}}_{\varepsilon hk}$ instead of $\boldsymbol{f}_h^{i+1/2}$ and $\overline{\boldsymbol{f}}_{hk}$, respectively. □

6.7. Uniqueness of discrete solutions

In this section, we prove a uniqueness result of the solution $\boldsymbol{m}_h^{i+1} \in \boldsymbol{\mathcal{S}}_h$ of Algorithm 6.2.1. The techniques of this section are inspired by [Pro01, Lemma 4.4], where a uniqueness result for an analytical solution of an equivalent reformulation of LLG (2.3a) is proved. So far, uniqueness of the discrete solution $\boldsymbol{m}_h^{i+1}$ required

$$\textit{the CFL-type condition} \quad k = \mathbf{o}(h^2)$$

and was a bi-product of the convergence results of the fixed-point iteration for the solution of the non-linear system from the variational formulation (6.2); see, e.g., [Bar06, BP06, BBP08, BPS09] and the latter section. In Theorem 6.7.1 below, we prove that, essentially, the weaker assumption that

$$\textit{no finite time blow-up} \qquad \text{and} \qquad k = \mathbf{o}(h)$$

suffice to establish uniqueness of $\boldsymbol{m}_h^{i+1}$.

Theorem 6.7.1 (Uniqueness of solutions)**.** *Consider the IMEX midpoint scheme from Algorithm 6.2.1 for the discretization of LLG* (2.3)*. Suppose that*

- *the approximations* $\boldsymbol{m}_h^0$ *are uniformly bounded* **(M1)***;*
- *the approximation operators* $\boldsymbol{\pi}_h$ *are linear* **(D2)** *and uniformly bounded* **(D3)***;*
- *the approximation operators* $\boldsymbol{\Pi}_h$ *satisfy the Lipschitz-type condition* **(M2)***;*
- *there holds the mild CFL-type condition* $k = \mathbf{o}(h)$*;*
- *there is no finite time blow-up in the sense that*

$$\sup_{h,k>0} \|\nabla \overline{\boldsymbol{m}}_{hk}\|_{\boldsymbol{L}^\infty(\omega_T)} \leq C_\nabla < \infty. \tag{6.48}$$

Then, there exists $k_0 > 0$*, which depends only on* $\boldsymbol{m}^0$*,* $C_{\mathbf{ex}}$*,* α*,* $\boldsymbol{\pi}(\cdot)$*,* $\boldsymbol{\Pi}(\cdot)$*,* $C_{\mathbf{mesh}}$*, and* C_∇ *such that for all* $k < k_0$ *the sequences* $(\boldsymbol{m}_h^i)_{i=0}^M$ *of approximations are unique.*

The actual proof, is essentially based on the following lemma.

Lemma 6.7.2. *There exists a constant* $C > 0$*, which depends only on* $C_{\mathbf{mesh}}$*, such that*

$$\langle \boldsymbol{\mu}_h \times \Delta_h \boldsymbol{\psi}_h, \boldsymbol{\psi}_h \rangle_h \leq C\, h^{-1} \, \|\nabla \boldsymbol{\mu}_h\|_{\boldsymbol{L}^\infty(\omega)} \, \|\boldsymbol{\psi}_h\|_h^2 \quad \textit{for all } \boldsymbol{\mu}_h, \boldsymbol{\psi}_h \in \boldsymbol{\mathcal{S}}_h.$$

Proof. Let $\boldsymbol{\psi}_h \in \boldsymbol{\mathcal{S}}_h$ be arbitrary. We denote the standard nodal interpolation operator corresponding to $\boldsymbol{\mathcal{S}}_h$ with $\boldsymbol{\mathcal{I}}_h$. Then, we use an implicit trick from [BP06, p. 1410]: Since the definition (6.20) of the approximate $\boldsymbol{L}^2$-scalar product $\langle \cdot, \cdot \rangle_h$ depends only on the nodal values of the arguments, we can apply $\boldsymbol{\mathcal{I}}_h$ to the arguments. Then, the definition (3.11) of the discrete Laplacian Δ_h yields that

$$\begin{aligned} \langle \boldsymbol{\mu}_h \times \Delta_h \boldsymbol{\psi}_h, \boldsymbol{\psi}_h \rangle_h &= \langle \boldsymbol{\psi}_h \times \boldsymbol{\mu}_h, \Delta_h \boldsymbol{\psi}_h \rangle_h \\ &= \langle \boldsymbol{\mathcal{I}}_h(\boldsymbol{\psi}_h \times \boldsymbol{\mu}_h), \Delta_h \boldsymbol{\psi}_h \rangle_h = -\langle \nabla \boldsymbol{\mathcal{I}}_h(\boldsymbol{\psi}_h \times \boldsymbol{\mu}_h), \nabla \boldsymbol{\psi}_h \rangle_{\boldsymbol{L}^2(\omega)}. \end{aligned}$$

The approximation properties of $\boldsymbol{\mathcal{I}}_h$ (see Proposition 3.1.7) and $(\mathbf{a} \times \mathbf{b}) \cdot \mathbf{a} = 0$ for vectors $\mathbf{a}, \mathbf{b} \in \mathbb{R}^3$ further yield that

$$\begin{aligned} &\langle \boldsymbol{\mu}_h \times \Delta_h \boldsymbol{\psi}_h, \boldsymbol{\psi}_h \rangle_h = \\ &\quad = -\langle \nabla(\boldsymbol{\psi}_h \times \boldsymbol{\mu}_h), \nabla \boldsymbol{\psi}_h \rangle_{\boldsymbol{L}^2(\omega)} + \langle \nabla(1 - \boldsymbol{\mathcal{I}}_h)(\boldsymbol{\psi}_h \times \boldsymbol{\mu}_h), \nabla \boldsymbol{\psi}_h \rangle_{\boldsymbol{L}^2(\omega)} \\ &\quad = -\langle \boldsymbol{\psi}_h \times \nabla \boldsymbol{\mu}_h, \nabla \boldsymbol{\psi}_h \rangle_{\boldsymbol{L}^2(\omega)} + \sum_{K \in \mathcal{T}_h} \langle \nabla(1 - \boldsymbol{\mathcal{I}}_h)(\boldsymbol{\psi}_h \times \boldsymbol{\mu}_h), \nabla \boldsymbol{\psi}_h \rangle_{\boldsymbol{L}^2(K)} \\ &\quad \lesssim \|\nabla \boldsymbol{\mu}_h\|_{\boldsymbol{L}^\infty(\omega)} \|\boldsymbol{\psi}_h\|_{\boldsymbol{L}^2(\omega)} \|\nabla \boldsymbol{\psi}_h\|_{\boldsymbol{L}^2(\omega)} + h \sum_{K \in \mathcal{T}_h} \|\boldsymbol{\psi}_h \times \boldsymbol{\mu}_h\|_{\boldsymbol{H}^2(K)} \|\nabla \boldsymbol{\psi}_h\|_{\boldsymbol{L}^2(K)}. \end{aligned}$$

Since it holds elementwise that $D^2 \boldsymbol{\psi}_h = D^2 \boldsymbol{\mu}_h = \mathbf{0}$, we get from the latter estimate that

$$\begin{aligned} &\langle \boldsymbol{\mu}_h \times \Delta_h \boldsymbol{\psi}_h, \boldsymbol{\psi}_h \rangle_h \\ &\qquad \lesssim \|\nabla \boldsymbol{\mu}_h\|_{\boldsymbol{L}^\infty(\omega)} \|\boldsymbol{\psi}_h\|_{\boldsymbol{L}^2(\omega)} \|\nabla \boldsymbol{\psi}_h\|_{\boldsymbol{L}^2(\omega)} + h \sum_{K \in \mathcal{T}_h} \|\nabla \boldsymbol{\mu}_h\|_{\boldsymbol{L}^\infty(K)} \|\boldsymbol{\psi}_h\|_{\boldsymbol{H}^1(K)}^2. \end{aligned}$$

With an inverse estimate (see Proposition 3.1.8), the latter estimate yields that

$$\langle \boldsymbol{\mu}_h \times \Delta_h \boldsymbol{\psi}_h, \boldsymbol{\psi}_h \rangle_h \lesssim h^{-1} \|\nabla \boldsymbol{\mu}_h\|_{\boldsymbol{L}^\infty(\omega)} \|\boldsymbol{\psi}_h\|^2_{\boldsymbol{L}^2(\omega)}.$$

Together with the norm equivalence relation $\|\cdot\|_h \simeq \|\cdot\|_{\boldsymbol{L}^2(\omega)}$ from Lemma 3.3.1(i), this concludes the proof. □

We have everything at hand for the actual proof of Theorem 6.7.1.

Proof of Theorem 6.7.1. We split the proof into the following five steps.

Step 1. We collect auxiliary notations and results: Fix $i \in \{0, \dots, M-1\}$ and let $\boldsymbol{m}_h^{i+1}, \widetilde{\boldsymbol{m}}_h^{i+1} \in \boldsymbol{\mathcal{S}}_h$ both solve the discrete variational formulation (6.2). By abuse of notation, we define

$$\boldsymbol{m}_h^{i+1/2} := \frac{1}{2}\left(\boldsymbol{m}_h^{i+1} + \boldsymbol{m}_h^i\right) \in \boldsymbol{\mathcal{S}}_h, \quad \text{and} \quad \widetilde{\boldsymbol{m}}_h^{i+1/2} := \frac{1}{2}\left(\widetilde{\boldsymbol{m}}_h^{i+1} + \boldsymbol{m}_h^i\right) \in \boldsymbol{\mathcal{S}}_h. \tag{6.49a}$$

Moreover, we define the mean value of the differences as

$$\boldsymbol{d}_h^{i+1/2} := \boldsymbol{m}_h^{i+1/2} - \widetilde{\boldsymbol{m}}_h^{i+1/2} = \frac{1}{2}\boldsymbol{m}_h^{i+1} - \frac{1}{2}\widetilde{\boldsymbol{m}}_h^{i+1} \in \boldsymbol{\mathcal{S}}_h. \tag{6.49b}$$

For given $\boldsymbol{\mu}_h \in \boldsymbol{\mathcal{S}}_h$, we recall from (6.28a) the notion of the approximate effective field and dissipative effects

$$\begin{aligned}\boldsymbol{\mathcal{H}}_h^i(\boldsymbol{\mu}_h) &:= C_{\mathbf{ex}} \Delta_h \boldsymbol{\mu}_h + \boldsymbol{\mathcal{P}}_h \boldsymbol{\pi}_h^{\boldsymbol{\Theta}}(2\boldsymbol{\mu}_h - \boldsymbol{m}_h^i, \boldsymbol{m}_h^i, \boldsymbol{m}_h^{i-1}) \\ &\quad + \boldsymbol{\mathcal{P}}_h \boldsymbol{f}_h^{i+1/2} + \boldsymbol{\mathcal{P}}_h \boldsymbol{\Pi}_h^{\boldsymbol{\Theta}}(2\boldsymbol{\mu}_h - \boldsymbol{m}_h^i, \boldsymbol{m}_h^i, \boldsymbol{m}_h^{i-1}) \in \boldsymbol{\mathcal{S}}_h.\end{aligned}$$

Finally, since $\boldsymbol{m}_h^{i+1}$ and $\widetilde{\boldsymbol{m}}_h^{i+1}$ both solve the discrete variational formulation (6.2), Theorem 6.5.1(a) applies and we obtain uniform boundedness in the sense that

$$\begin{aligned}&\|\widetilde{\boldsymbol{m}}_h^{i+1/2}\|_{\boldsymbol{L}^\infty(\omega)} + \|\boldsymbol{m}_h^{i+1/2}\|_{\boldsymbol{L}^\infty(\omega)} \\ &\quad \le \frac{1}{2}\|\boldsymbol{m}_h^{i+1}\|_{\boldsymbol{L}^\infty(\omega)} + \frac{1}{2}\|\widetilde{\boldsymbol{m}}_h^{i+1}\|_{\boldsymbol{L}^\infty(\omega)} + \|\boldsymbol{m}_h^i\|_{\boldsymbol{L}^\infty(\omega)} \\ &\quad = 2\|\boldsymbol{m}_h^i\|_{\boldsymbol{L}^\infty(\omega)} = 2\|\boldsymbol{m}_h^0\|_{\boldsymbol{L}^\infty(\omega)} \overset{\textbf{(M1)}}{\lesssim} 1.\end{aligned} \tag{6.50}$$

Step 2. We estimate $\|\boldsymbol{d}_h^{i+1/2}\|_h$: Following the lines of Section 6.6.1, we rewrite the discrete variational formulation (6.2) with the notations from **Step 1**. Since $\boldsymbol{m}_h^{i+1}$ and $\widetilde{\boldsymbol{m}}_h^{i+1}$ both solve (6.2), we get for $\boldsymbol{\mu}_h \in \{\boldsymbol{m}_h^{i+1/2}, \widetilde{\boldsymbol{m}}_h^{i+1/2}\}$, that

$$\frac{2}{k}\langle \boldsymbol{\mu}_h, \boldsymbol{\varphi}_h \rangle_h + \langle \boldsymbol{\mu}_h \times \boldsymbol{\mathcal{H}}_h^i(\boldsymbol{\mu}_h), \boldsymbol{\varphi}_h \rangle_h + \frac{2\alpha}{k}\langle \boldsymbol{\mu}_h \times \boldsymbol{m}_h^i, \boldsymbol{\varphi}_h \rangle_h = \frac{2}{k}\langle \boldsymbol{m}_h^i, \boldsymbol{\varphi}_h \rangle_h,$$

for all $\boldsymbol{\varphi}_h \in \boldsymbol{\mathcal{S}}_h$. From the latter equation, we obtain that

$$\begin{aligned}\frac{2}{k}\langle \boldsymbol{d}_h^{i+1/2}, \boldsymbol{\varphi}_h \rangle_h &= -\langle \boldsymbol{m}_h^{i+1/2} \times \boldsymbol{\mathcal{H}}_h^i(\boldsymbol{m}_h^{i+1/2}), \boldsymbol{\varphi}_h \rangle_h + \langle \widetilde{\boldsymbol{m}}_h^{i+1/2} \times \boldsymbol{\mathcal{H}}_h^i(\widetilde{\boldsymbol{m}}_h^{i+1/2}), \boldsymbol{\varphi}_h \rangle_h \\ &\quad - \frac{2\alpha}{k}\langle \boldsymbol{d}_h^{i+1/2} \times \boldsymbol{m}_h^i, \boldsymbol{\varphi}_h \rangle_h \quad \text{for all } \boldsymbol{\varphi}_h \in \boldsymbol{\mathcal{S}}_h.\end{aligned}$$

We test the latter equation with $\boldsymbol{\varphi}_h := \boldsymbol{d}_h^{i+1/2}$. Since

$$\widetilde{\boldsymbol{m}}_h^{i+1/2} \overset{(6.49b)}{=} \boldsymbol{m}_h^{i+1/2} - \boldsymbol{d}_h^{i+1/2} \tag{6.51}$$

and $(\mathbf{a} \times \mathbf{b}) \cdot \mathbf{a} = 0$ for vectors $\mathbf{a}, \mathbf{b} \in \mathbb{R}^3$, we obtain that

$$\begin{aligned} \frac{2}{k}\|\boldsymbol{d}_h^{i+1/2}\|_h^2 &= -\langle \boldsymbol{m}_h^{i+1/2} \times \boldsymbol{\mathcal{H}}_h^i(\boldsymbol{m}_h^{i+1/2}), \boldsymbol{d}_h^{i+1/2}\rangle_h + \langle \widetilde{\boldsymbol{m}}_h^{i+1/2} \times \boldsymbol{\mathcal{H}}_h^i(\widetilde{\boldsymbol{m}}_h^{i+1/2}), \boldsymbol{d}_h^{i+1/2}\rangle_h \\ &\overset{(6.51)}{=} -\langle \boldsymbol{m}_h^{i+1/2} \times \boldsymbol{\mathcal{H}}_h^i(\boldsymbol{m}_h^{i+1/2}), \boldsymbol{d}_h^{i+1/2}\rangle_h + \langle \boldsymbol{m}_h^{i+1/2} \times \boldsymbol{\mathcal{H}}_h^i(\widetilde{\boldsymbol{m}}_h^{i+1/2}), \boldsymbol{d}_h^{i+1/2}\rangle_h \\ &= -\langle \boldsymbol{m}_h^{i+1/2} \times \big[\boldsymbol{\mathcal{H}}_h^i(\boldsymbol{m}_h^{i+1/2}) - \boldsymbol{\mathcal{H}}_h^i(\widetilde{\boldsymbol{m}}_h^{i+1/2})\big], \boldsymbol{d}_h^{i+1/2}\rangle_h. \end{aligned} \tag{6.52}$$

With the auxiliary notations from **Step 1**, it holds that

$$\boldsymbol{\mathcal{H}}_h^i(\boldsymbol{m}_h^{i+1/2}) \;-\; \boldsymbol{\mathcal{H}}_h^i(\widetilde{\boldsymbol{m}}_h^{i+1/2}) \;:=\; C_{\mathbf{ex}}\Delta_h \boldsymbol{d}_h^{i+1/2} \;+\; \boldsymbol{\mathcal{R}}_h,$$

where the residual term $\boldsymbol{\mathcal{R}}_h$ is defined as

$$\begin{aligned} \boldsymbol{\mathcal{R}}_h := \boldsymbol{\mathcal{P}}_h\boldsymbol{\pi}_h^{\boldsymbol{\Theta}}(\boldsymbol{m}_h^{i+1}, \boldsymbol{m}_h^i, \boldsymbol{m}_h^{i-1}) - \boldsymbol{\mathcal{P}}_h\boldsymbol{\pi}_h^{\boldsymbol{\Theta}}(\widetilde{\boldsymbol{m}}_h^{i+1}, \boldsymbol{m}_h^i, \boldsymbol{m}_h^{i-1}) \\ + \boldsymbol{\mathcal{P}}_h\boldsymbol{\Pi}_h^{\boldsymbol{\Theta}}(\boldsymbol{m}_h^{i+1}, \boldsymbol{m}_h^i, \boldsymbol{m}_h^{i-1}) - \boldsymbol{\mathcal{P}}_h\boldsymbol{\Pi}_h^{\boldsymbol{\Theta}}(\widetilde{\boldsymbol{m}}_h^{i+1}, \boldsymbol{m}_h^i, \boldsymbol{m}_h^{i-1}) \in \boldsymbol{\mathcal{S}}_h. \end{aligned} \tag{6.53}$$

The combination of the latter three equations then yields that

$$\begin{aligned} \|\boldsymbol{d}_h^{i+1/2}\|_h^2 &\overset{(6.52)}{=} -\frac{C_{\mathbf{ex}}}{2} k\,\langle \boldsymbol{m}_h^{i+1/2} \times \Delta_h \boldsymbol{d}_h^{i+1/2}, \boldsymbol{d}_h^{i+1/2}\rangle_h - \frac{1}{2} k\,\langle \boldsymbol{m}_h^{i+1/2} \times \boldsymbol{\mathcal{R}}_h, \boldsymbol{d}_h^{i+1/2}\rangle_h \\ &=: -\frac{C_{\mathbf{ex}}}{2}\, T_1 - \frac{1}{2}\, T_2. \end{aligned} \tag{6.54}$$

Step 3. We estimate T_1: From Lemma 6.7.2, we get that

$$\begin{aligned} T_1 &\overset{(6.54)}{=} k\,\langle \boldsymbol{m}_h^{i+1/2} \times \Delta_h \boldsymbol{d}_h^{i+1/2}, \boldsymbol{d}_h^{i+1/2}\rangle_h \lesssim\; kh^{-1}\,\|\nabla \boldsymbol{m}_h^{i+1/2}\|_{\boldsymbol{L}^\infty(\omega)}\,\|\boldsymbol{d}_h^{i+1/2}\|_h^2 \\ &\leq\; kh^{-1}\,\|\nabla \overline{\boldsymbol{m}}_{hk}\|_{\boldsymbol{L}^\infty(\omega_T)}\,\|\boldsymbol{d}_h^{i+1/2}\|_h^2 \overset{(6.48)}{\lesssim} kh^{-1}\,\|\boldsymbol{d}_h^{i+1/2}\|_h^2. \end{aligned}$$

Step 4. We estimate T_2: If we employ the explicit approaches **(A2)** with $i > 0$ or **(A3)** for $\boldsymbol{\pi}_h^{\boldsymbol{\Theta}}$ and $\boldsymbol{\Pi}_h^{\boldsymbol{\Theta}}$, then $\boldsymbol{\mathcal{R}}_h = \mathbf{0}$ and there is nothing to do. For the implicit approach **(A1)** and **(A2)** with $i = 0$, the residual term becomes

$$\boldsymbol{\mathcal{R}}_h \overset{(6.53)}{=} \boldsymbol{\mathcal{P}}_h\boldsymbol{\pi}_h(\boldsymbol{m}_h^{i+1/2}) - \boldsymbol{\mathcal{P}}_h\boldsymbol{\pi}_h(\widetilde{\boldsymbol{m}}_h^{i+1/2}) + \boldsymbol{\mathcal{P}}_h\boldsymbol{\Pi}_h(\boldsymbol{m}_h^{i+1/2}) - \boldsymbol{\mathcal{P}}_h\boldsymbol{\Pi}_h(\widetilde{\boldsymbol{m}}_h^{i+1/2}). \tag{6.55}$$

We estimate that

$$\begin{aligned} T_2 &\overset{(6.54)}{=} k\,\langle \boldsymbol{d}_h^{i+1/2} \times \boldsymbol{m}_h^{i+1/2}, \boldsymbol{\mathcal{R}}_h\rangle_h \\ &\lesssim k\,\|\boldsymbol{m}_h^{i+1/2}\|_{\boldsymbol{L}^\infty(\omega)}\,\|\boldsymbol{d}_h^{i+1/2}\|_h\,\|\boldsymbol{\mathcal{R}}_h\|_h \overset{(6.50)}{\leq} k\,\|\boldsymbol{d}_h^{i+1/2}\|_h\,\|\boldsymbol{\mathcal{R}}_h\|_h. \end{aligned}$$

To estimate $\|\boldsymbol{\mathcal{R}}_h\|_h$, the boundedness statement of $\boldsymbol{\mathcal{P}}_h$ from Lemma 3.3.3 yields for the approaches **(A1)** or **(A2)** with $i = 0$ that

$$\begin{aligned}\|\boldsymbol{\mathcal{R}}_h\|_h &\overset{(6.55)}{\leq} \|\boldsymbol{\mathcal{P}}_h\boldsymbol{\pi}_h(\boldsymbol{m}_h^{i+1/2}) - \boldsymbol{\mathcal{P}}_h\boldsymbol{\pi}_h(\widetilde{\boldsymbol{m}}_h^{i+1/2})\|_h + \|\boldsymbol{\mathcal{P}}_h\boldsymbol{\Pi}_h(\boldsymbol{m}_h^{i+1/2}) - \boldsymbol{\mathcal{P}}_h\boldsymbol{\Pi}_h(\widetilde{\boldsymbol{m}}_h^{i+1/2})\|_h \\ &\leq \|\boldsymbol{\pi}_h(\boldsymbol{m}_h^{i+1/2}) - \boldsymbol{\pi}_h(\widetilde{\boldsymbol{m}}_h^{i+1/2})\|_{\boldsymbol{L}^2(\omega)} + \|\boldsymbol{\Pi}_h(\boldsymbol{m}_h^{i+1/2}) - \boldsymbol{\Pi}_h(\widetilde{\boldsymbol{m}}_h^{i+1/2})\|_{\boldsymbol{L}^2(\omega)}.\end{aligned} \tag{6.56}$$

For the first term on the right-hand side of (6.56), we get that

$$\begin{aligned}\|\boldsymbol{\pi}_h(\boldsymbol{m}_h^{i+1/2}) - \boldsymbol{\pi}_h(\widetilde{\boldsymbol{m}}_h^{i+1/2})\|_{\boldsymbol{L}^2(\omega)} &\overset{\textbf{(D2)}}{=} \|\boldsymbol{\pi}_h(\boldsymbol{m}_h^{i+1/2} - \widetilde{\boldsymbol{m}}_h^{i+1/2})\|_{\boldsymbol{L}^2(\omega)} \\ &\overset{\textbf{(D3)}}{\lesssim} \|\boldsymbol{m}_h^{i+1/2} - \widetilde{\boldsymbol{m}}_h^{i+1/2}\|_{\boldsymbol{L}^2(\omega)} \overset{(6.49b)}{=} \|\boldsymbol{d}_h^{i+1/2}\|_{\boldsymbol{L}^2(\omega)}.\end{aligned}$$

For the second term on the right-hand side of (6.56), we get that

$$\begin{aligned}&\|\boldsymbol{\Pi}_h(\boldsymbol{m}_h^{i+1/2}) - \boldsymbol{\Pi}_h(\widetilde{\boldsymbol{m}}_h^{i+1/2})\|_{\boldsymbol{L}^2(\omega)} \\ &\overset{\textbf{(M2)}}{\lesssim} h^{-1}\left[1 + \|\boldsymbol{m}_h^{i+1/2}\|_{\boldsymbol{L}^\infty(\omega)} + \|\widetilde{\boldsymbol{m}}_h^{i+1/2}\|_{\boldsymbol{L}^\infty(\omega)}\right] \|\boldsymbol{m}_h^{i+1/2} - \widetilde{\boldsymbol{m}}_h^{i+1/2}\|_{\boldsymbol{L}^2(\omega)} \\ &\overset{(6.50)}{\lesssim} h^{-1}\,\|\boldsymbol{m}_h^{i+1/2} - \widetilde{\boldsymbol{m}}_h^{i+1/2}\|_{\boldsymbol{L}^2(\omega)} \overset{(6.49b)}{=} h^{-1}\,\|\boldsymbol{d}_h^{i+1/2}\|_{\boldsymbol{L}^2(\omega)}.\end{aligned}$$

Together with the norm equivalence relation $\|\cdot\|_h \simeq \|\cdot\|_{\boldsymbol{L}^2(\omega)}$ from Lemma 3.3.1(i), we arrive at

$$T_2 \lesssim kh^{-1}\,\|\boldsymbol{d}_h^{i+1/2}\|_h^2.$$

Step 5. We combine **Step 1**–**Step 4** and obtain that

$$\begin{aligned}0 &\overset{(6.54)}{=} \|\boldsymbol{d}_h^{i+1/2}\|_h^2 + \frac{C_{\mathbf{ex}}}{2}k\,\langle \boldsymbol{m}_h^{i+1/2} \times \Delta_h\boldsymbol{d}_h^{i+1/2}, \boldsymbol{d}_h^{i+1/2}\rangle_h + \frac{k}{2}\,\langle \boldsymbol{m}_h^{i+1/2} \times \boldsymbol{\mathcal{R}}_h, \boldsymbol{d}_h^{i+1/2}\rangle_h \\ &\geq \left(1 - Ckh^{-1}\right)\|\boldsymbol{d}_h^{i+1/2}\|_h^2,\end{aligned}$$

where $C > 0$ is independent of $h, k > 0$. With $k = \mathbf{o}(h)$ and for sufficiently small $k > 0$, the latter factor is positive and we obtain that $\boldsymbol{d}_h^{i+1/2} = \mathbf{0}$ and thus $\boldsymbol{m}_h^{i+1} = \widetilde{\boldsymbol{m}}_h^{i+1}$. This concludes the proof. □

Remark 6.7.3. *If the assumption* (6.48) *fails to hold, we cannot make the last estimate in* **Step 3** *of the latter proof. Arguing along the same lines, we arrive in this case at*

$$0 \geq \left(1 - Ckh^{-1}\left[1 + \|\nabla\overline{\boldsymbol{m}}_{hk}\|_{\boldsymbol{L}^\infty(\omega_T)}\right]\right)\|\boldsymbol{d}_h^{i+1/2}\|_h^2,$$

where $C > 0$ does not depend on $h, k > 0$. In order for the factor in the latter estimate to be positive, an inverse estimate (see Proposition 3.1.8) and Theorem 6.5.1(a) *yield that*

$$kh^{-1}\left[1 + \|\nabla\overline{\boldsymbol{m}}_{hk}\|_{\boldsymbol{L}^\infty(\omega_T)}\right] \lesssim kh^{-2}\,\|\overline{\boldsymbol{m}}_{hk}\|_{\boldsymbol{L}^\infty(\omega_T)} \lesssim kh^{-2}\,\|\boldsymbol{m}_h^0\|_{\boldsymbol{L}^\infty(\omega_T)} \overset{\textbf{(M1)}}{\lesssim} kh^{-2}.$$

Hence, without (6.48), *the statement of Theorem 6.7.1 remains valid under the CFL-type condition $k = \mathbf{o}(h^2)$. However, this is the classical bi-product of the convergence result of the fixpoint iteration; see, e.g., [BP06, BBP08, BPS09] or Theorem 6.6.12.*

7. Decoupled midpoint scheme for SDLLG

7.1. Introduction

In this chapter, we extend the (formally) second-order in time midpoint scheme from Chapter 6 to the SDLLG system (2.23).

As far as coupled LLG systems are concerned, the midpoint scheme was so far only extended to the coupling of LLG with the full Maxwell system [BBP08]. There, the implicit nature of the midpoint rule gives rise to a fully-coupled non-linear system for the approximations to the LLG variable and the Maxwell variables, which increases the computational complexity of the method.

For the coupled SDLLG system, the works [AHP$^+$14, ARB$^+$15, Rug16] formulate and analyze a first-order in time tangent plane scheme. In particular, these works employ an explicit Euler approach to the coupling term, which even decouples the computation of $\boldsymbol{m}_h^{i+1} \approx \boldsymbol{m}(t_{i+1})$ and $\boldsymbol{s}_h^{i+1} \approx \boldsymbol{s}(t_{i+1})$.

With the midpoint scheme for the coupling of LLG with the full Maxwell system [BBP08, Algorithm 1.2] and the corresponding tangent plane scheme for SDLLG [AHP$^+$14, ARB$^+$15, Rug16] at hand, the formulation and analysis of the corresponding midpoint scheme for (2.23) seems (relatively) straightforward. However, we identify the following issues:

- The straightforward fully coupled approach in the virtue of [BBP08] gives rise to a numerically expensive fully coupled system for the computation of $\boldsymbol{m}_h^{i+1} \approx \boldsymbol{m}(t_{i+1})$ and $\boldsymbol{s}_h^{i+1} \approx \boldsymbol{s}(t_{i+1})$. The explicit Euler-approach from the first-order tangent plane [AHP$^+$14, ARB$^+$15, Rug16] for the coupling term is feasible, however, reduces the superior (formal) convergence order of the midpoint scheme from second to first order in time.

- Surprisingly, the implicit midpoint approach for the spin diffusion equation prevents an easy combination of the techniques of, e.g., [AHP$^+$14, ARB$^+$15, Rug16, PRS18] and Chapter 6, respectively, for the verification of the energy estimate (2.27).

7.1.1. Contributions

In this chapter, we make the following contributions, which are novel and have not been published elsewhere.

- We extend the midpoint scheme for plain LLG from [PRS18] and Chapter 6, respectively, to the setting of SDLLG (2.23).

- We employ an explicit second-order in time approach for the coupling term, which decouples the computations of $\boldsymbol{m}_h^{i+1} \approx \boldsymbol{m}(t_{i+1})$ and $\boldsymbol{s}_h^{i+1} \approx \boldsymbol{s}(t_{i+1})$. In particular, this greatly reduces the computational complexity of the overall integrator.

- We prove well-posedness and unconditional convergence of our extension of the midpoint scheme towards a weak solution of SDLLG in the sense of Definition 2.2.4(i)–(iv); see Section 7.3.
- Under the CFL-type condition $k = \mathcal{O}(h^2)$, we prove convergence towards a physical weak solution in the sense of Definition 2.2.4(i)–(v); see Section 7.3.5.

Note that the own work [DPP+17] makes corresponding contributions for the (almost) second-order tangent plane scheme for ELLG; see Chapter 5. Moreover, we stress that our implementation for the numerical experiments of this work does not yet include the proposed midpoint scheme for SDLLG, i.e., we have no means to underpin the theoretical findings of this chapter with numerical experiments.

7.2. Algorithm

In this section, we formulate an extension of the IMEX midpoint scheme for plain LLG to SDLLG (2.23), which computes approximations

$$\boldsymbol{\mathcal{S}}_h \ni \boldsymbol{m}_h^i \approx \boldsymbol{m}(t_i) \quad \text{and} \quad \boldsymbol{\mathcal{S}}_h^\Omega \ni \boldsymbol{s}_h^i \approx \boldsymbol{s}(t_i) \quad \text{for all } i = 0, \dots, M.$$

For the LLG part (2.23a), we proceed as in Section 6, where we extended [BP06] from $\boldsymbol{h}_{\mathrm{eff}}(\boldsymbol{m}) = \Delta \boldsymbol{m}$ and $\boldsymbol{\Pi}(\boldsymbol{m}) = \boldsymbol{0}$ to our setting of LLG (2.3). For the spin diffusion part (2.23b), we adapt the decoupled tangent plane scheme for SDLLG from [AHP+14, ARB+15, Rug16]. Moreover, we also build on the fully-coupled midpoint scheme for the coupled Maxwell-LLG system from [BBP08]. To formulate our algorithm, we adopt from Chapter 6 the implicit-explicit approaches

$$\boldsymbol{\pi}_h^{\boldsymbol{\Theta}}(\boldsymbol{m}_h^{i+1}, \boldsymbol{m}_h^i, \boldsymbol{m}_h^{i-1}) \approx \boldsymbol{\pi}(\boldsymbol{m}(t_i + k/2)) \quad \text{and} \quad \boldsymbol{\Pi}_h^{\boldsymbol{\Theta}}(\boldsymbol{m}_h^{i+1}, \boldsymbol{m}_h^i, \boldsymbol{m}_h^{i-1}) \approx \boldsymbol{\Pi}(\boldsymbol{m}(t_i + k/2))$$

from **(A1)**–**(A3)**. Accordingly, we define the coupling term $\boldsymbol{s}_h^{i,\boldsymbol{\Theta}}$ with one of the following three options:

(C1) The implicit and formally second-order in time midpoint approach [BBP08]

$$\boldsymbol{s}_h^{i,\boldsymbol{\Theta}} := \boldsymbol{s}_h^{i+1/2} \in \boldsymbol{\mathcal{S}}_h^\Omega.$$

(C2) The explicit and formally second-order in time Adams–Bashforth approach

$$\boldsymbol{\mathcal{S}}_h^\Omega \ni \boldsymbol{s}_h^{i,\boldsymbol{\Theta}} := \begin{cases} \boldsymbol{s}_h^{i+1/2} & \text{for } i = 0, \\ \frac{3}{2}\, \boldsymbol{s}_h^i - \frac{1}{2}\, \boldsymbol{s}_h^{i-1} & \text{else.} \end{cases}$$

(C3) The explicit and formally first-order in time Euler approach [AHP+14, ARB+15, Rug16]

$$\boldsymbol{s}_h^{i,\boldsymbol{\Theta}} := \boldsymbol{s}_h^i \in \boldsymbol{\mathcal{S}}_h^\Omega.$$

Moreover, we introduce the approximation to the spin current $\boldsymbol{j}$ as

$$\boldsymbol{\mathcal{S}}_h^\Omega \ni \boldsymbol{j}_h^i \approx \boldsymbol{j}(t_i) \quad \text{for all } i \in \{0, 1, \ldots, M\}.$$

Finally, given $\boldsymbol{\mu} \in \boldsymbol{L}^\infty(\omega)$, we recall from (2.24) the $\boldsymbol{\mu}$-dependent bilinear form

$$\begin{aligned}\boldsymbol{a}(\boldsymbol{\mu}; \boldsymbol{\zeta}_1, \boldsymbol{\zeta}_2) := \langle D_0 \nabla \boldsymbol{\zeta}_1, \nabla \boldsymbol{\zeta}_2 \rangle_{\boldsymbol{L}^2(\Omega)} - \beta\beta' \langle D_0 (\boldsymbol{\mu} \otimes \boldsymbol{\mu}) \nabla \boldsymbol{\zeta}_1, \nabla \boldsymbol{\zeta}_2 \rangle_{\boldsymbol{L}^2(\omega)} \\ + \langle D_0 \boldsymbol{\zeta}_1, \boldsymbol{\zeta}_2 \rangle_{\boldsymbol{L}^2(\Omega)} + \langle D_0 (\boldsymbol{\zeta}_1 \times \boldsymbol{\mu}), \boldsymbol{\zeta}_2 \rangle_{\boldsymbol{L}^2(\omega)} \quad \text{for all } \boldsymbol{\zeta}_1, \boldsymbol{\zeta}_2 \in \boldsymbol{H}^1(\Omega),\end{aligned}$$

where, for the sake of readability, we suppose exact evaluation of $D_0 \in \boldsymbol{L}^\infty(\Omega)$ with $D_0 \geq D > 0$. With these preparations, we are ready to formulate our algorithm.

Algorithm 7.2.1 (MPS for SDLLG)**. Input:** *Approximations* $\boldsymbol{m}_h^{-1} := \boldsymbol{m}_h^0 \in \boldsymbol{\mathcal{S}}_h$ *and* $\boldsymbol{s}_h^{-1} := \boldsymbol{s}_h^0 \in \boldsymbol{\mathcal{S}}_h^\Omega$.
Loop: *For* $i = 0, \ldots, M-1$*, find* $\boldsymbol{m}_h^{i+1} \in \boldsymbol{\mathcal{S}}_h$ *and* $\boldsymbol{s}_h^{i+1} \in \boldsymbol{\mathcal{S}}_h^\Omega$ *such that for all* $\boldsymbol{\varphi}_h \in \boldsymbol{\mathcal{S}}_h$*, it holds that*

$$\begin{aligned}&\langle \mathrm{d_t} \boldsymbol{m}_h^{i+1}, \boldsymbol{\varphi}_h \rangle_h = \\ &\quad - C_{\mathbf{ex}} \langle \boldsymbol{m}_h^{i+1/2} \times \Delta_h \boldsymbol{m}_h^{i+1/2}, \boldsymbol{\varphi}_h \rangle_h - \langle \boldsymbol{m}_h^{i+1/2} \times \boldsymbol{\mathcal{P}}_h \boldsymbol{\pi}_h^{\boldsymbol{\Theta}}(\boldsymbol{m}_h^{i+1}, \boldsymbol{m}_h^i, \boldsymbol{m}_h^{i-1}), \boldsymbol{\varphi}_h \rangle_h \\ &\quad - \langle \boldsymbol{m}_h^{i+1/2} \times \boldsymbol{\mathcal{P}}_h \boldsymbol{\Pi}_h^{\boldsymbol{\Theta}}(\boldsymbol{m}_h^{i+1}, \boldsymbol{m}_h^i, \boldsymbol{m}_h^{i-1}), \boldsymbol{\varphi}_h \rangle_h - \langle \boldsymbol{m}_h^{i+1/2} \times \boldsymbol{\mathcal{P}}_h \boldsymbol{f}_h^{i+1/2}, \boldsymbol{\varphi}_h \rangle_h \\ &\quad - \langle \boldsymbol{m}_h^{i+1/2} \times \boldsymbol{\mathcal{P}}_h \boldsymbol{s}_h^{i,\boldsymbol{\Theta}}, \boldsymbol{\varphi}_h \rangle_h + \alpha \langle \boldsymbol{m}_h^{i+1/2} \times \mathrm{d_t} \boldsymbol{m}_h^{i+1}, \boldsymbol{\varphi}_h \rangle_h\end{aligned} \tag{7.1a}$$

and for all $\boldsymbol{\zeta}_h \in \boldsymbol{\mathcal{S}}_h^\Omega$*, it holds that*

$$\begin{aligned}&\langle \mathrm{d_t} \boldsymbol{s}_h^{i+1}, \boldsymbol{\zeta}_h \rangle_{\boldsymbol{L}^2(\Omega)} + \boldsymbol{a}(\boldsymbol{m}_h^{i+1/2}; \boldsymbol{s}_h^{i+1/2}, \boldsymbol{\zeta}_h) = \\ &\qquad \beta \langle \boldsymbol{m}_h^{i+1/2} \otimes \boldsymbol{j}_h^{i+1/2}, \nabla \boldsymbol{\zeta}_h \rangle_{\boldsymbol{L}^2(\Omega)} + \beta \langle \boldsymbol{j}_h^{i+1/2} \cdot \boldsymbol{n}, \boldsymbol{m}_h^{i+1/2} \cdot \boldsymbol{\zeta}_h \rangle_{\boldsymbol{L}^2(\partial\Omega \cap \partial\omega)}.\end{aligned} \tag{7.1b}$$

Output: *Approximations* $\boldsymbol{m}_h^i \approx \boldsymbol{m}(t_i)$ *and* $\boldsymbol{s}_h^i \approx \boldsymbol{s}(t_i)$. □

Remark 7.2.2. (i) *The explicit approaches* **(C2)** *for* $i > 0$ *and* **(C3)** *decouple the time-stepping in the latter Algorithm. Then, the coupling term* $\boldsymbol{s}_h^{i,\boldsymbol{\Theta}}$ *in the LLG part* (7.1a) *plays the role of another, explicitly available contribution to the dissipative effects. In particular, we can successively solve the non-linear LLG part for* $\boldsymbol{m}_h^{i+1}$ *and the linear spin diffusion part* (7.1b) *for* $\boldsymbol{s}_h^{i+1}$.

(ii) *To solve the non-linear system from the LLG part* (7.1a) *from* (i)*, we suggest the fixed-point iteration for plain LLG from Section 6.6. Under the CFL-type condition* $k = \mathbf{o}(h^2)$*, the fixed-point iterates converge towards a unique solution. In Section 7.2.1 we formulate the resulting (inexact) decoupled algorithm.*

(iii) *With* $\boldsymbol{s}_h^{i,\boldsymbol{\Theta}} = \boldsymbol{s}_h^{i+1/2}$ *from the implicit approaches, the system* (7.1) *is non-linear and fully-coupled, but admits a solution; see Theorem 7.3.1*(a) *for details. However, not even under the CFL-type condition* $k = \mathbf{o}(h^2)$*, we succeeded in proving uniqueness or convergence of the corresponding fixed-point iteration. This is due to the fact that the bilinear form* $\boldsymbol{a}(\boldsymbol{m}_h^{i+1/2}; \cdot, \cdot)$ *in the spin diffusion part* (7.1b) *depends on the sought* $\boldsymbol{m}_h^{i+1}$.

(iv) *In practice, we suggest to solve the spin diffusion part* (7.1b) *for the unknown* $\boldsymbol{\sigma}_h := \boldsymbol{s}_h^{i+1/2} \in \boldsymbol{\mathcal{S}}_h^\Omega$, *i.e., compute the unique* $\boldsymbol{\sigma}_h \in \boldsymbol{\mathcal{X}}_h$ *such that*

$$\begin{aligned} &2\,\langle \boldsymbol{\sigma}_h, \boldsymbol{\zeta}_h \rangle_{\boldsymbol{L}^2(\Omega)} + k\,\boldsymbol{a}(\boldsymbol{m}_h^{i+1/2}; \boldsymbol{\sigma}_h, \boldsymbol{\zeta}_h) \\ &\quad = 2\,\langle \boldsymbol{s}_h^i, \boldsymbol{\zeta}_h \rangle_{\boldsymbol{L}^2(\Omega)} + \beta k\,\langle \boldsymbol{m}_h^{i+1/2} \otimes \boldsymbol{j}_h^{i+1/2}, \nabla \boldsymbol{\zeta}_h \rangle_{\boldsymbol{L}^2(\Omega)} \\ &\qquad + \beta k\,\langle \boldsymbol{j}_h^{i+1/2} \cdot \boldsymbol{n}, \boldsymbol{m}_h^{i+1/2} \cdot \boldsymbol{\zeta}_h \rangle_{\boldsymbol{L}^2(\partial\Omega \cap \partial\omega)} \quad \textit{for all } \boldsymbol{\zeta}_h \in \boldsymbol{\mathcal{S}}_h^\Omega. \end{aligned}$$

In particular, this system is linear in $\boldsymbol{\sigma}_h$ *and* $\boldsymbol{s}_h^{i+1} := 2\boldsymbol{\sigma}_h - \boldsymbol{s}_h^i$ *solves the spin diffusion part* (7.1b).

7.2.1. Decouple the (inexact) time-stepping

In this section, we present one time-step of Algorithm 7.2.1 in its ideal form. For $i > 0$, we exploit the advantages of the explicit second-order in time approaches and employ the explicit second-order Adams–Bashforth approach

$$\boldsymbol{s}_h^{i,\boldsymbol{\Theta}} = \frac{3}{2}\,\boldsymbol{s}_h^i - \frac{1}{2}\,\boldsymbol{s}_h^{i-1}, \tag{7.2a}$$

from **(C2)** for the coupling term as well as the explicit Adams–Bashforth approaches

$$\boldsymbol{\pi}_h^{\boldsymbol{\Theta}}(\boldsymbol{m}_h^{i+1}, \boldsymbol{m}_h^i, \boldsymbol{m}_h^{i-1}) = \frac{3}{2}\,\boldsymbol{\pi}_h(\boldsymbol{m}_h^i) - \frac{1}{2}\,\boldsymbol{\pi}_h(\boldsymbol{m}_h^{i-1}), \quad \text{and} \tag{7.2b}$$

$$\boldsymbol{\Pi}_h^{\boldsymbol{\Theta}}(\boldsymbol{m}_h^{i+1}, \boldsymbol{m}_h^i, \boldsymbol{m}_h^{i-1}) = \frac{3}{2}\,\boldsymbol{\Pi}_h(\boldsymbol{m}_h^i) - \frac{1}{2}\,\boldsymbol{\Pi}_h(\boldsymbol{m}_h^{i-1}) \tag{7.2c}$$

from **(A2)** for the lower-order terms. In particular, $\boldsymbol{s}_h^{i,\boldsymbol{\Theta}}$ is independent of the sought $\boldsymbol{s}_h^{i+1}$ and can be interpreted as a further, explicitly available dissipative effect. This way, we decouple the time-stepping and can compute sequentially $\boldsymbol{m}_h^{i+1}$ and $\boldsymbol{s}_h^{i+1}$. Following Remark 7.2.2(i), we employ a fixed-point iteration for the inexact solution of the LLG part (7.1a). Moreover, we employ the nodewise systems of Section 6.6.3. To this end, we recall from (6.28a) the notion of the approximate effective field and dissipative effects $\boldsymbol{\mathcal{H}}_h^i(\cdot)$, which, in the setting of (7.2) reads

$$\begin{aligned} \boldsymbol{\mathcal{H}}_h^i(\boldsymbol{\mu}_h) := C_{\mathbf{ex}}\Delta_h\boldsymbol{\mu}_h + \frac{3}{2}\,\boldsymbol{\mathcal{P}}_h\boldsymbol{\pi}_h(\boldsymbol{m}_h^i) - \frac{1}{2}\,\boldsymbol{\mathcal{P}}_h\boldsymbol{\pi}_h(\boldsymbol{m}_h^{i-1}) + \boldsymbol{\mathcal{P}}_h\boldsymbol{f}_h^{i+1/2} \\ + \frac{3}{2}\,\boldsymbol{\mathcal{P}}_h\boldsymbol{\Pi}_h(\boldsymbol{m}_h^i) - \frac{1}{2}\,\boldsymbol{\mathcal{P}}_h\boldsymbol{\Pi}_h(\boldsymbol{m}_h^{i-1}) + \frac{3}{2}\,\boldsymbol{\mathcal{P}}_h\boldsymbol{s}_h^i - \frac{1}{2}\,\boldsymbol{\mathcal{P}}_h\boldsymbol{s}_h^{i-1} \in \boldsymbol{\mathcal{S}}_h. \end{aligned} \tag{7.3}$$

Algorithm 7.2.3 (Inexact decoupled second-order MPS for SDLLG, $i > 0$)**. Input.** $i > 0$ *with approximations* $\boldsymbol{\mathcal{S}}_h \ni \boldsymbol{m}_h^i \approx \boldsymbol{m}(t_i)$, $\boldsymbol{\mathcal{S}}_h \ni \boldsymbol{m}_h^{i-1} \approx \boldsymbol{m}(t_{i-1})$ *and* $\boldsymbol{\mathcal{S}}_h^\Omega \ni \boldsymbol{s}_h^i \approx \boldsymbol{s}(t_i)$, $\boldsymbol{\mathcal{S}}_h^\Omega \ni \boldsymbol{s}_h^{i-1} \approx \boldsymbol{s}(t_{i-1})$, *iteration tolerance* $\varepsilon > 0$. *Iterate the following steps* (a)–(e)*:*

(a) *Set* $\boldsymbol{\mu}_h^{(0)} := \boldsymbol{m}_h^i$ *and compute* $\boldsymbol{\mathcal{H}}_h^i(\boldsymbol{\mu}_h^{(0)}) \in \boldsymbol{\mathcal{S}}_h$; *see Lemma 6.6.6.*

(b) **Loop.** *For* $\ell = 1, 2, \ldots$, *repeat the following steps* (b-i)–(b-ii) *until*

$$\|\Delta_h\boldsymbol{\mu}_h^{(\ell+1)} - \Delta_h\boldsymbol{\mu}_h^{(\ell)}\|_h < \frac{\varepsilon}{C_{\mathbf{ex}}}:$$

(b-i) *Compute* $\boldsymbol{\mu}_h^{(\ell+1)} \in \boldsymbol{\mathcal{S}}_h$ *via the nodewise systems*

$$\mathbf{A}_j^{(\ell)} \left[\boldsymbol{\mu}_h^{(\ell+1)}(\boldsymbol{z}_j)\right] = \boldsymbol{m}_h^i(\boldsymbol{z}_j) \quad \textit{for all } j = 1, \dots, N,$$

where $\mathbf{A}_j^{(\ell)} \in \mathbb{R}^{3\times 3}$ *are the nodewise defined matrices*

$$\mathbf{A}_j^{(\ell)} := \mathbf{I} - \frac{k}{2}\big[\big(\boldsymbol{\mathcal{H}}_h^i(\boldsymbol{\mu}_h^{(\ell)})\big)(\boldsymbol{z}_j)\big]_\times - \frac{\alpha k}{2}\big[\,\boldsymbol{m}_h^i(\boldsymbol{z}_j)\big]_\times.$$

(b-ii) *Compute* $\boldsymbol{\mathcal{H}}_h^i(\boldsymbol{\mu}_h^{(\ell+1)}) \in \boldsymbol{\mathcal{S}}_h$*; see Lemma 6.6.6.*

(c) *Set* $\boldsymbol{m}_h^{i+1} := 2\boldsymbol{\mu}_h^{(\ell+1)} - \boldsymbol{m}_h^i \in \boldsymbol{\mathcal{S}}_h$.

(d) *Find* $\boldsymbol{\sigma}_h \in \boldsymbol{\mathcal{S}}_h^\Omega$ *such that*

$$\begin{aligned} 2\,\langle \boldsymbol{\sigma}_h, \boldsymbol{\zeta}_h\rangle_{\boldsymbol{L}^2(\Omega)} &+ k\,\boldsymbol{a}(\boldsymbol{m}_h^{i+1/2}; \boldsymbol{\sigma}_h, \boldsymbol{\zeta}_h) \\ &= 2\,\langle \boldsymbol{s}_h^i, \boldsymbol{\zeta}_h\rangle_{\boldsymbol{L}^2(\Omega)} + \beta k\,\langle \boldsymbol{m}_h^{i+1/2} \otimes \boldsymbol{j}_h^{i+1/2}, \nabla\boldsymbol{\zeta}_h\rangle_{\boldsymbol{L}^2(\Omega)} + \beta k\,\langle \boldsymbol{j}_h^{i+1/2}\cdot\boldsymbol{n}, \boldsymbol{m}_h^{i+1/2}\cdot\boldsymbol{\zeta}_h\rangle_{\boldsymbol{L}^2(\partial\Omega\cap\partial\omega)}, \end{aligned}$$

for all $\boldsymbol{\zeta}_h \in \boldsymbol{\mathcal{S}}_h^\Omega$.

(e) *Set* $\boldsymbol{s}_h^{i+1} := 2\boldsymbol{\sigma}_h - \boldsymbol{s}_h^i \in \boldsymbol{\mathcal{S}}_h^\Omega$.

Output. *Approximations* $\boldsymbol{m}_h^{i+1} \approx \boldsymbol{m}(t_{i+1})$ *and* $\boldsymbol{s}_h^{i+1} \approx \boldsymbol{s}(t_{i+1})$. □

Proposition 7.2.4 (Convergence of fixed-point iteration)**.** *Consider the fixed-point iteration from Algorithm 7.2.3. The fixed-point iterates* $(\boldsymbol{\mu}_h^{(\ell)})_{\ell=0}^\infty$ *are well-defined. There exists a constant* $C > 0$*, which depends only on* $C_{\mathbf{ex}}$ *and* $C_{\mathbf{mesh}}$*, such that, for all* $h, k > 0$*, which satisfy the CFL-type condition*

$$\big(\,1 + \|\boldsymbol{m}_h^i\|_{\boldsymbol{L}^\infty(\omega)}^2\big)\,k\,h^{-2} \,<\, C,$$

the sequence of iterates $(\boldsymbol{\mu}_h^{(\ell)})_{\ell=0}^\infty$ *is a contraction in* $\boldsymbol{L}^2(\omega)$*. Then, there exists a unique* $\boldsymbol{\mu}_h \in \boldsymbol{\mathcal{S}}_h$ *such that*

$$\boldsymbol{\mu}_h^{(\ell)} \to \boldsymbol{\mu}_h \quad \textit{in } \boldsymbol{L}^2(\omega) \quad \textit{as } \ell \to \infty.$$

In particular, $\boldsymbol{m}_h^{i+1} := 2\boldsymbol{\mu}_h - \boldsymbol{m}_h^i$ *is the unique solution of the LLG-part* (7.1a).

Proof. The $\boldsymbol{s}_h^i$- and $\boldsymbol{s}_h^{i-1}$-terms in the functional $\boldsymbol{\mathcal{H}}_h^i(\cdot)$ from (7.3) play the role of another explicitly available dissipative effect. Hence, the proof follows as for plain LLG–see Proposition 6.6.2, Proposition 6.6.3, and Remark 6.6.4 (iii). □

7.3. Main result

In this section, we formulate and prove a convergence result for our midpoint scheme for SDLLG. Recall that for plain LLG, we extended in Chapter 6 the convergence result from [BP06] to our extended setting of LLG. For coupled equations, a similar convergence result is proved in [BBP08] for a fully coupled midpoint scheme for Maxwell-LLG. For SDLLG, similar results for the first-order tangent plane scheme are proved in [AHP⁺14, Rug16]. Our result combines and extends the latter findings for our midpoint scheme for SDLLG. To this end, we require the following additional assumptions:

(S1) Uniform boundedness of $\boldsymbol{m}_h^0$: For all $h > 0$, it holds that $\beta\beta' \|\boldsymbol{m}_h^0\|^2_{\boldsymbol{L}^\infty(\Omega)} \leq \gamma < 1$.

(S2) Weak consistency of $\boldsymbol{s}_h^0$: It holds that $\boldsymbol{s}_h^0 \rightharpoonup \boldsymbol{s}^0$ in $\boldsymbol{L}^2(\Omega)$ as $h \to 0$.

(S3) Strong consistency of $(\boldsymbol{j}_h^i)_{i=0}^M$: The postprocessed output $\overline{\boldsymbol{j}}_{hk} \in L^2(0,T;\boldsymbol{H}^1(\Omega))$ of $(\boldsymbol{j}_h^i)_{i=0}^M$ satisfies that

$$\overline{\boldsymbol{j}}_{hk} \to \boldsymbol{j} \quad \text{in } L^2(0,T;\boldsymbol{H}^1(\Omega)) \quad \text{as } h,k \to 0.$$

For the stronger statement from Theorem 7.3.1(c) below, we additionally require the following assumption:

(CFL) CFL-type condition: It holds that $k = \mathcal{O}(h^2)$.

With these preparations, we are ready to formulate our theorem.

Theorem 7.3.1 (Convergence of MPS for SDLLG)**.** *Consider Algorithm 7.2.1 for the discretization of SDLLG* (2.23)*. Then, the following three assertions* (a)–(c) *hold true:*

(a) *Suppose that*

- *the approximations $\boldsymbol{m}_h^0$ satisfy* **(S1)**
- *the approximation operators $\boldsymbol{\pi}_h$ are linear* **(D2)***;*
- *the approximation operators $\boldsymbol{\Pi}_h$ satisfy the Lipschitz-type condition* **(M2)***.*

Then, Algorithm 7.2.1 is well-posed and for all $i \in \{0,\dots,M-1\}$, it holds that

$$|\boldsymbol{m}_h^{i+1}(z)| = |\boldsymbol{m}_h^0(z)| \quad \textit{for all nodes } \boldsymbol{z} \in \mathcal{N}_h.$$

In particular, it holds that $\|\boldsymbol{m}_h^i\|_h = \|\boldsymbol{m}_h^0\|_h$ and $\|\boldsymbol{m}_h^i\|_{\boldsymbol{L}^\infty(\omega)} = \|\boldsymbol{m}_h^0\|_{\boldsymbol{L}^\infty(\omega)}$ for all $i \in \{0,\dots,M\}$.

(b) *Suppose that*

- *$\boldsymbol{\pi}_h$, $(\boldsymbol{f}_h^i)_{i=0}^M$, and $\boldsymbol{\Pi}_h$ satisfy the assumptions of Theorem 6.5.1*(b) *for plain LLG;*
- *the approximations $\boldsymbol{m}_h^0$ satisfy* **(D1)** *and* **(S1)***;*
- *the approximations $\boldsymbol{s}_h^0$ satisfy* **(S2)***;*
- *the approximations $(\boldsymbol{j}_h^i)_{i=0}^M$ are strongly consistent* **(S3)***;*

- *the general coupling approach* $\boldsymbol{s}_h^{i,\boldsymbol{\Theta}}$ *is defined by one of the three options* **(C1)**–**(C3)**.

Then, there exists a subsequence of the postprocessed output $\boldsymbol{m}_{hk}$ *and* $\boldsymbol{s}_{hk}$ *from Algorithm 7.2.1, and a weak solution*

$$\boldsymbol{m} \in L^\infty(0,T;\boldsymbol{H}^1(\omega)) \cap \boldsymbol{H}^1(\omega_T) \quad \text{and}$$
$$\boldsymbol{s} \in L^\infty(0,T;\boldsymbol{L}^2(\Omega)) \cap W(0,T;\boldsymbol{L}^2(\Omega),\boldsymbol{H}^1(\Omega))$$

of SDLLG (2.23) *in the sense of Definition 2.2.4*(i)–(iv) *such that*

$$\boldsymbol{m}_{hk} \rightharpoonup \boldsymbol{m} \quad \text{in } \boldsymbol{H}^1(\omega_T) \quad \text{and} \quad \boldsymbol{s}_{hk} \rightharpoonup \boldsymbol{s} \quad \text{in } \boldsymbol{L}^2(\Omega_T) \quad \text{as } h,k \to 0.$$

(c) *Additionally to the assumptions from* (b), *suppose that* $\boldsymbol{m}_h^0$ *satisfies* **(D1$^+$)** *and that there holds the CFL-type condition* **(CFL)**. *Then,* $(\boldsymbol{m},\boldsymbol{s})$ *from* (b) *is a physical weak solution in the sense of Definition 2.2.4*(i)–(v), *i.e., it additionally satisfies the stronger energy estimate* (2.27).

Remark 7.3.2. (i) *Uniform boundedness* **(S1)** *of* $\boldsymbol{m}_h^0$ *for Theorem 7.3.1 is stronger than the corresponding uniform boundedness* **(M1)** *in Theorem 6.5.1 for plain LLG. We already require* **(S1)** *to prove that Algorithm 7.2.1 is well-posed. Moreover, since* $0 < \beta, \beta' < 1$, **(S1)** *allows the natural case that* $\boldsymbol{m}_h^0 \in \boldsymbol{\mathcal{M}}_h$.

(ii) *In contrast to the unconditional convergence results from [AHP$^+$14, Rug16] for the first-order tangent plane scheme for SDLLG, we require the CFL-type condition* $k = \mathcal{O}(h^2)$ *to prove Theorem 7.3.1*(c).

(iii) *For the validity of the assumptions for our exemplary contributions to* $\boldsymbol{\pi}_h$ *and* $\boldsymbol{\Pi}_h$, *the situation is precisely the same as in Remark 6.5.2*(ii)–(iv) *for plain LLG.*

(iv) *Recall from Remark 7.2.2*(ii) *that for the implicit approaches* $\boldsymbol{s}_h^{i,\boldsymbol{\Theta}} = \boldsymbol{s}_h^{i+1/2}$ *convergence of a corresponding fixed-point iteration —even under the CFL-type condition* $k = \mathbf{o}(h^2)$— *remains mathematically open.*

We split the proof of Theorem 7.3.1 into the following subsections. In Section 7.3.1, we prove well-posedness (a). To prove (b), we use a standard energy argument (see, e.g., [Eva10]), which consists of the following three steps:

- We derive a discrete energy bound for the output of Algorithm 7.2.1; see Section 7.3.2.
- We extract weakly convergent subsequences and identify the limits; see Section 7.3.3.
- We verify that the limit $(\boldsymbol{m},\boldsymbol{s})$ is a weak solution of SDLLG in the sense of Definition 2.2.4(i)–(iv) and thus conclude the proof of (b); see Section 7.3.4.

In Section 7.3.5, we prove (c). To this end, we extend the concept of the postprocessed output to the coupling term $\boldsymbol{s}_h^{i,\boldsymbol{\Theta}}$ and write

$$\boldsymbol{s}_{hk}^{\boldsymbol{\Theta}}(t) := \boldsymbol{s}_h^{i,\boldsymbol{\Theta}} \quad \text{for } t \in [t_i, t_{i+1}), \quad \text{where} \quad i \in \{0,1,\ldots,M-1\}. \tag{7.4}$$

7.3.1. Well-posedness

In this section, we prove Theorem 7.3.1(a), i.e., we show that Algorithm 7.2.1 is well-posed. Essentially, the proof is contained in the following adaption of [BPS09, Lemma 5.1]. It is based on a corollary of the Brouwer fixed-point theorem (see Theorem B.2.5).

Proposition 7.3.3 (Well-posedness of MPS for SDLLG, one time-step). *Suppose linearity* **(D2)** *of* $\boldsymbol{\pi}_h$ *as well as the Lipschitz-type continuity* **(M2)** *of* $\boldsymbol{\Pi}_h$. *Let* $i \in \{0, \dots, M-1\}$. *Let* $\boldsymbol{m}_h^i, \boldsymbol{m}_h^{i-1} \in \boldsymbol{\mathcal{S}}_h$ *with*

$$\beta\beta' \, \|\boldsymbol{m}_h^i\|_{\boldsymbol{L}^\infty(\omega)}^2 \;\le\; \gamma \;<\; 1. \tag{7.5}$$

and $\boldsymbol{s}_h^i, \boldsymbol{s}_h^{i-1} \in \boldsymbol{\mathcal{S}}_h^\Omega$. *Then, there exist* $\boldsymbol{m}_h^{i+1} \in \boldsymbol{\mathcal{S}}_h$ *and* $\boldsymbol{s}_h^{i+1} \in \boldsymbol{\mathcal{S}}_h^\Omega$, *which solve the discrete variational formulation* (7.1). *Moreover,*

$$|\boldsymbol{m}_h^{i+1}(\boldsymbol{z})| = |\boldsymbol{m}_h^i(\boldsymbol{z})| \quad \text{for all nodes } \boldsymbol{z} \in \mathcal{N}_h.$$

In particular, it holds that $\|\boldsymbol{m}_h^{i+1}\|_{\boldsymbol{L}^\infty(\omega)} = \|\boldsymbol{m}_h^i\|_{\boldsymbol{L}^\infty(\omega)}$ *as well as* $\|\boldsymbol{m}_h^{i+1}\|_h = \|\boldsymbol{m}_h^i\|_h$.

Proof. We split the proof into the following five steps.

Step 1. We make preliminary definitions: We define the product space $\boldsymbol{X}_h := \boldsymbol{\mathcal{S}}_h \times \boldsymbol{\mathcal{S}}_h^\Omega$, endow it with the inner product

$$\langle(\boldsymbol{\varphi}_h, \boldsymbol{\zeta}_h), (\widetilde{\boldsymbol{\varphi}}_h, \widetilde{\boldsymbol{\zeta}}_h)\rangle_{\boldsymbol{X}_h} := \langle \boldsymbol{\varphi}_h, \widetilde{\boldsymbol{\varphi}}_h\rangle_h + \langle \boldsymbol{\zeta}_h, \widetilde{\boldsymbol{\zeta}}_h\rangle_{\boldsymbol{L}^2(\Omega)} \quad \text{for all } (\boldsymbol{\varphi}_h, \boldsymbol{\zeta}_h), (\widetilde{\boldsymbol{\varphi}}_h, \widetilde{\boldsymbol{\zeta}}_h) \in \boldsymbol{X}_h \tag{7.6}$$

and denote the corresponding norm with $\|\cdot\|_{\boldsymbol{X}_h}$. Let $\boldsymbol{\mathcal{I}}_h : \boldsymbol{C}(\overline{\omega}) \to \boldsymbol{\mathcal{S}}_h$ and $\boldsymbol{\mathcal{I}}_h^\Omega : \boldsymbol{C}(\overline{\Omega}) \to \boldsymbol{\mathcal{S}}_h^\Omega$ be the nodal interpolants corresponding to $\boldsymbol{\mathcal{S}}_h$ and $\boldsymbol{\mathcal{S}}_h^\Omega$, respectively. Given $\boldsymbol{\varphi}_h \in \boldsymbol{\mathcal{S}}_h$ and $\boldsymbol{\zeta}_h \in \boldsymbol{\mathcal{S}}_h^\Omega$, let $\mathbf{A}(\boldsymbol{\varphi}_h; \boldsymbol{\zeta}_h) \in \boldsymbol{\mathcal{S}}_h^\Omega$ be the unique solution of

$$\langle \mathbf{A}(\boldsymbol{\varphi}_h; \boldsymbol{\zeta}_h), \boldsymbol{\psi}_h\rangle_{\boldsymbol{L}^2(\Omega)} = \mathbf{a}(\boldsymbol{\varphi}_h; \boldsymbol{\zeta}_h, \boldsymbol{\psi}_h) \quad \text{for all } \boldsymbol{\psi}_h \in \boldsymbol{\mathcal{S}}_h^\Omega. \tag{7.7a}$$

Given $\boldsymbol{\varphi}_h \in \boldsymbol{\mathcal{S}}_h$, let $\mathbf{R}(\boldsymbol{\varphi}_h) \in \boldsymbol{\mathcal{S}}_h^\Omega$ be the unique solution of

$$\begin{aligned}\langle \mathbf{R}(\boldsymbol{\varphi}_h), \boldsymbol{\zeta}_h\rangle_{\boldsymbol{L}^2(\Omega)} = &-\beta\langle \boldsymbol{\varphi}_h \otimes \boldsymbol{j}_h^{i+1/2}, \nabla\boldsymbol{\zeta}_h\rangle_{\boldsymbol{L}^2(\Omega)} \\ &- \beta\langle \boldsymbol{j}_h^{i+1/2} \cdot \boldsymbol{n}, \boldsymbol{\varphi}_h \cdot \boldsymbol{\zeta}_h\rangle_{\boldsymbol{L}^2(\partial\Omega\cap\partial\omega)} \quad \text{for all } \boldsymbol{\zeta}_h \in \boldsymbol{\mathcal{S}}_h^\Omega.\end{aligned} \tag{7.7b}$$

Step 2. We define an auxiliary mapping $\boldsymbol{\mathcal{F}}(\cdot,\cdot)$ on $\boldsymbol{X}_h$ via

$$\boldsymbol{\mathcal{F}} : \boldsymbol{X}_h \to \boldsymbol{X}_h : (\boldsymbol{\varphi}_h, \boldsymbol{\zeta}_h) \mapsto \begin{pmatrix} \boldsymbol{\mathcal{F}}^{(1)}(\boldsymbol{\varphi}_h, \boldsymbol{\zeta}_h) \\ \boldsymbol{\mathcal{F}}^{(2)}(\boldsymbol{\varphi}_h, \boldsymbol{\zeta}_h) \end{pmatrix}, \tag{7.8a}$$

where the mappings $\boldsymbol{\mathcal{F}}^{(1)}$ and $\boldsymbol{\mathcal{F}}^{(2)}$ are defined in the following: To this end, let $(\boldsymbol{\varphi}_h, \boldsymbol{\zeta}_h) \in \boldsymbol{X}_h$ and set

$$\boldsymbol{\mathcal{F}}^{(1)}(\boldsymbol{\varphi}_h, \boldsymbol{\zeta}_h) := \frac{2}{k}(\boldsymbol{\varphi}_h - \boldsymbol{m}_h^i) + \boldsymbol{\mathcal{I}}_h\big(\boldsymbol{\varphi}_h \times \boldsymbol{\mathcal{R}}_h^i(\boldsymbol{\varphi}_h, \boldsymbol{\zeta}_h)\big) \in \boldsymbol{\mathcal{S}}_h, \tag{7.8b}$$

where the residual $\boldsymbol{\mathcal{R}}_h^i(\cdot,\cdot)$ is defined as

$$\begin{aligned}\boldsymbol{\mathcal{R}}_h^i(\boldsymbol{\varphi}_h,\boldsymbol{\zeta}_h) := C_{\mathbf{ex}}\Delta_h\boldsymbol{\varphi}_h + \boldsymbol{\mathcal{P}}_h\boldsymbol{\pi}_h^{\boldsymbol{\Theta}}(2\boldsymbol{\varphi}_h - \boldsymbol{m}_h^i, \boldsymbol{m}_h^i, \boldsymbol{m}_h^{i-1}) + \boldsymbol{\mathcal{P}}_h\boldsymbol{f}_h^{i+1/2} \\ + \boldsymbol{\mathcal{P}}_h\boldsymbol{\Pi}_h^{\boldsymbol{\Theta}}(2\boldsymbol{\varphi}_h - \boldsymbol{m}_h^i, \boldsymbol{m}_h^i, \boldsymbol{m}_h^{i-1}) + \boldsymbol{\mathcal{P}}_h\big[\,\boldsymbol{\Theta}^{(1)}\boldsymbol{\zeta}_h + \boldsymbol{\Theta}^{(2)}\boldsymbol{s}_h^i + \boldsymbol{\Theta}^{(3)}\boldsymbol{s}_h^{i-1}\,\big] \\ - \frac{2\alpha}{k}(\boldsymbol{\varphi}_h - \boldsymbol{m}_h^i) \in \boldsymbol{\mathcal{S}}_h,\end{aligned}$$

and $\boldsymbol{\Theta}^{(1)}, \boldsymbol{\Theta}^{(2)}, \boldsymbol{\Theta}^{(3)} \in \mathbb{R}$ depend on the specific approach **(C1)**–**(C3)** to the coupling term $\boldsymbol{s}_h^{i,\boldsymbol{\Theta}}$. Next, we set

$$\begin{aligned}\boldsymbol{\mathcal{F}}^{(2)}(\boldsymbol{\varphi}_h,\boldsymbol{\zeta}_h) := \frac{2}{k}(\boldsymbol{\zeta}_h - \boldsymbol{s}_h^i) + \mathbf{A}\Big(\min\Big\{1, \frac{\|\boldsymbol{m}_h^i\|_{\boldsymbol{L}^\infty(\omega)}}{\|\boldsymbol{\varphi}_h\|_{\boldsymbol{L}^\infty(\omega)}}\Big\}\boldsymbol{\varphi}_h;\boldsymbol{\zeta}_h\Big) \\ + \mathbf{R}\Big(\min\Big\{1, \frac{\|\boldsymbol{m}_h^i\|_{\boldsymbol{L}^\infty(\omega)}}{\|\boldsymbol{\varphi}_h\|_{\boldsymbol{L}^\infty(\omega)}}\Big\}\boldsymbol{\varphi}_h\Big) \in \boldsymbol{\mathcal{S}}_h^\Omega. \qquad (7.8c)\end{aligned}$$

where, for $\boldsymbol{\varphi}_h = \mathbf{0}$, we interpret $\min\{1, \frac{\|\boldsymbol{m}_h^i\|_{\boldsymbol{L}^\infty(\omega)}}{\|\boldsymbol{\varphi}_h\|_{\boldsymbol{L}^\infty(\omega)}}\} = 1$. With linearity **(D2)** of $\boldsymbol{\pi}_h$ as well as the Lipschitz-type continuity **(M2)** of $\boldsymbol{\Pi}_h$, the auxiliary mapping $\boldsymbol{\mathcal{F}}^{(1)} : \boldsymbol{X}_h \to \boldsymbol{\mathcal{S}}_h$ is continuous for all general time-stepping approaches **(A1)**–**(A3)**. Moreover, $\boldsymbol{\mathcal{F}}^{(2)} : \boldsymbol{X}_h \to \boldsymbol{\mathcal{S}}_h^\Omega$ is continuous for all coupling approaches **(C1)**–**(C3)**. Altogether, $\boldsymbol{\mathcal{F}} : \boldsymbol{X}_h \to \boldsymbol{X}_h$ is continuous.

Step 3. We emphasize the special meaning of $\min\{1, \frac{\|\boldsymbol{m}_h^i\|_{\boldsymbol{L}^\infty(\omega)}}{\|\boldsymbol{\varphi}_h\|_{\boldsymbol{L}^\infty(\omega)}}\}$ in the definition of $\boldsymbol{\mathcal{F}}$: In particular, it holds that

$$\Big\|\min\Big\{1, \frac{\|\boldsymbol{m}_h^i\|_{\boldsymbol{L}^\infty(\omega)}}{\|\boldsymbol{\varphi}_h\|_{\boldsymbol{L}^\infty(\omega)}}\Big\}\boldsymbol{\varphi}_h\Big\|_{\boldsymbol{L}^\infty(\omega)} \le \|\boldsymbol{m}_h^i\|_{\boldsymbol{L}^\infty(\omega)}. \qquad (7.9)$$

Together with the uniform ellipticity property of $\boldsymbol{a}(\boldsymbol{m}_h^{i+1/2};\cdot,\cdot)$ from Lemma 2.2.3(ii), we obtain that

$$\begin{aligned}&\langle\mathbf{A}(\min\Big\{1, \frac{\|\boldsymbol{m}_h^i\|_{\boldsymbol{L}^\infty(\omega)}}{\|\boldsymbol{\varphi}_h\|_{\boldsymbol{L}^\infty(\omega)}}\Big\}\boldsymbol{\varphi}_h;\boldsymbol{\zeta}_h),\boldsymbol{\zeta}_h\rangle_{\boldsymbol{L}^2(\Omega)} \overset{(7.7a)}{=} \mathbf{a}\Big(\min\Big\{1, \frac{\|\boldsymbol{m}_h^i\|_{\boldsymbol{L}^\infty(\omega)}}{\|\boldsymbol{\varphi}_h\|_{\boldsymbol{L}^\infty(\omega)}}\Big\}\boldsymbol{\varphi}_h;\boldsymbol{\zeta}_h,\boldsymbol{\zeta}_h\Big) \\ &\ge \Big(1 - \beta\beta'\Big[\min\Big\{1, \frac{\|\boldsymbol{m}_h^i\|_{\boldsymbol{L}^\infty(\omega)}}{\|\boldsymbol{\varphi}_h\|_{\boldsymbol{L}^\infty(\omega)}}\Big\}\Big]^2\|\boldsymbol{\varphi}_h\|^2_{\boldsymbol{L}^\infty(\omega)}\Big)D\,\|\boldsymbol{\zeta}_h\|^2_{\boldsymbol{H}^1(\Omega)} \\ &\overset{(7.9)}{\ge} \big(1 - \beta\beta'\|\boldsymbol{m}_h^i\|^2_{\boldsymbol{L}^\infty(\omega)}\big)D\,\|\boldsymbol{\zeta}_h\|^2_{\boldsymbol{H}^1(\Omega)} \overset{(7.5)}{\ge} (1-\gamma)\,D\,\|\boldsymbol{\zeta}_h\|^2_{\boldsymbol{H}^1(\Omega)}. \qquad (7.10a)\end{aligned}$$

Moreover, we obtain the crucial uniform boundedness property

$$\begin{aligned}&\|\mathbf{R}\Big(\min\Big\{1, \frac{\|\boldsymbol{m}_h^i\|_{\boldsymbol{L}^\infty(\omega)}}{\|\boldsymbol{\varphi}_h\|_{\boldsymbol{L}^\infty(\omega)}}\Big\}\boldsymbol{\varphi}_h\Big)\|_{\widetilde{\boldsymbol{H}}^{-1}(\Omega)} \\ &\quad\overset{(7.7b)}{\le} 2\beta\,\Big\|\min\Big\{1, \frac{\|\boldsymbol{m}_h^i\|_{\boldsymbol{L}^\infty(\omega)}}{\|\boldsymbol{\varphi}_h\|_{\boldsymbol{L}^\infty(\omega)}}\Big\}\boldsymbol{\varphi}_h\Big\|_{\boldsymbol{L}^\infty(\omega)}\|\boldsymbol{j}_h^{i+1/2}\|_{\boldsymbol{H}^1(\Omega)}. \\ &\quad\overset{(7.9)}{\le} 2\beta\,\|\boldsymbol{m}_h^i\|_{\boldsymbol{L}^\infty(\omega)}\,\|\boldsymbol{j}_h^{i+1/2}\|_{\boldsymbol{H}^1(\Omega)}. \qquad (7.10b)\end{aligned}$$

Step 4. We state the key-property of $\boldsymbol{\mathcal{F}}(\cdot,\cdot)$: Note that for $\boldsymbol{\varphi}_h \in \boldsymbol{\mathcal{S}}_h$, with $\|\boldsymbol{\varphi}_h\|_{\boldsymbol{L}^\infty(\omega)} \leq \|\boldsymbol{m}_h^i\|_{\boldsymbol{L}^\infty(\omega)}$, we obtain that

$$\min\Big\{ 1, \frac{\|\boldsymbol{m}_h^i\|_{\boldsymbol{L}^\infty(\omega)}}{\|\boldsymbol{\varphi}_h\|_{\boldsymbol{L}^\infty(\omega)}} \Big\} = 1. \tag{7.11}$$

In particular, let $(\boldsymbol{\varphi}_h, \boldsymbol{\zeta}_h) \in \boldsymbol{\mathcal{S}}_h \times \boldsymbol{\mathcal{S}}_h^\Omega$ with $\|\boldsymbol{\varphi}_h\|_{\boldsymbol{L}^\infty(\omega)} \leq \|\boldsymbol{m}_h^i\|_{\boldsymbol{L}^\infty(\omega)}$ and $\boldsymbol{\mathcal{F}}(\boldsymbol{\varphi}_h, \boldsymbol{\zeta}_h) = (\mathbf{0}, \mathbf{0})^T$. By design, $\boldsymbol{m}_h^{i+1} := 2\boldsymbol{\varphi}_h - \boldsymbol{m}_h^i$ and $\boldsymbol{s}_h^{i+1} := 2\boldsymbol{\zeta}_h - \boldsymbol{s}_h^i$ are then a solution of the discrete variational formulation (7.1).

Step 5. We show the existence of $(\boldsymbol{\varphi}_h, \boldsymbol{\zeta}_h) \in \boldsymbol{X}_h$ with $\boldsymbol{\mathcal{F}}(\boldsymbol{\varphi}_h, \boldsymbol{\zeta}_h) = (\mathbf{0}, \mathbf{0})^T$: To that end, we apply the Brouwer fixed-point theorem (see Theorem B.2.5). Let $(\boldsymbol{\varphi}_h, \boldsymbol{\zeta}_h) \in \boldsymbol{X}_h$ and test $\boldsymbol{\mathcal{F}}(\boldsymbol{\varphi}_h, \boldsymbol{\zeta}_h)$ with $(\boldsymbol{\varphi}_h, \boldsymbol{\zeta}_h)$. Since $(\mathbf{a} \times \mathbf{b}) \cdot \mathbf{a} = \mathbf{0}$ for all vectors $\mathbf{a}, \mathbf{b} \in \mathbb{R}^3$, the $\boldsymbol{\mathcal{R}}_h^i(\cdot)$-contribution in $\boldsymbol{\mathcal{F}}^{(1)}$ cancels out and we obtain that

$$\begin{aligned}
&\langle \boldsymbol{\mathcal{F}}(\boldsymbol{\varphi}_h, \boldsymbol{\zeta}_h), (\boldsymbol{\varphi}_h, \boldsymbol{\zeta}_h) \rangle_{\boldsymbol{X}_h} \overset{(7.6)}{=} \langle \boldsymbol{\mathcal{F}}^{(1)}(\boldsymbol{\varphi}_h, \boldsymbol{\zeta}_h), \boldsymbol{\varphi}_h \rangle_h + \langle \boldsymbol{\mathcal{F}}^{(2)}(\boldsymbol{\varphi}_h, \boldsymbol{\zeta}_h), \boldsymbol{\zeta}_h \rangle_{\boldsymbol{L}^2(\Omega)} \\
&\overset{(7.8)}{=} \frac{2}{k}\,\|\boldsymbol{\varphi}_h\|_h^2 - \frac{2}{k}\langle \boldsymbol{m}_h^i, \boldsymbol{\varphi}_h \rangle_h + \frac{2}{k}\,\|\boldsymbol{\zeta}_h\|_{\boldsymbol{L}^2(\Omega)}^2 - \frac{2}{k}\,\langle \boldsymbol{s}_h^i, \boldsymbol{\zeta}_h \rangle_{\boldsymbol{L}^2(\Omega)} \\
&\quad + \langle \mathbf{A}(\min\Big\{ 1, \frac{\|\boldsymbol{m}_h^i\|_{\boldsymbol{L}^\infty(\omega)}}{\|\boldsymbol{\varphi}_h\|_{\boldsymbol{L}^\infty(\omega)}} \Big\} \boldsymbol{\varphi}_h; \boldsymbol{\zeta}_h), \boldsymbol{\zeta}_h \rangle_{\boldsymbol{L}^2(\Omega)} + \langle \mathbf{R}(\min\Big\{ 1, \frac{\|\boldsymbol{m}_h^i\|_{\boldsymbol{L}^\infty(\omega)}}{\|\boldsymbol{\varphi}_h\|_{\boldsymbol{L}^\infty(\omega)}} \Big\} \boldsymbol{\varphi}_h), \boldsymbol{\zeta}_h \rangle_{\boldsymbol{L}^2(\Omega)} \\
&= \frac{2}{k}\,\|(\boldsymbol{\varphi}_h, \boldsymbol{\zeta}_h)\|_{\boldsymbol{X}_h}^2 - \frac{2}{k}\,\langle (\boldsymbol{m}_h^i, \boldsymbol{s}_h^i), (\boldsymbol{\varphi}_h, \boldsymbol{\zeta}_h) \rangle_{\boldsymbol{X}_h} \\
&\quad + \langle \mathbf{A}(\min\Big\{ 1, \frac{\|\boldsymbol{m}_h^i\|_{\boldsymbol{L}^\infty(\omega)}}{\|\boldsymbol{\varphi}_h\|_{\boldsymbol{L}^\infty(\omega)}} \Big\} \boldsymbol{\varphi}_h; \boldsymbol{\zeta}_h), \boldsymbol{\zeta}_h \rangle_{\boldsymbol{L}^2(\Omega)} + \langle \mathbf{R}(\min\Big\{ 1, \frac{\|\boldsymbol{m}_h^i\|_{\boldsymbol{L}^\infty(\omega)}}{\|\boldsymbol{\varphi}_h\|_{\boldsymbol{L}^\infty(\omega)}} \Big\} \boldsymbol{\varphi}_h), \boldsymbol{\zeta}_h \rangle_{\boldsymbol{L}^2(\Omega)}.
\end{aligned}$$

With the estimates (7.10) for the last two terms and an inverse estimate (see Proposition 3.1.8), we obtain that

$$\begin{aligned}
&\langle \boldsymbol{\mathcal{F}}(\boldsymbol{\varphi}_h, \boldsymbol{\zeta}_h), (\boldsymbol{\varphi}_h, \boldsymbol{\zeta}_h) \rangle_{\boldsymbol{X}_h} \\
&\geq \frac{2}{k}\,\|(\boldsymbol{\varphi}_h, \boldsymbol{\zeta}_h)\|_{\boldsymbol{X}_h} \big(\|(\boldsymbol{\varphi}_h, \boldsymbol{\zeta}_h)\|_{\boldsymbol{X}_h} - \|(\boldsymbol{m}_h^i, \boldsymbol{s}_h^i)\|_{\boldsymbol{X}_h} \big) \\
&\qquad + (1-\gamma)\, D \|\boldsymbol{\zeta}_h\|_{\boldsymbol{H}^1(\Omega)}^2 - 2\beta \|\boldsymbol{m}_h^i\|_{\boldsymbol{L}^\infty(\omega)} \|\boldsymbol{j}_h^{i+1/2}\|_{\boldsymbol{H}^1(\Omega)} \|\boldsymbol{\zeta}_h\|_{\boldsymbol{H}^1(\Omega)} \\
&\geq \frac{2}{k}\,\|(\boldsymbol{\varphi}_h, \boldsymbol{\zeta}_h)\|_{\boldsymbol{X}_h} \big(\|(\boldsymbol{\varphi}_h, \boldsymbol{\zeta}_h)\|_{\boldsymbol{X}_h} - \|(\boldsymbol{m}_h^i, \boldsymbol{s}_h^i)\|_{\boldsymbol{X}_h} \big) \\
&\qquad - 2C\beta h^{-1} \|\boldsymbol{m}_h^i\|_{\boldsymbol{L}^\infty(\omega)} \|\boldsymbol{j}_h^{i+1/2}\|_{\boldsymbol{H}^1(\Omega)}\, \|\boldsymbol{\zeta}_h\|_{\boldsymbol{L}^2(\Omega)} \\
&\geq \frac{2}{k}\,\|(\boldsymbol{\varphi}_h, \boldsymbol{\zeta}_h)\|_{\boldsymbol{X}_h} \big(\|(\boldsymbol{\varphi}_h, \boldsymbol{\zeta}_h)\|_{\boldsymbol{X}_h} - \|(\boldsymbol{m}_h^i, \boldsymbol{s}_h^i)\|_{\boldsymbol{X}_h} - C\beta k h^{-1} \|\boldsymbol{m}_h^i\|_{\boldsymbol{L}^\infty(\omega)} \|\boldsymbol{j}_h^{i+1/2}\|_{\boldsymbol{H}^1(\Omega)} \big),
\end{aligned}$$

where the constant $C > 0$ is independent of h and k and stems from the inverse estimate. Since $\gamma < 1$, we conclude from the latter estimate that there exists $r > 0$ (which depends on h) such that

$$\langle \boldsymbol{\mathcal{F}}(\boldsymbol{\varphi}_h, \boldsymbol{\zeta}_h), (\boldsymbol{\varphi}_h, \boldsymbol{\zeta}_h) \rangle_{\boldsymbol{X}_h} \geq 0 \quad \text{if } \|(\boldsymbol{\varphi}_h, \boldsymbol{\zeta}_h)\|_{\boldsymbol{X}_h} \geq r.$$

Consequently, the Brouwer fixed-point theorem (see Theorem B.2.5) yields the existence of a pair $(\boldsymbol{\varphi}_h, \boldsymbol{\zeta}_h) \in \boldsymbol{\mathcal{S}}_h \times \boldsymbol{\mathcal{S}}_h^\Omega$ with $\|(\boldsymbol{\varphi}_h, \boldsymbol{\zeta}_h)\|_{\boldsymbol{X}_h} < r$ and $\boldsymbol{\mathcal{F}}(\boldsymbol{\varphi}_h, \boldsymbol{\zeta}_h) = (\mathbf{0}, \mathbf{0})^T$.

Step 6. We combine **Step 1**–**Step 5** and set $\boldsymbol{m}_h^{i+1} := 2\boldsymbol{\varphi}_h - \boldsymbol{m}_h^i$ as well as $\boldsymbol{s}_h^{i+1} := 2\boldsymbol{\zeta}_h - \boldsymbol{s}_h^i$. As in Proposition 6.5.3 for plain LLG, we get that $|\boldsymbol{m}_h^{i+1}(\boldsymbol{z})| = |\boldsymbol{m}_h^i(\boldsymbol{z})|$ for all nodes $\boldsymbol{z} \in \mathcal{N}_h$. Hence,

$$\|\boldsymbol{\varphi}_h\|_{\boldsymbol{L}^\infty(\omega)} = \frac{1}{2}\|\boldsymbol{m}_h^{i+1} + \boldsymbol{m}_h^i\|_{\boldsymbol{L}^\infty(\omega)} \leq \frac{1}{2}\|\boldsymbol{m}_h^{i+1}\|_{\boldsymbol{L}^\infty(\omega)} + \frac{1}{2}\|\boldsymbol{m}_h^i\|_{\boldsymbol{L}^\infty(\omega)} = \|\boldsymbol{m}_h^i\|_{\boldsymbol{L}^\infty(\omega)}.$$

In particular, it holds (7.11). Altogether, **Step 4** concludes the proof. □

Proof of Theorem 7.3.1(a). With the uniform boundedness property **(S1)** of $\boldsymbol{m}_h^0$, Proposition 7.3.3 and an induction argument on $i = 0, \ldots, M-1$ proves well-posedness and

$$|\boldsymbol{m}_h^{i+1}(\boldsymbol{z})| = |\boldsymbol{m}_h^0(\boldsymbol{z})| \quad \text{for all nodes } \boldsymbol{z} \in \mathcal{N}_h.$$

Therefore,

$$\|\boldsymbol{m}_h^{i+1}\|_h = \|\boldsymbol{m}_h^0\|_h \quad \text{and} \quad \|\boldsymbol{m}_h^{i+1}\|_{\boldsymbol{L}^\infty(\omega)} = \|\boldsymbol{m}_h^0\|_{\boldsymbol{L}^\infty(\omega)}.$$

This concludes the proof. □

7.3.2. Discrete energy bound

In this section, we derive a discrete energy bound, which represents the mathematical core of the proof. Recall that in the corresponding Lemma 6.5.4 for plain LLG, we combined and extended the techniques from [BP06] for the midpoint scheme with $\boldsymbol{h}_{\text{eff}}(\boldsymbol{m}) := \Delta\boldsymbol{m}$ and $\boldsymbol{\Pi}(\boldsymbol{m}) = \boldsymbol{0}$ with the techniques from [AKT12, BSF$^+$14] for the tangent plane scheme with lower-order terms. For SDLLG (2.23), [AHP$^+$14, Rug16] prove corresponding results for the first-order tangent plane scheme for SDLLG. For the SDLLG setting of Algorithm 7.2.1, we combine and extend the techniques from Lemma 6.5.4 for the LLG part (2.3a) with the techniques of [AHP$^+$14, Rug16] for the spin diffusion part (2.3b).

Lemma 7.3.4 (Discrete energy bound)**.** *Let the assumptions of Theorem 7.3.1*(b) *be satisfied and let $k > 0$ be sufficiently small. Then, the following assertions* (i)–(ii) *hold true:*

(i) *For all $i = 0, \ldots, M-1$, it holds that*

$$\begin{aligned}
&\frac{C_{\mathbf{ex}}}{2}\,\mathrm{d_t}\,\|\nabla\boldsymbol{m}_h^{i+1}\|^2_{\boldsymbol{L}^2(\omega)} + \alpha\|\,\mathrm{d_t}\boldsymbol{m}_h^{i+1}\|_h^2 \\
&\quad = \langle \mathrm{d_t}\boldsymbol{m}_h^{i+1}, \boldsymbol{\pi}_h^{\boldsymbol{\Theta}}(\boldsymbol{m}_h^{i+1}, \boldsymbol{m}_h^i, \boldsymbol{m}_h^{i-1})\rangle_{\boldsymbol{L}^2(\omega)} + \langle \mathrm{d_t}\boldsymbol{m}_h^{i+1}, \boldsymbol{f}_h^{i+1/2}\rangle_{\boldsymbol{L}^2(\omega)} \\
&\qquad + \langle \mathrm{d_t}\boldsymbol{m}_h^{i+1}, \boldsymbol{\Pi}_h^{\boldsymbol{\Theta}}(\boldsymbol{m}_h^{i+1}, \boldsymbol{m}_h^i, \boldsymbol{m}_h^{i-1})\rangle_{\boldsymbol{L}^2(\omega)} + c\langle \mathrm{d_t}\boldsymbol{m}_h^{i+1}, \boldsymbol{s}_h^{i,\boldsymbol{\Theta}}\rangle_{\boldsymbol{L}^2(\omega)}.
\end{aligned}$$

(ii) *There exists a constant $C > 0$, which depends only on T, ω, Ω, $\boldsymbol{m}^0$, α, $C_{\mathbf{ex}}$, $\boldsymbol{\pi}(\cdot)$, $\boldsymbol{f}$, $\boldsymbol{\Pi}(\cdot)$, $\boldsymbol{s}^0$, c, β, β', D_0, $\boldsymbol{j}$, and $C_{\mathbf{mesh}}$, such that, for all $j = 0, \ldots, M$, it holds that*

$$\begin{aligned}
&\|\nabla\boldsymbol{m}_h^j\|^2_{\boldsymbol{L}^2(\omega)} + k\sum_{i=0}^{j-1}\|\,\mathrm{d_t}\boldsymbol{m}_h^{i+1}\|_h^2 \\
&\quad + \|\boldsymbol{s}_h^j\|^2_{\boldsymbol{L}^2(\Omega)} + k\sum_{i=0}^{j-1}\|\nabla\boldsymbol{s}_h^{i+1/2}\|^2_{\boldsymbol{L}^2(\Omega)} + k\sum_{i=0}^{j-1}\|\,\mathrm{d_t}\boldsymbol{s}_h^{i+1}\|^2_{\widetilde{\boldsymbol{H}}^{-1}(\Omega)} \leq C < \infty.
\end{aligned}$$

Proof. (i) follows like for plain LLG; see the proof of Lemma 6.5.4. We split the remainder of the proof into the following six steps.

Step 1. We bound the third and fourth term in (ii). To this end, we test the spin diffusion part (7.1b) with $\boldsymbol{\zeta}_h := k\boldsymbol{s}_h^{i+1/2}$ and obtain that

$$\begin{aligned}&\frac{1}{2}\,\|\boldsymbol{s}_h^{i+1}\|^2_{\boldsymbol{L}^2(\Omega)} - \frac{1}{2}\,\|\boldsymbol{s}_h^{i}\|^2_{\boldsymbol{L}^2(\Omega)} + k\,\boldsymbol{a}(\boldsymbol{m}_h^{i+1/2};\boldsymbol{s}_h^{i+1/2},\boldsymbol{s}_h^{i+1/2})\\ &\overset{(7.1\text{b})}{=} \beta k\langle \boldsymbol{m}_h^{i+1/2}\otimes \boldsymbol{j}_h^{i+1/2}, \nabla \boldsymbol{s}_h^{i+1/2}\rangle_{\boldsymbol{L}^2(\Omega)} + k\langle \boldsymbol{j}_h^{i+1/2}\cdot\boldsymbol{n}, \boldsymbol{m}_h^{i+1/2}\cdot\boldsymbol{s}_h^{i+1/2}\rangle_{\boldsymbol{L}^2(\partial\Omega\cap\partial\omega)}.\end{aligned} \tag{7.12}$$

Moreover, we infer the uniform boundedness

$$\begin{aligned}\|\boldsymbol{m}_h^{i+1/2}\|_{\boldsymbol{L}^\infty(\omega)} &\le \frac{1}{2}\|\boldsymbol{m}_h^{i+1}\|_{\boldsymbol{L}^\infty(\omega)} + \frac{1}{2}\|\boldsymbol{m}_h^{i}\|_{\boldsymbol{L}^\infty(\omega)}\\ &\overset{\text{(a)}}{=} \|\boldsymbol{m}_h^{0}\|_{\boldsymbol{L}^\infty(\omega)} \overset{\textbf{(S1)}}{\le} (\beta\beta')^{-1/2}\,(1-\gamma)^{1/2} < \infty.\end{aligned} \tag{7.13}$$

The trace inequality and the Young inequality yield for arbitrary $\delta > 0$, that

$$\begin{aligned}&\frac{1}{2}\,\|\boldsymbol{s}_h^{i+1}\|^2_{\boldsymbol{L}^2(\Omega)} - \frac{1}{2}\,\|\boldsymbol{s}_h^{i}\|^2_{\boldsymbol{L}^2(\Omega)} + k\,\boldsymbol{a}(\boldsymbol{m}_h^{i+1/2};\boldsymbol{s}_h^{i+1/2},\boldsymbol{s}_h^{i+1/2})\\ &\overset{(7.12)}{\lesssim} \frac{k}{\delta}\,\|\boldsymbol{m}_h^{i+1/2}\|^2_{\boldsymbol{L}^\infty(\omega)}\,\|\boldsymbol{j}_h^{i+1/2}\|^2_{\boldsymbol{H}^1(\Omega)} + \delta k\,\|\boldsymbol{s}_h^{i+1/2}\|^2_{\boldsymbol{H}^1(\Omega)}\\ &\overset{(7.13)}{\lesssim} \frac{k}{\delta}\,\|\boldsymbol{j}_h^{i+1/2}\|^2_{\boldsymbol{H}^1(\Omega)} + \delta k\,\|\boldsymbol{s}_h^{i+1/2}\|^2_{\boldsymbol{H}^1(\Omega)}.\end{aligned}$$

With the uniform boundedness statement (7.13) for $\boldsymbol{m}_h^{i+1/2}$, the ellipticity of the bilinear form $\boldsymbol{a}(\boldsymbol{m}_h^{i+1/2};\cdot,\cdot)$ from Lemma 2.2.3(ii) yields that

$$\begin{aligned}\boldsymbol{a}(\boldsymbol{m}_h^{i+1/2};\boldsymbol{s}_h^{i+1/2},\boldsymbol{s}_h^{i+1/2}) &\ge \big(1-\beta\beta'\|\boldsymbol{m}_h^{i+1/2}\|^2_{\boldsymbol{L}^\infty(\omega)}\big)\,D\,\|\boldsymbol{s}_h^{i+1/2}\|^2_{\boldsymbol{H}^1(\Omega)}\\ &\overset{(7.13)}{\ge} (1-\gamma)D\,\|\boldsymbol{s}_h^{i+1/2}\|^2_{\boldsymbol{H}^1(\Omega)}.\end{aligned}$$

The combination of the latter two equations yields that

$$\begin{aligned}&\frac{1}{2}\,\|\boldsymbol{s}_h^{i+1}\|^2_{\boldsymbol{L}^2(\Omega)} - \frac{1}{2}\,\|\boldsymbol{s}_h^{i}\|^2_{\boldsymbol{L}^2(\Omega)} + (1-\gamma)Dk\,\|\boldsymbol{s}_h^{i+1/2}\|^2_{\boldsymbol{H}^1(\Omega)}\\ &\lesssim \frac{k}{\delta}\,\|\boldsymbol{j}_h^{i+1/2}\|^2_{\boldsymbol{H}^1(\Omega)} + \delta k\,\|\boldsymbol{s}_h^{i+1/2}\|^2_{\boldsymbol{H}^1(\Omega)}.\end{aligned} \tag{7.14}$$

We sum this estimate over $i = 0,\dots,j-1$. The telescopic sum property proves that

$$\begin{aligned}&\frac{1}{2}\,\|\boldsymbol{s}_h^{j}\|^2_{\boldsymbol{L}^2(\Omega)} + (1-\gamma)D\,k\sum_{i=0}^{j-1}\|\boldsymbol{s}_h^{i+1/2}\|^2_{\boldsymbol{H}^1(\Omega)}\\ &\lesssim \frac{1}{2}\,\|\boldsymbol{s}_h^{0}\|^2_{\boldsymbol{L}^2(\Omega)} + \frac{k}{\delta}\sum_{i=0}^{j-1}\|\boldsymbol{j}_h^{i+1/2}\|^2_{\boldsymbol{H}^1(\Omega)} + \delta k\sum_{i=0}^{j-1}\|\boldsymbol{s}_h^{i+1/2}\|^2_{\boldsymbol{H}^1(\Omega)}.\end{aligned}$$

If we choose δ in the latter estimate small enough, we can absorb the last term to the left-hand side and arrive at

$$\begin{aligned}\|\boldsymbol{s}_h^j\|_{\boldsymbol{L}^2(\Omega)}^2 + k\sum_{i=0}^{j-1}\|\boldsymbol{s}_h^{i+1/2}\|_{\boldsymbol{H}^1(\Omega)}^2 &\lesssim \|\boldsymbol{s}_h^0\|_{\boldsymbol{L}^2(\Omega)}^2 + k\sum_{i=0}^{j-1}\|\boldsymbol{j}_h^{i+1/2}\|_{\boldsymbol{H}^1(\Omega)}^2 \\ &\overset{\textbf{(S2)}}{\lesssim} 1 + k\sum_{i=0}^{j-1}\|\boldsymbol{j}_h^{i+1/2}\|_{\boldsymbol{H}^1(\Omega)}^2 \leq 1 + \int_0^T \|\overline{\boldsymbol{j}}_{hk}\|_{\boldsymbol{H}^1(\Omega)}^2\,\mathrm{d}t \overset{\textbf{(S3)}}{\lesssim} 1.\end{aligned} \tag{7.15}$$

Step 2. We bound the first two terms in (ii): To this end, we sum (i) over $i = 0, \ldots, j-1$. The telescopic sum property yields that

$$\begin{aligned}\chi^{(j)} &:= \frac{C_{\mathbf{ex}}}{2}\,\|\nabla \boldsymbol{m}_h^j\|_{\boldsymbol{L}^2(\omega)}^2 + \alpha k\sum_{i=0}^{j-1}\|\,\mathrm{d}_t\boldsymbol{m}_h^{i+1}\|_h^2 \\ &\overset{\text{(i)}}{=} \frac{C_{\mathbf{ex}}}{2}\,\|\nabla \boldsymbol{m}_h^0\|_{\boldsymbol{L}^2(\Omega)}^2 + k\sum_{i=0}^{j-1}\langle \mathrm{d}_t\boldsymbol{m}_h^{i+1}, \boldsymbol{\pi}_h^{\boldsymbol{\Theta}}(\boldsymbol{m}_h^{i+1}, \boldsymbol{m}_h^i, \boldsymbol{m}_h^{i-1})\rangle_{\boldsymbol{L}^2(\omega)} \\ &\quad + k\sum_{i=0}^{j-1}\langle \mathrm{d}_t\boldsymbol{m}_h^{i+1}, \boldsymbol{f}_h^{i+1/2}\rangle_{\boldsymbol{L}^2(\omega)} + k\sum_{i=0}^{j-1}\langle \mathrm{d}_t\boldsymbol{m}_h^{i+1}, \boldsymbol{\Pi}_h^{\boldsymbol{\Theta}}(\boldsymbol{m}_h^{i+1}, \boldsymbol{m}_h^i, \boldsymbol{m}_h^{i-1})\rangle_{\boldsymbol{L}^2(\omega)} \\ &\quad + c\,k\sum_{i=0}^{j-1}\langle \mathrm{d}_t\boldsymbol{m}_h^{i+1}, \boldsymbol{s}_h^{i,\boldsymbol{\Theta}}\rangle_{\boldsymbol{L}^2(\omega)} =: S_1 + \cdots + S_5,\end{aligned} \tag{7.16}$$

i.e., $\chi^{(j)}$ covers the first two terms in (ii). In the following steps, we estimate $S_1, \ldots, S_5$. Then, our goal is to absorb as many terms as possible to $\chi^{(j)}$ and to apply the discrete Gronwall lemma afterwards.

Step 3. We estimate $S_1, \ldots, S_4$: Following the lines of the proof of Lemma 6.5.4, we get for arbitrary $\delta > 0$, that

$$\sum_{\ell=1}^{4}|S_\ell| \lesssim 1 + \frac{1}{\delta} + \delta k\sum_{i=0}^{j-1}\|\,\mathrm{d}_t\boldsymbol{m}_h^{i+1}\|_{\boldsymbol{L}^2(\omega)}^2 + \frac{k}{\delta}\sum_{i=0}^{j}\|\nabla\boldsymbol{m}_h^i\|_{\boldsymbol{L}^2(\omega)}^2.$$

Step 4. We estimate S_5: For arbitrary $\delta > 0$, the Young inequality yields that

$$S_5 \overset{(7.16)}{=} c\,k\sum_{i=0}^{j-1}\langle \mathrm{d}_t\boldsymbol{m}_h^{i+1}, \boldsymbol{s}_h^{i,\boldsymbol{\Theta}}\rangle_{\boldsymbol{L}^2(\omega)} \lesssim 1 + \delta k\sum_{i=0}^{j-1}\|\,\mathrm{d}_t\boldsymbol{m}_h^{i+1}\|_{\boldsymbol{L}^2(\omega)}^2 + \frac{k}{\delta}\sum_{i=0}^{j-1}\|\boldsymbol{s}_h^{i,\boldsymbol{\Theta}}\|_{\boldsymbol{L}^2(\Omega)}^2.$$

For either of the general coupling approaches **(C1)**–**(C3)**, we infer from **Step 1** that

$$\frac{k}{\delta}\sum_{i=0}^{j-1}\|\boldsymbol{s}_h^{i,\boldsymbol{\Theta}}\|_{\boldsymbol{L}^2(\Omega)}^2 \lesssim \frac{k}{\delta}\sum_{i=0}^{j}\|\boldsymbol{s}_h^i\|_{\boldsymbol{L}^2(\Omega)}^2 \lesssim \frac{1}{\delta}.$$

Altogether, the latter two equations prove that

$$S_5 \lesssim 1 + \frac{1}{\delta} + \delta k\sum_{i=0}^{j-1}\|\,\mathrm{d}_t\boldsymbol{m}_h^{i+1}\|_{\boldsymbol{L}^2(\omega)}^2.$$

Step 5. We combine **Step 1**–**Step 4** and obtain that

$$\chi^{(j)} \overset{(7.16)}{=} \frac{C_{\mathbf{ex}}}{2} \|\nabla \boldsymbol{m}_h^j\|_{\boldsymbol{L}^2(\omega)}^2 + \alpha k \sum_{i=0}^{j-1} \| \mathrm{d}_t \boldsymbol{m}_h^{i+1}\|_h^2$$
$$\lesssim 1 + \frac{1}{\delta} + \delta k \sum_{i=0}^{j-1} \| \mathrm{d}_t \boldsymbol{m}_h^{i+1}\|_{\boldsymbol{L}^2(\omega)}^2 + \frac{k}{\delta} \sum_{i=0}^{j} \|\nabla \boldsymbol{m}_h^i\|_{\boldsymbol{L}^2(\omega)}^2.$$

If we choose δ in the latter estimate small enough, we can absorb $\delta k \sum_{i=0}^{j-1} \| \mathrm{d}_t \boldsymbol{m}_h^{i+1}\|_{\boldsymbol{L}^2(\omega)}^2$ to the left-hand side. Then, we choose $k > 0$ sufficiently small such that we can absorb $k\|\nabla \boldsymbol{m}_h^j\|_{\boldsymbol{L}^2(\omega)}^2$ from the last term to the left-hand side. Altogether, we arrive at

$$\chi^{(j)} \lesssim 1 + k \sum_{i=0}^{j-1} \|\nabla \boldsymbol{m}_h^i\|_{\boldsymbol{L}^2(\omega)}^2 \overset{(7.16)}{\lesssim} 1 + k \sum_{i=0}^{j-1} \chi^{(i)} \quad \text{for all } j \in \{1, \dots, M-1\} \tag{7.17a}$$

and additionally note that

$$\chi^{(0)} \overset{(7.16)}{=} \frac{C_{\mathbf{ex}}}{2} \|\nabla \boldsymbol{m}_h^0\|_{\boldsymbol{L}^2(\omega)} \overset{\textbf{(D1)}}{\lesssim} 1. \tag{7.17b}$$

Hence, (7.17) fits in the setting of the discrete Gronwall lemma (see Lemma B.3.1). This yields that

$$\chi^{(j)} \lesssim \exp\Big(\sum_{i=0}^{j-1} k\Big) \lesssim \exp(T) < \infty \quad \text{for all } j = 1, \dots, M.$$

Step 6. To bound the last term in (ii), we follow [AHP+14, Proposition 17]: Let $\mathbb{P}_{\boldsymbol{\mathcal{S}}_h^\Omega}$ be the $\boldsymbol{L}^2$-orthogonal projection onto $\boldsymbol{\mathcal{S}}_h^\Omega$. Together with the continuity of $\mathbf{a}(\boldsymbol{m}_h^{i+1/2};\cdot,\cdot)$ from Lemma 2.2.3(i), we obtain for $\boldsymbol{\zeta} \in \boldsymbol{H}^1(\Omega)$ that

$$\langle \mathrm{d}_t \boldsymbol{s}_h^{i+1}, \boldsymbol{\zeta}\rangle_{\tilde{\boldsymbol{H}}^{-1}(\Omega)\times \boldsymbol{H}^1(\Omega)} = \langle \mathrm{d}_t \boldsymbol{s}_h^{i+1}, \boldsymbol{\zeta}\rangle_{\boldsymbol{L}^2(\Omega)} = \langle \mathrm{d}_t \boldsymbol{s}_h^{i+1}, \big(\mathbb{P}_{\boldsymbol{\mathcal{S}}_h^\Omega}\boldsymbol{\zeta}\big)\rangle_{\boldsymbol{L}^2(\Omega)}$$
$$\overset{(7.1b)}{=} -\boldsymbol{a}(\boldsymbol{m}_h^{i+1/2}; \boldsymbol{s}_h^{i+1/2}, \big(\mathbb{P}_{\boldsymbol{\mathcal{S}}_h^\Omega}\boldsymbol{\zeta}\big)) + \beta\langle \boldsymbol{m}_h^{i+1/2} \otimes \boldsymbol{j}_h^{i+1/2}, \nabla\big(\mathbb{P}_{\boldsymbol{\mathcal{S}}_h^\Omega}\boldsymbol{\zeta}\big)\rangle_{\boldsymbol{L}^2(\Omega)}$$
$$+ \beta\langle \boldsymbol{j}_h^{i+1/2} \cdot \boldsymbol{n}, \boldsymbol{m}_h^{i+1/2} \cdot \big(\mathbb{P}_{\boldsymbol{\mathcal{S}}_h^\Omega}\boldsymbol{\zeta}\big)\rangle_{\boldsymbol{L}^2(\partial\Omega\cap\partial\omega)}$$
$$\lesssim \big(1 + \|\boldsymbol{m}_h^{i+1/2}\|_{\boldsymbol{L}^\infty(\omega)} + \|\boldsymbol{m}_h^{i+1/2}\|_{\boldsymbol{L}^\infty(\omega)}^2\big) \|\boldsymbol{s}_h^{i+1/2}\|_{\boldsymbol{H}^1(\Omega)} \|\big(\mathbb{P}_{\boldsymbol{\mathcal{S}}_h^\Omega}\boldsymbol{\zeta}\big)\|_{\boldsymbol{H}^1(\Omega)}$$
$$+ \|\boldsymbol{m}_h^{i+1/2}\|_{\boldsymbol{L}^\infty(\omega)} \|\boldsymbol{j}_h^{i+1/2}\|_{\boldsymbol{H}^1(\Omega)} \|\big(\mathbb{P}_{\boldsymbol{\mathcal{S}}_h^\Omega}\boldsymbol{\zeta}\big)\|_{\boldsymbol{H}^1(\Omega)}$$
$$\overset{(7.13)}{\lesssim} \big(\|\boldsymbol{j}_h^{i+1/2}\|_{\boldsymbol{H}^1(\Omega)} + \|\boldsymbol{s}_h^{i+1/2}\|_{\boldsymbol{H}^1(\Omega)}\big) \|\big(\mathbb{P}_{\boldsymbol{\mathcal{S}}_h^\Omega}\boldsymbol{\zeta}\big)\|_{\boldsymbol{H}^1(\Omega)}.$$

Since the family of meshes $(\mathcal{T}_h^\Omega)_{h>0}$ is quasi-uniform, $\mathbb{P}_{\boldsymbol{\mathcal{S}}_h^\Omega}$ is $\boldsymbol{H}^1(\Omega)$-stable. This yields that

$$\langle \mathrm{d}_t \boldsymbol{s}_h^{i+1}, \boldsymbol{\zeta}\rangle_{\tilde{\boldsymbol{H}}^{-1}(\Omega)\times \boldsymbol{H}^1(\Omega)} \lesssim \big(\|\boldsymbol{j}_h^{i+1/2}\|_{\boldsymbol{H}^1(\Omega)} + \|\boldsymbol{s}_h^{i+1/2}\|_{\boldsymbol{H}^1(\Omega)}\big) \|\big(\mathbb{P}_{\boldsymbol{\mathcal{S}}_h^\Omega}\boldsymbol{\zeta}\big)\|_{\boldsymbol{H}^1(\Omega)}$$
$$\lesssim \big(\|\boldsymbol{j}_h^{i+1/2}\|_{\boldsymbol{H}^1(\Omega)} + \|\boldsymbol{s}_h^{i+1/2}\|_{\boldsymbol{H}^1(\Omega)}\big) \|\boldsymbol{\zeta}\|_{\boldsymbol{H}^1(\Omega)} \quad \text{for all } \boldsymbol{\zeta} \in \boldsymbol{H}^1(\Omega).$$

Together with the Young inequality, we conclude that

$$\| \mathrm{d_t} \boldsymbol{s}_h^{i+1} \|^2_{\widetilde{\boldsymbol{H}}^{-1}(\Omega)} \lesssim \| \boldsymbol{j}_h^{i+1/2} \|^2_{\boldsymbol{H}^1(\Omega)} + \| \boldsymbol{s}_h^{i+1/2} \|^2_{\boldsymbol{H}^1(\Omega)}.$$

We sum the latter estimate over $i = 0, \dots, j-1$ and obtain with **Step 1** that

$$\begin{aligned} k \sum_{i=0}^{j-1} \| \mathrm{d_t} \boldsymbol{s}_h^{i+1} \|^2_{\widetilde{\boldsymbol{H}}^{-1}(\Omega)} &\lesssim k \sum_{i=0}^{j-1} \| \boldsymbol{j}_h^{i+1/2} \|^2_{\boldsymbol{H}^1(\Omega)} + k \sum_{i=0}^{j-1} \| \boldsymbol{s}_h^{i+1/2} \|^2_{\boldsymbol{H}^1(\Omega)} \\ &\overset{(7.15)}{\lesssim} 1 + k \sum_{i=0}^{j-1} \| \boldsymbol{j}_h^{i+1/2} \|^2_{\boldsymbol{H}^1(\Omega)} \overset{\textbf{(S3)}}{\lesssim} 1. \end{aligned}$$

Altogether, this shows (ii) and concludes the proof. ☐

7.3.3. Extraction of weakly convergent subsequences

In this section, we exploit the discrete energy bound from Lemma 7.3.4 and extract weakly convergent subsequences of the postprocessed output of our midpoint scheme for SDLLG. Note that the result is somewhat weaker then the corresponding results from [AHP+14, Rug16] for the tangent plane scheme for SDLLG (2.23); see, e.g., [AHP+14, Proposition 21]. In contrast to [AHP+14, Proposition 21], we can only exploit

$$k \sum_{i=0}^{M-1} \| \nabla \boldsymbol{s}_h^{i+1/2} \|^2_{\boldsymbol{L}^2(\Omega)} \lesssim 1 \qquad \text{instead of} \qquad k \sum_{i=0}^{M} \| \nabla \boldsymbol{s}_h^{i} \|^2_{\boldsymbol{L}^2(\Omega)} \lesssim 1.$$

As a consequence, the stronger convergence statement from (ix) below holds only for $\overline{\boldsymbol{s}}_{hk}$.

Lemma 7.3.5 (Convergence properties)**.** *Let the assumptions of Theorem 7.3.1*(b) *be satisfied. Then, there exist subsequences of the postprocessed output*

$$\boldsymbol{m}_{hk}^{\star} \in \{ \boldsymbol{m}_{hk}^{=}, \boldsymbol{m}_{hk}^{-}, \boldsymbol{m}_{hk}^{+}, \overline{\boldsymbol{m}}_{hk}, \boldsymbol{m}_{hk} \}, \quad \textit{and} \tag{7.18a}$$

$$\boldsymbol{s}_{hk}^{\star} \in \{ \boldsymbol{s}_{hk}^{=}, \boldsymbol{s}_{hk}^{-}, \boldsymbol{s}_{hk}^{+}, \overline{\boldsymbol{s}}_{hk}, \boldsymbol{s}_{hk}, \boldsymbol{s}_{hk}^{\boldsymbol{\Theta}} \} \tag{7.18b}$$

of Algorithm 7.2.1 as well as functions

$$\begin{aligned} \boldsymbol{m} &\in L^\infty(0,T; \boldsymbol{H}^1(\omega)) \cap \boldsymbol{H}^1(\omega_T), \quad \textit{and} \\ \boldsymbol{s} &\in L^\infty(0,T; \boldsymbol{L}^2(\Omega)) \cap W(0,T; \boldsymbol{L}^2(\Omega), \boldsymbol{H}^1(\Omega)) \end{aligned}$$

such that the following convergence properties (i)–(x) *hold true simultaneously for the same subsequence as $h, k \to 0$:*

(i) $\boldsymbol{m}_{hk} \rightharpoonup \boldsymbol{m}$ *in* $\boldsymbol{H}^1(\omega_T)$.

(ii) $\boldsymbol{m}_{hk}^{\star} \overset{\star}{\rightharpoonup} \boldsymbol{m}$ *in* $L^\infty(0,T; \boldsymbol{H}^1(\omega))$.

(iii) $\boldsymbol{m}_{hk}^{\star} \rightharpoonup \boldsymbol{m}$ *in* $\boldsymbol{L}^2(0,T; \boldsymbol{H}^1(\omega))$.

(iv) $\boldsymbol{m}_{hk}^{\star} \to \boldsymbol{m}$ *in* $\boldsymbol{L}^2(\omega_T)$.

(v) $\boldsymbol{m}_{hk}^{\star}(t) \to \boldsymbol{m}(t)$ *in* $\boldsymbol{L}^2(\omega)$ *a.e. for* $t \in (0,T)$.

(vi) $\boldsymbol{m}_{hk}^{\star} \to \boldsymbol{m}$ *pointwise a.e. in* ω_T.

(vii) $\boldsymbol{s}_{hk}^{\star} \rightharpoonup \boldsymbol{s}$ *in* $\boldsymbol{L}^2(\Omega_T)$.

(viii) $\boldsymbol{s}_{hk}^{\star} \overset{\star}{\rightharpoonup} \boldsymbol{s}$ *in* $L^\infty(0,T;\boldsymbol{L}^2(\Omega))$.

(ix) $\overline{\boldsymbol{s}}_{hk} \rightharpoonup \boldsymbol{s}$ *in* $L^2(0,T;\boldsymbol{H}^1(\Omega))$,

(x) $\partial_t \boldsymbol{s}_{hk} \rightharpoonup \partial_t \boldsymbol{s}$ *in* $L^2(0,T;\widetilde{\boldsymbol{H}}^{-1}(\Omega))$.

Proof. From the definition (3.3) of the postprocessed output, we get that

$$\|\boldsymbol{m}_{hk}^{\star}\|_{\boldsymbol{L}^\infty(\omega_T)} \overset{\text{(a)}}{\leq} \|\boldsymbol{m}_h^0\|_{\boldsymbol{L}^\infty(\omega)} \overset{\textbf{(S1)}}{\lesssim} 1.$$

With the discrete energy bound from Lemma 7.3.4, the definition of the postprocessed output yields that

$$\|\boldsymbol{m}_{hk}\|_{\boldsymbol{H}^1(\omega_T)} + \|\boldsymbol{m}_{hk}^{\star}\|_{L^\infty(0,T;\boldsymbol{H}^1(\omega))} \lesssim 1, \quad \text{and} \tag{7.19a}$$

$$\|\boldsymbol{s}_{hk}^{\star}\|_{L^\infty(0,T;\boldsymbol{L}^2(\Omega))} + \|\overline{\boldsymbol{s}}_{hk}\|_{L^2(0,T;\boldsymbol{H}^1(\Omega))} + \|\partial_t \boldsymbol{s}_{hk}\|_{L^2(0,T;\widetilde{\boldsymbol{H}}^{-1}(\Omega))} \lesssim 1. \tag{7.19b}$$

From (7.19a), we conclude (i)–(vi) like in the proof of Lemma 6.5.5(i)–(vi) for plain LLG. Next, we prove (vii) and (ix)–(x). With the uniform bound (7.19b), the Eberlein–Šmulian theorem (see Theorem B.2.2) yields existence of

$$\boldsymbol{s}^{=}, \boldsymbol{s}^{-}, \boldsymbol{s}^{+}, \boldsymbol{s}^{\boldsymbol{\Theta}} \in \boldsymbol{L}^2(\Omega_T), \quad \overline{\boldsymbol{s}} \in L^2(0,T;\boldsymbol{H}^1(\Omega)),$$
$$\boldsymbol{s} \in \boldsymbol{L}^2(\Omega_T), \quad \text{and} \quad \widetilde{\boldsymbol{s}} \in L^2(0,T;\widetilde{\boldsymbol{H}}^{-1}(\Omega))$$

as well as subsequences of the postprocessed output such that there hold the convergences

$$\boldsymbol{s}_{hk}^{=} \rightharpoonup \boldsymbol{s}^{=}, \quad \boldsymbol{s}_{hk}^{-} \rightharpoonup \boldsymbol{s}^{-}, \quad \boldsymbol{s}_{hk}^{+} \rightharpoonup \boldsymbol{s}^{+} \quad \text{and} \quad \boldsymbol{s}_{hk}^{\boldsymbol{\Theta}} \rightharpoonup \boldsymbol{s}^{\boldsymbol{\Theta}} \quad \text{in } \boldsymbol{L}^2(\Omega_T), \tag{7.20a}$$

$$\overline{\boldsymbol{s}}_{hk} \rightharpoonup \overline{\boldsymbol{s}} \quad \text{in } L^2(0,T;\boldsymbol{H}^1(\Omega)), \quad \text{and} \tag{7.20b}$$

$$\boldsymbol{s}_{hk} \rightharpoonup \boldsymbol{s} \quad \text{in } \boldsymbol{L}^2(\Omega_T) \quad \text{as well as} \quad \partial_t \boldsymbol{s}_{hk} \rightharpoonup \boldsymbol{w} \quad \text{in } L^2(0,T;\widetilde{\boldsymbol{H}}^{-1}(\Omega)) \tag{7.20c}$$

as $h,k \to 0$. In a first step, we show $\boldsymbol{w} = \partial_t \boldsymbol{s}$. Upon extraction of another subsequence, the uniform bound (7.19b) yields existence of $\widetilde{\boldsymbol{s}} \in \boldsymbol{H}^1(0,T;\widetilde{\boldsymbol{H}}^{-1}(\Omega))$ such that

$$\boldsymbol{s}_{hk} \rightharpoonup \widetilde{\boldsymbol{s}} \quad \text{in } \boldsymbol{H}^1(0,T;\widetilde{\boldsymbol{H}}^{-1}(\Omega)) \quad \text{as } h,k \to 0,$$

i.e., in particular, it holds that

$$\boldsymbol{s}_{hk} \rightharpoonup \widetilde{\boldsymbol{s}} \quad \text{and} \quad \partial_t \boldsymbol{s}_{hk} \rightharpoonup \partial_t \widetilde{\boldsymbol{s}} \quad \text{in } \boldsymbol{L}^2(0,T;\widetilde{\boldsymbol{H}}^{-1}(\Omega)) \quad \text{as } h,k \to 0.$$

However, since weak convergence in $\boldsymbol{L}^2(\Omega_T)$ implies weak convergence in $L^2(0,T;\widetilde{\boldsymbol{H}}^{-1}(\Omega))$ and since weak limits are unique, we obtain with (7.20c) that $\boldsymbol{s} = \widetilde{\boldsymbol{s}}$ as well as $\boldsymbol{w} = \partial_t \widetilde{\boldsymbol{s}} = \partial_t \boldsymbol{s}$. Next, we identify the limits from (7.20). To this end, denote by $\boldsymbol{s}^{\star}$ the corresponding limit of the postprocessed output $\boldsymbol{s}_{hk}^\star$. First, note that the definitions of the postprocessed output and the discrete time-derivative directly yield that

$$\|\boldsymbol{s}_{hk} - \boldsymbol{s}_{hk}^\star\|_{L^2(0,T;\widetilde{\boldsymbol{H}}^{-1}(\Omega))} \lesssim k\,\|\partial_t \boldsymbol{s}_{hk}\|_{L^2(0,T;\widetilde{\boldsymbol{H}}^{-1}(\Omega))} \to 0 \quad \text{as } h,k \to 0. \tag{7.21}$$

For $\boldsymbol{\varphi} \in L^2(0,T;\boldsymbol{H}^1(\Omega))$, we then obtain with the convergences from (7.20) that

$$\begin{aligned} &\Big| \int_0^T \langle \boldsymbol{s} - \boldsymbol{s}_{hk}^\star, \boldsymbol{\varphi} \rangle_{\widetilde{\boldsymbol{H}}^{-1}(\Omega)\times \boldsymbol{H}^1(\Omega)} \,\mathrm{d}t \Big| \\ &\leq \quad \Big| \int_0^T \langle \boldsymbol{s} - \boldsymbol{s}_{hk}, \boldsymbol{\varphi} \rangle_{\widetilde{\boldsymbol{H}}^{-1}(\Omega)\times \boldsymbol{H}^1(\Omega)} \,\mathrm{d}t \Big| \\ &\qquad + \|\boldsymbol{s}_{hk} - \boldsymbol{s}_{hk}^\star\|_{L^2(0,T;\widetilde{\boldsymbol{H}}^{-1}(\Omega))} \|\boldsymbol{\varphi}\|_{L^2(0,T;\boldsymbol{H}^1(\Omega))} \overset{(7.21)}{\to} 0 \quad \text{as } h,k \to 0. \end{aligned}$$

With the uniqueness of weak limits we conclude that $\boldsymbol{s}^\star = \boldsymbol{s}$ in $L^2(0,T;\widetilde{\boldsymbol{H}}^{-1}(\Omega))$ and hence $\boldsymbol{s}^\star = \boldsymbol{s}$ a.e. in Ω_T as well as $\boldsymbol{s} \in W(0,T;\boldsymbol{L}^2(\Omega),\boldsymbol{H}^1(\Omega))$. Altogether, this proves (vii) and (ix)–(x). Finally, we prove (viii). With (7.19b), the Alaoglu theorem (see Theorem B.2.3) allows the further extraction of subsequences of the postprocessed output $\boldsymbol{s}_{hk}^\star$, which are weak* convergent in $L^\infty(0,T;\boldsymbol{L}^2(\Omega))$. Since this implies weak convergence in $\boldsymbol{L}^2(\Omega_T)$, the common limit is $\boldsymbol{s}$ from (vii). Altogether, this concludes the proof. □

As for plain LLG, we note a direct consequence of the latter convergence properties for $\boldsymbol{m}_{hk}^*$ and anticipate the verification of Definition 2.2.4(i) for the proof of Theorem 7.3.1(b). The proof follows the lines of Lemma 6.5.6 for plain LLG.

Lemma 7.3.6 ($|\boldsymbol{m}| = 1$ a.e. in ω_T)**.** *Let the assumptions of Theorem 7.3.1*(b) *be satisfied. Then,* $\boldsymbol{m} \in L^\infty(0,T;\boldsymbol{H}^1(\omega)) \cap \boldsymbol{H}^1(\omega_T)$ *from Lemma 7.3.5 satisfies* $|\boldsymbol{m}| = 1$ *a.e. in* ω_T. □

7.3.4. Convergence to weak solution

In this section, we prove Theorem 7.3.1(b). Recall that the proof of Theorem 6.5.1(b) for plain LLG combines and extends the techniques of [BP06] for the midpoint scheme with $\boldsymbol{h}_{\mathrm{eff}}(\boldsymbol{m}) = \Delta \boldsymbol{m}$ and $\boldsymbol{\Pi}(\boldsymbol{m}) = \boldsymbol{0}$ with [AKT12, BSF$^+$14] from the tangent plane scheme for the lower-order terms. Moreover, note that [AHP$^+$14, Rug16] prove a corresponding result for the tangent plane scheme for the coupled SDLLG system; see, e.g., [AHP$^+$14, Theorem 12]. We adapt the ideas of these works for the setting of our midpoint scheme.

Proof of Theorem 7.3.1(b)*.* We show that

$$\boldsymbol{m} \in L^\infty(0,T;\boldsymbol{H}^1(\omega)) \cap \boldsymbol{H}^1(\omega_T), \quad \text{and} \tag{7.22a}$$

$$\boldsymbol{s} \in L^\infty(0,T;\boldsymbol{L}^2(\Omega)) \cap W(0,T;\boldsymbol{L}^2(\Omega),\boldsymbol{H}^1(\Omega)), \tag{7.22b}$$

from Lemma 7.3.5 are a weak solution in the sense of Definition 2.2.4(i)–(iv). The combination of (7.22) and Lemma 7.3.6 already yields Definition 2.2.4(i)–(ii), and we split the remaining verifications into the following five steps.

Step 1. We verify Definition 2.2.4(iii), i.e., $\boldsymbol{m}(0) = \boldsymbol{m}^0$ and $\boldsymbol{s}(0) = \boldsymbol{s}^0$ in the sense of traces: We conclude $\boldsymbol{m}(0) = \boldsymbol{m}^0$ as in **Step 1** in the proof of Theorem 6.5.1(b) for plain LLG. The verification of $\boldsymbol{s}(0) = \boldsymbol{s}^0$ follows the same lines: On the one hand, note that

$$\boldsymbol{s}_{hk}(0) = \boldsymbol{s}_h^0 \overset{\textbf{(S2)}}{\rightharpoonup} \boldsymbol{s}^0 \quad \text{in } \boldsymbol{L}^2(\Omega) \quad \text{as } h, k \to 0.$$

On the other hand, the convergence properties of Lemma 7.3.5 imply that

$$\boldsymbol{s}_{hk} \rightharpoonup \boldsymbol{s} \quad \text{in } H^1((0,T), \widetilde{\boldsymbol{H}}^{-1}(\Omega)) \quad \text{as } h, k \to 0.$$

With the continuity of the trace operator, we infer from the latter equation that

$$\boldsymbol{s}_{hk}(0) \rightharpoonup \boldsymbol{s}(0) \quad \text{in } \widetilde{\boldsymbol{H}}^{-1}(\Omega) \quad \text{as } h, k \to 0.$$

Since the injection $\boldsymbol{L}^2(\Omega) \subset \widetilde{\boldsymbol{H}}^{-1}(\Omega)$ is continuous, the uniqueness of limits verifies Definition 2.2.4(iii).

Step 2. We verify Definition 2.2.4(iv), i.e., $(\boldsymbol{m}, \boldsymbol{s})$ satisfies the variational formulation (2.26). To this end, we proceed similarly to the proof of Theorem 6.5.1(b) for plain LLG. Let $\boldsymbol{\varphi} \in \boldsymbol{C}^\infty(\overline{\omega_T})$ and $\boldsymbol{\zeta} \in \boldsymbol{C}^\infty(\overline{\Omega_T})$. Moreover, let $\boldsymbol{\mathcal{I}}_h$ and $\boldsymbol{\mathcal{I}}_h^\Omega$ be the nodal interpolants corresponding to $\boldsymbol{\mathcal{S}}_h$ and $\boldsymbol{\mathcal{S}}_h^\Omega$, respectively. Define

$$\boldsymbol{\varphi}_h(t) := \boldsymbol{\mathcal{I}}_h(\boldsymbol{\varphi}(t)) \quad \text{and} \quad \boldsymbol{\zeta}_h(t) := \boldsymbol{\mathcal{I}}_h^\Omega(\boldsymbol{\zeta}(t)) \quad \text{for } t \in [0,T].$$

For $t \in [t_i, t_{i+1})$ with $i \in \{0, \dots, M-1\}$, we test the corresponding discrete variational formulation (7.1) with $\boldsymbol{\varphi}_h(t)$ and $\boldsymbol{\zeta}_h(t)$ and integrate over $[0,T]$. With the definition of the postprocessed output, we get an LLG part

$$\begin{aligned}
I_{hk}^1 &:= \int_0^T \langle \partial_t \boldsymbol{m}_{hk}, \boldsymbol{\varphi}_h \rangle_h \,\mathrm{d}t \\
&\overset{(7.1)}{=} -C_{\mathbf{ex}} \int_0^T \langle \overline{\boldsymbol{m}}_{hk} \times \Delta_h \overline{\boldsymbol{m}}_{hk}, \boldsymbol{\varphi}_h \rangle_h \,\mathrm{d}t - \int_0^T \langle \overline{\boldsymbol{m}}_{hk} \times \boldsymbol{\mathcal{P}}_h \boldsymbol{\pi}_h^{\boldsymbol{\Theta}}(\boldsymbol{m}_{hk}^+, \boldsymbol{m}_{hk}^-, \boldsymbol{m}_{hk}^=), \boldsymbol{\varphi}_h \rangle_h \,\mathrm{d}t \\
&\quad - \int_0^T \langle \overline{\boldsymbol{m}}_{hk} \times \boldsymbol{\mathcal{P}}_h \overline{\boldsymbol{f}}_{hk}, \boldsymbol{\varphi}_h \rangle_h \,\mathrm{d}t - \int_0^T \langle \overline{\boldsymbol{m}}_{hk} \times \boldsymbol{\mathcal{P}}_h \boldsymbol{\Pi}_h^{\boldsymbol{\Theta}}(\boldsymbol{m}_{hk}^+, \boldsymbol{m}_{hk}^-, \boldsymbol{m}_{hk}^=), \boldsymbol{\varphi}_h \rangle_h \,\mathrm{d}t \\
&\quad - c \int_0^T \langle \overline{\boldsymbol{m}}_{hk} \times \boldsymbol{\mathcal{P}}_h \boldsymbol{s}_{hk}^{\boldsymbol{\Theta}}, \boldsymbol{\varphi}_h \rangle_h \,\mathrm{d}t + \alpha \int_0^T \langle \overline{\boldsymbol{m}}_{hk} \times \partial_t \boldsymbol{m}_{hk}, \boldsymbol{\varphi}_h \rangle_h \,\mathrm{d}t \\
&=: -C_{\mathbf{ex}} I_{hk}^2 - I_{hk}^3 - I_{hk}^4 - I_{hk}^5 - c I_{hk}^6 + \alpha I_{hk}^7.
\end{aligned} \tag{7.23a}$$

and a spin diffusion part

$$\begin{aligned}
I_{hk}^8 + I_{hk}^9 &:= \int_0^T \langle \partial_t \boldsymbol{s}_{hk}, \boldsymbol{\zeta}_h \rangle_{\widetilde{\boldsymbol{H}}^{-1}(\Omega) \times \boldsymbol{H}^1(\Omega)} \,\mathrm{d}t + \int_0^T \boldsymbol{a}(\overline{\boldsymbol{m}}_{hk}, \overline{\boldsymbol{s}}_{hk}, \boldsymbol{\zeta}_h) \,\mathrm{d}t \\
&= \beta \int_0^T \langle \overline{\boldsymbol{m}}_{hk} \otimes \overline{\boldsymbol{j}}_{hk}, \nabla \boldsymbol{\zeta}_h \rangle_{\boldsymbol{L}^2(\omega)} \,\mathrm{d}t - \beta \int_0^T \langle \overline{\boldsymbol{j}}_{hk} \cdot \boldsymbol{n}, \overline{\boldsymbol{m}}_{hk} \cdot \boldsymbol{\zeta}_h \rangle_{\boldsymbol{L}^2(\partial\Omega \cap \partial\omega)} \,\mathrm{d}t \\
&=: \beta I_{hk}^{10} - \beta I_{hk}^{11}.
\end{aligned} \tag{7.23b}$$

In the following, we show convergence of the integrals $I_{hk}^1,\dots,I_{hk}^{11}$ towards their continuous counterparts in the variational formulation (2.26).

Step 3. We collect some auxiliary results: From standard approximation properties of the nodal interpolants (see Proposition 3.1.7), we get for $p \in (3/2, \infty]$ and $q \in [1, \infty]$ that

$$\boldsymbol{\varphi}_h \to \boldsymbol{\varphi} \quad \text{in } L^q(0,T;\boldsymbol{W}^{1,p}(\omega)), \quad \text{and} \tag{7.24a}$$

$$\boldsymbol{\zeta}_h \to \boldsymbol{\zeta} \quad \text{in } L^q(0,T;\boldsymbol{W}^{1,p}(\Omega)) \quad \text{as } h,k \to 0. \tag{7.24b}$$

As in **Step 3** of the proof of Theorem 6.5.1(b) for plain LLG, we infer from the convergence properties from Lemma 7.3.5 and (7.24b) that

$$\boldsymbol{\mathcal{I}}_h(\overline{\boldsymbol{m}}_{hk} \times \boldsymbol{\varphi}_h) \to \boldsymbol{m} \times \boldsymbol{\varphi} \quad \text{in } \boldsymbol{L}^2(\omega_T) \quad \text{and} \tag{7.25a}$$

$$\overline{\boldsymbol{m}}_{hk} \times \boldsymbol{\zeta}_h \to \boldsymbol{m} \times \boldsymbol{\zeta} \quad \text{in } \boldsymbol{L}^2(\omega_T) \quad \text{as } h,k \to 0. \tag{7.25b}$$

Together with the convergence properties from Lemma 7.3.5, we obtain that

$$\overline{\boldsymbol{m}}_{hk} \otimes \overline{\boldsymbol{m}}_{hk} \;\to\; \boldsymbol{m} \otimes \boldsymbol{m} \quad \text{in } \boldsymbol{L}^2(\omega_T), \tag{7.26a}$$

$$\overline{\boldsymbol{m}}_{hk} \cdot \boldsymbol{\zeta}_h \overset{(7.24b)}{\rightharpoonup} \boldsymbol{m} \cdot \boldsymbol{\zeta} \quad \text{in } \boldsymbol{L}^2(0,T;\boldsymbol{H}^1(\omega)), \tag{7.26b}$$

$$\overline{\boldsymbol{m}}_{hk} \otimes \overline{\boldsymbol{j}}_{hk} \overset{\textbf{(S3)}}{\rightharpoonup} \boldsymbol{m} \otimes \boldsymbol{j} \quad \text{in } \boldsymbol{L}^2(\omega_T) \tag{7.26c}$$

as $h, k \to 0$. Here, (7.26a)–(7.26b) follow as in [Rug16, Chapter 5] and rely on $|\boldsymbol{m}| = 1$ a.e. in ω_T (see Lemma 7.3.6) and on the uniform bound

$$\|\overline{\boldsymbol{m}}_{hk}\|_{\boldsymbol{L}^\infty(\omega_T)} \le \max_{i=0,\dots,M} \|\boldsymbol{m}_h^i\|_{\boldsymbol{L}^\infty(\omega)} \overset{\text{(a)}}{=} \|\boldsymbol{m}_h^0\|_{\boldsymbol{L}^\infty(\omega)} \overset{\textbf{(S2)}}{\lesssim} 1. \tag{7.27}$$

However, instead of (7.26c), the corresponding [Rug16, Lemma 5.1.12] verifies strong convergence and requires the additional assumption $\boldsymbol{j} \in \boldsymbol{L}^\infty(\Omega_T)$ for that. To see our weaker (and sufficient) (7.26c), we conclude from (7.27) and **(S3)** on the one hand that $\|\overline{\boldsymbol{m}}_{hk} \otimes \overline{\boldsymbol{j}}_{hk}\|_{\boldsymbol{L}^2(\omega_T)} \lesssim 1$. On the other hand, we get with the convergence properties from Lemma 7.3.5 for all $\widetilde{\boldsymbol{\zeta}} \in \boldsymbol{C}^\infty(\overline{\Omega_T})$ that

$$\begin{aligned}
&\int_0^T \langle \overline{\boldsymbol{m}}_{hk} \otimes \overline{\boldsymbol{j}}_{hk}, \widetilde{\boldsymbol{\zeta}} \rangle_{\boldsymbol{L}^2(\omega)} \,\mathrm{d}t - \int_0^T \langle \boldsymbol{m} \otimes \boldsymbol{j}, \widetilde{\boldsymbol{\zeta}} \rangle_{\boldsymbol{L}^2(\omega)} \,\mathrm{d}t \\
&\quad = \int_0^T \langle (\overline{\boldsymbol{m}}_{hk} - \boldsymbol{m}) \otimes \overline{\boldsymbol{j}}_{hk}, \widetilde{\boldsymbol{\zeta}} \rangle_{\boldsymbol{L}^2(\omega)} \,\mathrm{d}t + \int_0^T \langle \boldsymbol{m} \otimes (\overline{\boldsymbol{j}}_{hk} - \boldsymbol{j}), \widetilde{\boldsymbol{\zeta}} \rangle_{\boldsymbol{L}^2(\omega)} \,\mathrm{d}t \\
&\quad \lesssim \|\overline{\boldsymbol{m}}_{hk} - \boldsymbol{m}\|_{\boldsymbol{L}^2(\omega_T)} \|\overline{\boldsymbol{j}}_{hk}\|_{\boldsymbol{L}^2(\Omega_T)} \|\widetilde{\boldsymbol{\zeta}}\|_{\boldsymbol{L}^\infty(\Omega_T)} + \|\overline{\boldsymbol{j}}_{hk} - \boldsymbol{j}\|_{\boldsymbol{L}^2(\Omega_T)} \|\boldsymbol{m}\|_{\boldsymbol{L}^2(\omega_T)} \|\widetilde{\boldsymbol{\zeta}}\|_{\boldsymbol{L}^\infty(\Omega_T)} \\
&\quad \lesssim \|\overline{\boldsymbol{m}}_{hk} - \boldsymbol{m}\|_{\boldsymbol{L}^2(\omega_T)} + \|\overline{\boldsymbol{j}}_{hk} - \boldsymbol{j}\|_{\boldsymbol{L}^2(\Omega_T)} \overset{\textbf{(S3)}}{\to} 0 \quad \text{as } h,k \to 0.
\end{aligned}$$

Together with Lemma B.2.1, this verifies (7.26c).

Step 4. We deal with the LLG part (7.23a): For the coupling term I_{hk}^6, recall the convergence property from Lemma 7.3.5(vii). Moreover, recall from the definition (3.10) that the approximate $\boldsymbol{L}^2$-product $\langle\cdot,\cdot\rangle_h$ depends only on the nodal values of the arguments. From the definition (3.12) of the quasi-$\boldsymbol{L}^2$-projection $\boldsymbol{\mathcal{P}}_h$, we obtain that

$$
\begin{aligned}
I_{hk}^6 &\overset{(7.23a)}{=} \int_0^T \langle \overline{\boldsymbol{m}}_{hk} \times \boldsymbol{\mathcal{P}}_h \boldsymbol{s}_{hk}^{\boldsymbol{\Theta}}, \boldsymbol{\varphi}_h\rangle_h \,\mathrm{d}t = -\int_0^T \langle \boldsymbol{\mathcal{I}}_h(\overline{\boldsymbol{m}}_{hk} \times \boldsymbol{\varphi}_h), \boldsymbol{\mathcal{P}}_h \boldsymbol{s}_{hk}^{\boldsymbol{\Theta}}\rangle_h \,\mathrm{d}t \\
&= \quad -\int_0^T \langle \boldsymbol{\mathcal{I}}_h(\overline{\boldsymbol{m}}_{hk} \times \boldsymbol{\varphi}_h), \boldsymbol{s}_{hk}^{\boldsymbol{\Theta}}\rangle_{\boldsymbol{L}^2(\omega)} \,\mathrm{d}t \overset{(7.25a)}{\to} -\int_0^T \langle \boldsymbol{m} \times \boldsymbol{\varphi}, \boldsymbol{s}\rangle_{\boldsymbol{L}^2(\omega)} \,\mathrm{d}t \\
&= \quad \int_0^T \langle \boldsymbol{m} \times \boldsymbol{s}, \boldsymbol{\varphi}\rangle_{\boldsymbol{L}^2(\omega)} \,\mathrm{d}t \quad \text{as } h,k \to 0.
\end{aligned}
$$

For I_{hk}^1, I_{hk}^2, I_{hk}^4 and I_{hk}^7, we follow the lines of the proof of Theorem 6.5.1(b) for plain LLG and obtain that

$$
\begin{aligned}
I_{hk}^1 &\overset{(7.23a)}{=} \int_0^T \langle \partial_t \boldsymbol{m}_{hk}, \boldsymbol{\varphi}_h\rangle_h \,\mathrm{d}t \to \int_0^T \langle \partial_t \boldsymbol{m}, \boldsymbol{\varphi}\rangle_{\boldsymbol{L}^2(\omega)} \,\mathrm{d}t, \\
I_{hk}^2 &\overset{(7.23a)}{=} \int_0^T \langle \overline{\boldsymbol{m}}_{hk} \times \Delta_h \overline{\boldsymbol{m}}_{hk}, \boldsymbol{\varphi}_h\rangle_h \,\mathrm{d}t \to -\int_0^T \langle \boldsymbol{m} \times \nabla \boldsymbol{m}, \nabla \boldsymbol{\varphi}\rangle_{\boldsymbol{L}^2(\omega)} \,\mathrm{d}t, \\
I_{hk}^4 &\overset{(7.23a)}{=} \int_0^T \langle \overline{\boldsymbol{m}}_{hk} \times \boldsymbol{\mathcal{P}}_h \overline{\boldsymbol{f}}_{hk}, \boldsymbol{\varphi}_h\rangle_h \,\mathrm{d}t \to \int_0^T \langle \boldsymbol{m} \times \boldsymbol{f}, \boldsymbol{\varphi}\rangle_{\boldsymbol{L}^2(\omega)} \,\mathrm{d}t, \text{ and} \\
I_{hk}^7 &\overset{(7.23a)}{=} \int_0^T \langle \overline{\boldsymbol{m}}_{hk} \times \partial_t \boldsymbol{m}_{hk}, \boldsymbol{\varphi}_h\rangle_h \,\mathrm{d}t \to \int_0^T \langle \boldsymbol{m} \times \partial_t \boldsymbol{m}, \boldsymbol{\varphi}\rangle_{\boldsymbol{L}^2(\omega)} \,\mathrm{d}t
\end{aligned}
$$

as $h,k \to 0$. For I_{hk}^3 and I_{hk}^5, recall from plain LLG that we required the convergence properties from Lemma 6.5.5 and the weak consistencies **(D4)** for $\boldsymbol{\pi}_h$ and **(D7)** for $\boldsymbol{\Pi}_h$ to derive the weak consistencies from Lemma 6.5.7 for $\boldsymbol{\pi}_h^{\boldsymbol{\Theta}}$ and $\boldsymbol{\Pi}_h^{\boldsymbol{\Theta}}$. Hence, with Lemma 7.3.5 (i)–(vi), we get in the same way that

$$
\begin{aligned}
I_{hk}^3 &\overset{(7.23a)}{=} \int_0^T \langle \overline{\boldsymbol{m}}_{hk} \times \boldsymbol{\mathcal{P}}_h \boldsymbol{\pi}_h^{\boldsymbol{\Theta}}(\boldsymbol{m}_{hk}^+, \boldsymbol{m}_{hk}^-, \boldsymbol{m}_{hk}^=), \boldsymbol{\varphi}_h\rangle_h \,\mathrm{d}t \to \int_0^T \langle \boldsymbol{m} \times \boldsymbol{\pi}(\boldsymbol{m}), \boldsymbol{\varphi}\rangle_{\boldsymbol{L}^2(\omega)} \,\mathrm{d}t, \text{ and} \\
I_{hk}^5 &\overset{(7.23a)}{=} \int_0^T \langle \overline{\boldsymbol{m}}_{hk} \times \boldsymbol{\mathcal{P}}_h \boldsymbol{\Pi}_h^{\boldsymbol{\Theta}}(\boldsymbol{m}_{hk}^+, \boldsymbol{m}_{hk}^-, \boldsymbol{m}_{hk}^=), \boldsymbol{\varphi}_h\rangle_h \,\mathrm{d}t \to \int_0^T \langle \boldsymbol{m} \times \boldsymbol{\Pi}(\boldsymbol{m}), \boldsymbol{\varphi}\rangle_{\boldsymbol{L}^2(\omega)} \,\mathrm{d}t
\end{aligned}
$$

as $h,k \to 0$.

Step 5. We deal with the spin diffusion part similarly as in [AHP+14, Rug16]: We start with I_{hk}^8, I_{hk}^{10}, and I_{hk}^{11} and derive from the convergence properties from Lemma 7.3.5 and **Step 3** that

$$
\begin{aligned}
I_{hk}^8 &\overset{(7.23b)}{=} \int_0^T \langle \partial_t \boldsymbol{s}_{hk}, \boldsymbol{\zeta}_h\rangle_{\widetilde{\boldsymbol{H}}^{-1}(\Omega)\times \boldsymbol{H}^1(\Omega)} \,\mathrm{d}t \overset{(7.24b)}{\to} \int_0^T \langle \partial_t \boldsymbol{s}, \boldsymbol{\zeta}\rangle_{\widetilde{\boldsymbol{H}}^{-1}(\Omega)\times \boldsymbol{H}^1(\Omega)} \,\mathrm{d}t, \\
I_{hk}^{10} &\overset{(7.23b)}{=} \int_0^T \langle \overline{\boldsymbol{m}}_{hk} \otimes \overline{\boldsymbol{j}}_{hk}, \nabla \boldsymbol{\zeta}_h\rangle_{\boldsymbol{L}^2(\omega)} \,\mathrm{d}t \overset{(7.26c)}{\to} \int_0^T \langle \boldsymbol{m} \otimes \boldsymbol{j}, \nabla \boldsymbol{\zeta}\rangle_{\boldsymbol{L}^2(\omega)} \,\mathrm{d}t \quad \text{and} \\
I_{hk}^{11} &\overset{(7.23b)}{=} \int_0^T \langle \overline{\boldsymbol{j}}_{hk} \cdot \boldsymbol{n}, \overline{\boldsymbol{m}}_{hk} \cdot \boldsymbol{\zeta}_h\rangle_{\boldsymbol{L}^2(\partial\Omega\cap\partial\omega)} \,\mathrm{d}t \overset{(7.26b)}{\rightharpoonup} \int_0^T \langle \boldsymbol{j} \cdot \boldsymbol{n}, \boldsymbol{m} \cdot \boldsymbol{\zeta}\rangle_{\boldsymbol{L}^2(\partial\Omega\cap\partial\omega)} \,\mathrm{d}t \text{ as } h,k \to 0.
\end{aligned}
$$

For I_{hk}^9, the definition (2.24) of the bilinear form $\mathbf{a}(\overline{\boldsymbol{m}}_{hk};\cdot,\cdot)$ unveils that

$$\begin{aligned}
I_{hk}^9 &\overset{(7.23b)}{=} \int_0^T \boldsymbol{a}(\overline{\boldsymbol{m}}_{hk}, \overline{\boldsymbol{s}}_{hk}, \boldsymbol{\zeta}_h)\,\mathrm{d}t \\
&= \int_0^T \langle D_0 \nabla \overline{\boldsymbol{s}}_{hk}, \nabla \boldsymbol{\zeta}_h \rangle_{\boldsymbol{L}^2(\Omega)}\,\mathrm{d}t - \beta\beta' \int_0^T \langle D_0 (\overline{\boldsymbol{m}}_{hk} \otimes \overline{\boldsymbol{m}}_{hk}) \nabla \overline{\boldsymbol{s}}_{hk}, \nabla \boldsymbol{\zeta}_h \rangle_{\boldsymbol{L}^2(\omega)}\,\mathrm{d}t \\
&\quad + \int_0^T \langle D_0 \overline{\boldsymbol{s}}_{hk}, \boldsymbol{\zeta}_h \rangle_{\boldsymbol{L}^2(\Omega)}\,\mathrm{d}t + \int_0^T \langle D_0 (\overline{\boldsymbol{s}}_{hk} \times \overline{\boldsymbol{m}}_{hk}), \boldsymbol{\zeta}_h \rangle_{\boldsymbol{L}^2(\omega)}\,\mathrm{d}t \\
&=: I_{hk}^{\mathbf{a},1} - \beta\beta' I_{hk}^{\mathbf{a},2} + I_{hk}^{\mathbf{a},3} + I_{hk}^{\mathbf{a},4}.
\end{aligned}$$

We exploit the convergence properties from Lemma 7.3.5 and **Step 3** and obtain with $D_0 \in \boldsymbol{L}^\infty(\Omega)$ that

$$\begin{aligned}
I_{hk}^{\mathbf{a},1} &= \int_0^T \langle D_0 \nabla \overline{\boldsymbol{s}}_{hk}, \nabla \boldsymbol{\zeta}_h \rangle_{\boldsymbol{L}^2(\Omega)}\,\mathrm{d}t \overset{(7.24b)}{\to} \int_0^T \langle D_0 \nabla \boldsymbol{s}, \nabla \boldsymbol{\zeta} \rangle_{\boldsymbol{L}^2(\Omega)}\,\mathrm{d}t, \\
I_{hk}^{\mathbf{a},3} &= \int_0^T \langle D_0 \overline{\boldsymbol{s}}_{hk}, \boldsymbol{\zeta}_h \rangle_{\boldsymbol{L}^2(\Omega)}\,\mathrm{d}t \overset{(7.24b)}{\to} \int_0^T \langle D_0 \boldsymbol{s}, \boldsymbol{\zeta} \rangle_{\boldsymbol{L}^2(\Omega)}\,\mathrm{d}t \quad \text{and} \\
I_{hk}^{\mathbf{a},2} &= \int_0^T \langle D_0 (\overline{\boldsymbol{m}}_{hk} \otimes \overline{\boldsymbol{m}}_{hk}) \nabla \overline{\boldsymbol{s}}_{hk}, \nabla \boldsymbol{\zeta}_h \rangle_{\boldsymbol{L}^2(\omega)}\,\mathrm{d}t \overset{(7.24b)}{\to} \int_0^T \langle D_0 (\boldsymbol{m} \otimes \boldsymbol{m}) \nabla \boldsymbol{s}, \nabla \boldsymbol{\zeta} \rangle_{\boldsymbol{L}^2(\omega)}\,\mathrm{d}t
\end{aligned}$$

as $h, k \to 0$. Finally, we get with $D_0 \in \boldsymbol{L}^\infty(\Omega)$ that

$$\begin{aligned}
I_{hk}^{\mathbf{a},4} &= -\int_0^T \langle \overline{\boldsymbol{s}}_{hk}, D_0 (\overline{\boldsymbol{m}}_{hk} \times \boldsymbol{\zeta}_h) \rangle_{\boldsymbol{L}^2(\omega)}\,\mathrm{d}t \overset{(7.25b)}{\to} -\int_0^T \langle \boldsymbol{s}, D_0 (\boldsymbol{m} \times \boldsymbol{\zeta}) \rangle_{\boldsymbol{L}^2(\omega)}\,\mathrm{d}t \\
&= \int_0^T \langle D_0 (\boldsymbol{s} \times \boldsymbol{m}), \boldsymbol{\zeta} \rangle_{\boldsymbol{L}^2(\omega)}\,\mathrm{d}t \quad \text{as } h, k \to 0.
\end{aligned}$$

Altogether, we get that

$$I_{hk}^9 = \int_0^T \boldsymbol{a}(\overline{\boldsymbol{m}}_{hk}, \overline{\boldsymbol{s}}_{hk}, \boldsymbol{\zeta}_h)\,\mathrm{d}t \to \int_0^T \boldsymbol{a}(\boldsymbol{m}, \boldsymbol{s}, \boldsymbol{\zeta})\,\mathrm{d}t \quad \text{as } h, k \to 0.$$

The combination of **Step 1**–**Step 5** concludes the proof. □

7.3.5. Stronger energy estimate

In this section, we prove Theorem 7.3.1(c), i.e., under stronger assumptions, the solution $(\boldsymbol{m}, \boldsymbol{s})$ from (b) also satisfies the stronger energy estimate (2.27). The proof builds on two lemmas which improve

- the statements about the boundedness of the discrete energy (Lemma 7.3.7);
- the convergence property of the postprocessed output (Lemma 7.3.8).

Roughly, our analysis follows [AHP+14, Rug16], where a corresponding result is proved for the tangent plane scheme for SDLLG. For the midpoint scheme, however, the situation seems to be more involved and we additionally require the CFL-type condition

$$\text{CFL-type condition} \quad k = \mathcal{O}(h^2).$$

We start with the stronger result about the boundedness of the discrete energy. To this end, we adapt the corresponding techniques from [AHP+14, Rug16].

Lemma 7.3.7 (Stronger discrete energy bound)**.** *Let the assumptions of Theorem 7.3.1*(b) *be satisfied. Let $k > 0$ be sufficiently small and suppose* **(CFL)**, *i.e., it holds that $k = \mathcal{O}(h^2)$. Then, there exists a constant $C > 0$, which depends only on T, ω, Ω, $\boldsymbol{m}^0$, α, $C_{\mathbf{ex}}$, $\boldsymbol{\pi}(\cdot)$, $\boldsymbol{f}$, $\boldsymbol{\Pi}(\cdot)$, $\boldsymbol{s}^0$, c, β, β', D_0, $\boldsymbol{j}$, and $C_{\mathbf{mesh}}$ such that, for all $j \in \{1, \dots, M\}$, it holds that*

$$\|\boldsymbol{s}_h^j\|_{\boldsymbol{L}^2(\Omega)}^2 + k \sum_{i=0}^{j} \|\nabla \boldsymbol{s}_h^i\|_{\boldsymbol{L}^2(\Omega)}^2 + \sum_{i=0}^{j-1} \|\boldsymbol{s}_h^{i+1} - \boldsymbol{s}_h^i\|_{\boldsymbol{L}^2(\Omega)}^2 \le C < \infty. \tag{7.28}$$

Proof. We split the proof into the following four steps.

Step 1. We test the spin diffusion part (7.1b) with $\boldsymbol{\zeta}_h := k\boldsymbol{s}_h^{i+1}$. Then, the Young inequality and the trace inequality yield for any $\delta > 0$ that

$$\begin{aligned} &\langle \boldsymbol{s}_h^{i+1} - \boldsymbol{s}_h^i, \boldsymbol{s}_h^{i+1} \rangle_{\boldsymbol{L}^2(\Omega)} + k\,\mathbf{a}(\boldsymbol{m}_h^{i+1/2}; \boldsymbol{s}_h^{i+1/2}, \boldsymbol{s}_h^{i+1}) \\ &\overset{(7.1b)}{=} \beta k \langle \boldsymbol{m}_h^{i+1/2} \otimes \boldsymbol{j}_h^{i+1/2}, \nabla \boldsymbol{s}_h^{i+1} \rangle_{\boldsymbol{L}^2(\Omega)} + k \langle \boldsymbol{j}_h^{i+1/2} \cdot \boldsymbol{n}, \boldsymbol{m}_h^{i+1/2} \cdot \boldsymbol{s}_h^{i+1} \rangle_{\boldsymbol{L}^2(\partial\Omega \cap \partial\omega)}. \end{aligned} \tag{7.29}$$

As in **Step 1** of the proof of Lemma 7.3.4, we get the uniform boundedness property

$$\begin{aligned} \|\boldsymbol{m}_h^{i+1/2}\|_{\boldsymbol{L}^\infty(\omega)} &\le \frac{1}{2}\|\boldsymbol{m}_h^{i+1}\|_{\boldsymbol{L}^\infty(\omega)} + \frac{1}{2}\|\boldsymbol{m}_h^i\|_{\boldsymbol{L}^\infty(\omega)} \\ &\overset{(a)}{=} \|\boldsymbol{m}_h^0\|_{\boldsymbol{L}^\infty(\omega)} \overset{\textbf{(S1)}}{\le} (\beta\beta')^{-1/2}(1-\gamma)^{1/2} < \infty. \end{aligned} \tag{7.30}$$

With the Young inequality this yields for arbitrary $\delta > 0$ that

$$\langle \boldsymbol{s}_h^{i+1} - \boldsymbol{s}_h^i, \boldsymbol{s}_h^{i+1} \rangle_{\boldsymbol{L}^2(\Omega)} + k\,\mathbf{a}(\boldsymbol{m}_h^{i+1/2}; \boldsymbol{s}_h^{i+1/2}, \boldsymbol{s}_h^{i+1}) \overset{(7.30)}{\lesssim} \frac{k}{\delta}\,\|\boldsymbol{j}_h^{i+1/2}\|_{\boldsymbol{H}^1(\Omega)}^2 + \delta k\,\|\boldsymbol{s}_h^{i+1}\|_{\boldsymbol{H}^1(\Omega)}^2.$$

With $\boldsymbol{s}_h^{i+1/2} = \boldsymbol{s}_h^{i+1} - (k/2)\,\mathrm{d_t}\boldsymbol{s}_h^{i+1}$, we obtain that

$$\begin{aligned} &\langle \boldsymbol{s}_h^{i+1} - \boldsymbol{s}_h^i, \boldsymbol{s}_h^{i+1} \rangle_{\boldsymbol{L}^2(\Omega)} + k\,\mathbf{a}(\boldsymbol{m}_h^{i+1/2}; \boldsymbol{s}_h^{i+1}, \boldsymbol{s}_h^{i+1}) \\ &\overset{(7.30)}{\lesssim} \frac{k}{\delta}\,\|\boldsymbol{j}_h^{i+1/2}\|_{\boldsymbol{H}^1(\Omega)}^2 + \delta k\,\|\boldsymbol{s}_h^{i+1}\|_{\boldsymbol{H}^1(\Omega)}^2 + k^2\,\mathbf{a}(\boldsymbol{m}_h^{i+1/2}; \mathrm{d_t}\boldsymbol{s}_h^{i+1}, \boldsymbol{s}_h^{i+1}). \end{aligned}$$

In the following, we exploit Lemma 2.2.3 and estimate both terms involving the bilinear form $\mathbf{a}(\boldsymbol{m}_h^{i+1/2}; \cdot, \cdot)$.

Step 2. We estimate $\mathbf{a}(\boldsymbol{m}_h^{i+1/2}; \boldsymbol{s}_h^{i+1}, \boldsymbol{s}_h^{i+1})$ from below: With the ellipticity statement of the bilinear form $\mathbf{a}(\boldsymbol{m}_h^{i+1/2}, \cdot, \cdot)$ from Lemma 2.2.3(ii), we obtain that

$$\begin{aligned} \mathbf{a}(\boldsymbol{m}_h^{i+1/2}; \boldsymbol{s}_h^{i+1}, \boldsymbol{s}_h^{i+1}) &\ge D\left(1 - \beta\beta'\|\boldsymbol{m}_h^{i+1/2}\|_{\boldsymbol{L}^\infty(\Omega)}^2\right)\|\boldsymbol{s}_h^{i+1}\|_{\boldsymbol{H}^1(\Omega)}^2 \\ &\overset{(7.30)}{\ge} D\left(1 - \beta\beta'\|\boldsymbol{m}_h^0\|_{\boldsymbol{L}^\infty(\Omega)}^2\right)\|\boldsymbol{s}_h^{i+1}\|_{\boldsymbol{H}^1(\Omega)}^2 \overset{\textbf{(S1)}}{\ge} D\,(1-\gamma)\,\|\boldsymbol{s}_h^{i+1}\|_{\boldsymbol{H}^1(\Omega)}^2. \end{aligned} \tag{7.31}$$

Step 3. We estimate $k^2\mathbf{a}(\boldsymbol{m}_h^{i+1/2}; \mathrm{d_t}\boldsymbol{s}_h^{i+1}, \boldsymbol{s}_h^{i+1})$ from above: With the continuity statement of the bilinear form $\mathbf{a}(\boldsymbol{m}_h^{i+1/2}, \cdot, \cdot)$ from Lemma 2.2.3(i) and with $D_0 \in \boldsymbol{L}^\infty(\Omega)$, we get that

$$
\begin{aligned}
&\mathbf{a}(\boldsymbol{m}_h^{i+1/2}; \mathrm{d_t}\boldsymbol{s}_h^{i+1}, \boldsymbol{s}_h^{i+1}) \\
&\quad\le \|D_0\|_{\boldsymbol{L}^\infty(\Omega)}\big(1 + \|\boldsymbol{m}_h^{i+1/2}\|_{\boldsymbol{L}^\infty(\Omega)} + \|\boldsymbol{m}_h^{i+1/2}\|^2_{\boldsymbol{L}^\infty(\Omega)}\big)\| \mathrm{d_t}\boldsymbol{s}_h^{i+1}\|_{\boldsymbol{H}^1(\Omega)}\|\boldsymbol{s}_h^{i+1}\|_{\boldsymbol{H}^1(\Omega)} \\
&\quad\overset{(7.30)}{\le} \|D_0\|_{\boldsymbol{L}^\infty(\Omega)}\big(1 + \|\boldsymbol{m}_h^{0}\|_{\boldsymbol{L}^\infty(\Omega)} + \|\boldsymbol{m}_h^{0}\|^2_{\boldsymbol{L}^\infty(\Omega)}\big)\| \mathrm{d_t}\boldsymbol{s}_h^{i+1}\|_{\boldsymbol{H}^1(\Omega)}\|\boldsymbol{s}_h^{i+1}\|_{\boldsymbol{H}^1(\Omega)} \\
&\quad\overset{\textbf{(S1)}}{\lesssim} \| \mathrm{d_t}\boldsymbol{s}_h^{i+1}\|_{\boldsymbol{H}^1(\Omega)}\, \|\boldsymbol{s}_h^{i+1}\|_{\boldsymbol{H}^1(\Omega)}.
\end{aligned}
$$

With an inverse estimate (see Proposition 3.1.8), we obtain that

$$
\begin{aligned}
\| \mathrm{d_t}\boldsymbol{s}_h^{i+1}\|^2_{\boldsymbol{L}^2(\Omega)} &= \langle \mathrm{d_t}\boldsymbol{s}_h^{i+1}, \mathrm{d_t}\boldsymbol{s}_h^{i+1}\rangle_{\boldsymbol{L}^2(\Omega)} = \langle \mathrm{d_t}\boldsymbol{s}_h^{i+1}, \mathrm{d_t}\boldsymbol{s}_h^{i+1}\rangle_{\widetilde{\boldsymbol{H}}^{-1}(\Omega)\times\boldsymbol{H}^1(\Omega)} \\
&\le \| \mathrm{d_t}\boldsymbol{s}_h^{i+1}\|_{\widetilde{\boldsymbol{H}}^{-1}(\Omega)}\, \| \mathrm{d_t}\boldsymbol{s}_h^{i+1}\|_{\boldsymbol{H}^1(\Omega)} \lesssim h^{-1}\, \| \mathrm{d_t}\boldsymbol{s}_h^{i+1}\|_{\widetilde{\boldsymbol{H}}^{-1}(\Omega)}\, \| \mathrm{d_t}\boldsymbol{s}_h^{i+1}\|_{\boldsymbol{L}^2(\Omega)},
\end{aligned}
$$

i.e., $\| \mathrm{d_t}\boldsymbol{s}_h^{i+1}\|_{\boldsymbol{L}^2(\Omega)} \lesssim h^{-1}\, \| \mathrm{d_t}\boldsymbol{s}_h^{i+1}\|_{\widetilde{\boldsymbol{H}}^{-1}(\Omega)}$. Hence, another application of an inverse estimate shows that $\| \mathrm{d_t}\boldsymbol{s}_h^{i+1}\|_{\boldsymbol{H}^1(\omega)} \lesssim h^{-2}\| \mathrm{d_t}\boldsymbol{s}_h^{i+1}\|_{\widetilde{\boldsymbol{H}}^{-1}(\Omega)}$. With the Young inequality, this yields for arbitrary $\delta > 0$ that

$$
\begin{aligned}
k^2\, \mathbf{a}(\boldsymbol{m}_h^{i+1/2}; \mathrm{d_t}\boldsymbol{s}_h^{i+1}, \boldsymbol{s}_h^{i+1}) &\lesssim (kh^{-2})\, k\, \| \mathrm{d_t}\boldsymbol{s}_h^{i+1}\|_{\widetilde{\boldsymbol{H}}^{-1}(\Omega)}\, \|\boldsymbol{s}_h^{i+1}\|_{\boldsymbol{H}^1(\Omega)} \\
&\overset{\textbf{(CFL)}}{\lesssim} k\| \mathrm{d_t}\boldsymbol{s}_h^{i+1}\|_{\widetilde{\boldsymbol{H}}^{-1}(\Omega)}\, \|\boldsymbol{s}_h^{i+1}\|_{\boldsymbol{H}^1(\Omega)} \lesssim \frac{k}{\delta}\, \| \mathrm{d_t}\boldsymbol{s}_h^{i+1}\|^2_{\widetilde{\boldsymbol{H}}^{-1}(\Omega)} + \delta k\, \|\boldsymbol{s}_h^{i+1}\|^2_{\boldsymbol{H}^1(\Omega)}.
\end{aligned}
$$

Step 4. We combine **Step 1**–**Step 3** and obtain that

$$
\begin{aligned}
&\langle \boldsymbol{s}_h^{i+1} - \boldsymbol{s}_h^{i}, \boldsymbol{s}_h^{i+1}\rangle_{\boldsymbol{L}^2(\Omega)} + D\,(1-\gamma)\, k\, \|\boldsymbol{s}_h^{i+1}\|^2_{\boldsymbol{H}^1(\Omega)} \\
&\quad\lesssim \frac{k}{\delta}\, \|\boldsymbol{j}_h^{i+1/2}\|^2_{\boldsymbol{H}^1(\Omega)} + \delta k\, \|\boldsymbol{s}_h^{i+1}\|^2_{\boldsymbol{H}^1(\Omega)} + \frac{k}{\delta}\, \| \mathrm{d_t}\boldsymbol{s}_h^{i+1}\|^2_{\widetilde{\boldsymbol{H}}^{-1}(\Omega)}.
\end{aligned}
$$

We sum in the latter estimate over $i = 0, \dots, j-1$ and obtain with Lemma 7.3.4 that

$$
\begin{aligned}
&\sum_{i=0}^{j-1} \langle \boldsymbol{s}_h^{i+1} - \boldsymbol{s}_h^{i}, \boldsymbol{s}_h^{i+1}\rangle_{\boldsymbol{L}^2(\Omega)} + D\,(1-\gamma)\, k \sum_{i=0}^{j-1} \|\boldsymbol{s}_h^{i+1}\|^2_{\boldsymbol{H}^1(\Omega)} \\
&\quad\lesssim \frac{k}{\delta} \sum_{i=0}^{j-1} \|\boldsymbol{j}_h^{i+1/2}\|^2_{\boldsymbol{H}^1(\Omega)} + \delta k \sum_{i=0}^{j-1} \|\boldsymbol{s}_h^{i+1}\|^2_{\boldsymbol{H}^1(\Omega)} + \frac{k}{\delta} \sum_{i=0}^{j-1} \| \mathrm{d_t}\boldsymbol{s}_h^{i+1}\|^2_{\widetilde{\boldsymbol{H}}^{-1}(\Omega)} \\
&\quad\overset{\textbf{(S2)}}{\lesssim} \frac{1}{\delta} + \delta k \sum_{i=0}^{j-1} \|\boldsymbol{s}_h^{i+1}\|^2_{\boldsymbol{H}^1(\Omega)}.
\end{aligned}
$$

For $\delta > 0$ small enough, we can absorb the last term into the left-hand side. With Abel's summation by parts (see Lemma B.3.3), we get that

$$
\sum_{i=0}^{j-1} \langle \boldsymbol{s}_h^{i+1} - \boldsymbol{s}_h^{i}, \boldsymbol{s}_h^{i+1}\rangle_{\boldsymbol{L}^2(\Omega)} = \frac{1}{2}\, \|\boldsymbol{s}_h^{j}\|^2_{\boldsymbol{L}^2(\Omega)} - \frac{1}{2}\|\boldsymbol{s}_h^{0}\|^2_{\boldsymbol{L}^2(\Omega)} + \frac{1}{2} \sum_{i=0}^{j-1} \|\boldsymbol{s}_h^{i+1} - \boldsymbol{s}_h^{i}\|^2_{\boldsymbol{L}^2(\Omega)}.
$$

Combining the latter three equations, we obtain that

$$\|\boldsymbol{s}_h^j\|_{\boldsymbol{L}^2(\Omega)}^2 + \sum_{i=0}^{j-1} \|\boldsymbol{s}_h^{i+1} - \boldsymbol{s}_h^i\|_{\boldsymbol{L}^2(\Omega)}^2 + k \sum_{i=0}^{j-1} \|\boldsymbol{s}_h^{i+1}\|_{\boldsymbol{H}^1(\Omega)}^2 \lesssim 1 + \|\boldsymbol{s}_h^0\|_{\boldsymbol{L}^2(\Omega)}^2 \overset{\textbf{(S3)}}{\lesssim} 1.$$

Finally, an inverse estimate yields that

$$k \, \|\nabla \boldsymbol{s}_h^0\|_{\boldsymbol{L}^2(\omega)}^2 \lesssim kh^{-2} \, \|\boldsymbol{s}_h^0\|_{\boldsymbol{L}^2(\omega)}^2 \overset{\textbf{(S2)}}{\lesssim} kh^{-2} \overset{\textbf{(CFL)}}{\lesssim} 1,$$

and the combination of the latter two equations concludes the proof. □

With the latter lemma at hand, we proceed to prove additional convergence properties for the postprocessed output of our midpoint scheme for SDLLG. A corresponding result for the tangent plane scheme for SDLLG is proved as part of [AHP$^+$14, Proposition 15] or [Rug16, Proposition 5.1.11].

Lemma 7.3.8 (Additional convergence properties)**.** *Let the assumptions of Theorem 7.3.1*(b) *be satisfied. Moreover, suppose* **(CFL)***, i.e., it holds that $k = \mathcal{O}(h^2)$. Let*

$$\boldsymbol{s}_{hk}^\star \in \{\boldsymbol{s}_{hk}^=, \boldsymbol{s}_{hk}^-, \boldsymbol{s}_{hk}^+, \overline{\boldsymbol{s}}_{hk}, \boldsymbol{s}_{hk}, \boldsymbol{s}_{hk}^{\boldsymbol{\Theta}}\}$$

be the postprocessed output of Algorithm 7.2.1. Then, upon further extraction of another subsequence, it holds that

$$\boldsymbol{s}_{hk}^\star \to \boldsymbol{s} \quad \textit{in } \boldsymbol{L}^2(\Omega_T) \quad \textit{as } h, k \to 0.$$

Proof. With the stronger discrete energy bound from Lemma 7.3.7, the Eberlein–Šmulian theorem (see Theorem B.2.2) allows to further extract a subsequence of the postprocessed output $\boldsymbol{s}_{hk}$ such that $\boldsymbol{s}_{hk} \rightharpoonup \boldsymbol{s}$ in $L^2(0,T;\boldsymbol{H}^1(\Omega))$ as $h,k \to 0$. Recalling from Lemma 7.3.5(x) that $\partial_t \boldsymbol{s}_{hk} \rightharpoonup \partial_t \boldsymbol{s}$ in $L^2(0,T;\widetilde{\boldsymbol{H}}^{-1}(\Omega))$ as $h,k \to 0$, we altogether get that

$$\boldsymbol{s}_{hk} \rightharpoonup \boldsymbol{s} \quad \text{in } W(0,T;\boldsymbol{L}^2(\Omega),\boldsymbol{H}^1(\Omega)) \quad \text{as } h,k \to 0.$$

From this, we get with the Aubin-Lions lemma (see Lemma 2.1.8) that $\boldsymbol{s}_{hk} \to \boldsymbol{s}$ in $\boldsymbol{L}^2(\Omega_T)$ as $h,k \to 0$. Moreover, the stronger discrete energy bound from Lemma 7.3.7 yields that

$$\|\boldsymbol{s}_{hk} - \boldsymbol{s}_{hk}^\star\|_{\boldsymbol{L}^2(\Omega_T)}^2 \lesssim k \sum_{j=0}^{M-1} \|\boldsymbol{s}_h^{i+1} - \boldsymbol{s}_h^i\|_{\boldsymbol{L}^2(\Omega)}^2 \lesssim k \to 0 \quad \text{as } h,k \to 0. \tag{7.32}$$

Altogether, this concludes the proof. □

We come to the actual proof of Theorem 7.3.1(c). With the additional convergence result from Lemma 7.3.8, our starting position in terms of convergence properties of the postprocessed output is now the same as that in [AHP$^+$14, Rug16] for the tangent plane scheme for SDLLG. Hence, the following proof combines the techniques of Section 6.5.5 for the midpoint scheme for plain LLG with [AHP$^+$14, Rug16] for the tangent plane scheme for SDLLG.

Proof of Theorem 7.3.1(c). Since the assumptions of (c) are stronger than those of (b), we only have to verify that $(\boldsymbol{m}, \boldsymbol{s})$ from (b) satisfies the energy estimate (2.27). To that end, recall from (2.25) the notion of the energy functional

$$\mathcal{E}_{\mathrm{LLG}}(\boldsymbol{m}) \overset{(2.25)}{=} \frac{C_{\mathbf{ex}}}{2}\|\nabla\boldsymbol{m}\|^2_{\boldsymbol{L}^2(\omega)} - \frac{1}{2}\langle\boldsymbol{\pi}(\boldsymbol{m}),\boldsymbol{m}\rangle_{\boldsymbol{L}^2(\omega)} - \langle\boldsymbol{f},\boldsymbol{m}\rangle_{\boldsymbol{L}^2(\omega)}. \tag{7.33}$$

Since we supposed in Section 2.2 that $\boldsymbol{f} \in C^1([0,T],\boldsymbol{L}^2(\omega))$, we can define $\boldsymbol{f}^i := \boldsymbol{f}(t_i)$ for $i \in \{0,\ldots,M\}$. Let $\tau \in [0,T)$ be arbitrary and let $j \in \{1,\ldots,M\}$ such that $t \in [t_{j-1}, t_j)$. With the discrete energy equality from Lemma 7.3.4(i) for all $i \in \{0,\ldots,j-1\}$, we obtain that

$$\begin{aligned}
&\mathcal{E}_{\mathrm{LLG}}(\boldsymbol{m}_h^{i+1}) - \mathcal{E}_{\mathrm{LLG}}(\boldsymbol{m}_h^{i}) \\
&\overset{(7.33)}{=} \frac{C_{\mathbf{ex}}}{2}k\,\mathrm{d_t}\,\|\nabla\boldsymbol{m}_h^{i+1}\|^2_{\boldsymbol{L}^2(\omega)} - \frac{1}{2}\langle\boldsymbol{\pi}(\boldsymbol{m}_h^{i+1}),\boldsymbol{m}_h^{i+1}\rangle_{\boldsymbol{L}^2(\omega)} + \frac{1}{2}\langle\boldsymbol{\pi}(\boldsymbol{m}_h^{i}),\boldsymbol{m}_h^{i}\rangle_{\boldsymbol{L}^2(\omega)} \\
&\qquad - \langle\boldsymbol{f}^{i+1},\boldsymbol{m}_h^{i+1}\rangle_{\boldsymbol{L}^2(\omega)} + \langle\boldsymbol{f}^{i},\boldsymbol{m}_h^{i}\rangle_{\boldsymbol{L}^2(\omega)} \\
&= \ -\alpha k\,\|\,\mathrm{d_t}\boldsymbol{m}_h^{i+1}\|_h^2 - \frac{1}{2}\langle\boldsymbol{\pi}(\boldsymbol{m}_h^{i+1}),\boldsymbol{m}_h^{i+1}\rangle_{\boldsymbol{L}^2(\omega)} + \frac{1}{2}\langle\boldsymbol{\pi}(\boldsymbol{m}_h^{i}),\boldsymbol{m}_h^{i}\rangle_{\boldsymbol{L}^2(\omega)} \\
&\qquad + k\,\langle\mathrm{d_t}\boldsymbol{m}_h^{i+1},\boldsymbol{\pi}_h^{\boldsymbol{\Theta}}(\boldsymbol{m}_h^{i+1},\boldsymbol{m}_h^{i},\boldsymbol{m}_h^{i-1})\rangle_{\boldsymbol{L}^2(\omega)} - \langle\boldsymbol{f}^{i+1},\boldsymbol{m}_h^{i+1}\rangle_{\boldsymbol{L}^2(\omega)} + \langle\boldsymbol{f}^{i},\boldsymbol{m}_h^{i}\rangle_{\boldsymbol{L}^2(\omega)} \\
&\qquad + k\,\langle\mathrm{d_t}\boldsymbol{m}_h^{i+1},\boldsymbol{f}_h^{i+1/2}\rangle_{\boldsymbol{L}^2(\omega)} + k\,\langle\mathrm{d_t}\boldsymbol{m}_h^{i+1},\boldsymbol{\Pi}_h^{\boldsymbol{\Theta}}(\boldsymbol{m}_h^{i+1},\boldsymbol{m}_h^{i},\boldsymbol{m}_h^{i-1})\rangle_{\boldsymbol{L}^2(\omega)} \qquad (7.34\mathrm{a}) \\
&\qquad + c\,k\langle\mathrm{d_t}\boldsymbol{m}_h^{i+1},\boldsymbol{s}_h^{i,\boldsymbol{\Theta}}\rangle_{\boldsymbol{L}^2(\omega)} \\
&=: \ -\alpha k\,\|\,\mathrm{d_t}\boldsymbol{m}_h^{i+1}\|_h^2 + \sum_{\ell=1}^{3} T_{\boldsymbol{\pi}}^{(\ell)} + \sum_{\ell=1}^{3} T_{\boldsymbol{f}}^{(\ell)} + k\,\langle\boldsymbol{\Pi}_h^{\boldsymbol{\Theta}}(\boldsymbol{m}_h^{i+1},\boldsymbol{m}_h^{i},\boldsymbol{m}_h^{i-1}),\mathrm{d_t}\boldsymbol{m}_h^{i+1}\rangle_{\boldsymbol{L}^2(\omega)} \\
&\qquad + c\,k\langle\mathrm{d_t}\boldsymbol{m}_h^{i+1},\boldsymbol{s}_h^{i,\boldsymbol{\Theta}}\rangle_{\boldsymbol{L}^2(\omega)}. \qquad (7.34\mathrm{b})
\end{aligned}$$

As in **Step 2** and **Step 3** of the proof of Theorem 6.5.1(c) for plain LLG, it holds that

$$\sum_{\ell=1}^{3} T_{\boldsymbol{\pi}}^{(\ell)} = k\,\langle\mathrm{d_t}\boldsymbol{m}_h^{i+1},\boldsymbol{\pi}_h^{\boldsymbol{\Theta}}(\boldsymbol{m}_h^{i+1},\boldsymbol{m}_h^{i},\boldsymbol{m}_h^{i-1}) - \boldsymbol{\pi}(\boldsymbol{m}_h^{i+1/2})\rangle_{\boldsymbol{L}^2(\omega)} \quad \text{and} \tag{7.34c}$$

$$\sum_{\ell=1}^{3} T_{\boldsymbol{f}}^{(\ell)} = k\,\langle\mathrm{d_t}\boldsymbol{m}_h^{i+1},\boldsymbol{f}_h^{i+1/2} - \boldsymbol{f}^{i+1/2}\rangle_{\boldsymbol{L}^2(\omega)} - k\,\langle\mathrm{d_t}\boldsymbol{f}^{i+1},\boldsymbol{m}_h^{i+1/2}\rangle_{\boldsymbol{L}^2(\omega)}. \tag{7.34d}$$

Then, summation in (7.34) over $i = 0, \dots, j-1$ yields that

$$\begin{aligned}
&\mathcal{E}_{\mathrm{LLG}}\,(\boldsymbol{m}_h^j) + \alpha k \sum_{i=0}^{j-1} \|\, \mathrm{d_t}\boldsymbol{m}_h^{i+1}\|_h^2 + k \sum_{i=0}^{j-1} \langle \mathrm{d_t}\boldsymbol{f}^{i+1}, \boldsymbol{m}_h^{i+1/2}\rangle_{\boldsymbol{L}^2(\omega)} \\
&\quad - k \sum_{i=0}^{j-1} \langle \boldsymbol{\Pi}_h^{\boldsymbol{\Theta}}(\boldsymbol{m}_h^{i+1}, \boldsymbol{m}_h^i, \boldsymbol{m}_h^{i-1}), \mathrm{d_t}\boldsymbol{m}_h^{i+1}\rangle_{\boldsymbol{L}^2(\omega)} - ck \sum_{i=0}^{j-1} \langle \boldsymbol{s}_h^{i,\boldsymbol{\Theta}}, \mathrm{d_t}\boldsymbol{m}_h^{i+1}\rangle_{\boldsymbol{L}^2(\omega)} \\
&= \mathcal{E}_{\mathrm{LLG}}\,(\boldsymbol{m}_h^0) + k \sum_{i=0}^{j-1} \langle \mathrm{d_t}\boldsymbol{m}_h^{i+1}, \boldsymbol{\pi}_h^{\boldsymbol{\Theta}}(\boldsymbol{m}_h^{i+1}, \boldsymbol{m}_h^i, \boldsymbol{m}_h^{i-1}) - \boldsymbol{\pi}(\boldsymbol{m}_h^{i+1/2})\rangle_{\boldsymbol{L}^2(\omega)} \\
&\quad + k \sum_{i=0}^{j-1} \langle \mathrm{d_t}\boldsymbol{m}_h^{i+1}, \boldsymbol{f}_h^{i+1/2} - \boldsymbol{f}^{i+1/2}\rangle_{\boldsymbol{L}^2(\omega)}. \qquad (7.35)
\end{aligned}$$

The norm equivalence relation $\|\cdot\|_{\boldsymbol{L}^2(\omega)} \le \|\cdot\|_h$ from Lemma 3.3.1(i) and the definition of the postprocessed output yield that

$$\begin{aligned}
&\mathcal{E}_{\mathrm{LLG}}\,(\boldsymbol{m}_{hk}^+) + \alpha \int_0^{t_j} \|\partial_t \boldsymbol{m}_{hk}\|_{\boldsymbol{L}^2(\omega)}^2 \,\mathrm{d}t + \int_0^{t_j} \langle \partial_t \boldsymbol{f}_k, \overline{\boldsymbol{m}}_{hk}\rangle_{\boldsymbol{L}^2(\omega)} \,\mathrm{d}t \\
&\quad - \int_0^{t_j} \langle \boldsymbol{\Pi}_h^{\boldsymbol{\Theta}}(\boldsymbol{m}_{hk}^+, \boldsymbol{m}_{hk}^-, \boldsymbol{m}_{hk}^=), \partial_t \boldsymbol{m}_{hk}\rangle_{\boldsymbol{L}^2(\omega)} \,\mathrm{d}t - c \int_0^{t_j} \langle \boldsymbol{s}_{hk}^{\boldsymbol{\Theta}}, \partial_t \boldsymbol{m}_{hk}\rangle_{\boldsymbol{L}^2(\omega)} \,\mathrm{d}t \\
&\overset{(3.10)}{\le} \mathcal{E}_{\mathrm{LLG}}\,(\boldsymbol{m}_h^0) + \int_0^{t_j} \langle \partial_t \boldsymbol{m}_{hk}, \boldsymbol{\pi}_h^{\boldsymbol{\Theta}}(\boldsymbol{m}_{hk}^+, \boldsymbol{m}_{hk}^-, \boldsymbol{m}_{hk}^=) - \boldsymbol{\pi}(\overline{\boldsymbol{m}}_{hk})\rangle_{\boldsymbol{L}^2(\omega)} \,\mathrm{d}t \\
&\quad + \int_0^{t_j} \langle \partial_t \boldsymbol{m}_{hk}, \overline{\boldsymbol{f}}_{hk} - \overline{\boldsymbol{f}}_k\rangle_{\boldsymbol{L}^2(\omega)} \,\mathrm{d}t\,. \qquad (7.36)
\end{aligned}$$

For the terms with $\boldsymbol{\pi}_h^{\boldsymbol{\Theta}}$ and $\boldsymbol{\Pi}_h^{\boldsymbol{\Theta}}$, recall from plain LLG that we required the convergence properties from Lemma 6.5.5 and the strong consistencies **(D4$^+$)** for $\boldsymbol{\pi}_h$ and **(D7$^+$)** for $\boldsymbol{\Pi}_h$ to derive the strong consistencies from Lemma 6.5.8. Hence, with Lemma 7.3.5 (i)–(vi), we get in the same way that

$$\begin{aligned}
\int_0^{t_j} \langle \partial_t \boldsymbol{m}_{hk}, \boldsymbol{\pi}_h^{\boldsymbol{\Theta}}(\boldsymbol{m}_{hk}^+, \boldsymbol{m}_{hk}^-, \boldsymbol{m}_{hk}^=) - \boldsymbol{\pi}(\overline{\boldsymbol{m}}_{hk})\rangle_{\boldsymbol{L}^2(\omega)} \,\mathrm{d}t \to 0, \quad \text{and} \\
\int_0^{t_j} \langle \boldsymbol{\Pi}_h^{\boldsymbol{\Theta}}(\boldsymbol{m}_{hk}^+, \boldsymbol{m}_{hk}^-, \boldsymbol{m}_{hk}^=), \partial_t \boldsymbol{m}_{hk}\rangle_{\boldsymbol{L}^2(\omega)} \,\mathrm{d}t \to \int_0^T \langle \boldsymbol{\Pi}(\boldsymbol{m}), \partial_t \boldsymbol{m}\rangle_{\boldsymbol{L}^2(\omega)} \,\mathrm{d}t,
\end{aligned}$$

as $h, k \to 0$. The last term on the right-hand side vanishes with the strong consistency as for plain LLG as $h, k \to 0$. For the coupling term, we infer from the additional convergence property of Lemma 7.3.8 that

$$c \int_0^{t_j} \langle \boldsymbol{s}_{hk}^{\boldsymbol{\Theta}}, \partial_t \boldsymbol{m}_{hk}\rangle_{\boldsymbol{L}^2(\omega)} \,\mathrm{d}t \to c \int_0^{\tau} \langle \boldsymbol{s}, \partial_t \boldsymbol{m}\rangle_{\boldsymbol{L}^2(\omega)} \,\mathrm{d}t \quad \text{as } h, k \to 0.$$

With the latter convergences at hand, the remainder of the proof employs standard lower semi-continuity arguments and follows the lines of the **Step 5** of the proof of the corresponding Theorem 6.5.1(c) for plain LLG. □

A. Lower-order terms

A.1. Assumption verification for $\boldsymbol{\pi}$

Proposition A.1.1 (Uniaxial anisotropy). *The uniaxial anisotropy* $\boldsymbol{\pi}$ *from* (2.7) *satisfies* **(L1)**–**(L3)** *and* **(T6)**, *i.e.,* $\boldsymbol{\pi}$ *is linear, bounded, self-adjoint, and* $\boldsymbol{L}^3$*-stable.*

Proof. **(L1)**, **(L2)** and **(T6)** are direct consequences of $|\mathbf{a}| = 1$. To verify **(L3)**, the definition (2.7) of the anisotropy contribution $\boldsymbol{\pi}$ yields, that

$$\int_\omega \boldsymbol{\pi}(\boldsymbol{\varphi})\,\boldsymbol{\psi}\,\mathrm{d}\boldsymbol{x} \overset{(2.7)}{=} \int_\omega (\mathbf{a}\cdot\boldsymbol{\varphi})\,(\mathbf{a}\cdot\boldsymbol{\psi})\,\mathrm{d}\boldsymbol{x} \overset{(2.7)}{=} \int_\omega \boldsymbol{\varphi}\,\boldsymbol{\pi}(\boldsymbol{\psi})\,\mathrm{d}\boldsymbol{x} \quad \text{for all } \boldsymbol{\varphi},\boldsymbol{\psi}\in\boldsymbol{L}^2(\omega).$$

This concludes the proof. □

Proposition A.1.2 (Stray field, [Pra04, Proposition 3.4, Theorem 5.2]). *The stray field* $\boldsymbol{\pi}$ *from* (2.11) *is well-defined and satisfies* **(L1)**–**(L3)** *and* **(T6)**, *i.e.,* $\boldsymbol{\pi}$ *is linear, bounded, self-adjoint, and* $\boldsymbol{L}^3$*-stable.* □

A.2. Assumption verification for $\boldsymbol{\pi}_h$

Proposition A.2.1 (Approximate anisotropy). *The approximate uniaxial anisotropy* $\boldsymbol{\pi}_h$ *from* (3.16) *satisfies* **(D2)**, **(D3)**, *and* **(D4⁺)**, *i.e.,* $\boldsymbol{\pi}_h$ *is linear, uniformly bounded in* $\boldsymbol{L}^2(\omega)$, *and satisfies the strong consistency condition.* □

Proposition A.2.2 (Approximate stray field with Fredkin–Koehler). *The approximate stray field* $\boldsymbol{\pi}_h$ *from Section 3.4.5 satisfies* **(D2)**, **(D3)**, *and* **(D4⁺)**, *i.e.,* $\boldsymbol{\pi}_h$ *is linear, uniformly bounded in* $\boldsymbol{L}^2(\omega)$, *and satisfies the strong consistency condition.*

Proof. The linearity **(D2)** is obvious from Algorithm 3.4.3. In [BSF⁺14, Proposition 4.2], **(D3)** and **(D4)** are proved with the Scott–Zhang projection [SZ90], instead of the $L^2(\partial\omega)$-orthogonal projection in Algorithm 3.4.3(b). Since $\mathcal{T}_h$ is quasi-uniform, we obtain, in particular, that the $L^2(\partial\omega)$-orthogonal projection onto $\mathcal{S}_h^{\partial\omega} := \mathcal{S}_h|_{\partial\omega}$ is (uniformly) $\boldsymbol{H}^1(\partial\omega)$-stable. Then, [Gol12, Section 4.3] implies that **(D3)** and **(D4)** are also valid for the $L^2(\partial\omega)$-orthogonal projection. □

A.3. Assumption verification for $\boldsymbol{\Pi}_h$

A.3.1. Approximate Zhang–Li field

In the following proposition, we verify the assumptions of this work for the approximate Zhang–Li field $\boldsymbol{\Pi}_h$ from (3.18) and the corresponding approximate derivative $\boldsymbol{D}_h$

from (4.12). For (i), we elaborate and extend the corresponding arguments of [PRS18, Section 4.2], [DPP+17, Section 7.2.2] and [Rug16, Section 5.2.2]. For (ii), we reorganize and extend [DPP+17, Section 7.2.2]. For (iii), we follow [PRS18, Remark 14(vii)]. Whenever necessary, we transfer those arguments from the postprocessed outputs $\boldsymbol{m}_{hk}^{\star}$ and $\boldsymbol{v}_{hk}^{-}$ to our general framework. For the sake of readability, we recall the approximate Zhang–Li field from (3.18): For $\boldsymbol{\varphi}_h \in \boldsymbol{\mathcal{S}}_h$, we have

$$\boldsymbol{\Pi}_h(\boldsymbol{\varphi}_h) := \boldsymbol{\varphi}_h \times (\boldsymbol{u} \cdot \nabla)\,\boldsymbol{\varphi}_h + \beta\,(\boldsymbol{u} \cdot \nabla)\,\boldsymbol{\varphi}_h \in \boldsymbol{L}^2(\omega), \tag{A.1a}$$

where $\boldsymbol{u} \in \boldsymbol{L}^\infty(\omega)$ and $\beta \in [0,1]$. For the tangent plane scheme, we additionally recall the corresponding approximation operator of the formal derivative from (4.12): For $\boldsymbol{\varphi}_h, \boldsymbol{\psi}_h \in \boldsymbol{\mathcal{S}}_h$, we have

$$\boldsymbol{D}_h(\boldsymbol{\varphi}_h, \boldsymbol{\psi}_h) := \boldsymbol{\psi}_h \times (\boldsymbol{u} \cdot \nabla)\,\boldsymbol{\varphi}_h + \boldsymbol{\varphi}_h \times (\boldsymbol{u} \cdot \nabla)\,\boldsymbol{\psi}_h + \beta\,(\boldsymbol{u} \cdot \nabla)\,\boldsymbol{\psi}_h \in \boldsymbol{L}^2(\omega). \tag{A.1b}$$

Proposition A.3.1 (Approximate Zhang–Li field)**.** *Consider the approximate Zhang–Li field* $\boldsymbol{\Pi}_h$ *and the corresponding approximate derivative operator* $\boldsymbol{D}_h$ *from* (A.1)*. Then, the following three assertions* (i)–(iii) *hold true:*

(i) **General:** *The operator* $\boldsymbol{\Pi}_h$ *satisfies* **(D6)** *and* **(D7)***.*

(ii) **TPS:** *The operator* $\boldsymbol{D}_h$ *satisfies* **(T3)** *and* **(T4)***.*

(iii) **MPS:** *The operator* $\boldsymbol{\Pi}_h$ *satisfies* **(M2)***.*

Proof. To prove (i), we conclude uniform boundedness **(D6)** from

$$\begin{aligned}\|\boldsymbol{\Pi}_h(\boldsymbol{\varphi}_h)\|_{\boldsymbol{L}^2(\omega)} &\overset{\text{(A.1a)}}{\lesssim} \|\boldsymbol{\varphi}_h\|_{\boldsymbol{L}^\infty(\omega)}\,\|\boldsymbol{u}\|_{\boldsymbol{L}^\infty(\omega)}\,\|\nabla\boldsymbol{\varphi}_h\|_{\boldsymbol{L}^2(\omega)} + \beta\,\|\boldsymbol{u}\|_{\boldsymbol{L}^\infty(\omega)}\,\|\nabla\boldsymbol{\varphi}_h\|_{\boldsymbol{L}^2(\omega)} \\ &\lesssim \big(1 + \|\boldsymbol{\varphi}_h\|_{\boldsymbol{L}^\infty(\omega)}\big)\,\|\boldsymbol{\varphi}_h\|_{\boldsymbol{H}^1(\omega)} \quad \text{for all } \boldsymbol{\varphi}_h \in \boldsymbol{\mathcal{S}}_h. \end{aligned} \tag{A.2}$$

Next, we verify weak consistency **(D7)**: To this end, let $\boldsymbol{\varphi} \in \boldsymbol{H}^1(\omega_T) \cap \boldsymbol{L}^\infty(\omega_T)$ and let the sequence $(\boldsymbol{\varphi}_{hk})_{h,k>0} \subset \boldsymbol{L}^2(0,T;\boldsymbol{\mathcal{S}}_h)$ satisfy that

$$\boldsymbol{\varphi}_{hk} \to \boldsymbol{\varphi} \quad \text{in } \boldsymbol{L}^2(\omega_T) \quad \text{and} \quad \nabla\boldsymbol{\varphi}_{hk} \rightharpoonup \nabla\boldsymbol{\varphi} \quad \text{in } \boldsymbol{L}^2(\omega_T), \quad \text{as } h,k \to 0, \tag{A.3}$$

Moreover, let $(\boldsymbol{\varphi}_{hk})_{h,k>0}$ be uniformly bounded, i.e., it holds that $\|\boldsymbol{\varphi}_{hk}\|_{\boldsymbol{L}^\infty(\omega_T)} \lesssim 1$. With Lemma B.2.1, and the uniform boundedness

$$\|\boldsymbol{\Pi}_h(\boldsymbol{\varphi}_{hk})\|_{\boldsymbol{L}^2(\omega_T)} \overset{\text{(A.2)}}{\lesssim} \big(1 + \|\boldsymbol{\varphi}_{hk}\|_{\boldsymbol{L}^\infty(\omega_T)}\big)\,\|\nabla\boldsymbol{\varphi}_{hk}\|_{\boldsymbol{L}^2(\omega_T)} \lesssim 1,$$

it only remains to show for all $\boldsymbol{\zeta} \in \boldsymbol{C}^\infty(\overline{\omega_T})$ that

$$\int_0^T \langle \boldsymbol{\Pi}_h(\boldsymbol{\varphi}_{hk}), \boldsymbol{\zeta}\rangle_{\boldsymbol{L}^2(\omega)}\,\mathrm{d}\boldsymbol{x} \to \int_0^T \langle \boldsymbol{\Pi}(\boldsymbol{\varphi}), \boldsymbol{\zeta}\rangle_{\boldsymbol{L}^2(\omega)}\,\mathrm{d}\boldsymbol{x} \quad \text{as } h,k \to 0. \tag{A.4}$$

To that end, let $\boldsymbol{\zeta} \in \boldsymbol{C}^\infty(\overline{\omega_T})$. We get that

$$\begin{aligned}
&\int_0^T \langle \mathbf{\Pi}_h(\boldsymbol{\varphi}_{hk}), \boldsymbol{\zeta}\rangle_{\boldsymbol{L}^2(\omega)} \,\mathrm{d}t \\
&\overset{\text{(A.1a)}}{=} \int_0^T \langle \boldsymbol{\varphi}_{hk} \times (\boldsymbol{u}\cdot\nabla)\,\boldsymbol{\varphi}_{hk}, \boldsymbol{\zeta}\rangle_{\boldsymbol{L}^2(\omega)} \,\mathrm{d}t + \beta \int_0^T \langle (\boldsymbol{u}\cdot\nabla)\,\boldsymbol{\varphi}_{hk}, \boldsymbol{\zeta}\rangle_{\boldsymbol{L}^2(\omega)} \,\mathrm{d}t \\
&= \; -\int_0^T \langle (\boldsymbol{u}\cdot\nabla)\,\boldsymbol{\varphi}_{hk}, \boldsymbol{\varphi}_{hk} \times \boldsymbol{\zeta}\rangle_{\boldsymbol{L}^2(\omega)} \,\mathrm{d}t + \beta \int_0^T \langle (\boldsymbol{u}\cdot\nabla)\,\boldsymbol{\varphi}_{hk}, \boldsymbol{\zeta}\rangle_{\boldsymbol{L}^2(\omega)} \,\mathrm{d}t =: -I^1_{hk} + \beta I^2_{hk}.
\end{aligned}$$

Since $\boldsymbol{\zeta} \in \boldsymbol{C}^\infty(\overline{\omega_T})$, we obtain that

$$\boldsymbol{\varphi}_{hk} \times \boldsymbol{\zeta} \overset{\text{(A.3)}}{\to} \boldsymbol{\varphi} \times \boldsymbol{\zeta} \quad \text{in } \boldsymbol{L}^2(\omega_T) \quad \text{as } h, k \to 0,$$

and with the latter equation, we prove that

$$\begin{aligned}
I^1_{hk} &\to \int_0^T \langle (\boldsymbol{u}\cdot\nabla)\,\boldsymbol{\varphi}, \boldsymbol{\varphi} \times \boldsymbol{\zeta}\rangle_{\boldsymbol{L}^2(\omega)} \,\mathrm{d}t = -\int_0^T \langle \boldsymbol{\varphi} \times (\boldsymbol{u}\cdot\nabla)\,\boldsymbol{\varphi}, \boldsymbol{\zeta}\rangle_{\boldsymbol{L}^2(\omega)} \,\mathrm{d}t, \\
I^2_{hk} &\to \int_0^T \langle (\boldsymbol{u}\cdot\nabla)\,\boldsymbol{\varphi}, \boldsymbol{\zeta}\rangle_{\boldsymbol{L}^2(\omega)} \,\mathrm{d}t, \quad \text{as } h, k \to 0.
\end{aligned}$$

The combination of the latter three equations verifies (A.4). This shows **(D7)** and proves (i).

For (ii), linearity in the second argument **(T3)** is obvious from the definition (A.1b) of $\boldsymbol{D}_h$. For uniform boundedness **(T4)**, let $\boldsymbol{\varphi}_h \in \boldsymbol{\mathcal{M}}_h$ and $\boldsymbol{\psi}_h \in \boldsymbol{\mathcal{S}}_h$. From $(\mathbf{a} \times \mathbf{b}) \cdot \mathbf{a} = \mathbf{0}$, we obtain for vectors $\mathbf{a}, \mathbf{b} \in \mathbb{R}^3$ that

$$\begin{aligned}
\langle \boldsymbol{D}_h(\boldsymbol{\varphi}_h, \boldsymbol{\psi}_h), \boldsymbol{\psi}_h\rangle &\overset{\text{(A.1b)}}{=} \langle \boldsymbol{\varphi}_h \times (\boldsymbol{u}\cdot\nabla)\,\boldsymbol{\psi}_h, \boldsymbol{\psi}_h\rangle_{\boldsymbol{L}^2(\omega)} + \beta\,\langle (\boldsymbol{u}\cdot\nabla)\,\boldsymbol{\psi}_h, \boldsymbol{\psi}_h\rangle_{\boldsymbol{L}^2(\omega)} \\
&\lesssim \big(\,\|\boldsymbol{\varphi}_h\|_{\boldsymbol{L}^\infty(\omega)} + \beta\,\big)\,\|\boldsymbol{u}\|_{\boldsymbol{L}^\infty(\omega)}\,\|\nabla\boldsymbol{\psi}_h\|_{\boldsymbol{L}^2(\omega)}\,\|\boldsymbol{\psi}_h\|_{\boldsymbol{L}^2(\omega)} \\
&\lesssim \|\boldsymbol{\psi}_h\|_{\boldsymbol{L}^2(\omega)}\,\|\boldsymbol{\psi}_h\|_{\boldsymbol{H}^1(\omega)},
\end{aligned}$$

which verifies the first part of **(T4)**. For the second part, let $\boldsymbol{\varphi}_h, \widetilde{\boldsymbol{\varphi}}_h \in \boldsymbol{\mathcal{M}}_h$. Then,

$$\begin{aligned}
&\|\boldsymbol{D}_h(\boldsymbol{\varphi}_h, \widetilde{\boldsymbol{\varphi}}_h)\|_{\boldsymbol{L}^2(\omega)} \\
&\overset{\text{(A.1b)}}{\leq} \|\widetilde{\boldsymbol{\varphi}}_h \times (\boldsymbol{u}\cdot\nabla)\,\boldsymbol{\varphi}_h\|_{\boldsymbol{L}^2(\omega)} + \|\boldsymbol{\varphi}_h \times (\boldsymbol{u}\cdot\nabla)\,\widetilde{\boldsymbol{\varphi}}_h\|_{\boldsymbol{L}^2(\omega)} + \beta\,\|(\boldsymbol{u}\cdot\nabla)\,\widetilde{\boldsymbol{\varphi}}_h\|_{\boldsymbol{L}^2(\omega)} \\
&\leq \|\widetilde{\boldsymbol{\varphi}}_h\|_{\boldsymbol{L}^\infty(\omega)}\,\|\nabla\boldsymbol{\varphi}_h\|_{\boldsymbol{L}^2(\omega)} + \|\boldsymbol{\varphi}_h\|_{\boldsymbol{L}^\infty(\omega)}\,\|\nabla\widetilde{\boldsymbol{\varphi}}_h\|_{\boldsymbol{L}^2(\omega)} + \beta\,\|\nabla\widetilde{\boldsymbol{\varphi}}_h\|_{\boldsymbol{L}^2(\omega)} \\
&\lesssim \|\boldsymbol{\varphi}_h\|_{\boldsymbol{H}^1(\omega)} + \|\widetilde{\boldsymbol{\varphi}}_h\|_{\boldsymbol{H}^1(\omega)}.
\end{aligned}$$

Altogether, this verifies **(T4)**.

For (iii), we have to show the Lipschitz-type continuity **(M2)**. To this end, let $\boldsymbol{\varphi}_h, \boldsymbol{\psi}_h \in$

$\boldsymbol{\mathcal{S}}_h$. Then, we obtain that

$$
\begin{aligned}
&\|\boldsymbol{\Pi}_h(\boldsymbol{\varphi}_h) - \boldsymbol{\Pi}_h(\boldsymbol{\psi}_h)\|_{\boldsymbol{L}^2(\omega)} \\
&\overset{\text{(A.1b)}}{\leq} \|\boldsymbol{\varphi}_h \times (\boldsymbol{u}\cdot\nabla)\boldsymbol{\varphi}_h - \boldsymbol{\psi}_h \times (\boldsymbol{u}\cdot\nabla)\boldsymbol{\psi}_h\|_{\boldsymbol{L}^2(\omega)} + \beta\,\|(\boldsymbol{u}\cdot\nabla)\big[\boldsymbol{\varphi}_h - \boldsymbol{\psi}_h\big]\|_{\boldsymbol{L}^2(\omega)} \\
&\lesssim \|\big[\boldsymbol{\varphi}_h - \boldsymbol{\psi}_h\big] \times (\boldsymbol{u}\cdot\nabla)\boldsymbol{\varphi}_h\|_{\boldsymbol{L}^2(\omega)} + \|\boldsymbol{\psi}_h \times (\boldsymbol{u}\cdot\nabla)\big[\boldsymbol{\varphi}_h - \boldsymbol{\psi}_h\big]\|_{\boldsymbol{L}^2(\omega)} \\
&\qquad + \beta\,\|\boldsymbol{u}\|_{\boldsymbol{L}^\infty(\omega)}\,\|\nabla\boldsymbol{\varphi}_h - \nabla\boldsymbol{\psi}_h\|_{\boldsymbol{L}^2(\omega)} \\
&\lesssim \|\boldsymbol{u}\|_{\boldsymbol{L}^\infty(\omega)}\,\|\nabla\boldsymbol{\varphi}_h\|_{\boldsymbol{L}^\infty(\omega)}\,\|\boldsymbol{\varphi}_h - \boldsymbol{\psi}_h\|_{\boldsymbol{L}^2(\omega)} \\
&\qquad + \big(\,\|\boldsymbol{u}\|_{\boldsymbol{L}^\infty(\omega)}\,\|\boldsymbol{\psi}_h\|_{\boldsymbol{L}^\infty(\omega)} + \beta\,\big)\,\|\nabla\boldsymbol{\varphi}_h - \nabla\boldsymbol{\psi}_h\|_{\boldsymbol{L}^2(\omega)}.
\end{aligned}
$$

With an inverse estimate (see Proposition 3.1.8), we altogether get that

$$
\|\boldsymbol{\Pi}_h(\boldsymbol{\varphi}_h) - \boldsymbol{\Pi}_h(\boldsymbol{\psi}_h)\|_{\boldsymbol{L}^2(\omega)} \lesssim h^{-1}\,\big(\,1 + \|\boldsymbol{\varphi}_h\|_{\boldsymbol{L}^\infty(\omega)} + \|\boldsymbol{\psi}_h\|_{\boldsymbol{L}^\infty(\omega)}\,\big)\,\|\boldsymbol{\varphi}_h - \boldsymbol{\psi}_h\|_{\boldsymbol{L}^2(\omega)}.
$$

This shows **(M2)** and concludes the proof. □

The weak consistency property **(T5)** for the approximate derivative does not hold for $\boldsymbol{D}_h$ from (A.1b). Throughout the proof of Theorem 4.5.1(b), the assumption **(T5)** is not required until the convergence (4.52). However, in the specific situation of Lemma 4.5.4, the following proposition let us bypass the missing **(T5)**; see also Remark 4.5.8.

Proposition A.3.2 (Bypass missing **(T5)** in (4.52))**.** *Consider the approximate approximate derivative operator $\boldsymbol{D}_h$ from* (A.1) *of the Zhang–Li field from* (3.18)*. Let the assumptions from Theorem 4.5.1*(b) *be satisfied. Let $\boldsymbol{\mathcal{I}}_h$ be the nodal interpolant corresponding to $\boldsymbol{\mathcal{S}}_h$. Then, for all $\boldsymbol{\varphi} \in \boldsymbol{C}^\infty(\overline{\omega_T})$, it holds that*

$$
\int_0^T \langle \boldsymbol{D}_h(\boldsymbol{m}_{hk}^-, k\boldsymbol{v}_{hk}^-), \boldsymbol{\mathcal{I}}_h(\boldsymbol{m}_{hk}^- \times \boldsymbol{\varphi})\rangle_{\boldsymbol{L}^2(\omega)}\,\mathrm{d}t \to 0, \quad \textit{and} \tag{A.5a}
$$

$$
\int_0^T \langle \boldsymbol{D}_h(\boldsymbol{m}_{hk}^-, \boldsymbol{m}_{hk}^- - \boldsymbol{m}_{hk}^{=}), \boldsymbol{\mathcal{I}}_h(\boldsymbol{m}_{hk}^- \times \boldsymbol{\varphi})\rangle_{\boldsymbol{L}^2(\omega)}\,\mathrm{d}t \to 0, \quad \textit{as } h,k \to 0. \tag{A.5b}
$$

Proof. With the assumptions from Theorem 4.5.1(b), we have, in particular, available the convergence properties of the postprocessed output from Lemma 4.5.4. Lemma 4.5.6 implies that the limit $\boldsymbol{m}$ satisfies $|\boldsymbol{m}| = 1$ a.e. in ω_T. The nodewise normalization in the update from Algorithm 4.2.1(c) yields that $\|\boldsymbol{m}_{hk}^-\|_{\boldsymbol{L}^\infty(\omega_T)} = 1$ and for $\boldsymbol{\varphi} \in \boldsymbol{C}^\infty(\overline{\omega_T})$ that

$$
\widehat{\boldsymbol{\varphi}}_{hk} := \boldsymbol{\mathcal{I}}_h(\boldsymbol{m}_{hk}^- \times \boldsymbol{\varphi}) \quad \text{satisfies} \quad \|\widehat{\boldsymbol{\varphi}}_{hk}\|_{\boldsymbol{L}^\infty(\omega_T)} \leq \|\boldsymbol{\varphi}\|_{\boldsymbol{L}^\infty(\omega_T)}. \tag{A.6}
$$

First, we show (A.5a): With linearity **(T3)** of $\boldsymbol{D}_h$ in the second argument (cf. Proposition A.3.1(ii)), we obtain that

$$
\begin{aligned}
I_{hk}^1 &:= \Big| \int_0^T \langle \boldsymbol{D}_h(\boldsymbol{m}_{hk}^-, k\boldsymbol{v}_{hk}^-), \widehat{\boldsymbol{\varphi}}_{hk}\rangle_{\boldsymbol{L}^2(\omega)}\,\mathrm{d}t \Big| = \Big| k\int_0^T \langle \boldsymbol{D}_h(\boldsymbol{m}_{hk}^-, \boldsymbol{v}_{hk}^-), \widehat{\boldsymbol{\varphi}}_{hk}\rangle_{\boldsymbol{L}^2(\omega)}\,\mathrm{d}t \Big| \\
&\overset{\text{(A.1b)}}{\leq} k\int_0^T \big|\langle \boldsymbol{v}_{hk}^- \times (\boldsymbol{u}\cdot\nabla)\,\boldsymbol{m}_{hk}^-, \widehat{\boldsymbol{\varphi}}_{hk}\rangle_{\boldsymbol{L}^2(\omega)}\big|\,\mathrm{d}t + k\int_0^T \big|\langle \boldsymbol{m}_{hk}^- \times (\boldsymbol{u}\cdot\nabla)\,\boldsymbol{v}_{hk}^-, \widehat{\boldsymbol{\varphi}}_{hk}\rangle_{\boldsymbol{L}^2(\omega)}\big|\,\mathrm{d}t \\
&\quad + \beta k \int_0^T \big|\langle (\boldsymbol{u}\cdot\nabla)\,\boldsymbol{v}_{hk}^-, \widehat{\boldsymbol{\varphi}}_{hk}\rangle_{\boldsymbol{L}^2(\omega)}\big|\,\mathrm{d}t \\
&\overset{\text{(A.6)}}{\lesssim} k\,\|\boldsymbol{v}_{hk}^-\|_{\boldsymbol{L}^2(\omega_T)}\,\|\boldsymbol{u}\|_{\boldsymbol{L}^\infty(\omega)}\,\|\nabla\boldsymbol{m}_{hk}^-\|_{\boldsymbol{L}^2(\omega_T)}\,\|\widehat{\boldsymbol{\varphi}}_{hk}\|_{\boldsymbol{L}^\infty(\omega_T)} \\
&\quad + k\,\big(1 + \|\boldsymbol{m}_{hk}^-\|_{\boldsymbol{L}^\infty(\omega_T)}\big)\,\|\boldsymbol{u}\|_{\boldsymbol{L}^\infty(\omega)}\,\|\nabla\boldsymbol{v}_{hk}^-\|_{\boldsymbol{L}^2(\omega_T)}\,\|\widehat{\boldsymbol{\varphi}}_{hk}\|_{\boldsymbol{L}^\infty(\omega_T)}.
\end{aligned}
$$

With $\|\boldsymbol{m}_{hk}^-\|_{\boldsymbol{L}^\infty(\omega_T)} = 1$ and uniform boundedness from (A.6), we get that

$$
I_{hk}^1 \lesssim k\,\|\boldsymbol{v}_{hk}^-\|_{\boldsymbol{L}^2(\omega_T)}\,\|\nabla\boldsymbol{m}_{hk}^-\|_{\boldsymbol{L}^2(\omega_T)}\,\|\boldsymbol{\varphi}\|_{\boldsymbol{L}^\infty(\omega_T)} + k\,\|\nabla\boldsymbol{v}_{hk}^-\|_{\boldsymbol{L}^2(\omega_T)}\,\|\boldsymbol{\varphi}\|_{\boldsymbol{L}^\infty(\omega_T)}.
$$

With the convergence properties from Lemma 4.5.4, this yields that $I_{hk}^1 \to 0$ as $h, k \to 0$ and thus proves (A.5a).

Next, we show (A.5b): We obtain that

$$
\begin{aligned}
I_{hk}^2 &:= \int_0^T \langle \boldsymbol{D}_h(\boldsymbol{m}_{hk}^-, \boldsymbol{m}_{hk}^- - \boldsymbol{m}_{hk}^=), \widehat{\boldsymbol{\varphi}}_{hk}\rangle_{\boldsymbol{L}^2(\omega)}\,\mathrm{d}t \\
&\overset{\text{(A.1b)}}{=} \int_0^T \langle [\boldsymbol{m}_{hk}^- - \boldsymbol{m}_{hk}^=] \times (\boldsymbol{u}\cdot\nabla)\,\boldsymbol{m}_{hk}^-, \widehat{\boldsymbol{\varphi}}_{hk}\rangle_{\boldsymbol{L}^2(\omega)}\,\mathrm{d}t \\
&\quad + \int_0^T \langle \boldsymbol{m}_{hk}^- \times (\boldsymbol{u}\cdot\nabla)[\boldsymbol{m}_{hk}^- - \boldsymbol{m}_{hk}^=], \widehat{\boldsymbol{\varphi}}_{hk}\rangle_{\boldsymbol{L}^2(\omega)}\,\mathrm{d}t \\
&\quad + \beta\int_0^T \langle (\boldsymbol{u}\cdot\nabla)[\boldsymbol{m}_{hk}^- - \boldsymbol{m}_{hk}^=], \widehat{\boldsymbol{\varphi}}_{hk}\rangle_{\boldsymbol{L}^2(\omega)}\,\mathrm{d}t =: I_{hk}^{2,A} + I_{hk}^{2,B} + I_{hk}^{2,C}.
\end{aligned}
\tag{A.7}
$$

First, we deal with $I_{hk}^{2,A}$: With $\|\boldsymbol{m}_{hk}^-\|_{\boldsymbol{L}^\infty(\omega_T)} = 1$ and uniform boundedness (A.6), we get that

$$
|I_{hk}^{2,A}| \overset{\text{(A.7)}}{\lesssim} \|\boldsymbol{u}\|_{\boldsymbol{L}^\infty(\omega)}\,\|\boldsymbol{m}_{hk}^- - \boldsymbol{m}_{hk}^=\|_{\boldsymbol{L}^2(\omega_T)}\,\|\nabla\boldsymbol{m}_{hk}^-\|_{\boldsymbol{L}^2(\omega_T)}\,\|\boldsymbol{\varphi}\|_{\boldsymbol{L}^\infty(\omega_T)}.
$$

The convergence properties of Lemma 4.5.4 then yield that $I_{hk}^{2,A} \to 0$ as $h, k \to 0$. For $I_{hk}^{2,B}$, we get as in **Step 3** of the proof of Theorem 4.5.1(b) that

$$
\widehat{\boldsymbol{\varphi}}_{hk} \overset{\text{(A.6)}}{\to} \boldsymbol{m}\times\boldsymbol{\varphi} \quad \text{in } \boldsymbol{L}^2(\omega_T) \quad \text{as } h, k \to 0
$$

With $\|\boldsymbol{m}_{hk}^-\|_{\boldsymbol{L}^\infty(\omega_T)} = \|\boldsymbol{m}\|_{\boldsymbol{L}^\infty(\omega_T)} = 1$ and the uniform boundedness (A.6), we similarly obtain that

$$
\boldsymbol{m}_{hk}^- \times \boldsymbol{\varphi}_{hk} \to \boldsymbol{m}\times(\boldsymbol{m}\times\boldsymbol{\varphi}) \quad \text{in } \boldsymbol{L}^2(\omega_T) \quad \text{as } h, k \to 0.
$$

The latter two convergences and the convergence properties of Lemma 4.5.4 yield that

$$I_{hk}^{2,B} \overset{(A.7)}{=} -\int_0^T \langle (\boldsymbol{u}\cdot\nabla)\big[\boldsymbol{m}_{hk}^- - \boldsymbol{m}_{hk}^=\big], \boldsymbol{m}_{hk}^- \times \widehat{\boldsymbol{\varphi}}_{hk}\rangle_{\boldsymbol{L}^2(\omega)}\,\mathrm{d}t \to 0 \quad \text{as } h,k \to 0.$$

With $\boldsymbol{\varphi}_{hk}$ instead of $\boldsymbol{m}_{hk}^- \times \boldsymbol{\varphi}_{hk}$, in the latter arguments, we get in the same way that $I_{hk}^{2,C} \to 0$ as $h,k \to 0$. Altogether, this shows (A.5b) and concludes the proof. □

A.3.2. Approximate Slonczewksi field

In the following proposition, we verify the assumptions of this work for the approximate Slonczewski field $\boldsymbol{\Pi}_h$ from (3.19) and the corresponding approximate derivative $\boldsymbol{D}_h$ from (4.13). Morally, we reorganize [DPP+17, Section 7.2.1]. For (i) and (iii), we also refer to [Rug16, Section 5.2.1]. Whenever necessary, we transfer the arguments in the latter references from the postprocessed outputs $\boldsymbol{m}_{hk}^\star$ and $\boldsymbol{v}_{hk}^-$ to our general framework. For the sake of readability, we recall the approximate Slonczewski field from (3.19): For $\boldsymbol{\varphi}_h \in \boldsymbol{\mathcal{S}}_h$, we have

$$\boldsymbol{\Pi}_h(\boldsymbol{\varphi}_h) := \mathcal{G}(\boldsymbol{\varphi}_h \cdot \mathbf{p})\,\boldsymbol{\varphi}_h \times \mathbf{p} \in \boldsymbol{L}^2(\omega) \tag{A.8a}$$

For the tangent plane scheme, we additionally recall the corresponding approximation operator of the formal derivative from (4.13): For $\boldsymbol{\varphi}_h, \boldsymbol{\psi}_h \in \boldsymbol{\mathcal{S}}_h$, we have

$$\boldsymbol{D}_h(\boldsymbol{\varphi}_h, \boldsymbol{\psi}_h) := \big[\mathcal{G}'(\boldsymbol{\varphi}_h \cdot \mathbf{p})\,\boldsymbol{\psi}_h \cdot \mathbf{p}\big]\boldsymbol{\varphi}_h \times \mathbf{p} + \mathcal{G}(\boldsymbol{\varphi}_h \cdot \mathbf{p})\,\boldsymbol{\psi}_h \times \mathbf{p} \in \boldsymbol{L}^2(\omega). \tag{A.8b}$$

Proposition A.3.3 (Approximate Slonczewski field)**.** *Consider the approximate Slonczewski-field $\boldsymbol{\Pi}_h$ from* (3.19) *and the corresponding approximate derivative $\boldsymbol{D}_h$ from* (A.8)*. Then, the following three assertions* (i)–(iii) *hold true:*

(i) **General:** *The operator $\boldsymbol{\Pi}_h$ satisfies* **(D6)** *and* **(D7$^+$)***.*

(ii) **TPS:** *The operator $\boldsymbol{D}_h$ satisfies* **(T3)***,* **(T4$^+$)** *and* **(T5$^+$)***.*

(iii) **MPS:** *The operator $\boldsymbol{\Pi}_h$ satisfies* **(M2)***.*

Proof. To show (i), we need to verify **(D6)**. To this end, $\mathcal{G} \in C_0^1(\mathbb{R})$ and $|\mathbf{p}| = 1$ yield that

$$\begin{aligned}\|\boldsymbol{\Pi}_h(\boldsymbol{\varphi}_h)\|_{\boldsymbol{L}^2(\omega)} &\overset{(A.8a)}{\lesssim} \|\mathcal{G}(\boldsymbol{\varphi}_h\cdot\mathbf{p})\,\boldsymbol{\varphi}_h \times \mathbf{p}\|_{\boldsymbol{L}^2(\omega)} \\ &\lesssim \|\mathcal{G}\|_{L^\infty(\mathbb{R})}\,\|\boldsymbol{\varphi}_h\|_{\boldsymbol{L}^2(\omega)} \lesssim \|\boldsymbol{\varphi}_h\|_{\boldsymbol{L}^2(\omega)} \quad \text{for all } \boldsymbol{\varphi}_h \in \boldsymbol{\mathcal{S}}_h,\end{aligned}$$

i.e., there even holds a stronger estimate than in **(D6)**. To verify the strong consistency condition **(D7$^+$)** we follow [Rug16, Section 5.2.1]: Let $\boldsymbol{\varphi} \in \boldsymbol{L}^2(\omega_T)$ and $(\boldsymbol{\varphi}_{hk})_{h,k>0} \subset \boldsymbol{L}^2(0,T,\boldsymbol{\mathcal{S}}_h)$ with

$$\|\boldsymbol{\varphi}_{hk}\|_{\boldsymbol{L}^\infty(\omega_T)} \lesssim 1 \quad \text{and} \quad \boldsymbol{\varphi}_{hk} \to \boldsymbol{\varphi} \quad \text{in } \boldsymbol{L}^2(\omega_T) \quad \text{as } h,k > 0. \tag{A.9}$$

Then, $\mathcal{G} \in C_0^1(\mathbb{R})$ is, in particular, Lipschitz-continuous and

$$
\begin{aligned}
\|\mathbf{\Pi}_h(\boldsymbol{\varphi}_{hk}) - \mathbf{\Pi}(\boldsymbol{\varphi})\|_{\boldsymbol{L}^2(\omega_T)} &= \|\mathcal{G}(\boldsymbol{\varphi}_{hk}\cdot\mathbf{p})\,\boldsymbol{\varphi}_{hk}\times\mathbf{p} - \mathcal{G}(\boldsymbol{\varphi}\cdot\mathbf{p})\,\boldsymbol{\varphi}\times\mathbf{p}\|_{\boldsymbol{L}^2(\omega_T)} \\
&\le \|\big[\mathcal{G}(\boldsymbol{\varphi}_{hk}\cdot\mathbf{p}) - \mathcal{G}(\boldsymbol{\varphi}\cdot\mathbf{p})\big]\,(\boldsymbol{\varphi}_{hk}\times\mathbf{p})\|_{\boldsymbol{L}^2(\omega_T)} + \|\mathcal{G}(\boldsymbol{\varphi}\cdot\mathbf{p})\big[\boldsymbol{\varphi}_{hk}-\boldsymbol{\varphi}\big]\times\mathbf{p}\|_{\boldsymbol{L}^2(\omega)} \\
&\lesssim \|\mathcal{G}\|_{W^{1,\infty}(\mathbb{R})}\,\|\boldsymbol{\varphi}_{hk}-\boldsymbol{\varphi}\|_{\boldsymbol{L}^2(\omega_T)}\,\|\boldsymbol{\varphi}_{hk}\times\mathbf{p}\|_{\boldsymbol{L}^\infty(\omega_T)} + \|\mathcal{G}\|_{L^\infty(\mathbb{R})}\,\|\boldsymbol{\varphi}_{hk}-\boldsymbol{\varphi}\|_{\boldsymbol{L}^2(\omega_T)} \\
&\overset{\text{(A.9)}}{\lesssim} \|\boldsymbol{\varphi}_{hk}-\boldsymbol{\varphi}\|_{\boldsymbol{L}^2(\omega_T)} \overset{\text{(A.9)}}{\to} 0 \quad \text{as } h,k\to 0.
\end{aligned} \tag{A.10}
$$

This show **(D7⁺)** and concludes the proof of (ii).

Similarly to **(D7⁺)**, we verify **(M2)** and thus prove (iii). To this end, let $\boldsymbol{\varphi}_h, \boldsymbol{\psi}_h \in \boldsymbol{\mathcal{S}}_h$. Since we defined $\mathbf{\Pi}_h := \mathbf{\Pi}|_{\boldsymbol{\mathcal{S}}_h}$ in (A.8a), we can repeat the computations of (A.10) and similarly get that

$$
\begin{aligned}
&\|\mathbf{\Pi}_h(\boldsymbol{\varphi}_h) - \mathbf{\Pi}_h(\boldsymbol{\psi}_h)\|_{\boldsymbol{L}^2(\omega)} \\
&\quad\overset{\text{(A.8a)}}{\lesssim} \|\mathcal{G}\|_{W^{1,\infty}(\mathbb{R})}\,\|\boldsymbol{\varphi}_h\times\mathbf{p}\|_{\boldsymbol{L}^\infty(\omega)}\,\|\boldsymbol{\varphi}_h-\boldsymbol{\psi}_h\|_{\boldsymbol{L}^2(\omega)} + \|\mathcal{G}\|_{L^\infty(\mathbb{R})}\,\|\boldsymbol{\varphi}_h-\boldsymbol{\psi}_h\|_{\boldsymbol{L}^2(\omega)} \\
&\quad\lesssim \big(1 + \|\boldsymbol{\varphi}_h\|_{\boldsymbol{L}^\infty(\omega)}\big)\,\|\boldsymbol{\varphi}_h-\boldsymbol{\psi}_h\|_{\boldsymbol{L}^2(\omega)},
\end{aligned}
$$

which verifies an even stronger estimate than that of **(M2)**.

Finally, we prove (ii). Linearity in the second argument **(T3)** of $\boldsymbol{D}_h$ is obvious from the definition (A.8b). To show strong uniform boundedness **(T4⁺)** of $\boldsymbol{D}_h$, let $\boldsymbol{\varphi}_h \in \boldsymbol{\mathcal{M}}_h$ and $\boldsymbol{\psi}_h \in \boldsymbol{\mathcal{S}}_h$. We get that

$$
\begin{aligned}
\|\boldsymbol{D}_h(\boldsymbol{\varphi}_h,\boldsymbol{\psi}_h)\|_{\boldsymbol{L}^2(\omega)} &\overset{\text{(A.8b)}}{\lesssim} \|\big[\mathcal{G}'(\boldsymbol{\varphi}_h\cdot\mathbf{p})\,\boldsymbol{\psi}_h\cdot\mathbf{p}\big]\boldsymbol{\varphi}_h\times\mathbf{p}\|_{\boldsymbol{L}^2(\omega)} + \|\mathcal{G}(\boldsymbol{\varphi}_h\cdot\mathbf{p})\,\boldsymbol{\psi}_h\times\mathbf{p}\|_{\boldsymbol{L}^2(\omega)} \\
&\lesssim \|\mathcal{G}'\|_{L^\infty(\mathbb{R})}\,\|\boldsymbol{\psi}_h\|_{\boldsymbol{L}^2(\omega)}\,\|\boldsymbol{\varphi}_h\|_{\boldsymbol{L}^\infty(\omega)} + \|\mathcal{G}\|_{L^\infty(\mathbb{R})}\,\|\boldsymbol{\psi}_h\|_{\boldsymbol{L}^2(\omega)} \qquad \text{(A.11)} \\
&\lesssim \big(1 + \|\boldsymbol{\varphi}_h\|_{\boldsymbol{L}^\infty(\omega)}\big)\,\|\boldsymbol{\psi}_h\|_{\boldsymbol{L}^2(\omega)}, \qquad \text{(A.12)}
\end{aligned}
$$

i.e., there even holds a stronger statement than **(T4⁺)**. Finally, we show **(T5⁺)**: To this end, let $(\boldsymbol{\varphi}_{hk})_{h,k>0} \subset L^2(0,T;\boldsymbol{\mathcal{S}}_h)$ and $(\boldsymbol{\psi}_{hk})_{h,k>0} \subset L^2(0,T;\boldsymbol{\mathcal{S}}_h)$, such that

$$
\|\boldsymbol{\varphi}_{hk}\|_{\boldsymbol{L}^\infty(\omega)} \lesssim 1 \quad \text{and} \quad \boldsymbol{\psi}_{hk} \to \mathbf{0} \quad \text{in } \boldsymbol{L}^2(\omega_T) \quad \text{as } h,k\to 0. \tag{A.13}
$$

Repeating the estimates of (A.11) with $\|\cdot\|_{\boldsymbol{L}^2(\omega_T)}$ instead of $\|\cdot\|_{\boldsymbol{L}^2(\omega)}$, we show that

$$
\|\boldsymbol{D}_h(\boldsymbol{\varphi}_{hk},\boldsymbol{\psi}_{hk})\|_{\boldsymbol{L}^2(\omega_T)} \lesssim \big(1 + \|\boldsymbol{\varphi}_h\|_{\boldsymbol{L}^\infty(\omega)}\big)\,\|\boldsymbol{\psi}_{hk}\|_{\boldsymbol{L}^2(\omega_T)} \overset{\text{(A.13)}}{\to} 0 \quad \text{as } h,k\to 0.
$$

Altogether, this shows **(T5⁺)** and concludes the proof. □

B. Auxiliary results

B.1. Tangent plane scheme

Lemma B.1.1 ([Bar05, Lemma 3.2]). *Let $\mathcal{I}_h$ be the nodal interpolant corresponding to $\mathcal{S}_h$, where the underlying mesh satisfies the angle condition* **(T1)**. *Let $\varphi_h \in \mathcal{S}_h$ with $|\varphi_h(z)| \geq 1$ for all nodes $z \in \mathcal{N}_h$. Then, it holds that*

$$\Big\| \nabla \mathcal{I}_h\Big(\frac{\varphi_h}{|\varphi_h|}\Big)\Big\|_{L^2(\omega)} \leq \|\nabla \varphi_h\|_{L^2(\omega)}. \qquad \square$$

Lemma B.1.2 ([Gol12, Lemma 3.1.1]). *Let $p \in [1, \infty)$. Then, there exists a constant $C > 0$, which depends only on $C_{\mathbf{mesh}}$ and p, such that*

$$C^{-1} \|\varphi_h\|_{L^p(\omega)} \leq h^3 \Bigg(\sum_{z \in \mathcal{N}_h} |\varphi_h(z)|^p\Bigg)^{1/p} \leq C \|\varphi_h\|_{L^p(\omega)} \quad \text{for all } \varphi_h \in \mathcal{S}_h. \qquad \square$$

Remark B.1.3. *Lemma B.1.2 is a generalization of Lemma 3.3.1 for $p = 2$.*

Lemma B.1.4. *Let $m_h^i \in \mathcal{M}_h$ and $v_h^i \in \mathcal{K}_h(m_h^i)$. Define $m_h^{i+1} \in \mathcal{M}_h$ via*

$$m_h^{i+1}(z) := \frac{m_h^i(z) + k v_h^i(z)}{|m_h^i(z) + k v_h^i(z)|} \quad \text{for all nodes } z \in \mathcal{N}_h.$$

Then, the following two assertions (i)–(ii) *hold true:*

(i) *For all nodes $z \in \mathcal{N}_h$, it holds that*

$$|m_h^{i+1}(z) - m_h^i(z)| \leq \frac{1}{2} k\, |v_h^i(z)| \quad \text{and} \quad |m_h^{i+1}(z) - m_h^i(z) - k v_h^i(z)| \leq \frac{1}{2} k^2\, |v_h^i(z)|.$$

(ii) *Let $p \in [1, \infty)$. Then, there exists a constant $C > 0$, which depends only on $C_{\mathbf{mesh}}$ and p, such that*

$$\| \mathrm{d_t} m_h^{i+1}\|_{L^p(\omega)} \leq C\, \|v_h^i\|_{L^p(\omega)} \quad \text{and} \quad \| \mathrm{d_t} m_h^{i+1} - v_h^i\|_{L^p(\omega)} \lesssim Ck\, \|v_h^i\|_{L^{2p}(\omega)}.$$

Proof. For the proof of (i), see, e.g., [AJ06, Section 3.1] or [Gol12, Lemma 3.3.2, 3.3.3]. (ii) is a direct consequence of Lemma B.1.2. $\square$

B.2. Functional analysis

Lemma B.2.1 ([Yos95, Chapter V.1, Theorem 3]). *Let B be a Banach space with corresponding norm $\|\cdot\|_B$ and $(x_\ell)_{\ell=1}^\infty \subset B$ as well as $x \in B$. It holds that $x_\ell \rightharpoonup x$ in B as $\ell \to \infty$ if and only if the following two conditions* (A) *and* (B) *are satisfied:*

(A) *It holds that $\sup_{\ell\in\mathbb{N}} \|x_\ell\|_B < \infty$.*

(B) *There exists a dense set $D \subset B'$, such that*

$$f(x_\ell) \to f(x) \quad \text{as } \ell \to \infty \quad \text{for all } f \in D. \qquad \square$$

Theorem B.2.2 (Eberlein–Šmulian theorem, [Yos95, p. 141]). *Let B be a reflexive Banach space with corresponding norm $\|\cdot\|_B$. Let $(x_\ell)_{\ell=1}^\infty \subset B$, such that*

$$\sup_{\ell\in\mathbb{N}} \|x_\ell\| < \infty.$$

Then, there exists $x \in B$ and a subsequence $(x_{\ell_k})_{k=1}^\infty$ such that $x_{\ell_k} \rightharpoonup x$ in B as $k \to \infty$. $\square$

Theorem B.2.3 (Banach–Alaoglu theorem, [Rud91, Theorem 3.17]). *Let B be a separable Banach space with dual space B'. Denote the norm corresponding to B' by $\|\cdot\|_{B'}$. Let $(f_\ell)_{\ell=1}^\infty \subset B'$ such that*

$$\sup_{\ell\in\mathbb{N}} \|f_\ell\|_{B'} < \infty.$$

Then, there exists $f \in B'$ and a subsequence $(f_{\ell_k})_{k=1}^\infty$ such that $f_{\ell_k} \overset{*}{\rightharpoonup} x$ in B' as $k \to \infty$. $\square$

Theorem B.2.4 (Lax–Milgram theorem, [Yos95, Section III.7]). *Let H be a Hilbert space with corresponding norm $\|\cdot\|_H$. Let $S : H \times H \to \mathbb{R}$ be a sesquilinear form, which is continuous in the sense that there exists a constant $C_{cont} > 0$ such that*

$$|S(x, y)| \le C_{cont} \|x\|_H \|y\|_H \quad \text{for all } x, y \in H,$$

and coercive in the sense that there exists a constant $C_{coer} > 0$ such that

$$S(x, x) \ge C_{coer} \|x\|_H^2 \quad \text{for all } x \in H.$$

Let $f \in H'$. Then, there exists a unique $x_f \in H$, such that

$$S(x_f, y) = F(y) \quad \text{for all } y \in H. \qquad \square$$

Theorem B.2.5 (Brouwer fixed-point theorem[1], [Eva10, p. 529]). *Let $d \in \mathbb{N}$ and let $F : \mathbb{R}^d \to \mathbb{R}^d$ be continuous. Suppose there exists $r > 0$, such that*

$$F(\mathbf{x}) \cdot \mathbf{x} \ge 0 \quad \text{for all } \mathbf{x} \in \mathbb{R}^d \text{ with } |\mathbf{x}| = r.$$

Then, there exists $\mathbf{x}_0 \in \mathbb{R}^d$ with $|\mathbf{x}_0| < r$ and $F(\mathbf{x}_0) = \mathbf{0}$. $\square$

[1] Note that this result is often only considered a corollary of the actual Brouwer fixed-point theorem. We refer to, e.g., [Eva10, p. 463] for the classical formulation.

Theorem B.2.6 (Banach fixed-point theorem, [Wer11, p. 166])**.** *Let B be a Banach space with corresponding norm $\|\cdot\|_B$. Let $q \in (0,1)$. Let $\mathcal{F} : B \to B$ be a mapping, such that*

$$\|\mathcal{F}(u) - \mathcal{F}(v)\|_B \le q\,\|u - v\|_B \quad \text{for all } u, v \in B.$$

Then, $\mathcal{F}$ has a unique fixed-point $x \in B$, i.e., $\mathcal{F}(x) = x$. In particular, for any initial value $x_0 \in B$, the sequence $(x_\ell)_{\ell \in \mathbb{N}_0} \subset B$ defined via $x_{\ell+1} := \mathcal{F}(x_\ell)$ for all $\ell \in \mathbb{N}_0$ satisfies that

$$x_\ell \to x \quad \text{in } B \quad \text{as } \ell \to \infty. \qquad \square$$

B.3. Other

Lemma B.3.1 (Discrete Gronwall lemma, [QV94, Lemma 1.4.2])**.** *Let $\alpha_0 > 0$ and let $(\beta_i)_{i=0}^\infty, (\gamma_i)_{i=0}^\infty$ be non-negative sequences. Suppose that*

$$\gamma_0 \le \alpha_0 \quad \text{and} \quad \gamma_i \le \alpha_0 + \sum_{j=0}^{i-1} \beta_j \gamma_j \quad \text{for all } i \ge 1.$$

Then, it holds that

$$\gamma_i \le \alpha_0 \exp\left(\sum_{j=0}^{i-1} \beta_j\right) \quad \text{for all } i \ge 1. \qquad \square$$

Lemma B.3.2 (Young's inequality, [Eva10, p. 706])**.** *Let $a, b \in \mathbb{R}$. For $\delta > 0$, it holds that*

$$ab \le \delta a^2 + \frac{b^2}{4\delta}. \qquad \square$$

Lemma B.3.3 (Abel's summation by parts, [Bar15, Lemma 3.8])**.** *Let H be a Hilbert space with the corresponding scalar product $\langle \cdot, \cdot \rangle_H$ and the corresponding norm $\|\cdot\|_H$. Let $j \in \mathbb{N}$ and $(x_i)_{i=0}^j \in H$. Then, it holds that*

$$\sum_{i=0}^{j-1} \langle x_{i+1} - x_i, x_i \rangle_H = \frac{1}{2}\,\|x_j\|_H^2 - \frac{1}{2}\,\|x_0\|_H^2 + \sum_{i=0}^{j-1} \|x_{i+1} - x_i\|_H^2. \qquad \square$$

List of Figures

List of Tables

List of Assumptions

Time-stepping approaches (TPS)

Plain LLG ($\pi_h^D(v_h^i; m_h^i, m_h^{i-1})$).

Coupled ELLG system ($h_h^{i,\Theta}$).

Time-stepping approaches (MPS)

Plain LLG ($\pi_h^\Theta(m_h^{i+1}, m_h^i, m_h^{i-1})$).

Coupled SDLLG system ($s_h^{i,\Theta}$).

Literaturverzeichnis

[AdBH14] F. Alouges, A. de Bouard, and A. Hocquet. A semi-discrete scheme for the stochastic Landau-Lifshitz equation. *Stoch. Partial Differ. Equ. Anal. Comput.*, 2(3):281–315, 2014.

[AEB+13] C. Abert, L. Exl, F. Bruckner, A. Drews, and D. Suess. magnum.fe: A micromagnetic finite-element simulation code based on FEniCS. *J. Magn. Magn. Mater.*, 345:29 – 35, 2013.

[AF03] R. A. Adams and J. J. F. Fournier. *Sobolev spaces*, volume 140 of *Pure and Applied Mathematics (Amsterdam)*. Elsevier/Academic Press, Amsterdam, second edition, 2003.

[AGL05] J. Ahrens, B. Geveci, and C. Law. *ParaView: An End-User Tool for Large Data Visualization.* Visualization Handbook, Elsevier, 2005.

[AHP+14] C. Abert, G. Hrkac, M. Page, D. Praetorius, M. Ruggeri, and D. Suess. Spin-polarized transport in ferromagnetic multilayers: an unconditionally convergent FEM integrator. *Comput. Math. Appl.*, 68(6):639–654, 2014.

[AJ06] F. Alouges and P. Jaisson. Convergence of a finite element discretization for the Landau-Lifshitz equations in micromagnetism. *Math. Models Methods Appl. Sci.*, 16(2):299–316, 2006.

[AKST14] F. Alouges, E. Kritsikis, J. Steiner, and J.-C. Toussaint. A convergent and precise finite element scheme for Landau-Lifschitz-Gilbert equation. *Numer. Math.*, 128(3):407–430, 2014.

[AKT12] F. Alouges, E. Kritsikis, and J.-C. Toussaint. A convergent finite element approximation for Landau-Lifschitz-Gilbert equation. *Physica B*, 407:1345–1349, 2012.

[Alo08] F. Alouges. A new finite element scheme for Landau-Lifchitz equations. *Discrete Contin. Dyn. Syst. Ser. S*, 1(2):187–196, 2008.

[ARB+15] C. Abert, M. Ruggeri, F. Bruckner, C. Vogler, G. Hrkac, D. Praetorius, and D. Suess. A three-dimensional spin-diffusion model for micromagnetics. *Sci. Rep.*, (5):14855, 2015.

[AS92] F. Alouges and A. Soyeur. On global weak solutions for Landau-Lifshitz equations: existence and nonuniqueness. *Nonlinear Anal.*, 18(11):1071–1084, 1992.

[Bar05] S. Bartels. Stability and convergence of finite-element approximation schemes for harmonic maps. *SIAM J. Numer. Anal.*, 43(1):220–238, 2005.

[Bar06] S. Bartels. Constraint preserving, inexact solution of implicit discretizations of Landau–Lifshitz–Gilbert equations and consequences for convergence. *Proc. Appl. Math. Mech.*, 6(1):19–22, 2006.

[Bar15] S. Bartels. *Numerical methods for nonlinear partial differential equations*, volume 47 of *Springer Series in Computational Mathematics*. Springer, Cham, 2015.

[BBNP14] Ľ. Baňas, Z. Brzeźniak, M. Neklyudov, and A. Prohl. *Stochastic ferromagnetism*, volume 58 of *De Gruyter Studies in Mathematics*. De Gruyter, Berlin, 2014.

[BBP08] Ľ. Baňas, S. Bartels, and A. Prohl. A convergent implicit finite element discretization of the Maxwell-Landau-Lifshitz-Gilbert equation. *SIAM J. Numer. Anal.*, 46(3):1399–1422, 2008.

[BBP13] Ľ. Baňas, Z. Brzeźniak, and A. Prohl. Computational studies for the stochastic Landau-Lifshitz-Gilbert equation. *SIAM J. Sci. Comput.*, 35(1):B62–B81, 2013.

[Ber96] L. Berger. Emission of spin waves by a magnetic multilayer traversed by a current. *Phys. Rev. B*, 54:9353–9358, Oct 1996.

[BKP08] S. Bartels, J. Ko, and A. Prohl. Numerical analysis of an explicit approximation scheme for the Landau-Lifshitz-Gilbert equation. *Math. Comp.*, 77(262):773–788, 2008.

[BMS09] G. Bertotti, I. D. Mayergoyz, and C. Serpico. *Nonlinear magnetization dynamics in nanosystems*. Elsevier Series in Electromagnetism. Elsevier B. V., Amsterdam, 2009.

[BP06] S. Bartels and A. Prohl. Convergence of an implicit finite element method for the Landau-Lifshitz-Gilbert equation. *SIAM J. Numer. Anal.*, 44(4):1405–1419, 2006.

[BP07] S. Bartels and A. Prohl. Constraint preserving implicit finite element discretization of harmonic map flow into spheres. *Math. Comp.*, 76(260):1847–1859, 2007.

[BP08] S. Bartels and A. Prohl. Convergence of an implicit, constraint preserving finite element discretization of p-harmonic heat flow into spheres. *Numer. Math.*, 109(4):489–507, 2008.

[BPP15] Ľ. Baňas, M. Page, and D. Praetorius. A convergent linear finite element scheme for the Maxwell-Landau-Lifshitz-Gilbert equations. *Electron. Trans. Numer. Anal.*, 44:250–270, 2015.

[BPPR14] Ľ. Baňas, M. Page, D. Praetorius, and J. Rochat. A decoupled and unconditionally convergent linear FEM integrator for the Landau-Lifshitz-Gilbert equation with magnetostriction. *IMA J. Numer. Anal.*, 34(4):1361–1385, 2014.

[BPS09] Ľ. Baňas, A. Prohl, and M. Slodička. Modeling of thermally assisted magnetodynamics. *SIAM J. Numer. Anal.*, 47(1):551–574, 2008/09.

[BPS12] Ľ. Baňas, A. Prohl, and M. Slodička. Numerical scheme for augmented Landau-Lifshitz equation in heat assisted recording. *J. Comput. Appl. Math.*, 236(18):4775–4787, 2012.

[Bra07] D. Braess. *Finite elements*. Cambridge University Press, Cambridge, third edition, 2007. Theory, fast solvers, and applications in elasticity theory, Translated from the German by Larry L. Schumaker.

[BS08] S. C. Brenner and L. R. Scott. *The mathematical theory of finite element methods*, volume 15 of *Texts in Applied Mathematics*. Springer, New York, third edition, 2008.

[BSF$^+$14] F. Bruckner, D. Suess, M. Feischl, T. Führer, P. Goldenits, M. Page, D. Praetorius, and M. Ruggeri. Multiscale modeling in micromagnetics: existence of solutions and numerical integration. *Math. Models Methods Appl. Sci.*, 24(13):2627–2662, 2014.

[CF98] G. Carbou and P. Fabrie. Time average in micromagnetism. *J. Differential Equations*, 147(2):383–409, 1998.

[CF01] G. Carbou and P. Fabrie. Regular solutions for Landau-Lifschitz equation in a bounded domain. *Differential Integral Equations*, 14(2):213–229, 2001.

[Cim08] I. Cimrák. A survey on the numerics and computations for the Landau-Lifshitz equation of micromagnetism. *Arch. Comput. Methods Eng.*, 15(3):277–309, 2008.

[Cim09] I. Cimrák. Convergence result for the constraint preserving mid-point scheme for micromagnetism. *J. Comput. Appl. Math.*, 228(1):238–246, 2009.

[DL92] R. Dautray and J.-L. Lions. *Mathematical analysis and numerical methods for science and technology. Vol. 5*. Springer-Verlag, Berlin, 1992. Evolution problems. I, With the collaboration of Michel Artola, Michel Cessenat and Hélène Lanchon, Translated from the French by Alan Craig.

[DP99] M. J. Donahue and D. G. Porter. OOMMF user's guide, Version 1.0. Interagency Report NISTIR 6376, National Institute of Standards and Technology, Gaithersburg, MD, 1999.

[DPP$^+$17] G. Di Fratta, C.-M. Pfeiler, D. Praetorius, M. Ruggeri, and B. Stiftner. Linear second order IMEX-type integrator for the (eddy current) Landau–Lifshitz–Gilbert equation, 2017. Extended preprint available at arXiv:1711.10715.

[DS14] E. Dumas and F. Sueur. On the weak solutions to the Maxwell-Landau-Lifshitz equations and to the Hall-Magneto-Hydrodynamic equations. *Commun. Math. Phys.*, 330:1179–1225, 2014.

[Edw65] R. E. Edwards. *Functional analysis. Theory and applications*. Holt, Rinehart and Winston, New York-Toronto-London, 1965.

[EG04] A. Ern and J.-L. Guermond. *Theory and practice of finite elements*, volume 159 of *Applied Mathematical Sciences*. Springer-Verlag, New York, 2004.

[EHM+18] L. Exl, M. Hochsteger, N. Mauser, C.-M. Pfeiler, D. Praetorius, M. Ruggeri, J. Schöberl, and B. Stiftner. Computational micromagnetics with `NGS/Py`. In preparation, 2018.

[Eva10] L. C. Evans. *Partial differential equations*, volume 19 of *Graduate Studies in Mathematics*. American Mathematical Society, Providence, RI, second edition, 2010.

[FK90] D. Fredkin and T. Koehler. Hybrid method for computing demagnetizing fields. *IEEE Trans. Magn.*, 26(2):415–417, 1990.

[FT17] M. Feischl and T. Tran. The eddy current-LLG equations: FEM-BEM coupling and a priori error estimates. *SIAM J. Numer. Anal.*, 55(4):1786–1819, 2017.

[Gil55] T. L. Gilbert. A Lagrangian formulation of the gyromagnetic equation of the magnetization fields. *Phys. Rev.*, 100:1243, 1955. Abstract only.

[GLT16] B. Goldys, K.-N. Le, and T. Tran. A finite element approximation for the stochastic Landau-Lifshitz-Gilbert equation. *J. Differential Equations*, 260(2):937–970, 2016.

[Gol12] P. Goldenits. *Konvergente numerische Integration der Landau-Lifshitz-Gilbert Gleichung.* PhD thesis (in German), TU Wien, Institute for Analysis and Scientific Computing, 2012.

[GW07] C. J. García-Cervera and X.-P. Wang. Spin-polarized transport: existence of weak solutions. *Discrete Contin. Dyn. Syst. Ser. B*, 7(1):87–100, 2007.

[HS98] A. Hubert and R. Schäfer. *Magnetic domains; the analysis of magnetic microstructures.* Springer, Berlin, 1998. Corrected Printing 2000.

[Kem14] J. Kemetmüller. Numerische Integration der Landau-Lifschitz-Gilbert-Gleichung. Master thesis (in German), TU Wien, Institute for Analysis and Scientific Computing, 2014.

[KP06] M. Kružík and A. Prohl. Recent developments in the modeling, analysis, and numerics of ferromagnetism. *SIAM Rev.*, 48(3):439–483, 2006.

[KPP+18] J. Kraus, C.-M. Pfeiler, D. Praetorius, M. Ruggeri, and B. Stiftner. Iterative solution and preconditioning for the tangent plane scheme in computational micromagnetism. In preparation, 2018.

[LL08] L. Landau and E. Lifschitz. On the theory of the dispersion of magnetic permeability in ferromagnetic bodies. *Ukr. J. Phys.*, (53), 2008. Special Issue, Reprinted from Phys. Zeitsch. der Sow. 8, pp. 153–169 (1935).

[LPPT15] K.-N. Le, M. Page, D. Praetorius, and T. Tran. On a decoupled linear FEM integrator for eddy-current-LLG. *Appl. Anal.*, 94(5):1051–1067, 2015.

[LT13] K.-N. Le and T. Tran. A convergent finite element approximation for the quasi-static Maxwell-Landau-Lifshitz-Gilbert equations. *Comput. Math. Appl.*, 66(8):1389–1402, 2013.

[Maz11] V. Maz'ya. *Sobolev spaces with applications to elliptic partial differential equations*, volume 342 of *Grundlehren der Mathematischen Wissenschaften*. Springer, Heidelberg, augmented edition, 2011.

[McL00] W. McLean. *Strongly elliptic systems and boundary integral equations*. Cambridge University Press, Cambridge, 2000.

[Mon03] P. Monk. *Finite element methods for Maxwell's equations*. Numerical Mathematics and Scientific Computation. Oxford University Press, New York, 2003.

[mum] μMAG – Micromagnetic Modeling Activity Group. National Institute for Standards and Technology (NIST). `https://www.ctcms.nist.gov/~rdm/mumag.org.html`. Accessed: 2018-03-21.

[Néd86] J.-C. Nédélec. A new family of mixed finite elements in $\mathbf{R}^3$. *Numer. Math.*, 50(1):57–81, 1986.

[ngs] NGSolve finite element library. `https://ngsolve.org/`. Accessed: 2018-04-19.

[Pag13] M. Page. *On dynamical Micromagnetism*. PhD thesis, TU Wien, Institute for Analysis and Scientific Computing, 2013.

[Pfe17] C.-M. Pfeiler. Lineare IMEX-integration zweiter Ordnung für die nichtlineare Landau–Lifshitz–Gilbert-gleichung. Master thesis (in German), TU Wien, Institute for Analysis and Scientific Computing, 2017.

[Pra04] D. Praetorius. Analysis of the operator Δ^{-1}div arising in magnetic models. *Z. Anal. Anwendungen*, 23(3):589–605, 2004.

[Pro01] A. Prohl. *Computational micromagnetism*. Advances in Numerical Mathematics. B. G. Teubner, Stuttgart, 2001.

[PRS18] D. Praetorius, M. Ruggeri, and B. Stiftner. Convergence of an implicit–explicit midpoint scheme for computational micromagnetics. *Comput. Math. Appl.*, 75(5):1719–1738, 2018.

[QV94] A. Quarteroni and A. Valli. *Numerical approximation of partial differential equations*, volume 23 of *Springer Series in Computational Mathematics*. Springer, Berlin, 1994.

[Rie] A. Rieder. Coupling NGsolve to BEM++. `https://github.com/arieder/ngbem`. Accessed: 2018-02-27.

[Rou05] T. Roubíček. *Nonlinear partial differential equations with applications*, volume 153 of *International Series of Numerical Mathematics*. Birkhäuser Verlag, Basel, 2005.

[Rud91] Walter Rudin. *Functional analysis.* International Series in Pure and Applied Mathematics. McGraw-Hill, Inc., New York, second edition, 1991.

[Rug16] M. Ruggeri. *Coupling and numerical integration of the Landau–Lifshitz–Gilbert equation.* PhD thesis, TU Wien, Institute for Analysis and Scientific Computing, 2016.

[Saa03] Yousef Saad. *Iterative methods for sparse linear systems.* Society for Industrial and Applied Mathematics, Philadelphia, PA, second edition, 2003.

[ŚBA+15] W. Śmigaj, T. Betcke, S. Arridge, J. Phillips, and M. Schweiger. Solving boundary integral problems with BEM++. *ACM Trans. Math. Software*, 41(2):Art. 6, 40, 2015.

[Slo96] J. C. Slonczewski. Current-driven excitation of magnetic multilayers. *J. Magn. Magn. Mater.*, 159(1):L1 – L7, 1996.

[SS11] S. A. Sauter and C. Schwab. *Boundary element methods*, volume 39 of *Springer Series in Computational Mathematics.* Springer-Verlag, Berlin, 2011. Translated and expanded from the 2004 German original.

[SZ90] L. Ridgway Scott and Shangyou Zhang. Finite element interpolation of nonsmooth functions satisfying boundary conditions. *Math. Comp.*, 54(190):483–493, 1990.

[TNMS05] A. Thiaville, Y. Nakatani, J. Miltat, and Y. Suzuki. Micromagnetic understanding of current-driven domain wall motion in patterned nanowires. *EPL (Europhysics Letters)*, 69(6):990, 2005.

[Vis85] A. Visintin. On Landau-Lifshitz' equations for ferromagnetism. *Japan J. Appl. Math.*, 2(1):69–84, 1985.

[Wer11] D. Werner. *Funktionalanalysis.* Springer-Verlag, Berlin, 7th revised and extended edition, 2011. (in German).

[Yos95] K. Yosida. *Functional analysis.* Classics in Mathematics. Springer-Verlag, Berlin, 1995. Reprint of the sixth (1980) edition.

[Zei90] E. Zeidler. *Nonlinear functional analysis and its applications. II/A.* Springer-Verlag, New York, 1990. Linear monotone operators, Translated from the German by the author and Leo F. Boron.

[ZL04] S. Zhang and Z. Li. Roles of nonequilibrium conduction electrons on the magnetization dynamics of ferromagnets. *Phys. Rev. Lett.*, 93(12):127204, 2004.

Curriculum Vitae

Personal details

Name	**Bernhard Erwin Stiftner**
Date of birth	November 12, 1988
Place of birth	Vienna
Nationality	Austrian
Email	bernhard.stiftner@asc.tuwien.ac.at
Homepage	http://www.asc.tuwien.ac.at/~bstiftner/

Education/Working experience

since 03/2015	PhD student, Supervisor: Dirk Praetorius, Member of WWTF research project Thermally controlled magnetization dynamics (Grant: MA14-44), TU Vienna, Austria.
09/2013–03/2014	Internship at Robert Bosch GmbH in R & D, Schwieberdingen, Germany.
11/2012–11/2015	Master studies, Technical Mathematics, TU Vienna, Austria.
03/2008–11/2012	Bachelor studies, Mathematics in Technology and Sciences, TU Vienna, Austria.
09/1999–06/2007	Highschool/Middle school, Theresianische Akademie, Vienna, Austria.
09/1995–06/1999	Elementary school, Salvatorschule, Vienna, Austria.

Scientific publications/Preprints

G. Gantner, A. Haberl, D. Praetorius, and B. Stiftner. *Rate optimal adaptive FEM with inexact solver for nonlinear operators*, accepted for publication in IMA Journal of Numerical Analysis (2017). Published online first, DOI: drx050.

D. Praetorius, M. Ruggeri, and B. Stiftner. *Convergence of an implicit-explicit midpoint scheme for computational micromagnetics*, Computers & Mathematics with Applications, 75 (2018), 1719-1738.

G. Di Fratta, C.-M. Pfeiler, D. Praetorius, M. Ruggeri, and B. Stiftner. *Linear second order IMEX-type integrator for the (eddy current) Landau–Lifshitz–Gilbert equation*, 2017. Extended preprint available at arXiv:1711.10715.

G. Hrkac, C.-M. Pfeiler, D. Praetorius, M. Ruggeri, A. Segatti, and B. Stiftner. *Convergent tangent plane integrators for the simulation of chiral magnetic skyrmion dynamics*, 2018. Preprint available at arXiv:1712.03795v2.

Proceedings

G. Gantner, A. Haberl, D. Praetorius, and B. Stiftner. *Rate optimal adaptive FEM with inexact solver for strongly monotone operators*, Oberwolfach Workshop on Adaptive Algorithms, Oberwolfach, 18.09.2016-24.09.2016, Oberwolfach Report, European Mathematical Society, 44/2016 (2016). Preprint available at asc20x2016.

M. Ruggeri, D. Praetorius, and B. Stiftner. *Coupling and numerical integration of the Landau-Lifshitz-Gilbert equation*, Oberwolfach Mini-Workshop: Mathematics of Magnetoelastic Materials, Oberwolfach, 30.10.2016-05.11.2016, Oberwolfach Report, European Mathematical Society, 51/2016 (2016). Preprint available at OWR_2016_51.

Scientific talks

SolveLLG - A simulation tool for micromagnetics, NGSolve User Meeting, TU Wien, Wien, 14.06.2017-16.06.2017. link

Numerical integration of the Landau-Lifshitz-Gilbert equation, 11th International Conference on Large-Scale Scientific Computations, Sozopol, Bulgaria, 05.06.2017-09.06.2017. link

Numerical integration of the Landau-Lifshitz-Gilbert equation, 10th Workshop on Analysis and Advanced Numerical Methods for Partial Differential Equations (not only) for Junior Scientists, Paleochora, Greece, 02.10.2017-06.10.2017. link

Numerical integration of the Landau-Lifshitz-Gilbert equation, Invited talk at Oberseminar Numerische Mathematik, Universität Duisburg-Essen, 20.06.2017.

Linear second order implicit-explicit time integration of the (eddy-currents-) Landau-Lifschitz-Gilbert equation, 13th Austrian Numerical Analysis Day, Salzburg, 04./05.05.2017. link

An extended midpoint scheme for the Landau-Lifschitz-Gilbert equation in computational micromagnetics, 9th Workshop on Analysis and Advanced Numerical Methods for Partial Differential Equations (not only) for Junior Scientists, Strobl, 04.07.2016-08.07.2016. link

An extended midpoint scheme for the Landau-Lifschitz-Gilbert equation in computational micromagnetics, 12th Austrian Numerical Analysis Day, Innsbruck, 28./29.04.2016. link

Supervised thesis

C. Pfeiler. *Lineare IMEX-Integration zweiter Ordnung für die nichtlineare Landau-Lifshitz-Gilbert-Gleichung* (Supervisors: D. Praetorius, M. Ruggeri, B. Stiftner), Diploma thesis, Institute for Analysis and Scientific Computing, 2018, Examination: 24.01.2018.

Academic thesis

B. Stiftner. *A-Posteriori-Fehlerschätzer des Discontinuous-Galerkin-Verfahrens für die Space-Time-Diskretisierung der Wärmeleitungsgleichung* (Supervisor: M. Melenk), Diploma thesis, Institute for Analysis and Scientific Computing, 2015, Examination: 13.03.2015.

Teaching experience

Introduction to programming for Technical Mathematics (EPROG). link

Vienna, on June 15, 2018

____
Bernhard Erwin Stiftner